NONLINEAR FINITE ELEMENT ANALYSIS OF PILED RAFT FOUNDATION

THESIS

Submitted in partial fulfillment
of the requirements for the degree of
DOCTOR OF PHILOSOPHY

By

ANSHUMAN

Under the Supervision of

Dr. D.K.MAHARAJ

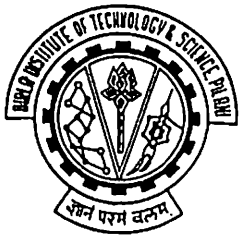

BIRLA INSTITUTE OF TECHNOLOGY AND SCIENCE
PILANI (RAJASTHAN)

2004

ACKNOWLEDGEMENTS

I wish to express deep sense of gratitude and sincere thanks to my thesis supervisor Dr D K Maharaj for his able guidance, encouragement and suggestions throughout the period of this research work. It has been a great privilege for me to work under his guidance

Much appreciation is expressed to Prof. Rajiv Gupta, Dean EHD, and Dr. K. Srinivas Raju, Group Leader, Civil Engineering Group, who were the members of Doctoral Advisory Committee (DAC), for their kind suggestions, moral support and assistance.

Gratitude is also accorded to BITS, Pilani for providing all the necessary facilities to complete the research work. My special thanks go to Prof. S. Venkateswaran, Vice Chancellor, B.I.T.S. for giving me an opportunity to do research at the Institute. I also thank Prof. L. K. Maheshwari, Director, B.I.T.S., Prof. K. E. Raman Deputy Director, B.I.T.S., Prof. V. S. Rao, Deputy Director, B.I.T.S. and Prof. A. K. Sarkar, Dean Instruction Division and Faculty Division-I, for providing the necessary infrastructure and other facilities.

I also express my gratitude for the kind and affectionate enquiries about the work and the encouragement given by Prof. Ravi Prakash, Dean, Research and Consultancy Division and Mr. Sanjay D. Pohekar of the same Division.

The contributions of Prof. H. S. Moondra, of Civil Engineering Group are acknowledged with appreciation. Special thanks and appreciation is extended to him for his invaluable advice and moral support throughout the study.

Once again I would like to add a word of thanks to Dr. A. P. Singh, Dr. P. K. Gupta, Mr.A.Vasan, Mr. Manish Kewalramani, Mr. Rajendra Khapre and Mr. Rahul

Ralegaonkar and all other colleagues in the Civil Engineering Group for their valuable time and support extended to me at the time of my need

Finally a very special expression of appreciation is extended to my father, Shri Ram Shankar Srivastava, mother, Smt Sheela Srivastava and all family members. Without their encouragement, patience, and understanding this endeavor would not have been possible. I would like to record my special affection and thanks to my wife Aarti, whose constant persuasion and moral support has been a source of inspiration to me. I also thank my daughter Ananya for having cheerfully sacrificing the time that rightfully belonged to her.

ABSTRACT

This thesis deals with the nonlinear finite element analysis to understand the behaviour of raft foundation and piled raft foundation under axisymmetric and plane strain condition. The nonlinear finite element analysis has been carried out for both the foundations by varying parameters like raft diameter/width, length of pile, load, raft thickness, soil modulus, and spacing between the piles. The raft, pile and soil have been discretized into four noded isoparametric finite elements. The soil has been modeled as Von-Mises elasto-plastic material. The nonlinear finite element equations have been solved by Modified Newton Raphson iterative procedure. Uniformly distributed load has been considered to act on the foundation. The uniformly distributed load considered has been applied as concentrated load on the respective nodes on the foundation in the nonlinear finite element analysis.

The load transfer mechanism in piled raft foundation is different than the conventional piled foundation. Based on the yielding pattern of soil it has been found that in piled raft foundation, the load transfer starts first at the tip of pile then it moves upward. In case of piled raft foundation with rigid raft, the yielding of soil is seen first near the tip and in between the boundary piles and then it moves towards the centre piles. When the spacing between the piles is very small, the yielding pattern of soil shows that the piles in group are having block behaviour. When the spacing between the piles is large, the soil element in between the piles are also found to yield even at the initial load steps.

In case of an axisymmetric piled raft foundation with large thickness of raft, the boundary piles carry maximum load followed by the intermediate piles while the centre piles carry minimum load. Similar results are found in case of piled raft foundation under plane strain condition. For initial load steps, the raft takes most of the load. With increase in load steps the load gets transferred to the piles. This is true when the piles are of larger length with respect to diameter/width of the raft. For piled raft foundation in which pile is small compared to the raft size, the piles first reaches to its ultimate capacity and then the raft.

The nonlinear finite element method predicts the load settlement curves, which resembles with the observed field behaviour. The load carrying capacity of raft increases with increase in thickness of raft, diameter/width of raft, length of pile and soil modulus. The effect of addition of piles even of length equal to the diameter/width of raft has been found to increase the load carrying capacity of raft significantly. The effect of increase in spacing has been found to decrease the load carrying capacity of piled raft foundation. The effect of increase in diameter/width of raft keeping the pile spacing same has been found to increase the overall load carrying capacity significantly.

When the thickness of raft is very small (0.1 to 0.5 metre) dish shape of deflection is seen for the axisymmetric raft foundation. For the raft foundation under plane strain condition, maximum deflection is found at the centre and minimum at the edge of the raft. Differential settlement is found maximum in this case. With increase in thickness of raft this differential settlement reduces and at high thickness of raft, this differential settlement is found almost zero. This differential settlement of raft is also found to reduce with increase in length of pile and found almost zero at larger length of pile.

The axial force in pile has been found maximum in the top of pile and minimum at the bottom of the pile for all load steps. At higher load steps the axial load distribution curves have been found to overlap each other showing that the piles have reached to almost its ultimate load carrying capacity. The effect of increase in soil modulus has been found to increase the axial load in pile. This is because the frictional resistance offered is more in stiff soil than in soft soil. In case of piles in a piled raft foundation under plane strain condition, in some cases the axial force in the pile has been found to increase first, then decreasing with depth and then increases near the tip of the pile. This may be due to the bending of pile.

The effect of increase in spacing has been found to increase the load carrying capacity of pile showing that the mobilization of frictional resistance increases with increase in spacing between the piles.

The prediction of load, for permissible settlement, can be achieved using load settlement curves produced. Similarly for the allowable load, the settlement experienced can be found. This is true for both raft and piled raft foundation under axisymmetric and plane strain condition. From the parameters thickness of raft, diameter/raft size, pile length, spacing between piles, soil modulus, load applied, and settlement, any one unknown parameter can be obtained if the other six parameters are known.

The application of load settlement curves shows that for permissible settlement, an option can be selected between raft and piled raft foundation depending upon the load coming from the superstructure. From the load settlement curves obtained and on the basis of permissible settlement, load has been calculated and converted into uniformly distributed load, it is found form the computations that a 20 to75 storey multistoreyed building can be constructed on piled raft for the soil range considered in this thesis.

TABLE OF CONTENTS

ACKNOWLEDGEMENTS			(i)
ABSTRACT			(iii)
LIST OF FIGURES			(ix)
LIST OF TABLES			(xix)
NOTATIONS			(xx)
CHAPTER 1 INTRODUCTION			
1.1		General	1
1.2		Load Transfer Mechanism in Piled Raft Foundation	1
1.3		Nonlinear Finite Element Analysis	2
1.4		Load Settlement Curves	3
1.5		Scope of Present Work	3
CHAPTER 2 LITERATURE REVIEW			
2.1		Introduction	4
2.2		Linear Analysis	4
2.3		Nonlinear Analysis	12
2.4		Model Study	18
2.5		Field Measurements	20
2.6		Summary	25
CHAPTER 3 FINITE ELEMENT FORMULATION			
3.1		Introduction	27
3.2		Finite Element Formulation for the Model	27
	3.2.1	Stiffness Matrix	27
	3.2.1.1	Plane Strain Problem	27
	3.2.1.2	Axisymmetric Problem	30
	3.2.2	Constitutive Model	32
	3.2.3	Elastoplastic Constitutive Matrix	32
	3.2.4	Equilibrium Equation for an element and for the complete structure	34
3.3		Modified Newton Raphson Iterative Procedure	35
CHAPTER 4 VALIDATION OF THE FINITE ELEMENT MODEL			
4.1		Introduction	37
4.2		Validation under Plane Strain Condition	37
	4.2.1	Definition of the Problem	37
	4.2.2	Comparison of Load-Settlement Curve	38
4.3		Validation Under Axisymmetric Condition	39
	4.3.1	Definition of the Problem	39
	4.3.2	Comparison of Load Settlement Curve	39
CHAPTER 5 NONLINEAR FINITE ELEMENT ANALYSIS FOR AXISYMEETRIC PILED RAFT FOUNDATION			
5.1		Introduction	41
5.2		Definition of Problem	41
5.3		Detailed Parametric Study	41
5.4		Analysis of Axisymmetric Raft	41

5.5 Analysis of Axisymmetric Piled Raft Foundation 42
5.6 Results and Discussions 43
5.6.1 Load Settlement Curves for Raft 43
5.6.1.1 Effect of Raft Thickness 43
5.6.1.2 Effect of Soil Modulus 45
5.6.1.3 Effect of Raft Diameter 51
5.6.2 Load Settlement Curves for Piled Raft Foundation 55
5.6.2.1 Effect of Length of Pile 55
5.6.2.2 Effect of Soil Modulus 58
5.6.2.3 Effect of Spacing 58
5.6.2.4 Effect of Raft Diameter 66
5.6.3 Axial Load Distribution 76
5.6.4 Settlement Profile for Raft Foundation 99
5.6.4.1 Effect of Raft Thickness 99
5.6.4.2 Effect of Soil Modulus 105
5.6.5 Settlement Profile For Raft in a Piled Raft Foundation 105
5.6.5.1 Effect of Pile Length 105
5.6.5.2 Effect of Soil Modulus 117
5.6.6 Yielding of Soil in a Piled Raft Foundation 148

CHAPTER 6 NONLINEAR FINITE ELEMENT ANALYSIS OF PILED RAFT FOUNDATION UNDER PLANE STRAIN CONDITION

6.1 Introduction 165
6.2 Definition of Problem 165
6.3 Detailed Parametric Study 165
6.4 Analysis of Raft 165
6.5 Analysis of Piled Raft Foundation 166
6.6 Results and Discussions 167
6.6.1 Load Settlement Curves for Raft 167
6.6.1.1 Effect of Thickness 167
6.6.1.2 Effect of Soil Modulus 169
6.6.1.3 Effect of Width of Raft 175
6.6.2 Load Settlement Curves for Piled Raft Foundation 181
6.6.2.1 Effect of Pile Length 181
6.6.2.2 Effect of Spacing 186
6.6.3 Axial Load Distribution 213
6.6.4 Settlement Profile 220
6.6.4.1 Settlement Profile for Raft 220
6.6.4.2 Settlement Profile for Piled Raft Foundation 237
6.6.5 Yielding of Soil 249

CHAPTER 7 APPLICATION OF LOAD SETTLEMENT CURVE

7.1 Introduction 271
7.2 Examples 271
7.2.1 Axisymmetric Piled Raft Foundation 271
7.2.1.1 Example-1 271
7.2.1.2 Example-2 272
7.2.1.3 Example-3 276

7.2.1.4 Example-4 278
7.2.1.5 Example-5 281
7.2.2 Piled Raft Foundation Under Plane Strain Condition 283
7.2.2.1 Example-1 283
7.2.2.2 Example-2 287
7.2.2.3 Example-3 290
CHAPTER 8 SUMMARY AND CONCLUSIONS
8.1 Summary & Conclusions 295
FUTURE EXTENSION OF THE WORK 298
REFERENCES 299
APPENDIX – I Description of Model Considered 307
APPENDIX – II Cost Analysis 311
APPENDIX – III FEM Software 314
APPENDIX – IV Discretization Details 317
APPENDIX – V List of Publications 319

LIST OF FIGURES

1.1 (a), (b), (c)	Raft, Pile and Piled Raft Foundation	2
3.1	A Four Noded Isoparametric Element (Plane Strain Condition)	28
3.2	A Four Noded Isoparametric Element (Axisymmetric Condition)	30
4.1	Definition of the Problem (After Whitman and Hoeg 1966)	38
4.2	Validation of 2D finite element model	38
4.3	Soil Conditions at University of Houston (After Kraft, 1981)	39
4.4	Validation of FE Model	40
5.1	Finite Element Discretization for Axisymmetric Raft	42
5.2	Finite Element Discretization for Axisymmetric Piled Raft Foundation	43
5.3 (a), (b), (c)	Load Settlement Curves for Various Raft Thickness (D =10 m)	44
5.4 (a), (b), (c)	Load Settlement Curves for Various Raft Thickness (D =20 m)	46
5.5 (a), (b), (c)	Effect of Soil Modulus on the Load Settlement Behaviour of Raft Foundation (D = 10 m)	47
5.6 (a), (b), (c)	Effect of Soil Modulus on the Load Settlement Behaviour of Raft Foundation (D = 20 m)	48
5.7 (a), (b), (c)	Effect of Soil Modulus on the Load Settlement Behaviour of Raft Foundation (D = 30 m)	49
5.8 (a), (b), (c)	Effect of Soil Modulus on the Load Settlement Behaviour of Raft Foundation (D = 40 m)	50
5.9 (a), (b), (c)	Load Settlement Curves for Various Thickness and Raft Size (Es = 22000 kN/m^2)	52
5.10 (a), (b), (c)	Load Settlement Curves for Various Thickness and Raft Size (Es = 76000 kN/m^2)	53
5.11 (a), (b), (c)	Load Settlement Curve for Various Thickness and Raft Size (Es = 130000 Kn/m^2)	54
5.12 (a), (b), (c)	Effect of Length of Pile on Load Settlement Behaviour of Piled Raft Foundation (D = 10 m, s/d = 2.5)	56
5.13 (a), (b), (c)	Effect of Length of Pile on Load Settlement Behaviour of Piled Raft Foundation (D = 10 m, s/d = 5)	57
5.14 (a), (b), (c)	Effect of Length of Pile on Load Settlement Behaviour of Piled Raft Foundation (D = 10 m, s/d = 7.5)	59
5.15 (a), (b), (c), (d)	Effect of Soil Modulus on the Load Settlement Behaviour of Piled Raft Foundation (D = 10 m, s/d = 2.5)	60
5.16 (a), (b), (c), (d)	Effect of Soil Modulus on the Load Settlement Behaviour of Piled Raft Foundation (D = 10 m, s/d = 5)	61
5.17 (a), (b), (c), (d)	Effect of Soil Modulus on the Load Settlement Behaviour of Piled Raft Foundation (D = 10 m, s/d = 7.5)	62

5.18 (a), (b), (c)	Effect of Spacing on the Load Settlement Behaviour of Piled Raft Foundation (D = 10 m E_s= 22000 kN/m^2)	63
5.19 (a), (b), (c)	Effect of Spacing on the Load Settlement Behaviour of Piled Raft Foundation (D = 10 m E_s= 76000 kN/m^2)	64
5.20 (a), (b), (c)	Effect of Spacing on the Load Settlement Behaviour of Piled Raft Foundation (D = 10 m E_s= 130000 kN/m^2)	65
5.21 (a), (b), (c)	Load Settlement Curve for Various Modulus and Pile Lengths (D = 20 m, s/d = 5)	67
5.22 (a), (b), (c)	Load Settlement Curve for Various Modulus and Pile Lengths (D = 20 m, s/d = 7.5)	68
5.23 (a), (b), (c)	Load Settlement Curve for Various Modulus and Pile Lengths (D = 20 m, s/d = 10)	69
5.24 (a), (b), (c), (d)	Load Settlement Curve for Various Modulus and Pile Lengths (D = 30 m, s/d = 5)	70
5.25 (a), (b), (c), (d)	Load Settlement Curve for Various Modulus and Pile Lengths (D = 30 m, s/d = 7.5)	71
5.26 (a), (b), (c), (d)	Load Settlement Curve for Various Modulus and Pile Lengths (D = 30 m, s/d = 10)	72
5.27 (a), (b), (c)	Effect of Soil Modulus on Load Settlement Behaviour of Piled Raft Foundation (D = 30 m, s/d = 5)	73
5.28 (a), (b), (c)	Effect of Soil Modulus on Load Settlement Behaviour of Piled Raft Foundation (D = 30 m, s/d = 7.5)	74
5.29 (a), (b), (c)	Effect of Soil Modulus on Load Settlement Behaviour of Piled Raft Foundation (D = 30 m, s/d = 10)	75
5.30 (a), (b), (c)	Load Settlement Curve for Various Soil Modulus and Pile Lengths (D = 40 m, s/d = 7.5)	77
5.31 (a), (b), (c)	Load Settlement Curve for Various Soil Modulus and Pile Lengths (D = 40 m, s/d = 10)	78
5.32 (a), (b), (c)	Load Settlement Curves for Various Soil Modulus and Pile Lengths (D = 40, s/d = 15)	78
5.33 (a), (b)	Load Settlement Curve for Various Soil Modulus and Pile Lengths (D = 50 m, s/d = 7.5)	80
5.34 (a), (b)	Load Settlement Curve for Various Soil Modulus and Pile Lengths (D = 50 m, s/d = 10)	81
5.35 (a), (b)	Load Settlement Curves for Various Soil Modulus and Pile Lengths (D = 50, s/d = 15)	82
5.36 (a), (b)	Axial Force Distribution in Piles (D = 10 m, E_s = 22000 kN/m^2, Load Step-1)	83
5.37 (a), (b)	Axial Force Distribution in Piles (D = 10 m, E_s = 22000 kN/m^2, Load Step-10)	85

5.38 (a), (b)	Axial Force Distribution in Center and End Piles (D = 10 m, L = 30 m, Es = 22000 kN/m^2, Load Step-1)	86
5.39 (a), (b)	Axial Force Distribution in Center and End Piles (D = 10 m, L = 30 m, E_s = 22000 kN/m^2, Load Step-10)	87
5.40 (a), (b)	Axial Force Distribution in Different Piles (D = 10 m, L = 10 m, s/d = 2.5, E_s = 22000 kN/m^2)	88
5.41 (a), (b), (c)	Axial Force Distribution in Different Piles (D = 10 m, L = 30 m, s/d = 2.5, E_s = 22000 kN/m^2)	89
5.42 (a), (b), (c)	Axial Force Distribution in Center and End Piles (D = 10 m, s/d = 2.5, L = 10 m, Load Step-1)	90
5.43 (a), (b), (c)	Axial Force Distribution in Center and End Pile (D = 10 m, s/d = 2.5, L = 10 m, Load Step-10)	92
5.44 (a), (b), (c)	Axial Force Distribution in Center and End Pile (D = 10 m, s/d = 2.5, L = 10 m, Load Step-10)	93
5.45 (a), (b), (c)	Axial Force Distributions in Piles for Different Load Steps (D = 10 m, s/d = 2.5, L =10 m, E_s = 130000 kN/m^2)	94
5.46 (a), (b), (c)	Axial Force Distribution in End Piles (D=10 m, s/d = 5, L = 10 m, E_s = 22000 kN/m^2)	96, 97
5.47 (a), (b), (c)	Axial Force Distribution in Middle and End Pile (D = 10 m, s/d = 5, L = 30 m, E_s = 22000 kN/m^2)	97, 98
5.48 (a), (b), (c)	Axial Force Distribution in End Pile (D = 10 m, L = 10 m, s/d = 5, E_s = 130000 kN/m^2)	100,101
5.49 (a), (b), (c)	Axial Force Distribution in Middle and End Pile (D = 10 m, s/d = 5, L = 30 m, E_s = 130000 kN/m^2)	101,102
5.50 (a), (b), (c)	Settlement Profile of Raft (D = 10 m, E_s = 22000 kN/m^2)	103
5.51 (a), (b), (c)	Settlement Profile of Raft (D = 10 m, E_s = 76000 kN/m^2)	104
5.52 (a), (b), (c)	Settlement Profile of Raft (D = 10 m, E_s = 130000 kN/m^2)	106
5.53 (a), (b), (c)	Settlement Profile of Raft (D = 20 m, E_s = 22000 kN/m^2)	107
5.54 (a), (b), (c)	Settlement Profile of Raft (D = 20 m, E_s = 76000 kN/m^2)	108
5.55 (a), (b), (c)	Settlement Profile of Raft (D = 20 m, E_s = 130000 kN/m^2)	109
5.56 (a), (b), (c)	Settlement Profile of Raft (D = 30 m, E_s = 22000 kN/m^2)	110
5.57 (a), (b), (c)	Settlement Profile of Raft (D = 30 m, E_s = 76000 kN/m^2)	111
5.58 (a), (b), (c)	Settlement Profile of Raft (D = 30 m, E_s = 130000 kN/m^2)	112
5.59 (a), (b), (c)	Settlement Profile of Raft (D = 40 m, E_s = 22000 kN/m^2)	113
5.60 (a), (b), (c)	Settlement Profile of Raft (D = 40 m, E_s = 76000 kN/m^2)	114

5.61 (a), (b), (c)	Settlement Profile of Raft ($D = 40$ m, $E_s = 130000$ kN/m^2)	115
5.62 (a), (b), (c)	Settlement Profile of Raft in Piled Raft Foundation ($D = 10$ m, $s/d = 2.5$, $E_s = 22000$ kN/m^2)	116
5.63 (a), (b), (c)	Settlement Profile of Raft in Piled Raft Foundation ($D = 10$ m, $s/d = 2.5$, $E_s = 76000$ kN/m^2)	118
5.64 (a), (b), (c)	Settlement Profile of Raft in Piled Raft Foundation ($D = 10$ m, $s/d = 2.5$, $E_s = 130000$ kN/m^2)	119
5.65 (a), (b), (c)	Settlement Profile of Raft in Piled Raft Foundation ($D = 10$ m, $s/d = 5$, $E_s = 22000$ kN/m^2)	120
5.66 (a), (b), (c)	Settlement Profile of Raft in Piled Raft Foundation ($D = 10$ m, $s/d = 5$, $E_s = 76000$ kN/m^2)	121
5.67 (a), (b), (c)	Settlement Profile of Raft in Piled Raft Foundation ($D = 10$ m, $s/d = 5$, $E_s = 130000$ kN/m^2)	122
5.68 (a), (b), (c)	Settlement Profile of Raft in Piled Raft Foundation ($D = 10$ m, $s/d = 7.5$, $E_s = 22000$ kN/m^2)	123
5.69 (a), (b), (c)	Settlement Profile of Raft in Piled Raft Foundation ($D = 10$ m, $s/d = 7.5$, $E_s = 76000$ kN/m^2)	124
5.70 (a), (b), (c)	Settlement Profile of Raft in Piled Raft Foundation ($D = 10$ m, $s/d = 7.5$, $E_s = 130000$ kN/m^2)	125
5.71 (a), (b), (c)	Settlement Profile of Raft in Piled Raft Foundation ($D = 20$ m, $s/d = 5$, $E_s = 22000$ kN/m^2)	126
5.72 (a), (b), (c)	Settlement Profile of Raft in Piled Raft Foundation ($D = 20$ m, $s/d = 5$, $E_s = 76000$ kN/m^2)	127
5.73 (a), (b), (c)	Settlement Profile of Raft in Piled Raft Foundation ($D = 20$ m, $s/d = 5$, $E_s = 130000$ kN/m^2)	128
5.74 (a), (b), (c)	Settlement Profile of Raft in Piled Raft Foundation ($D = 20$ m, $s/d = 7.5$, $E_s = 22000$ kN/m^2)	129
5.75 (a), (b), (c)	Settlement Profile of Raft in Piled Raft Foundation ($D = 20$ m, $s/d = 7.5$, $E_s = 76000$ kN/m^2)	130
5.76 (a), (b), (c)	Settlement Profile of Raft in Piled Raft Foundation ($D = 20$ m, $s/d = 7.5$, $E_s = 130000$ kN/m^2)	131
5.77 (a), (b), (c)	Settlement Profile of Raft in Piled Raft Foundation ($D = 20$ m, $s/d = 10$, $E_s = 22000$ kN/m^2)	133
5.78 (a), (b), (c)	Settlement Profile of Raft in Piled Raft Foundation ($D = 20$ m, $s/d = 10$, $E_s = 76000$ kN/m^2)	134
5.79 (a), (b), (c)	Settlement Profile of Raft in Piled Raft Foundation ($D = 20$ m, $s/d = 10$, $E_s = 130000$ kN/m^2)	135
5.80 (a), (b), (c)	Settlement Profile of Raft in Piled Raft Foundation ($D = 30$ m, $s/d = 5$, $E_s = 22000$ kN/m^2)	136
5.81 (a), (b), (c)	Settlement Profile of Raft in Piled Raft Foundation ($D = 30$ m, $s/d = 5$, $E_s = 76000$ kN/m^2)	137
5.82 (a), (b), (c)	Settlement Profile of Raft in Piled Raft Foundation ($D = 30$ m, $s/d = 5$, $E_s = 130000$ kN/m^2)	138
5.83 (a), (b), (c)	Settlement Profile of Raft in Piled Raft Foundation ($D = 30$ m, $s/d = 7.5$, $E_s = 22000$ kN/m^2)	139

5.84 (a), (b), (c)	Settlement Profile of Raft in Piled Raft Foundation (D = 30 m, s/d = 7.5, E_s = 76000 kN/m^2)	140
5.85 (a), (b), (c)	Settlement Profile of Raft in Piled Raft Foundation (D = 30 m, s/d = 7.5, E_s = 130000 kN/m^2)	141
5.86 (a), (b), (c)	Settlement Profile of Raft in Piled Raft Foundation (D = 30 m, s/d = 10, E_s = 22000 kN/m^2)	142
5.87 (a), (b), (c)	Settlement Profile of Raft in Piled Raft Foundation (D = 30 m, s/d = 10, E_s = 76000 kN/m^2)	143
5.88 (a), (b), (c)	Settlement Profile of Raft in Piled Raft Foundation (D = 30 m, s/d = 10, E_s = 130000 kN/m^2)	144
5.89 (a), (b), (c)	Settlement Profile of Raft in Piled Raft Foundation (D = 50 m, s/d = 7.5, E_s = 22000 kN/m^2)	145
5.90 (a), (b), (c)	Settlement Profile of Raft in Piled Raft Foundation (D = 50 m, s/d = 7.5, E_s = 76000 kN/m^2)	146
5.91 (a), (b), (c)	Settlement Profile of Raft in Piled Raft Foundation (D = 50 m, s/d = 7.5, E_s = 130000 kN/m^2)	147
5.92 (a), (b), (c)	Settlement Profile of Raft in Piled Raft Foundation (D = 50 m, s/d = 10, E_s = 22000 kN/m^2)	149
5.93 (a), (b), (c)	Settlement Profile of Raft in Piled Raft Foundation (D = 50 m, s/d = 10, E_s = 76000 kN/m^2)	150
5.94 (a), (b), (c)	Settlement Profile of Raft in Piled Raft Foundation (D = 50 m, s/d = 10, E_s = 130000 kN/m^2)	151
5.95 (a), (b), (c)	Settlement Profile of Raft in Piled Raft Foundation (D = 50 m, s/d = 15, E_s = 22000 kN/m^2)	152
5.96 (a), (b), (c)	Settlement Profile of Raft in Piled Raft Foundation (D = 50 m, s/d = 15, E_s = 76000 kN/m^2)	153
5.97(a), (b), (c)	Settlement Profile of Raft in Piled Raft Foundation (D = 50 m, s/d = 15, E_s = 130000 kN/m^2)	154
5.98 (a), (b)	Yielding of Soil in a Piled Raft Foundation Load Step- 5 & 7 (D = 10 m, s/d = 2.5, L = 10 m, t = 0.1 m, E_s = 22000 kN/m^2)	155
5.99 (a), (b)	Yielding of Soil in a Piled Raft Foundation Load Step-10 & 15 (D = 10 m, s/d = 2.5, L = 10 m, t = 0.1 m, E_s = 22000 kN/m^2)	155
5.100	Yielding of Soil in a Piled Raft Foundation Load Step-20 (D = 10 m, s/d = 2.5, L = 10 m, t = 0.1 m, E_s = 22000 kN/m^2)	157
5.101 (a), (b)	Yielding of Soil in a Piled Raft Foundation Load Step-5 & 7 (D = 10 m, s/d = 2.5, L = 10 m, t = 4.0 m, E_s = 22000 kN/m^2)	157
5.102 (a), (b)	Yielding of Soil in a Piled Raft Foundation Load Step-10 &15 (D = 10 m, s/d = 2.5, L = 10 m, t = 4.0 m, E_s = 22000 kN/m^2)	158
5.103	Yielding of Soil in a Piled Raft Foundation Load Step-20 (D = 10 m, s/d = 2.5, L = 10 m, t = 4.0 m, E_s = 22000kN/m^2)	158

5.104 (a), (b)	Yielding of Soil in a Piled Raft Foundation Load Step-5 & 7 (D = 30 m L = 30 m s/d = 7.5 t = 1.0 m Es = 130000 kN/m^2)	159
5.105 (a), (b)	Yielding of Soil in a Piled Raft Foundation Load Step-10 & 15 (D = 30 m L = 30 m s/d = 7.5 t = 1.0 m Es = 130000 kN/m^2)	159
5.106	Yielding of Soil in a Piled Raft Foundation Load Step-20 (D = 30 m L = 30 m s/d = 7.5 t = 1.0 m Es = 130000 kN/m^2)	160
5.107 (a), (b)	Yielding of Soil in a Piled Raft Foundation Load Step – 4 & 7(D = 30 m L = 90 m s/d = 7.5 t = 1.0 m Es = 22000 kN/m^2)	162
5.108 (a), (b)	Yielding of Soil in a Piled Raft Foundation Load Step–10& 15(D = 30 m L = 90 m s/d = 7.5 t = 1.0 m Es = 22000 N/m^2)	162
5.109	Yielding of Soil in a Piled Raft Foundation Load Step - 20 (D = 30 m L = 90 m s/d = 7.5 t = 1.0 m Es = 22000 kN/m^2)	163
5.110 (a), (b)	Yielding of Soil in a Piled Raft Foundation Load Step-5 & 7 (D = 30 m L = 90 m s/d = 7.5 t = 1.0 m Es = 130000 kN/m^2)	163
5.111 (a), (b)	Yielding of Soil in a Piled Raft Foundation Load Step-10& 15(D = 30 m L = 90 m s/d = 7.5 t = 1.0 m Es = 130000 kN/m^2)	164`
5.112	Yielding of Soil in a Piled Raft Foundation Load Step- 20 (D = 30 m L = 90 m s/d = 7.5 t = 1.0 m Es = 130000 kN/m^2)	164
6.1	Finite element discretization for raft under plane strain condition	166
6.2	Finite element discretization of piled raft: Plane strain condition	167
6.3 (a), (b), (c)	Load Settlement Curves for Raft Foundation (B = 10 m)	168
6.4 (a), (b), (c)	Load Settlement Curves for Raft Foundation (B = 20 m)	170
6.5 (a), (b), (c)	Load Settlement Curves for Raft Foundation (B = 30 m)	171
6.6 (a), (b), (c)	Load Settlement Curves for Raft Foundation (B = 40 m)	172
6.7 (a), (b), (c)	Load Settlement Curves for Raft Foundation (B = 50 m)	173
6.8 (a), (b), (c), (d), (e), (f)	Effects of Soil Modulus and Raft Thickness on Load Settlement Curves of Raft Foundation (B = 10 m)	174
6.9 (a), (b), (c), (d), (e), (f)	Effects of Soil Modulus and Raft Thickness on Load Settlement Curves of Raft Foundation (B = 20 m)	176
6.10 (a), (b), (c), (d), (e), (f)	Effects of Soil Modulus and Raft Thickness on Load Settlement Curves of Raft Foundation (B = 30 m)	177
6.11 (a), (b), (c), (d), (e), (f)	Effects of Soil Modulus and Raft Thickness on Load Settlement Curves of Raft Foundation (B = 40 m)	178
6.12 (a), (b), (c), (d), (e), (f)	Effects of Soil Modulus and Raft Thickness on Load Settlement Curves of Raft Foundation (B = 50 m)	179
6.13 (a), (b), (c), (d), (e), (f)	Effect of Raft Width on Load Settlement Curves of Raft Foundation (E_s = 22000 kN/m^2)	180
6.14 (a), (b), (c), (d), (e), (f)	Effect of Raft Width on Load Settlement Curves of Raft Foundation (E_s = 76000 kN/m^2)	182
6.15 (a), (b), (c)	Effect of Pile Length on Load Settlement Curves of Piled Raft Foundation (B = 10 m, s/d = 2.5)	183
6.16 (a), (b), (c)	Effect of Pile Length on Load Settlement Curves of Piled	184

	Raft Foundation (B = 10 m, s/d = 5)	
6.17 (a), (b), (c)	Effect of Pile Length on Load Settlement Curves of Piled Raft Foundation (B = 10 m, s/d = 7.5)	185
6.18 (a), (b), (c), (d)	Effect of Soil Modulus on Load Settlement Curves of Piled Raft Foundation (B = 10 m, s/d = 2.5)	187
6.19 (a), (b), (c), (d)	Effect of Soil Modulus on Load Settlement Curves of Piled Raft Foundation (B = 10 m, s/d = 5)	188
6.20 (a), (b), (c), (d)	Effect of Soil Modulus on Load Settlement Curves of Piled Raft Foundation (B = 10 m, s/d = 7.5)	189
6.21 (a), (b), (c)	Effect of Spacing on Load Settlement Curves of Piled Raft Foundation (B = 10 m, E_s = 22000 kN/m^2)	190
6.22 (a), (b), (c)	Effect of Spacing on Load Settlement Curves of Piled Raft Foundation (B = 10 m, E_s = 76000 kN/m^2)	191
6.23 (a), (b), (c)	Effect of Spacing on Load Settlement Curves of Piled Raft Foundation (B = 10 m, E_s = 130000 kN/m^2)	193
6.24 (a), (b), (c)	Effect of Pile Length Load Settlement Curves of Piled Raft Foundation (B = 20 m, s/d = 5)	194
6.25 (a), (b), (c)	Effect of Pile Length Load Settlement Curves of Piled Raft Foundation (B = 20 m, s/d = 7.5)	195
6.26 (a), (b), (c)	Effect of Pile Length Load Settlement Curves of Piled Raft Foundation (B = 20 m, s/d = 10)	196
6.27 (a), (b), (c), (d)	Effect of Soil Modulus Load Settlement Curves of Piled Raft Foundation (B = 20 m s/d = 5)	197
6.28 (a), (b), (c), (d)	Effect of Soil Modulus Load Settlement Curves of Piled Raft Foundation (B = 20 m s/d = 7.5)	198
6.29 (a), (b), (c), (d)	Effect of Soil Modulus Load Settlement Curves of Piled Raft Foundation (B = 20 m s/d = 10)	200
6.30 (a), (b), (c)	Effect of spacing Load Settlement Curves of Piled Raft Foundation (D = 20 m, E_s = 22000 kN/m^2)	201
6.31 (a), (b), (c)	Effect of spacing Load Settlement Curves of Piled Raft Foundation (D = 20 m, E_s = 76000 kN/m^2)	202
6.32 (a), (b), (c)	Effect of spacing Load Settlement Curves of Piled Raft Foundation (D = 20 m, E_s = 130000 kN/m^2)	203
6.33 (a), (b), (c)	Effect of Length of Pile Load Settlement Curves of Piled Raft Foundation (B = 30 m, s/d = 7.5)	204
6.34 (a), (b), (c)	Effect of Length of Pile Load Settlement Curves of Piled Raft Foundation (B = 30 m, s/d = 10)	205
6.35 (a), (b), (c), (d)	Effect of Soil Modulus on Load Settlement Curves of Piled Raft Foundation (B = 30 m s/d = 7.5)	207
6.36 (a), (b), (c), (d)	Effect of Soil Modulus on Load Settlement Curves of Piled Raft Foundation (B = 30 m s/d = 10)	208
6.37 (a), (b), (c)	Effect of Spacing on Load Settlement Curves of Piled Raft Foundation (B = 30 m, Es = 22000 kN/m^2)	209
6.38 (a), (b), (c)	Effect of Spacing on Load Settlement Curves of Piled Raft Foundation (B = 30 m, Es = 76000 kN/m^2)	210
6.39 (a), (b), (c)	Effect of Spacing on Load Settlement Curves of Piled Raft	211

	Foundation (B = 30 m, Es = 130000 kN/m^2)	
6.40 (a), (b), (c)	Effect of Pile Length on Load Settlement Curves of Piled Raft Foundation (B = 40 m, s/d = 7.5)	212
6.41 (a), (b), (c)	Effect of Pile Length on Load Settlement Curves of Piled Raft Foundation (B = 40 m, s/d = 10)	214
6.42 (a), (b), (c)	Effect of Pile Length on Load Settlement Curves of Piled Raft Foundation (B = 40 m, s/d = 15)	215
6.43 (a), (b), (c), (d)	Effect of Soil Modulus on Load Settlement Curves of Piled Raft Foundation (B = 40 m, s/d = 7.5)	216
6.44 (a), (b), (c), (d)	Effect of Soil Modulus on Load Settlement Curves of Piled Raft Foundation (B = 40 m, s/d = 10)	217
6.45 (a), (b), (c), (d)	Effect of Soil Modulus on Load Settlement Curves of Piled Raft Foundation (B = 40 m, s/d = 15)	218
6.46 (a), (b)	Axial Force Distribution in Pile (B = 30 m, Es = 130000 kN/m^2, Center Pile)	219
6.47 (a), (b)	Axial Force Distribution in Pile (B = 30 m, Es = 130000 kN/m^2, End Pile)	221
6.48 (a), (b)	Effect of Soil Modulus on Axial Force Distribution (B = 30 m, s/d = 10, Center Pile)	222
6.49 (a), (b)	Effect of Soil Modulus on Axial Force Distribution (D = 30 m, s/d = 10, End Pile)	223
6.50 (a), (b), (c)	Settlement Profile of Raft (B = 10 m, E_s = 76000 kN/m^2)	224
6.51 (a), (b), (c)	Settlement Profile of Raft (B = 10 m, E_s = 130000 kN/m^2)	226
6.52 (a), (b), (c)	Settlement Profile of Raft (B = 20 m Es = 22000 kN/m^2)	227
6.53 (a), (b), (c)	Settlement Profile of Raft (B = 20 m Es = 76000 kN/m^2)	228
6.54 (a), (b), (c)	Settlement Profile of Raft (B = 20 m Es = 130000 kN/m^2)	229
6.55 (a), (b), (c)	Settlement Profile of Raft (B = 30 m Es = 22000 kN/m^2)	230
6.56 (a), (b), (c)	Settlement Profile of Raft (B = 30 m Es = 76000 kN/m^2)	232
6.57 (a), (b), (c)	Settlement Profile of Raft (B = 30 m Es = 130000 kN/m^2)	233
6.58 (a), (b), (c)	Settlement Profile of Raft (B = 40 m Es = 22000 kN/m^2)	234
6.59 (a), (b), (c)	Settlement Profile of Raft (B = 40 m Es = 76000 kN/m^2)	235
6.60 (a), (b), (c)	Settlement Profile of Raft (B = 40 m Es = 130000 kN/m^2)	236
6.61 (a), (b), (c)	Settlement Profile of Raft (B = 50 m Es = 22000 kN/m^2)	238
6.62 (a), (b), (c)	Settlement Profile of Raft (B = 50 m Es = 76000 kN/m^2)	239
6.63 (a), (b), (c)	Settlement Profile of Raft (B = 50 m Es = 130000 kN/m^2)	240
6.64 (a), (b), (c)	Settlement Profile of Raft in Piled Raft Foundation (B = 10 m, s/d = 2.5, E_s = 22000 kN/m^2)	241
6.65 (a), (b), (c)	Settlement Profile of Raft in Piled Raft Foundation (B = 10 m, s/d = 2.5, E_s = 76000 kN/m^2)	242
6.66 (a), (b), (c)	Settlement Profile of Raft in Piled Raft Foundation (B = 10 m, s/d = 2.5, E_s = 130000 kN/m^2)	244
6.67 (a), (b), (c)	Settlement Profile of Raft in Piled Raft Foundation (B = 10 m, s/d = 5, E_s = 22000 kN/m^2)	245
6.68 (a), (b), (c)	Settlement Profile of Raft in Piled Raft Foundation (B = 10 m, s/d = 5, E_s = 76000 kN/m^2)	246

6.69 (a), (b), (c)	Settlement Profile of Raft in Piled Raft Foundation (B = 10 m, s/d = 5, E_s = 130000 kN/m^2)	247
6.70 (a), (b), (c)	Settlement Profile of Raft in Piled Raft Foundation (B = 10 m, s/d = 7.5, E_s = 22000 kN/m^2)	248
6.71 (a), (b), (c)	Settlement Profile of Raft in Piled Raft Foundation (B = 10 m, s/d = 7.5, E_s = 76000 kN/m^2)	250
6.72 (a), (b), (c)	Settlement Profile of Raft in Piled Raft Foundation (B = 10 m, s/d = 7.5, E_s = 130000 kN/m^2)	251
6.73 (a), (b)	Yielding of Soil, Load Step-3 & 5 (B = 10 m, L = 10 m, t = 0.1 m, s/d = 2.5, E_s = 22000 kN/m^2)	252
6.74 (a), (b)	Yielding of Soil, Load Step-7 & 10 (B = 10 m, L = 10 m, t = 0.1 m, s/d = 2.5, E_s = 22000 kN/m^2)	252
6.75 (a), (b)	Yielding of Soil, Load Step-3 & 5 (B = 10 m, L = 10 m, t = 1.0 m, s/d = 2.5, E_s = 22000 kN/m^2)	254
6.76 (a), (b)	Yielding of Soil, Load Step-7 & 10 (B = 10 m, L = 10 m, t = 1.0 m, s/d = 2.5, E_s = 22000 kN/m^2)	254
6.77 (a), (b)	Yielding of Soil, Load Step- 4 & 5 (B = 10 m, L = 10 m, t = 4.0 m, s/d = 2.5, E_s = 22000 kN/m^2)	255
6.78 (a), (b)	Yielding of Soil, Load Step-7 & 10 (B = 10 m, L = 10 m, t = 4.0 m, s/d = 2.5, E_s = 22000 kN/m^2)	255
6.79 (a), (b)	Yielding of Soil, Load Step-5 & 7 (B = 10 m, L = 10 m, t = 0.1 m, s/d = 2.5, E_s = 130000 kN/m^2)	256
6.80 (a), (b)	Yielding of Soil, Load Step-10 & 15 (B = 10 m, L = 10 m, t = 0.1 m, s/d = 2.5, E_s = 130000 kN/m^2)	258
6.81 (a), (b)	Yielding of Soil, Load Step-5 & 7 (B = 10 m, L = 10 m, t = 1.0 m, s/d = 2.5, E_s = 130000 kN/m^2)	258
6.82 (a), (b)	Yielding of Soil, Load Step-10 & 15 (B = 10 m, L = 10 m, t = 1.0 m, s/d = 2.5, E_s = 130000 kN/m^2)	259
6.83 (a), (b)	Yielding of Soil, Load Step-5 & 7 (B = 10 m, L = 30 m, t = 1.0 m, s/d = 2.5, E_s = 22000 kN/m^2)	259
6.84 (a), (b)	Yielding of Soil, Load Step-10 & 15 (B = 10 m, L = 30 m, t = 1.0 m, s/d = 2.5, E_s = 22000 kN/m^2)	260
6.85	Yielding of Soil, Load Step-20 (B = 10 m, L = 30 m, t = 1.0 m, s/d = 2.5, E_s = 22000 kN/m^2)	260

6.86 (a), (b)	Yielding of Soil, Load Step-6 & 8 (B = 10 m, L = 30 m, t = 4.0 m, s/d = 2.5, E_s = 130000 kN/m^2)	262
6.87 (a), (b)	Yielding of Soil, Load Step-10 & 15 (B = 10 m, L = 30 m, t = 4.0 m, s/d = 2.5, E_s = 130000 kN/m^2)	262
6.88 (a), (b)	Yielding of Soil, Load Step-3 & 5 (B = 10 m, L = 10 m, t = 0.1 m, s/d = 7.5, E_s = 22000 kN/m^2)	263
6.89 (a), (b)	Yielding of Soil, Load Step-8 & 10 (B = 10 m, L = 10 m, t = 0.1 m, s/d = 7.5, E_s = 22000 kN/m^2)	263
6.90 (a), (b)	Yielding of Soil, Load Step-4 & 7 (B = 10 m, L = 10 m, t = 1.0 m, s/d = 7.5, E_s = 130000 kN/m^2)	264
6.91 (a), (b)	Yielding of Soil, Load Step-10 & 15 (B = 10 m, L = 10 m, t = 1.0 m, s/d = 7.5, E_s = 130000 kN/m^2)	266
6.92 (a), (b)	Yielding of Soil, Load Step-4 & 6 (B = 10 m, L = 30 m, t = 1.0 m, s/d = 7.5, E_s = 22000 kN/m^2)	266
6.93 (a), (b)	Yielding of Soil, Load Step-9 & 12 (B = 10 m, L = 30 m, t = 1.0 m, s/d = 7.5, E_s = 22000 kN/m^2)	267
6.94	Yielding of Soil, Load Step-20 (B = 10 m, L = 30 m, t = 1.0 m, s/d = 7.5, E_s = 22000 kN/m^2)	267
6.95 (a), (b)	Yielding of Soil, Load Step-5 & 8 (B = 10 m, L = 30 m, t = 1.0 m, s/d = 7.5, E_s = 130000 kN/m^2)	268
6.96 (a), (b)	Yielding of Soil, Load Step-12 & 16 (B = 10 m, L = 30 m, t = 1.0 m, s/d = 7.5, E_s = 22000 kN/m^2)	268
6.97	Yielding of Soil, Load Step-20 (B = 10 m, L = 30 m, t = 1.0 m, s/d = 7.5, E_s = 22000 kN/m^2)	270
7.1	Load Settlement Curves (D = 10 m, s/d = 5 E_s = 22000 kN/m^2)	
7.2	Load Settlement Curves (D = 10 m, s/d = 5 E_s = 76000 kN/m^2)	
7.3 (a), (b)	Load Settlement Curves (D = 10 m, s/d = 5)	
7.4 (a), (b), (c)	Load Settlement Curves (D = 30 m s/d = 5)	
7.5 (a), (b)	Load Settlement Curves (D = 50 m s/d = 7.5)	
7.6 (a), (b), (c)	Load Settlement Curves (B = 20 m s/d = 5)	
7.7 (a), (b), (c)	Load Settlement Curves (B = 20 m s/d = 7.5)	
7.8 (a), (b), (c)	Load Settlement Curves (B = 20 m s/d = 10)	

LIST OF TABLES

Table No	Title	Page No.
7.1	Settlement for different length of Pile (D =10 m, s/d =5, E_s = 22000 kN/m^2)	272
7.2	Settlement for different length of Pile (D =10 m, s/d =5, E_s = 76000 kN/m^2)	274
7.3	Permissible Loads and Loading Intensity Obtained for Different Length of Pile and the Soil Modulus (D = 10 m, s/d = 5)	276
7.4	Permissible Loads and Loading Intensity Obtained for Different Length of Pile and the Soil Modulus (D = 30 m, s/d = 5)	278
7.5	Permissible Loads and Loading Intensity Obtained for Different Length of Pile and the Soil Modulus (D = 50 m, s/d = 7.5)	283
7.6	Permissible Loads and Loading Intensity Obtained for Different Length of Pile and the Soil Modulus (D = 20 m, s/d = 5) Plain Strain Condition	284
7.7	Permissible Loads and Loading Intensity Obtained for Different Length of Pile and the Soil Modulus (D = 20 m, s/d = 7.5) Plain Strain Condition	290
7.8	Permissible Loads and Loading Intensity Obtained for Different Length of Pile and the Soil Modulus (D = 20 m, s/d = 10) Plain Strain Condition	291

NOTATION

B	=	Width of raft
d	=	Diameter of pile
E_c	=	Elastic Modulus of concrete
E_s	=	Elastic Modulus of soil
L	=	Pile length
n	=	Number of pile
s	=	Spacing between piles.
t	=	Raft thickness
udl	=	Uniformly distributed load
W	=	Total load applied on piled raft system
z	=	Depth below ground level
μ_c	=	Poisson's ratio of concrete
μ_s	=	Poisson's ratio of soil
D	=	Diameter of Raft

BIRLA INSTITUTE OF TECHNOLOGY & SCIENCE

PILANI (RAJASTHAN)

CERTIFICATE

This is to certify that the thesis entitled "**Nonlinear Finite Element Analysis of Piled Raft Foundation**" and submitted by **Anshuman** ID No. **1997PHXF404** for award of Ph.D. Degree of the Institute, embodies original work done by him under my supervision.

D Maharaj

Signature in full of the Supervisor

Name in capital block letters: D.K.MAHARAJ

Designation: Assistant Professor

Date: 17-05-2004

CHAPTER 1

INTRODUCTION

1.1 GENERAL

Piled raft foundation (Figure 1.1 (a)) is a recent concept of foundation in which the total load coming from the structure is taken by pile and raft both. The pile carry load through skin friction while the raft carries the load through contact with the soil. Such piled raft foundations on thick clay deposit have been found successful in places like Frankfurt, London etc. There are many instances of piled raft being used to support structures among these being: The Hyde Park Cavalry Barracks in London, UK and Guy's Hospital in London, UK. In conventional piled foundation (Figure 1.1(b)) the contribution of raft is completely ignored which makes the piled foundation an uneconomical foundation. Also in conventional piled foundation, long piles are a must as the piles are to be extended upto the deep hard strata. On the other hand if only raft foundation (Figure 1.1(c)) is provided, very thick raft is needed which again increases the cost of the foundation. Such raft foundation undergoes excessive settlement as well. In such situation piled raft foundation is best solution in which the piles are not to be extended upto the deep hard strata, it can be terminated at higher elevation. Also such piled raft foundation undergoes lesser settlement than that of the raft foundation. Such piled raft foundation has been reported in literature (Hooper (1973), Frankee (1991) and Yamashita (1994)).

1.2 LOAD TRANSFER MECHANISM IN PILED RAFT FOUNDATION

The load transfer mechanism in piles in a piled raft foundation and that in conventional piles are different. In case of conventional pile foundation the frictional resistance develops from top of pile and moves downward while in piles in a piled raft foundation, the frictional resistance develops from tip of pile and moves upward. The complete mobilization of end bearing resistance is seen first in case of piles in a piled raft

foundation than in regular piles. On the other hand the complete mobilization of frictional resistance is first seen in regular piles than in piles in a piled raft foundation.

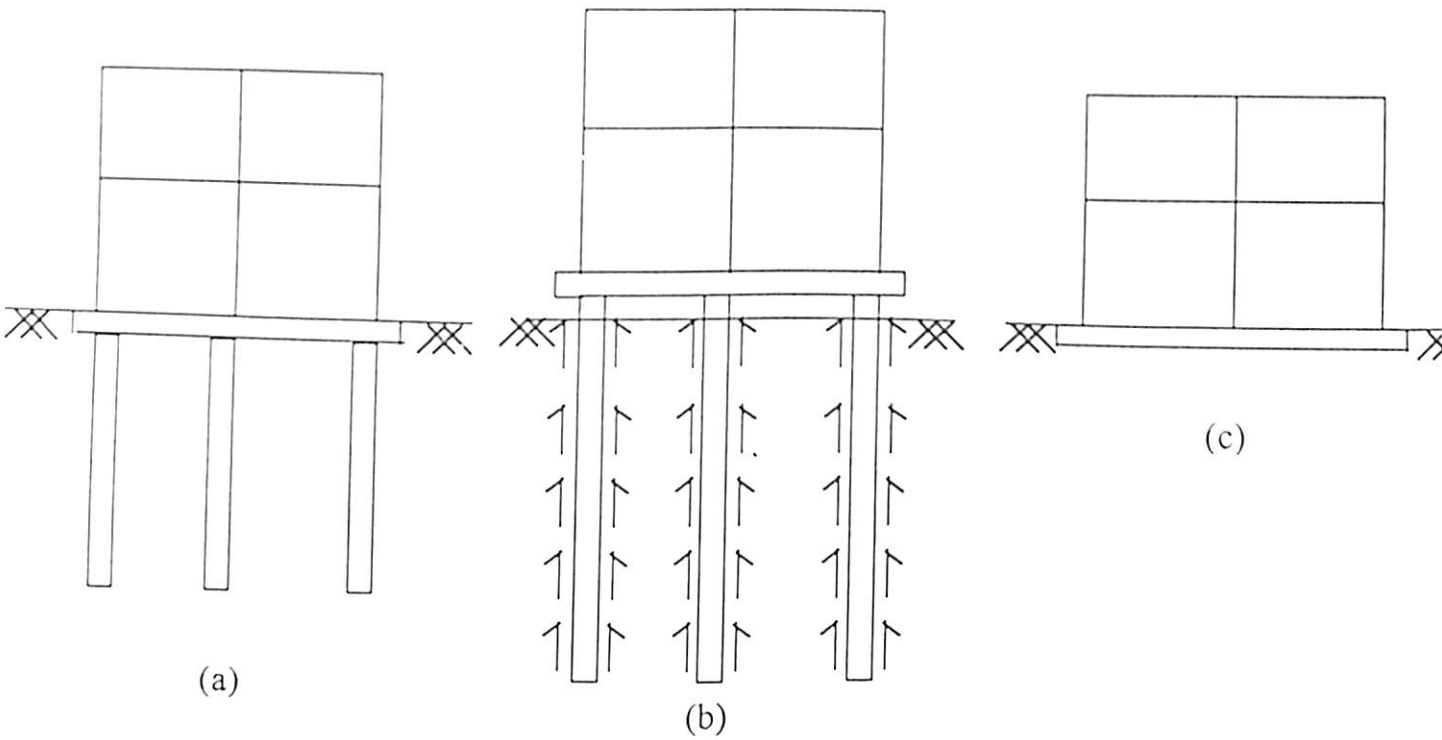

Figure 1.1 Piled Raft, Pile and Raft Foundation

1.3 NONLINEAR FINITE ELEMENT ANALYSIS

From literature, it is found that not much analytical work has been carried out to understand the behavior of piled raft foundation when loaded till failure. Very few literature reported piled raft foundation analysis under axisymmetric condition and plane strain condition. The load-settlement behaviour of piled raft foundation is still not well understood. The analytical work done is mostly based on linear elastic behaviour of soil. Thus, available literature indicate that a detailed nonlinear analysis of piled raft foundation under axisymmetric as well as plane strain condition considering elasto-plastic behaviour of soil is required. In the present research, piled raft foundation under axisymmetric as well as under plane strain condition have been analysed by nonlinear finite element method. The material nonlineraity of soil has been modeled by Von-Mises Yield Criterion. Modified Newton-Raphson Iterative

Procedure has been considered to solve the resulting nonlinear finite element equation. The stiffness matrix has been kept constant for each iteration in Modified Newton-Raphson Iterative Procedure.

1.4 LOAD SETTLEMENT CURVES

Based on nonlinear finite element analysis, load-settlement curves are produced which includes parameters like thickness of raft, diameter/width of raft, pile length, spacing between piles, and soil modulus. Thus, out of seven parameters; uniformly distributed load, settlement, thickness of raft, diameter of raft, pile length, spacing between piles, and soil modulus considered, if six parameters are known, the seventh can be arrived at.

1.5 SCOPE OF THE PRESENT WORK

The present research work has been aimed for detailed parametric study of piled raft foundation under axisymmetric and plane strain condition by nonlinear finite element analysis considering material nonlinearity of soil. This will be useful in understanding the behaviour of piled raft foundation for axial load distribution in pile, yielding of soil below raft and piled raft foundation, load settlement behaviour and settlement profile of the raft and piled raft foundation. Based on detailed parametric study, load-settlement curves are produced which will be very much useful for the designers as well as the researcher. The load-settlement curves can be used for predicting the load as well as settlement for a piled raft foundation if one of these two parameters is known for a known dimension of a piled raft foundation and the soil property. The load settlement curves produced will also be used for economical dimensioning of a piled raft foundation for known properties of soil and load coming on the piled raft foundation.

CHAPTER 2

LITERATURE REVIEW

2.1 INTRODUCTION

Work carried out in last two to three decades indicates that piled raft foundation is a promising economic solution for supporting high rise building on thick clay deposit. A number of researchers have carried out analytical study assuming elastic behaviour of the supporting soil. Very little work has been carried out on elasto-plastic behaviour. The behaviour of piled raft has been analysed in past both by model study and by actual monitoring of foundation in the field with instrumentation. The available literature is grouped into linear elastic analysis, nonlinear analysis, model study and field observations and a brief description of some of the important references is given in the following sections.

2.2 LINEAR ANALYSIS

Severn (1966) reported the finite element method for solving the mat foundation. The paper presents the derivation of stiffness matrix for plates, which include the effect of an elastic foundation. Stiffness matrix for beam on elastic foundation is also presented. The effect of foundation is assumed to consist two parts (a) the spring type reaction, which is directly proportional to the displacement, and (b) a spring-coupling action, which simulates shear resistance in the foundation.

Brown (1969) considered several methods of determination of reaction distributions and bending moment distribution for uniformly loaded smooth circular rafts of any flexibility on a deep isotropic elastic foundation. The method of analysis presented makes use of integral transforms and collocation. The results provided are found adequate as a basis of design.

Clough (1969) reported that the hexahedron element is distinctly superior to any tetrahedron assemblages in terms of performance both with regard to the individual

element properties and also in application to idealised structure systems. It is recommended that the 8 noded brick elements be used in standard programs for the analysis of general elastic solids.

Mattes and Poulos (1969) reported the effect of pile compressibility on the shear stress distribution along a pile. The compressibility of a pile modifies the distribution of shear stress along a pile as compared with an incompressible pile. As a pile becomes more compressible, the stresses near the top of the pile increase and the proportion of the load transferred to the base decreases. The influence of compressibility on the behaviour of a pile is likely to be significant for relatively slender piles but small for relatively short piles.

Butterfield and Banerjee (1971) presented elastic analysis of pile group considering the interaction of ground with pile cap. The load displacement behaviour of the system and the load distribution between the piles and the cap is analysed. The work is based on Mindlin's analysis for a point load embedded within a semi-infinite ideal elastic half space. It is found that the load sharing by pile cap ranges from 20% to 60% depending on pile spacing. It has also been found that maximum load is taken by corner pile followed by edge pile and least load is taken by center pile.

Lytton and Meyer (1971) presented a method of analysis which is based on the mechanics of beams-on-foundation, a simple enough for routine use by the design engineer, and uses the relevant properties of soil stiffness and soil profile in an elastic mathematical model of interaction problem. Typical results of this type of analysis are shown and recommendations are made on a proper choice of soil properties, soil profiles, and beam properties. The procedure adopted in this paper gives a better estimate of design quantities.

Hongladaromp *et al.* (1973) studied the interaction of a rectangular pile cap with subgrade to determine the sharing of load on piles and the subgrade. Employing the finite difference technique a parametric study was carried out. They found that the resistance of

the subgrade has considerable effect on settlement of footing and should be taken into consideration in the analysis Also it has considerable effect on the distribution of the column load

Hain and Lee (1974) reported that the most effective analytical technique for analysing the structure-raft-supporting soil system appears to be the substructure approach when the elements of the system can be treated as manifesting linear elastic behaviour The results of the linear elastic model are found to be consistent with the common observed concave settlement profile. Thus it is found that the linear elastic model should be used in preference to the Winkler's Model.

Balaam *et al.* (1975) developed a finite element analysis for an axially loaded pile in which the pile and soil are analysed as separate bodies and equilibrium as well as displacement compatibility at pile soil interface is then imposed to obtain a solution for the settlement of the pile. This analysis has been used to investigate the effects of installation of a pile on its load settlement behaviour. Installation of the pile has been simulated by introducing a zone of disturbed soil around the pile, having different strength and deformation properties from the undisturbed soil. The theoretical results indicate that the load settlement behaviour of the pile is influenced by the nature and extent of the disturbed zone, but to a lesser extent than the ultimate load of the pile, which almost depends entirely on the strength properties of the disturbed zone.

Brown and Wiesner (1975) presented results for load taken by piles, maximum displacements, differential displacements, and maximum positive and negative bending moments due to uniformly distributed load applied to a smooth strip footing which is supported by piles on a deep homogeneous isotropic elastic foundation. The results are presented for piles whose length to diameter ratio is 50; footings whose width is 5 times pile diameters on an incompressible foundation. Corrections for other pile length, footing widths and soil poisson's ratio are discussed.

Ottaviani (1975) applied finite element method to study the behaviour of vertically loaded single pile and pile groups in a homogeneous linearly elastic medium. Three-dimensional and axi-symmetric elements have been used in the analysis. Settlements are determined against ratio of pile to soil elastic modulli for single piles and for the 3 x 3 and 5 x 3 pile groups. The stress distributions in various piles and in the soil mass are also given. No relative displacements are allowed at the interfaces between the cap, the piles and the soil i.e., the various materials are considered as perfectly bonded to each other. The value of poisson's ratio has been kept constant for the soil as 0.45, so that the analysis is perfectly applicable to bored piles in undrained soil where the load transfer takes place mainly by lateral adhesion.

Fraser and Wardle (1976) analysed the behaviour of perfectly smooth, uniformly loaded rectangular raft of any rigidity resting on a homogeneous elastic layer which is underlain by a rough rigid base. Graphical solutions were presented which enable the determination of vertical displacement at the centre, edges and corner of the raft, and maximum bending moment in the raft. The solutions have been obtained by the finite element method with the interaction between raft and finite soil layer being incorporated through the use of surface elements. The author concluded that variations in raft rigidity, length/breadth ratio, soil layer depth and poisson's ratio can markedly effect both displacements and bending moments in raft foundations.

Hain and Lee (1978) analysed a piled raft considering the raft as a flexible elastic plate supported on compressible piles and soil as homogeneous/nonhomogeneous material. The ultimate load capacity of piles is taken into account by a load cut-off procedure, in which these piles are deleted from compatibility equation and their loads are held constant at the ultimate values in equilibrium equations. Thus, any excess load is redistributed to the adjacent piles. The effects of raft flexibility and rigidity on settlement, reaction pressure and bending moment have been studied for piled raft system.

Horvath (1983) developed a new mathematical model for analysing mat foundations under static loadings based on Reissner's concept of a simplified elastic continuum.

Horizontal normal and shear stresses are assumed to be zero throughout an elastic layer of finite thickness. Solutions for a constant Young's Modulus with depth as well as varying linearly and with square root of depth are discussed. The Reissner Simplified Continuum is shown to offer substantially better correlation with exact theory of elasticity solutions than does the commonly used modulus of subgrade reaction model.

Shukla (1984) presented a simplified method for design of mat foundations on elastic soil medium. The paper recommends methods to determine modulus of subgrade reaction and methods to calculate moments, shear forces, and deflections at critical points on mat with the help of charts. An example has also been given to show the use of charts.

Bowles (1986) reported a brief survey of computerized methods for mat design. The modulus of subgrade reaction is considered in some detail both in obtaining reasonable initial design estimates and simple methods to couple node effects. A mat example is reanalysed to illustrate the effect of simple coupling procedure. Several tables are given both to illustrate the validity of the finite grid method and for use in coupling procedure.

Bowles (1988) presented a method for computing the elastic settlement of a foundation on a sand deposit using conventional elastic settlement, adjusting the settlement influence factor. A reduced influence depth is suggested for settlement calculations. The value of the reduced influence depth is taken, as maximum of five times the width but not more than the stratum depth. A number of settlement cases are examined using this procedure and the cases examined show very good results using this suggested procedure.

Tomono *et al.* (1987) presented a simple model consisting of a rigid circular raft and a single pile. The method takes into account the interaction among the raft, pile and soil by combining the finite element method and the method based on Mindlin's first solution of elasticity. Comparison is made between the calculated values by the present method and those by axi-symmetric finite element method. As a result, the values calculated by the present method and those calculated by the finite element method prove a comparatively

good agreement with respect to the raft settlement and the load distribution between pile and raft. It is concluded that the present approximate approach provides a ground where the elastic modulus is constant or increasing in depth direction with a practically adequate accuracy.

Polo and Clemente (1988) presented a method of predicting pile-group settlements for cases in which piles are held together by means of rigid pile cap. Piles in the group have been considered to be of same material, length and diameter. The piles have been modeled as a hollow cylindrical insert in the interior of a homogeneous, linear, elastic, isotropic half space. Settlement influence and interaction factors are obtained. These factors are tabulated and can be used with the results of individual, full-scale, pile load tests to provide a very effective means of estimating pile-group settlements.

El-Mossallamy (1989) presented in his paper the pile-raft-soil interaction. The analysis was carried out under the assumption of linear elastic behaviour of raft, piles and half space, unsolved bond, i.e., no slip between piles and half space. The load sharing between pile and raft, the effect of length of piles in reducing settlement are discussed.

Kuwabara (1989) performed boundary element analysis based on elastic theory for behaviour of piled raft. Settlement and load transfer for a homogeneous isotropic elastic half space are compared with freestanding pile groups and single piles. The vertical load carried by the raft was found about 20-40% of the total applied load in case of L/d (Length to diameter ratio) < 50, s/d (spacing to diameter ratio) < 10, in an undrained condition. The result for load sharing has also been given for drained condition.

Chow (1992) presented a numerical analysis to study the behaviour of vertically loaded pile groups embedded in a nonhomogeneous soil with the pile cap in contact with the ground. The soil profile consists of soil with Young's modulus increasing linearly with depth. Parametric solutions are presented to show the influence of the Young's modulus variations on the behavior of the groups. The load displacement curve and load transfer behaviour of 3 x 3 pile group for computed and measured ones have been presented

Poulos (1993) presented the results of piled raft soil interaction analysis when the soil is subjected to either downward or upward vertical movements as a result of change in effective stress in the soil. The piled raft was analysed using simplified boundary element approach, in which the raft was represented as a series of rectangular elements resting on soil surface, and each of the piles was discretized into a series of shaft and base elements. For soils subjected to consolidation (downward) movement additional compressive loads are transferred to the piles by negative friction and the weight of the raft is also transferred to the piles for relatively small soil movements. For soils subjected to expansive (upward) movement additional tensile loads are transferred to the piles both because of the direct action of the expansive soil on pile and also because of additional pressure generated under side of the raft. Thus it is suggested that in circumstances where external vertical soil movements are likely to develop, the use of piled raft foundation is best avoided.

Pender (1994) compared the magnitude of the different contributions from pile group, raft base and raft sides to the overall stiffness of the foundation. It was found that the base interaction is most significant for vertical interaction and least significant for moment interaction; this is a reflection of the relatively small contribution the sidewalls make to the vertical stiffness and large contribution they make to the moment stiffness of an embedded raft.

Gandhi and Maharaj (1996) have reported the load sharing between pile and raft based on three-dimensional linear finite element method. Infinite piled forest model has been considered for piled raft foundation. The raft, pile and soil have been discretised by eight noded brick element. The effect of spacing, soil modulus and length of pile on load sharing between pile and raft have been discussed.

Clancy and Randolph (1996) developed hybrid method of analysis by which the complete analysis of larger foundation system may be performed. The paper outlines the hybrid finite element-elastic continuum method of piled raft analysis, and describes an approximate method for calculating overall foundation stiffness and load distribution.

Parametric studies using the hybrid method have been used to develop approximate methods for estimating differential settlement. Two case studies of piled raft foundation have been made for comparison with the approximate method developed

Burd and Frydman (1997) carried out a study of the bearing capacity of sand layers overlying clay soils for the case where the thickness of the sand layer is comparable to the width of a rigid foundation placed on the soil surface. A review of previous work is given and a discussion is presented of the dimensionless groups that govern the behaviour of this type of foundation. A parametric study is carried out using both finite element and finite difference methods. This study is based on the use of soil parameters obtained from an assessment of the range of values that might be expected to be appropriate for full-scale structures. The results of the parametric study are used to illustrate the mechanics of the system and also to develop charts that may be used directly in design. In particular, the results illustrate that the shear strength of the clay has an important influence on the mechanisms of load spread within the fill.

Aucilio and Counte (1999) deal with the one-dimensional consolidation of unsaturated soils due to the application of external loads. A simple equation is derived that enables one to predict the rate of settlement of shallow foundations with time. A series of examples is shown to demonstrate the feasibility and usefulness of the derived equation.

Noura *et.al* (2002) analysed settlement and differential settlement variability of a pair of foundations on random heterogeneous medium. The random soil properties of interest are the elastic modulus, and the Poisson ratio. The elastic modulus is modeled as a spatially random field by adopting the lognormal distribution, which enables analysing its large variability. Because soil poisson ratio is bounded in practice between two extreme values, its random field is obtained by using the Beta distribution. In this study, one proposes for the Beta field determination, a mapping technique on the probability distribution function diagram, by solving a non-linear equation. However, the mean and variance are unchanged through the mapping

operation. Because the soil Poisson ratio is a positive parameter, one prefers to perform the mapping operation with the probability function of the lognormal distribution. Also, the proposed technique can be used for other bounded soil properties such as the porosity. In this paper, settlement and differential settlement statistics prediction are carried out using Monte Carlo simulations combined with deterministic finite element method (DFEM). A performed parametric study shows that (i) as the variability of the elastic modulus increases as settlement and differential settlement statistics are important, also, settlement statistics decreases as the Poisson ratio variability increases, and differential settlement statistics do not seem be affected.

Liang *et al.* (2003) extended the concept of piled raft to a new type of foundation named composite piled raft in order to mobilize shallow soil to participate in the interaction of piled raft foundation sufficiently. In the system of composite piled raft, the short piles made of flexible materials were used to strengthen the shallow soft soil, while the long piles made of relatively rigid materials were used to reduce the settlements and the cushion beneath the raft was used to redistribute and adjust the stress ratio of piles to subsoil. Finite element method was applied to study the behavior of this new type of foundation subjected to vertical load. Influencing factors, which include ratio of length to diameter and elastic modulli of piles as well as thickness and elastic modulus of cushion, were studied in details. Load-sharing ratios of piles and subsoil as well as foundation settlement were also investigated in this paper. The conclusions had been successfully applied to some practical buildings in the coastal cities of China. The validity of the numerical results was examined through a seven-storey building observed in situ.

2.3 NONLINEAR ANALYSIS

Duncan and Chang (1970) developed a simple, practical procedure for representing the non-linear, stress dependent, inelastic stress-strain behaviour of soils. Accordingly, the values of required parameters may be derived from the results of standard laboratory triaxial tests. The relationship contains six parameters, whose values may be determined

readily from the results of a series of triaxial or plane strain compression tests involving primary loading, unloading and reloading. Two of these parameters are the Mohr-Coulomb strength parameters, c and ϕ, and the other four also have easily visualized physical significance. The behaviour of footings on sand and clay has shown that finite element stress analyses conducted using this relationship are in good agreement with observations and applicable theories.

Baguelin and Frank (1980) presented the use of the finite element method for determining the realistic modes of behaviour of piles, for single piles under lateral or axial static loads. For axial load, piles have been studied in ideal linear elastic media. The mechanism of shaft friction has been clarified and has been extended to non-linear media. The mobilisation of the shaft friction with the vertical displacements at a given depth is quantified, taking into account a remoulded zone of soil around the pile.

Desai (1981) used finite element method to analyse cap, piles and soil foundation. The cap was discretized as two dimensional plate elements and pile as one dimensional beam element. The stress-strain behaviour of soil was considered as nonlinear. The numerical predictions show satisfactory comparison with results from other finite element solutions and laboratory observations. It appears from the results that if the characteristics of loading, structure, and the soil are such that the stress levels remain in the linear range, the results from the present numerical procedure do not differ significantly in so far as load distribution is concerned. A parametric study is performed to identify the effects of changes of relative stiffness of cap, pile and soil medium. This study indicates that the relative stiffness of pile, soil and cap can have considerable influence on the distribution of load in piles in a pile group.

Madhav and Karmarker (1982) presented a simple method of estimating the settlement of circular or annular centrally loaded footings. In this method the elasto-plastic behaviour manifested through the contact pressure reaching yield value over certain regions of the footing has been incorporated. The results obtained have been found to agree closely

with those from FEM and experiments. Design charts have also been presented for ready use

Potts and Martins (1982) considered mobilisation of shear stress along a rough pile shaft in normally consolidated clay in terms of effective stresses acting in the clay. Predictions of the stress changes, which occur in the soil adjacent to the pile shaft on loading, are presented and shown in good agreement with some experimental results. The problem was analysed as axi-symmetric by finite element method. Isoparametric elements each with 8 nodes were used to discretize the pile and soil.

Siriwardane and Desai (1983) described computational procedures for implementing some constitutive models and introduced in three dimensional finite element procedures. The models considered were variable modulli, Drucker-Prager, critical state and Cap models. Consistent numerical schemes were presented with applications to number of problems. It was suggested that these procedures could provide successful results with advanced constitutive laws for three-dimensional analysis of a wide range of non-linear problems.

Poterasu and Mihalache (1985) presented analysis of stresses and displacement state in a foundation and soil. The foundation was subjected to a compressive force and a bending moment. For reinforced concrete foundation, Von-Mises criterion was used whereas for soil Drucker-Prager criterion was used. The analysis considered was for plane strain condition and the foundation and soil were discretized as 22 quadrilateral elements. The same problem was analysed by boundary element method. The boundary element method presented the advantage of a simpler discretization, that is, fewer the input data, lesser the computer time. Though the results of the stresses were better, the displacement values were far from the reality.

Kuppusamy (1985) suggested non-linear strain displacement relations in analysis for geotechnical engineering problems. The finite element method was used to analyse layered anisotropic soil media. The soil media was discretized as eight noded isotropic

brick element. The results of the analysis indicated that the displacements and stresses predicted by the non-linear theory differ significantly from those of the linear theory. Also the effect of anisotropy on the displacements and stresses is quite significant. It was therefore concluded that a realistic prediction of stresses and displacements for practical situations could only be accomplished by including geometric nonlinearity as well as the true material properties of the soil.

Chow (1987) presented a numerical method for the analysis of general three dimensional pile groups. The features of the pile-group model include battered piles, different pile sizes, non-uniform pile sections, soil nonlinearity, soil nonhomogeneity, and pile-soil-pile interaction. A typical six-pile group is analysed. The method has been used to analyse field and laboratory tests on groups of battered and vertical piles. The computed solutions are shown to be in good agreement with the measured data.

Zienkiewicz and Chen (1990) presented the theory of generalized plasticity in which yield and plastic potential surfaces need not be explicitly defined. They have shown how a very effective general model can be developed describing the behaviour of sands and of clays under monotonic or transient loading. The hierarchical structure of the model limits the number of parameters, which have to be experimentally determined for a given material to those strictly necessary for problem at hand.

Liu and Novak (1991) presented pile soil static interaction by the combination of finite and infinite elements. The pile and the near field soil medium were modeled by finite elements, whereas the far field soil medium was modeled by mapped infinite elements. The Drucker-Prager model (Drucker and Prager, 1952), which is an extension of the well-known Mohr-Coulomb criterion into three-dimensional situation, has been used in the analysis to simulate the soil behaviour. Axially loaded single pile and single pile with cap subjected to monotonic loading were investigated. The soil was assumed to be either elastic or elasto-plastic. A weak zone was introduced around the pile to approximately account for slip between the soil and pile.

Trochanis (1991) studied the effect of nonlinear soil behaviour on the axial and lateral response of piles due to monotonic and cyclic loading. The soil material was idealised as a Drucker-Prager elasto-plastic continuum and the interface elements were used to allow for slip and separation between the piles and the soil. Numerical results indicate that material nonlinearity can significantly affect pile and soil response. Pile-soil slippage is predominant under purely axial loading, while for lateral loads pile-soil separation is crucial factors.

Maharaj (1996) reported the elastic as well as elastoplastic analysis of piled raft foundation. The piled raft foundation has been analysed by three-dimensional linear as well as nonlinear finite element analysis using ANSYS Finite Element Software. Three models of piled raft foundation have been considered. First is the infinite pile forest model in which a single pile with equivalent area of raft has been considered for the analysis. Both elastic as well as elastoplastic analysis have been done. Second is the strip of piled raft foundation, which has been analysed for elastic analysis only. The third is the piled raft foundation with group of piles, which has been analysed by linear as well as nonlinear finite element analysis. The material nonlinearity of soil has been modeled by Drucker-Prager Yield Criterion. The raft, pile and soil have been discretized as eight noded brick finite elements. Design charts have been produced for load sharing between pile and raft from the infinite pile forest model. Load-settlement curves have been produced based on three-dimensional finite element analysis. The behaviour of piled raft foundation under three-dimensional finite element method has been well understood. The application of design charts for field problems have also been discussed.

Castelli and Maugeri (2002) proposed an approximate approach for the analysis of nonlinear response of vertically loaded pile groups. The nonlinear pile-soil-pile interaction is modeled by hyperbolic load-transfer functions. To evaluate the practical applicability of the proposed approach, a back analysis of a number of published case histories referring to single pile loading tests were carried out. To extend the solution of single pile to the case of a pile group, an equivalent pier interacting with surrounding soil by means of hyperbolic load transfer function was considered. The behaviour of three

full-scale instrumented pile groups was studied, and the computed results were found to compare well with the measured values.

Maharaj (2003) presents the results based on three dimensional nonlinear finite element analysis of piled raft foundation, which is under the application of uniformly distributed load. The raft, pile and soil have been discretized by eight noded brick elements. The soil has been idealised as a Drucker-Prager elastoplastic continuum. The load settlement curves for raft and piled raft have been presented. The effect of soil modulus and pile length on load settlement behaviour of raft and piled raft has also been presented. Based on the finite element analysis it has been found that the ultimate load carrying capacity of flexible raft increases with increase in soil modulus and length of pile. Piles of length even less than the width of a flexible raft have been found effective in reducing differential settlement. The increase in pile length has been found to reduce the overall settlement and differential settlement. The increase in soil modulus has been found to reduce the overall settlement. It has also been found that although the increase in soil modulus reduces the overall settlement, differential settlement increases with increase in soil modulus for the same overall settlement. The results based on three dimensional finite element model considered in this analysis compare well with published literature.

Maharaj and Gandhi (2003 a) presented detailed parametric study for piled raft foundation by finite element method using ANSYS Finite Element Software. A single pile with equivalent area of raft has been taken from infinite pile forest. Piled raft has been analysed considering one fourth of single pile with equivalent area of raft. The raft, pile and soil have been discretized as eight-noded brick elements. The parameters varied are pile length, pile spacing and soil modulus. Based on the above analyses design charts have been developed for obtaining load sharing between pile and raft. The design charts developed have been used to verify actual field measured data and found comparable. The result obtained from 3D finite element model considered compare well with the reported literature.

Maharaj and Gandhi (2003 b) present the results of three dimensional nonlinear finite element analysis of raft and piled raft foundation, which have been loaded till failure by ANSYS Finite Element Software. The raft, pile and soil have been discretized by eight noded brick elements. The soil has been modeled as Drucker-Prager elastoplastic medium. The analyses have been done for raft, piled raft, group of piles and individual pile. The load settlement behaviour of raft, piled raft, group of piles and single pile have been presented. The effect of thickness of raft and soil modulus on load settlement behaviour of raft and piled raft has also been presented. The axial load distribution for piles in piled raft foundation has been shown. Also the development of contact stress with increase in loading intensity has been presented for raft and contact stress-settlement curves have been shown for raft and piled raft. Addition of even small number of piles has been found to increase the load carrying capacity of raft foundation. The axial load distribution shows that piles in piled raft foundation reaches to its ultimate capacity earlier than the raft. The value of contact stress is found minimum at the center of raft and maximum at the corner. When the raft reaches to its ultimate load carrying capacity uniform contact stress is found below the raft except at a very very small zone at the corner of the raft. This uniform contact stress is found to be the maximum value, which can develop below raft and piled raft. The finite element result compare well with reported literature.

2.4 MODEL STUDY

Wiesner *et al.* (1980) presented a method of analysis of piled raft foundations in which the raft is represented as a thin plate supported by piles and an elastic continuum. Tests were performed on model piled rafts in a large tank filled with over consolidated clay. Settlement and moment results from these tests were compared with results from analysis. This suggests that theory based on the linearly elastic continuum can provide satisfactory predictions of the behavior of piled raft foundations on real soils provided that appropriate allowance is made for pile-bearing capacity.

Akinmusuru (1980) reported the interaction between cap, pile group and soil based on laboratory-scale model experiments. Due to interaction, the bending moments are induced in piles, and there is an increase in friction along the shaft of each pile. The percentage capacity change of the cap caused by the interaction is not significant. The change in both pile and cap capacities has been shown to be influenced by pile length and cap size

Cooke (1986) presented results of model test on unpiled rafts, free-standing piles and piled rafts of various sizes. These results were related with field measurements. The study suggest that at the same overall safety factors the settlements of the structures on piled rafts are likely to be comparable with the settlements of the structures on unpiled rafts of similar sizes. Since, piled raft foundations are frequently employed because the settlements of unpiled rafts are considered to be excessive, the small settlements that structures on these foundations normally experience are probably due to the fact that the safety factors in practice are higher than those assumed in design.

Byrne and Cassidy (2002) conducted a series of tests in a drum centrifuge with the aim of investigating the performance of typical offshore foundations on soft normally consolidated clay. The foundations consisted of spudcan footings and suction caissons. The main aim of the investigation was to compare how the performance changes as the foundation is varied. This is important when considering the use of a jack-up rig for a permanent facility, a concept that is increasingly being considered. In such a case there are concerns about the long-term suitability of the spudcan footing, with the amount of sustainable rotational fixity being of particular interest. A total of 64 experiments were carried out investigating areas that include a) comparing the vertical loading response in both compression and tension, b) using a fixed arm to apply predominantly horizontal loading, and c) using a hinged arm to apply a distinct ratio of horizontal to moment loading. Interestingly in the case of the spudcan footing considerable back-flow of the soil was observed during the installation phase.

2.5 FIELDS MEASUREMENTS

Zeevaert (1957) introduced new and interacting problems in foundation engineering for the forty-three-storey building Tower, Latino Americana in Mexico City. The foundation comprises of 41m x 16m raft with 83 concrete piles of length 24m and diameter 0.4m. The paper describes the general philosophy adopted in the design of the foundation of this building. A detailed description of the subsoil conditions and mechanical properties of the lacustrive deposits encountered at the site is given. Settlement observations are reported of the building of the ground surface and other deep-seated strata. The settlement observed for piled raft was 23mm. A comparison of observed and computed settlements is given in an attempt to predict the future behaviour of the foundation of the building.

Lambe (1968) reported measurements of pore water pressure and movement of foundations on the M.I.T Campus; identification and discussions of some of the fundamentals of foundation behaviour; comparison of predicted and measured performances. The main objectives were to assure that building foundations constructed on M.I.T Campus performed satisfactory; reduction in the chances of foundation construction damaging existing structures; and make possible foundations at a minimum cost to the institute. Most of the heave that occurred during foundation construction was caused by strains in the over consolidated soil immediately below the surface of the foundation, rather than in the normally consolidated softer clay below. Most of the heave was time-dependent. A comparison of predicted and measured performance showed an under prediction of initial head drop, an under prediction of rate of consolidation heave and excess pore pressure distribution, close prediction of the total head at the end of excavation period and over prediction in initial heave and consolidation heave.

Moore and Spencer (1969) predicted the settlement of a structure, which was erected on the surface of a thick layer of compressible soil. The different techniques adopted were conventional oedometer method; oedometer method with back pressuring and with load applied at constant strain rate; Skempton-Bjerrum method; Davis and Poulos method;

and Lambe stress path method. The first three methods based on oedometer testing under-estimated the observed settlement. The last three methods also yielded underestimates of the observed settlement but were closer to the true value.

D'Appolonia and Lambe (1971) evaluated case study of four buildings supported on end-bearing piles. The piles were driven in preaugered holes through a 100-ft thick deposit of medium to soft Boston blue clay to the bearing material, which is either sandy glacial, till or weathered shale. Movements were measured on these and adjacent buildings during and after construction. In addition, pore pressures and movements in the subsoil were observed. Driving displacement piles in clay generates large excess pore water pressures. Preaugering is an effective means for reducing excess pore water pressures caused by pile driving. Settlement of buildings, especially those on shallow foundations, adjacent to pile driving operations may be large.

Hooper (1973) studied the behaviour of piled raft foundation supporting a tower block in central London. The building is provided on piled raft foundation of plan area 618 m^2 with 51 bored concrete piles of length 25m and diameter 0.91m. The field measurements taken during several years are presented, together with the results of a detailed finite element analysis. The analysis is carried out assuming uniformly distributed load on the raft. The instruments used for measurement of pile load, contact pressure and settlement were pile load cell, earth pressure cell and level. The average settlement of the building measured was 18mm. Based on the field measurements the estimated proportions of load taken by piles and the raft at the end of construction were 60 % and 40 %. It was found that the long-term effect of consolidation is to increase the load carried by piles and to decrease raft contact pressure.

Cooke *et al.* (1981) investigated the behaviour of the piled raft foundation of size 43m x 19m with 351 bored cast in situ concrete piles of 13m length and 0.45m diameter of a 16 storey block of flats in North London in a 6 year period covering the erection and early life of the building. The observations showed that the load carried directly by the raft decreased from about 45% of the total at early stages of construction to 25% at the time

of occupation Load cells installed between the raft and selected piles demonstrated that piles around the periphery of the building carried loads approaching double the loads on piles in the interior of the group Vertical soil displacements beneath the building, was measured from the time the raft was cast. Surveys of the settlements of the external walls were made from the time the building was completed. From these observations it was found that, while the overall settlements were small and differential settlements negligible, the overall settlements were many times the settlement of a single pile measured in a short term loading test

Kay and Cavagnaro (1983) reported measurement of settlement of three structures on raft foundations. For two of these structures surveying techniques were used while for the third a borehole extensometer technique developed in the United Kingdom was used. The extensometer approach was found to be superior from a number of stand points, including accessibility during construction, convenience of measurement and accuracy of results.

Landva *et al.* (1987) reported a nine-storey structure constructed on raft foundation on a 30 m thick layer of clayey silt. Detailed soil investigations included conventional borings and self-boring pressure meter, field vane and flat dilatometer tests performed at the site. In addition to the field testing, undisturbed samples were obtained and tested in the laboratory to determine the compressibility and shear characteristics. To compare the performance of the foundation with design assumptions, instrumentation consisting of piezometers, contact pressure load cells and settlement points were installed. The foundation soil interaction was analysed using the stiffness method of foundation soil interaction analysis. It was concluded that the prediction of settlement on the basis of conventional consolidation tests grossly over estimates. The amount of settlement observed in the field measures showed that the raft has settled in a dish shaped manner. The contact pressure followed the trend of the settlement, highest recorded pressure being near the centre of the raft and the lowest pressure near the edges.

McKeen and Johnson (1990) conducted a study to investigate the simple rational methods for calculating the active zone depth and the edge moisture penetration distance in expansive soils. Analysis of soil-moisture diffusion indicated that the active zone depth is a function of the maximum suction change imposed, minimum suction change considered significant, climate frequency and field diffusion coefficient.

Franke (1991) discussed design of 4 buildings supported on piled raft in Germany. The analysis shows that compared to a raft foundation, piled raft reduces the settlement by about 50 %. He has reported actual measurements of pile head forces, contact pressure between raft and soil and the settlements of piled raft for some of these buildings. The instruments used were pressure cells, glotzl transducers and extensometer respectively. Time dependent load sharing and settlement of piled raft have been reported in graphical form.

Schwab *et al.* (1991) reported actual measurements of load sharing between piles and raft by instrumentation of piled raft foundations. The results of measurements carried out on several tall buildings in Frankfurt clay as done by Franke were reported here. The ultimate sharing was 45 % by raft and 55 % by pile

Hannink (1994) presented the results of settlement measurements of two projects in more detail. These projects offer data of the time settlement behaviour during the construction period, and of the stress distribution in the subsoil. Uncertainties however, continue to exist, especially in relation to the time dependency of the settlements. This underlines the necessity of continuing the measurements after completion of a high rise building. It was concluded that the final settlement of 100 m high buildings in Rotterdam with a smallest cross section of 25 to 30m would generally be restricted to 100 mm at maximum. It was strongly advised that consultants, contractors and local government increase their efforts to continue measurement programs after completion of the high rise building.

Poulos (1994) suggested the alternative design strategies for design of piled raft foundations, outlined the circumstances, which are favorable for their use and reviewed

various available methods of analysis of such foundations. It is suggested that significant saving in piling costs can be achieved by making allowance for the effect of raft in carrying load and reducing settlement, piles to operate at a factor of safety of unity and using piles of different length or stiffness.

Yamashita *et al.* (1994) reported a five storey building on piled raft foundation of size 24m x 23m with 20 piles of length 16m and diameter 0.75m. The results of field observations during construction and analytical study of the same building have been compared. At the time of completion of the building, the settlement measured was 10 to 20 mm and the load shared by piles was 49 %. Analytical simulation of the settlement behaviour of the building was presented taking into account the interaction between the piles, the soil and the raft, which compared favorably with the field observation.

Milovic (1998) showed the results of large settlements observed over several years in Belgrade for a hotel founded on four rectangular rafts with expansion joints of 1 m width, and for a silo group built on the right bank of the Danube River. The capacity of the silo group is 400 MN. The settlement calculation for these structures was made using deformation parameters deduced from cone penetration test results. The theoretical solution for stresses and displacements was obtained by the finite difference method. Observed and calculated settlements show satisfactory agreement.

Vincent Silvestri (2000) reports the results of a geotechnical investigation and a 3 year monitoring program of clay deposits in Montreal Island, on which are founded five typical residential buildings. The sites were provided with foundation wall elevation pins, ground movement plates, deep settlement points, piezometers and shallow water level gauges, aluminum tubes for the measurement of volumetric weights and water contents, and irrigation systems. Data recorded show that for the relatively dry summer of 1991 ground and foundation settlements were more pronounced on the nonirrigated sites.

Poulos (2001) reported that if the raft alone cannot satisfy the design requirements, it might be possible to enhance the performance of the raft by the addition of piles. The paper discusses the philosophy of using piles as the settlement reducers and conditions under which such an approach may be successful. Some of the characteristics of piled raft behaviour are discussed. Some typical applications of piled rafts are described, including comparisons between computed and measured foundation behaviour.

Sahara1 *et al* (2002) deals with the vertical behavior of a single model pile in sand in a pressurizing soil tank until the pile-soil system reaches an ultimate state, and presents the comparisons between the results of tests and the elasto-plastic analysis that was proposed by one of the authors. The analysis was based on the finite element method taking account of the elasto-plastic state corresponding to generalized strain in soil elements. On the other hand, the vertical loading tests were performed for three types of the pile model; the pile tip model subjected only to the bearing resistance at pile tip, the pile shaft model subjected only to skin friction and the entire pile model subjected to both types of resistance. As a result, it is found that prediction by the analysis is fairly in good agreement with the results of the tests.

2.6 SUMMARY

Based on detailed literature review it is found (Ottaviani, 1975, Hain and Lee 1978, etc.) that most of the analysis of piled raft considers linear elastic analysis with perfect bond between pile/soil interface. Ottaviani (1975), Kuwabara (1989) etc. have reported undrained condition. Kuppusamy (1985), Baguelin and Frank (1980), Chow (1987) and Sahara1 et al (2002) have reported soil nonlinearity. Few references only report elasto-plastic analysis (Liu and Novak (1991), Trochanis (1991), Poterasu and Mihalache (1985), Maharaj (1996), Maharaj and Gandhi (2003) mostly using Drucker Prager Yield criterion to idealise soil behaviour. Out of these Liu and Novak (1991) reports the analysis of pile-cap-soil interaction. The slip between pile and soil has been reported by Trochanis (1991) for piles only and Liu and Novak (1991) for pile-cap-soil interaction Field measurements as reported by Hooper (1973), Cooke (1981), Schweb (1991),

Franke (1991), Poulos (1994), Yamashita (1994) give very useful information for load transfer and settlement behaviour of piled raft. Poulos (1994) has also provided the design alternatives of piled raft foundation.

CHAPTER 3
FINITE ELEMENT FORMULATION

3.1 INTRODUCTION

In order to analyse a problem by finite element method, a finite element equation for the problem considered is to be obtained and after imposing the necessary boundary conditions the resulting equation is to be solved. In order to obtain the finite element equation for the problem the element stiffness matrix and load vector is to be obtained from which the finite element equation can be obtained. If material nonlinearity has been considered in the problem, the constitutive matrix corresponding to it must be considered in the formulation. The resulting nonlinear equation can then be solved by some of the iterative techniques. This chapter discusses the above aspects.

3.2 FORMULATION OF THE FINITE ELEMENT MODEL

The following section discusses the derivation of stiffness matrix for a four noded isoparametric finite element, the constitutive model, derivation of elastoplastic constitutive matrix, equilibrium equation for a finite element and the complete problem in nonlinear finite element method, and the Modified Newton Rapshon Iterative Procedure considered in the Finite Element Software's PSNLFEM and AXINLFEM developed by Maharaj (2000). Appendix-III discusses in brief about these softwares.

3.2.1 Element Stiffness Matrix

3.2.1.1 Plane strain problem

In case of isoparametric finite element the same shape function is used for representing the geometry and variation of element displacement. The formulation is given here for a four noded quadrilateral finite element. Figure 3.1 shows an isoparametric finite element in Cartesian and Natural coordinate system.

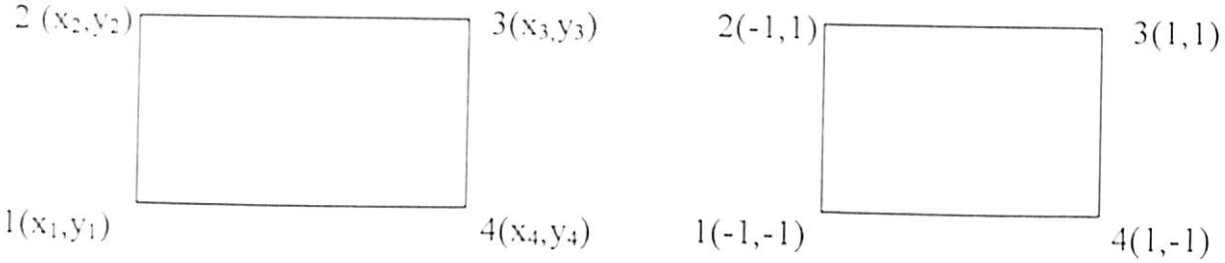

(a) Finite Element in Cartesian Coordinate System

(b) Finite Element in Natural Coordinate System

Figure 3.1 A Four Noded Isoparametric Element

The geometry of the element is expressed as

$$x = N_1x_1 + N_2x_2 + N_3x_3 + N_4x_4$$
$$y = N_1y_1 + N_2y_2 + N_3y_3 + N_4y_4 \qquad (3.1)$$

And the element displacement function is expressed as

$$u = N_1u_1 + N_2u_2 + N_3u_3 + N_4u_4$$
$$v = N_1v_1 + N_2v_2 + N_3v_3 + N_4v_4 \qquad (3.2)$$

Where N_1, N_2, N_3, N_4 are the shape functions at nodes 1,2,3 and 4 respectively. These shape functions are in natural coordinate system and can be obtained from the following expressions.

$$N_1 = \frac{(1-r)(1-s)}{4},\ N_2 = \frac{(1-r)(1+s)}{4},$$
$$N_3 = \frac{(1+r)(1+s)}{4},\ N_4 = \frac{(1+r)(1-s)}{4} \qquad (3.3)$$

The strain-displacement matrix can be obtained from the following expression

$$\begin{Bmatrix} \varepsilon_x \\ \varepsilon_y \\ \gamma_{xy} \end{Bmatrix} = \begin{bmatrix} \frac{\partial N_1}{\partial x} & 0 & \frac{\partial N_2}{\partial x} & 0 & \frac{\partial N_3}{\partial x} & 0 & \frac{\partial N_4}{\partial x} & 0 \\ 0 & \frac{\partial N_1}{\partial x} & 0 & \frac{\partial N_2}{\partial x} & 0 & \frac{\partial N_3}{\partial x} & 0 & \frac{\partial N_4}{\partial x} \\ \frac{\partial N_1}{\partial y} & \frac{\partial N_1}{\partial x} & \frac{\partial N_2}{\partial y} & \frac{\partial N_2}{\partial x} & \frac{\partial N_3}{\partial y} & \frac{\partial N_3}{\partial x} & \frac{\partial N_4}{\partial y} & \frac{\partial N_4}{\partial x} \end{bmatrix} \begin{Bmatrix} u_1 \\ v_1 \\ u_2 \\ v_2 \\ u_3 \\ v_3 \\ u_4 \\ v_4 \end{Bmatrix} \tag{3.4}$$

$$\{\varepsilon\} = [B_e]\ \{U_e\} \tag{3.5}$$

Each of the terms in the strain-displacement matrix can be obtained from the following relation between the Cartesian coordinate and the natural coordinate.

$$\begin{bmatrix} \frac{\partial N_1}{\partial x} & \frac{\partial N_2}{\partial x} & \frac{\partial N_3}{\partial x} & \frac{\partial N_4}{\partial x} \\ \frac{\partial N_1}{\partial x} & \frac{\partial N_2}{\partial x} & \frac{\partial N_3}{\partial x} & \frac{\partial N_4}{\partial x} \end{bmatrix} = \begin{bmatrix} z_{11} & z_{12} \\ z_{21} & z_{22} \end{bmatrix} \begin{bmatrix} \frac{\partial N_1}{\partial r} & \frac{\partial N_2}{\partial r} & \frac{\partial N_3}{\partial r} & \frac{\partial N_4}{\partial r} \\ \frac{\partial N_1}{\partial r} & \frac{\partial N_2}{\partial r} & \frac{\partial N_3}{\partial r} & \frac{\partial N_4}{\partial r} \end{bmatrix} \tag{3.6}$$

Where $\begin{bmatrix} z_{11} & z_{12} \\ z_{21} & z_{22} \end{bmatrix}$ is the inverse of the Jacobian matrix, which can be obtained from the following relation

$$\begin{bmatrix} z_{11} & z_{12} \\ z_{21} & z_{22} \end{bmatrix} = \begin{bmatrix} j_{11} & j_{12} \\ j_{21} & j_{22} \end{bmatrix}^{-1} \tag{3.7}$$

Where $\begin{bmatrix} j_{11} & j_{12} \\ j_{21} & j_{22} \end{bmatrix}$ is the jacobian matrix [J] and each of the terms of the Jacobian matrix can be defined as

$J_{11} = \partial x/\partial r$ $J_{12} = \partial y/\partial r$ $J_{21} = \partial x/\partial s$ and $J_{22} = \partial y/\partial s$ (3.8)

The stiffness matrix is expressed as

$$[K_e] = \int_{-1}^{+1}\int_{-1}^{+1} [B_e]^T [D][B_e] J| dr ds \tag{3.9}$$

The constitutive matrix [D] can be obtained from the following relation

$$\begin{Bmatrix} \sigma_x \\ \sigma_y \\ \tau_{xy} \end{Bmatrix} = \frac{E}{(1+\nu)(1-2\nu)} \begin{bmatrix} 1-\nu & \nu & 0 \\ \nu & 1-\nu & 0 \\ 0 & 0 & \frac{(1-2\nu)}{2} \end{bmatrix} \begin{Bmatrix} \varepsilon_x \\ \varepsilon_y \\ \gamma_{xy} \end{Bmatrix} \tag{3.10}$$

3.2.1.2 Axisymmetric problem

The formulation is given here for a four noded quadrilateral finite element Figure 3.2 below shows an isoparametric finite element in Cartesian and Natural coordinate system.

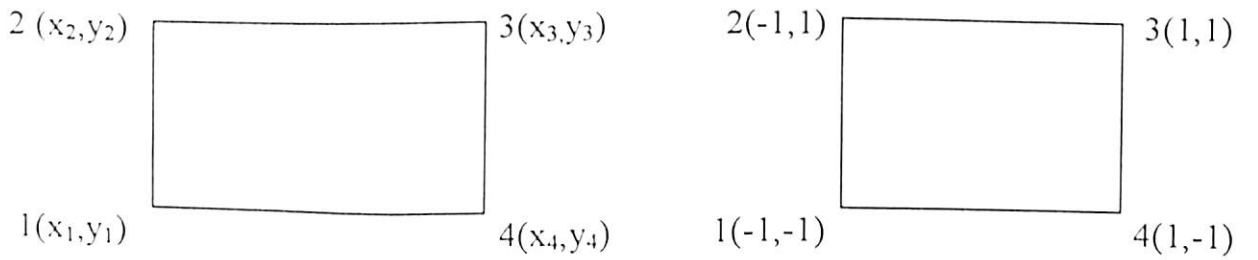

(a) Finite Element in Cartesian Coordinate System

(b) Finite Element in Natural Coordinate System

Figure 3.2 A Four Noded Isoparametric Element

The geometry of the element is expressed as

$$\begin{aligned} x &= N_1x_1 + N_2x_2 + N_3x_3 + N_4x_4 \\ y &= N_1y_1 + N_2y_2 + N_3y_3 + N_4y_4 \end{aligned} \tag{3.11}$$

And the element displacement function is expressed as

$$\begin{aligned} u &= N_1u_1 + N_2u_2 + N_3u_3 + N_4u_4 \\ v &= N_1v_1 + N_2v_2 + N_3v_3 + N_4v_4 \end{aligned} \tag{3.12}$$

Where N_1, N_2, N_3, N_4 are the shape functions at nodes 1,2,3 and 4 respectively. These shape functions are in natural coordinate system and can be obtained from the following expressions

$$N_1 = \frac{(1-r)(1-s)}{4},\ N_2 = \frac{(1-r)(1+s)}{4},$$
$$N_3 = \frac{(1+r)(1+s)}{4},\ N_4 = \frac{(1+r)(1-s)}{4} \tag{3.13}$$

The strain-displacement matrix can be obtained from the following expression

$$\begin{Bmatrix} \varepsilon_x \\ \varepsilon_y \\ \gamma_{xy} \\ \varepsilon_\theta \end{Bmatrix} = \begin{bmatrix} \frac{\partial N_1}{\partial x} & 0 & \frac{\partial N_2}{\partial x} & 0 & \frac{\partial N_3}{\partial x} & 0 & \frac{\partial N_4}{\partial x} & 0 \\ 0 & \frac{\partial N_1}{\partial y} & 0 & \frac{\partial N_2}{\partial y} & 0 & \frac{\partial N_3}{\partial y} & 0 & \frac{\partial N_4}{\partial y} \\ \frac{\partial N_1}{\partial y} & \frac{\partial N_1}{\partial x} & \frac{\partial N_2}{\partial y} & \frac{\partial N_2}{\partial x} & \frac{\partial N_3}{\partial y} & \frac{\partial N_3}{\partial x} & \frac{\partial N_4}{\partial y} & \frac{\partial N_4}{\partial x} \\ \frac{N_1}{x} & 0 & \frac{N_2}{x} & 0 & \frac{N_3}{x} & 0 & \frac{N_4}{x} & 0 \end{bmatrix} \begin{Bmatrix} u_1 \\ v_1 \\ u_2 \\ v_2 \\ u_3 \\ v_3 \\ u_4 \\ v_4 \end{Bmatrix} \tag{3.14}$$

$$\{\varepsilon\} = [B_e]\ \{U_e\} \tag{3.15}$$

The derivatives of shape function with respect to x and y in the strain-displacement matrix can be obtained from the following relation between the Cartesian coordinate and the natural coordinate.

$$\begin{bmatrix} \frac{\partial N_1}{\partial x} & \frac{\partial N_2}{\partial x} & \frac{\partial N_3}{\partial x} & \frac{\partial N_4}{\partial x} \\ \frac{\partial N_1}{\partial y} & \frac{\partial N_2}{\partial y} & \frac{\partial N_3}{\partial y} & \frac{\partial N_4}{\partial y} \end{bmatrix} = \begin{bmatrix} z_{11} & z_{12} \\ z_{21} & z_{22} \end{bmatrix} \begin{bmatrix} \frac{\partial N_1}{\partial r} & \frac{\partial N_2}{\partial r} & \frac{\partial N_3}{\partial r} & \frac{\partial N_4}{\partial r} \\ \frac{\partial N_1}{\partial s} & \frac{\partial N_2}{\partial s} & \frac{\partial N_3}{\partial s} & \frac{\partial N_4}{\partial s} \end{bmatrix} \tag{3.16}$$

Where $\begin{bmatrix} z_{11} & z_{12} \\ z_{21} & z_{22} \end{bmatrix}$ is the inverse of the Jacobian matrix, which can be obtained from the following relation

$$\begin{bmatrix} z_{11} & z_{12} \\ z_{21} & z_{22} \end{bmatrix} = \begin{bmatrix} j_{11} & j_{12} \\ j_{21} & j_{22} \end{bmatrix}^{-1} \tag{3.17}$$

Where $\begin{bmatrix} J_{11} & J_{12} \\ J_{21} & J_{22} \end{bmatrix}$ is the jacobian matrix [J] and each of the terms of the Jacobian matrix can be defined as

$J_{11}=\partial x/\partial r \quad J_{12}=\partial y/\partial r \quad J_{21}=\partial x/\partial s$ and $J_{22}=\partial y/\partial s$ (3.18)

The stiffness matrix is expressed as

$$[K_e]=\int_{-1}^{+1}\int_{-1}^{+1}[B_e]^T[D][B_e]2\pi x|J|drds \tag{3.19}$$

The elastic constitutive matrix [D] can be obtained from the following relation

$$\begin{Bmatrix}\sigma_x\\ \sigma_y\\ \tau_{xy}\\ \sigma_\theta\end{Bmatrix}=\frac{E}{(1+\nu)(1-2\nu)}\begin{bmatrix}1-\nu & \nu & \nu & 0\\ \nu & 1-\nu & \nu & 0\\ 0 & 0 & 0 & \frac{(1-2\nu)}{2}\\ \nu & \nu & 1-\nu & 0\end{bmatrix}\begin{Bmatrix}\varepsilon_x\\ \varepsilon_y\\ \gamma_{xy}\\ \varepsilon_\theta\end{Bmatrix} \tag{3.20}$$

$$\{\sigma\}=[D]\{\varepsilon\} \tag{3.21}$$

Where $\{\sigma\}$ is the stress vector and $\{\varepsilon\}$ is the strain vector for a finite element

3.2.2 Constitutive Model

In the finite element analysis the soil has been idealised as elastoplastic material by Von-Mises yield criterion. The criterion is given as

$$F = \sqrt{J_2} - \sigma_y = 0 \tag{3.22}$$

Where J_2 is the second invariant of deviatoric stress tensor and σ_y is the yield stress of material.

3.2.3 Elasto-Plastic Constitutive Matrix

The incremental stress-strain relation for an elastic element can be written as

$$\{d\sigma_e\}=[D]\{d\varepsilon_e^{el}\} \tag{3.23}$$

Where $\{d\sigma_e\}$ is the incremental elastic stress, $\{d\varepsilon_e^{el}\}$ is the incremental elastic strain

$[D]$ is the elastic constitutive matrix for an element under axisymmetric condition

The incremental elastic strain for a finite element can be expressed as

$$\{d\varepsilon_e^{el}\} = \{d\varepsilon_e\} - \{d\varepsilon_e^{pl}\} \tag{3.24}$$

Where $\{d\in_e\}$ is the incremental total strain, $\{d\varepsilon_e^{pl}\}$ is the incremental plastic strain for a finite element

By substituting equation (3.24) into equation (3.23), elasto-plastic stress-strain matrix for a finite element can be obtained as

$$\{d\sigma_e\} = [D](\{d\varepsilon_e\} - \{d\varepsilon_e^{pl}\}) \tag{3.25}$$

Where

$$\{d\varepsilon_e^{pl}\} = \lambda\left\{\frac{\partial Q}{\partial \sigma_e}\right\} \tag{3.26}$$

In the above equation Q is the plastic potential and λ is the plastic multiplier. In the formulation considered in this thesis Q=F. The plastic multiplier is given by

$$\lambda = \frac{\left\{\frac{\partial F}{\partial \sigma_e}\right\}^T [D]\{d\varepsilon_e\}}{\left\{\frac{\partial F}{\partial \sigma_e}\right\}^T [D]\left\{\frac{\partial F}{\partial \sigma_e}\right\}} \tag{3.27}$$

Putting equation (3.27) into equation (3.26) $\{d\varepsilon_e^{pl}\}$ can be written as

$$\{d\varepsilon_e^{pl}\} = \frac{\left\{\frac{\partial F}{\partial \sigma_e}\right\}\left\{\frac{\partial F}{\partial \sigma_e}\right\}^T [D]\{d\varepsilon_e\}}{\left\{\frac{\partial F}{\partial \sigma_e}\right\}^T [D]\left\{\frac{\partial F}{\partial \sigma_e}\right\}} \tag{3.28}$$

Hence from equation (3.24) the elastoplastic stress-strain relation can be written as

$$\{d\sigma_e\} = \left[[D] - \frac{[D]\left\{\frac{\partial F}{\partial \sigma_e}\right\}\left\{\frac{\partial F}{\partial \sigma_e}\right\}^T [D]}{\left\{\frac{\partial F}{\partial \sigma_e}\right\}^T [D]\left\{\frac{\partial F}{\partial \sigma_e}\right\}} \right] \{d\varepsilon_e\} \tag{3.29}$$

$$\{d\sigma_e\} = [D_{ep}]\{d\varepsilon_e\} \tag{3.30}$$

Where

$$[D_{ep}] = [D] - \frac{[D]\left\{\frac{\partial F}{\partial \sigma_e}\right\}\left\{\frac{\partial F}{\partial \sigma_e}\right\}^T [D]}{\left\{\frac{\partial F}{\partial \sigma_e}\right\}^T [D]\left\{\frac{\partial F}{\partial \sigma_e}\right\}} \tag{3.31}$$

3.2.4 Equilibrium equation for a finite element and the complete Problem in nonlinear finite element method

The equilibrium equation for a four noded isoparametric element as given below can be obtained using the principle of minimum potential energy

$$[K_e]\{U_e\} = \{F_e\} \tag{3.32}$$

where $[K_e]$ and $[F_e]$ are the stiffness matrix and load vector of a finite element and $[U_e]$ is the nodal displacement vector for an element The stiffness matrix for a finite element is given by

Under Plane strain condition

$$[K_e] = \int_{-1}^{+1}\int_{-1}^{+1} [B_e]^T [D_{ep}][B_e]|J|drds \tag{3.33}$$

Under Axisymmetric Condition

$$[K_e] = \int_{-1}^{+1}\int_{-1}^{+1} [B_e]^T [D_{ep}][B_e] 2\pi x |J| dr ds \tag{3.34}$$

Each term defined in stiffness matrix is same as in the stiffness matrix obtained for elastic analysis. Only the elastic constitutive matrix is to be replaced by elastoplastic constitutive matrix in the nonlinear finite element method. The force vector for an element is given by

$$\{F_e\} = \int_V [N_e]^T \{f_b\} dv + \int_V [N_e]^T \{f_s\} ds + \sum_{i=1}^{edof} f_i \tag{3.35}$$

In the element stiffness matrix and force vector;

$[B_e]$ is the strain-displacement matrix, $[D_{ep}]$ is the elasto-plastic constitutive matrix, $[N_e]$ is the shape function matrix for an element, $\{(f_b\}$ is the vector of body forces for an element, $\{f_s\}$ is the vector of surface traction for an element, f_i is the concentrated load acting at each nodal degree of freedom of an element, *edof* represents total degree of freedom for an element

The stiffness matrix and load vector for all the elements have been obtained using 2x2 Gauss quadrature [Zienkiwicz 1990] integration scheme.

The stiffness matrix and load vector for all the elements have been assembled to obtain the equations of equilibrium for the complete structure. The equilibrium equation for the complete structure can be expressed as

$$[K_s]\{U_s\} = \{F_s\} \tag{3.36}$$

Where $[K_s]$ is the stiffness matrix, $\{F_s\}$ is the load vector and $\{U_s\}$ is the nodal displacement vector for the complete structure.

3.3 Modified Newton-Raphson Iterative Procedure

The finite element discretization process yields a set of simultaneous equations.

$$[K_s]\{U_s\} = \{F_s\} \tag{3.37}$$

Where $[K_s]$ = Stiffness matrix

$\{U_s\}$ = Set of unknown displacements

$\{F_s\}$ = Set of applied loads

If the stiffness matrix $[K_s]$ is itself a function of unknown displacements or their derivatives, then the above equation is a nonlinear equation. The Modified Newton-Raphson method is an iterative process of solving the nonlinear equations and can be written as

$$[K_s]\{\Delta U_s\} = \{F_s\} - \{F_r\} \tag{3.38}$$

$$\{U_{s+1}\} = \{U_s\} + \{\Delta U_s\} \tag{3.39}$$

Where

$[K_s]$ = Tangent stiffness matrix

$[F_r]$ = Set of loads corresponding to stresses in all elements.

$[F_s]$-$[F_r]$ is the out of balance load vector. i.e. the amount the structural system is out of equilibrium

$\{U_{s+1}\}$ is the total displacement the structure undergoes after first iteration

$\{U_s\}$ are the displacement obtained at the zeroth iteration

$\{\Delta U_s\}$ are the displacement due to the unbalanced force after the first iteration.

The general algorithm proceeds as follows:

1. Assume $\{U_s\}$. $\{U_s\}$ are usually the converged solution from the previous iteration when iteration number is zero. At first iteration $\{U_s\} = \{0\}$.
2. $[K_s]$ is kept constant and the unbalanced force $\{F_s\text{-}F_r\}$ are computed.
3. The incremental $\{\Delta U_s\}$ is calculated for the unbalanced force.
4. $\{\Delta U_s\}$ is added to $\{U_s\}$ in order to obtain the next approximation $\{U_{s+1}\}$.

The solution is said to be converged and in equilibrium after a number of iterations when the unbalanced force $\{F_s\text{-}F_r\}$ becomes almost zero or near to the tolerance considered.

CHAPTER 4

VALIDATION OF THE FINITE ELEMENT MODEL

4.1 INTRODUCTION

Results obtained from experimental investigation is validated with the results obtained from numerical modeling while the results obtained from numerical modeling is validated with the results obtained from experimental investigation or the field observations. These validations are very important for both type of research whether it is experimental or it is analysed by numerical methods. The validation is accepted if the variation of the results from the two methods does not exceed from 10-20 %. In this chapter the results obtained for load settlement curves for piled raft foundation under axisymmetric condition and plane strain condition from the nonlinear finite element analysis have been validated with the results reported in literature.

4.2 VALIDATION UNDER PLANE STRAIN CONDITION

4.2.1 Definition of the Problem

The problem as analysed by Whitman and Hoeg (1966) and reported by Lambe and Whitman (1979) Figure 4.1, which has been analysed by finite difference method is reanalyzed by nonlinear finite element method using PSNLFEM software in the present research, modeling soil as Von-Mises elastoplastic material and comparison has been made for the load settlement curve. The number of elements used in the analysis is 100. The bottom nodes have been considered completely fixed. All the nodes and at the boundary edges have been allowed to undergo only vertical translation. The type soil reported is clay.

- Problem type: Plane Strain
- Type of load considered: Uniformly distributed load
- Width of application of load: 4.40 m
- Modulus of elasticity of soil (E_s) = 34480 kN/m^2

- Cohesion of soil (c) = 167.6 kN/m^2
- Poisson's ratio of soil= 0.30

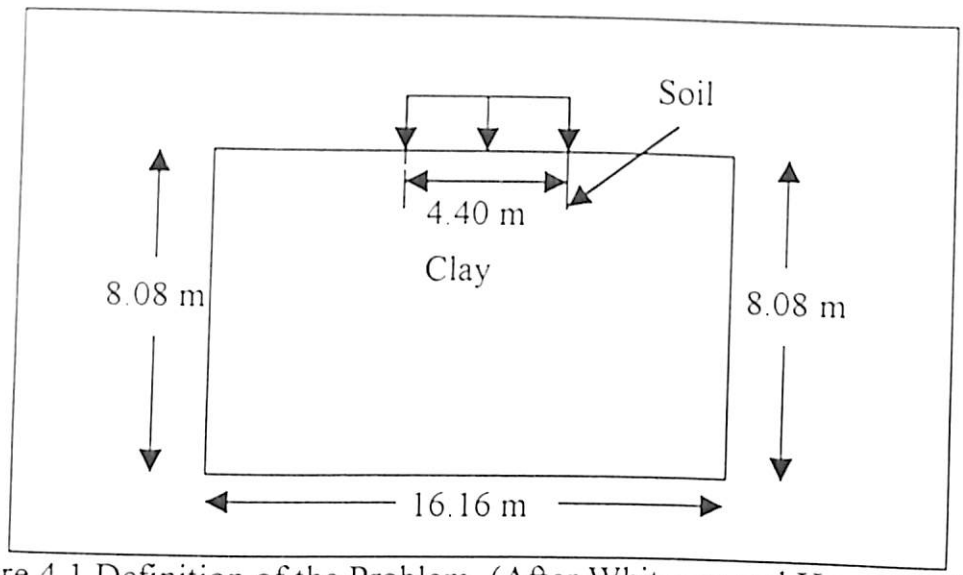

Figure 4.1 Definition of the Problem (After Whitman and Hoeg 1966)

4.2.2 Comparison of Load-Settlement Curve

Figure 4.2 shows the comparison of the load settlement curves as reported in literature and by the present nonlinear finite element model considered. The two results are in excellent agreement.

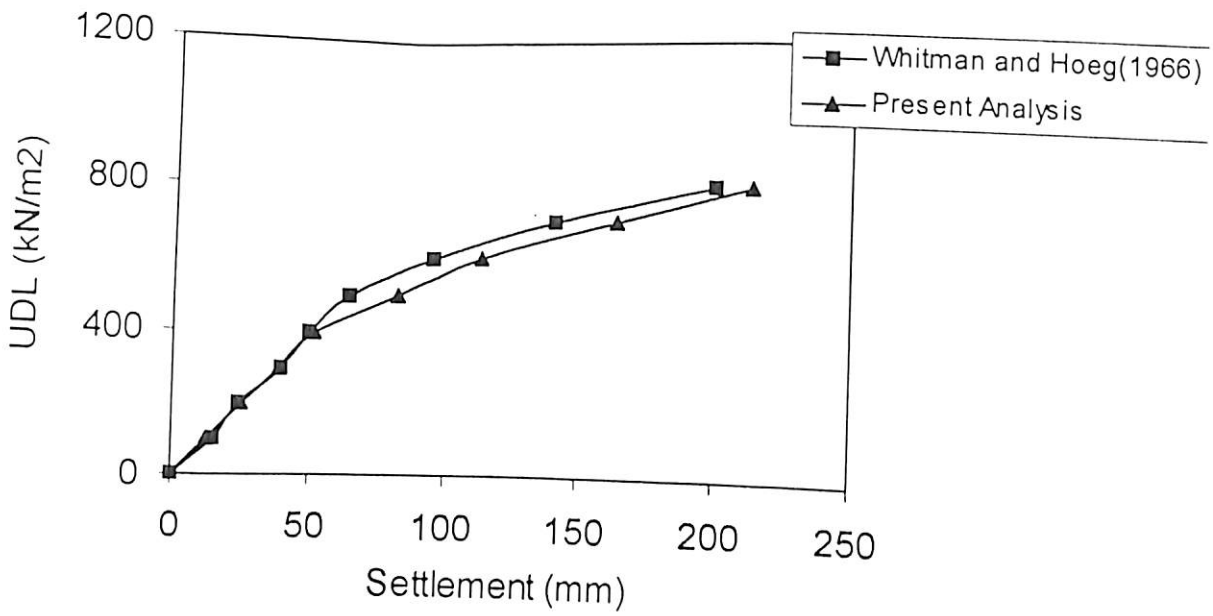

Figure 4.2. Validation of 2D finite element model

4.3 VALIDATION UNDER AXISYMMETRIC CONDITION

4.3.1 Definition of the Problem

The problem as reported by Kraft (1981), which is the field investigation of single pile at University of Housten, has been analysed by nonlinear finite element method under axisymmetric condition by AXINLFEM software. The number of elements used in the analysis is 400. The bottom nodes have been considered completely fixed. All the nodes at axis of symmetry and at the boundary edge have been allowed to undergo only vertical translation.

The pile is a closed ended steel pipe pile

- $(E_{steel})=2 \times 10^7$ kN/m^2
- The length of pile considered= 13 m
- Outer diameter of pile =0.273 m
- Thickness of hollow pile =. 00927 m
- Poisson's ratio of soil = 0.5
- Poisson's ratio considered in analysis = 0.45

The modulus of elasticity of soil (E_s) and the cohesion of the soil (C) has been taken and obtained from Figure 11 (Kraft (1981)), Figure 4.3 in this thesis.

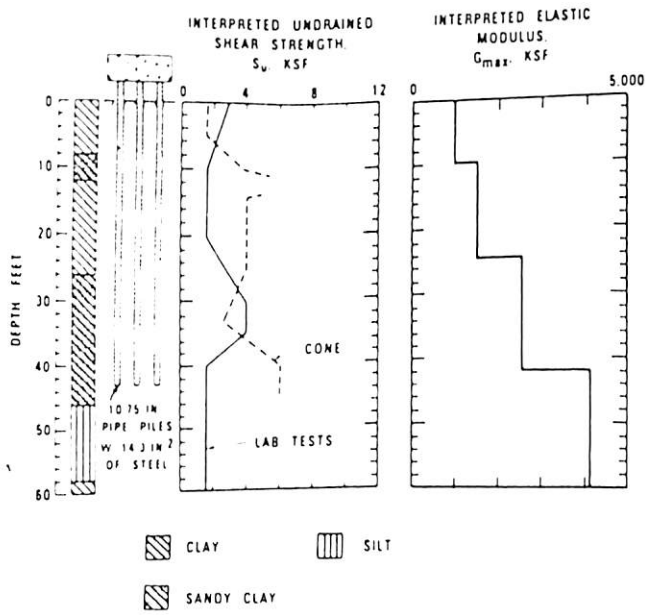

Figure.4.3 Soil Conditions at University of Houston (After Kraft, 1981)

4.3.2 Comparison of Load Settlement Curve

Figure 4.4 shows the load settlement curve as obtained by the present analysis and that reported by Kraft (1981). The two results are in excellent agreement.

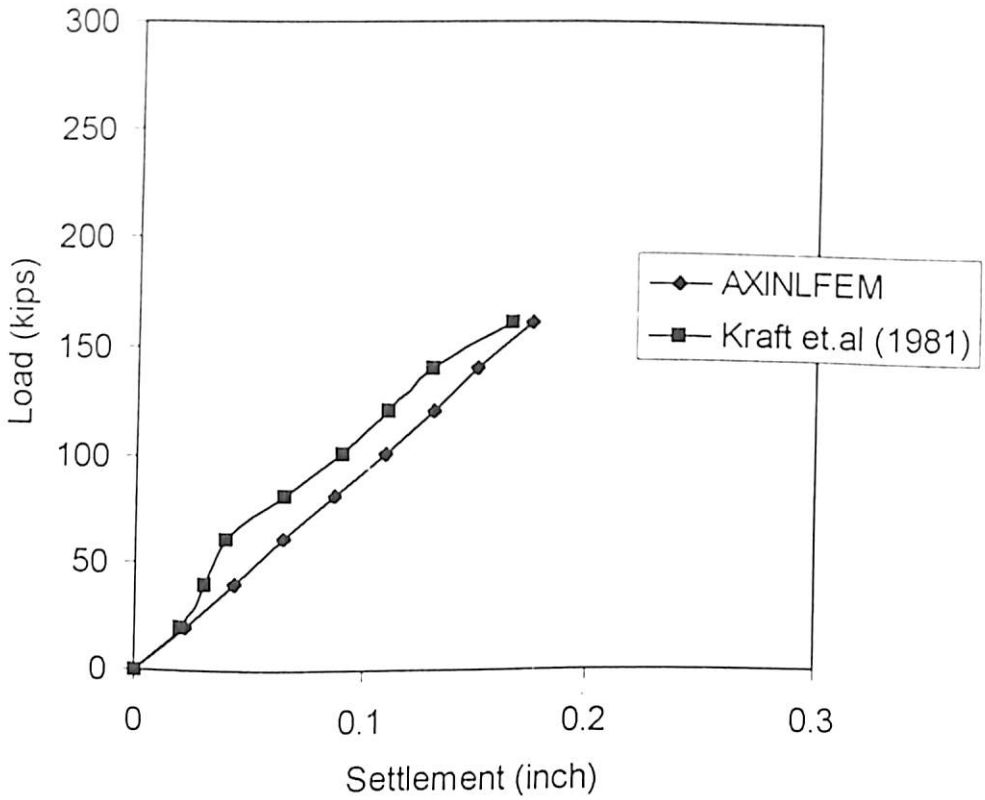

Figure 4.4. Validation of FE Model
(1 inch = 25.4 mm and 1 kip = 4.45 kN)

CHAPTER 5
NONLINEAR FINITE ELEMENT ANALYSIS FOR AXISYMETRIC PILED RAFT FOUNDATION

5.1 INTRODUCTION

An Axisymmetric raft and piled raft foundations are used widely for axisymmetric structures. In order to understand the behaviour of such foundations when loaded till failure, nonlinear finite element analysis has been done for axisymmetric raft and piled raft foundation.

5.2 DEFINITION OF PROBLEM

In order to understand the behaviour of raft and piled raft foundation nonlinear finite element analysis is carried out for raft and piled raft foundation by varying parameters such as raft diameter, length of pile, soil modulus, spacing between the piles.

5.3 DETAILED PARAMETRIC STUDY

Detailed Parametric study has been done for raft and piled raft by varying the following parameters:

Diameter of Raft =10, 20, 30, 40, 50 meters

Raft Thickness = 0.1m to 4.0 m

Length of Pile= 10, 20, 30, 40, 60, 90, 120 meter

Diameter of the Pile = 0.4 m

Soil Modulus =22000, 76000, 130000 kN/m^2

Poisson's Ratio for Soil = 0.45

Modulus of Raft and Pile Material = 20000000 kN/m^2

Poisson's Ratio of Raft and Pile Material = 0.30

5.4 ANALYSIS OF AXISYMMETRIC RAFT

AXINLFEM software has been used to analyse the axisymmetric raft foundation. The validation of the results obtained from this software has been shown in chapter 4. Figure 5.1 shows the finite element discretization considered for raft foundation. Appendix-IV includes the discretization details for a typical analysis. The raft and soil has been discretized into four noded isoparametric finite elements. The soil has been modeled as Von-Mises elasto-plastic material. From the centre of the raft a radial zone of soil equal

to 5 times the diameter of the raft has been considered. Below the raft, soil upto 200 meter has been considered.

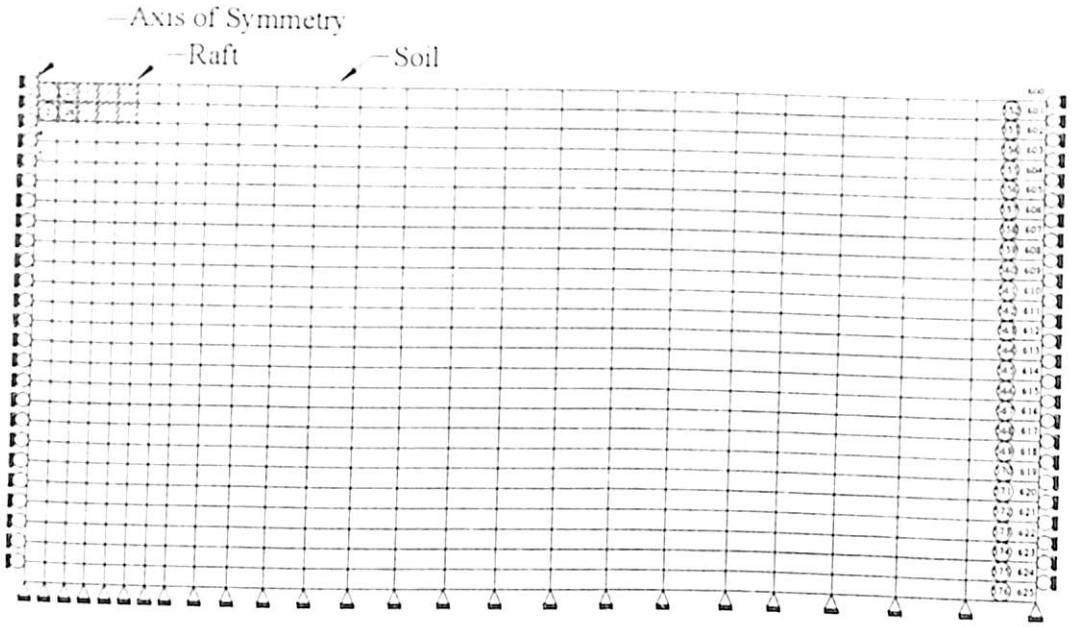

Figure 5.1 Finite Element Discretization for Axisymmetric Raft

5.5 ANALYSIS OF AXISYMMETRIC PILED RAFT FOUNDATION

Finite element analysis for axisymmetric piled raft foundations has been performed by AXINLFEM. The results obtained from AXINLFEM have been found in good agreement with standard finite element software. Each concentric row of piles in the piled raft foundation has been represented as an equivalent annulus of same volume. Finite element discretization for typical piled raft foundation with the surrounding soil and the soil strata below has been shown in Figure5.2. Appendix-IV includes the dimension of elements for a typical analysis. The raft, pile and soil have been discretized into four noded isoparametric finite elements. The number of nodes and elements considered are 625 and 576 respectively. The material nonlinearity of soil has been idealised by Von-Mises Yield Criterion, which is very suitable for clay under undrained condition. The depth of soil considered in the analysis is 200 meters. This depth has been kept constant for all the analyses. Soil domain equal to 5 times the diameter of the raft has been considered from the center of the raft in the lateral direction. The bottom nodes have been considered completely fixed. All the nodes at axis of symmetry and at the boundary edge have been allowed to undergo only vertical translation. Uniformly distributed load has been considered to act on the foundation.

The uniformly distributed load considered has been applied as concentrated load on the respective nodes on the foundation in the finite element analysis.

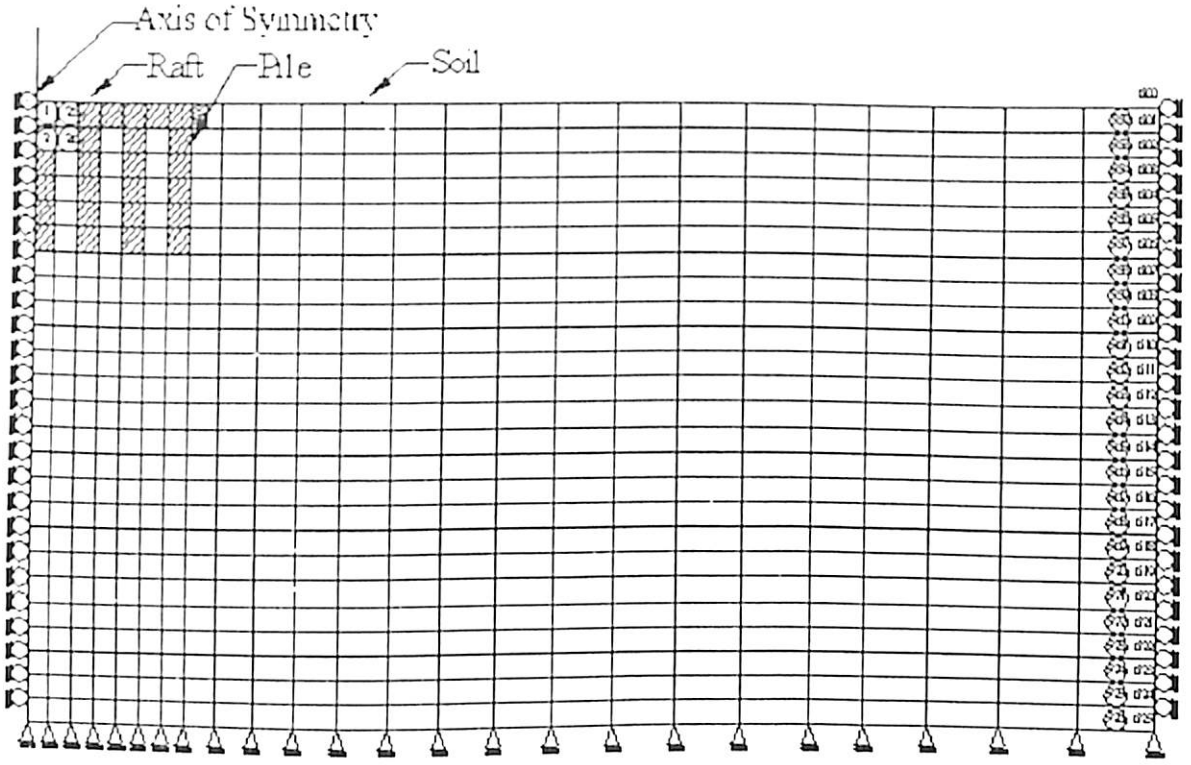

Figure 5.2 Finite Element Discretization for Axisymmetric Piled Raft Foundation

5.6 RESULTS AND DISCUSSION

5.6.1.Load Settlement Curves

5.6.1.1 Effect of raft thickness

Figure 5.3 (a) shows the effect of increase in thickness on load settlement behaviour of raft foundation of diameter 10 meters. The effect of increase in thickness of raft is to reduce the settlement of the raft foundation and increase the load carrying capacity of the raft foundation. The significant reduction in settlement and increase in load carrying capacity of the raft is found at a raft thickness of 4 meter.

Figures 5.3(b) and 5.3(c) show the effect of raft thickness on the load settlement behaviour of raft foundation of diameter 10 meter for different soil modulus. The nature of load settlement curves is similar as discussed above. Due to increase in soil modulus the overall settlement reduces at any thickness of the raft.

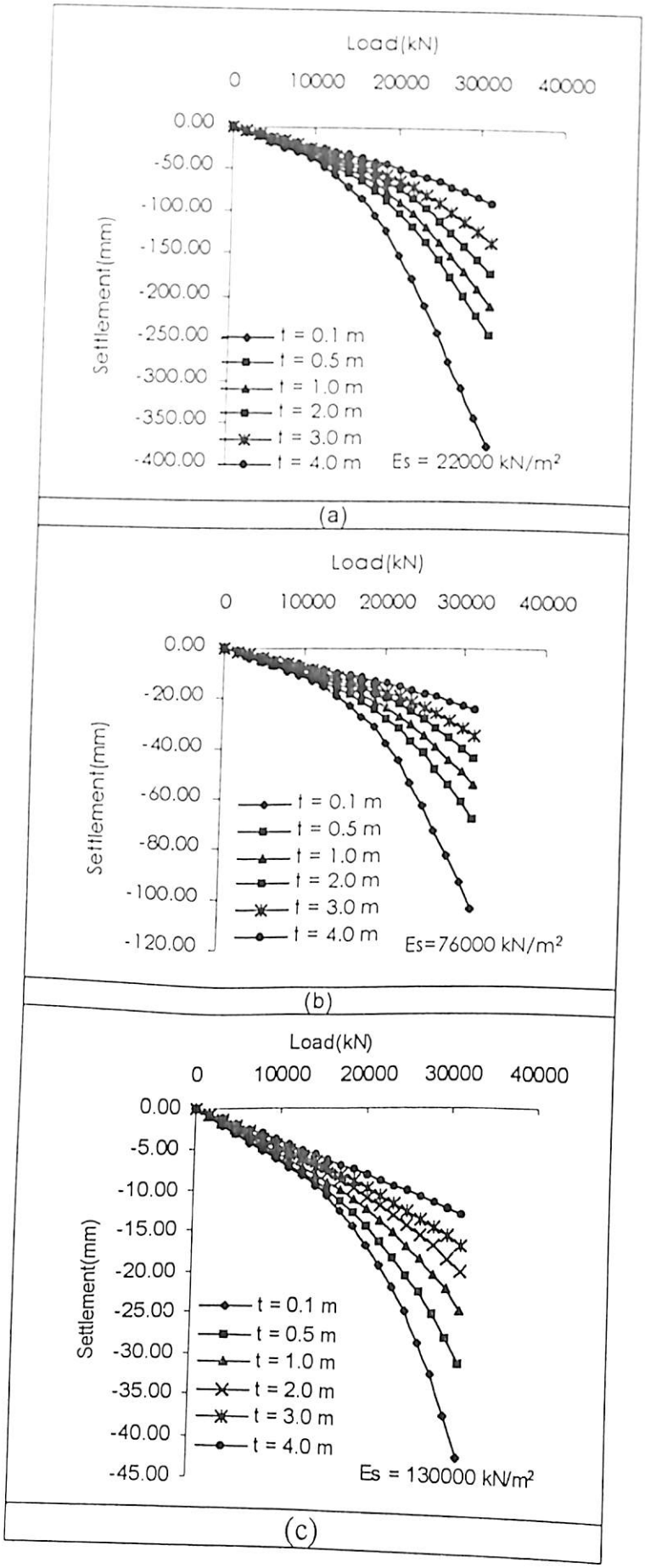

Figure 5.3 Load Settlement Curve for Raft of various thickness (D =10 m)

Figures 5.4 (a), (b), (c) show the effect of raft thickness on the load settlement behaviour of raft foundation of diameter 20 meter for different soil modulus. The effect of increase in thickness of raft is similar as discussed for smaller size (D = 10 m) of raft. For the considered range of thickness the load carrying capacity of the 20 meter diameter raft is more than that of the 10 meter raft. The effect of increase in soil modulus is to increase the load carrying capacity of the raft foundation.

5.6.1.2 Effect of soil modulus

Figures 5.5 (a), (b), (c), (d), (e) and (f) show the effect of soil modulus on the load settlement behaviour of raft of diameter 10 meter for different thickness of raft. At any thickness the effect of increase in soil modulus is to increase the load carrying capacity of raft foundation. In other words the load carrying capacity of raft in stiff clay is more than that in soft and medium stiff clay. The load carrying capacity of raft of minimum thickness is least while that with largest thickness is maximum.

Figures 5.6 (a), (b), (c), (d), (e), (f) show the effect of soil modulus on the load settlement behaviour of raft diameter 20 meter for different thickness of raft. It can be observed from the graphs that the settlement of the raft foundation decreases with increase in soil modulus of the soil.

Figures 5.7 (a), (b), (c), (d), (e), (f) show the effect of soil modulus on the load settlement behaviour of raft of diameter 30 meter for different thickness of raft. The effect of increase in soil modulus and thickness of raft is to increase the load carrying capacity of the raft foundation.

Figures 5.8 (a), (b), (c), (d), (e), (f) show the effect of soil modulus on the load settlement behaviour of raft of diameter 40 meter for different thickness of raft. It is observed from the graphs that load carrying capacity of the raft foundation increases with increase in soil modulus and raft thickness.

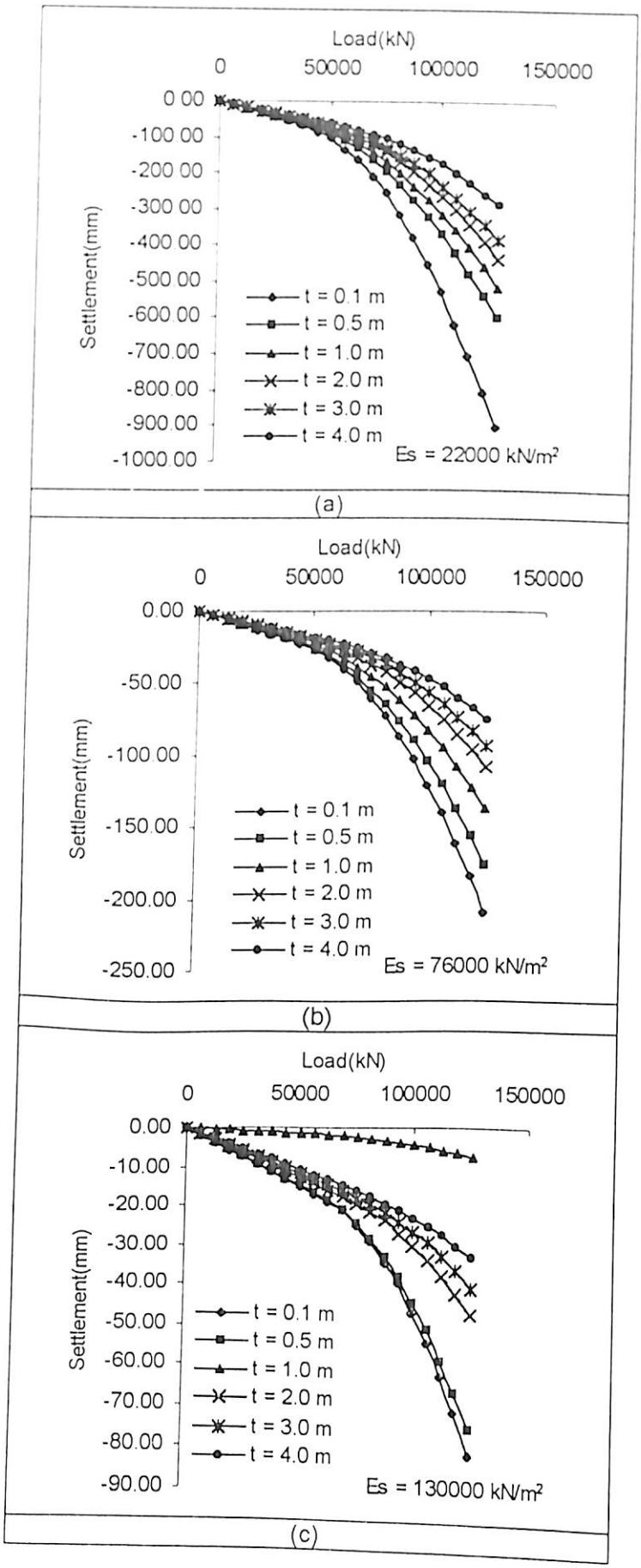

Figure 5.4 Load Settlement Curves for Various Raft Thickness (D =20 m)

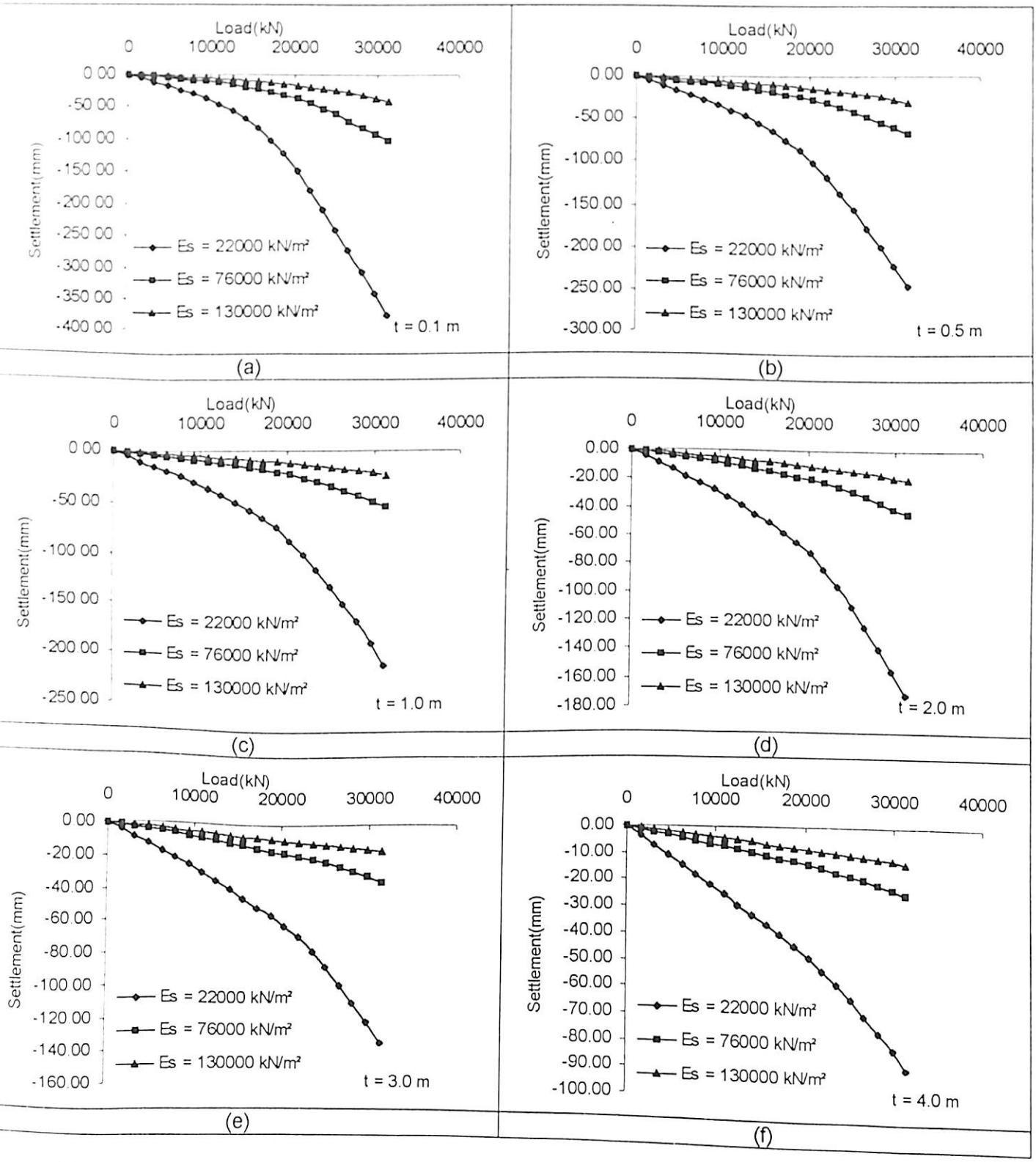

Figure 5.5 Effect of Soil Modulus on the Load Settlement Behaviour of Raft Foundation (D = 10 m)

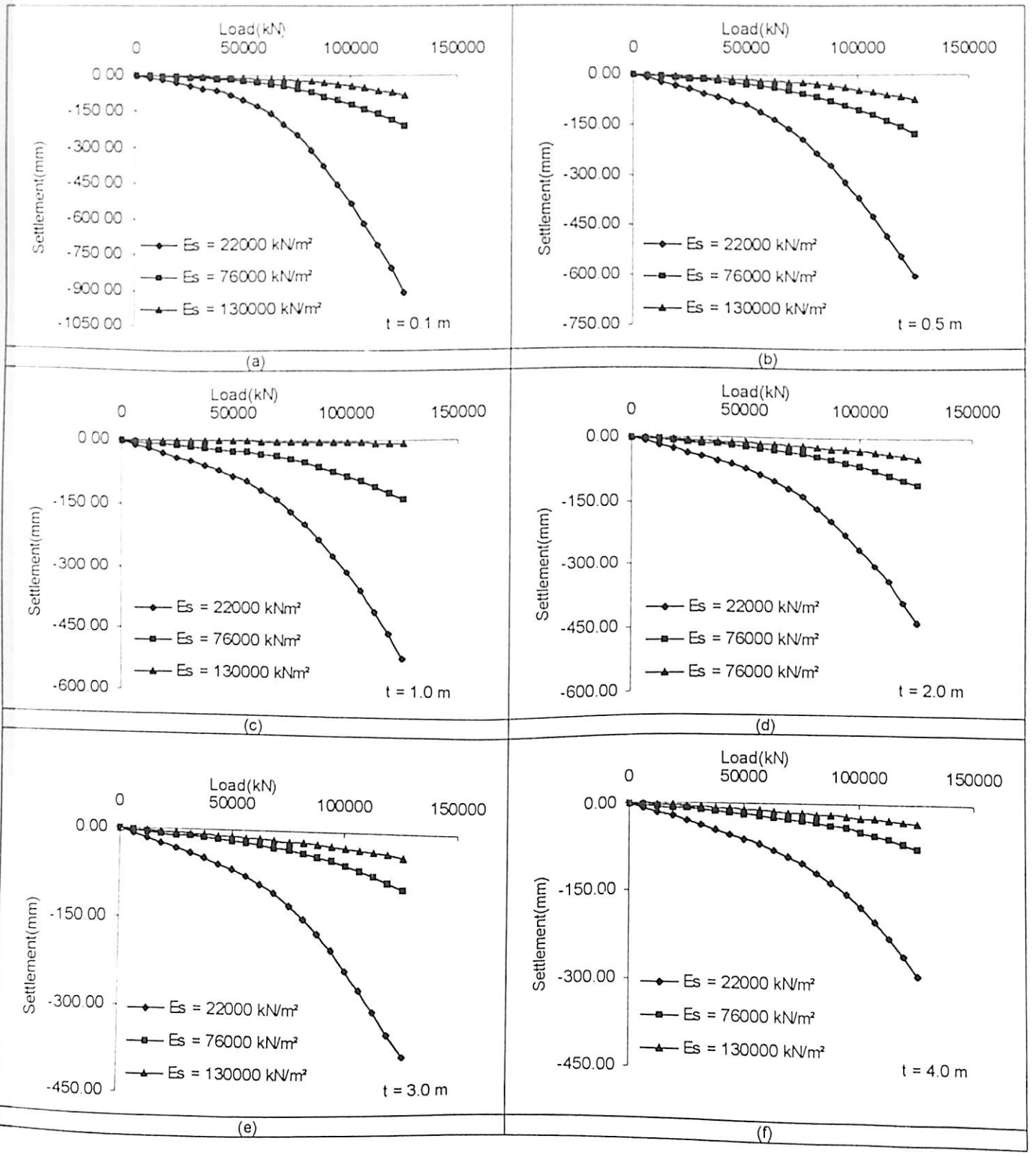

Figure 5.6 Effect of Soil Modulus on the Load Settlement Behaviour of Raft Foundation (D = 20 m)

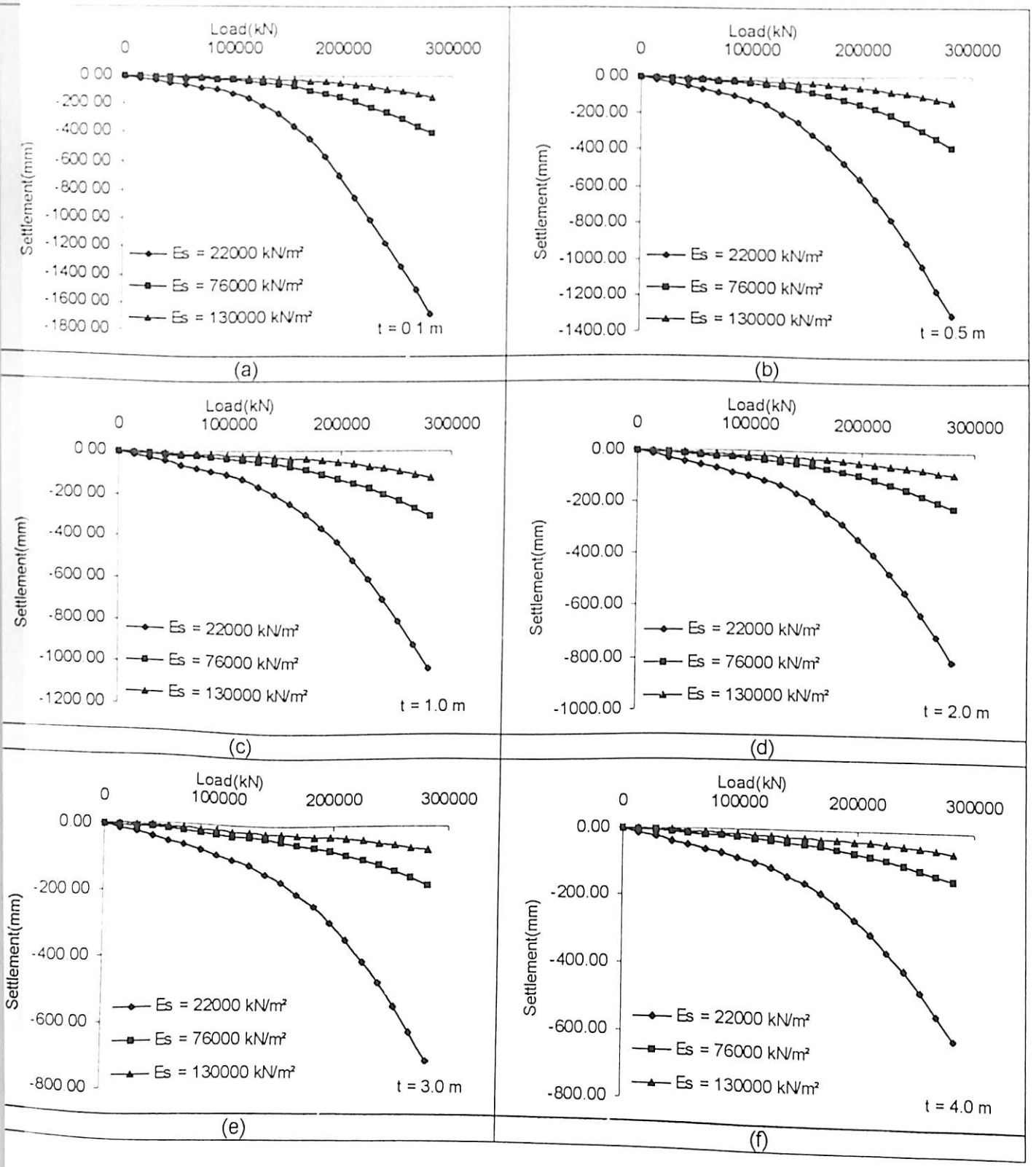

Figure 5.7 Effect of Soil Modulus on the Load Settlement Behaviour of Raft Foundation (D = 30 m)

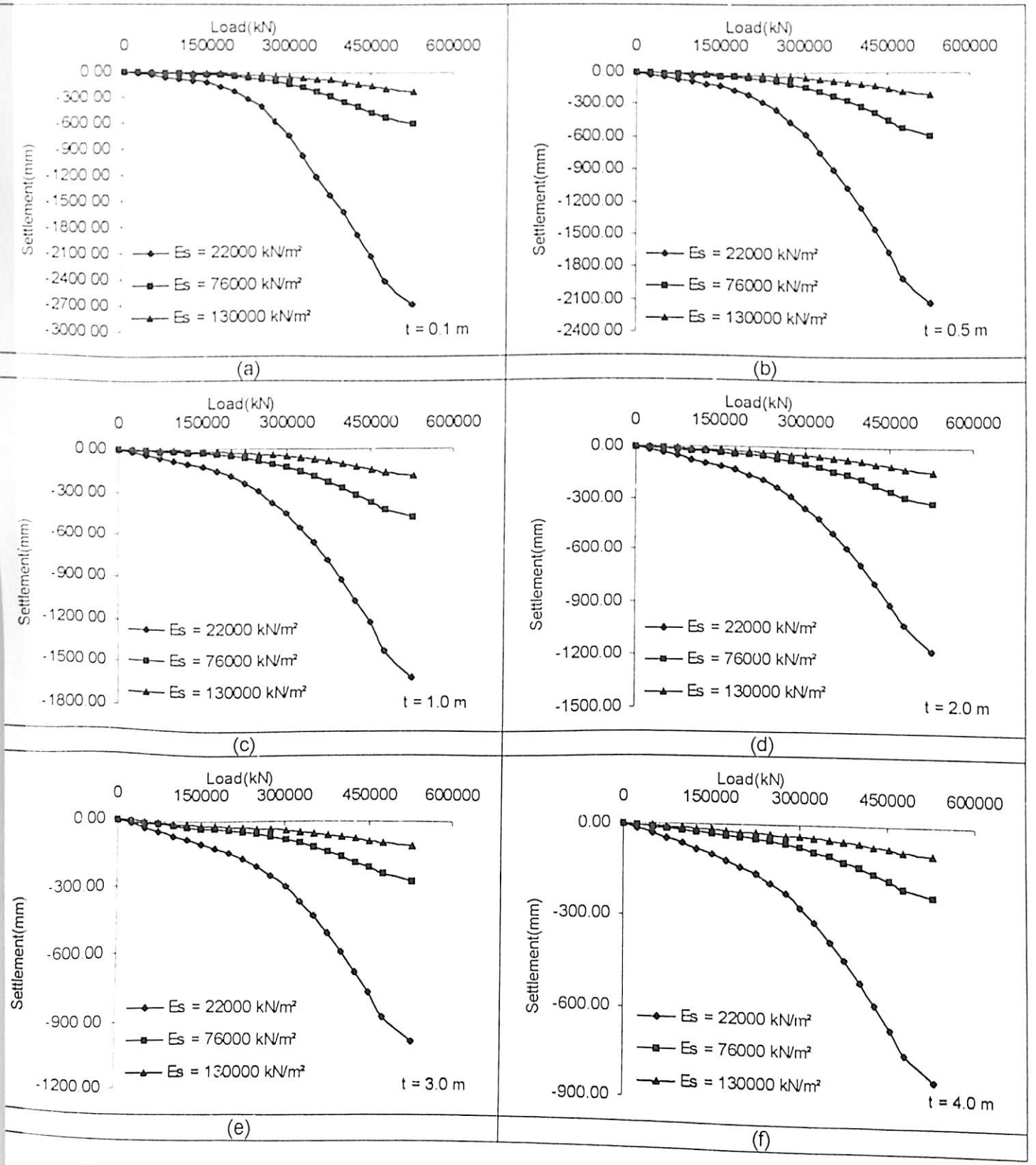

Figure 5.8 Effect of Soil Modulus on the Load Settlement Behaviour of Raft Foundation (D = 40 m)

5.6.1.3 Effect of Raft Diameter

Figure 5.9 shows the effect of raft diameter on the load settlement behaviour of raft foundation for different thickness of raft for soil modulus of 22000 kN/m^2. The load settlement curves obtained resembles with that reported by Maharaj (1996) and Maharaj and Gandhi (2003 b).The smaller raft reaches to its ultimate capacity at smaller settlement while the largest raft reaches to its ultimate capacity at very high settlement compared to the smaller size of the raft. Difference in load carrying capacity of different size of raft is more significant at higher loads.

Figure 5.10 shows the effect of raft diameter on the load settlement behaviour of raft foundation for different thickness of the raft for soil modulus of 76000 kN/m^2. The nature of the load settlement curve is similar as discussed above. The increase in size of the raft is to improve significantly the load carrying capacity of the raft. The smaller raft reaches to its ultimate capacity at smaller settlement while the largest raft reaches to its ultimate capacity at very high settlement compared to the smaller size of the raft. The load carrying capacity of raft is more than that for soil modulus 22000 kN/m^2.

Figure 5.11 shows the effect of raft diameter on the load settlement behaviour of raft foundation for different thickness of the raft for soil modulus of 130000 kN/m^2. The nature of the load settlement curves is similar as discussed earlier. With increase in size of the raft there is significant improvement in the load carrying capacity of the raft. The load carrying capacity of raft in this case is more than that discussed in Figure 5.10 due to the increase in soil modulus. In this case also the smaller raft reaches to its ultimate capacity at smaller settlement while the largest raft reaches to its ultimate capacity at very high settlement compared to the smaller size of the raft. The raft resting on soils with soil modulus 130000 kN/m^2 carries more loads when compared with rafts on soil modulus 22000 kN/m^2 and 76000 kN/m^2.

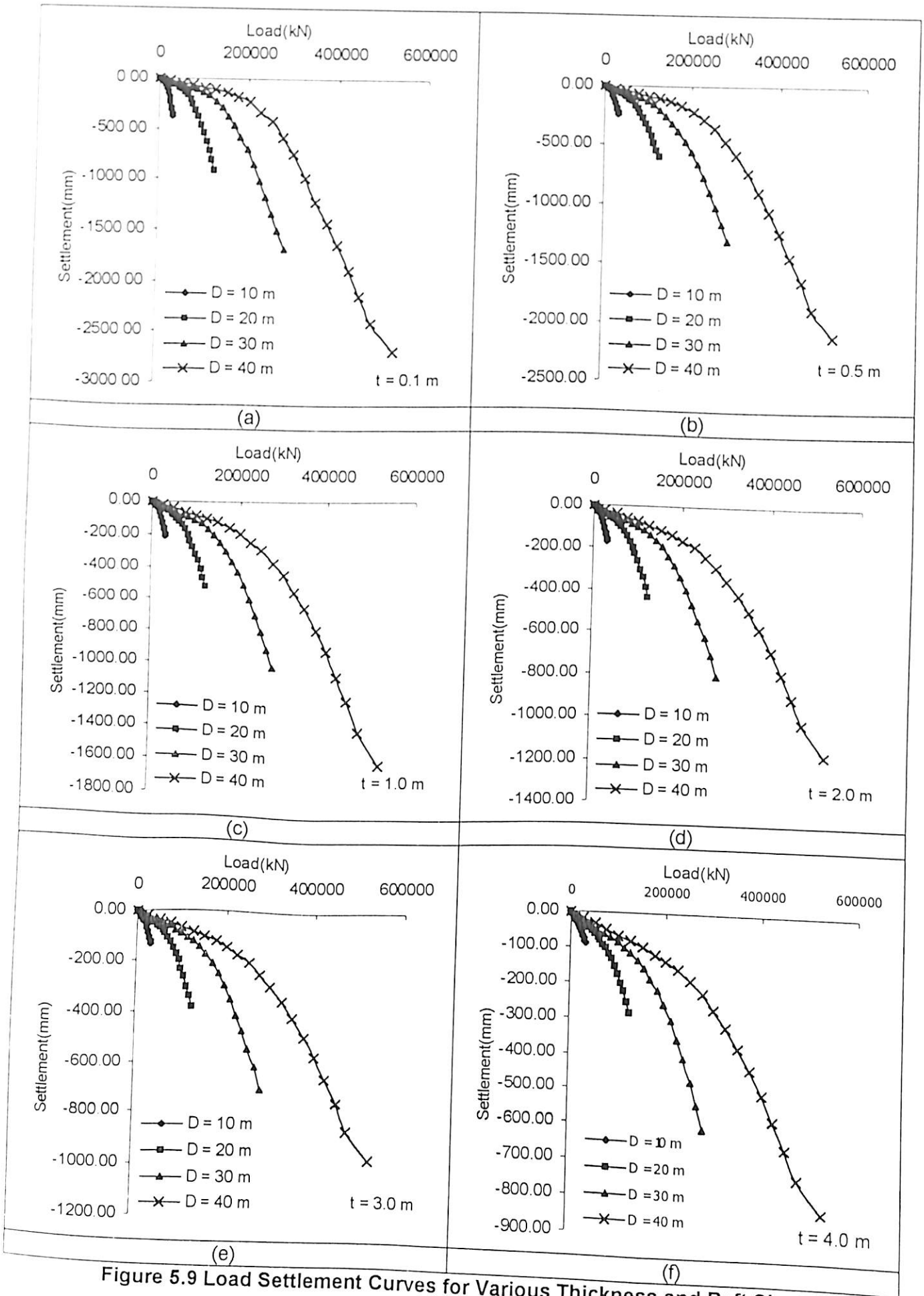

Figure 5.9 Load Settlement Curves for Various Thickness and Raft Size (Es = 22000 kN/m^2)

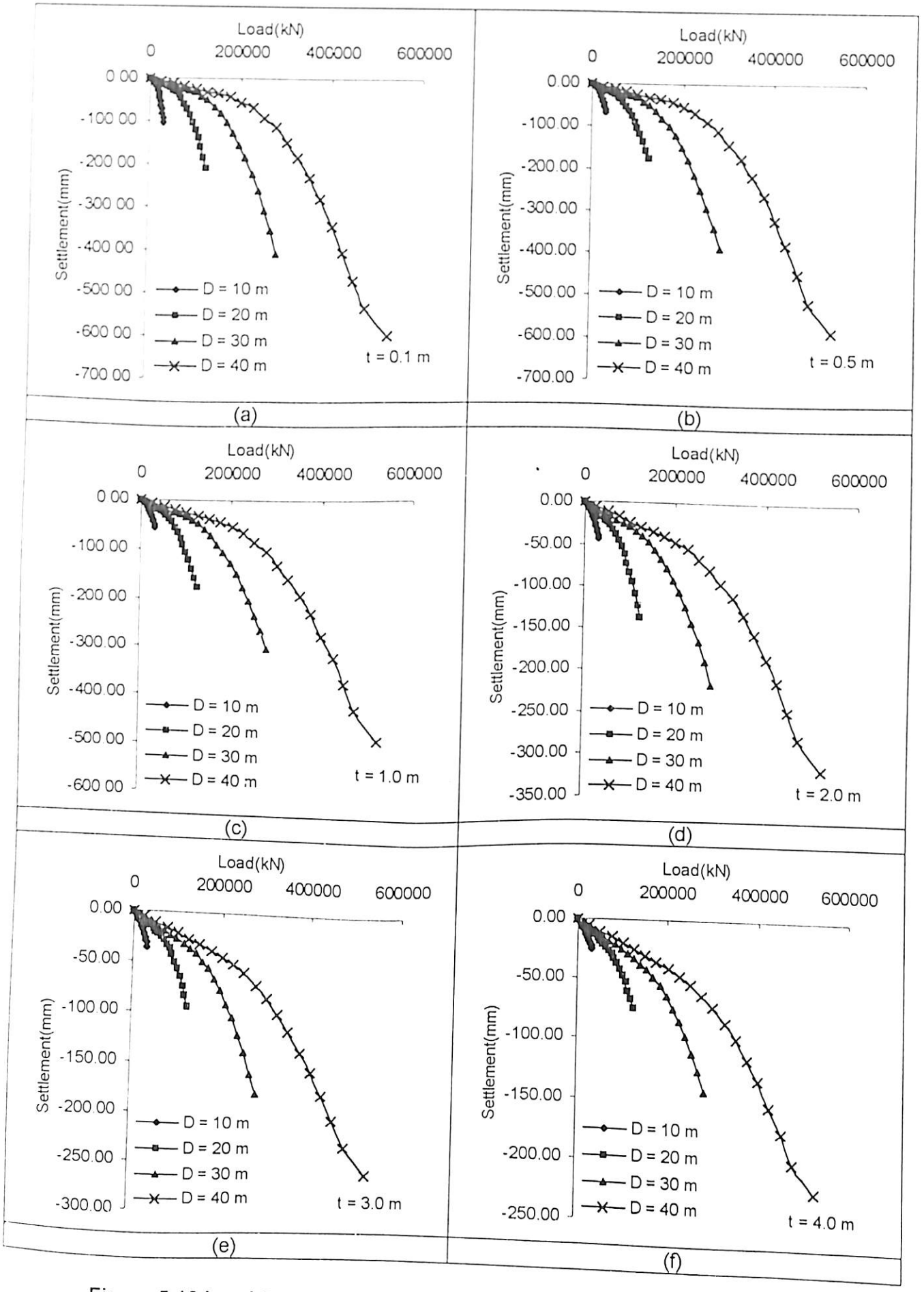

Figure 5.10 Load Settlement Curves for Various Thickness and Raft Size (Es = 76000 kN/m^2)

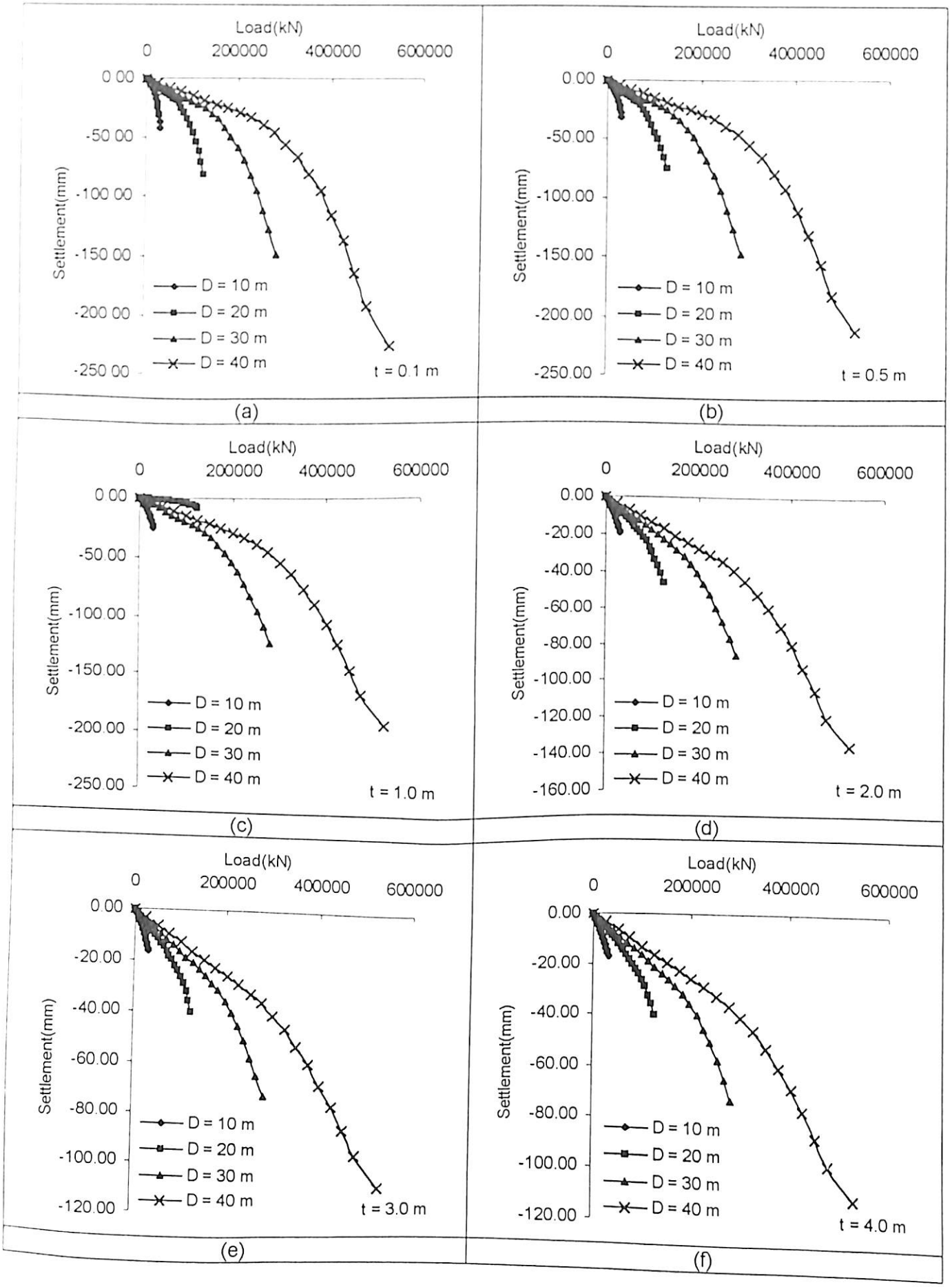

Figure 5.11 Load Settlement Curve for Various Thickness and Raft Size (Es = 130000 kN/m^2)

5.6.2 Load Settlement Curves for Piled Raft Foundation

5.6.2.1 Effect of length of pile

Figure 5.12 (a) shows the load settlement curves for piled raft foundation for varying length of piles. The effect of providing piles below a raft is to increase the load carrying capacity of raft foundation and decrease the settlement of raft foundation. With increase in length of pile significant increase in load carrying capacity of piled raft foundation is found. Initial portion of the load settlement curves for piled raft foundation for pile lengths 10,20 and 30 meter show overlap. This is due to the fact that for initial loads the raft takes most of the loads. Once the raft is fully loaded, the loads are transferred to the piles. It can be seen that piles of length even equal to the size of raft reduces the settlement of the raft foundation and at the same time increases the load carrying capacity of raft foundation.

Figures 5.12 (b), (c) show the load settlement curves for piled raft foundation of raft size 10 meter and varying pile lengths and varying soil modulus. A similar trend of load settlement curves as obtained earlier is seen even for these two cases. An increase in overlap range of load settlement curves is seen. This is due to the fact that when the modulus of soil increases the flexibility of raft as well as piles increases due to the soil structure interaction. In the beginning most of the load is carried by the raft and then it is transferred to the pile. Piles being compressible, even longer piles do not show much improvement in load carrying capacity due to its flexibility, which is due to soil structure interaction.

Figures 5.13 (a), (b), (c) show the load settlement curves for piled raft foundation when the piles are provided at center to center spacing of five times the diameter of the pile for varying pile lengths and soil modulus. As the spacing between the piles has been increased keeping the raft size same in the piled raft foundation, the number of piles in this case is less than in Figure 5.12. Comparison of Figure 5.13 and Figure 5.12 show that due to the increase in spacing between the piles the load carrying capacity of piled raft foundation decreases. The trend of load settlement curves of Figure 5.13 (a), (b), (c) is similar to 5.12.

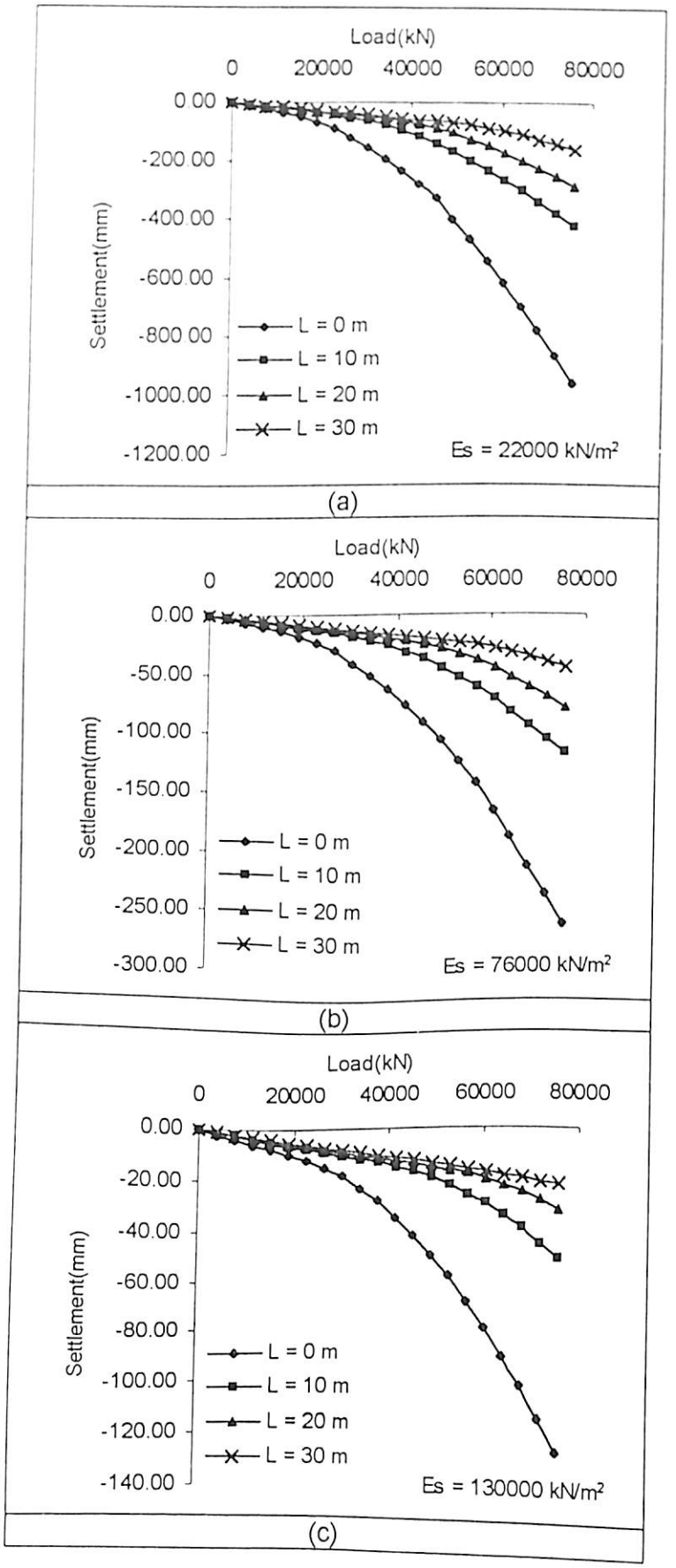

Figure 5.12 Effect of Length of Pile on Load Settlement Behaviour of Piled Raft Foundation (D = 10 m, s/d = 2.5)

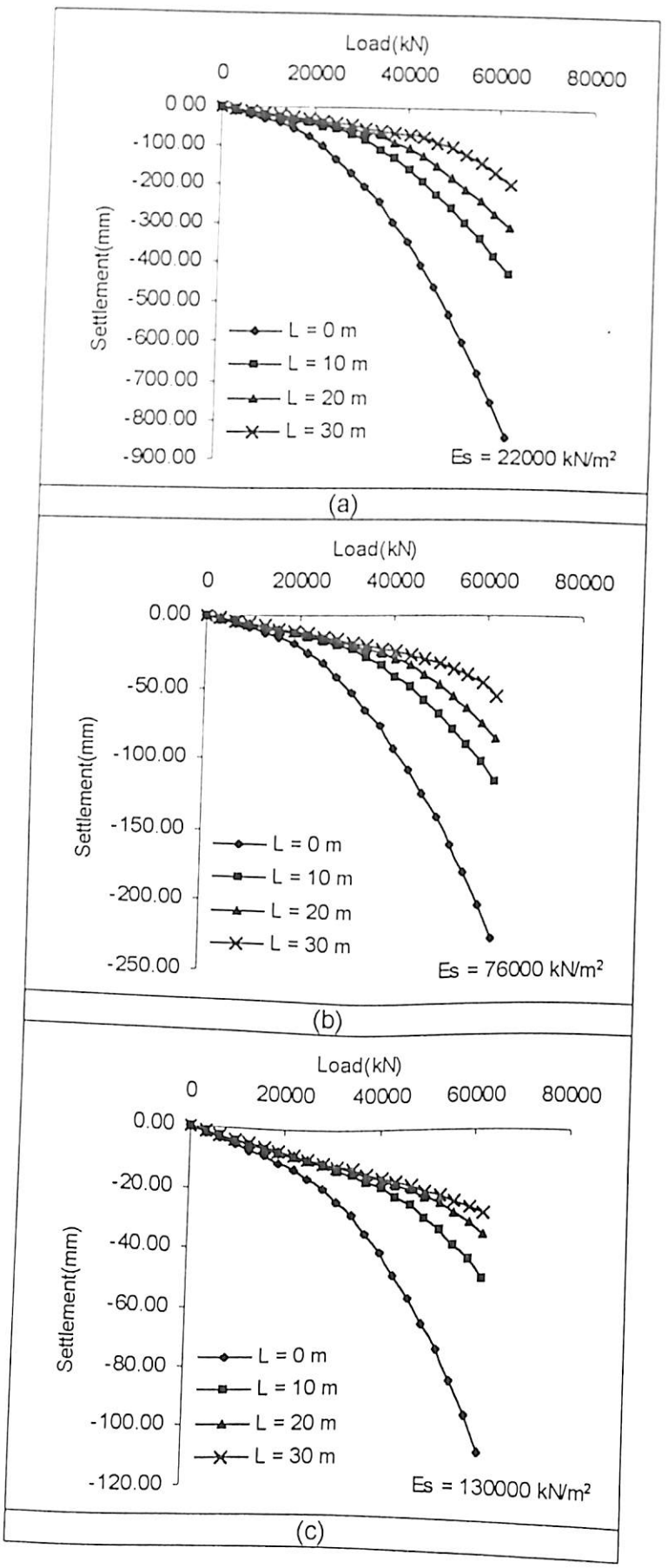

Figure 5.13 Effect of Length of Pile on Load Settlement Behaviour of Piled Raft Foundation (D = 10 m, s/d = 5)

Figures 5.14 (a), (b), (c) show the load settlement curves for piled raft foundation when the piles are at center to center spacing of seven and half times the diameter of pile. The load carrying capacity decreases with increase in spacing between the piles as is seen when Figures 5.12, 5.13, 5.14 are compared with each other.

5.6.2.2 Effect of soil modulus

Figures 5.15 (a), (b), (c), (d) show the effect of increase in soil modulus on the load settlement behaviour of piled raft foundation. The effect of increase in soil modulus is to increase the load carrying capacity and reduce the settlement of piled raft foundation. Although the load carrying capacity increases and settlement reduces due to the increase in soil modulus, the stiffness of the piled raft foundation as a whole decreases due to the soil structure interaction.

Figures 5.16 (a), (b), (c), (d) and Figures 5.17 (a), (b), (c), (d) show the load settlements curves for piled raft foundations for pile spacing equal to 5 and 7.5 times the diameter of the pile for varying soil modulus and pile length. With increase in spacing between the piles the overall stiffness of the piled raft foundation as a whole decreases. And the increase in soil modulus further reduces the overall stiffness of piled raft foundation. This reduction in stiffness can be observed from the increased overlap of load settlement curves when the soil modulus increases.

5.6.2.3 Effect of spacing

The load settlement curves have been plotted again to show the effect of increase in spacing between the piles on the load settlement behaviour of piled raft foundation. It can be seen from Figures 5.18 (a), (b), (c) that the effect of increase in spacing between the piles is to reduce the load carrying capacity of piled raft foundation.

Figures 5.19 (a), (b), (c) and Figures 5.20 (a), (b), (c) show the effect of increase in soil modulus for varying spacing between the piles. The effect of increase in spacing is to decrease the load carrying capacity while the increase in soil modulus is to increase the overall load carrying capacity of the piled raft foundation.

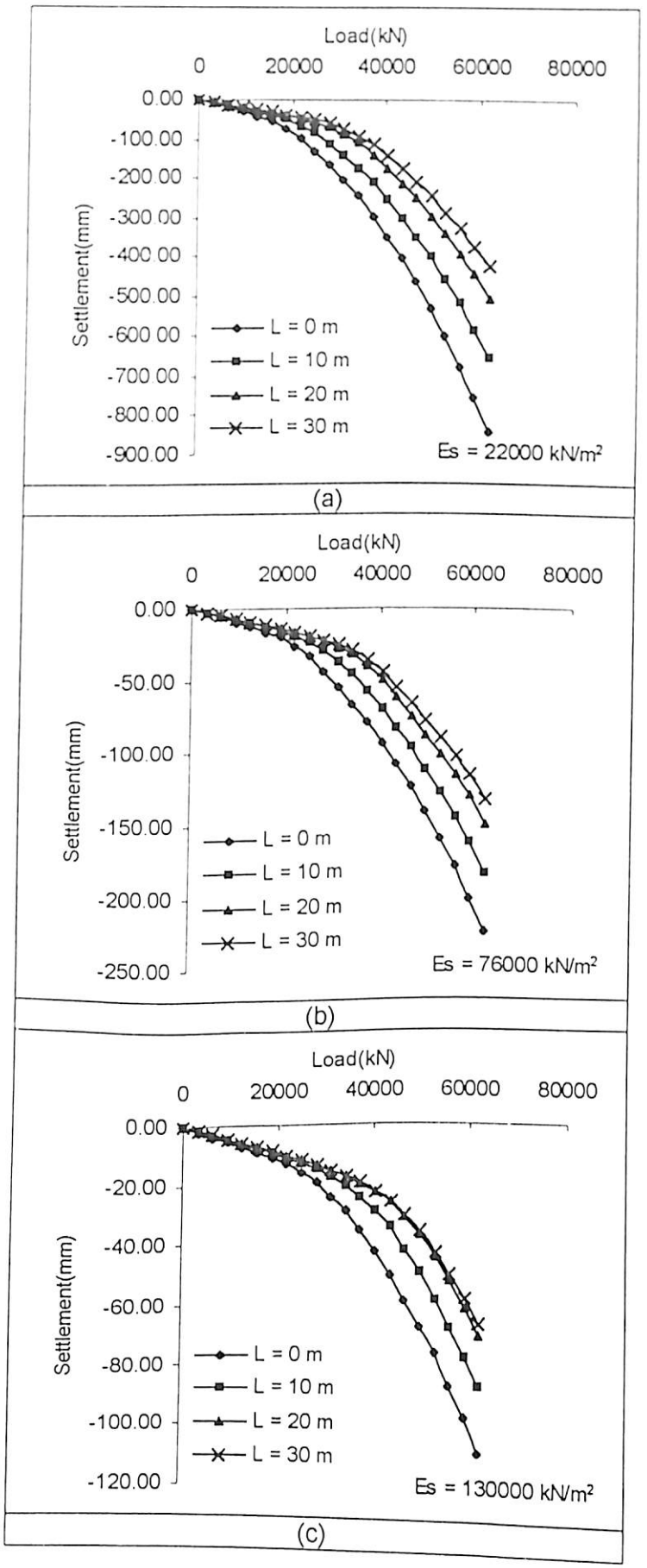

Figure 5.14 Effect of Length of Pile on Load Settlement Behaviour of Piled Raft Foundation
(D = 10 m, s/d = 7.5)

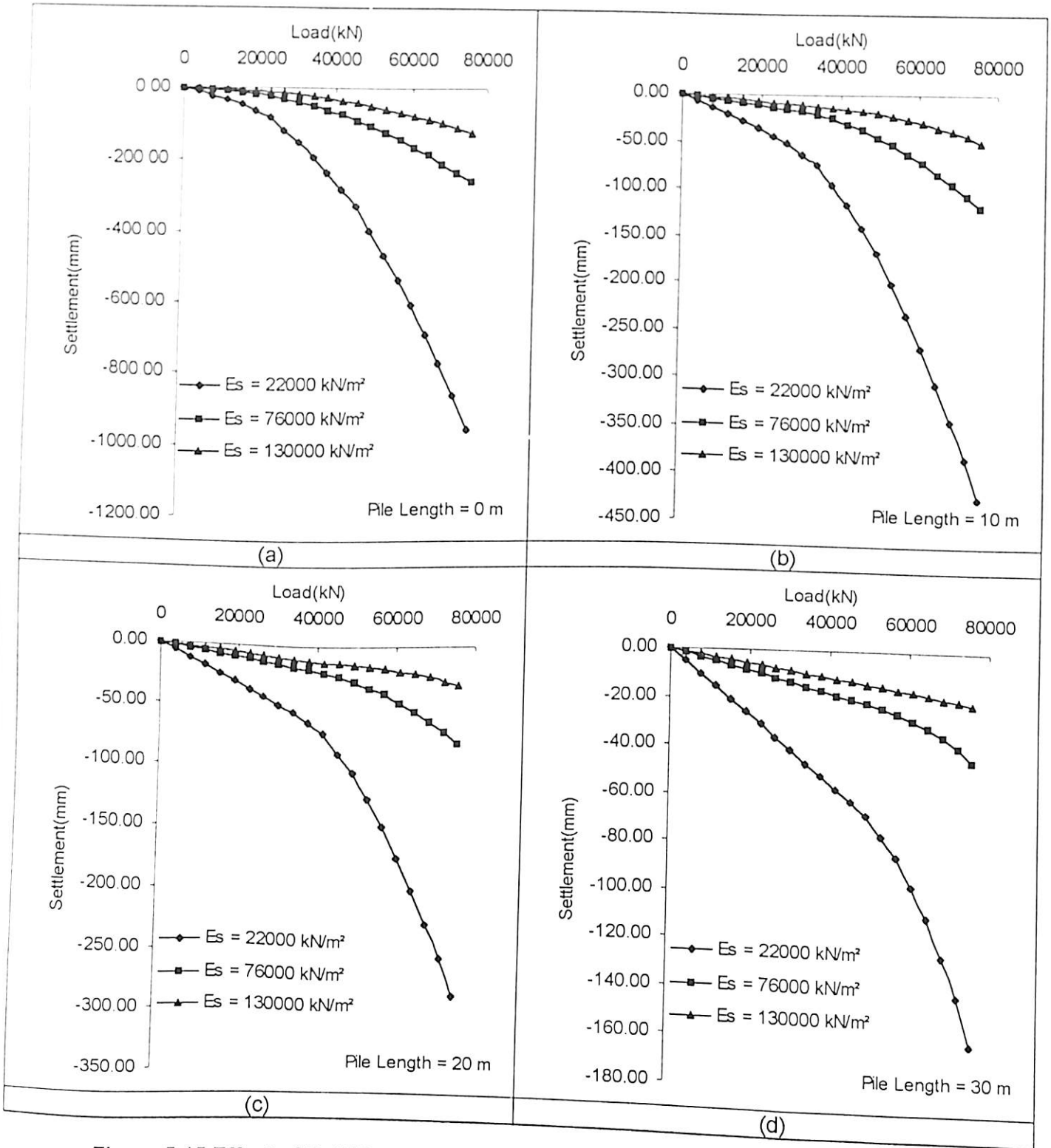

Figure 5.15 Effect of Soil Modulus on the Load Settlement Behaviour of Piled Raft Foundation
(D = 10 m, s/d = 2.5)

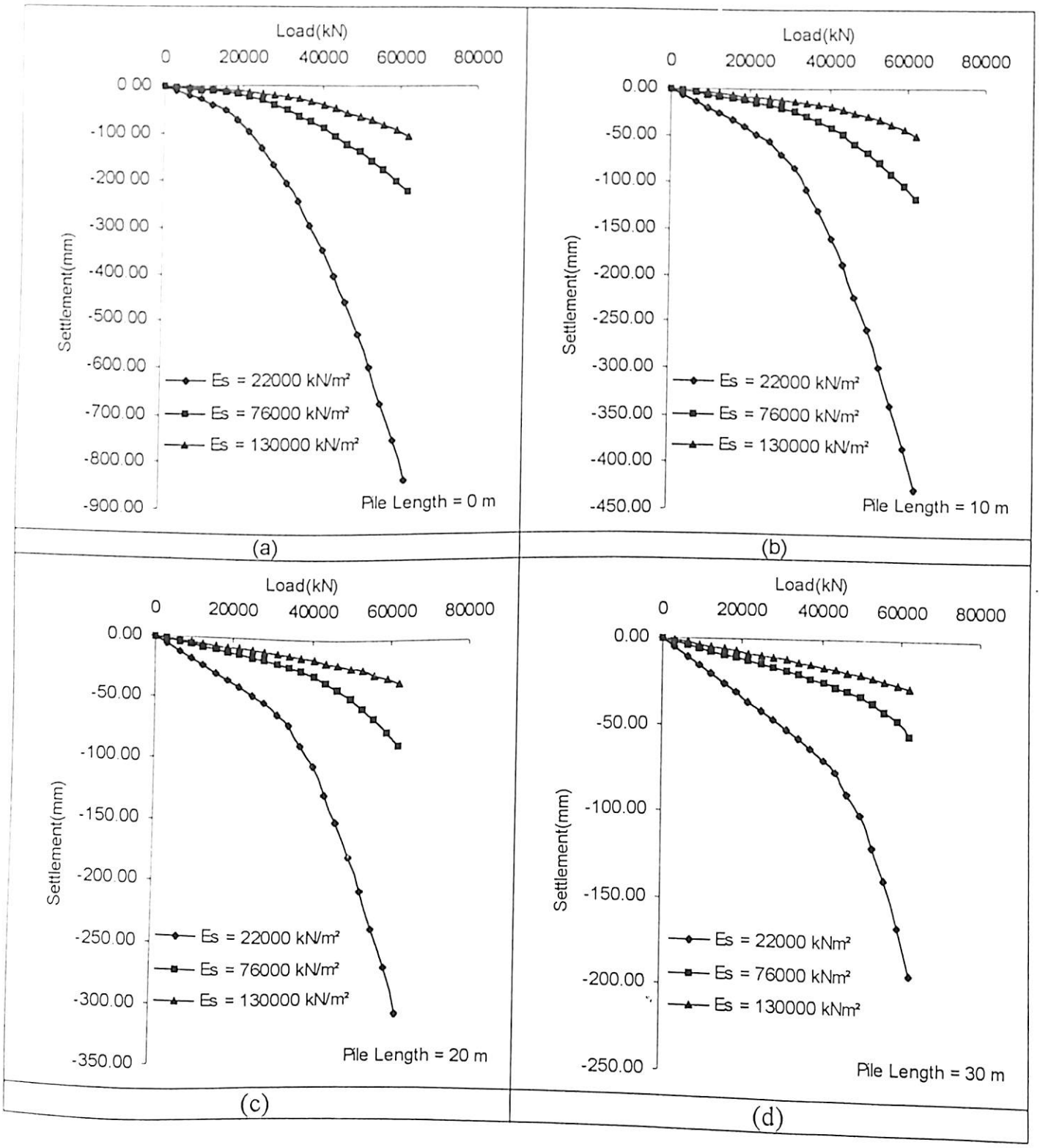

Figure 5.16 Effect of Soil Modulus on the Load Settlement Behaviour of Piled Raft Foundation (D = 10 m, s/d = 5)

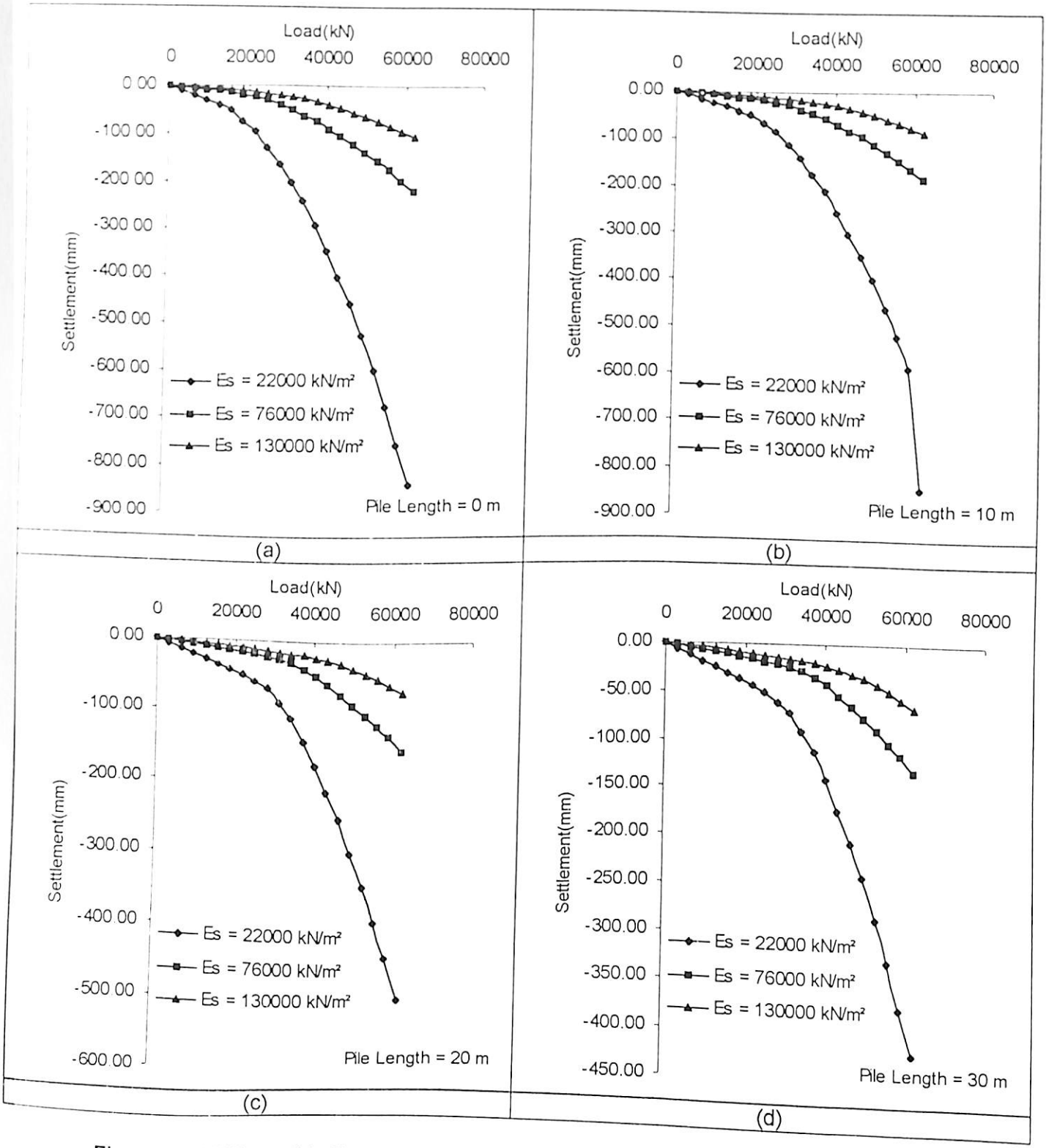

Figure 5.17 Effect of Soil Modulus on the Load Settlement Behaviour of Piled Raft Foundation
(D = 10 m, s/d = 7.5)

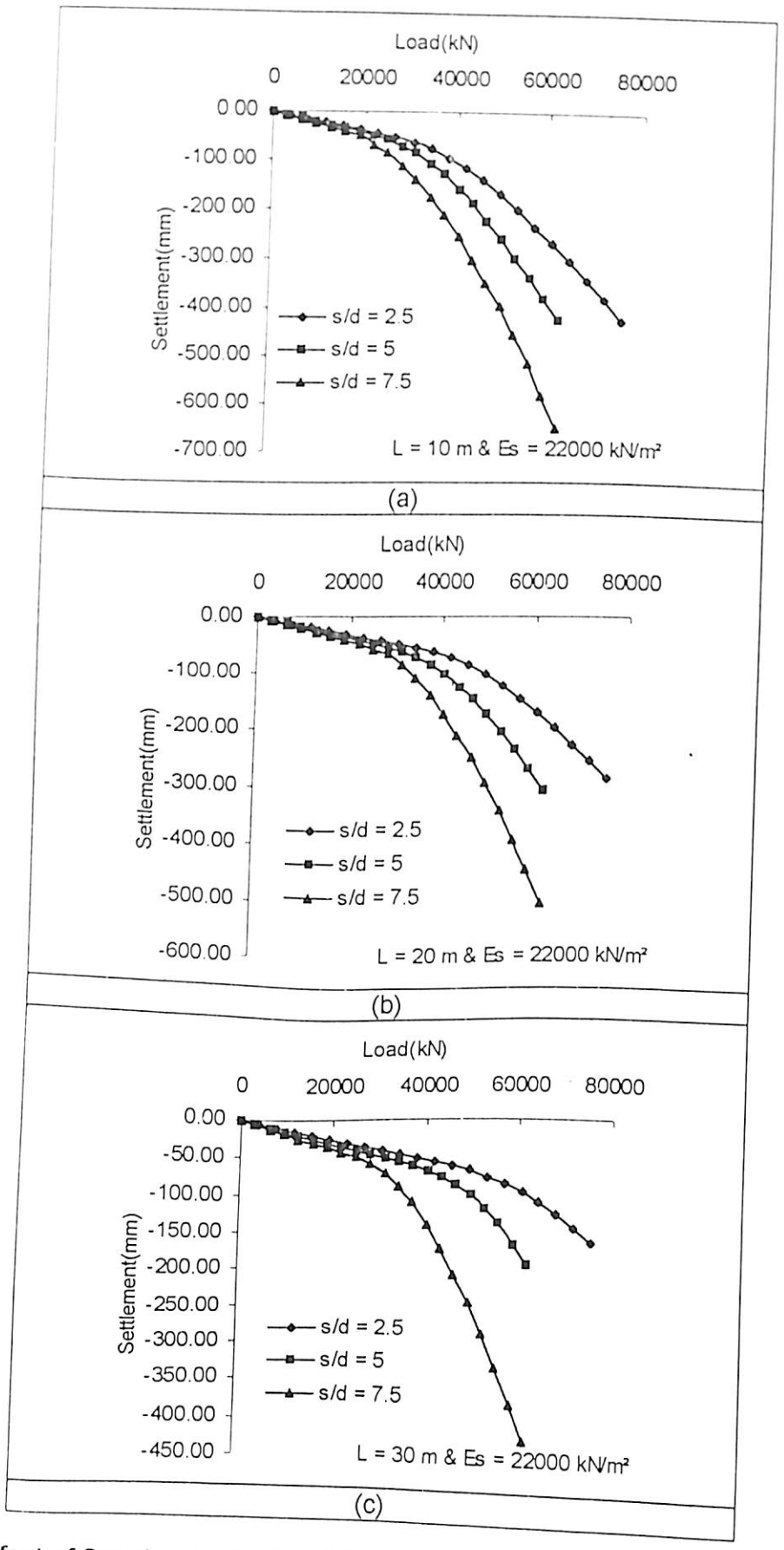

Figure 5.18 Effect of Spacing on the Load Settlement Behaviour of Piled Raft Foundation (D = 10 m)

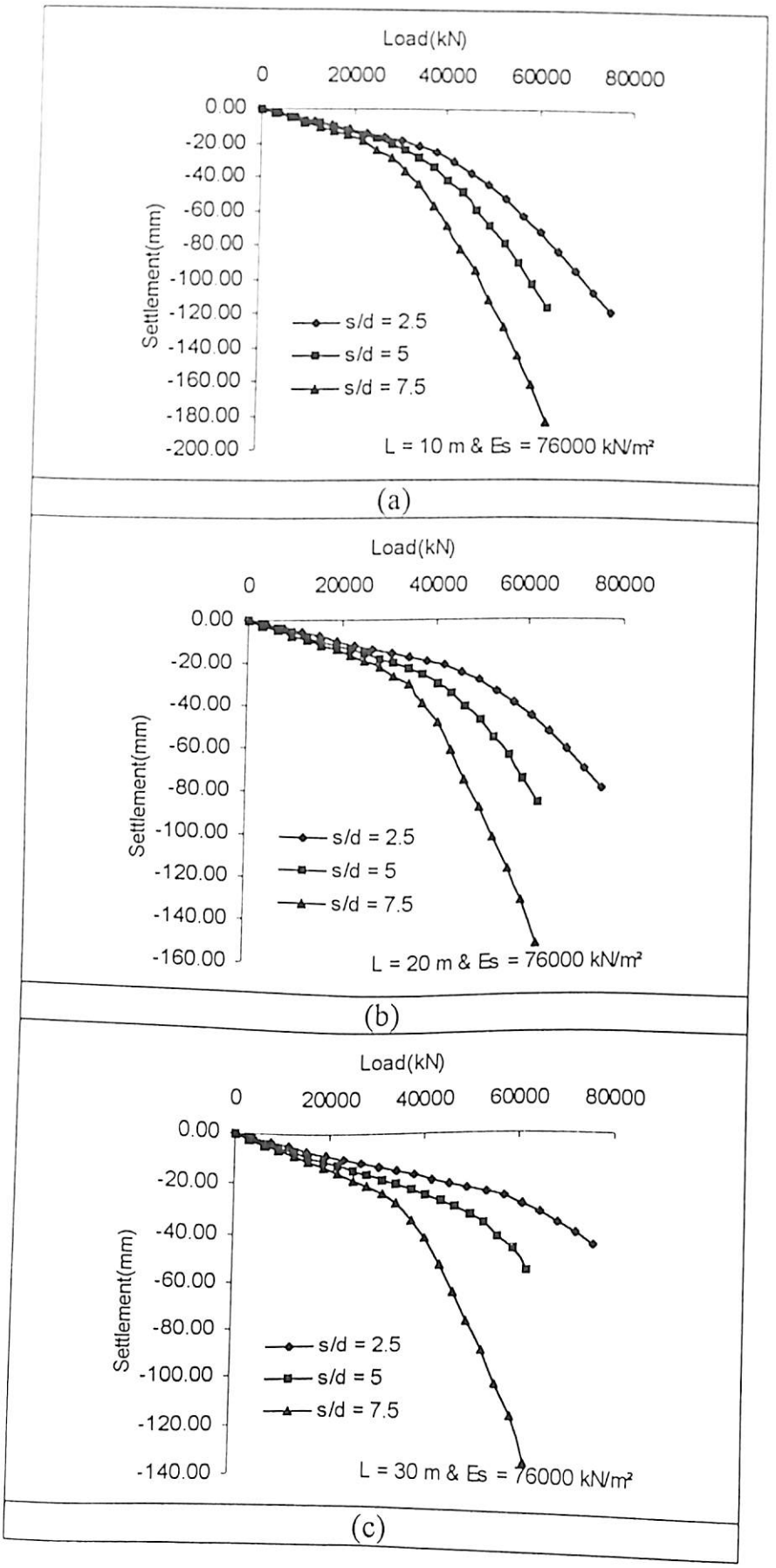

Figure 5.19 Effect of Spacing on the Load Settlement Behaviour of Piled Raft Foundation (D = 10 m)

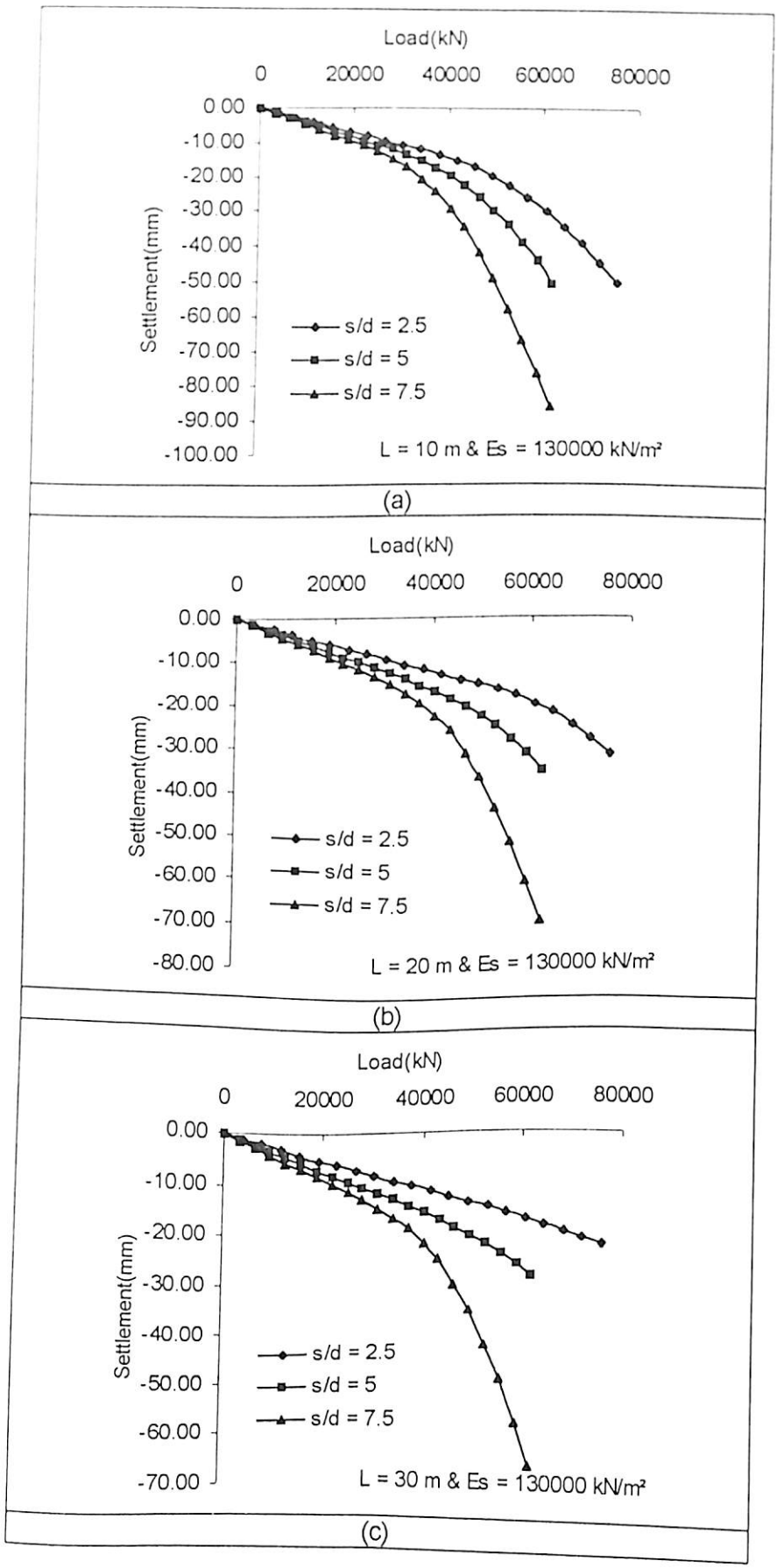

Figure 5.20 Effect of Spacing on the Load Settlement Behaviour of Piled Raft Foundation (D = 10 m)

Figures 5.21 (a), (b), (c), Figures 5.22 (a), (b), (c) and Figures 5.23 (a), (b), (c) show the load settlement curves for piled raft foundation of diameter 20 m and spacing to diameter ratio (s/d) of 5.0, 7.5 and 10. The effect of increase in spacing is to decrease the load carrying capacity of piled raft foundation. This increase is seen predominant at higher load on piled raft foundation. The effect of increase in length of pile is to increase the load carrying capacity of piled raft foundation. The effect of increase in soil modulus is to increase the load carrying capacity of piled raft foundation.

5.6.2.4 Load settlement curve for piled raft foundation for different diameter of the raft

Figures 5.24 (a), (b), (c) show the load settlement curves for a piled raft foundation of diameter 30 meter for different pile lengths. The effect of increase in length of pile is to increase the load carrying capacity of piled raft foundation. This effect is seen to be significant at higher load on piled raft foundation. When Figures 5.24 (a), (b), (c) are compared to each other it is found that the effect of increase in soil modulus is to increase the load carrying capacity of piled raft foundation.

Figures 5.25 (a), (b), (c) and Figures 5.26 (a), (b), (c) show the load settlement curves for piled raft foundation of diameter 30 m and spacing to diameter ratio (s/d) of 7.5 and 10. A similar trend of load settlement curves as seen above for Figure 5.24 is found in these cases. The effect of increase in spacing between the piles is to reduce the load carrying capacity of piled raft foundation.

Figures 5.27 (a), (b), (c), (d), Figures 5.28 (a), (b), (c), (d) and Figures 5.29 (a), (b), (c), (d) show the effect of soil modulus on the load settlement behaviour of piled raft foundation. The effect of increase in soil modulus is to increase the load carrying capacity of piled raft foundation. This is true for all lengths of pile considered in the analysis. When Figures 5.27, 5.28 and 5.29 are compared it is found that the effect of increase in spacing between the piles is to decrease the load carrying capacity of piled raft foundation.

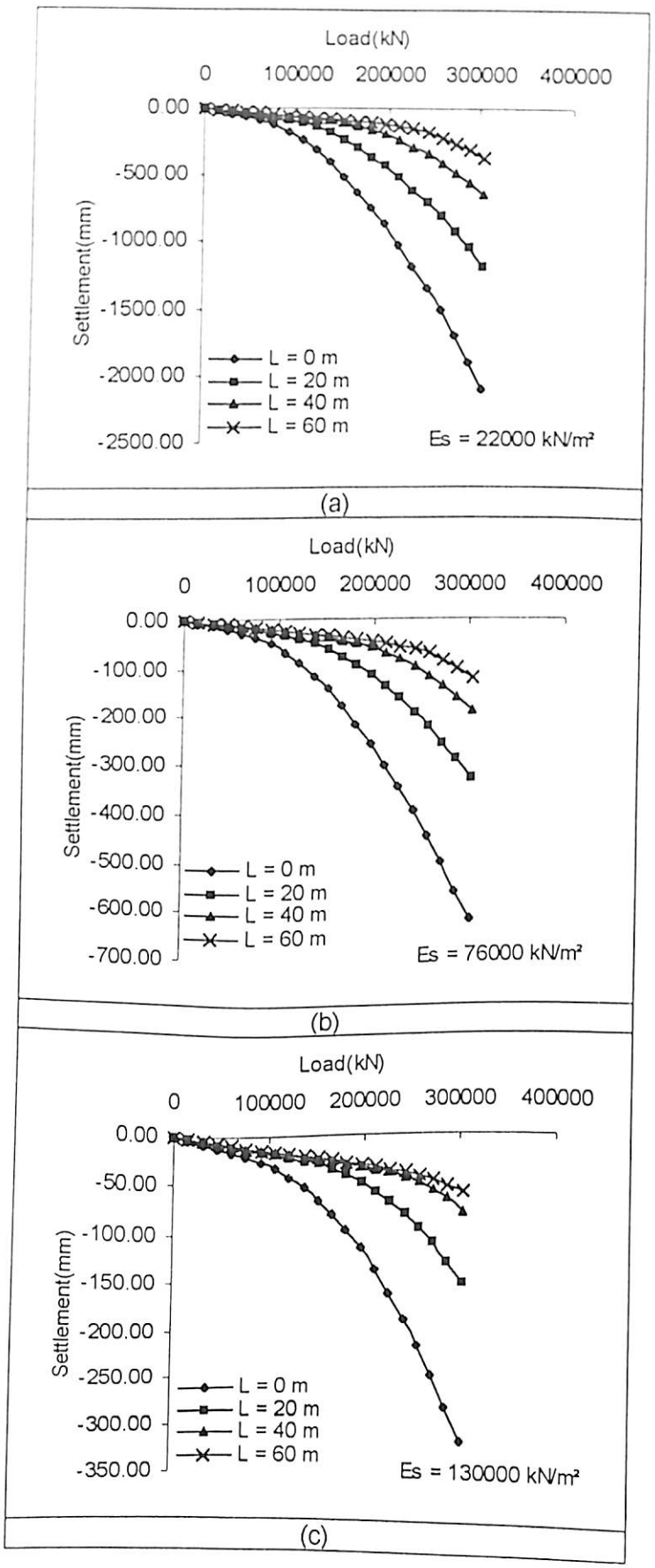

Figure 5.21 Load Settlement Curves for Various Modulus and Pile Lengths (D = 20 m, s/d = 5.0)

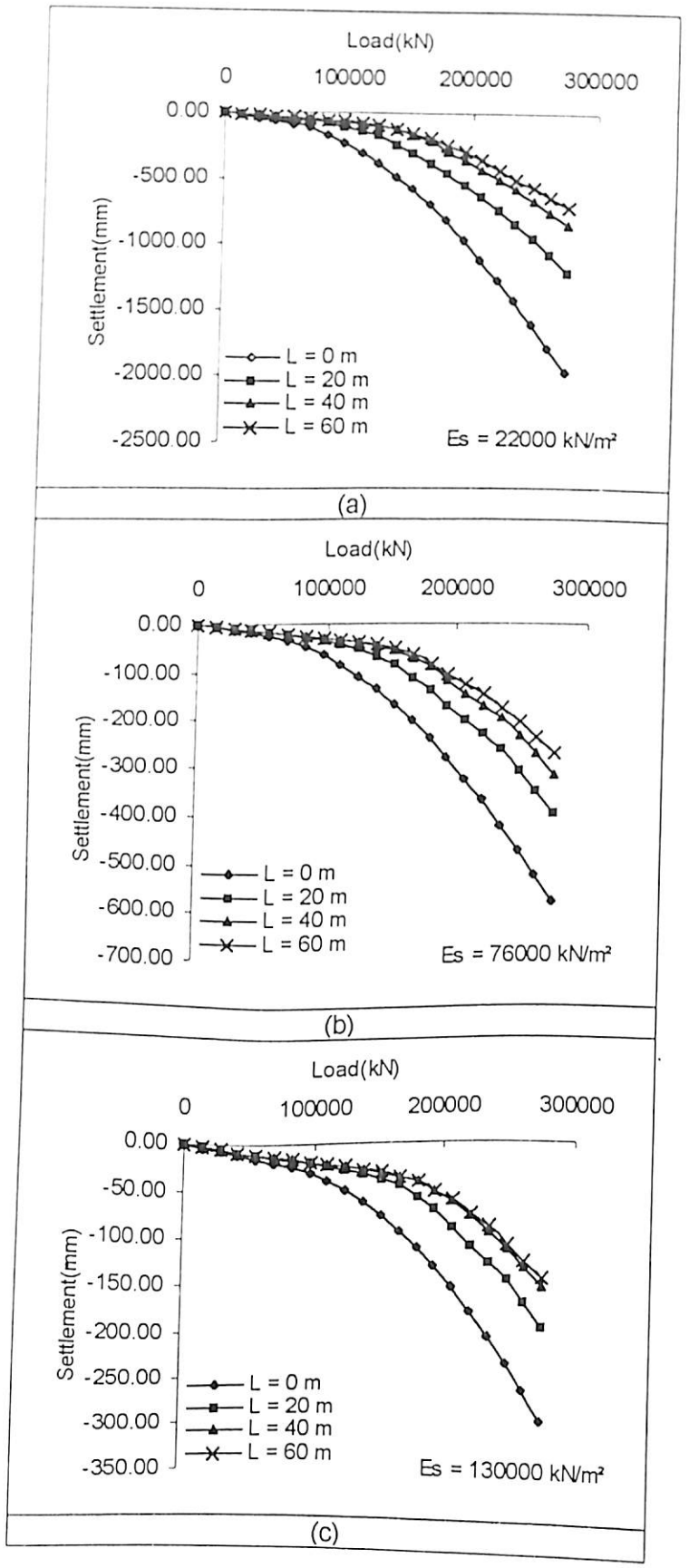

Figure 5.22 Load Settlement Curve for Various Modulus and Pile Lengths (D = 20 m, s/d = 7.5)

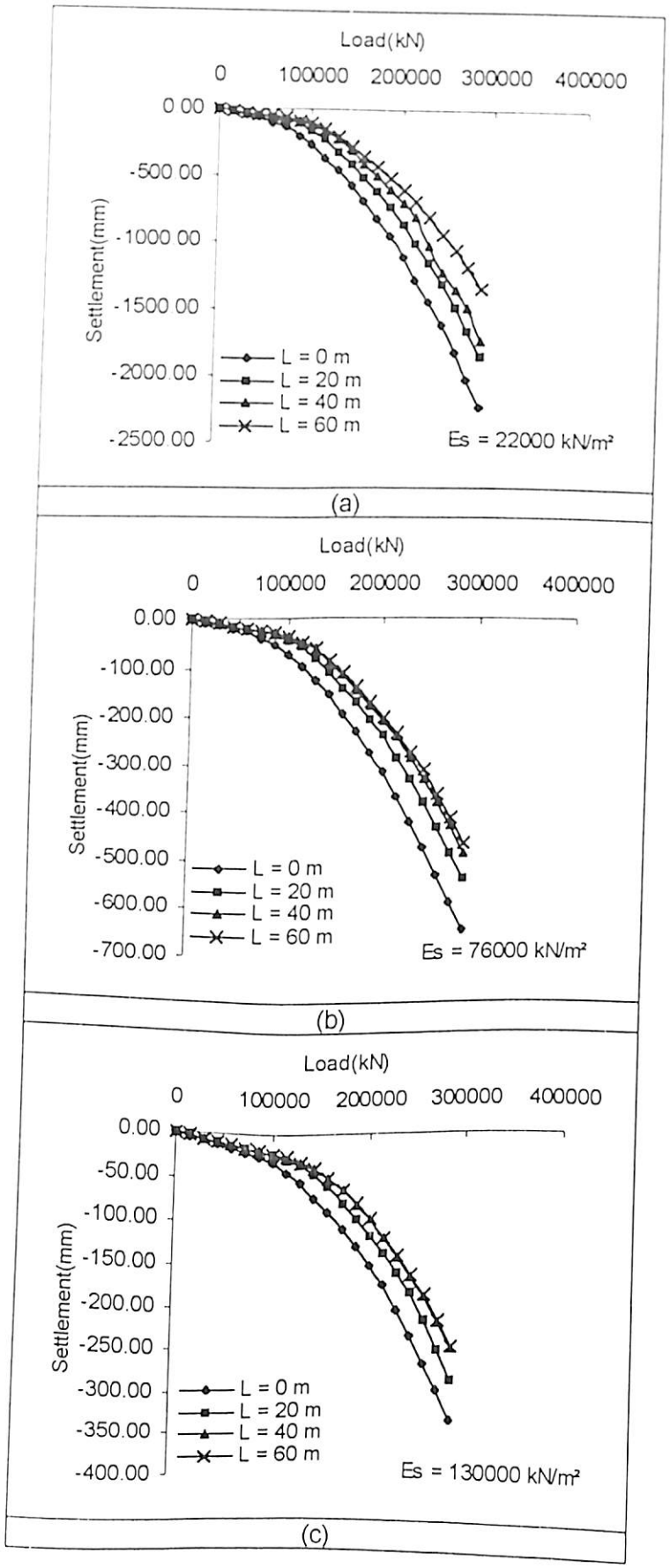

Figure 5.23 Load Settlement Curve for Various Modulus and Pile Lengths (D = 20 m, s/d = 10)

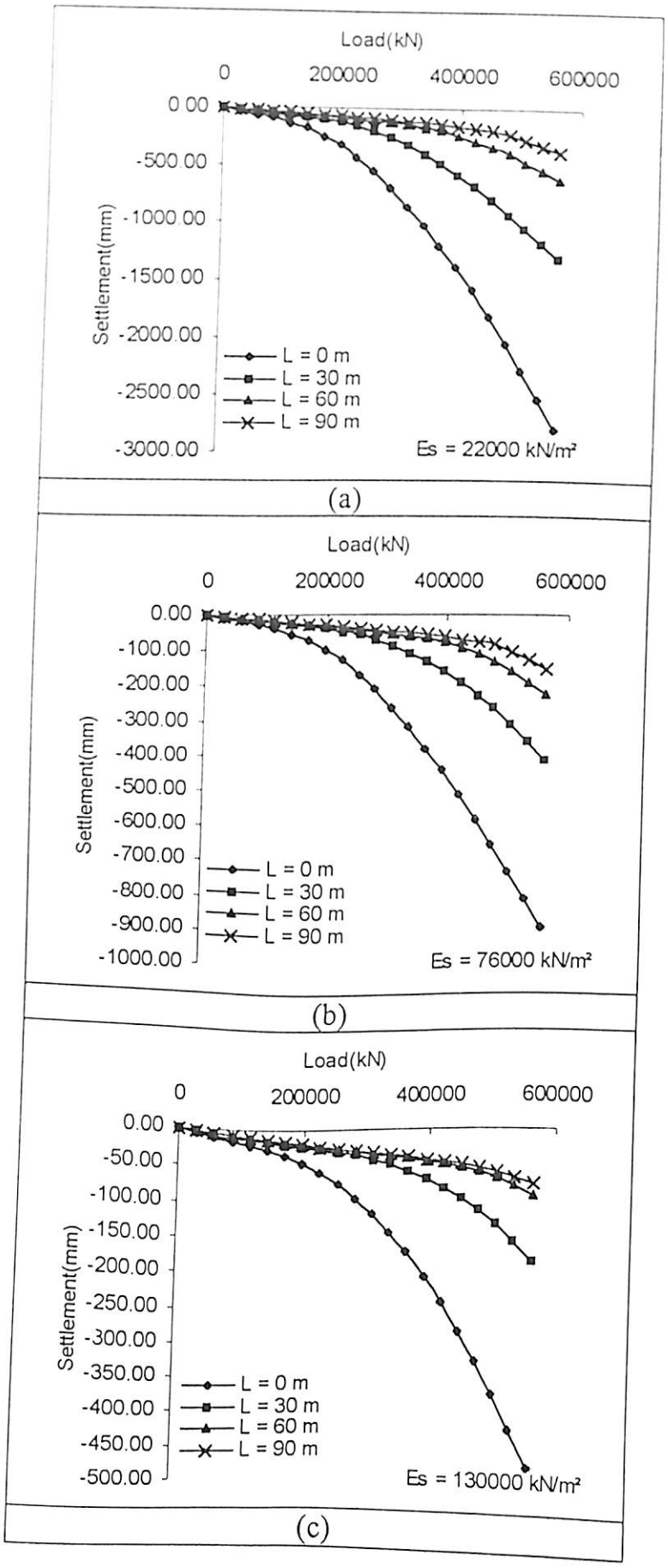

Figure 5.24 Load Settlement Curve for Various Modulus and Pile Lengths (D = 30 m, s/d = 5.0)

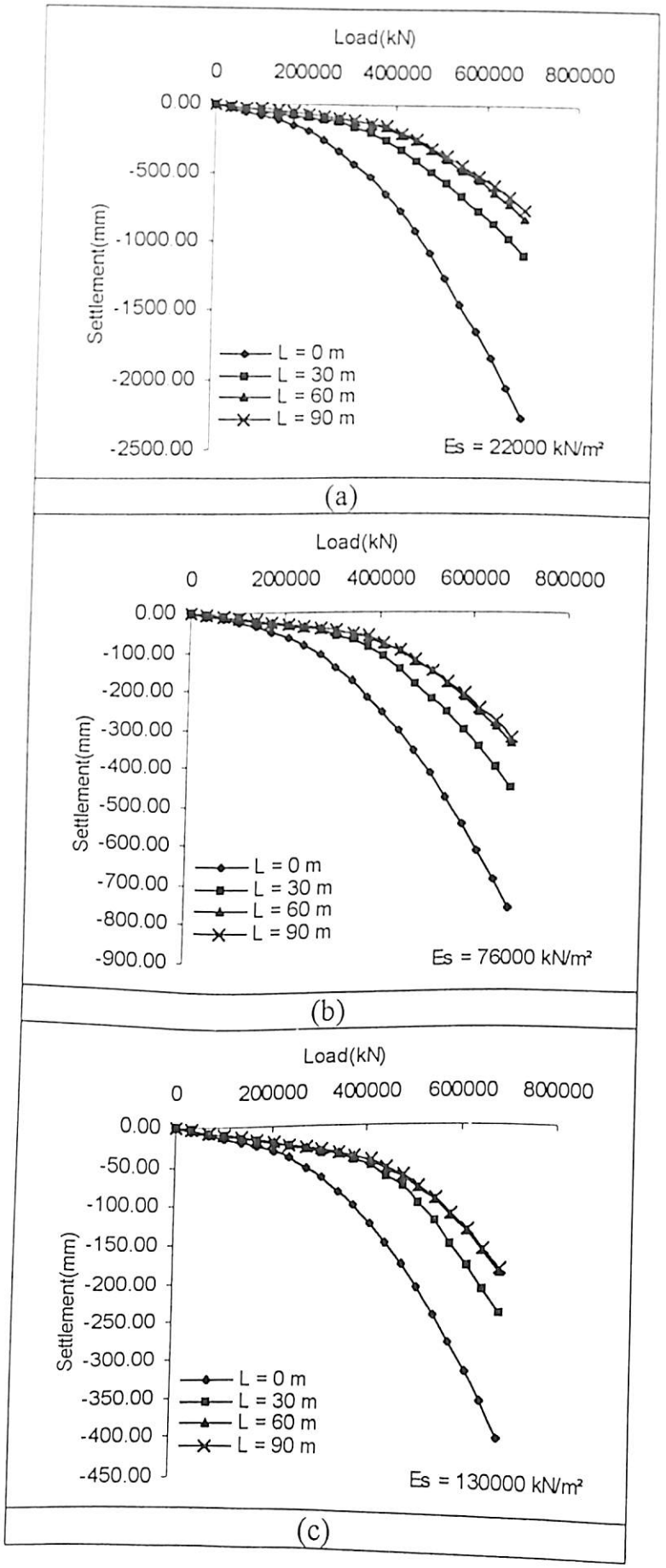

Figure 5.25 Load Settlement Curve for Various Modulus and Pile Lengths (D = 30 m, s/d = 7.5)

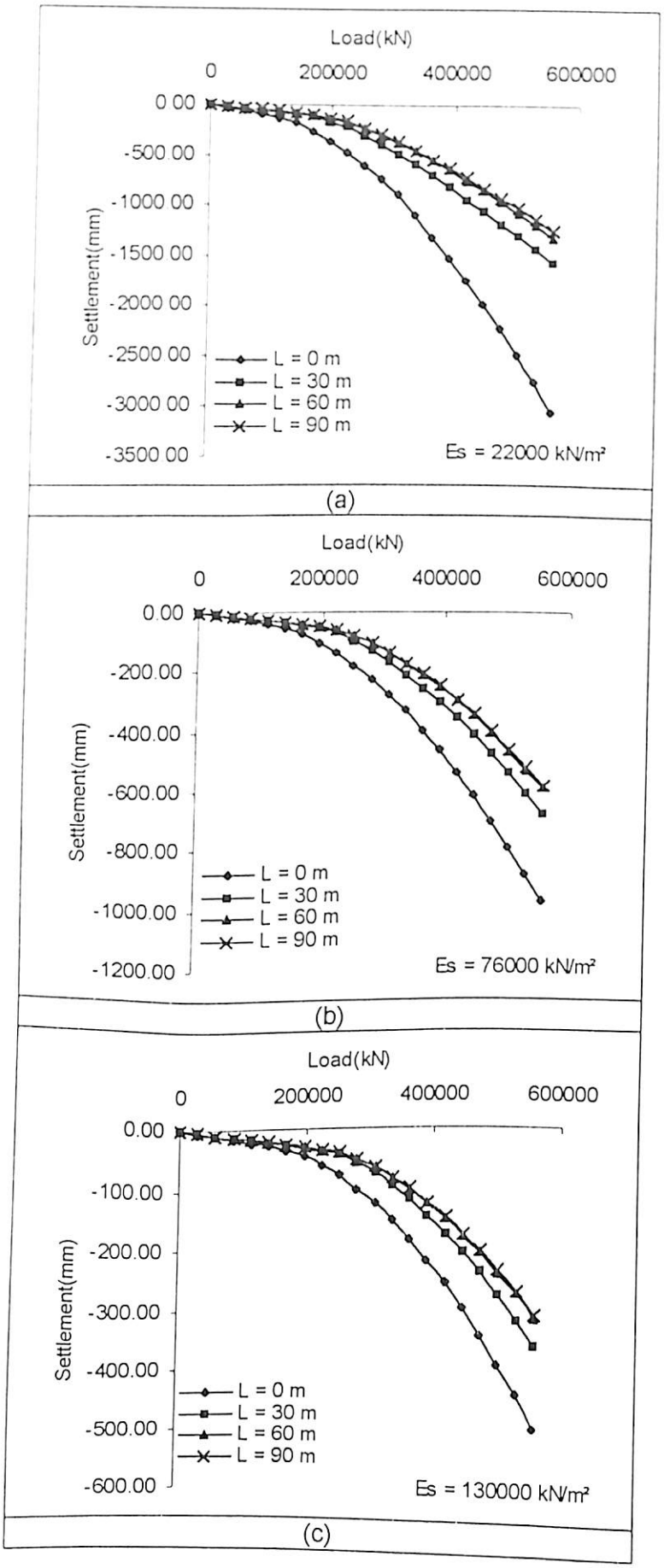

Figure 5.26 Load Settlement Curve for Various Modulus and Pile Lengths (D = 30 m, s/d = 10)

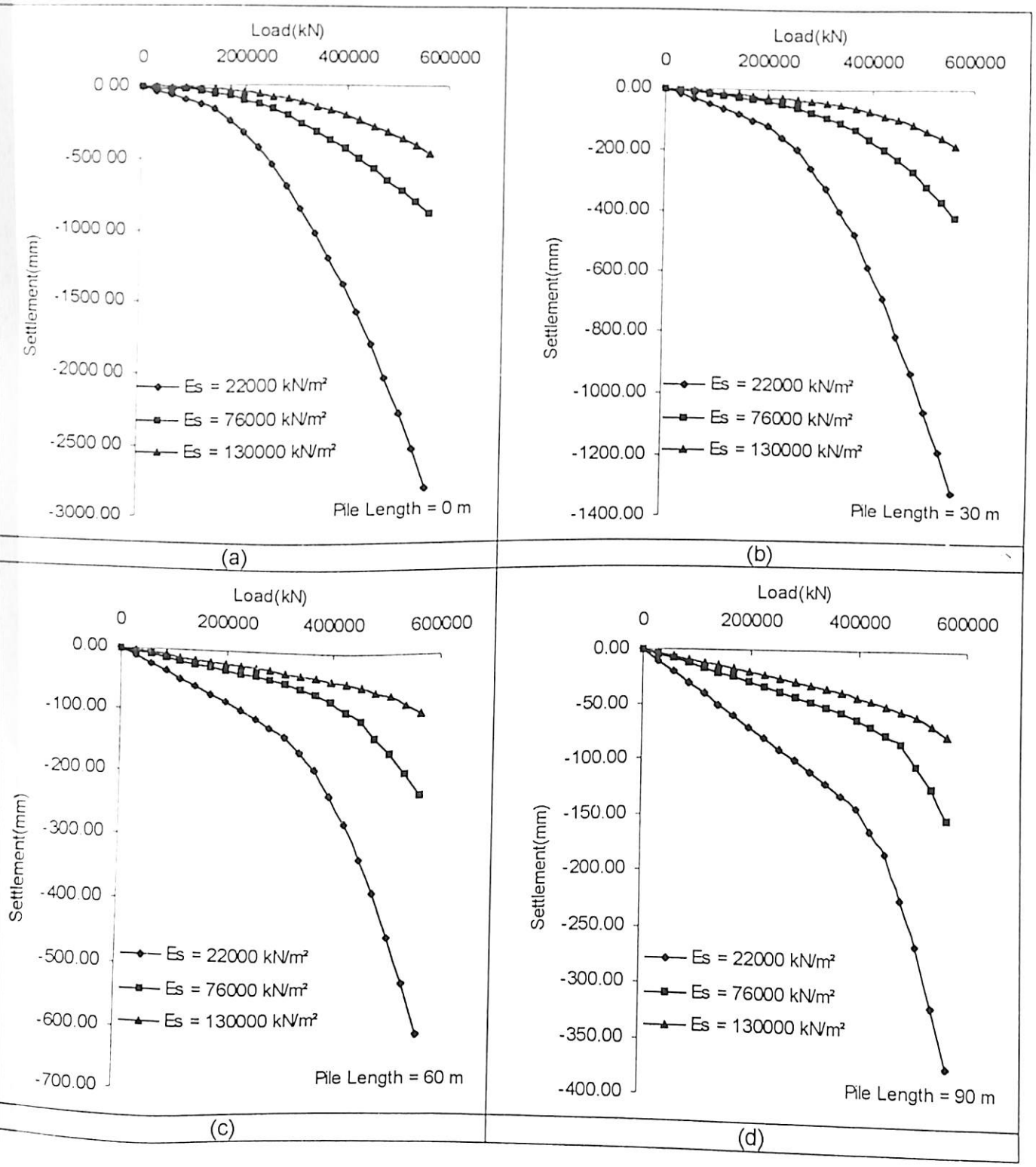

Figure 5.27 Effect of Soil Modulus on Load Settlement Behaviour of Piled Raft Foundation (D = 30 m, s/d = 5)

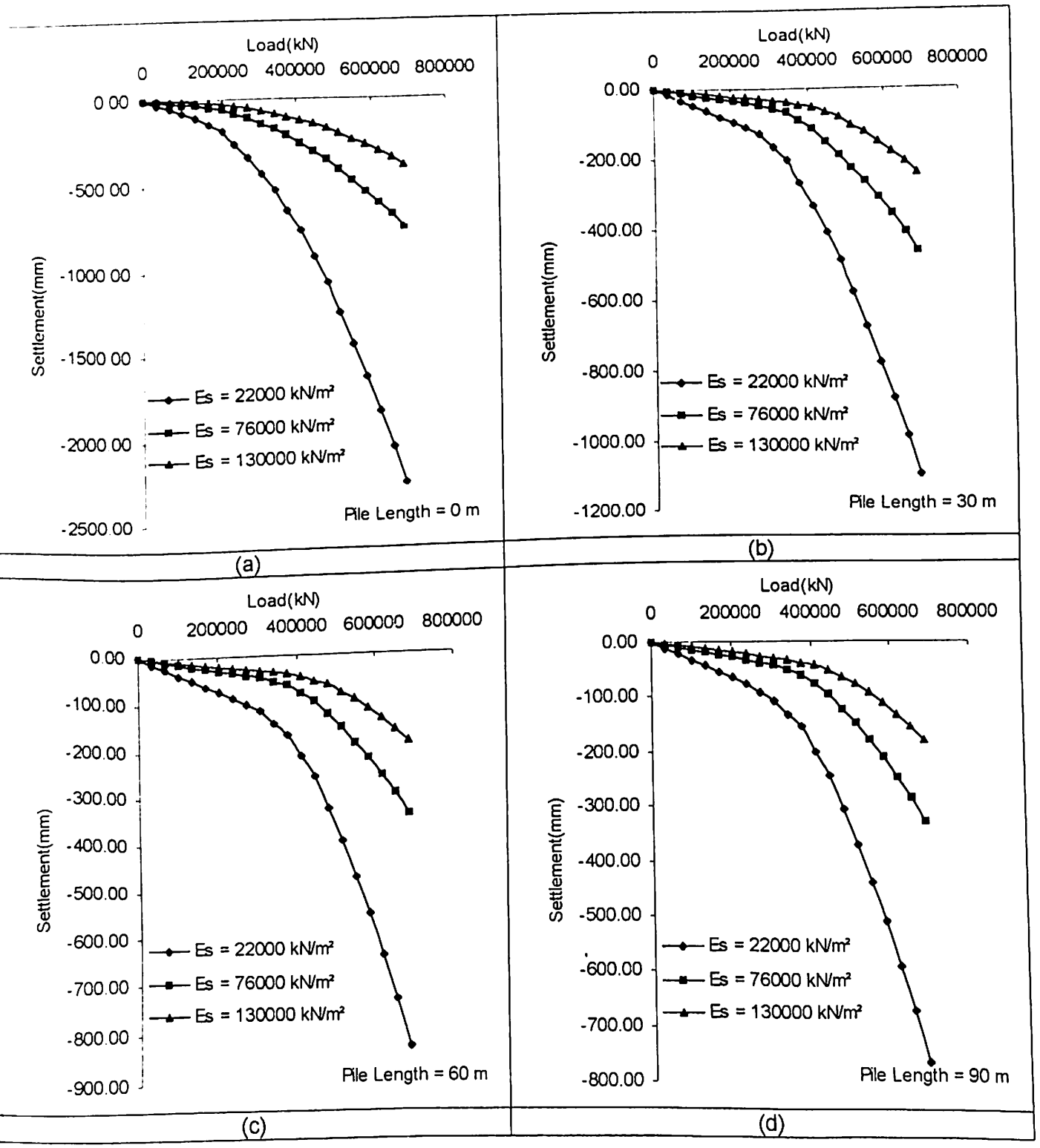

Figure 5.28 Effect of Soil Modulus on Load Settlement Behaviour of Piled Raft Foundation (D = 30 m, s/d = 7.5)

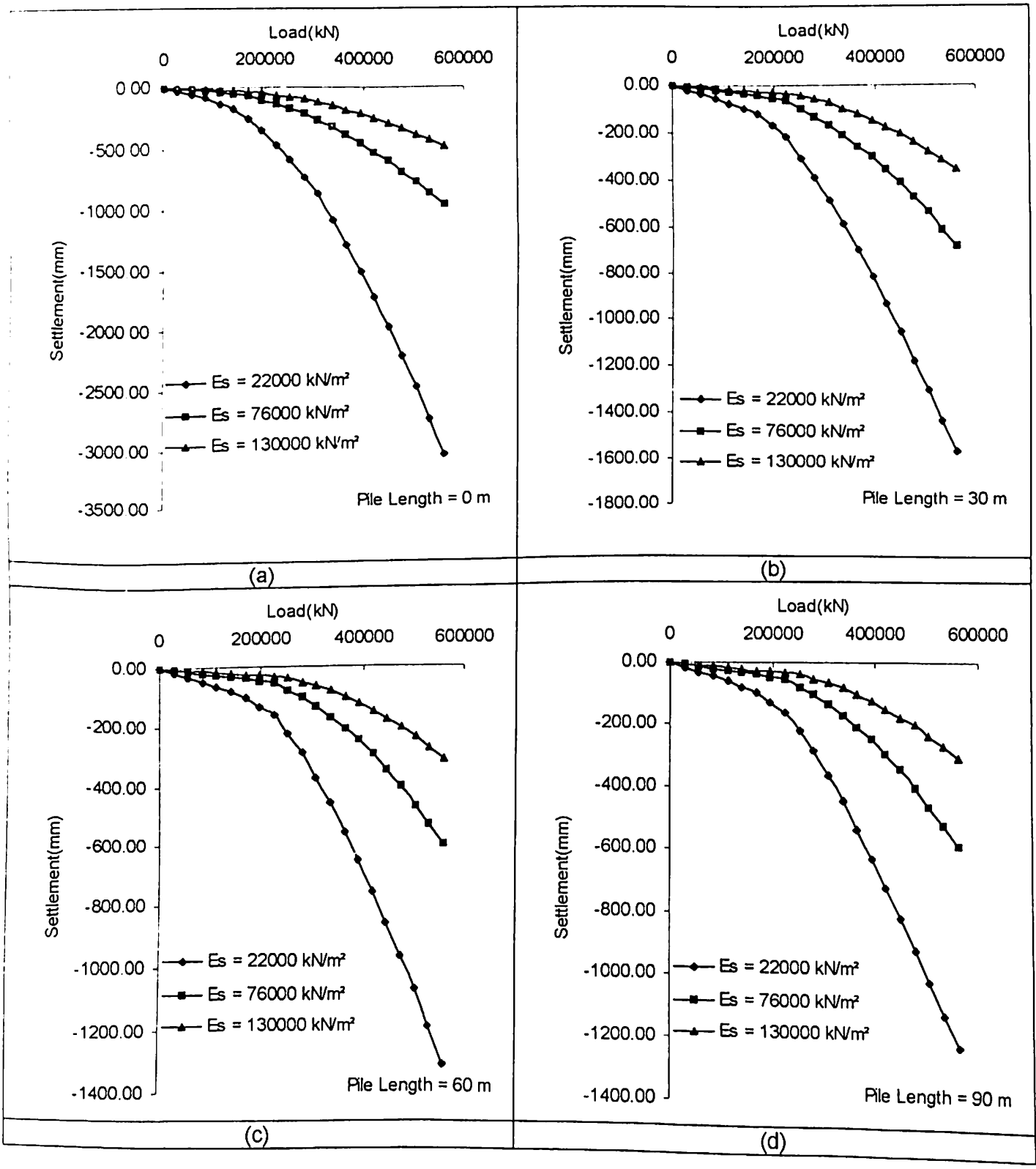

Figure 5.29 Effect of Soil Modulus on Load Settlement Behaviour of Piled Raft Foundation (D = 30 m, s/d = 10)

Figures 5.30 (a), (b), (c) Figures 5.31 (a), (b), (c) and Figures 5.32 (a), (b), (c) show the effect of pile length on the load settlement behaviour of piled raft foundation whose raft diameter is 40 meter for different soil modulus. The effect of increase in pile length is to increase the load carrying capacity of piled raft foundation. The effect of increase in soil modulus is to increase the load carrying capacity of piled raft foundation. This is true for all lengths of pile considered in the analysis. When Figures 5.30, 5.31, 5.32 are compared it is found that the effect of increase in spacing between the piles is to decrease the load carrying capacity of piled raft foundation.

Figure 5.33 (a), (b), (c), Figure 5.34 (a), (b), (c) and Figure 5.35 (a), (b), (c) show the load settlement curves for piled raft foundation of diameter 50 meter for varying pile lengths and spacing and soil modulus. The effect of increase in spacing is to decrease the load carrying capacity of piled raft foundation. The effect of increase in pile length and soil modulus is to increase the load carrying capacity of piled raft foundation.

5.6.3 Axial Load Distribution

Fig.5.36 (a), (b) show for first load step the effect of spacing on the axial load distribution of pile for raft diameter 10 meter, pile length equal to 10 meter for the center as well as the boundary pile for soil modulus of 22000 kN/m^2. In load step-1 the load applied are P=3756.981 kN for s/d=2.5, P = 3113.288 kN for s/d=5.0, and for s/d = 7.5, P = 3111.547 kN. After this load was applied in equal increments. For all spacing the axial load is maximum in the top portion and decreases with depth. The value is found to be minimum at the bottom of the pile. With increase in spacing the axial force in pile at all depth increases. This is due to the fact that the mobilization of skin friction has increased with increase in spacing between the piles. For all the above cases the boundary piles Figure 5.36 (a) carries more load than the center piles Figure 5.36 (b).

Figure. 5.37 (a), (b) show the axial load distribution for the same piles discussed above for load step 10. With increase in load step the axial load distribution has increased. This shows that with increase in load step more loads gets transferred to the piles. In the beginning most of the load is taken by the raft.

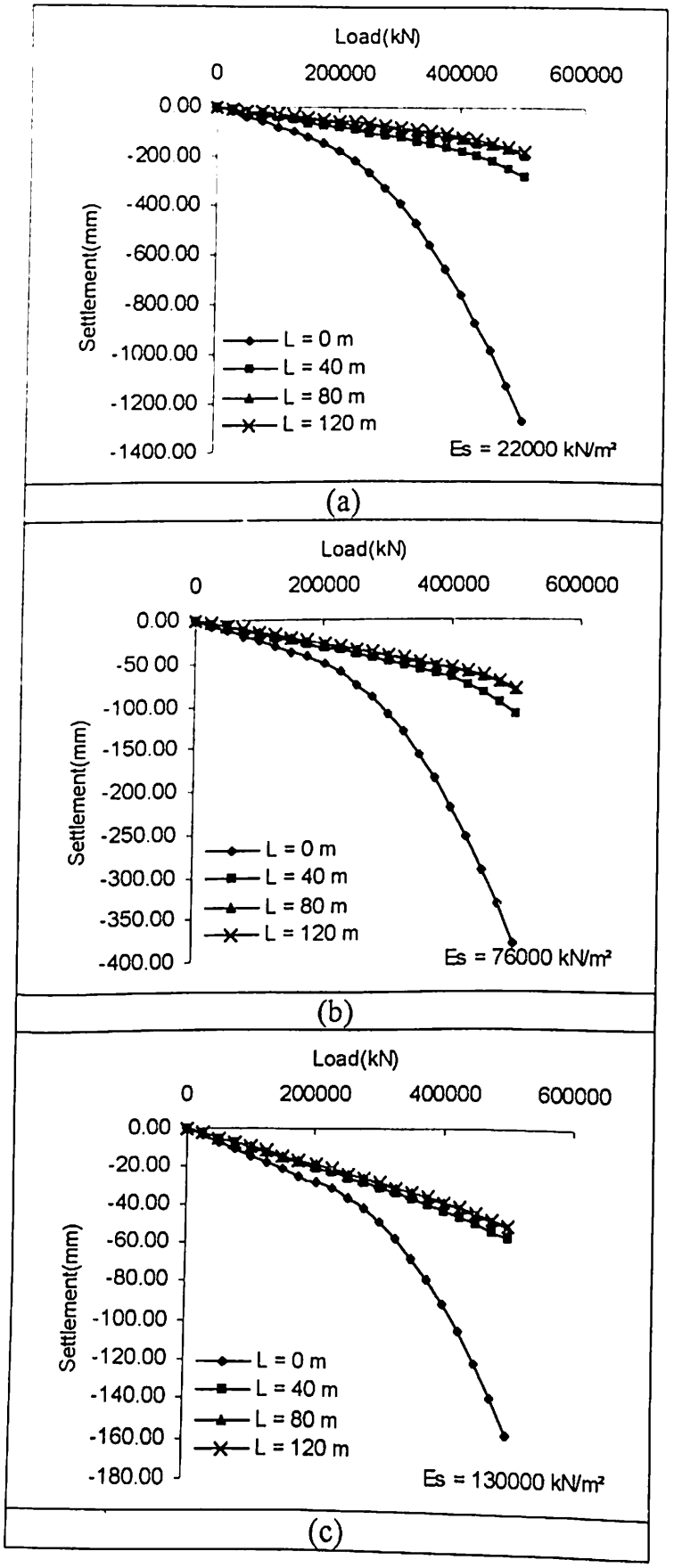

Figure 5.30 Load Settlement Curves for Various Soil Modulus and Pile Lengths (D = 40 m, s/d = 7.5)

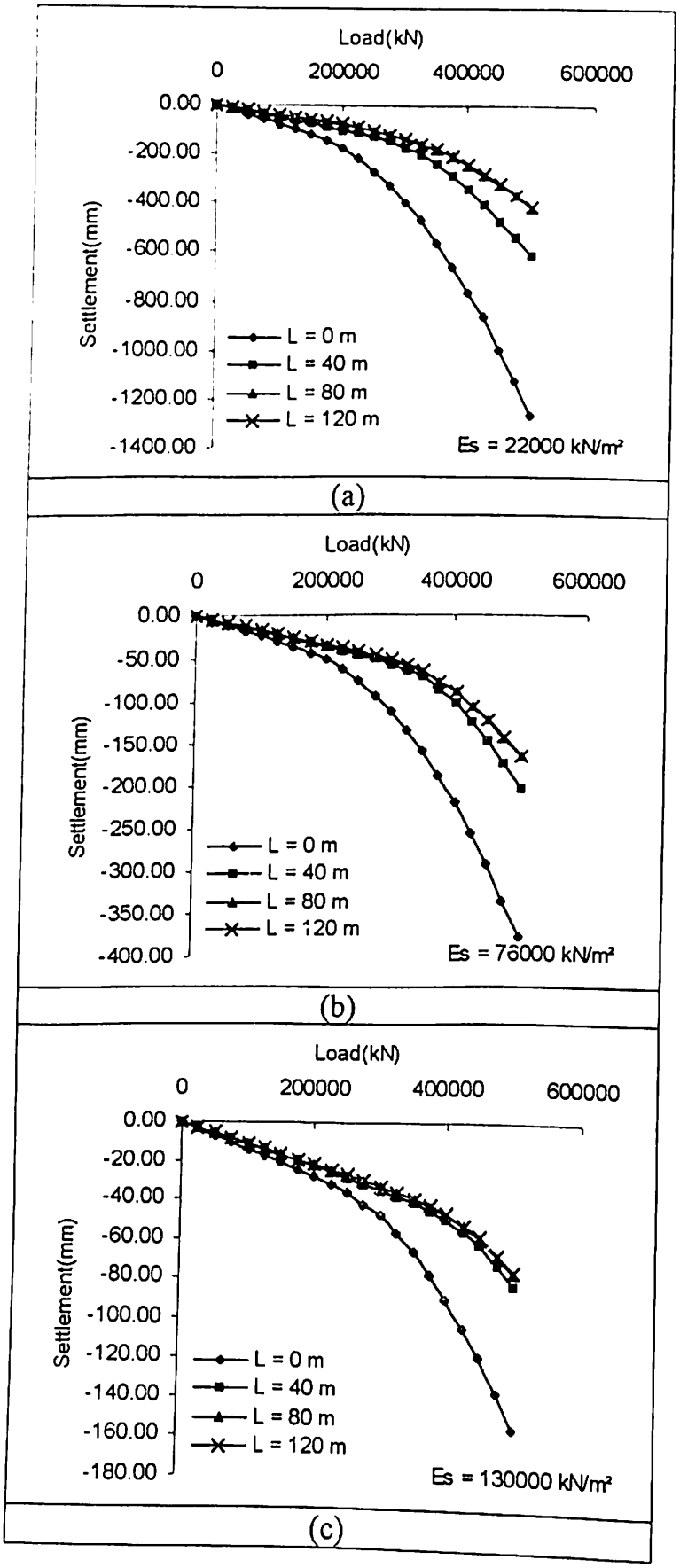

Figure 5.31 Load Settlement Curves for Various Soil Modulus and Pile Lengths (D = 40 m, s/d = 10)

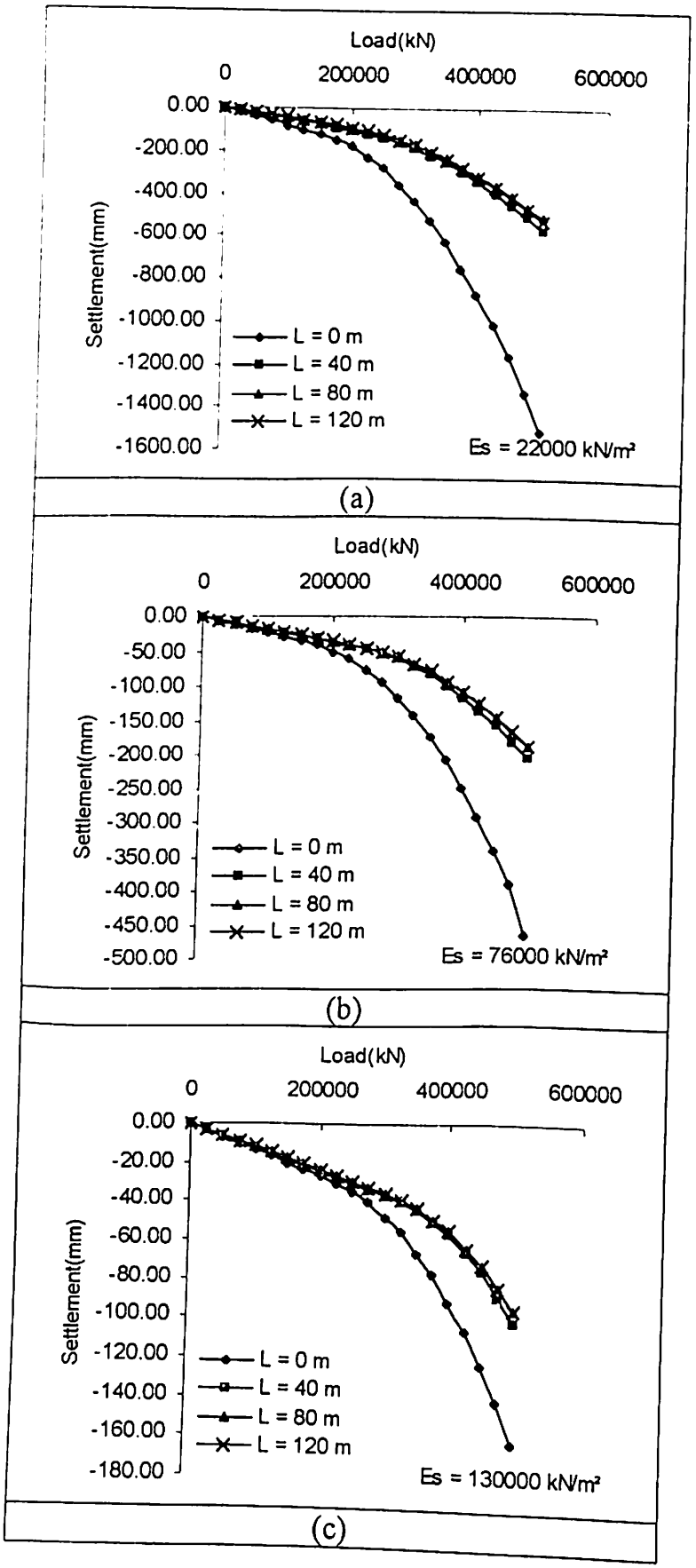

Figure 5.32 Load Settlement Curves for Various Soil Modulus and Pile Lengths (D = 40 m, s/d = 15)

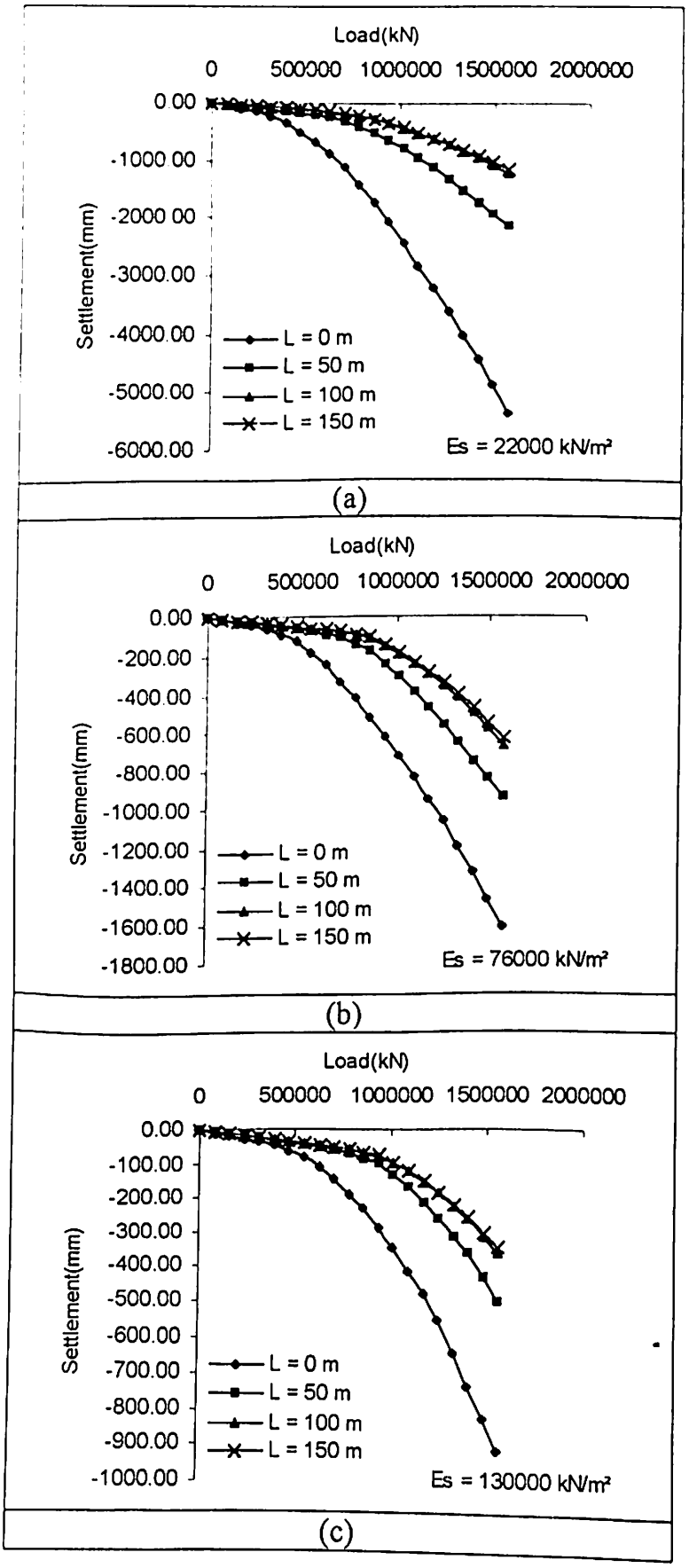

Figure 5.33 Load Settlement Curve for Various Soil Modulus and Pile Lengths (D = 50 m, s/d = 7.5)

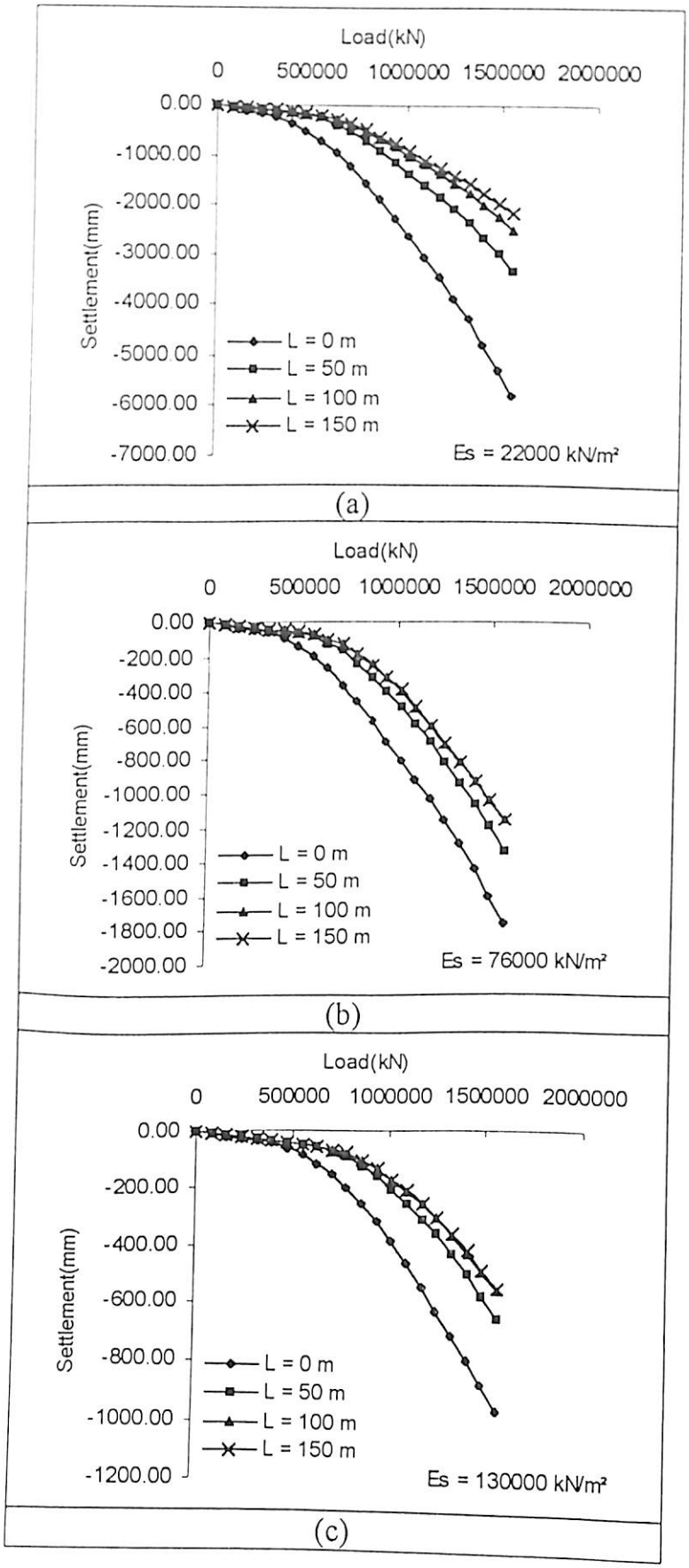

Figure 5.34 Load Settlement Curve for Various Soil Modulus and Pile Lengths (D = 50 m, s/d = 10)

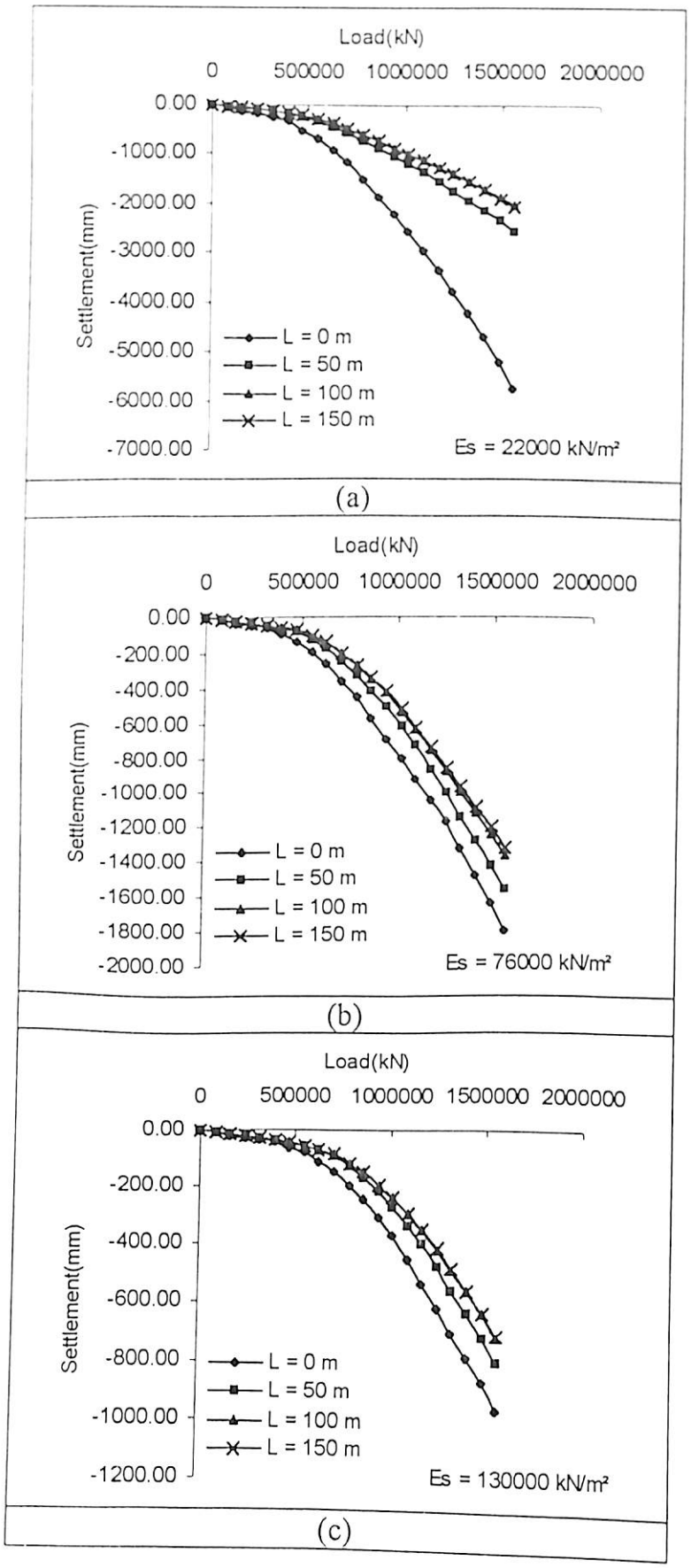

Figure 5.35 Load Settlement Curves for Various Soil Modulus and Pile Lengths (D = 50, s/d = 15)

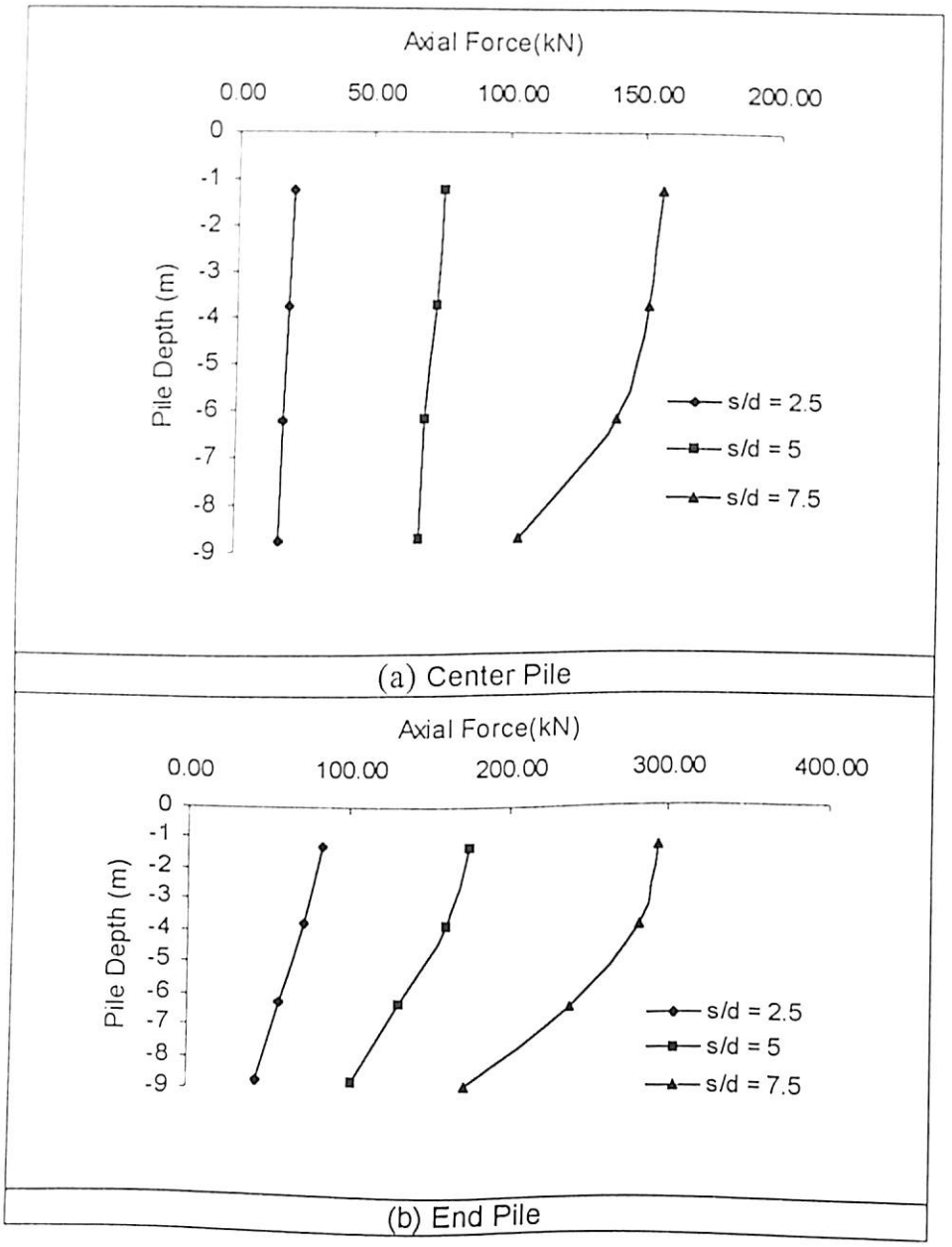

Figure 5.36 Axial Force Distribution in Piles
(D = 10 m, E_s = 22000 kN/m^2, Load Step-1)

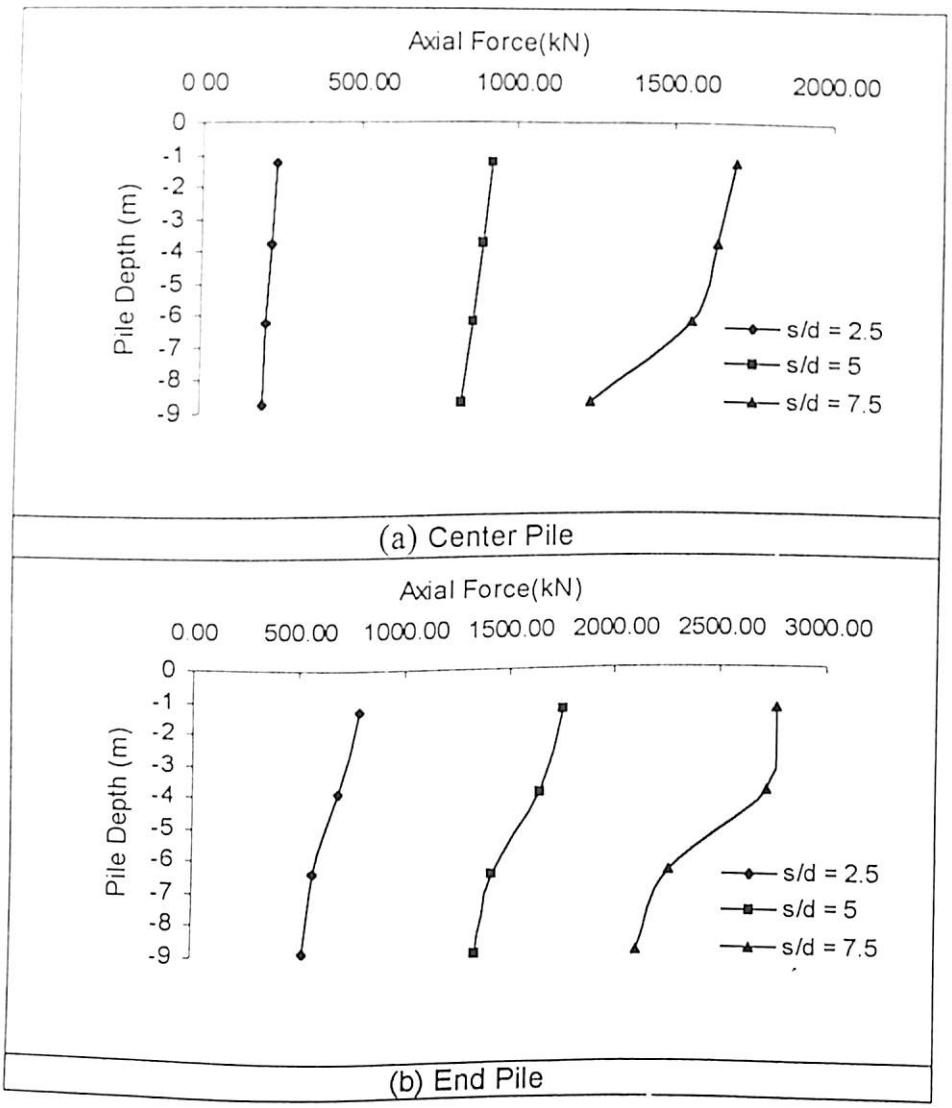

Figure 5.37 Axial Force Distribution in Piles
(D = 10 m, E_s = 22000 kN/m^2, Load Step-10)

Figures 5.38 (a), (b) show the effect of spacing on the axial force distribution for center and end pile of length 30 meter, raft diameter 10 meter and soil modulus of 22000 kN/m^2. The axial load is maximum in the top portion of pile and minimum in the bottom portion of the pile. The effect of increase in spacing is to increase the load carrying capacity of piles. When compared to Figure 5.36, it is found that the effect of increase in length of pile is to increase the load carrying capacity of pile.

Figure 5.39 (a), (b) show the axial force distribution for the same piles discussed above for load step 10. With increase in load step the axial force distribution has increased. This shows that with increase in load step more loads gets transferred to the piles. In the beginning most of the load is taken by the raft. The axial load carried by the end pile is more than that of the center pile.

Figure. 5.40 (a), (b) show the effect of location on the axial load distribution for piles of length 10 meter, diameter of raft 10 meter for soil modulus 22000 kN/m^2 spacing to diameter ratio (s/d) of 2.5 for load step 1 and 10. It can be seen that the center pile carries the minimum load while the end pile carry maximum load. The load carried by the other piles lie between the center piles and the boundary piles. When Figure. 5.40 (a) and 5.40 (b) are compared with each other it is found that the effect of increase in load step is to transfer more loads to the piles.

Figures 5.41 (a), (b) show the effect of location on the axial force distribution for piles of length 30 meter, diameter of raft 10 meter for soil modulus 22000 kN/m^2, spacing to diameter ratio (s/d) of 2.5 for load step 1 and 10. It can be seen that the center pile carries the minimum load while the end piles carry maximum load. The load carried by the other piles lie between the center piles and the end piles. When Figure 5.41(a) and 5.41(b) are compared with each other it is found that the effect of increase in load step is to transfer more load to the piles.

Figures 5.42 (a), (b) show the effect of soil modulus on the axial force distribution for center and end piles of length 10 meter, diameter 10 meter and load step 1.The effect of increase in soil modulus is to increase the load carrying capacity of piles in a piled raft foundation.

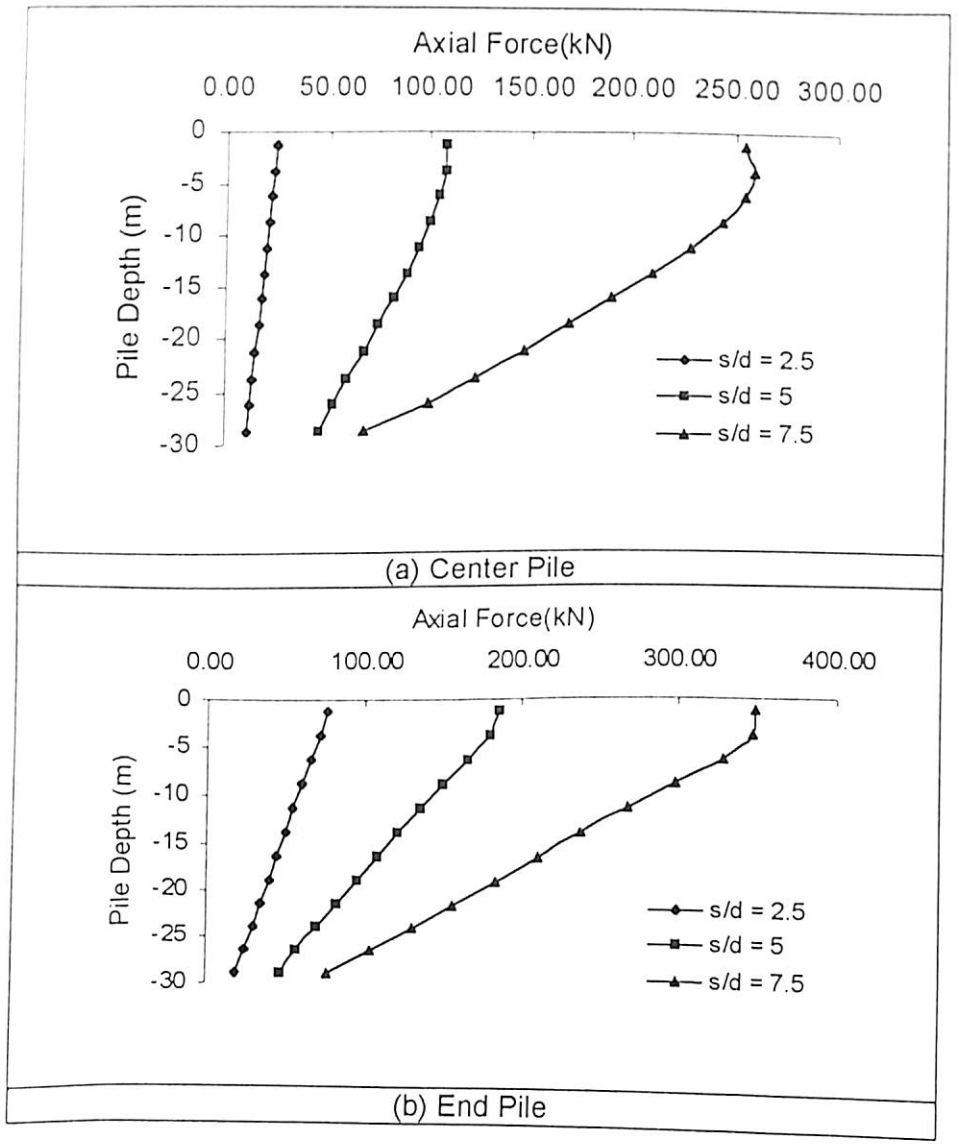

Figure 5.38 Axial Force Distribution in Center and End Piles (D = 10 m, L = 30 m, Es = 22000 kN/m^2, Load Step-1)

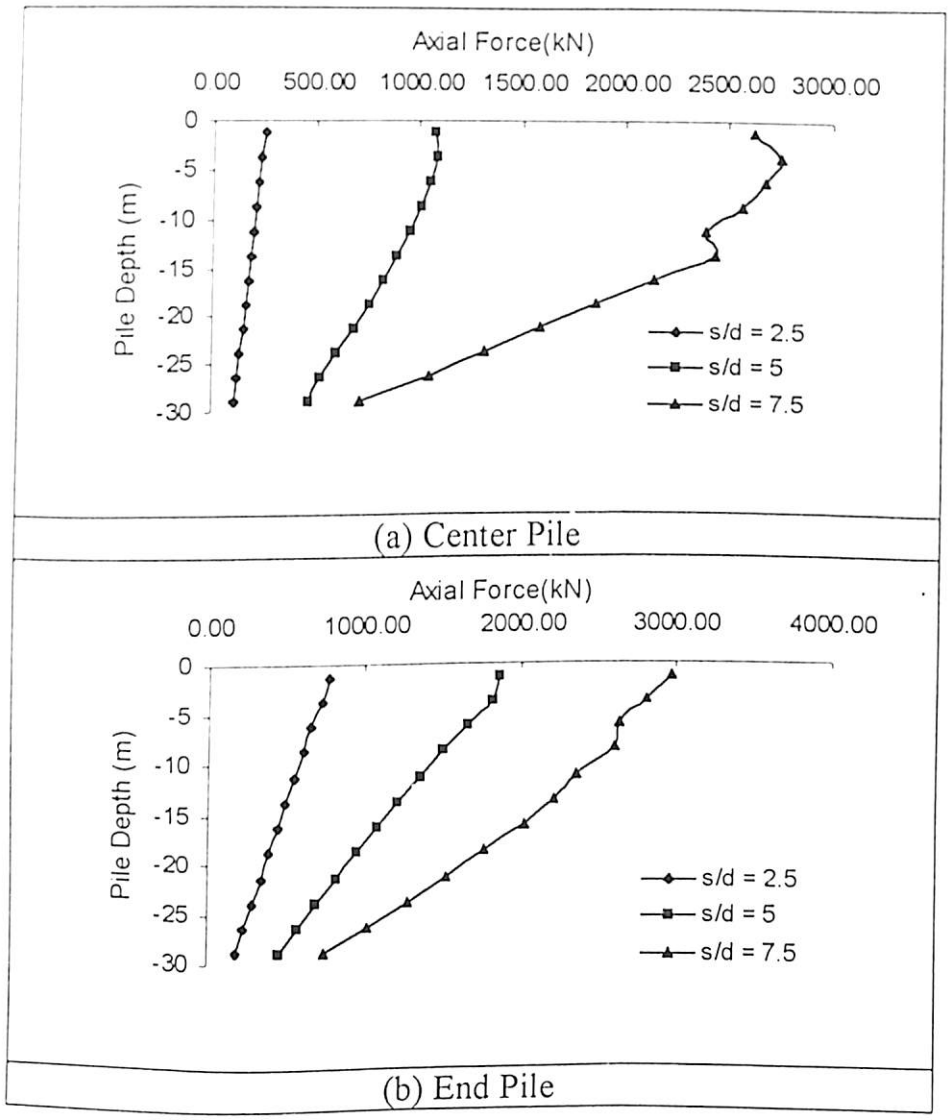

Figure 5.39 Axial Force Distribution in Center and End Piles (D = 10 m, L = 30 m, E_s = 22000 kN/m^2, Load Step-10)

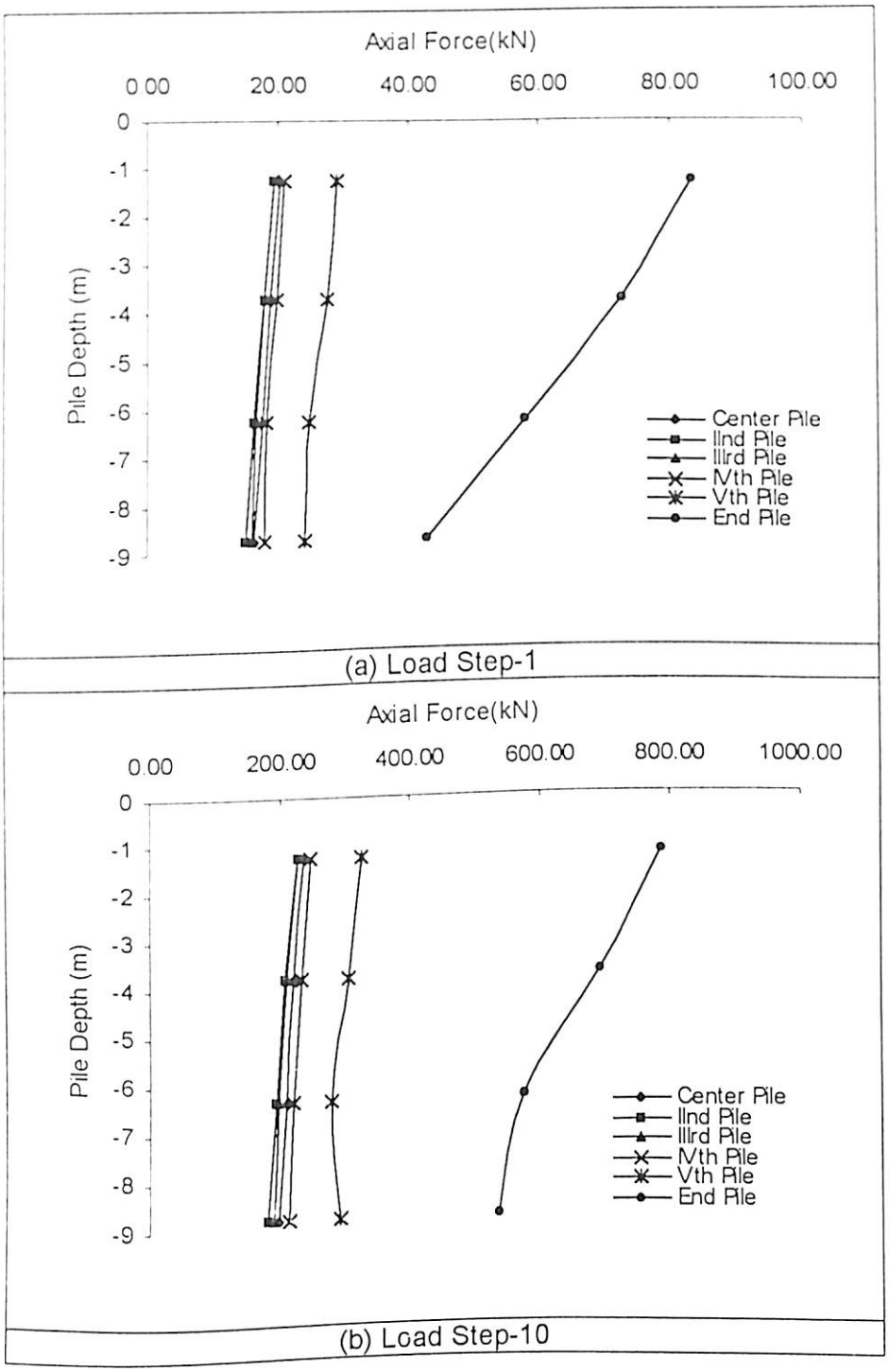

Figure 5.40 Axial Force Distribution in Different Piles (D = 10 m, L = 10 m, s/d = 2.5, E_s = 22000 kN/m^2)

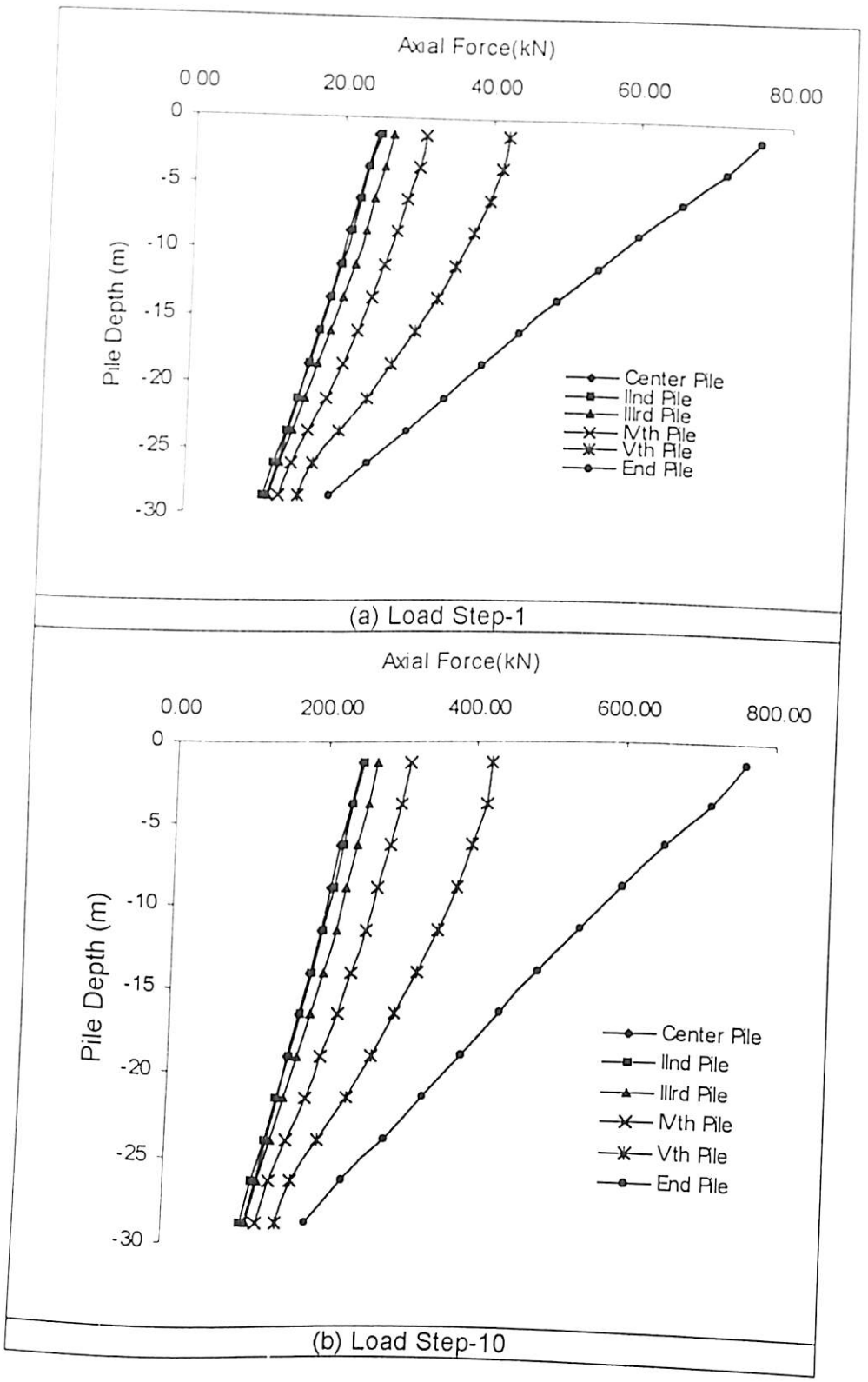

Figure 5.41 Axial Force Distribution in Different Piles
(D = 10 m, L = 30 m, s/d = 2.5, E_s = 22000 kN/m^2)

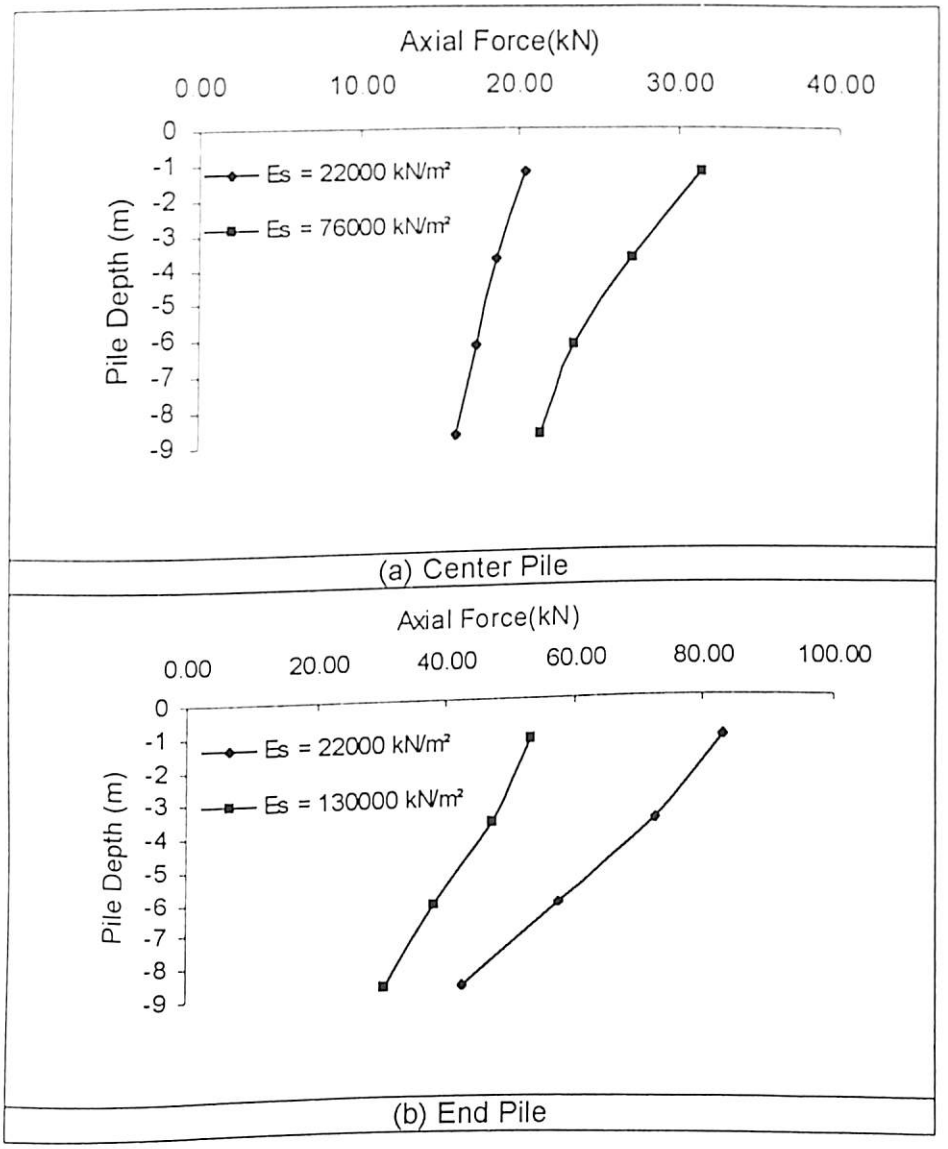

Figure 5.42 Axial Force Distribution in Center and End Piles (D = 10 m, s/d = 2.5, L = 10 m, Load Step-1)

The center piles carry minimum load while the end piles carry maximum load. This is due to the fact that the mobilisation of skin friction is maximum in the end piles than the center piles.

Figures 5.43 (a), (b) show the effect of soil modulus on the axial force distribution for center and end piles of length 10 meter, diameter 10 meter, load step 10.The effect of increase in soil modulus is to increase the load carrying capacity of piles in a piled raft foundation. The effect of increase in load step is to transfer more loads to the piles. The center piles carry minimum load while the end piles carry maximum load. This is due to the fact that the mobilisation of skin friction is maximum in the end piles than the center piles.

Figures 5.44 (a), (b), (c) show the axial load distribution in centre pile, middle pile and the boundary pile of length 10 meter at spacing to diameter ratio of 2.5 for varying load steps for a piled raft foundation whose raft diameter is 10 meter and is on a soil whose elastic modulus is 22000 kN/m^2. For all load steps the axial load in pile is maximum in the top portion and minimum in the lower portion. The percentage variation in axial load between the top and bottom portion increases with increase in load steps. This shows that the shear resistance offered by pile has increased with the increase in load step. Also at larger load steps the curves are seen to come closer to each other showing that the piles have reached to their ultimate capacity. When in Figures 5.44 (a), (b), (c) are compared it is found that the centre pile carries the least load followed by the middle pile while the end pile carries the maximum load.

Figures 5.45 (a), (b), (c) show the axial load distribution in centre pile, middle pile and the boundary pile of length 10 meter at spacing to diameter ratio of 2.5 for varying load steps for a piled raft foundation whose raft diameter is 10 meter and is on a soil whose elastic modulus is 130000 kN/m^2. For all load steps the axial load in pile is maximum in the top portion and minimum in the lower portion. The percentage variation in axial load between the top and bottom portion increases with increase in load steps. This shows that the shear resistance offered by pile has increased with the increase in

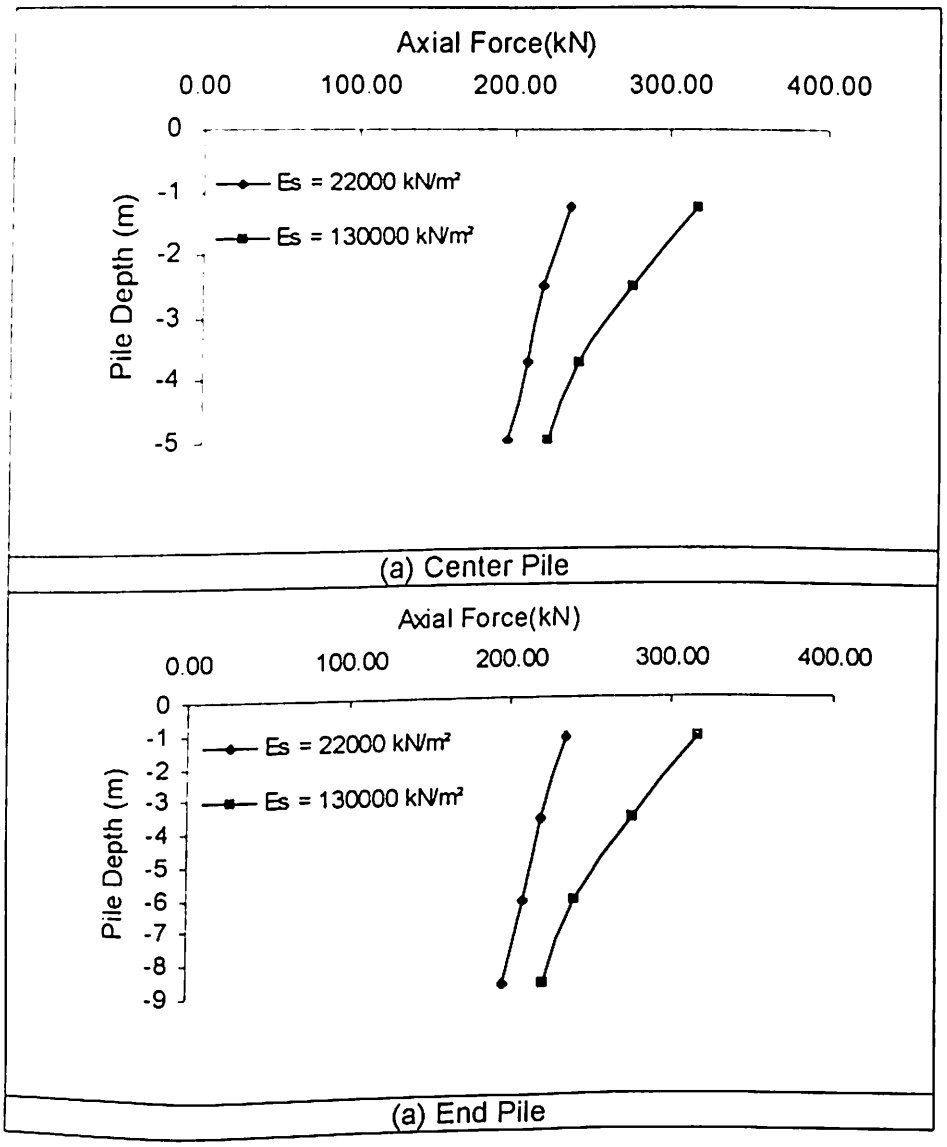

Figure 5.43 Axial Force Distribution in Center and End Pile (D = 10 m, s/d = 2.5, L = 10 m, Load Step-10)

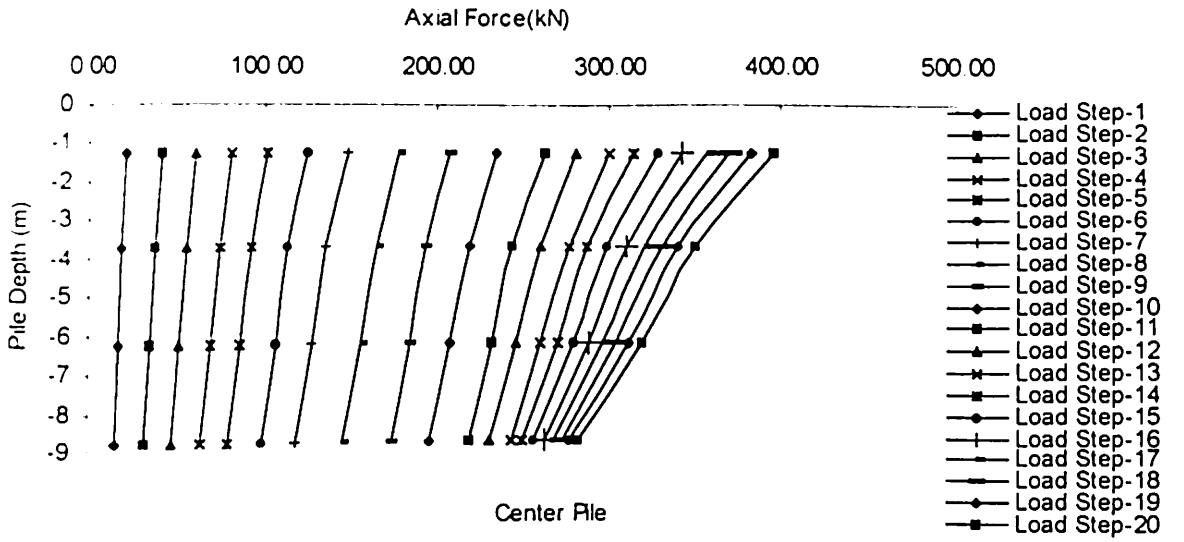

(a)

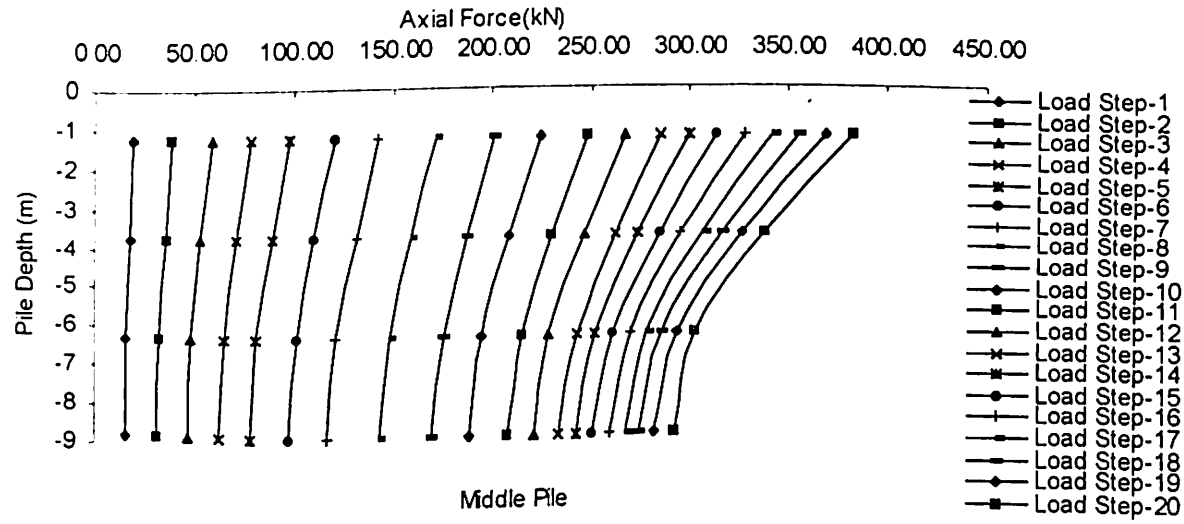

(b)

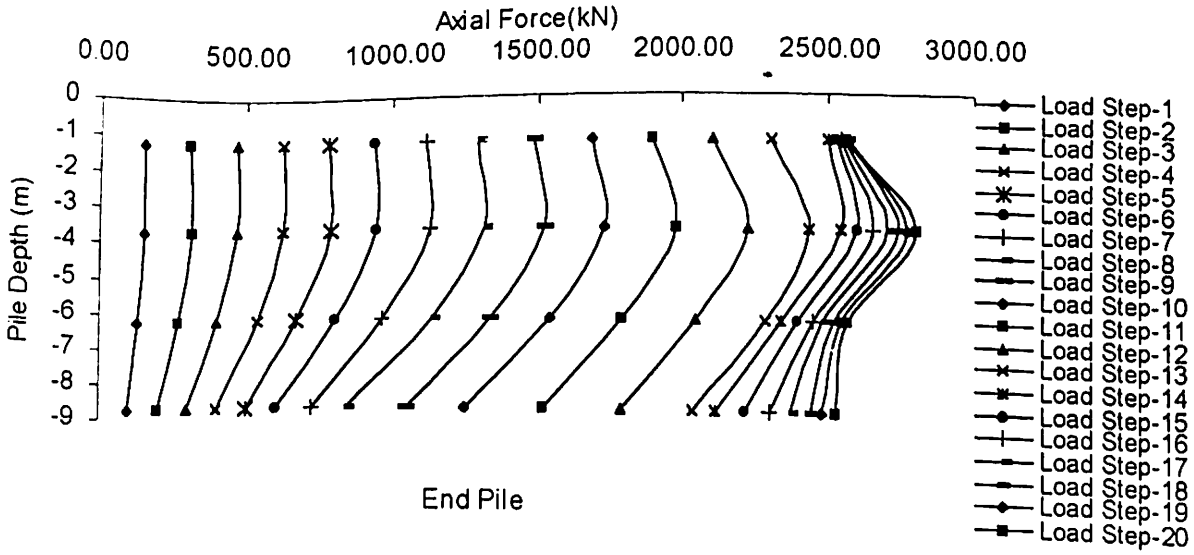

(c)

Figure 5.44 Axial Force Distributions in Piles for Different Load Steps (D = 10 m, s/d = 2.5, L =10 m, E_s = 22000 kN/m^2)

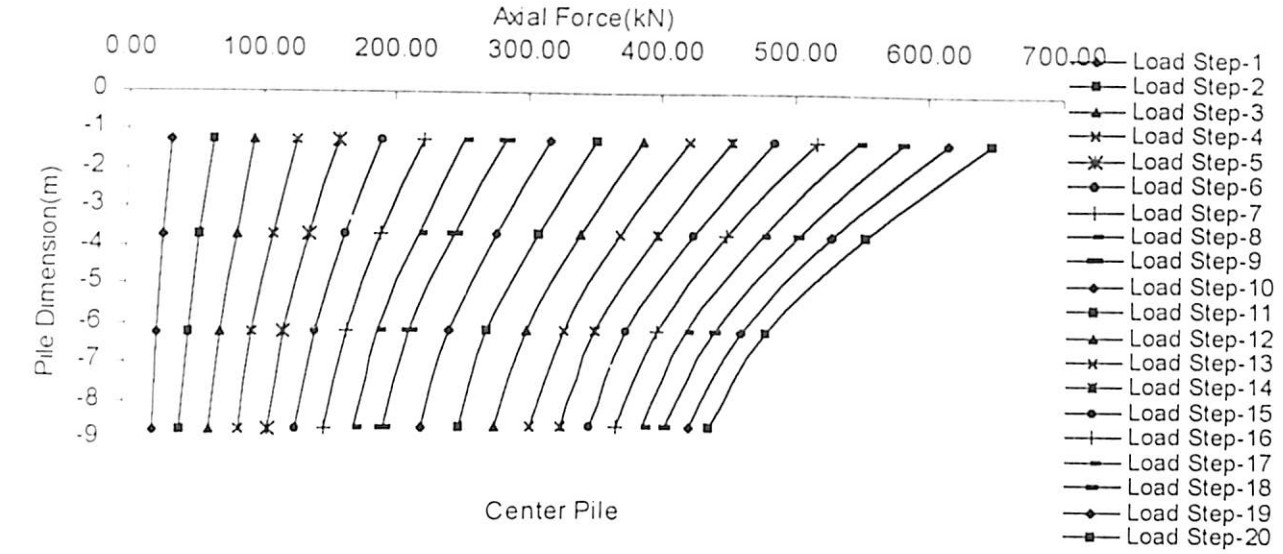

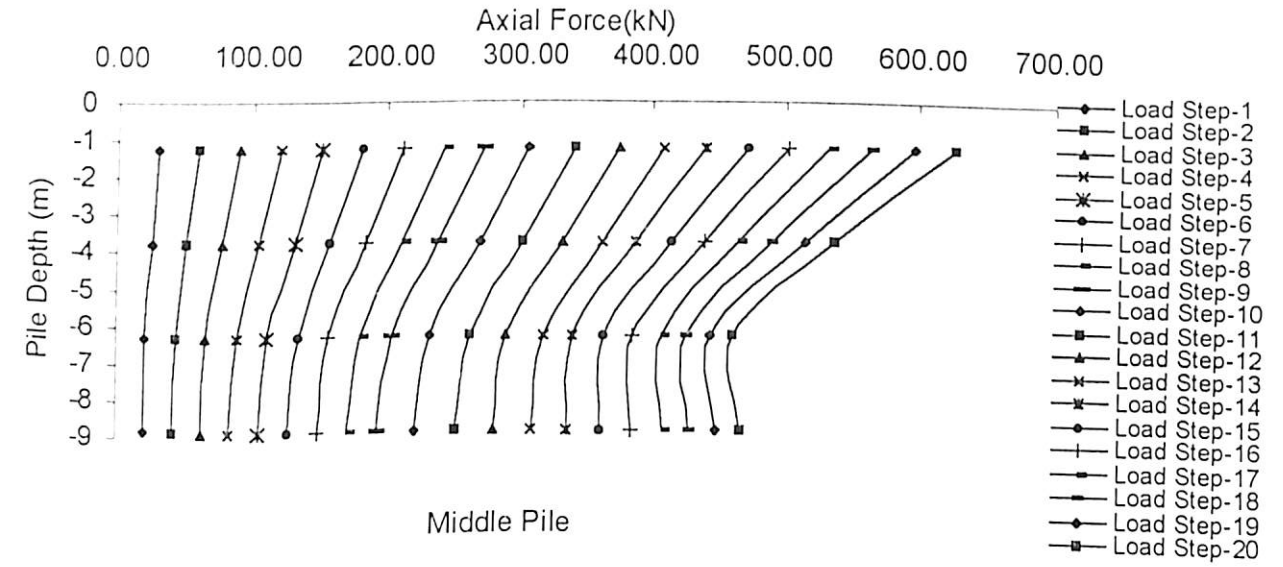

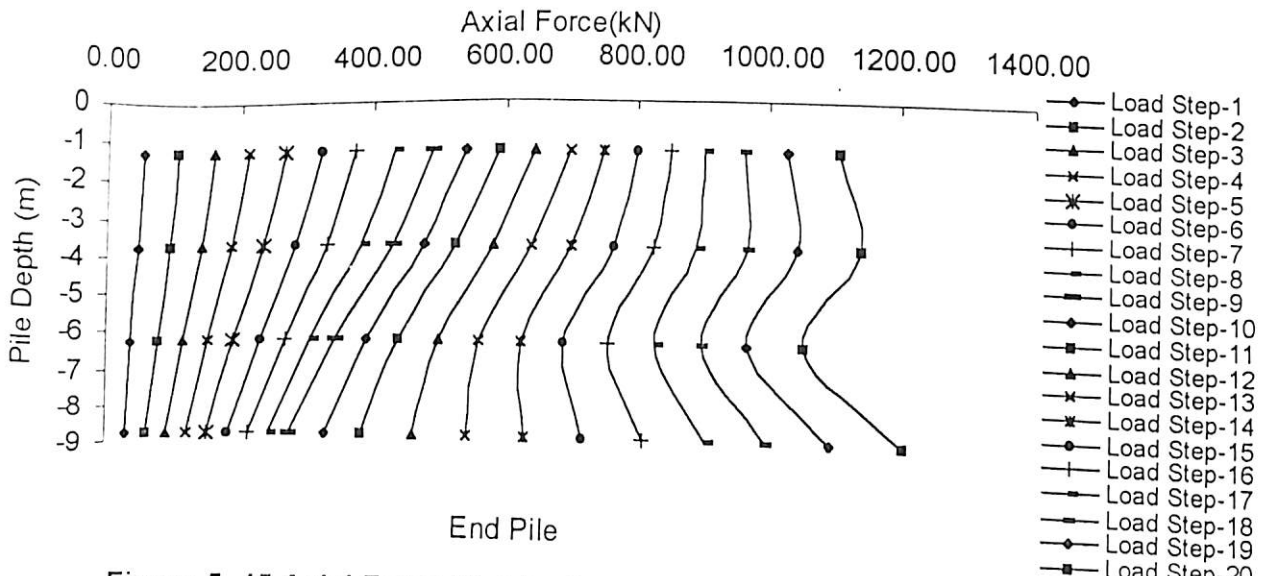

Figure 5. 45 Axial Force Distributions in Piles for Different Load Steps (D = 10 m, s/d = 2.5, L =10 m, E_s = 130000 kN/m^2)

load step. Also at larger load steps the curves are seen to come closer to each other showing that the piles have reached to their ultimate capacity. When in Figures 5.45 (a), (b), (c) are compared it is found that the centre pile carries the least load followed by the middle pile while the boundary pile carries the maximum load. When Figures 5.45 (a), (b), (c) are compared with Figures 5.44 (a), (b), (c) it is found that the effect of increase in soil modulus is to increase the axial load carrying capacity of all the piles.

Figures 5.46 (a), (b), (c) show the axial load distribution in centre pile, middle pile and the boundary pile of length 10 meter at spacing to diameter ratio of 5.0 for varying load steps for a piled raft foundation whose raft diameter is 10 meter and is on a soil whose elastic modulus is 22000 kN/m^2. For all load steps the axial load in pile is maximum in the top portion. For lower load steps the axial force decreases with depth and becomes minimum in the lower portion. For higher load steps the axial load first decreases and then increases. At larger load steps the curves are seen to come closer to each other showing that the piles have reached almost to their ultimate capacity. When in Figures 5.46, (a), (b), (c) are compared it is found that the centre pile carries the least load followed by the middle pile while the boundary pile carries the maximum load.

Figures 5.47 (a), (b), (c) show the axial load distribution in centre pile, middle pile and the boundary pile of length 30 meter at spacing to diameter ratio of 5.0 for varying load steps for a piled raft foundation whose raft diameter is 10 meter and is on a soil whose elastic modulus is 22000 kN/m^2. For all load steps the axial load in pile is maximum in the top portion and minimum in the bottom portion. The percentage variation in the load carried in the top and bottom portion increases with increase in load steps. At higher load steps the axial load distribution curves come very close to each other showing that the piles have reached almost to their ultimate capacity. When Figures 5.53, (a), (b), (c) are compared it is found that the centre pile carries the least load followed by the middle pile while the boundary pile carries the maximum load.

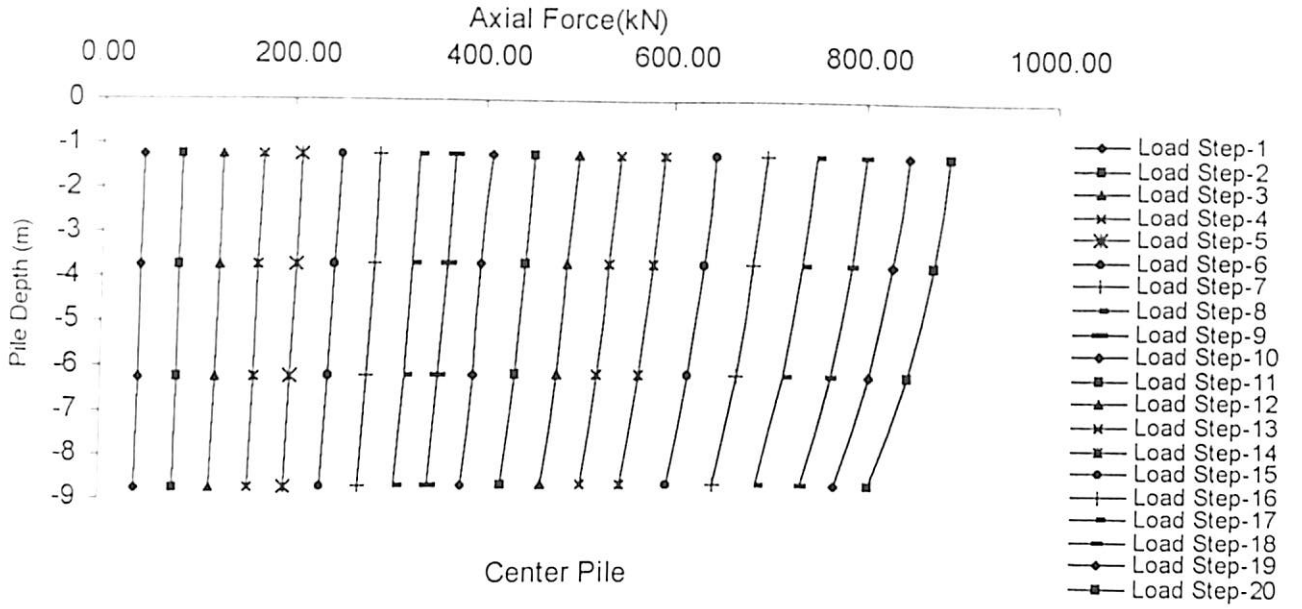

(a)

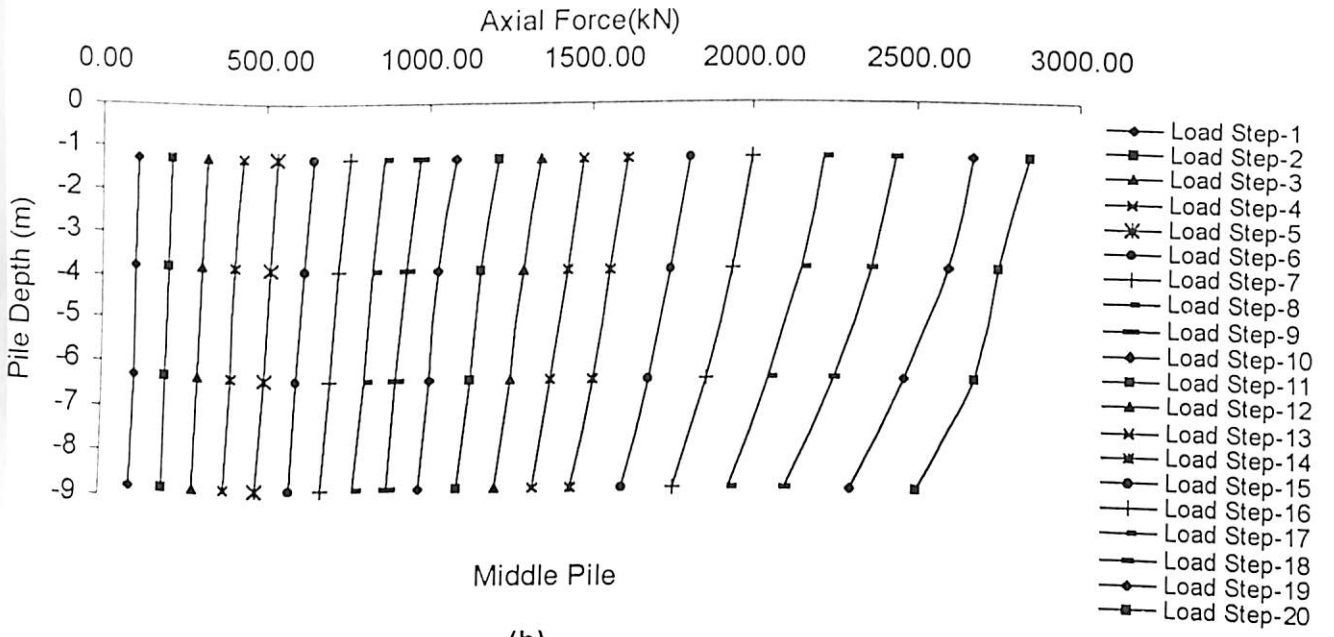

(b)

Figure 5.46 Axial Force Distribution in Center and Middle Piles (D=10 m, s/d = 5, L = 10 m, E_s = 22000 kN/m^2)

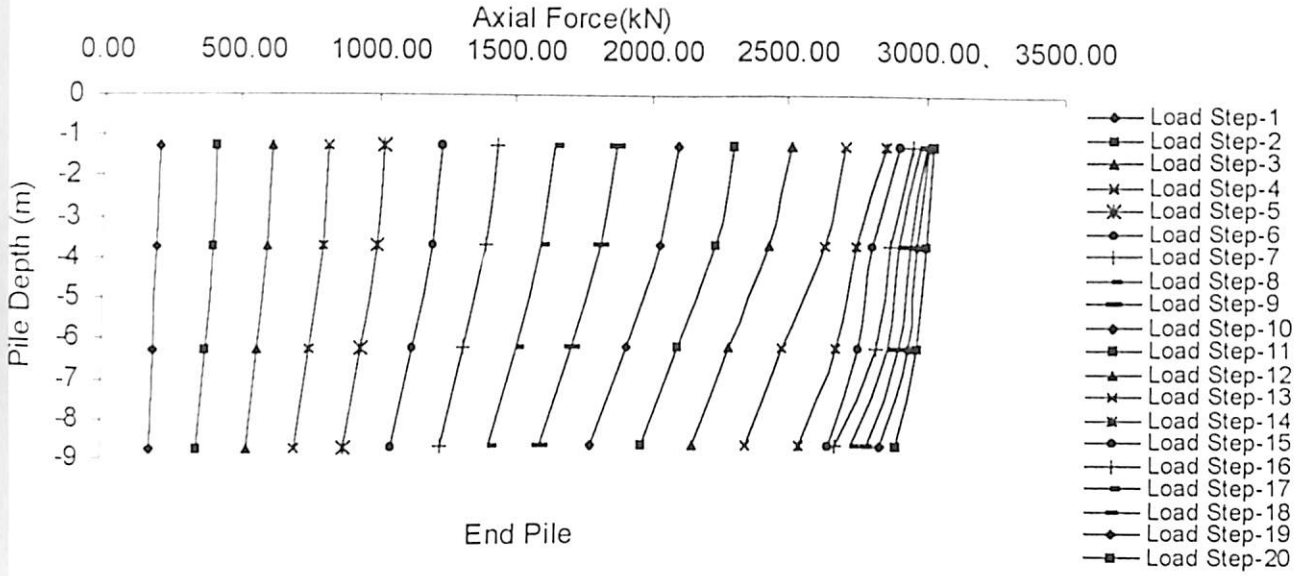

(c)

Figure 5.46 Axial Force Distribution in End Piles
(D=10 m, s/d = 5, L = 10 m, E_s = 22000 kN/m^2)

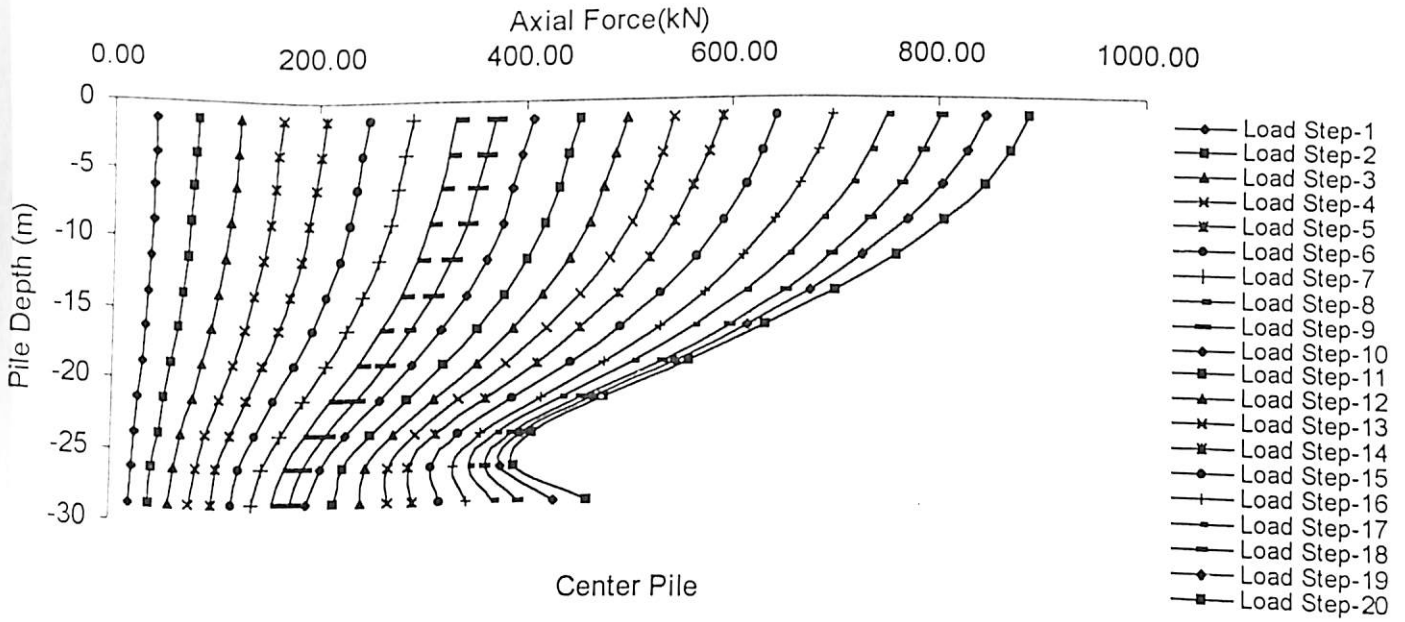

(a)

Figure 5.47 Axial Force Distribution in Center Pile
(D = 10 m, s/d = 5, L = 30 m, E_s = 22000 kN/m^2)

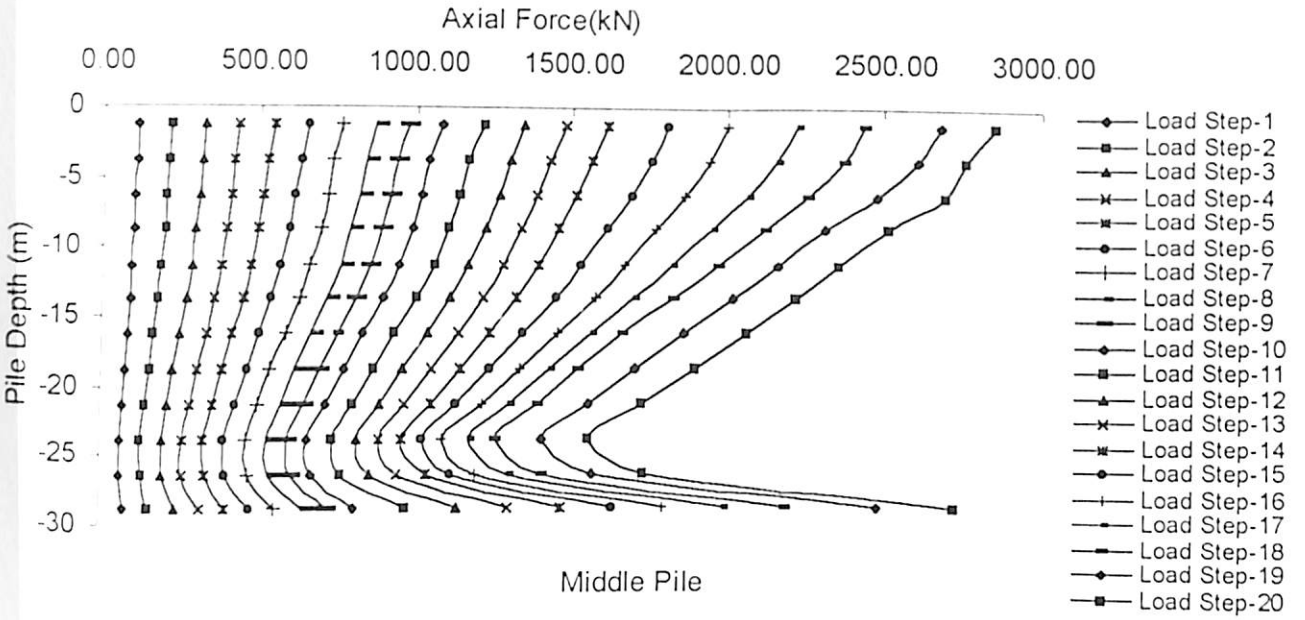

(b)

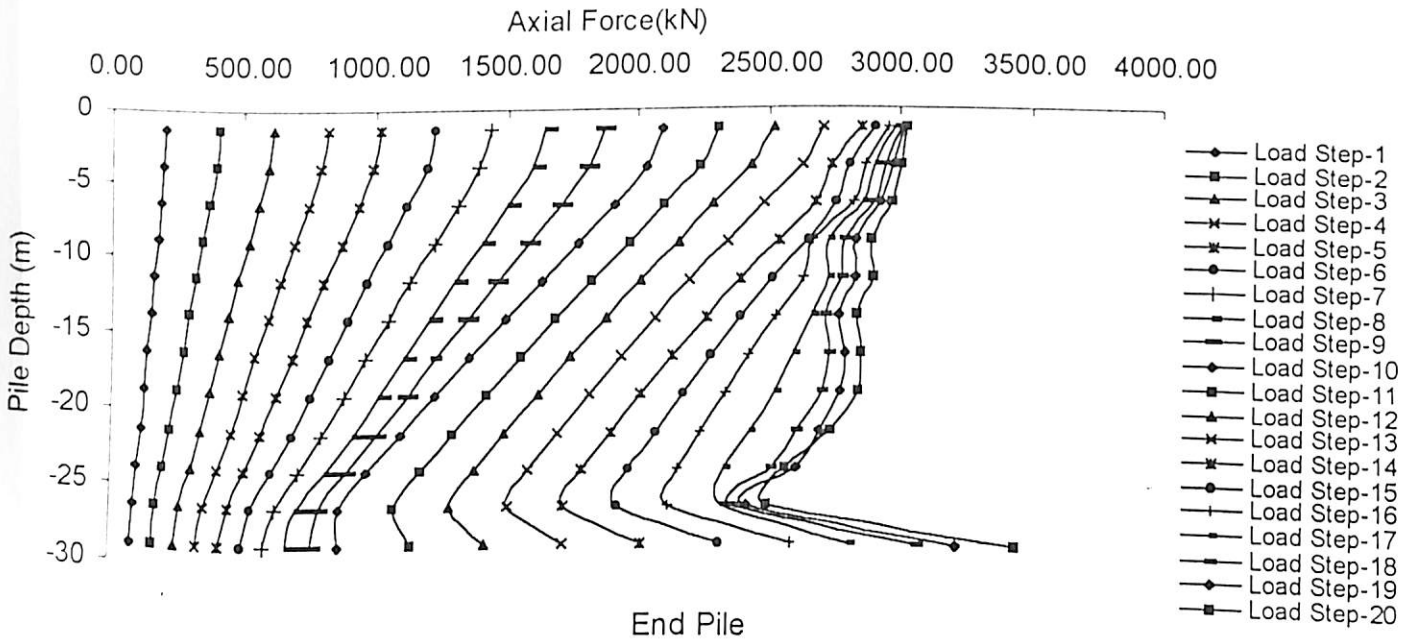

(c)

Figure 5.47 Axial Force Distribution in Middle and End Pile
(D = 10 m, s/d = 5, L = 30 m, E_s = 22000 kN/m^2)

Figures 5.48 (a), (b), (c) show the axial load distribution for centre, second and boundary pile for piles of length 10 meter, spacing to diameter ratio 5, raft diameter 10 meter and soil modulus 130000 kN/m^2. Axial load in pile is maximum in the top portion of pile and minimum in the bottom portion of the pile for the different load steps. At higher load steps for the centre pile and the second pile the axial load decreases with depth and then again increases. For the end piles at higher load steps the axial load first increases from the top then decreases and then slight increase is found.

Figures 5.49 (a), (b), (c) show the axial force distribution in centre, second and the end piles of length 30 meter, spacing to diameter ratio (s/d) 5, diameter of raft 10 meter and soil modulus 130000 kN/m^2. For each load step the axial load is maximum in the top portion of the pile and then decreases with depth. In the extreme top portion of the pile the axial load is found slightly less than the maximum for higher load steps. When centre piles, second concentric row of piles and the boundary piles are compared it is found that the centre piles carry the minimum load followed by the second concentric row of piles while the boundary piles carry the maximum load.

5.6.4 Settlement Profile for Raft

5.6.4.1 Effect of Raft Thickness

Figures 5.50 (a), (b), (c) show the settlement profile for the raft for different thickness of the raft and different soil modulus. When the thickness of the raft is 0.1 meter, the settlement is maximum at the center of the raft and decreases with increase in distance from the center of the raft. The settlement is maximum at the center of the raft and minimum at the edge of the raft. The raft is under maximum differential settlement. With increase in thickness of raft this differential settlement reduces and become almost negligible when the thickness of raft reaches to 4.0 meter. Even when the raft thickness reaches to 0.5 meter there is significant reduction in differential settlement. Figures 5.51 (a), (b), (c) show the settlement profile for soil modulus of 76000 kN/m^2. The effect of increase in thickness of raft is to decrease the differential settlement of the raft. With increase in soil modulus there is more curvature in the settlement profile, which shows that the raft behaves more flexible in this case. This is due

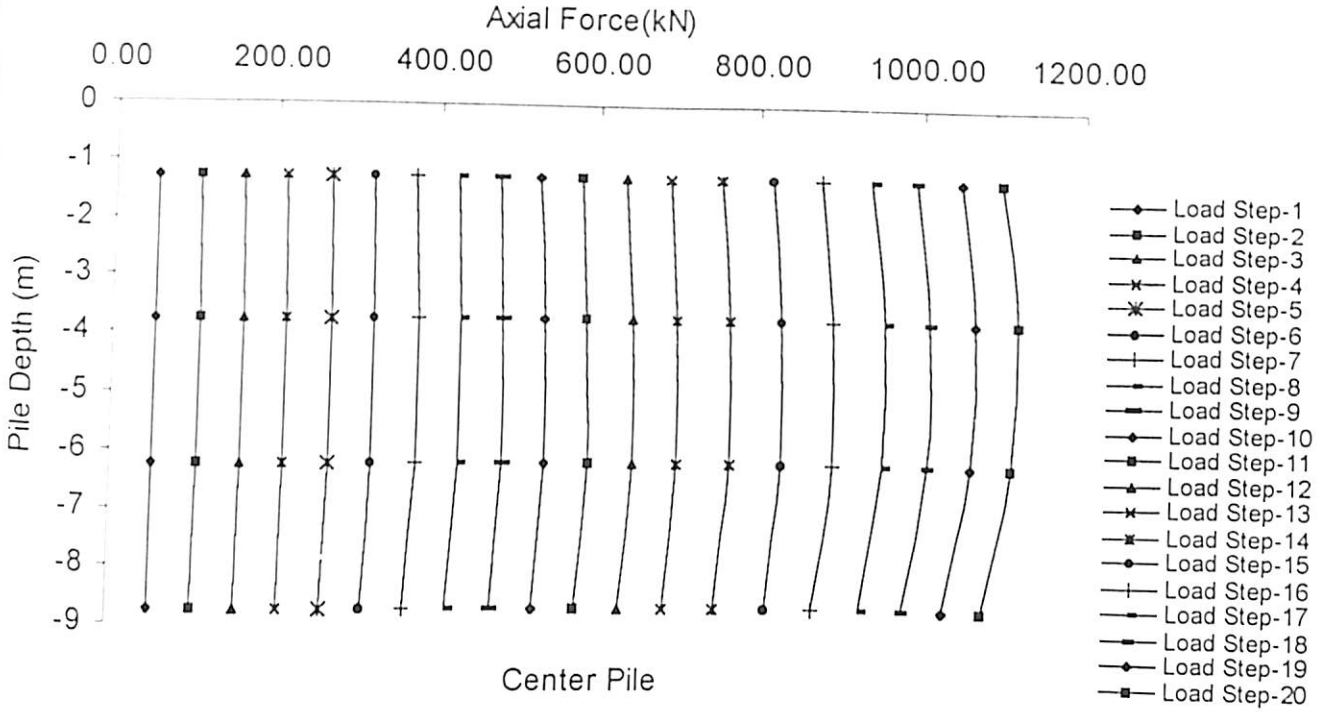

(a)

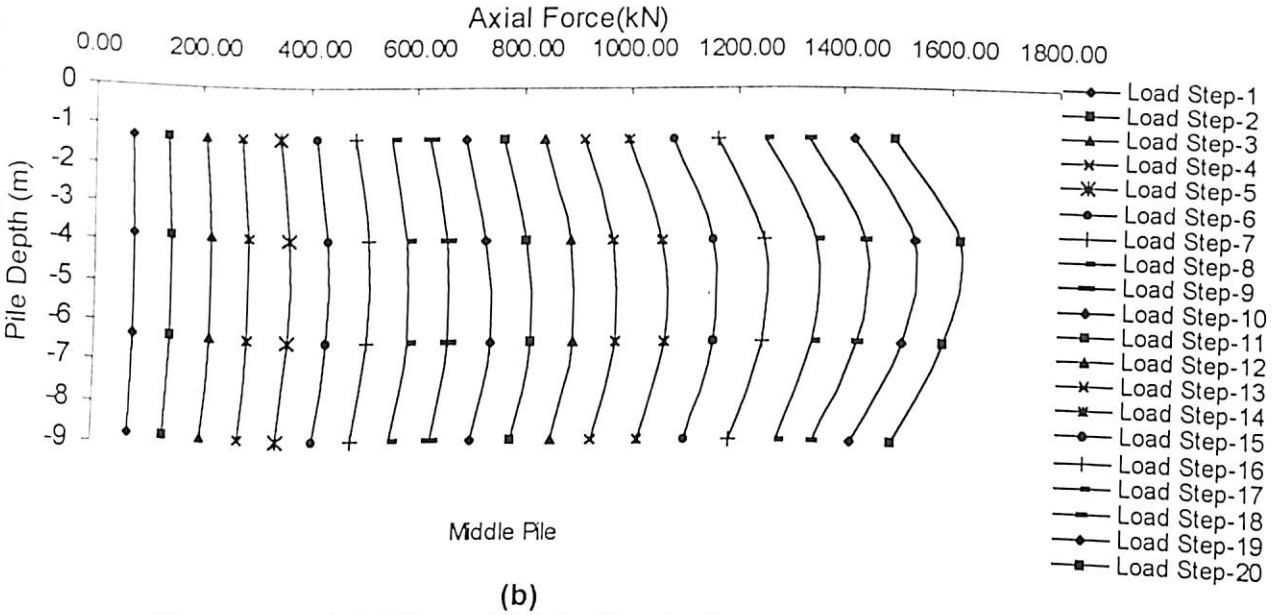

(b)

Figure 5.48 Axial Force Distribution in Center and Middle Pile (D = 10 m, L = 10 m, s/d = 5, E_s = 130000 kN/m^2)

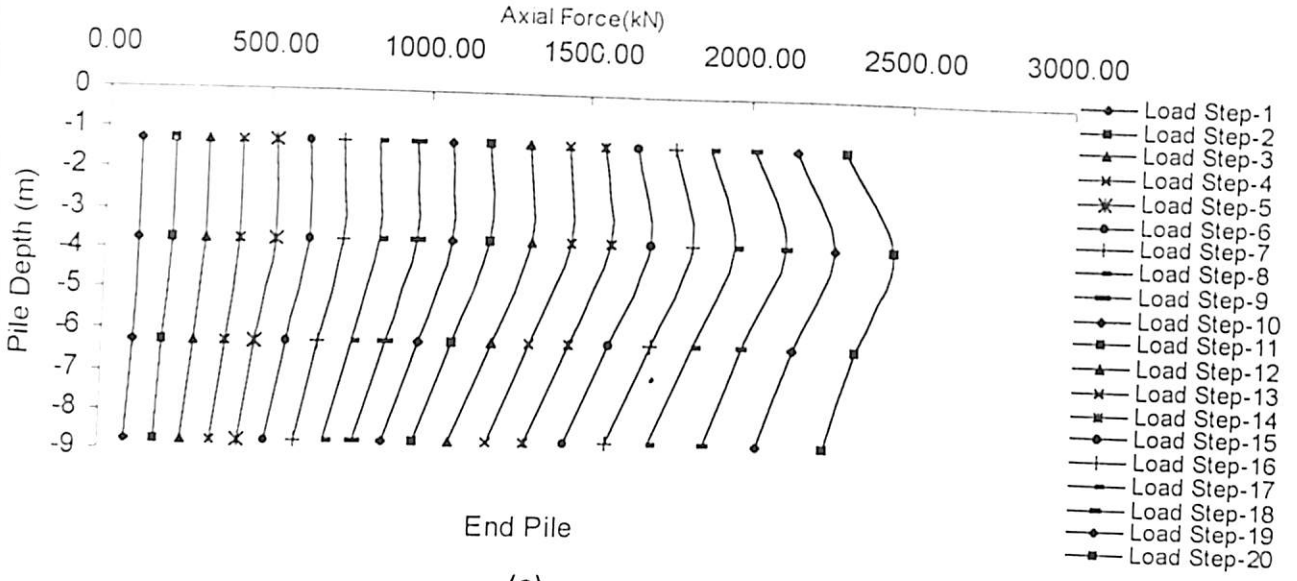

(c)

Figure 5.48 Axial Force Distribution in End Pile
(D = 10 m, L = 10 m, s/d = 5, E_s = 130000 kN/m^2)

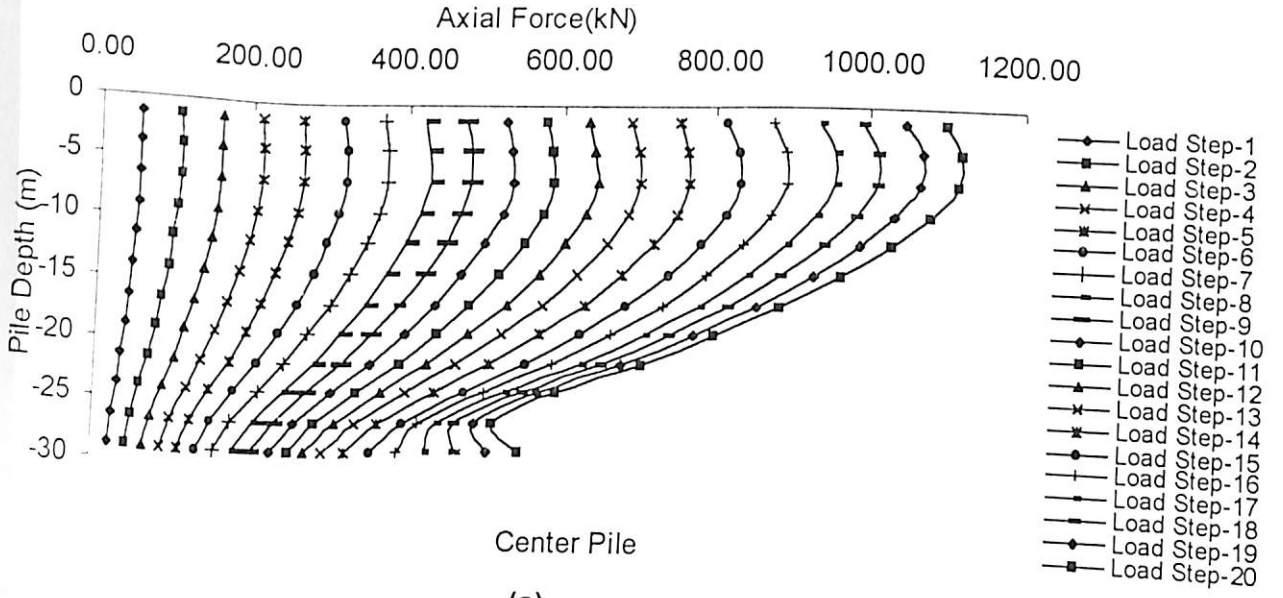

(a)

Figure 5.49 Axial Force Distribution in Center Pile
(D = 10 m, s/d = 5, L = 30, E_s = 130000 kN/m^2)

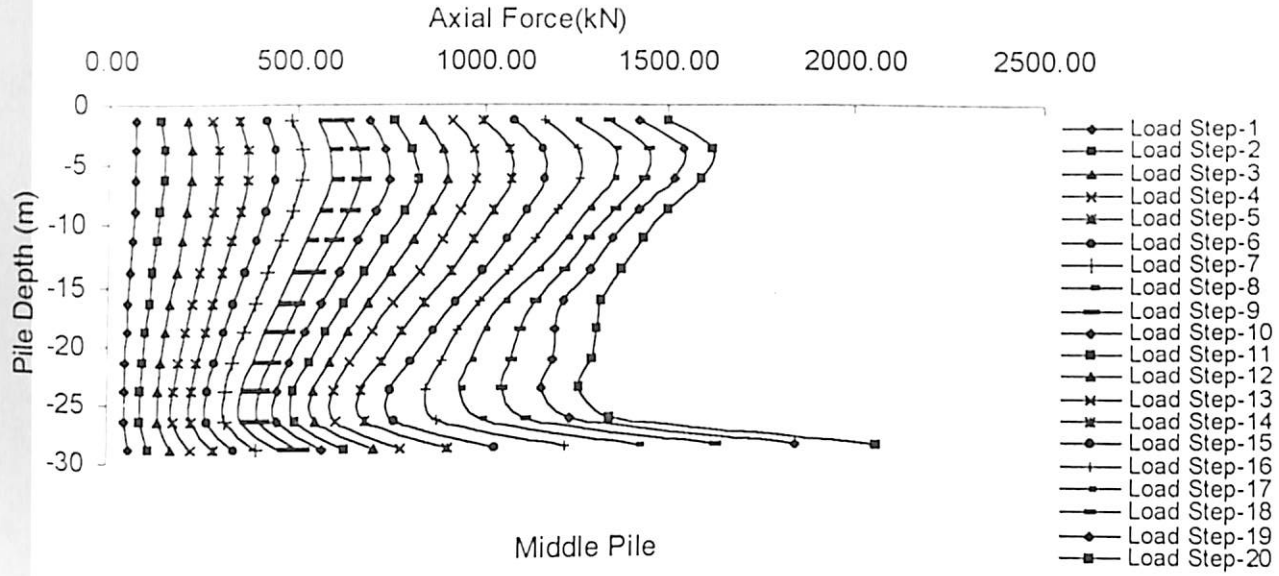

(b)

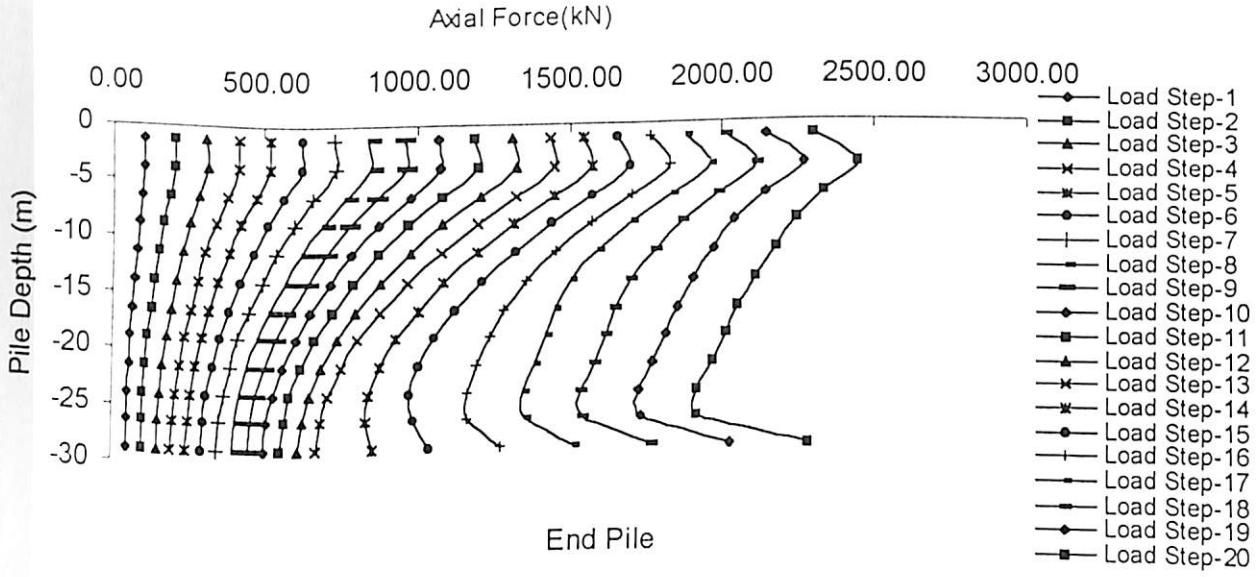

(c)

Figure 5.49 Axial Force Distribution in Middle and End Pile
(D = 10 m, s/d = 5, L = 30 m, E_s = 130000 kN/m^2)

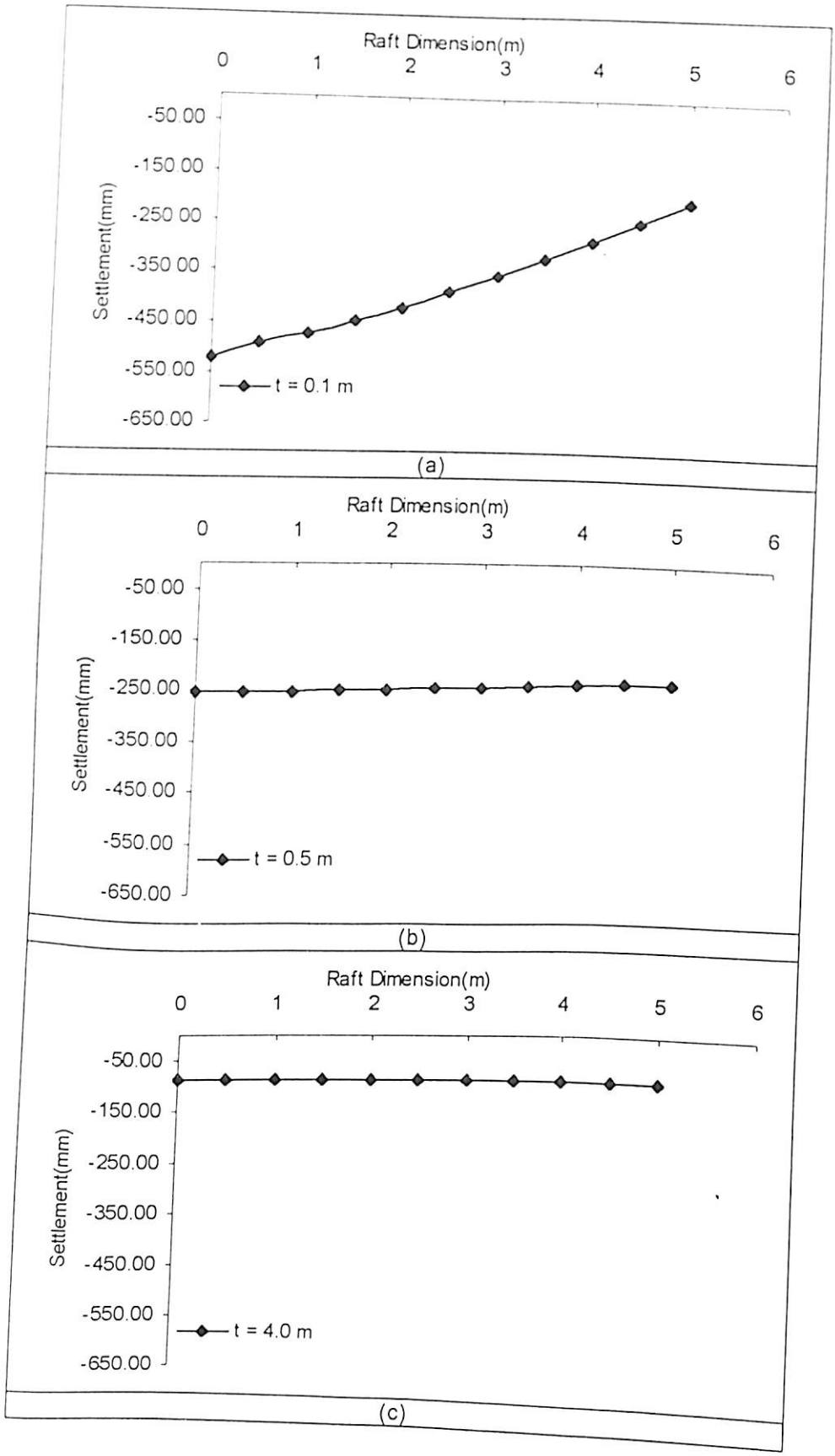

Figure 5.50 Settlement Profile for Raft
(D = 10 m, E_s = 22000 kN/m^2 P = 62801.6 kN)

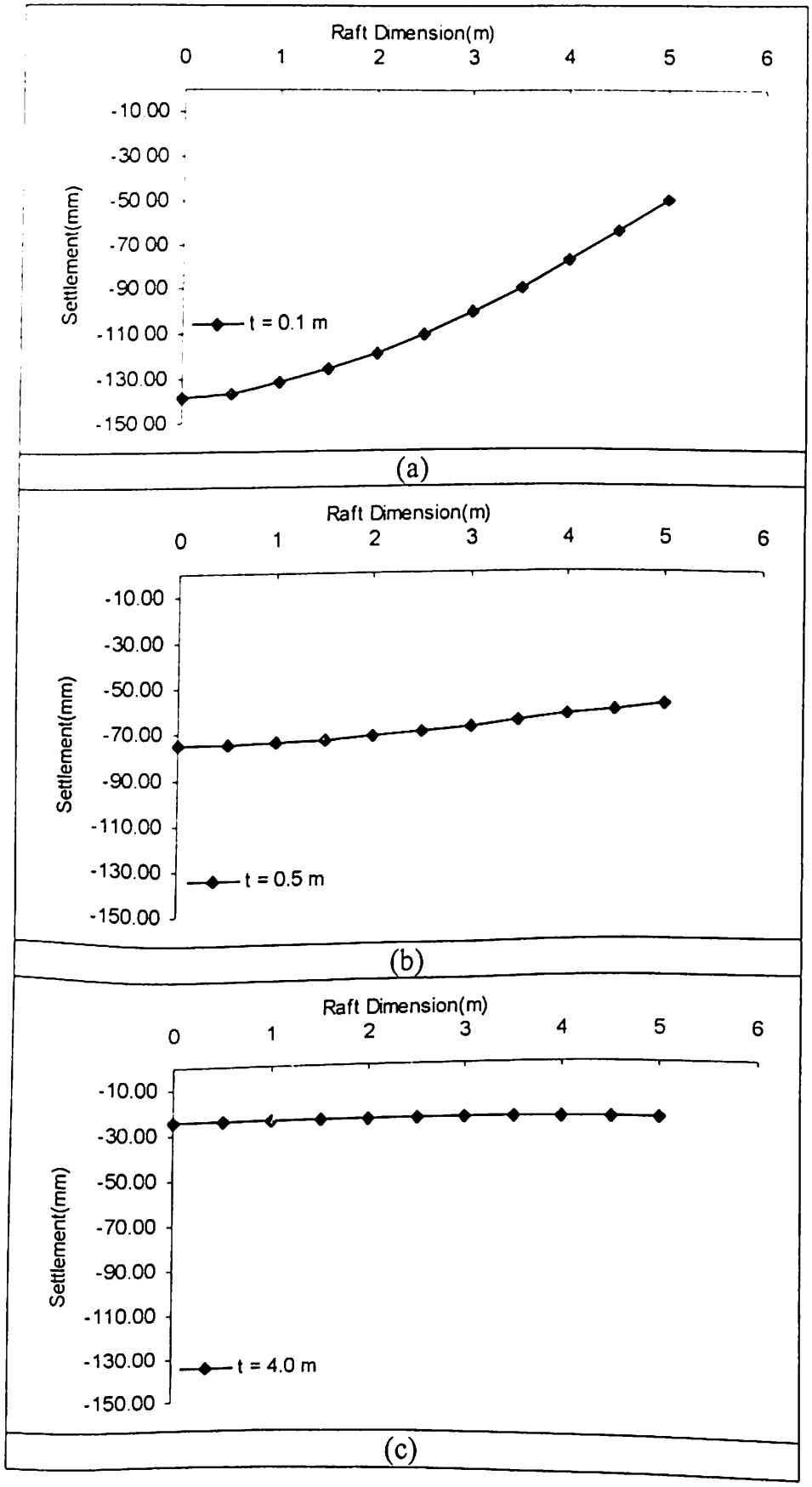

Figure 5.51 Settlement Profile for Raft
(D = 10 m, E_s = 76000 kN/m^2 P = 62801.6 kN)

to soil structure interaction. The overall settlement reduces with increase in soil modulus. Figures 5.52 (a), (b), (c) show the settlement profile for raft foundation for soil modulus of 13000 kN/m^2. The effect of increase in thickness of raft is to decrease the differential settlement.

Figures 5.53 (a), (b), (c) show the settlement profile for raft of diameter 20 meter for different thickness of the raft. The effect of increase in raft thickness is to decrease the differential settlement. But due to the increase in size of the raft, for the same thickness of raft, the differential settlement is more than that for the raft of diameter 10 meters.

5.6.4.2 Effect of Soil Modulus

The effect of increased soil modulus on the settlement profile of raft foundation has been shown in Figures 5.54 (a), (b), (c) and 5.55 (a), (b), (c). The differential settlement decreases with increase in thickness of raft but the raft shows more flexible behaviour with increase in soil modulus. This is due to the soil structure interaction.

Figures 5.56 (a), (b), (c) , 5.57 (a), (b), (c) and 5.58 (a), (b), (c) show the settlement profile for raft of diameter 30 meter for different soil modulus and different thickness of the raft. A similar explanation as explained above is true for this also. Due to the increased diameter of raft it undergoes more differential settlement than that for raft of diameter 10 and 20 meter.

Figures 5.59 (a), (b), (c), 5.60 (a), (b), (c) and 5.61 (a), (b), (c) show the settlement profile for raft of diameter 40 meter for different soil modulus and different thickness of the raft. A similar explanation as explained above is true for this case. Due to the increased diameter of raft it undergoes more differential settlement than that for raft of diameters 10, 20 and 30 meters.

5.6.5 Settlement Profile for Raft in a Piled Raft Foundation

5.6.5.1 Effect of Pile Length

Figures 5.62 (a), (b), (c) show the settlement profile for raft foundation of diameter 10 meters, E_s = 22000 kN/m^2 and spacing to diameter ratio of 2.5. Differential settlement can be seen for raft foundation when no pile is there as shown in Figure 5.62 (a). This differential settlement reduces

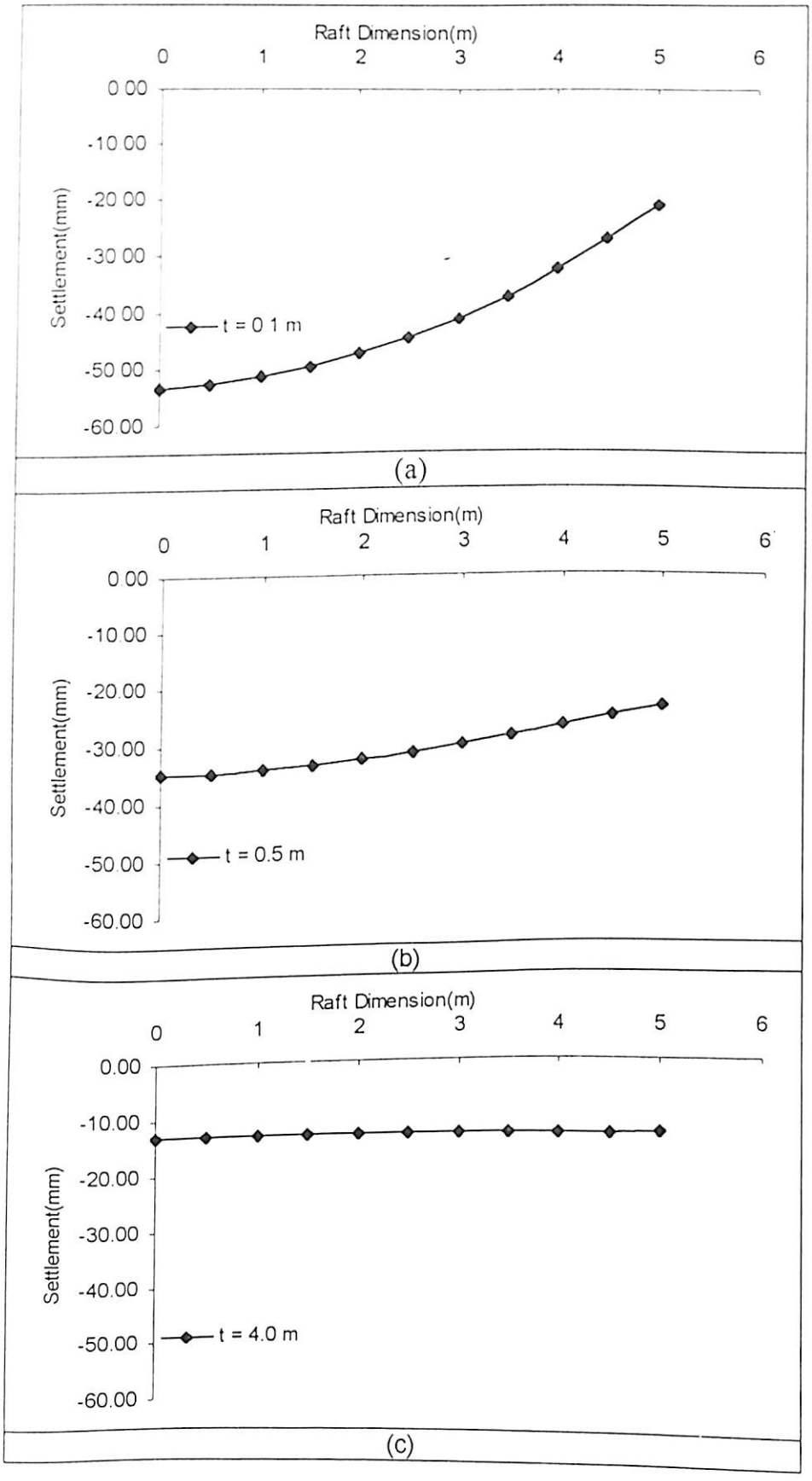

Figure 5.52 Settlement Profile of Raft
(D = 10m, E_s = 130000 kN/m^2 P = 62801.6 kN)

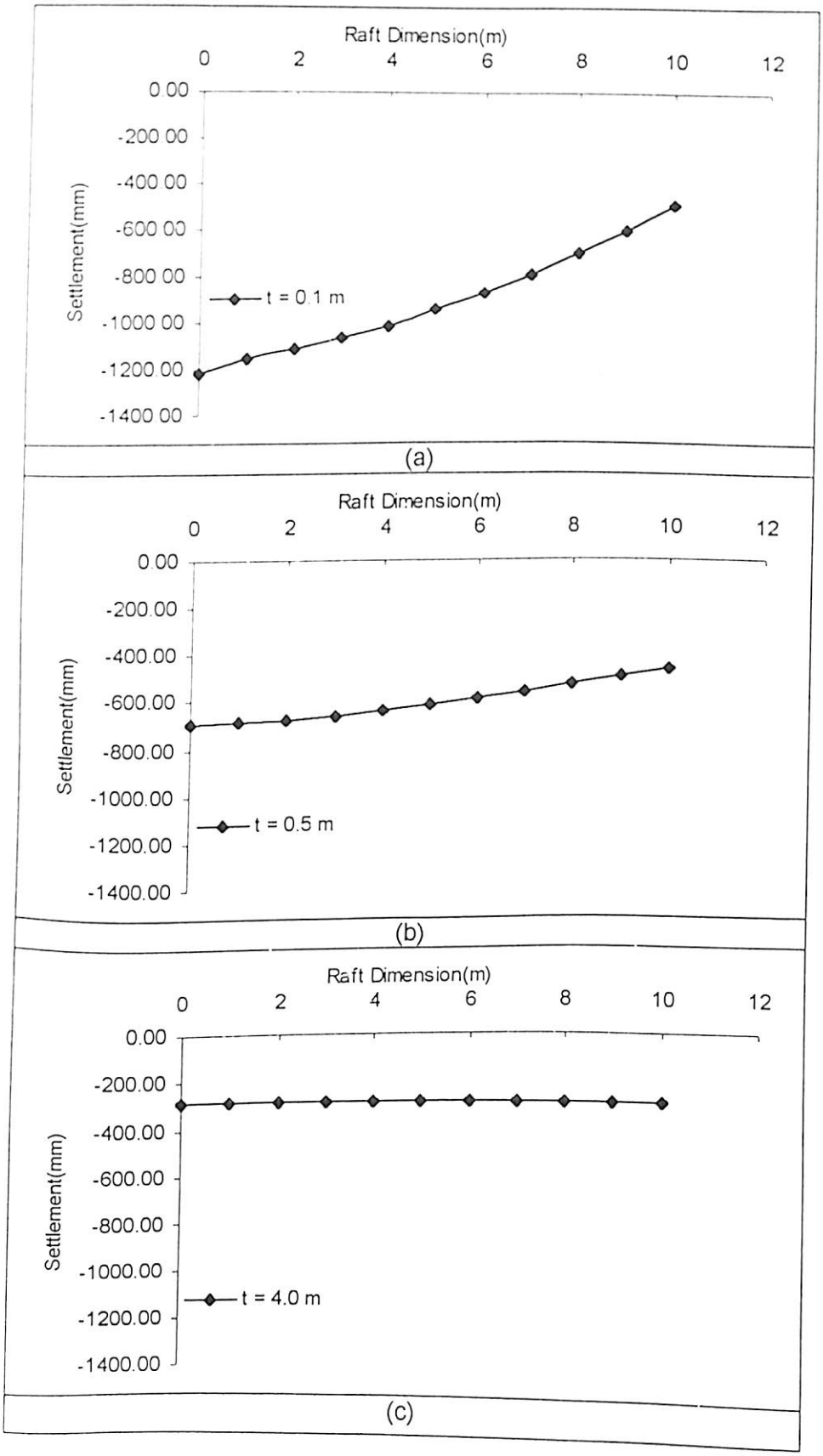

Figure 5.53 Settlement Profile of Raft
(D = 20 m, E_s = 22000 kN/m^2, P = 125660.6 kN)

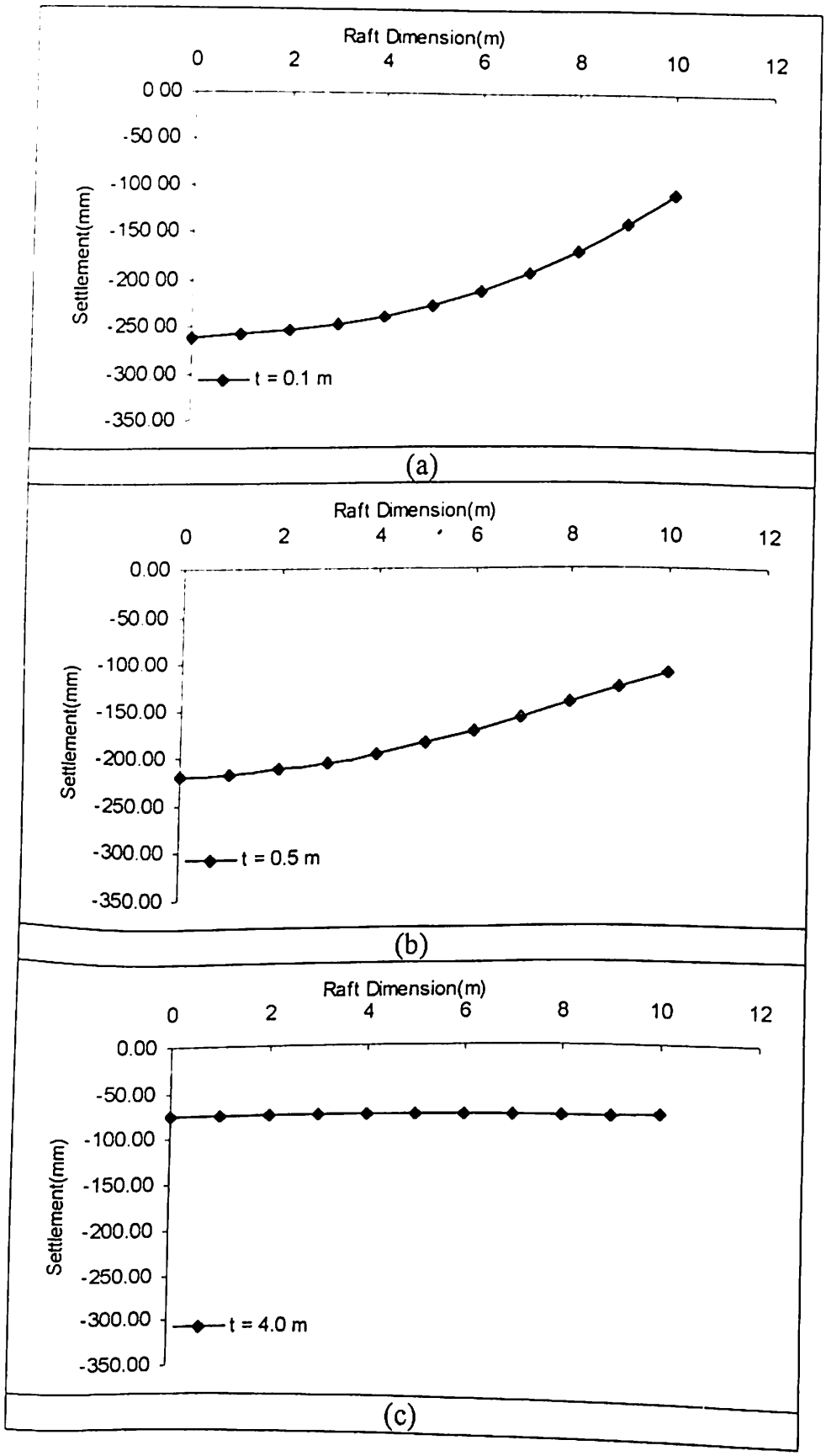

Figure 5.54 Settlement Profile of Raft
(D = 20 m, E_s = 76000 kN/m^2, P = 125660.6 kN)

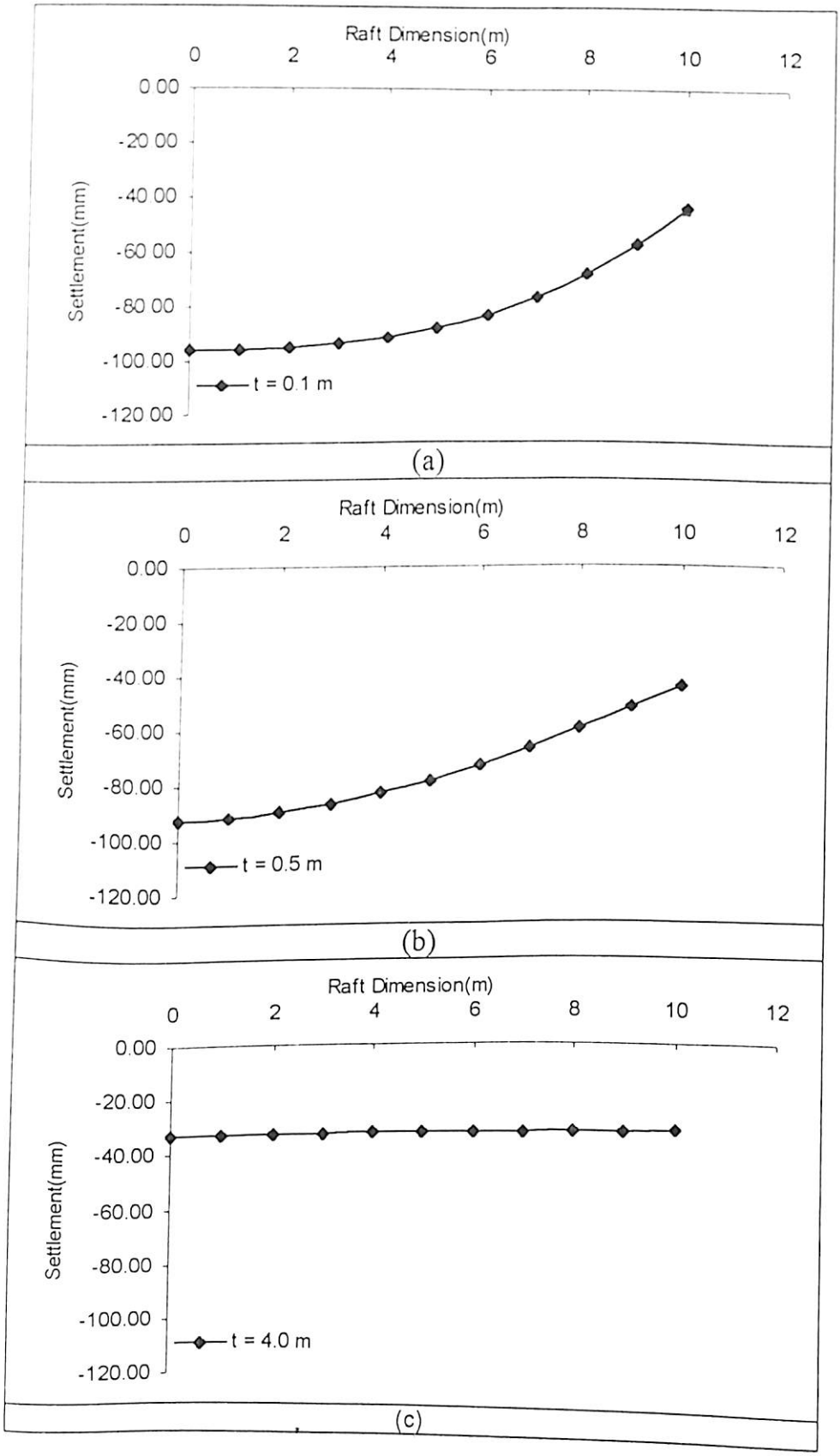

Figure 5.55 Settlement Profile of Raft
(D = 20 m, E_s = 130000 kN/m^2, P = 125660.6 kN)

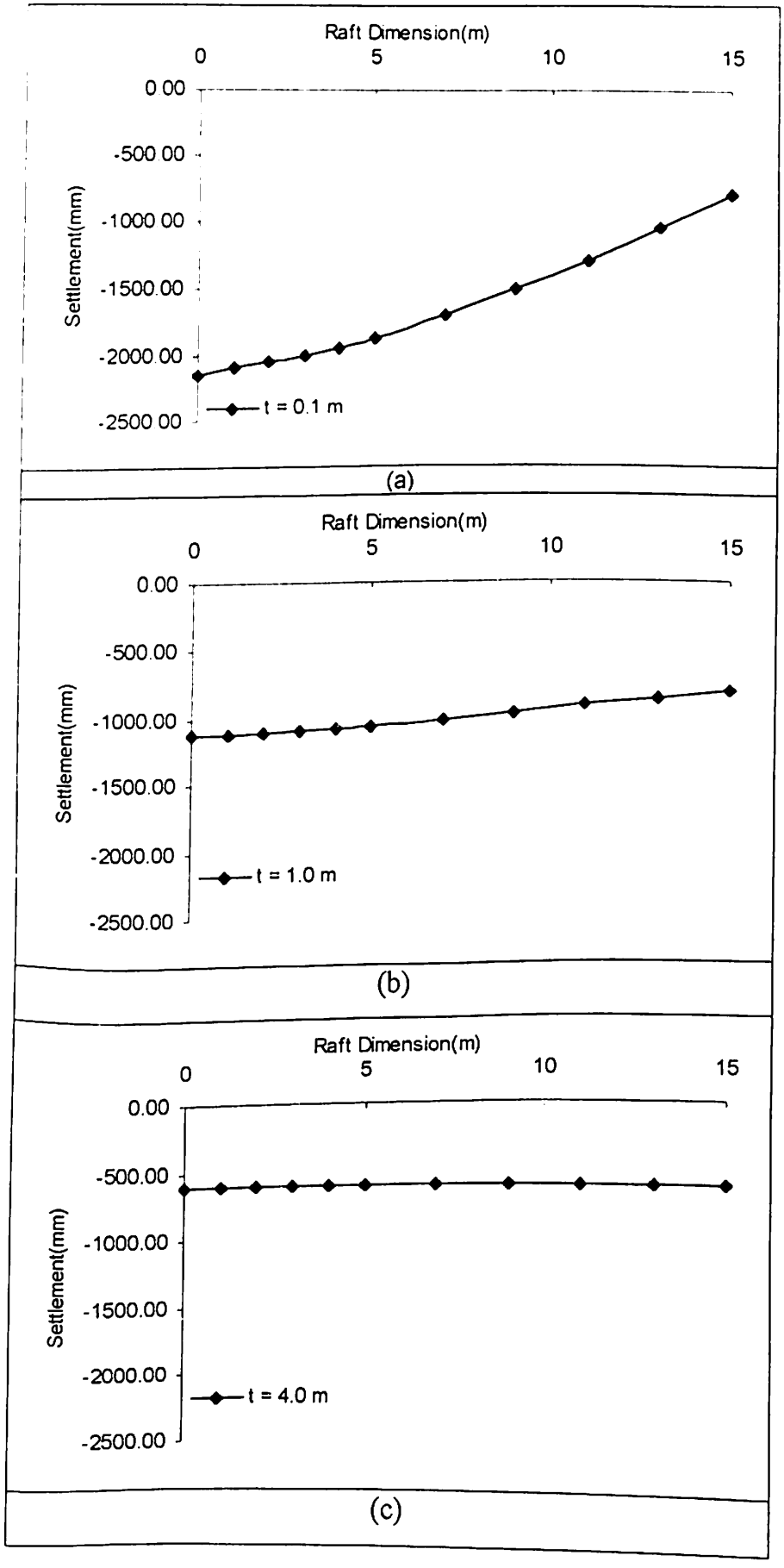

Figure 5.56 Settlement Profile of Raft
(D = 30 m, E_s = 22000 kN/m^2, P = 281800.9 kN)

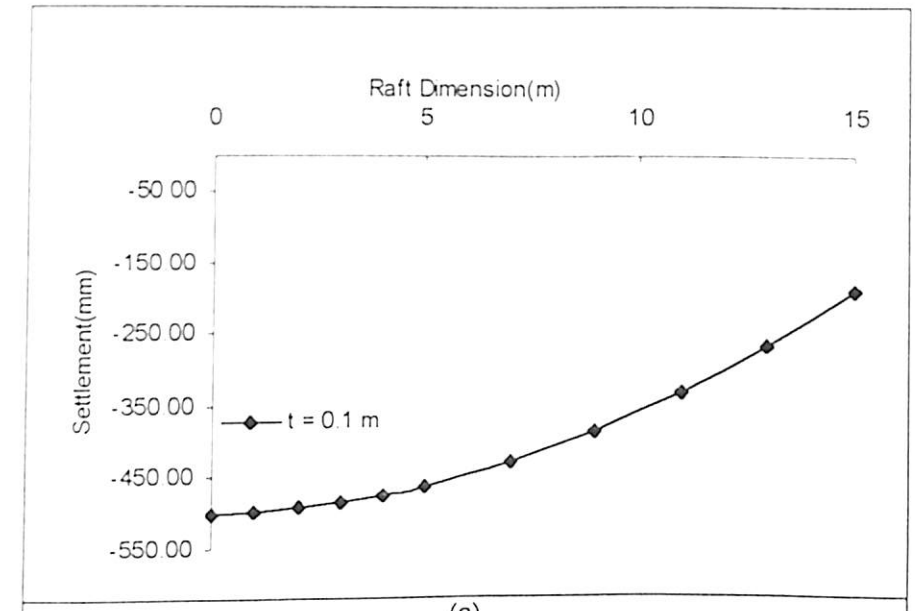

(a)

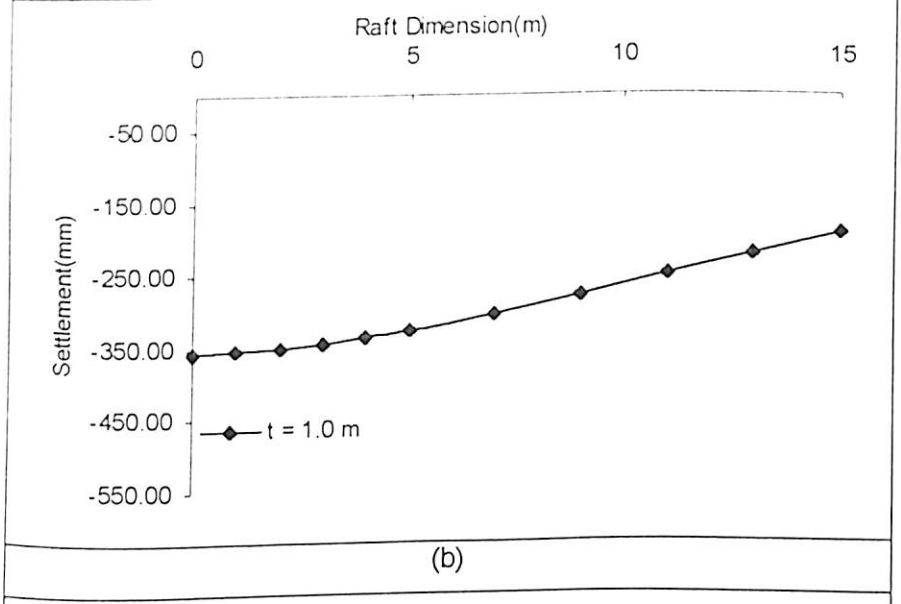

(b)

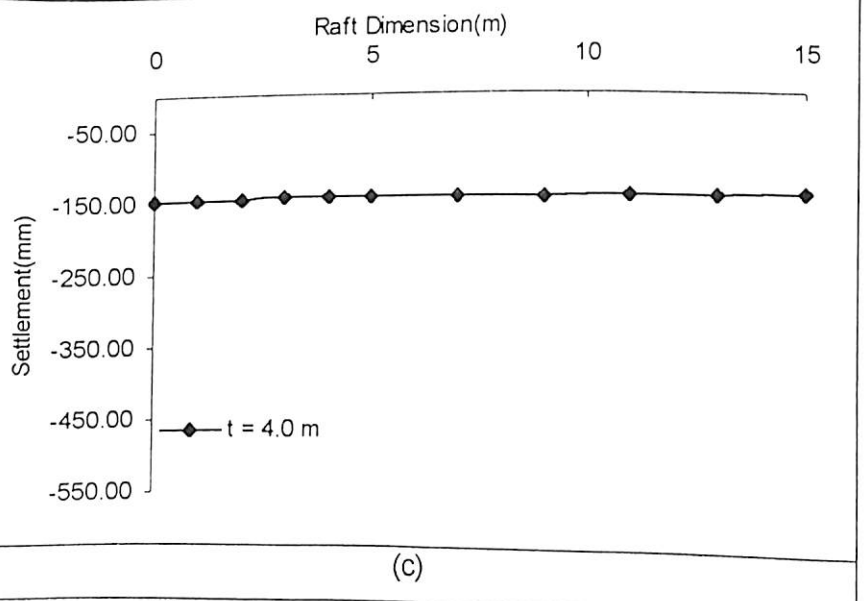

(c)

Figure 5.57 Settlement Profile of Raft
(D = 30 m, E_s = 76000 kN/m^2, P = 281800.9 kN)

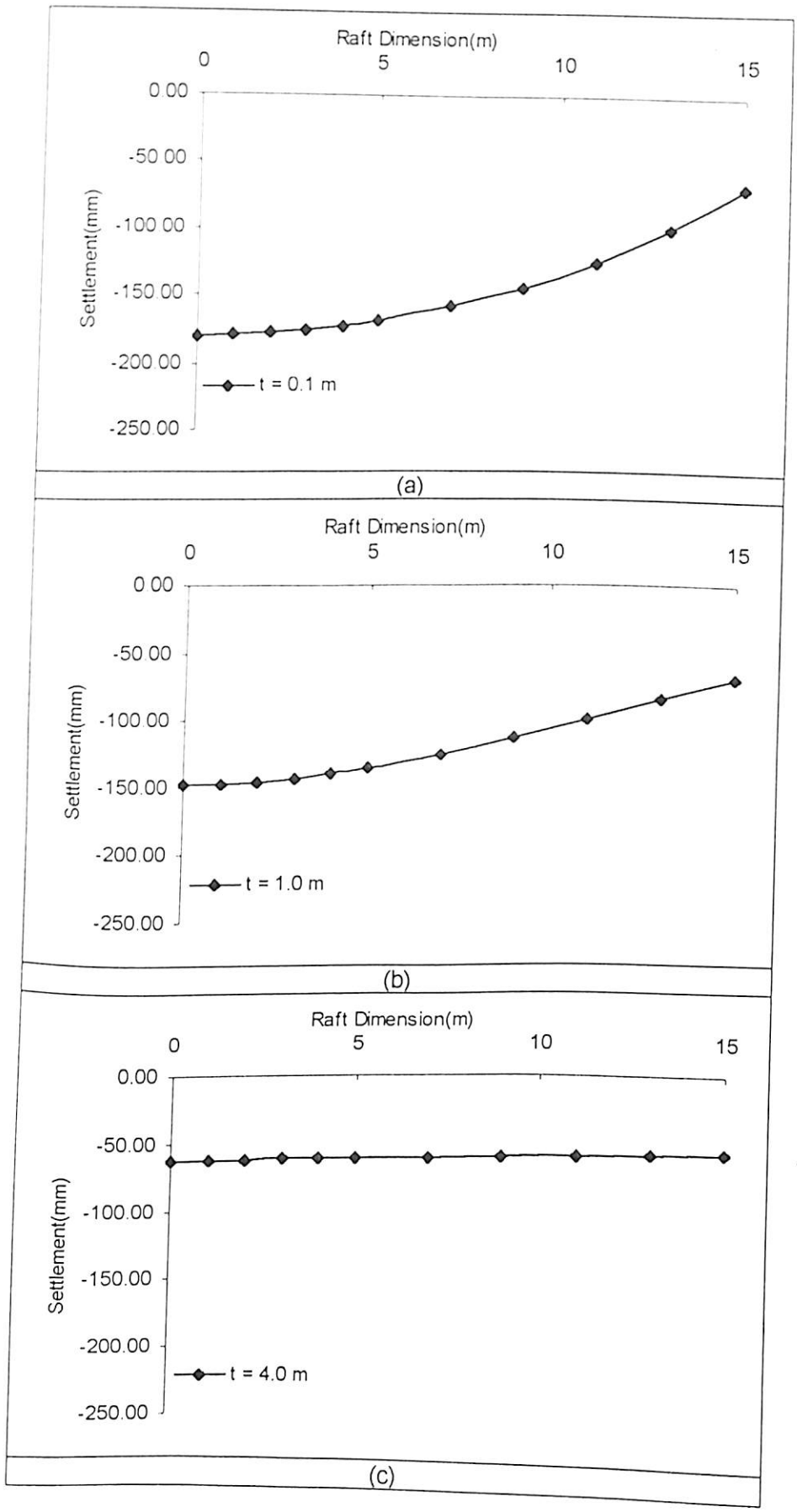

Figure 5.58 Settlement Profile of Raft
(D = 30 m, E_s = 130000 kN/m^2, P = 281800.9 kN)

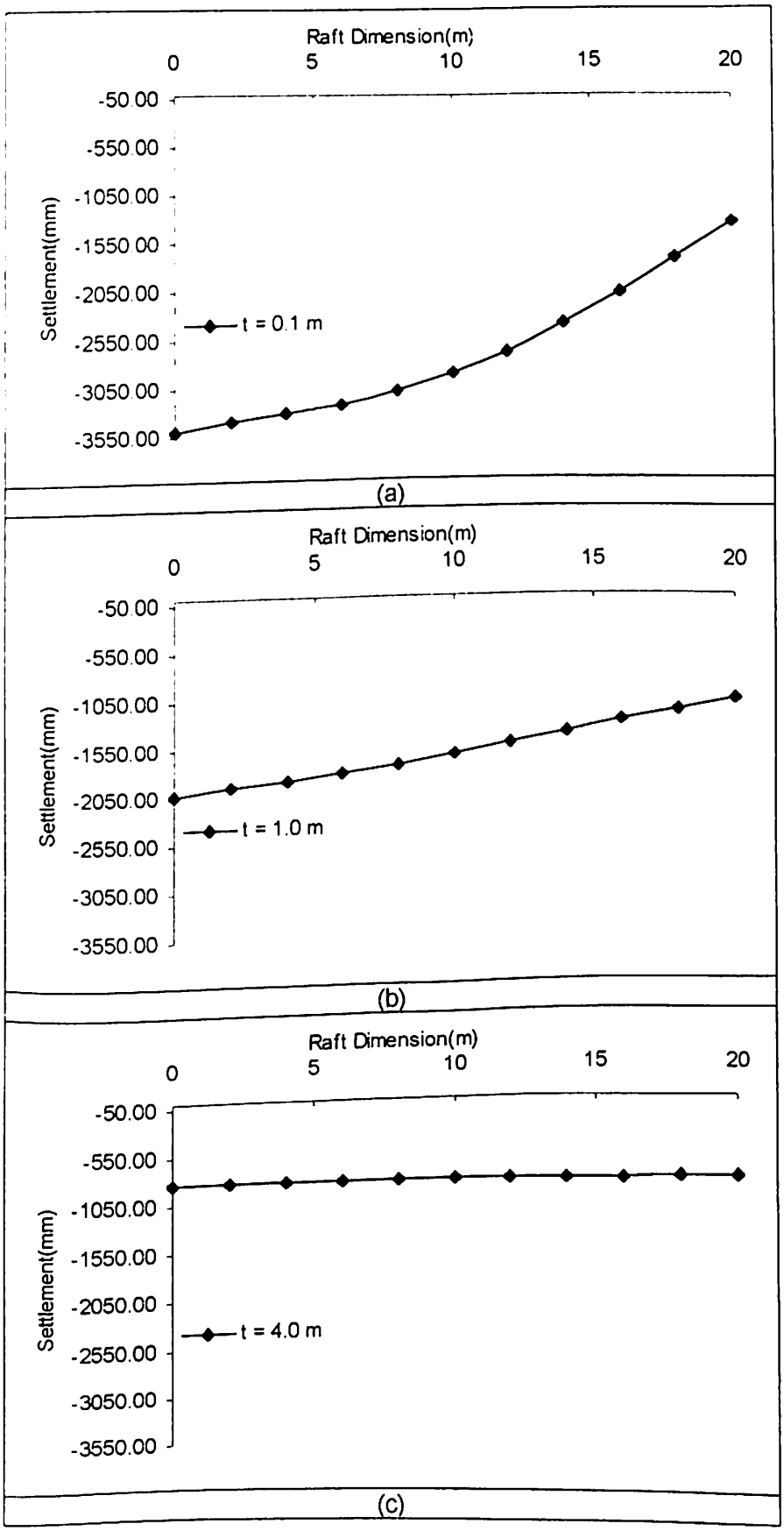

Figure 5.59 Settlement Profile of Raft
(D = 40 m, E_s = 22000 kN/m^2, P = 281800.9 kN)

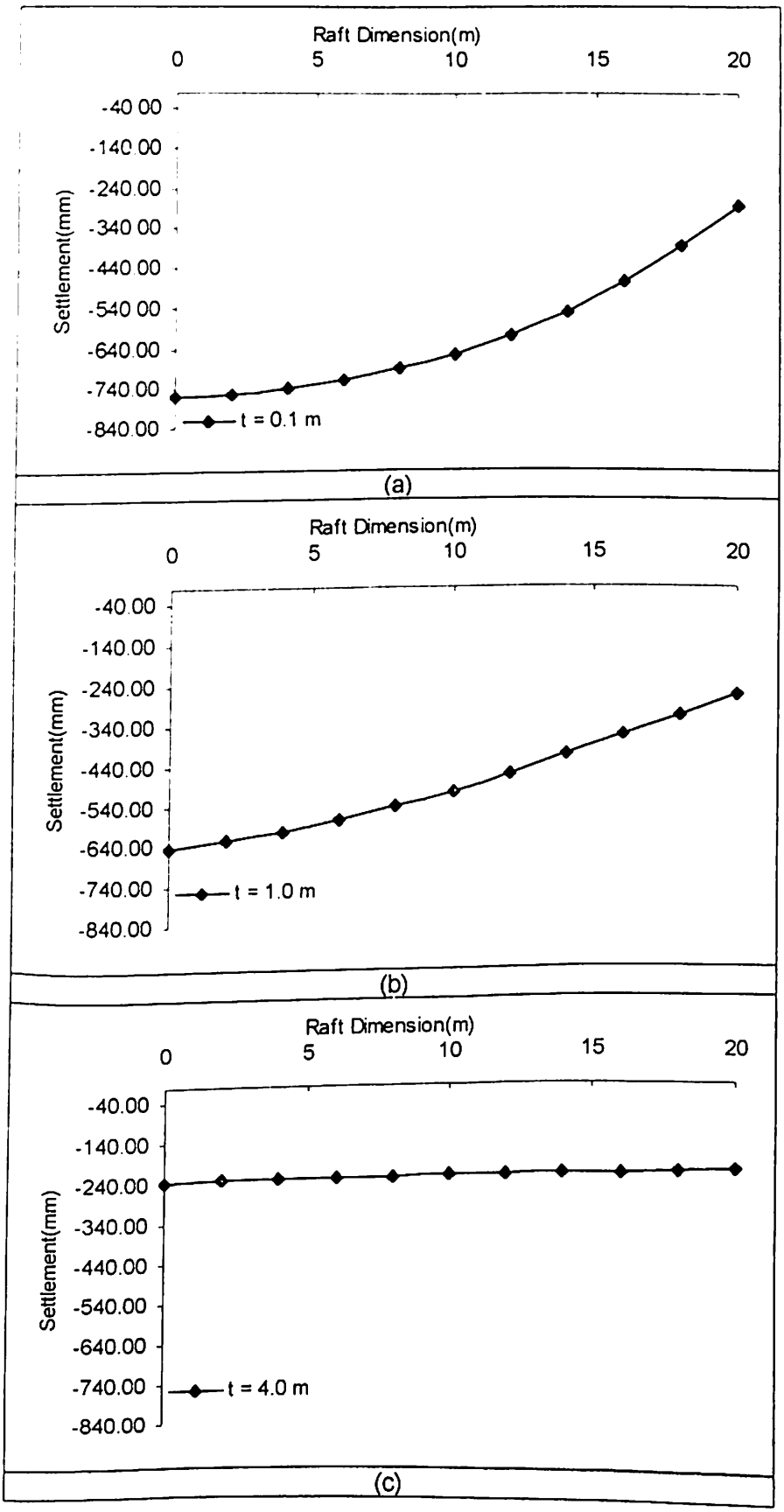

Figure 5.60 Settlement Profile of Raft
(D = 40 m, E_s = 76000 kN/m^2, P = 527598.1 kN)

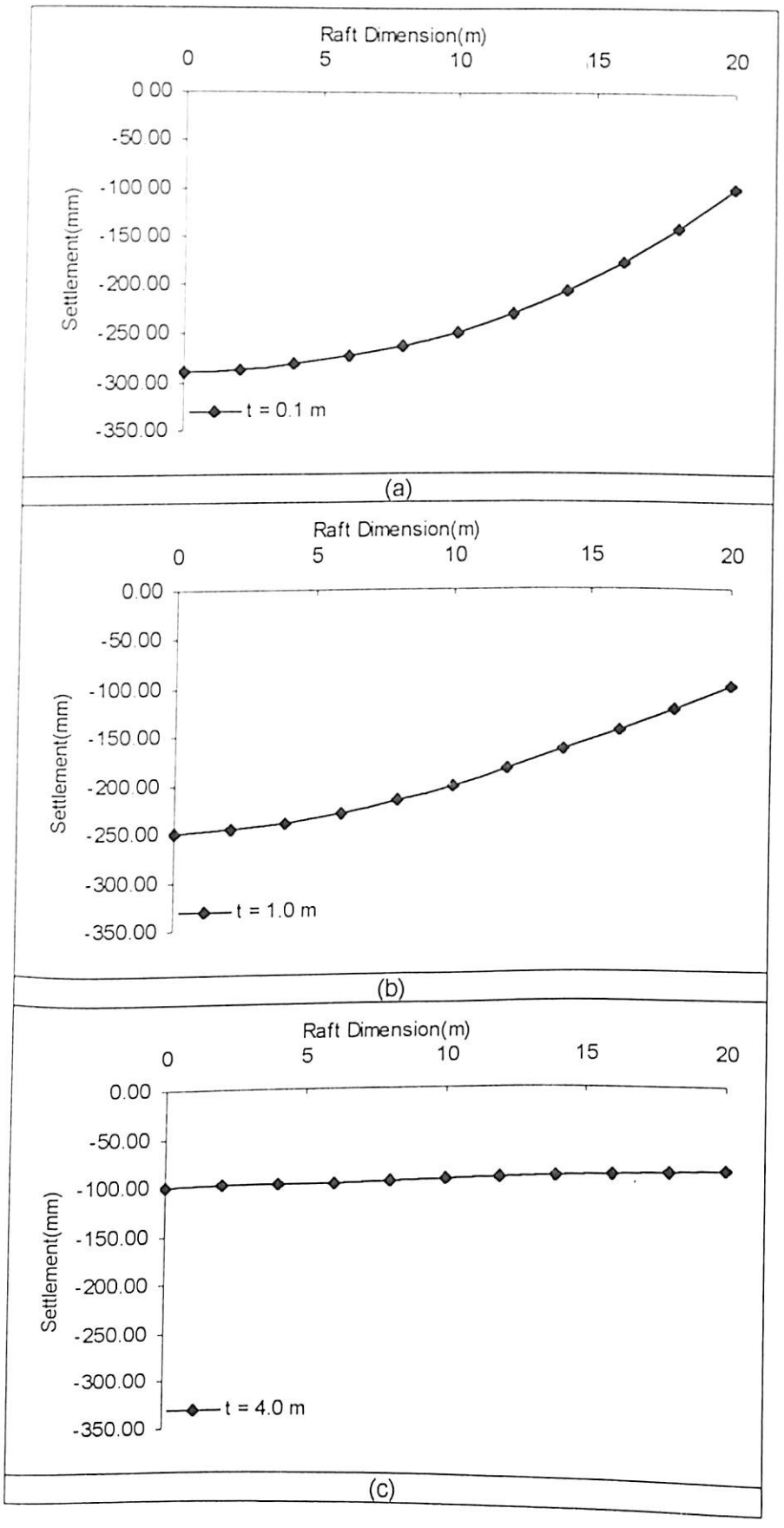

Figure 5.61 Settlement Profile of Raft
(D = 40 m, E_s = 130000 kN/m^2, P = 527598.1 kN)

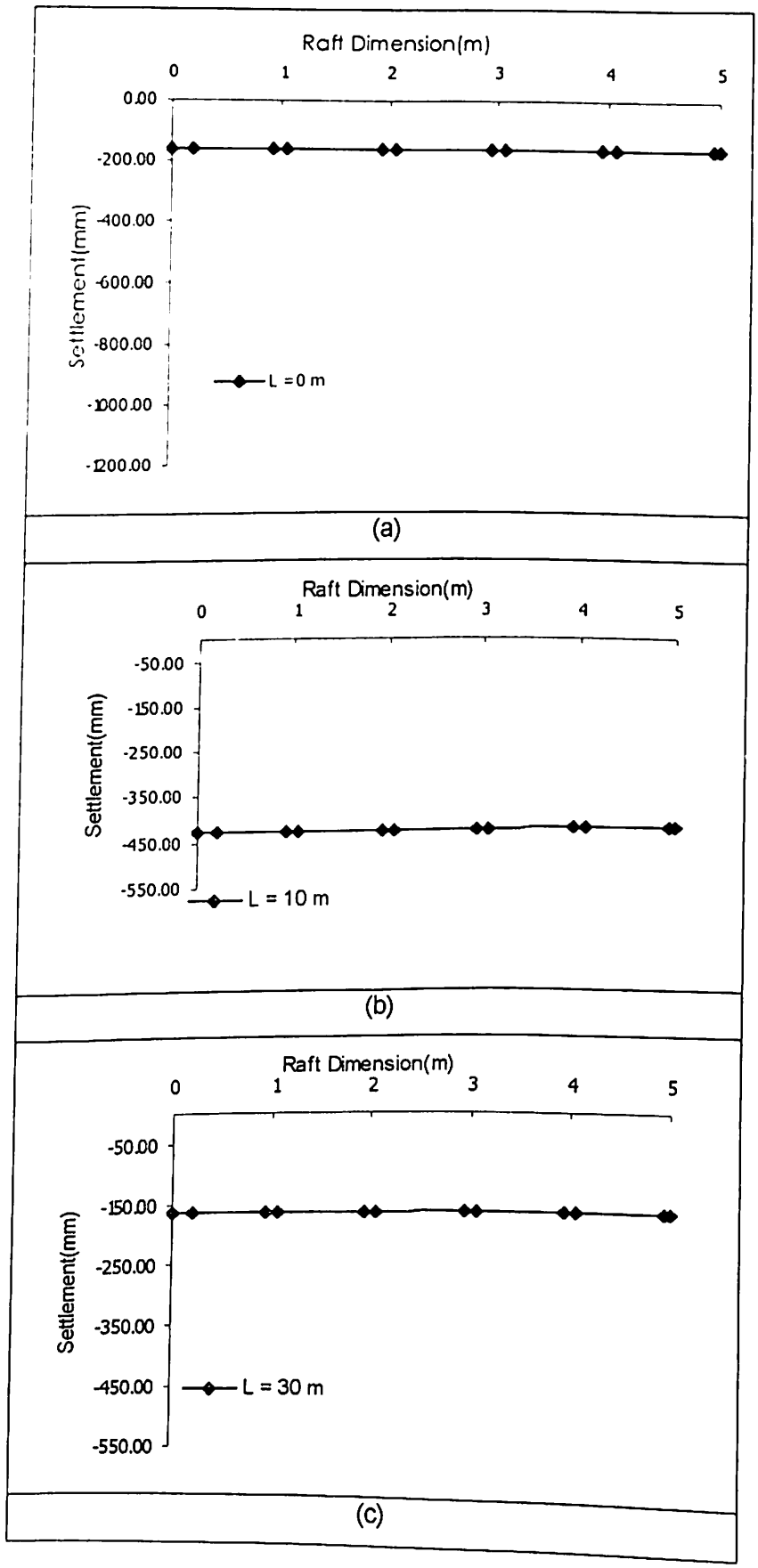

Figure 5.62 Settlement Profile of Raft in Piled Raft Foundation (D = 10 m, s/d = 2.5, E_s = 22000 kN/m^2, P = 527598.1 kN, t =1.0 m)

even when pile of length equal to the diameter of raft is provided below the raft (Figure 5.62 (b)). When pile of larger length is provided, no differential settlement is observed and the overall settlement is found to reduce.

5.6.5.2 Effect of Soil Modulus

Figures 5.63 (a), (b), (c) and Figures 5.64 (a), (b), (c) show the settlement profiles for different soil modulus of raft diameter 10 and s/d = 2.5. The effect of increase in soil modulus is found to reduce the overall settlement of piled raft foundation. The settlement profile is found similar as seen in Figure 5.62.

Figures 5.65 (a), (b), (c), Figures 5.66 (a), (b), (c) and Figures 5.67 (a), (b), (c) show the settlement profile for s/d=5 and for varying soil modulus for raft diameter 10 meter. The effect of increase in spacing is to increase the differential settlement and the overall settlement. With increase in length of pile differential settlement has almost become zero i.e. no differential settlement is there. The effect of increase in soil modulus is to reduce the overall settlement.

Figures 5.68 (a), (b), (c), Figures 5.69 (a), (b), (c) and Figures 5.70 (a), (b), (c) show the settlement profiles of raft diameter 10 meter and s/d=7.5. The effect of increase in spacing is to increase the overall settlement. With increase in length of pile the differential settlement reduces to almost zero. The effect of increase in soil modulus is to reduce the overall settlement of piled raft foundation.

Figures 5.71 (a), (b), (c), Figures 5.72 (a), (b, (c) and Figures 5.73 (a), (b), (c) show the settlement profiles for piled raft foundation whose raft diameter is 20 meter and spacing to diameter ratio of pile 5.0. Differential settlement is seen in the raft foundation, which reduces with addition of pile and becomes zero with increase in length of the pile. The effect of increase in soil modulus is to reduce the overall settlement.

Figures 5.74 (a), (b), (c), Figures 5.75 (a), (b, (c) and Figures 5.76 (a), (b), (c) show the settlement profiles for piled raft foundation whose raft diameter is 20 meter and spacing to diameter ratio of pile 7.5. Differential settlement is seen in the raft foundation, which

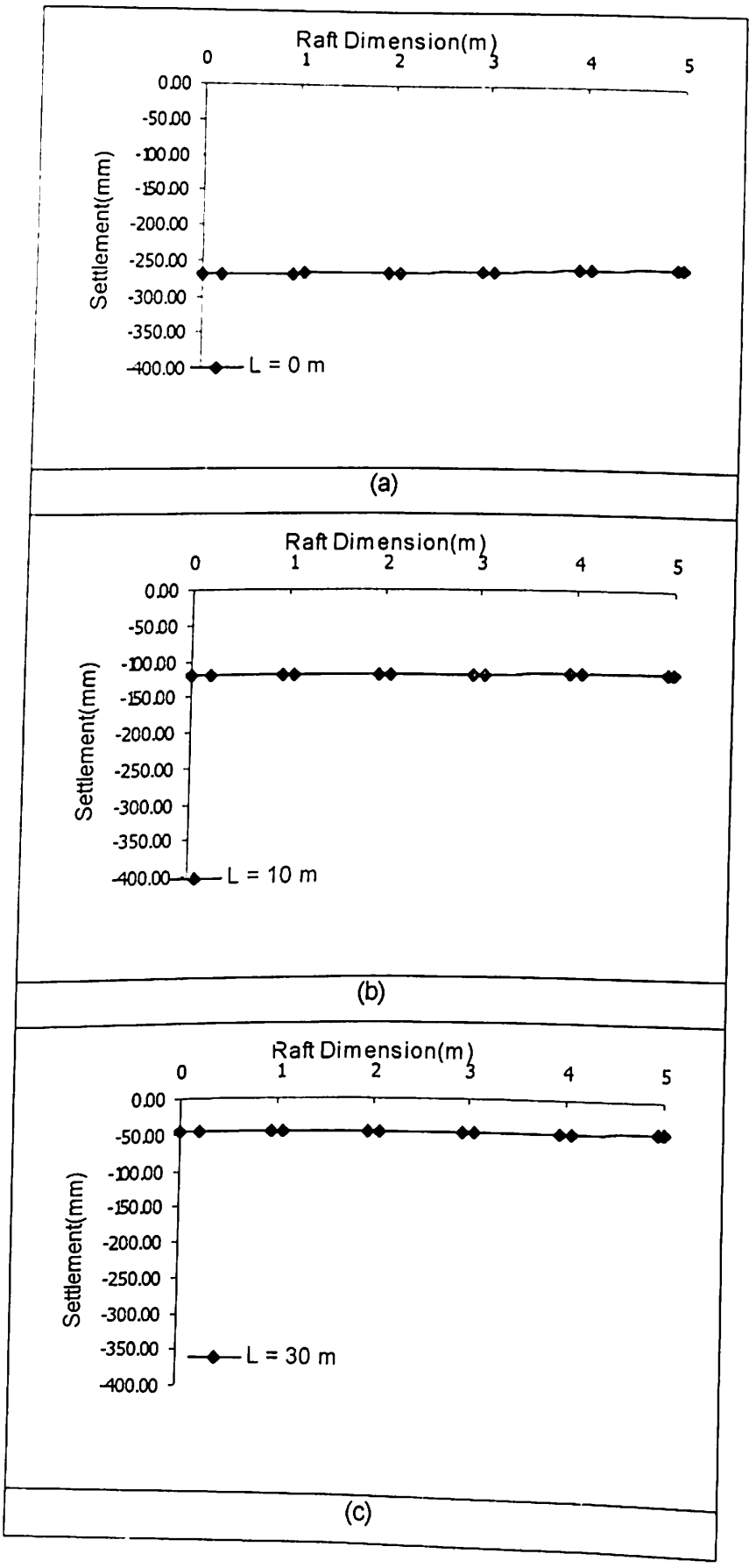

Figure 5.63 Settlement Profile of Raft in Piled Raft Foundation (D = 10 m, s/d = 2.5, E_s = 76000 kN/m^2, P = 75931.62 kN, t = 1.0 m)

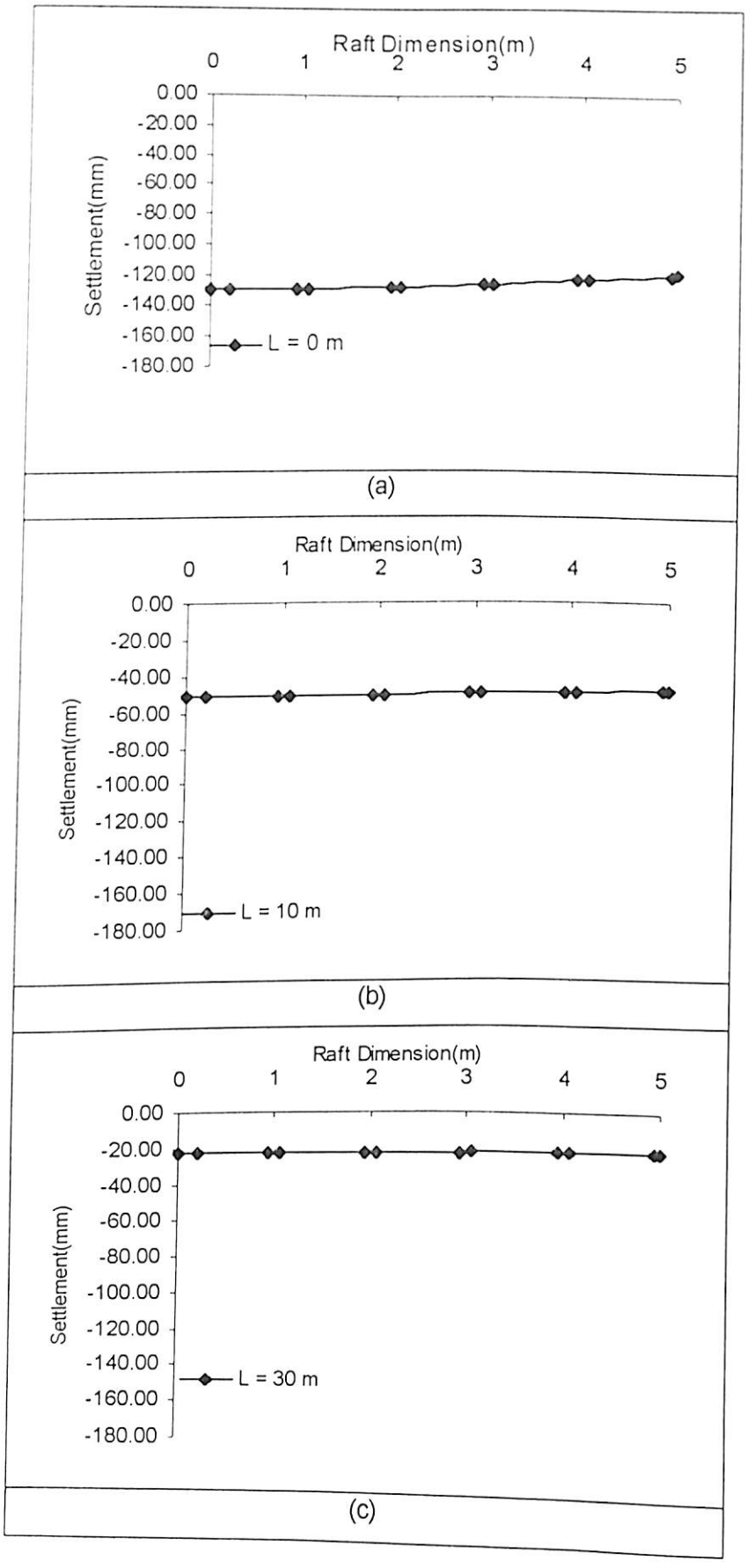

Figure 5.64 Settlement Profile of Raft in Piled Raft Foundation
(D = 10 m, s/d = 2.5, E_s = 130000 kN/m^2, P = 75931.62 kN, t = 1.0 m)

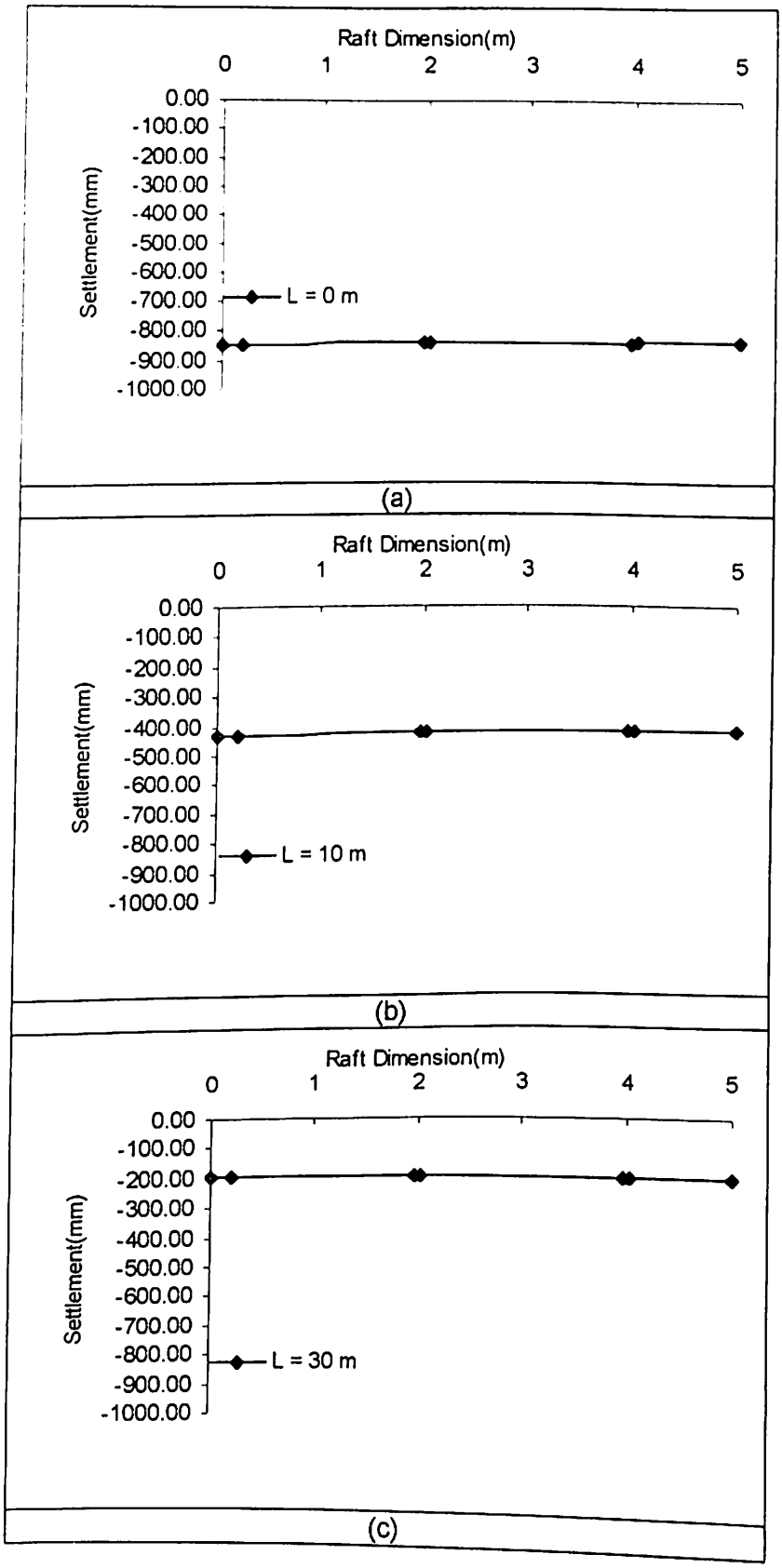

Figure 5.65 Settlement Profile of Raft in Piled Raft Foundation (D = 10 m, s/d = 5, E_s = 22000 kN/m^2, P = 62265.75 kN, t = 1.0 m)

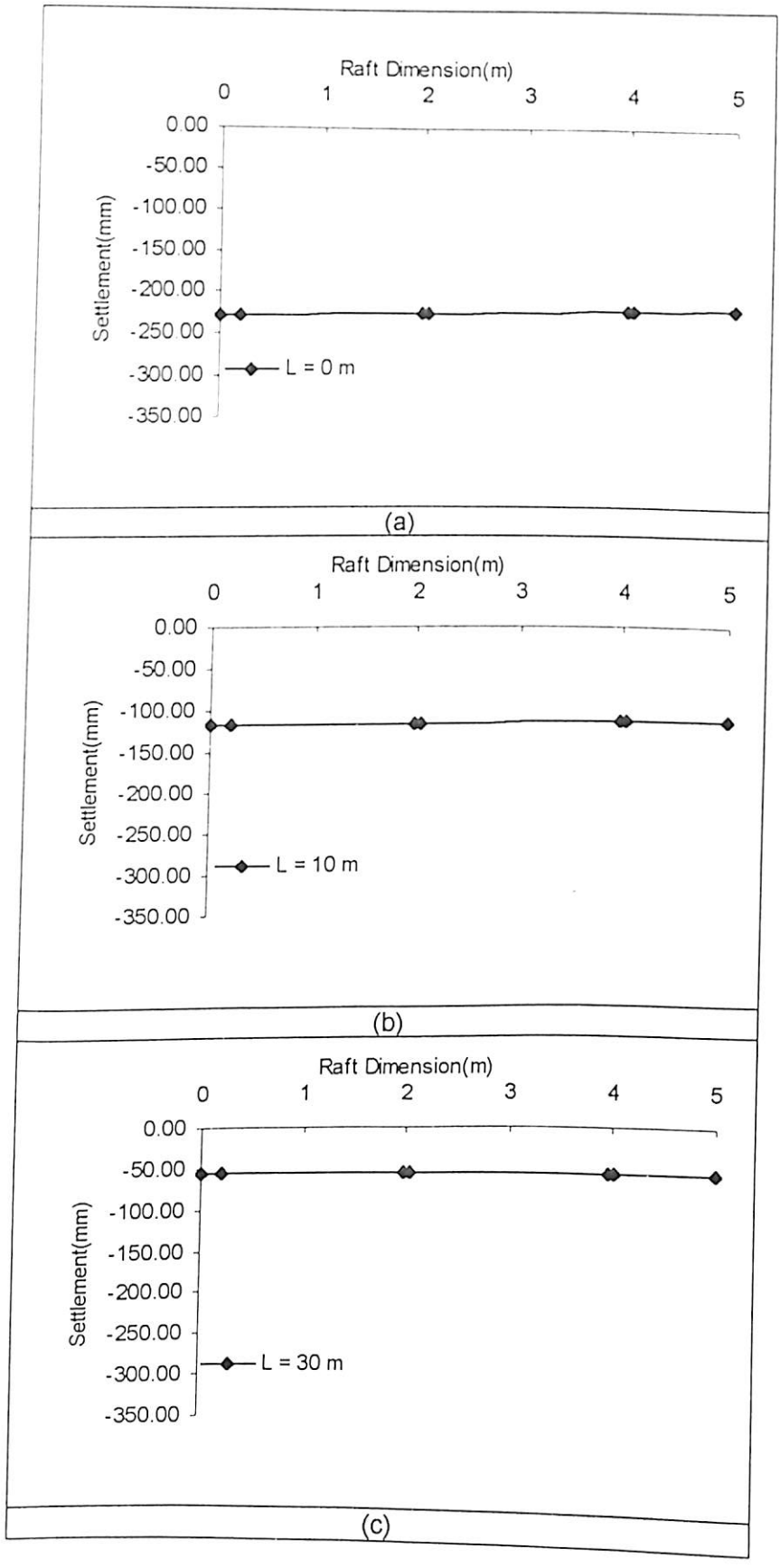

Figure 5.66 Settlement Profile of Raft in Piled Raft Foundation
(D = 10 m, s/d = 5, E_s = 76000 kN/m^2, P = 62265.75 kN, t = 1.0 m)

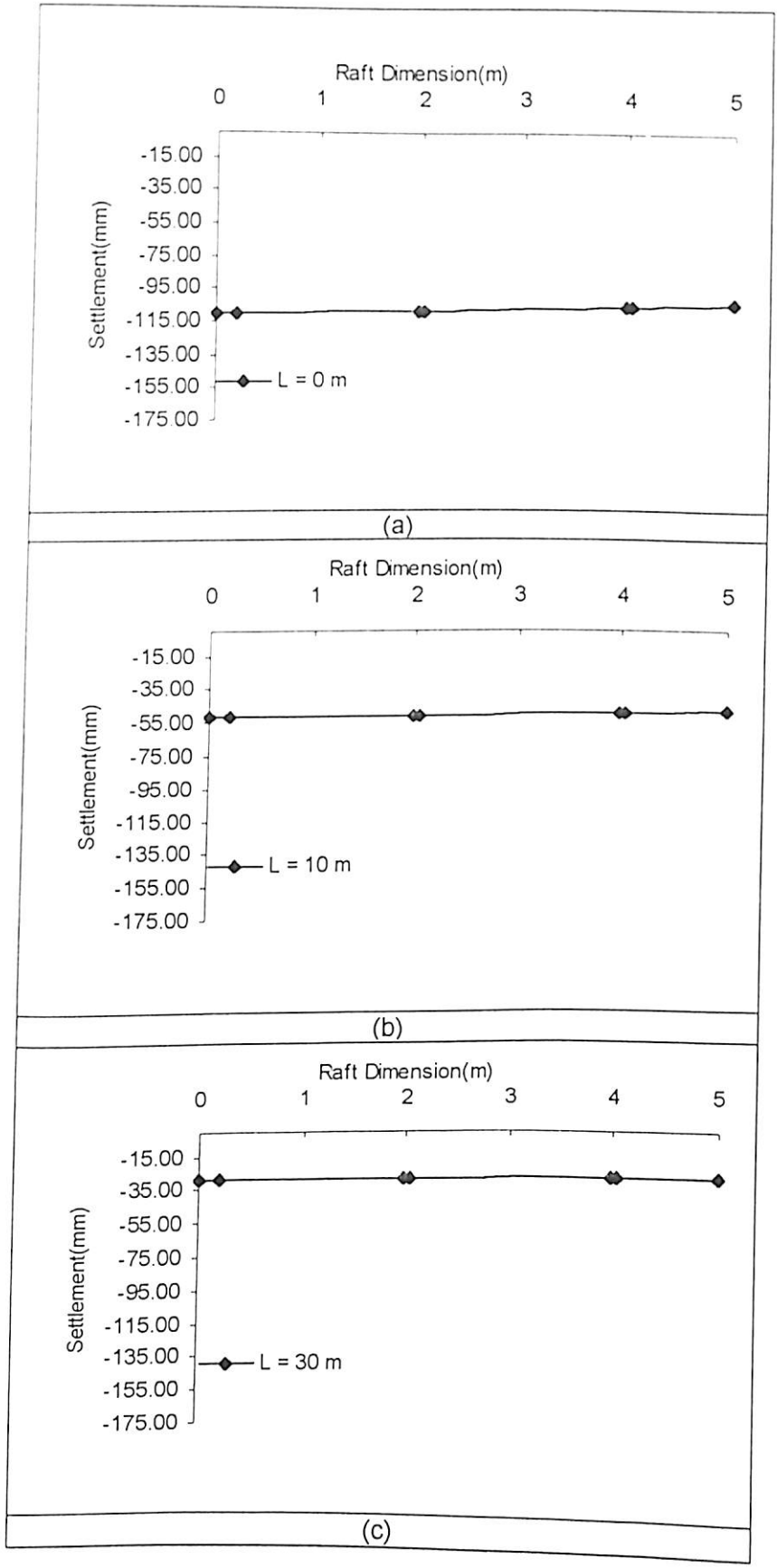

Figure 5.67 Settlement Profile of Raft in Piled Raft Foundation (D = 10 m, s/d = 5, E_s = 130000 kN/m^2, P = 62265.75 kN, t = 1.0 m)

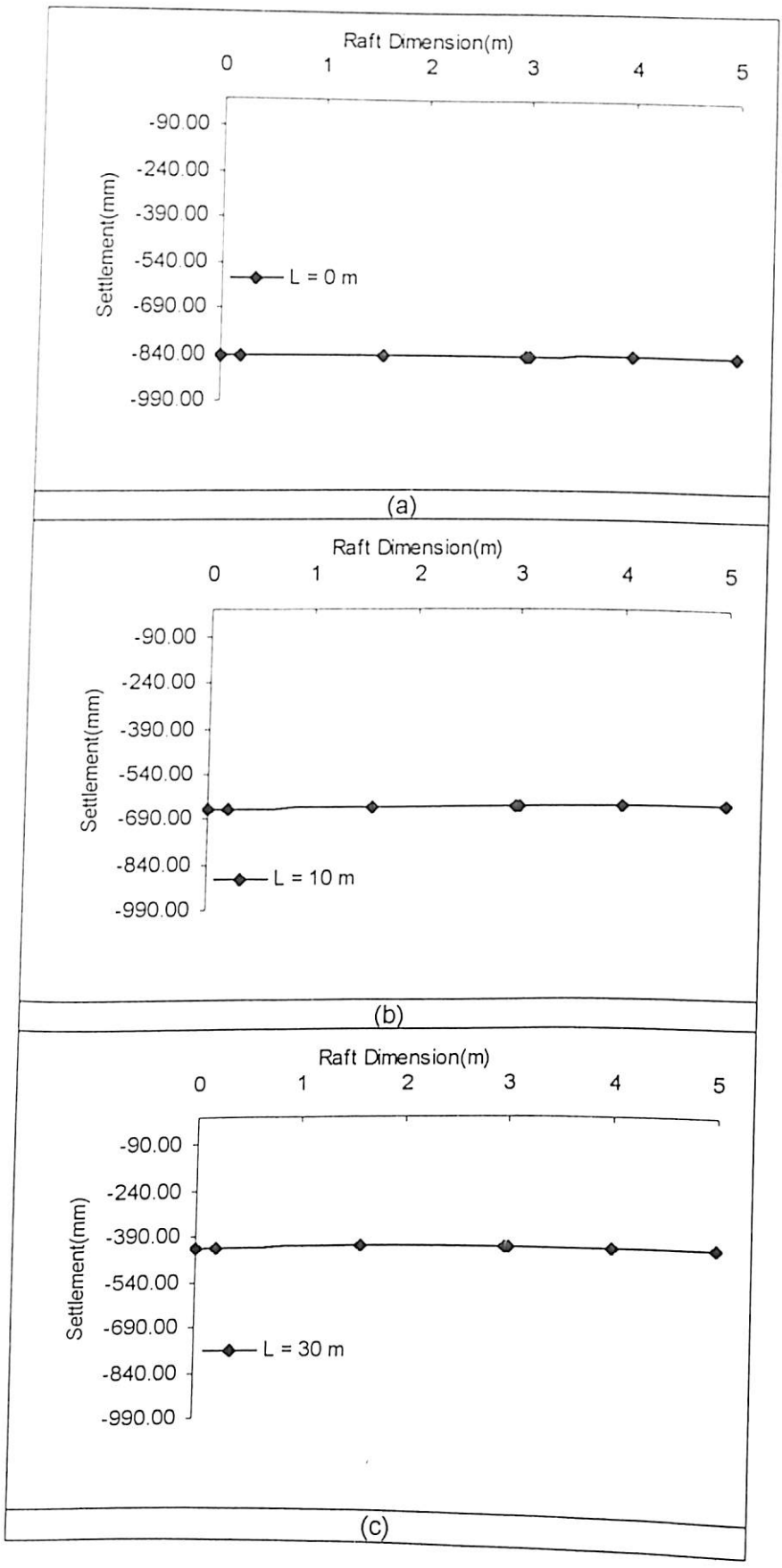

Figure 5.68 Settlement Profile of Raft in Piled Raft Foundation (D = 10 m, s/d =7.5, E_s = 22000 kN/m^2, P = 62230.94 kN, t = 1.0 m)

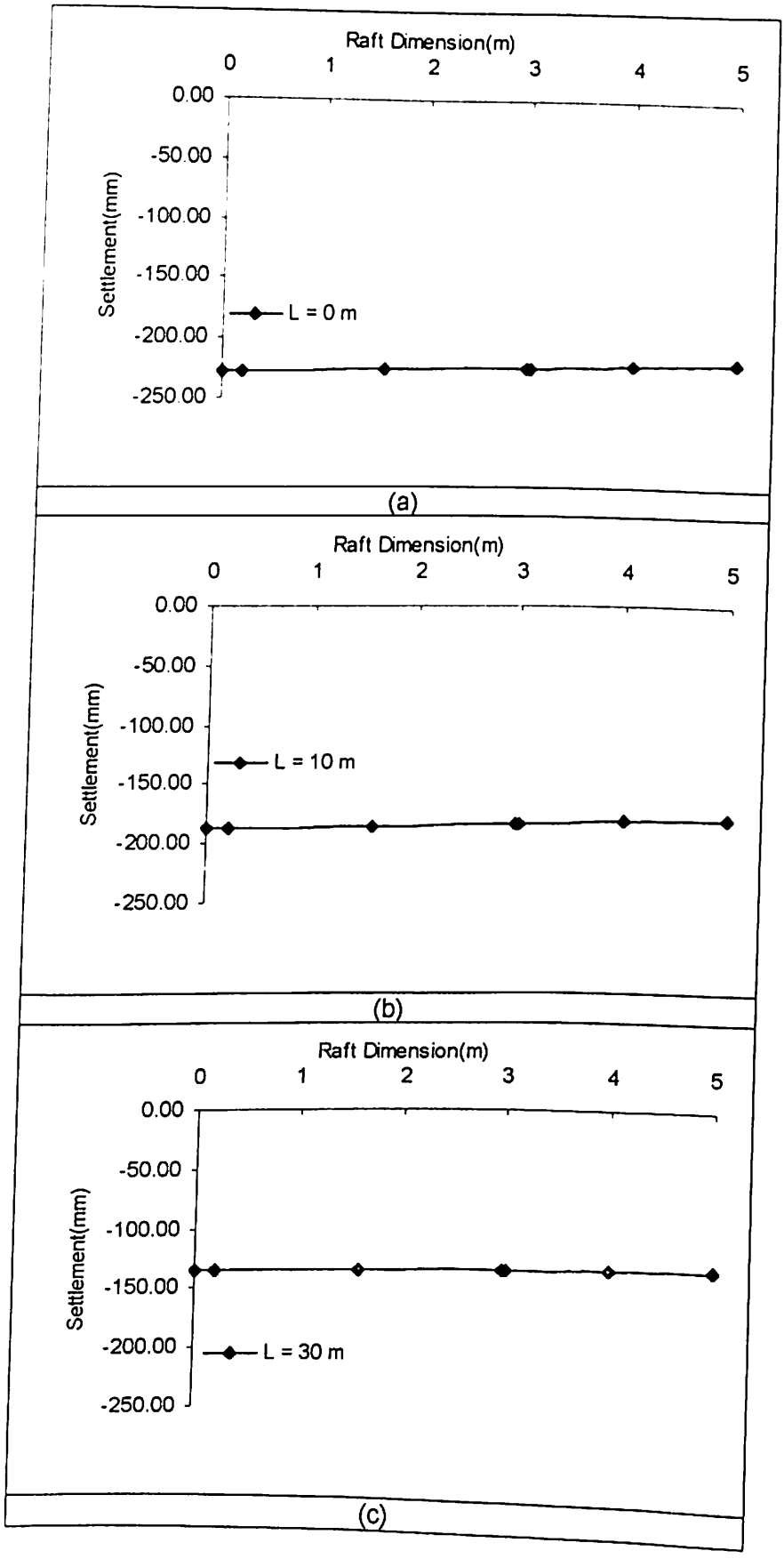

Figure 5.69 Settlement Profile of Raft in Piled Raft Foundation (D = 10 m, s/d =7.5, E_s = 76000 kN/m^2, P = 62230.94 kN, t = 1.0 m)

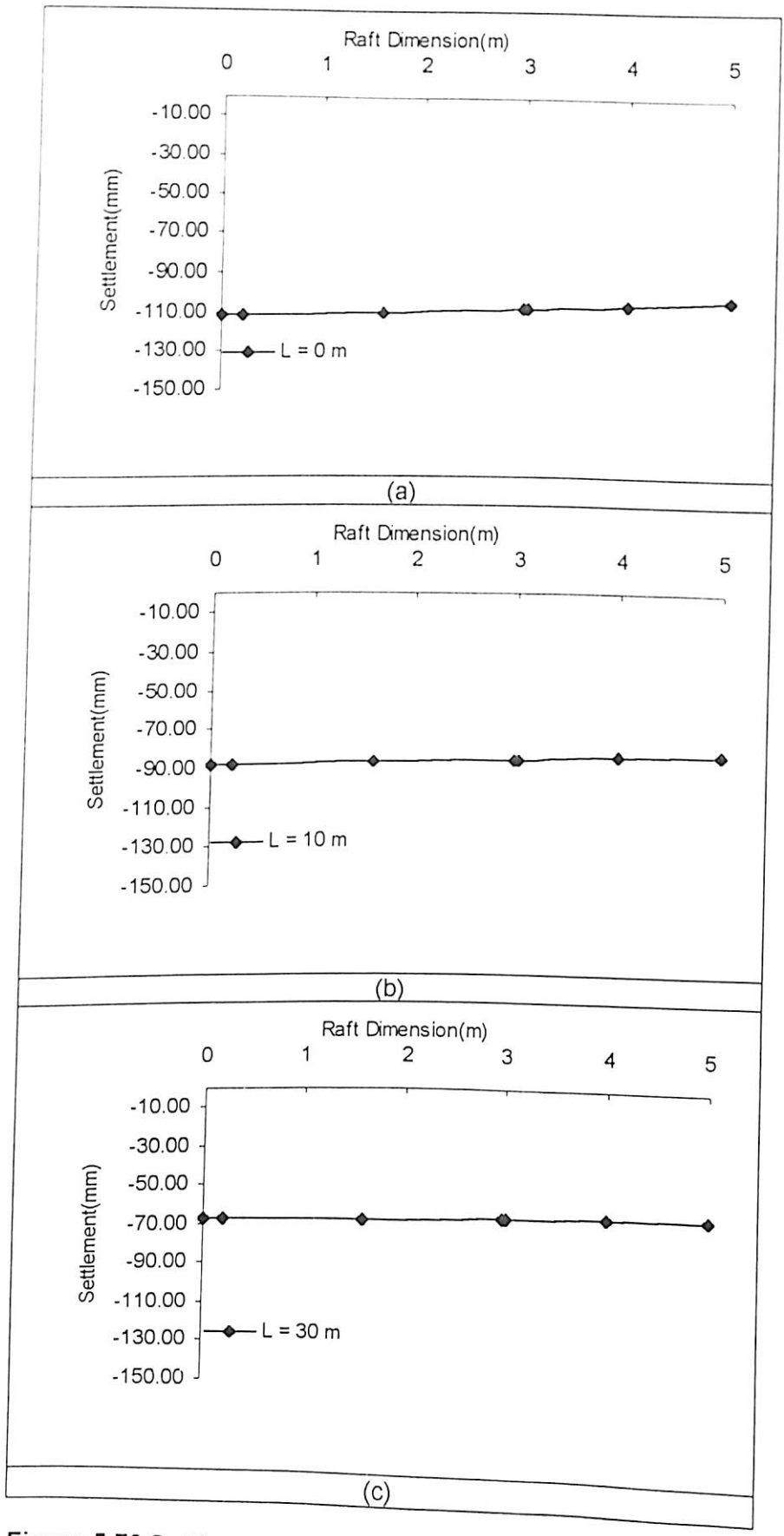

Figure 5.70 Settlement Profile of Raft in Piled Raft Foundation (D = 10 m, s/d =7.5, E_s =130000 kN/m^2, P = 62230.94 kN, t = 1.0 m)

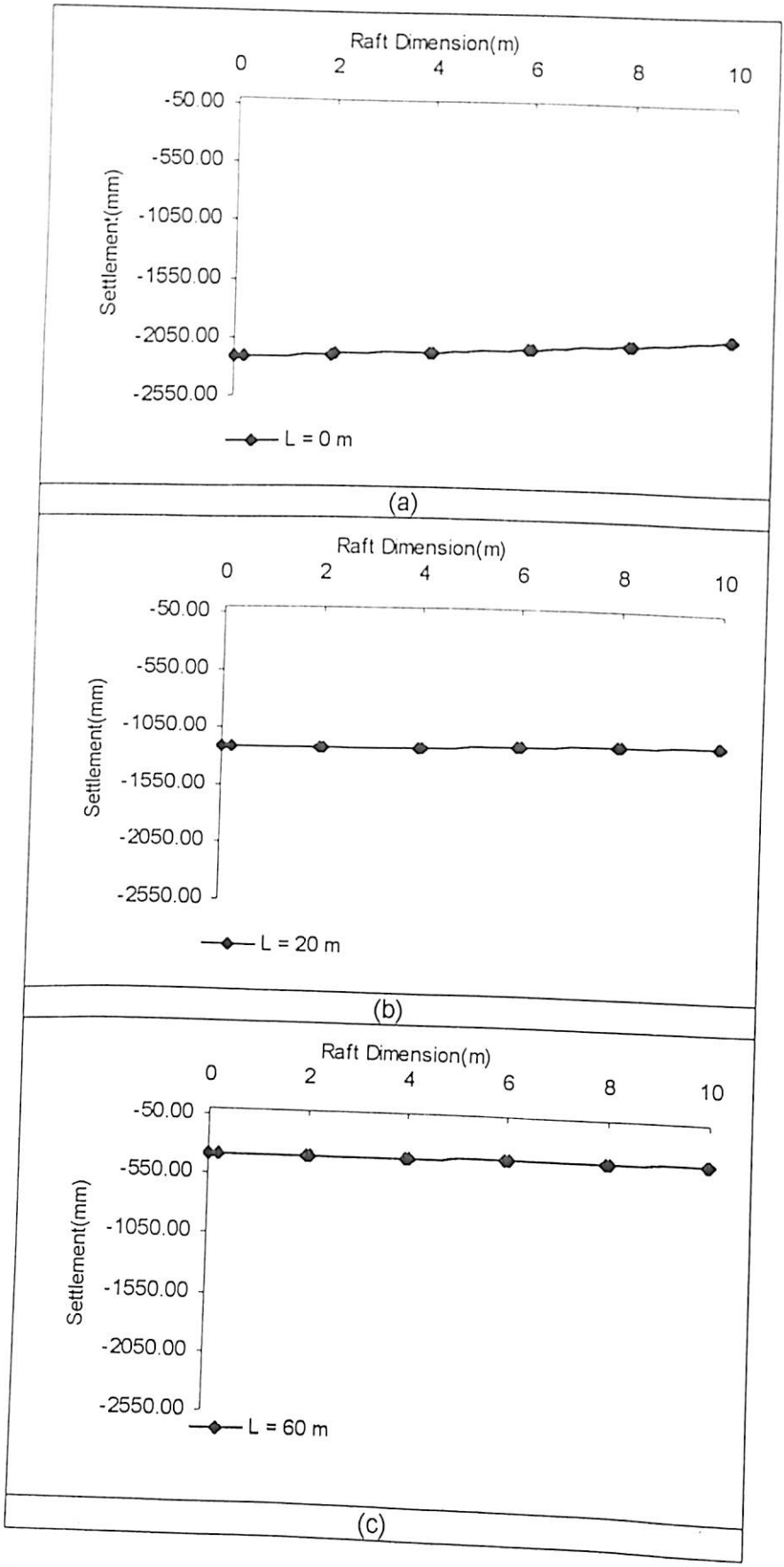

Figure 5.71 Settlement Profile of Raft in Piled Raft Foundation
(D = 20 m, s/d = 5, E_s = 22000 kN/m^2, P = 303557.6 kN, t = 1.0 m)

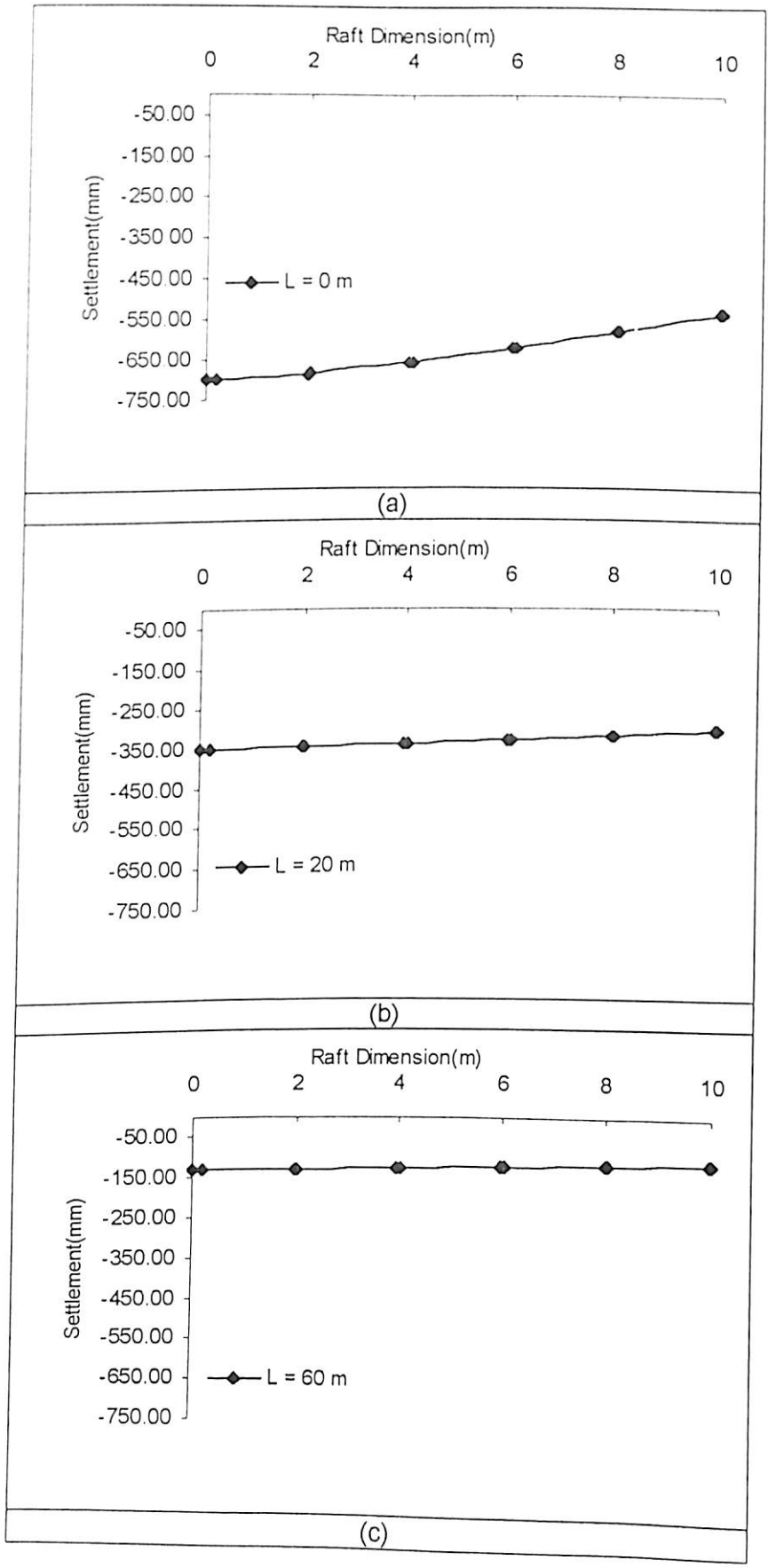

Figure 5.72 Settlement Profile of Raft in Piled Raft Foundation (D = 20 m, s/d = 5, E_s = 76000 kN/m^2, P = 303557.6 kN, t = 1.0 m)

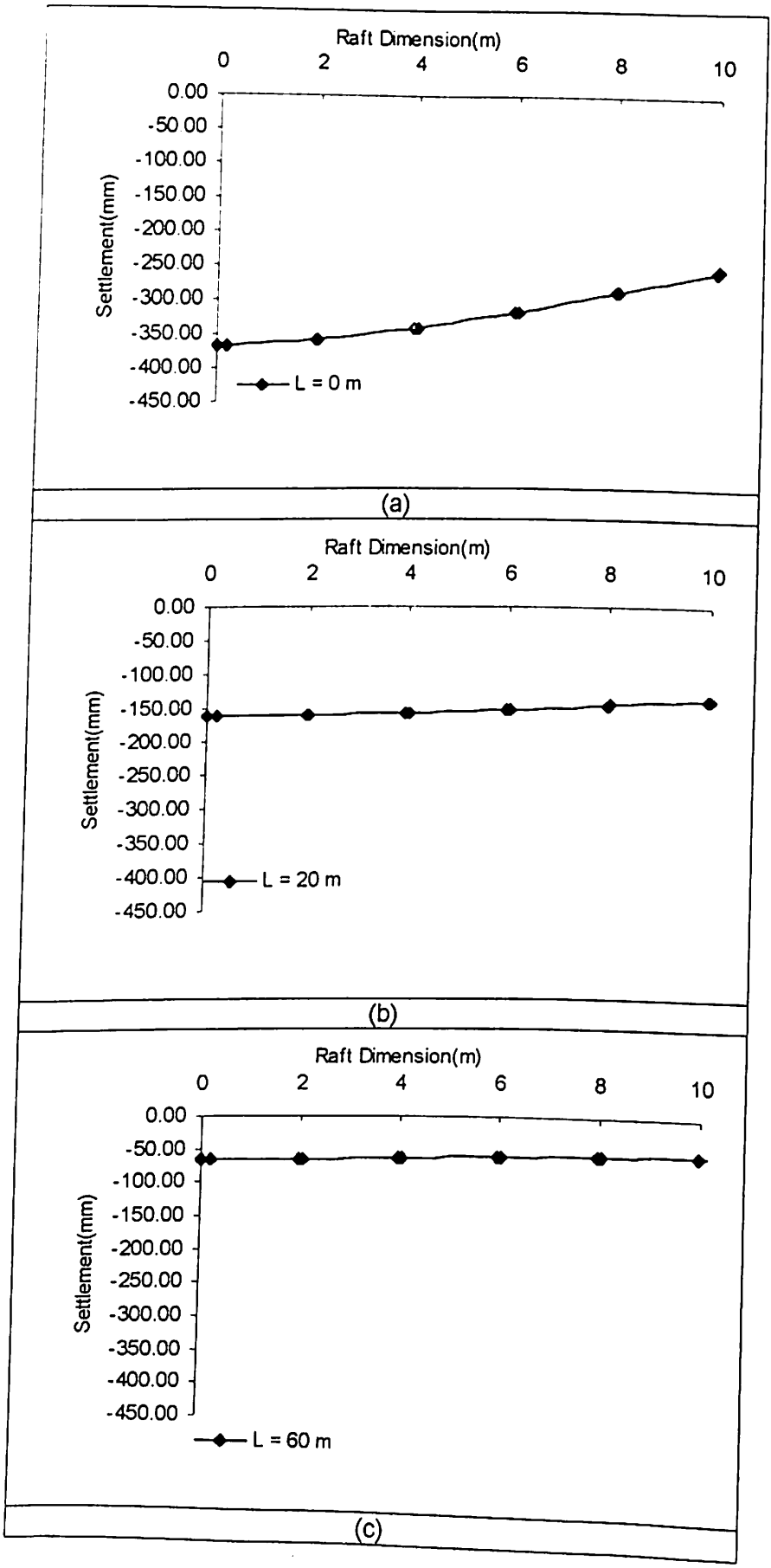

Figure 5.73 Settlement Profile of Raft in Piled Raft Foundation (D = 20 m, s/d = 5, E_s = 130000 kN/m^2, P = 303557.6 kN, t = 1.0 m)

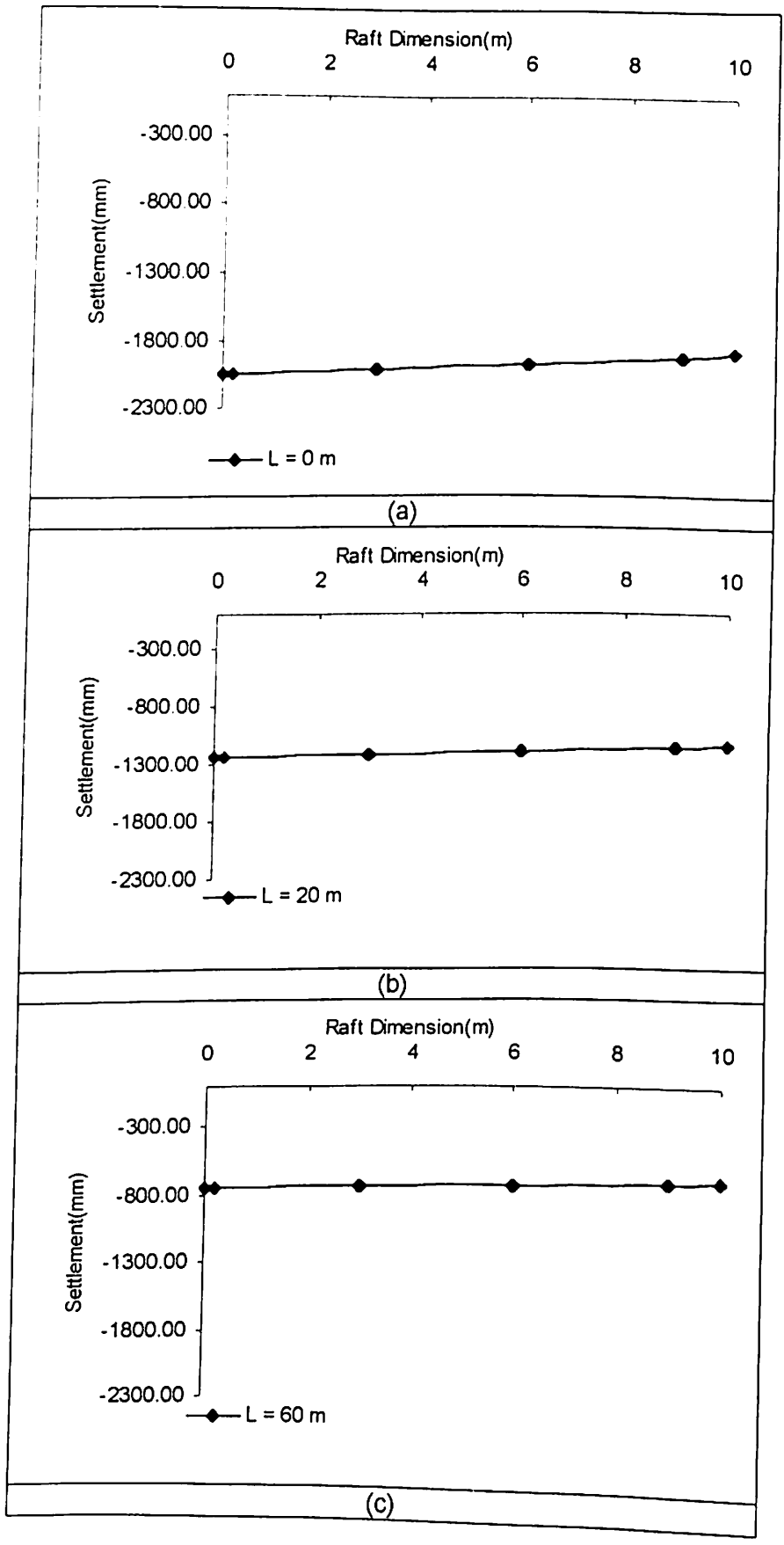

Figure 5.74 Settlement Profile of Raft in Piled Raft Foundation (D = 20 m, s/d = 7.5, E_s = 22000 kN/m^2, P = 276790.7 kN, t = 1.0 m)

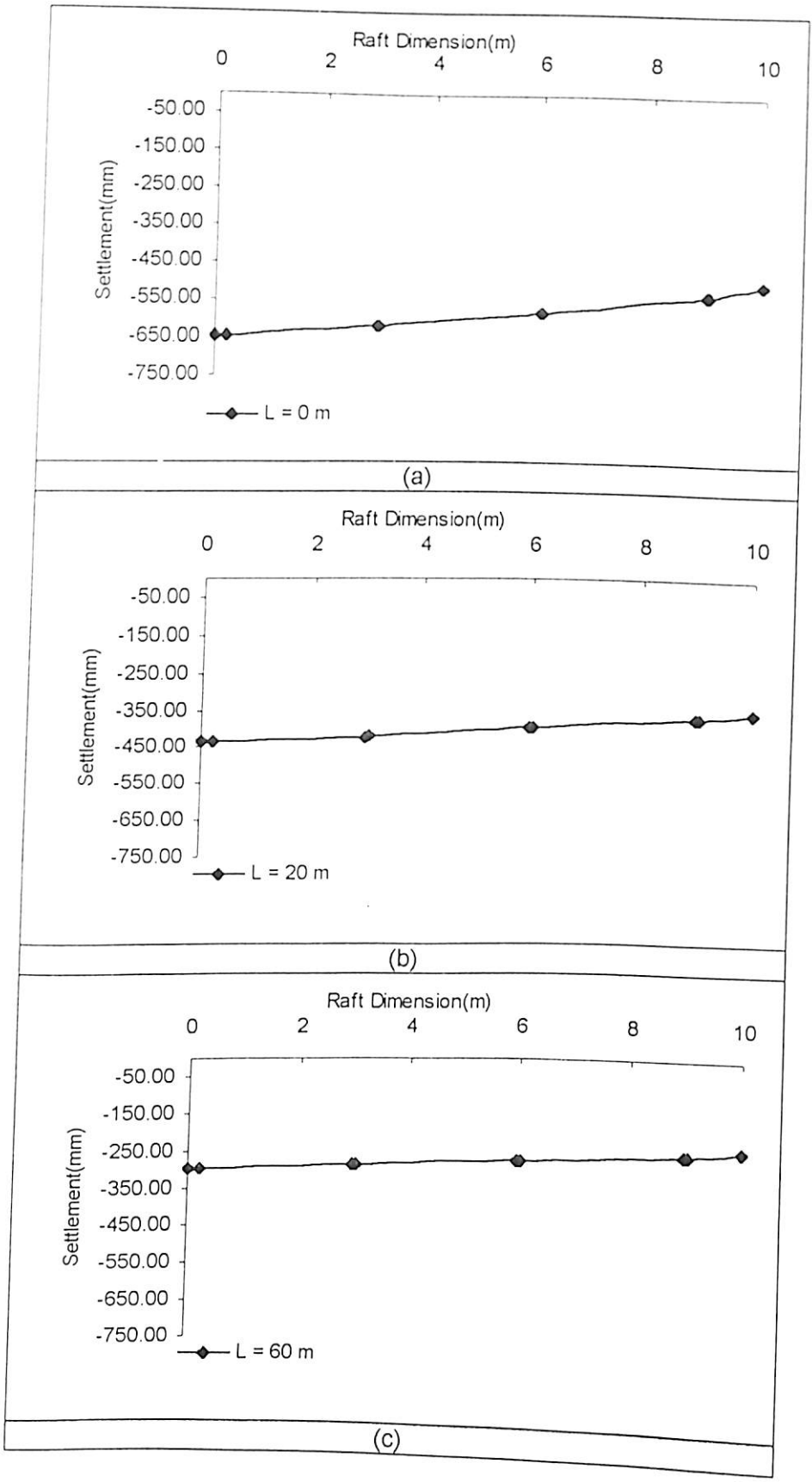

Figure 5.75 Settlement Profile of Raft in Piled Raft Foundation (D = 20 m, s/d = 7.5, E_s = 76000 kN/m^2, P = 276790.7 kN, t = 1.0 m)

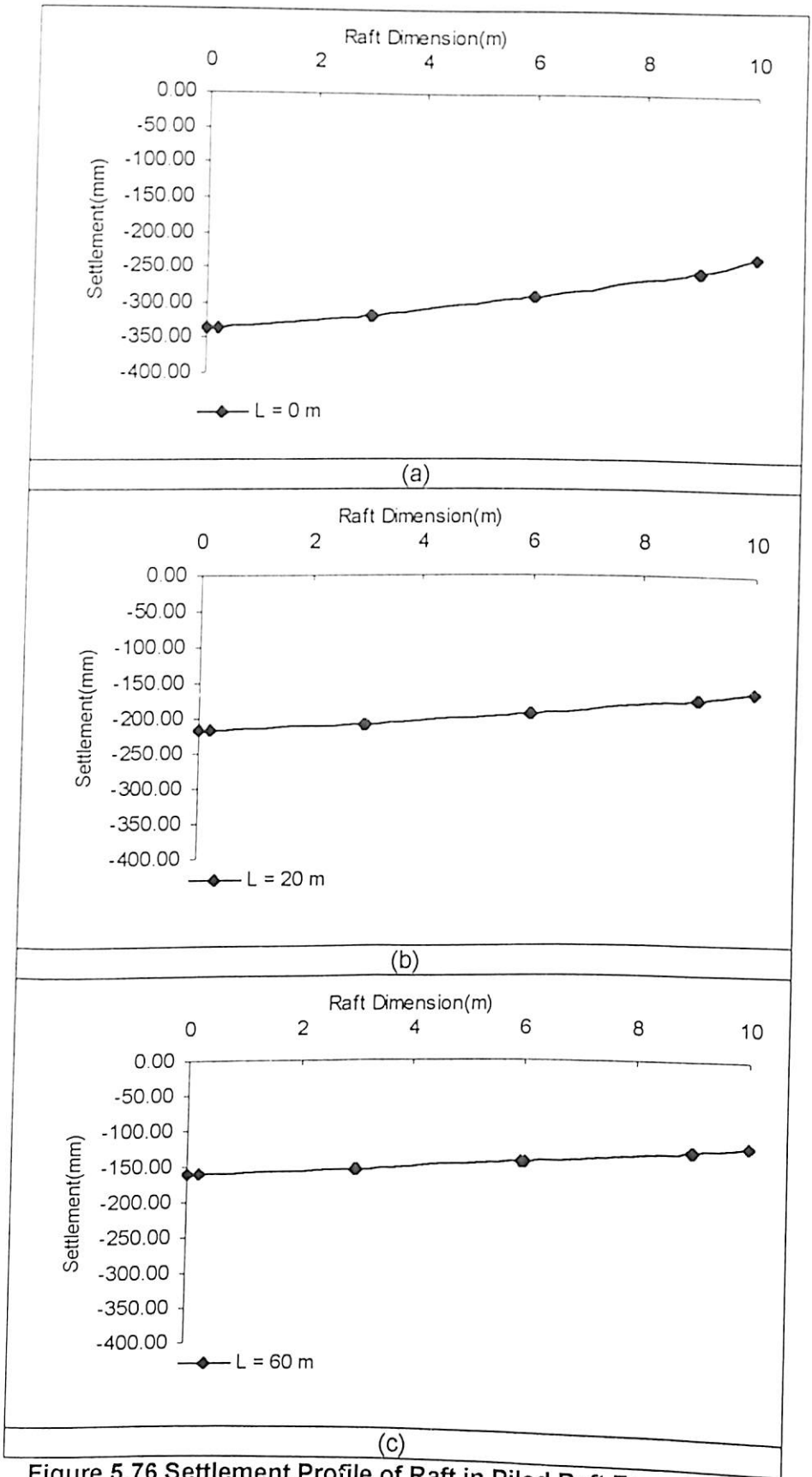

Figure 5.76 Settlement Profile of Raft in Piled Raft Foundation (D = 20 m, s/d = 7.5, E_s = 130000 kN/m^2, P = 276790.7 kN, t = 1.0 m)

reduces with addition of pile and becomes zero with increase in length of the pile. The effect of increase in soil modulus is to reduce the overall settlement.

Figures 5.77 (a), (b), (c), Figures 5.78 (a), (b), (c) and Figures 5.79 (a), (b), (c) show the settlement profiles for piled raft foundation whose raft diameter is 20 meter and spacing to diameter ratio of pile 10.0. Differential settlement is seen in the raft foundation, which reduces with addition of pile and becomes almost zero with increase in length of the pile. The effect of increase in soil modulus is to reduce the overall settlement.

Figures 5.80 (a), (b), (c), Figures 5.81 (a), (b, (c) and Figures 5.82 (a), (b), (c) show the settlement profiles for piled raft foundation whose raft diameter is 30 meter and spacing to diameter ratio of pile 5.0. Differential settlement is seen in the raft foundation, which reduces with addition of pile, and reduction is significant with increase in length of the pile.

Figures 5.83 (a), (b), (c), Figures 5.84 (a), (b, (c) and Figures 5.85 (a), (b), (c) show the settlement profiles for piled raft foundation whose raft diameter is 30 meter and spacing to diameter ratio of pile 7.5. As it can be seen from the settlement profile that overall settlement reduces with addition of pile, and also the differential settlement. The effect of ncrease in soil modulus is to reduce the overall

'igures 5.86 (a), (b), (c), Figures 5.87 (a), (b), (c) and Figures 5.88 (a), (b), (c) show the ettlement profiles for piled raft foundation whose raft diameter is 30 meter and spacing) diameter ratio of pile 10.0. Effect of addition of pile is found to decrease the overall ettlement as well as differential settlement The overall settlement decreases with ıcrease in soil modulus.

igures 5.89 (a), (b), (c), Figures 5.90 (a), (b), (c) and Figures 5.91 (a), (b), (c) show the ttlement profiles for piled raft foundation whose raft diameter is 50 meter and spacing diameter ratio of pile 7.5. Differential settlement is seen in the raft as well as the piled

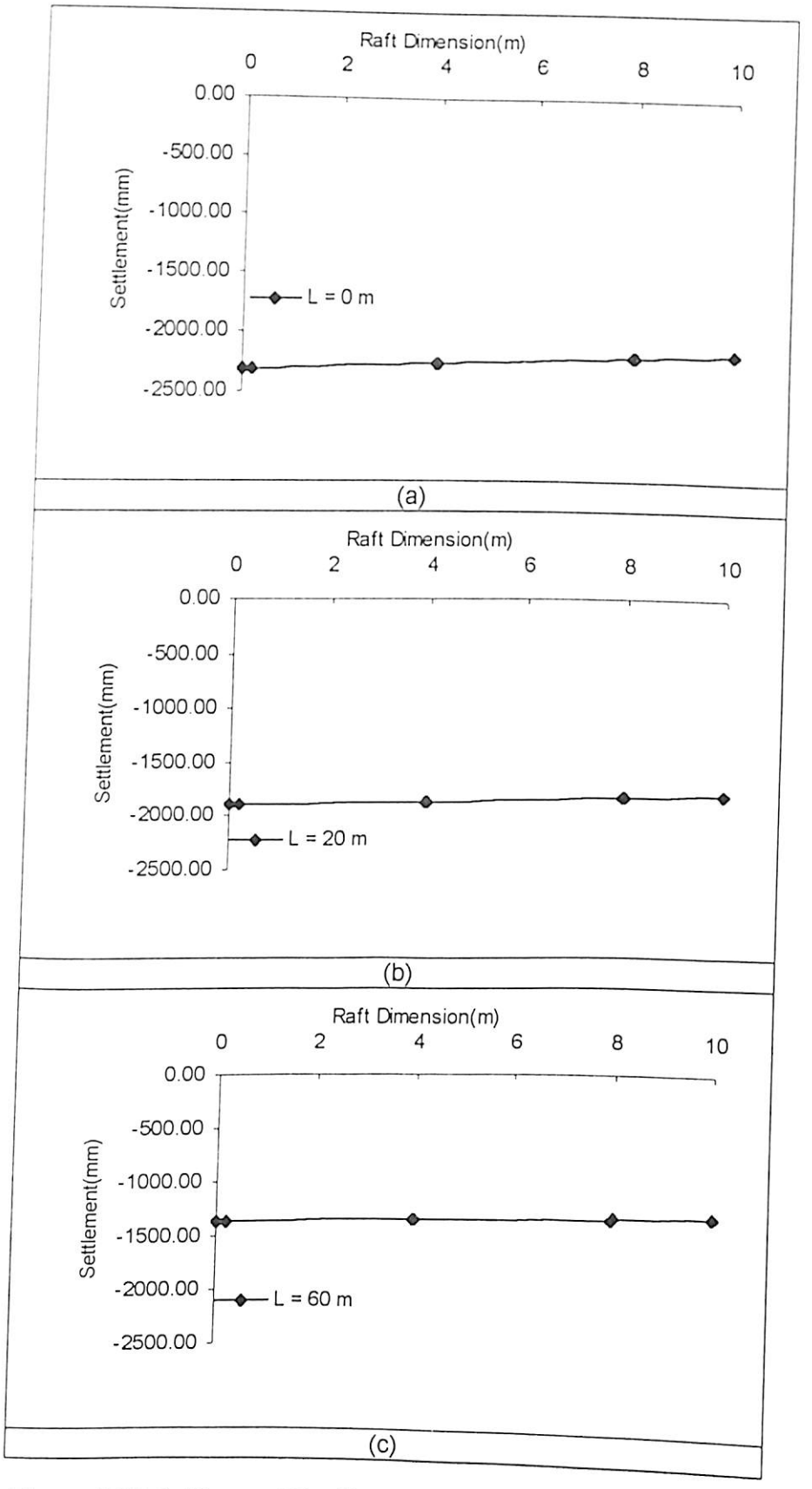

Figure 5.77 Settlement Profile of Raft in Piled Raft Foundation (D = 20 m, s/d = 10, E_s = 22000 kN/m^2, P = 288889.1 kN, t = 1.0 m)

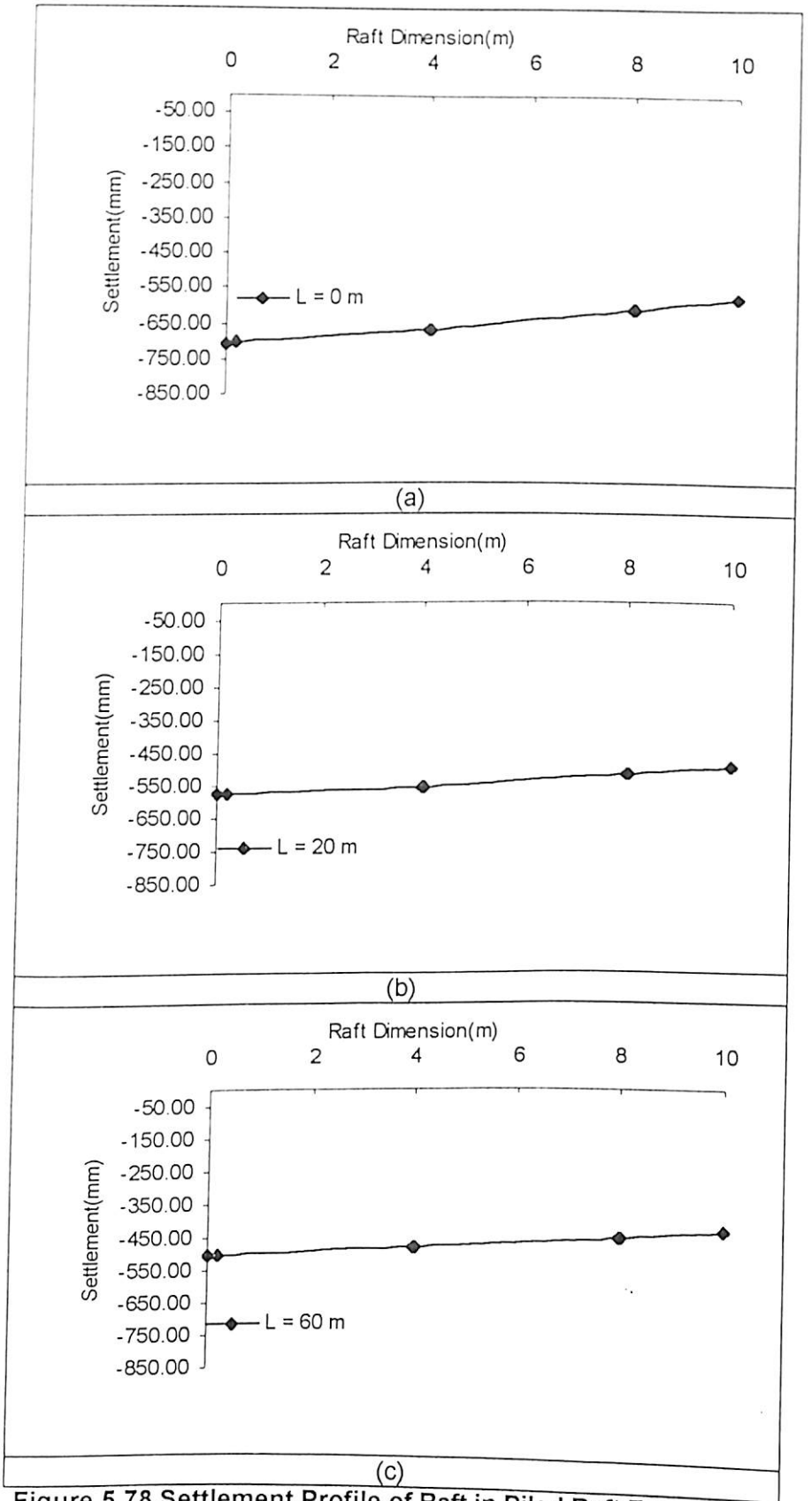

Figure 5.78 Settlement Profile of Raft in Piled Raft Foundation (D = 20 m, s/d = 10, E_s = 76000 kN/m^2, P = 288889.1 kN, t = 1.0 m)

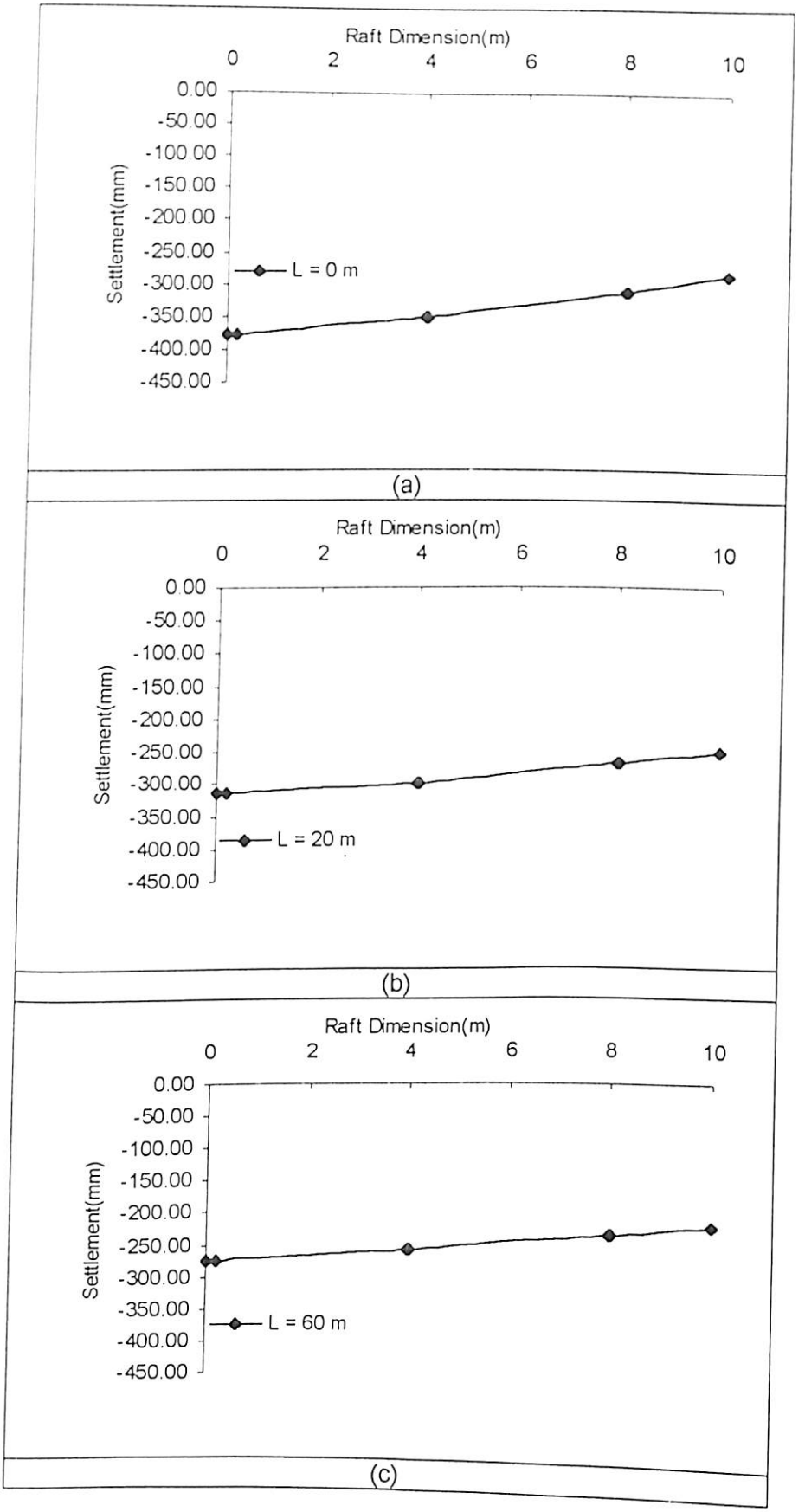

Figure 5.79 Settlement Profile of Raft in Piled Raft Foundation (D = 20 m, s/d = 10, E_s = 130000 kN/m^2, P = 288889.1 kN, t = 1.0 m)

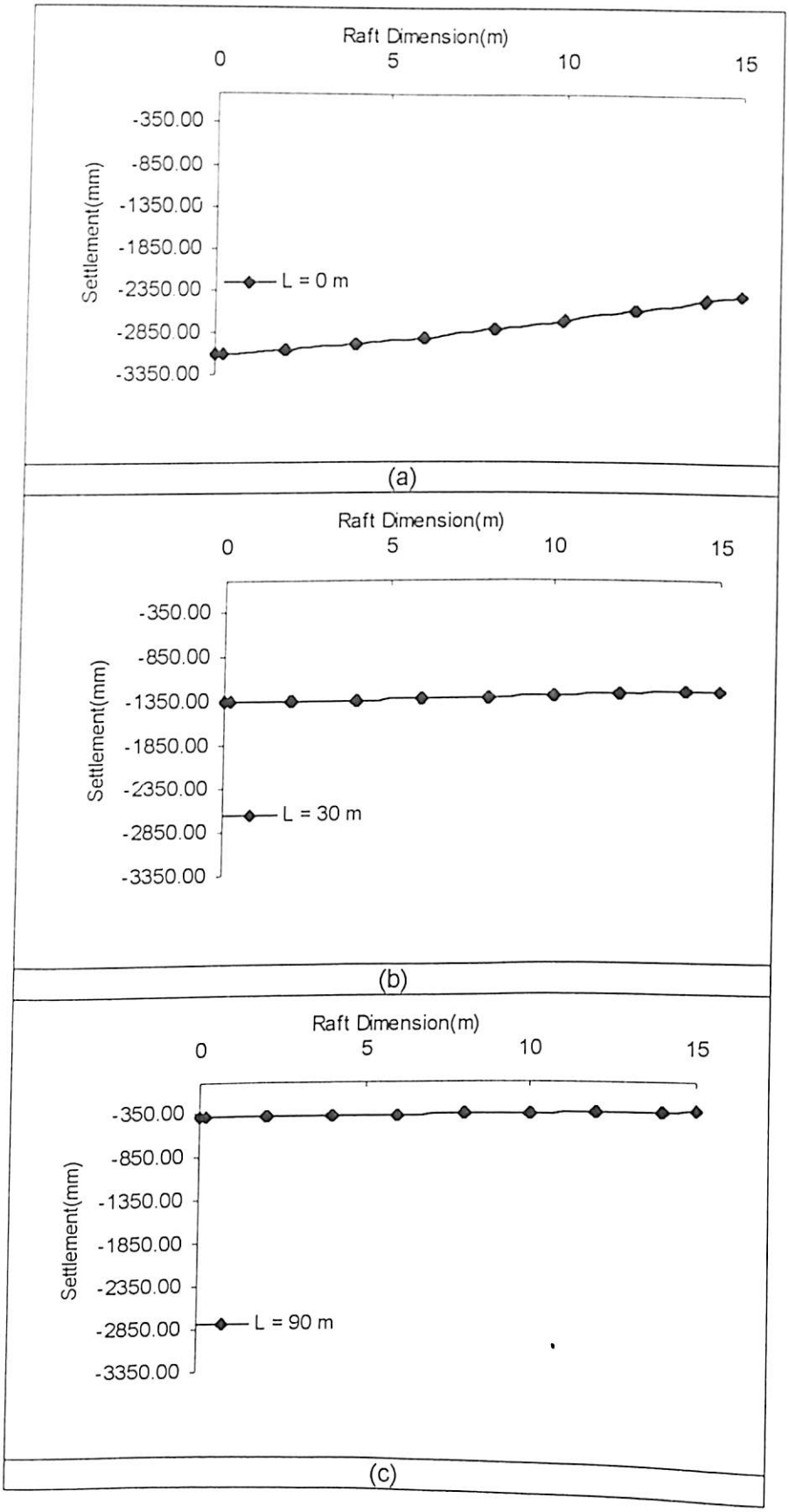

Figure 5.80 Settlement Profile of Raft in Piled Raft Foundation (D = 30 m, s/d = 5, E_s = 22000 kN/m^2, P = 564844.5 kN, t = 1.0 m)

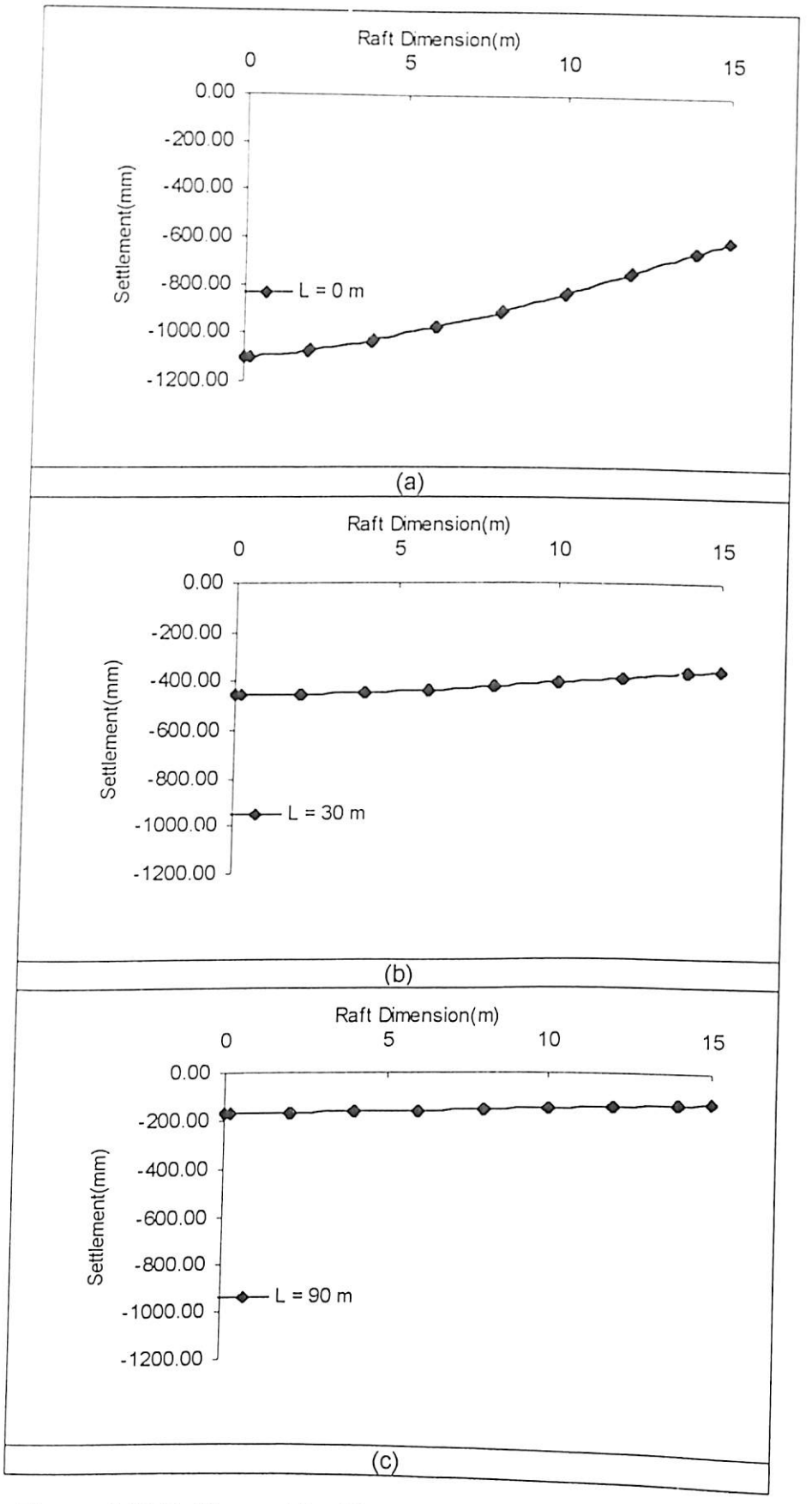

Figure 5.81 Settlement Profile of Raft in Piled Raft Foundation (D = 30 m, s/d = 5, E_s = 76000 kN/m^2, P = 564844.5 kN, t = 1.0 m)

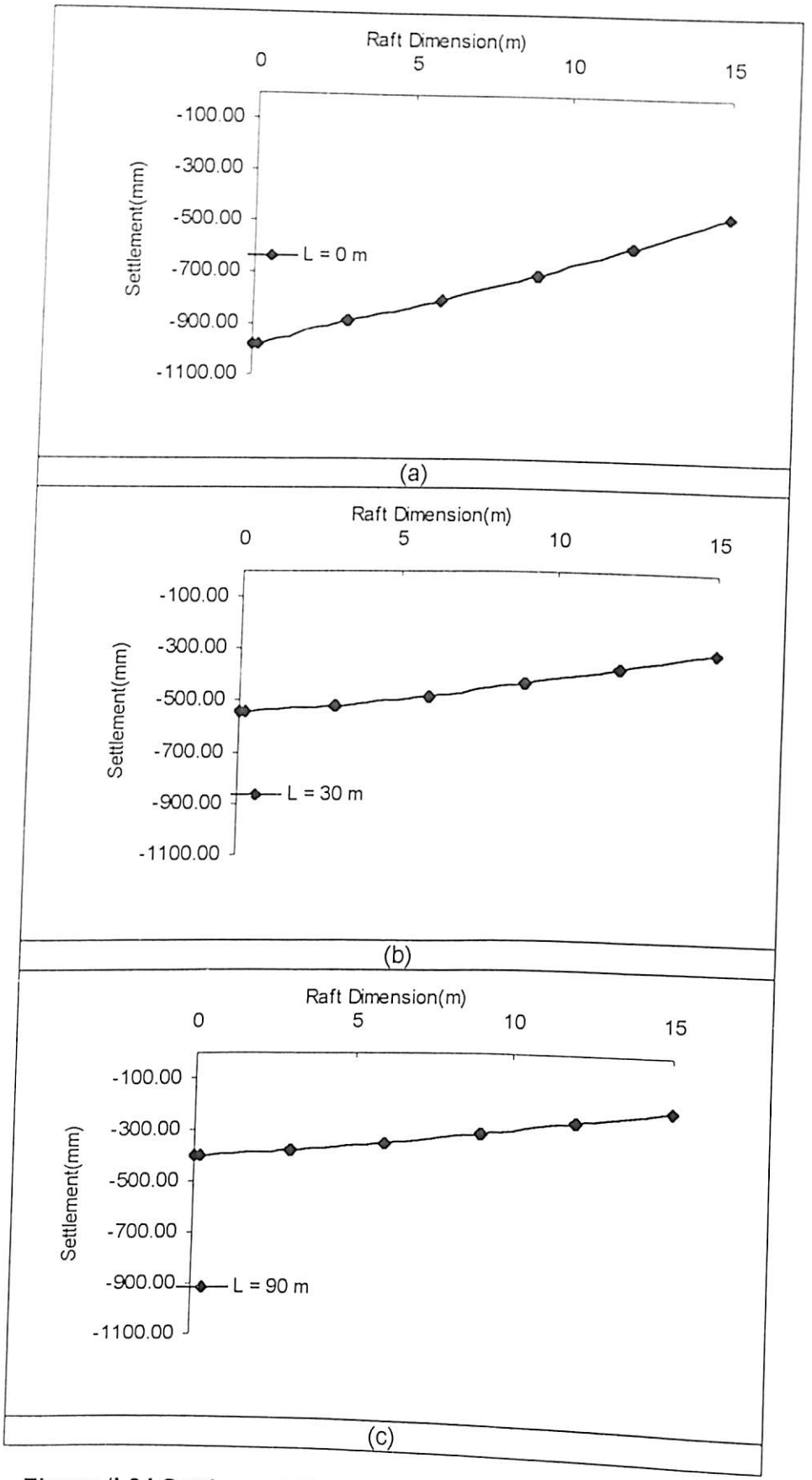

Figure 5.84 Settlement Profile of Raft in Piled Raft Foundation
(D = 30 m, s/d = 7.5, E_s = 76000 kN/m^2, , P = 686353.9 kN, t = 1.0 m)

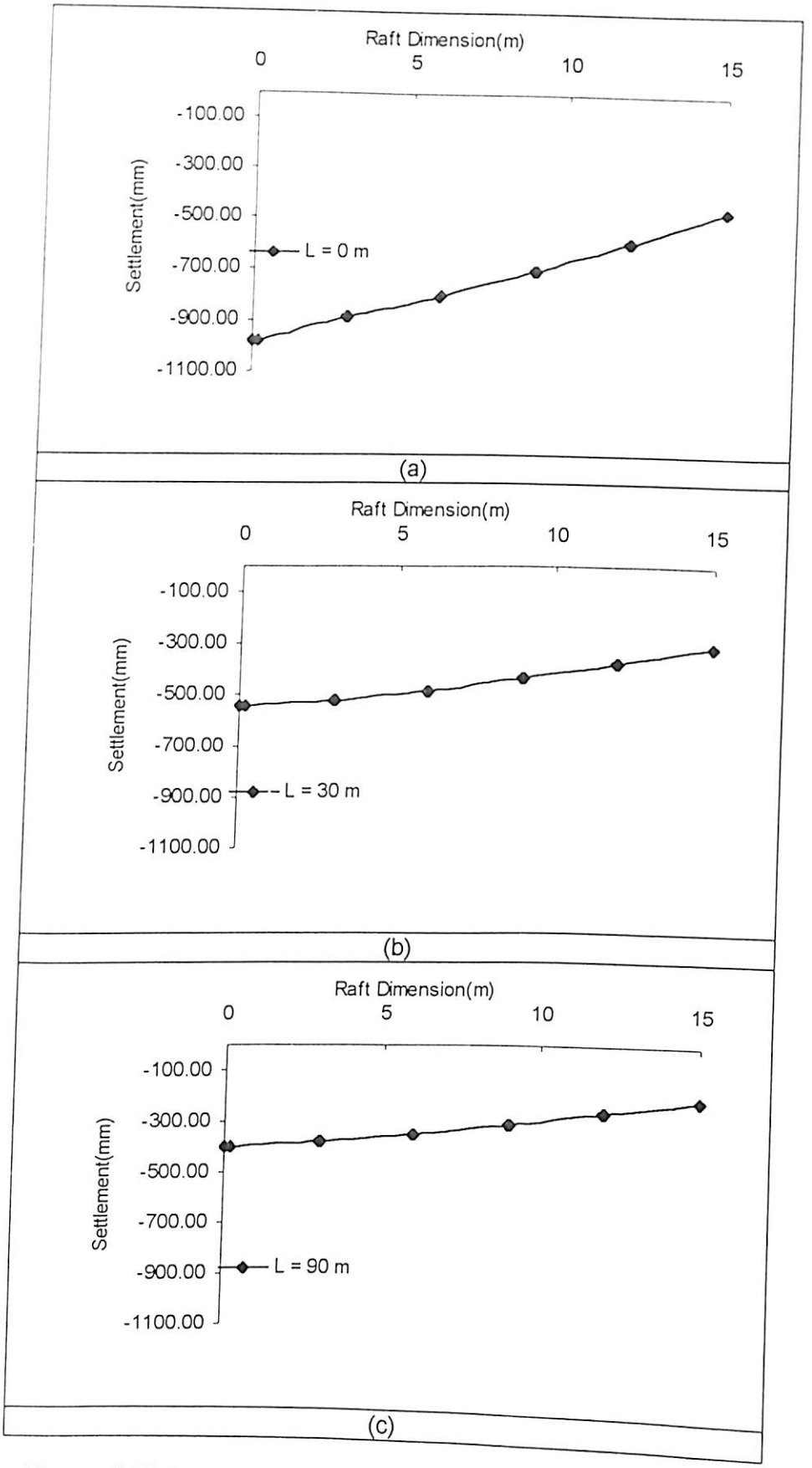

Figure 5.85 Settlement Profile of Raft in Piled Raft Foundation (D = 30 m, s/d = 7.5, E_s = 130000 kN/m^2, P = 686353.9 kN, t = 1.0 m)

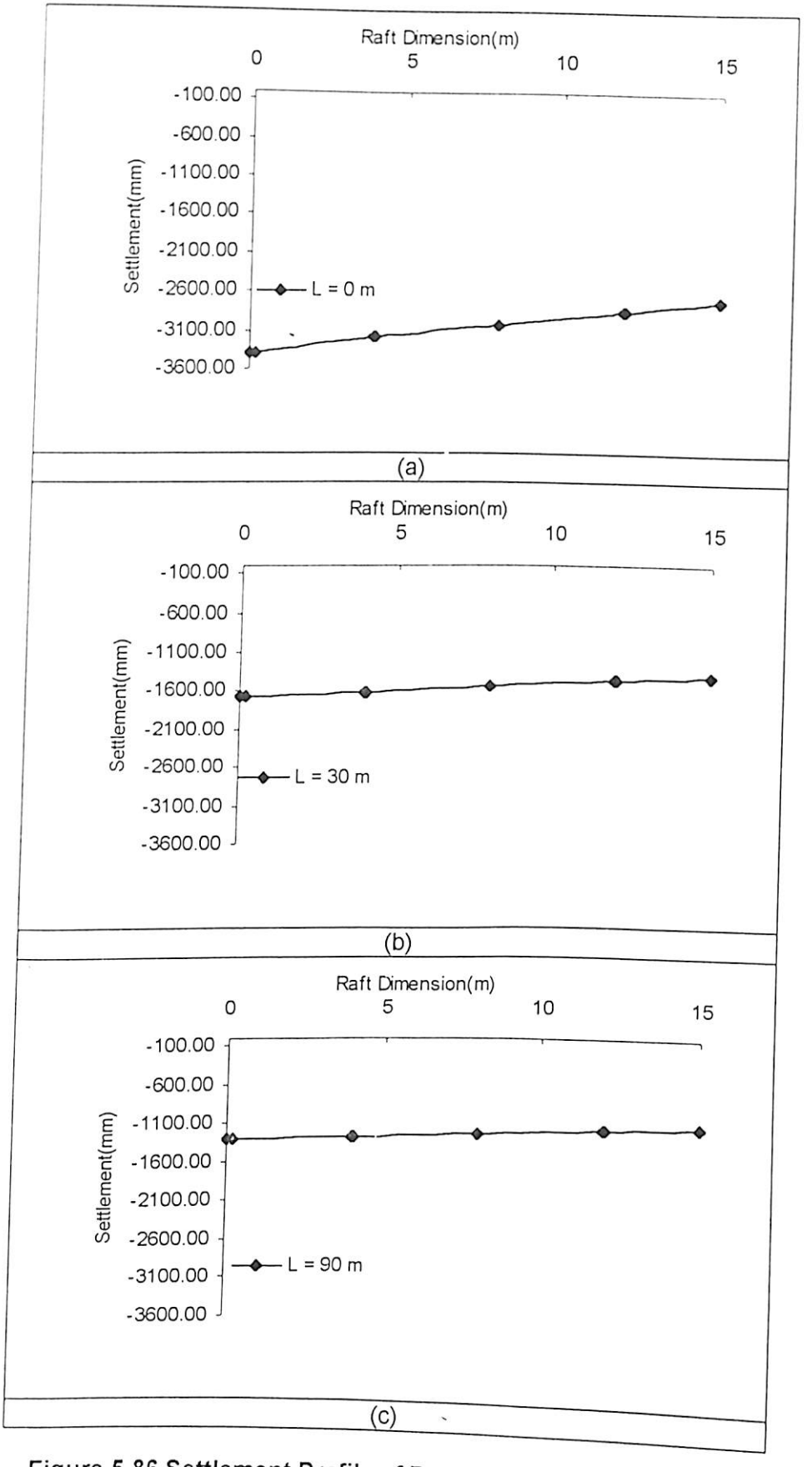

Figure 5.86 Settlement Profile of Raft in Piled Raft Foundation (D = 30 m, s/d = 10, E_s = 22000 kN/m^2, P = 686353.9 kN, t = 1.0 m)

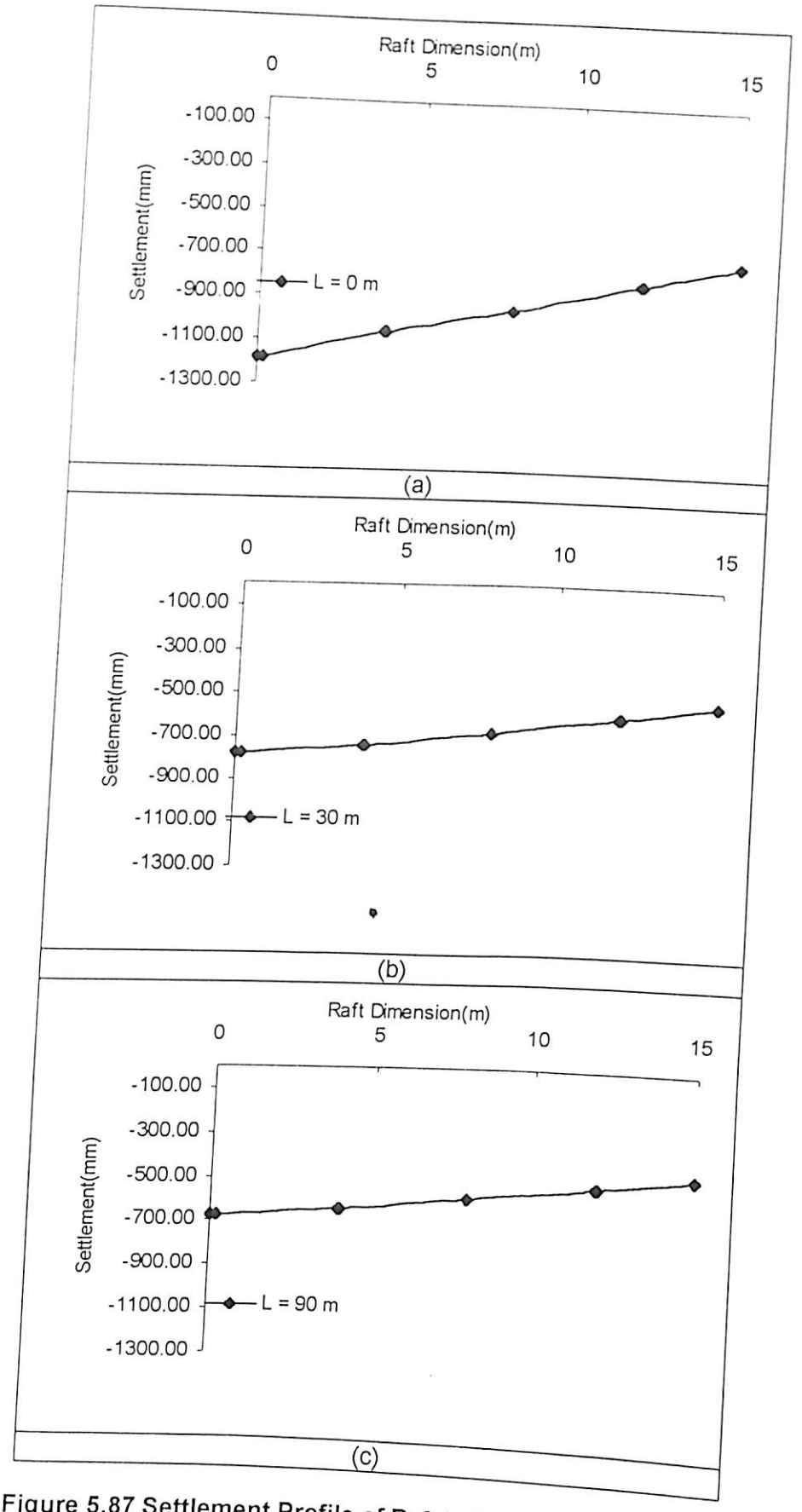

Figure 5.87 Settlement Profile of Raft in Piled Raft Foundation
(D = 30 m, s/d = 10, E_s = 76000 kN/m^2, P = 686353.9 kN, t = 1.0 m)

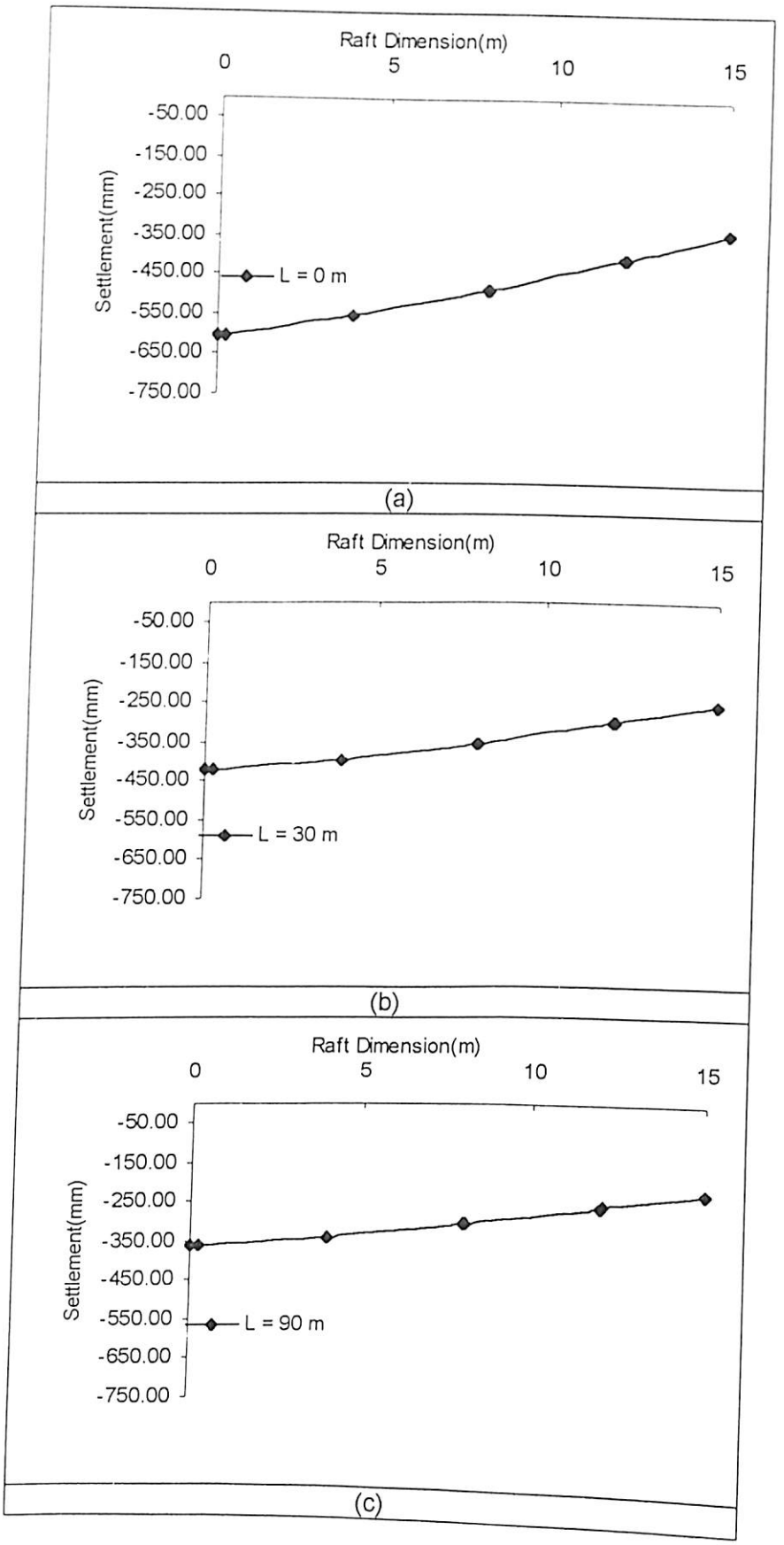

Figure 5.88 Settlement Profile of Raft in Piled Raft Foundation
(D = 30 m, s/d = 10, E_s = 130000 kN/m^2, P = 686353.9 kN, t = 1.0 m)

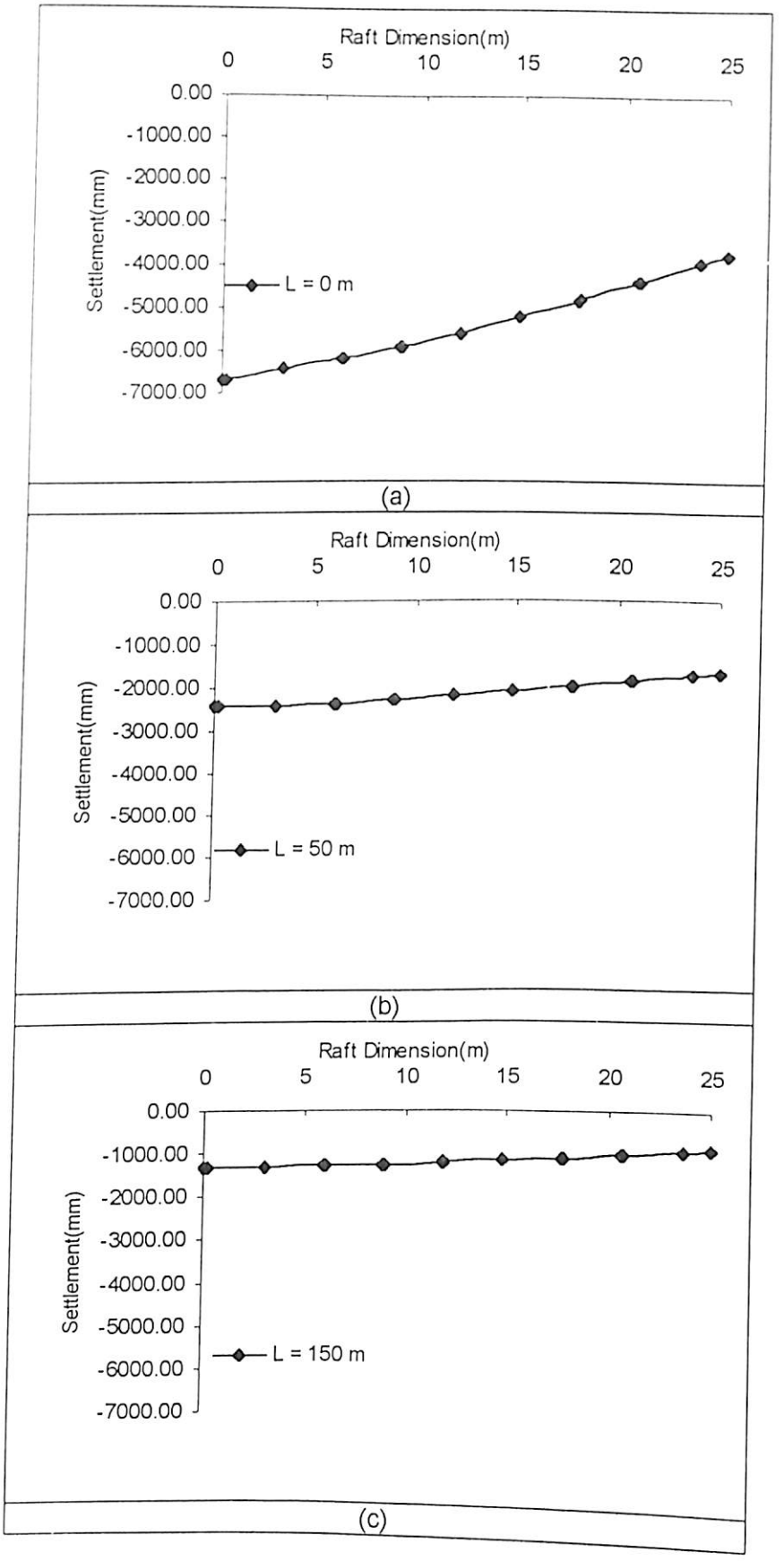

Figure 5.89 Settlement Profile of Raft in Piled Raft Foundation
(D = 50 m, s/d = 7.5, E_s = 22000 kN/m^2, t = 1.0 m)

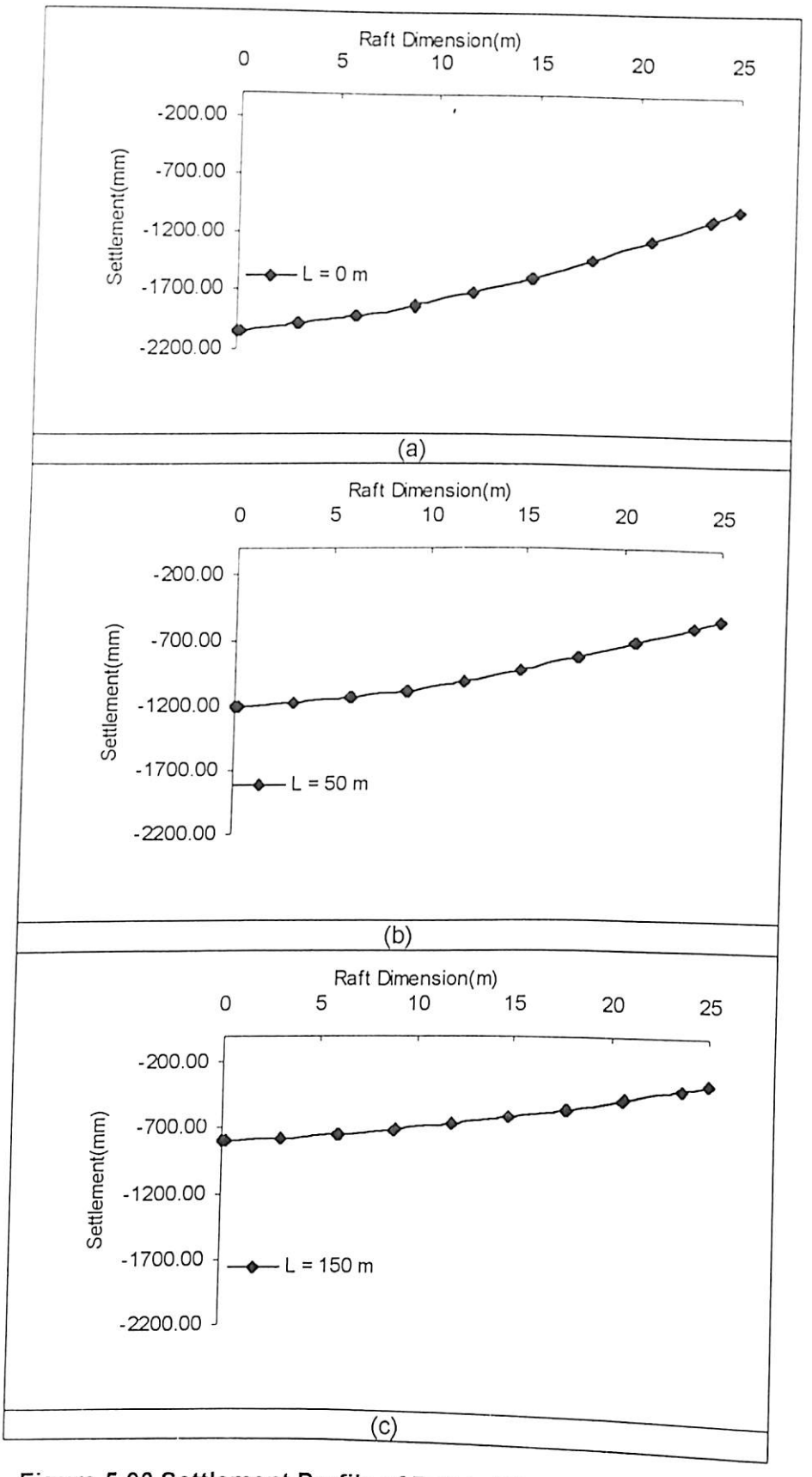

Figure 5.90 Settlement Profile of Raft in Piled Raft Foundation (D = 50 m, s/d = 7.5, E_s = 76000 kN/m^2, P = 1569694 kN, t = 1.0 m)

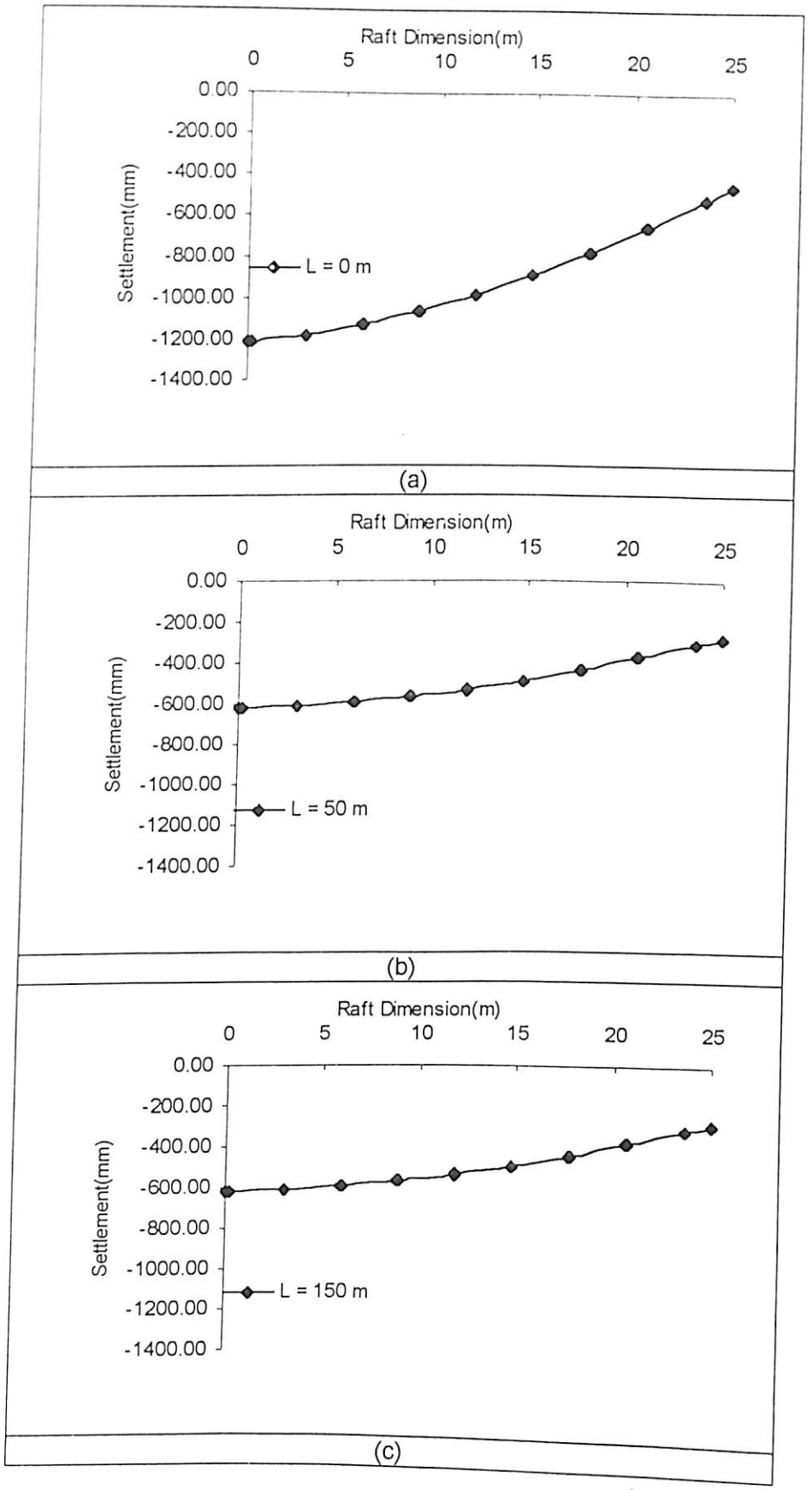

Figure 5.91 Settlement Profile of Raft in Piled Raft Foundation (D = 50 m, s/d = 7.5, E_s = 130000 kN/m^2, P = 1569694 kN, t = 1.0 m)

raft foundation, which reduces with addition of pile and with increase in length of pile. The effect of increase in soil modulus is to reduce the overall settlement.

Figures 5.92 (a), (b), (c), Figures 5.93 (a), (b), (c) and Figures 5.94 (a), (b), (c) show the settlement profiles for piled raft foundation whose raft diameter is 50 meter and spacing to diameter ratio of pile 10.0. Differential settlement is seen in the raft as well as the piled raft foundation, which reduces with addition of pile and with increase in length of pile. The effect of increase in soil modulus is to reduce the overall settlement.

Figures 5.95 (a), (b), (c), Figures 5.96 (a), (b), (c) and Figures 5.97 (a), (b), (c) show the settlement profiles for piled raft foundation whose raft diameter is 50 meter and spacing to diameter ratio of pile 15.0. Differential settlement is seen in the raft as well as the piled raft foundation, which reduces with addition of pile and with increase in length of pile. The effect of increase in soil modulus is to reduce the overall settlement.

5.6.6 Yielding of Soil in a Piled Raft Foundation

Figures 5.98 (a), (b) shows the development of yield stress in soil for a piled raft foundation of raft diameter 10 m, s/d equal to 2.5, raft thickness equal to 0.1 m and soil modulus of 22000 kN/m^2 for varying load steps. In load step 5, the yielding has started from the edge of the raft and from the tip of the boundary pile. In load step 7, he soil can be seen yielding from tip of pile and moving in upward direction. The soil lements below the pile tips have also yielded. The type of yielding shown in load step shows the block behaviour of the pile group. The result shows that when the piles re at very close spacing block behaviour is there in the group of piles.

gures 5.99 (a), (b) show the development of yielding at higher load steps (load step-) and 15). The yielding of soil has reached to the base of the pile and also below the il layers as has been seen in load step 7. From the same Figure it can be seen that e zone of yielding has spread in upward direction, lateral direction and also below previous layers of the yielded soil mass. The yielded zone can be seen of almost of b shape.

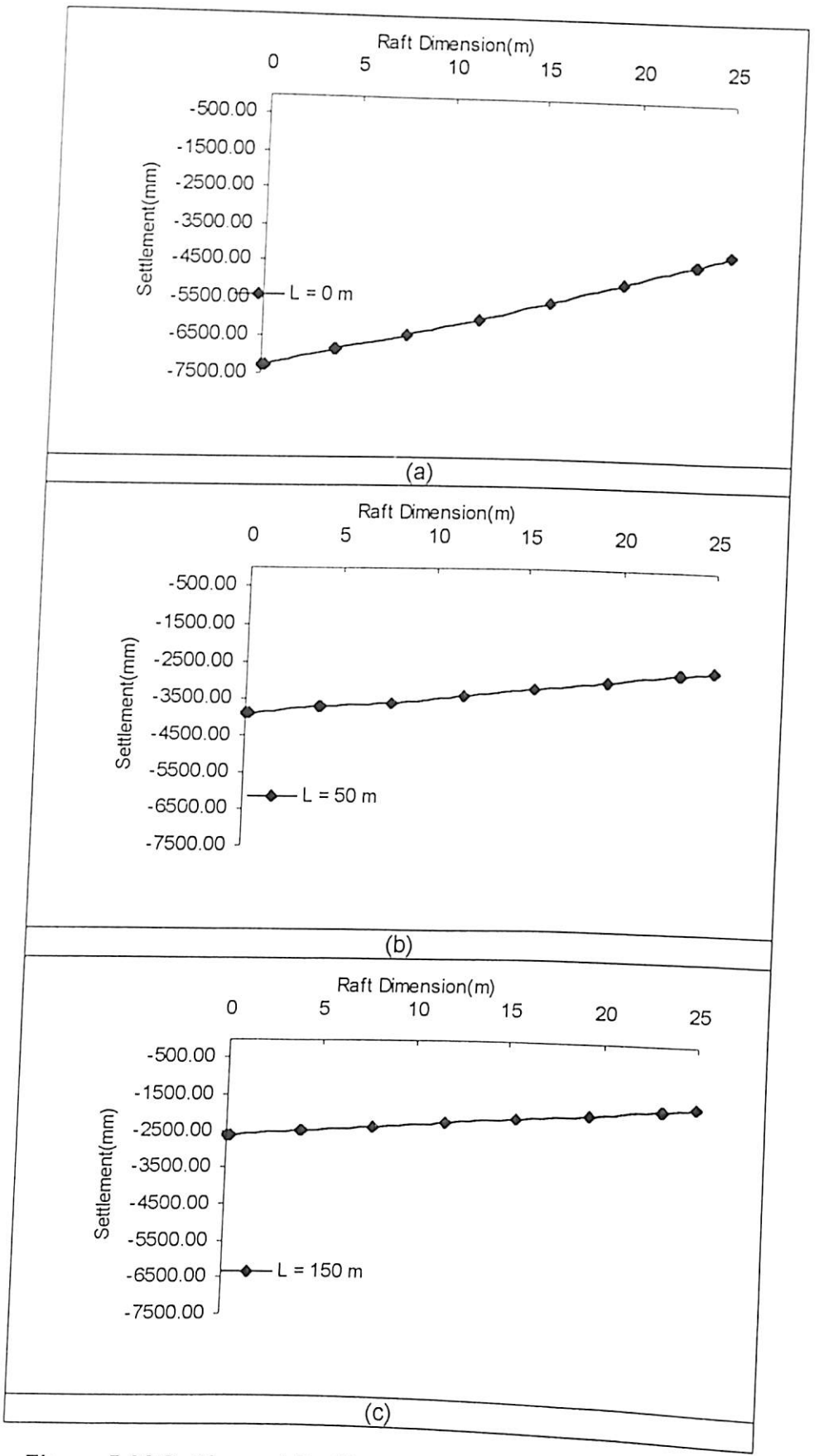

Figure 5.92 Settlement Profile of Raft in Piled Raft Foundation (D = 50 m, s/d = 10, E_s = 22000 kN/m^2, P = 1568820 kN, t = 1.0 m)

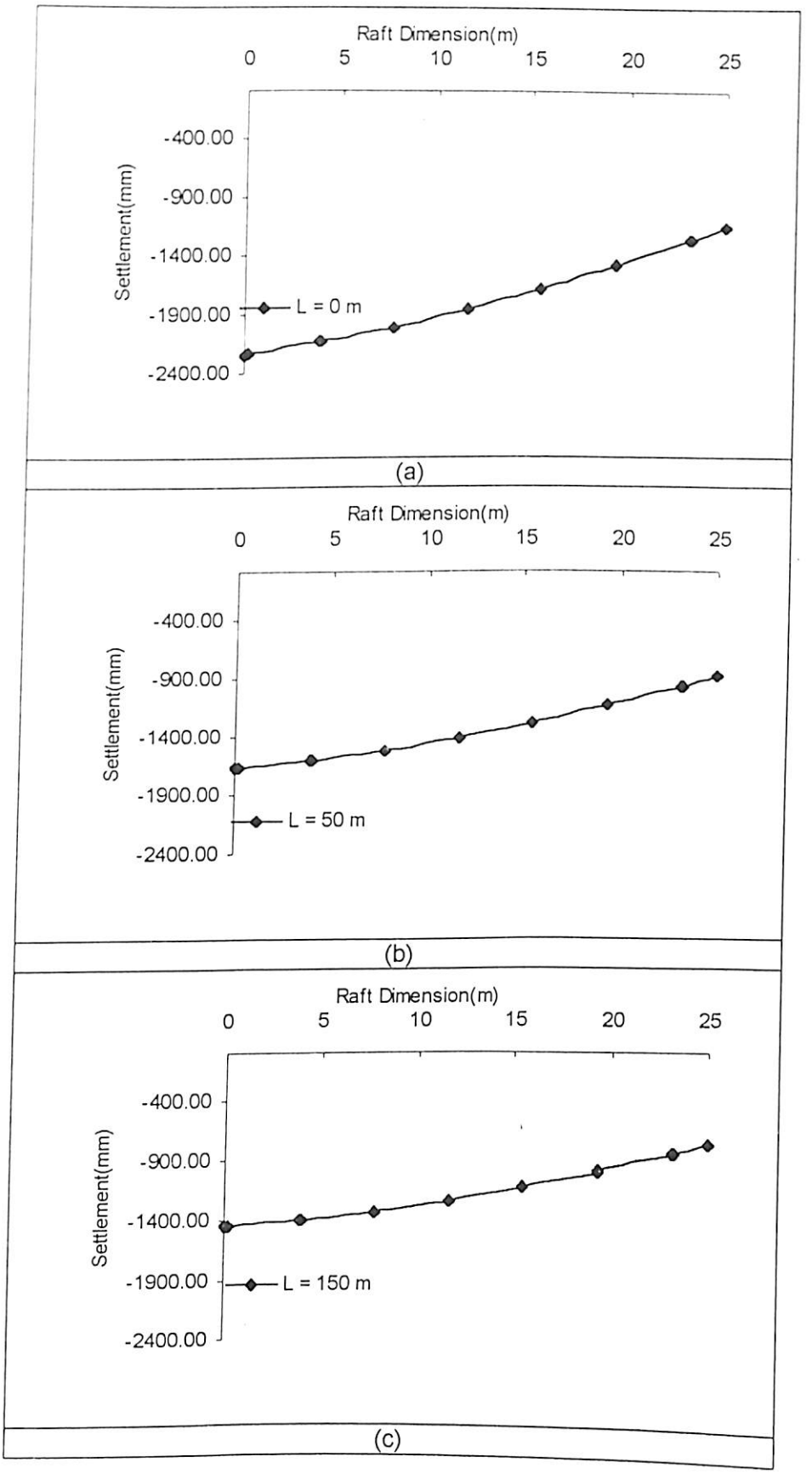

Figure 5.93 Settlement Profile of Raft in Piled Raft Foundation (D = 50 m, s/d = 10, E_s = 76000 kN/m^2, P = 1568820 kN, t = 1.0 m)

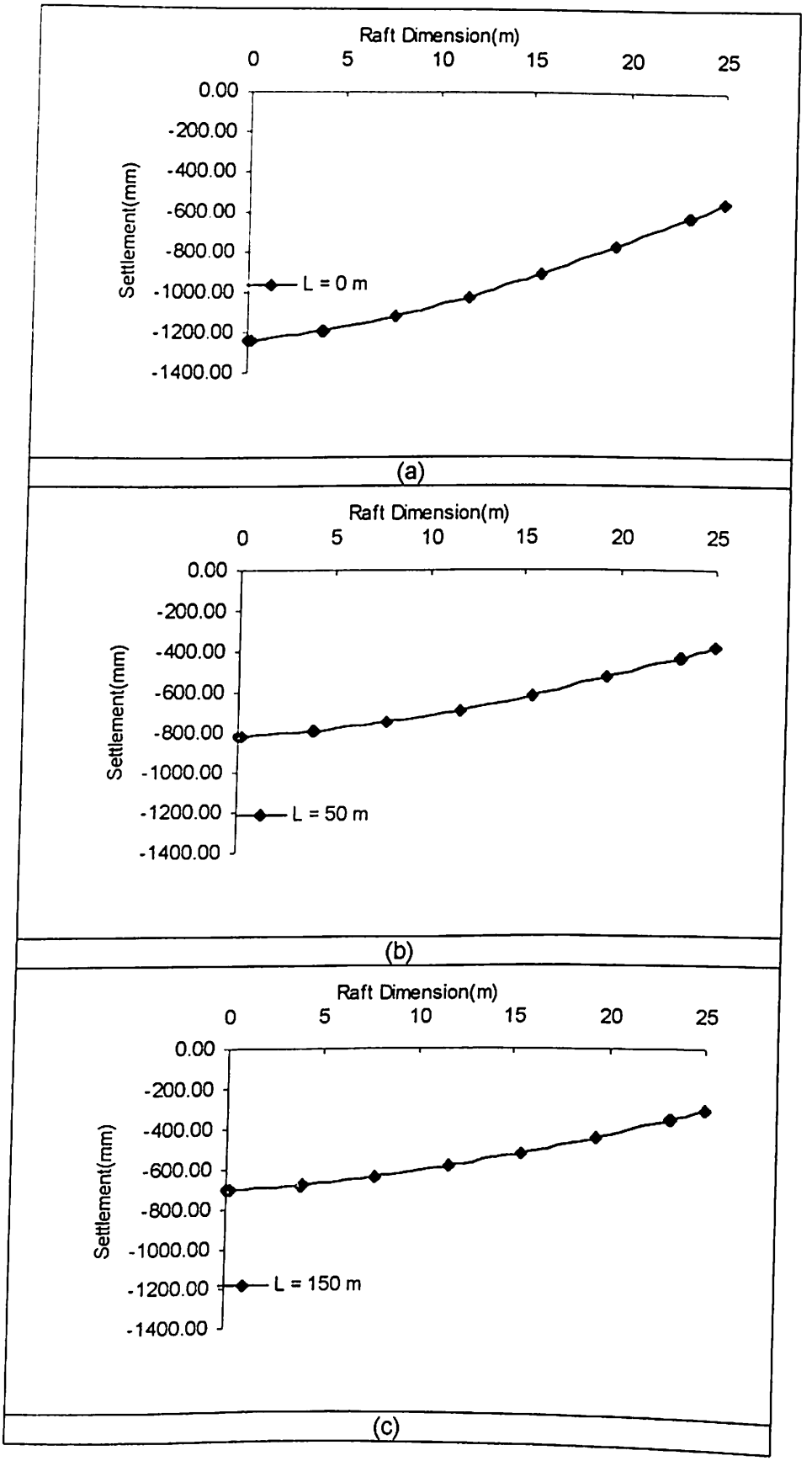

Figure 5.94 Settlement Profile of Raft in Piled Raft Foundation (D = 50 m, s/d = 10, E_s = 130000 kN/m^2, P = 1568820 kN, t = 1.0 m)

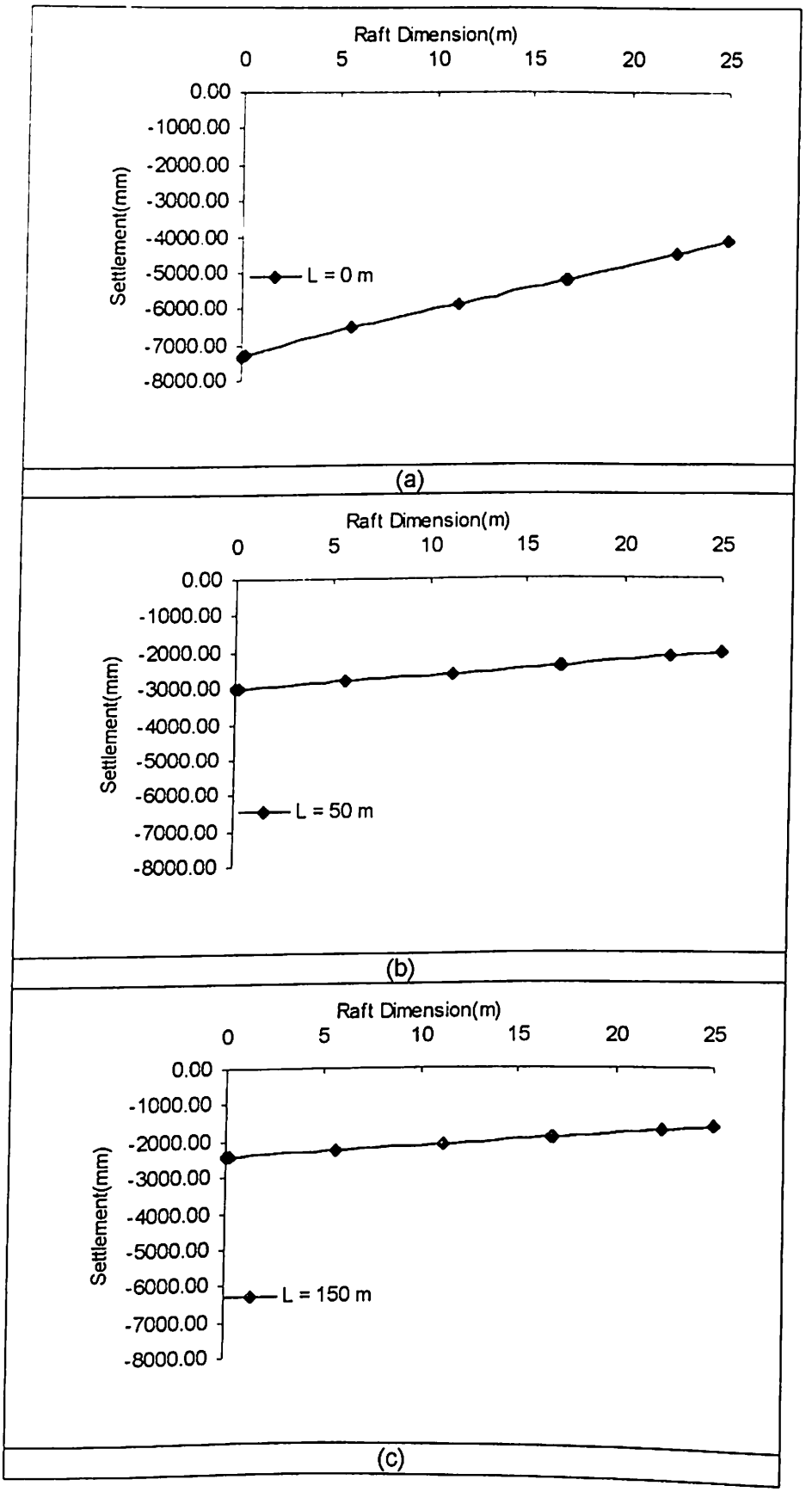

Figure 5.95 Settlement Profile of Raft in Piled Raft Foundation (D = 50 m, s/d = 15, E_s = 22000 kN/m^2, P = 1566289 kN, t = 1.0 m)

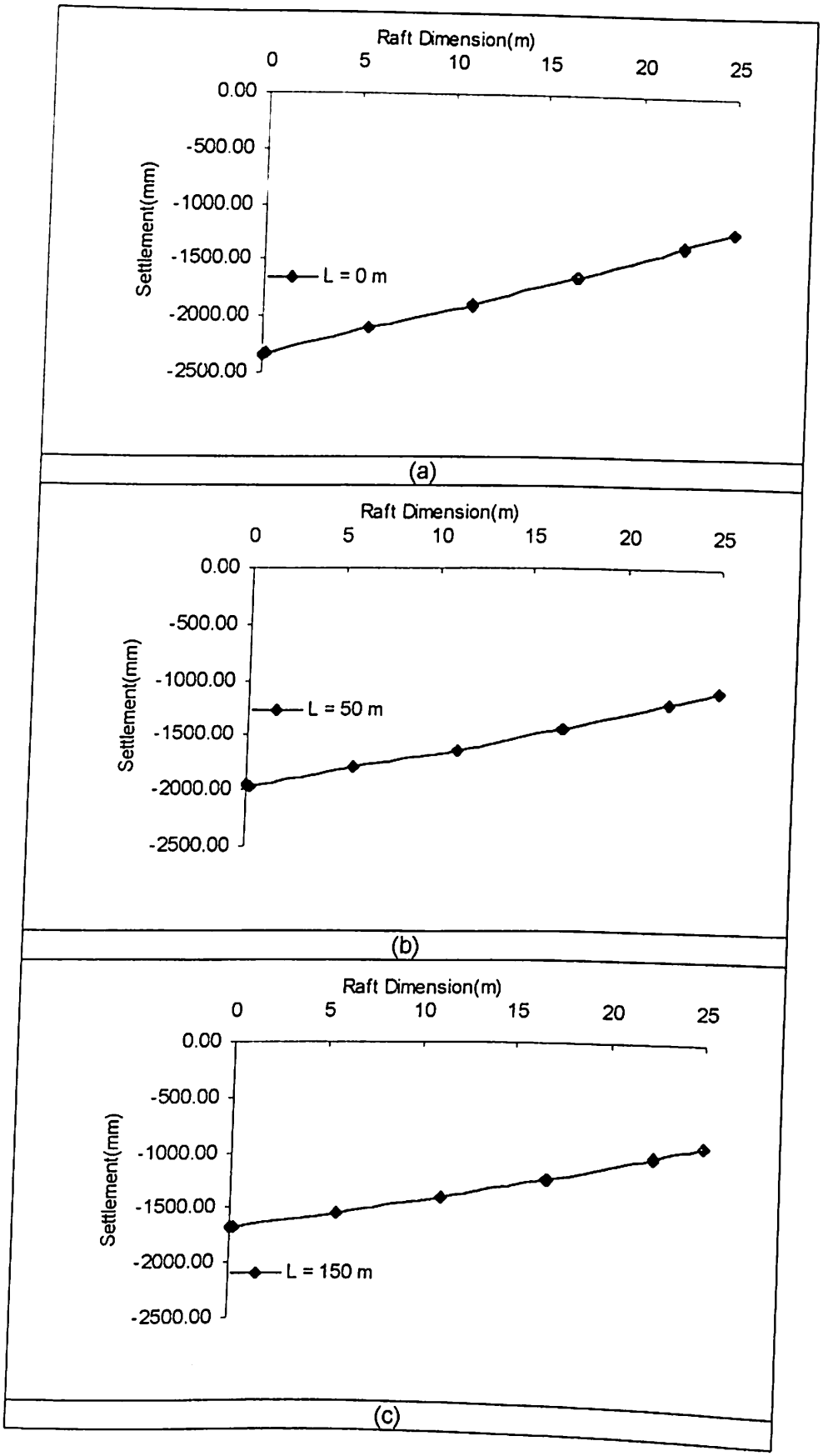

Figure 5.96 Settlement Profile of Raft in Piled Raft Foundation (D = 50 m, s/d = 15, E_s = 76000 kN/m^2, P = 1566289 kN, t = 1.0 m)

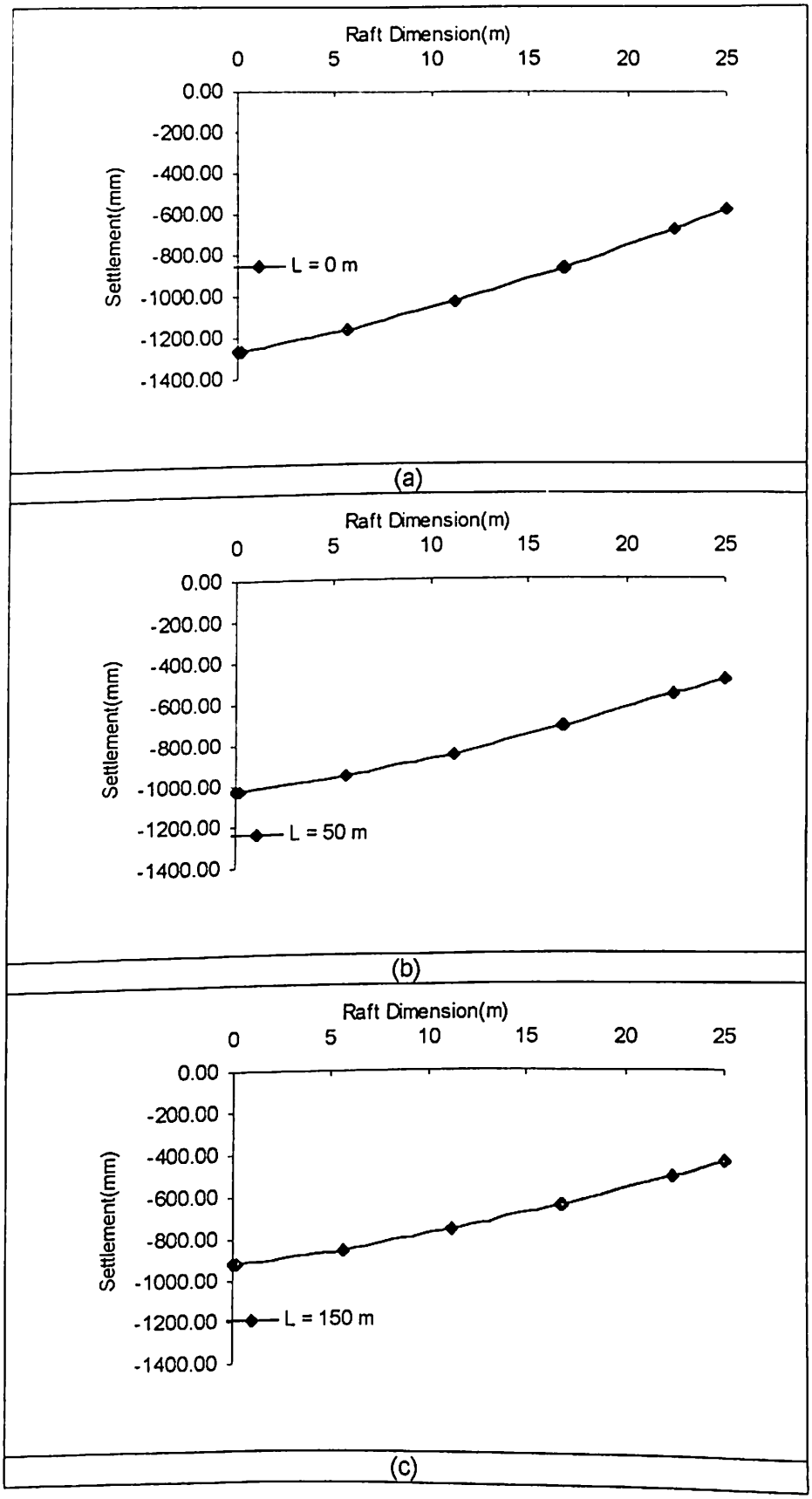

Figure 5.97 Settlement Profile of Raft in Piled Raft Foundation (D = 50 m, s/d = 15, E_s = 130000 kN/m^2, P = 1566289 kN, t = 1.0 m)

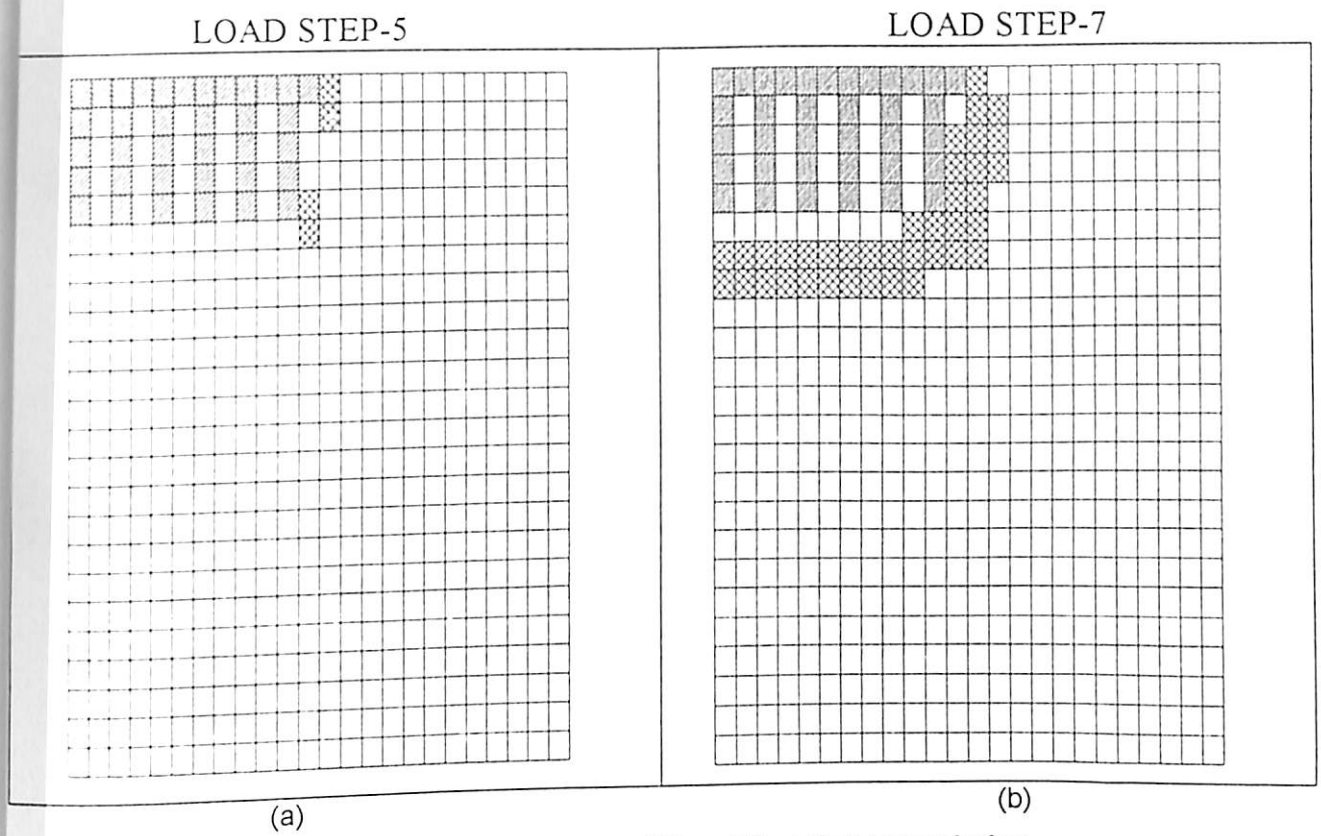

Figure 5.98 Yielding of Soil in a Piled Raft Foundation
(D = 10 m, s/d = 2.5, t = 0.1 m, E_s = 22000 kN/m^2)

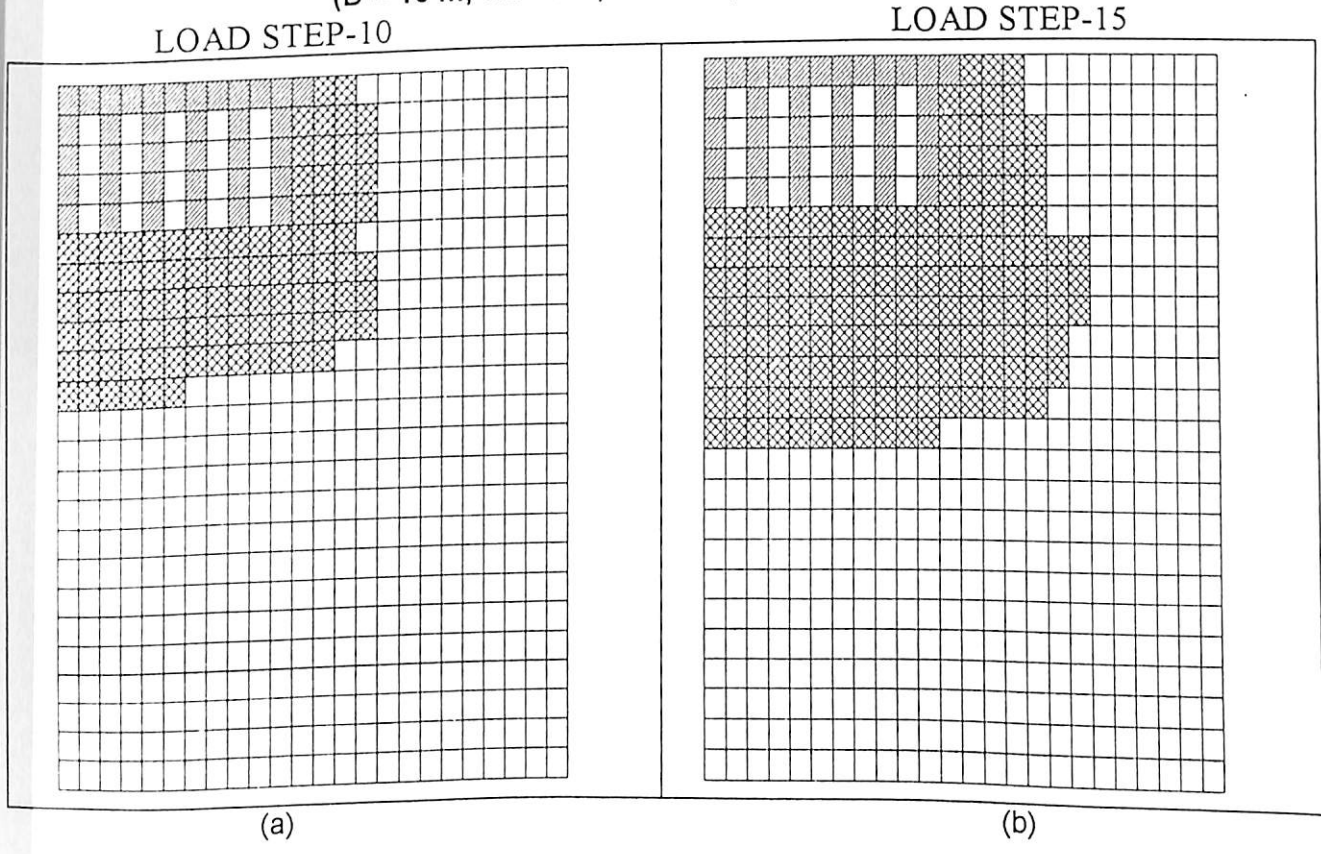

Figure 5.99 Yielding of Soil in a Piled Raft Foundation
(D = 10 m, s/d = 2.5, t = 0.1 m, E_s = 22000 kN/m^2)

Figure 5.100 shows the yielding of soil below a piled raft foundation for load step 20. The yielded soil can be seen to form a yielded bulb. The yielding has spread up to larger depth below the pile and also in the lateral direction. The zone of yielding is up to 15.5 m in the lateral direction and 23 meter below the pile. Comparison of Figures 5.98, 5.99, and 5.100 show that yielding starts from edge of raft and tip of the boundary pile and as the load is increased, this yielding spreads in horizontal and vertical direction and there is complete yielding of soil below the tip of pile and around the boundary of pile and the edge of the raft.

Figures 5.101 (a), (b) show the yielding of soil for an axisymmetric piled raft foundation for different load steps (5 & 7) for raft thickness of 4.0 metres, length of pile 10 metre, spacing to diameter ratio of 2.5 and soil modulus of 22000 kN/m^2. The yielding starts first from the tip of pile and with increase in load it also starts from the edge of the raft and the periphery of the pile.

Figures 5.102 (a), (b) show the yielding of soil in case of piled raft foundation for load steps of 10 and 15. With increase in load steps (10), the yielding of soil is seen to spared from tip of the boundary pile towards the center of the pile and also along the periphery of the boundary pile. With further increase in load step (15), the yielding is found to be up to a larger area below the tip of the pile. The yielding area also has increased in the lateral direction. Figure.5.103 shows the yielding of the soil for load step 20. Almost bulb shape of yielded zone of soil can be seen. The block behaviour is seen even in this case.

Figures 5.104 (a), (b) shows the yielding of soil for a piled raft foundation of raft diameter 30 metre, spacing to diameter ratio 7.5, soil modulus of 130000 kN/m^2 and raft thickness as 1.0 m. At load step 5, yielding of soil has started from the edge of the raft. This yielding can be seen to spread in the lateral direction from the periphery piles (load step 7). At load step 10 (Figure.5.105 (a)), the yielding of soil is seen to move in between the piles and also below the pile. At load step 15 (Figure.5.105 (b)), the yielded soil forms a bulb shape. Figure.5.106 shows the yielding of the soil, for load step 20 and a large zone of soil is found to be yielded.

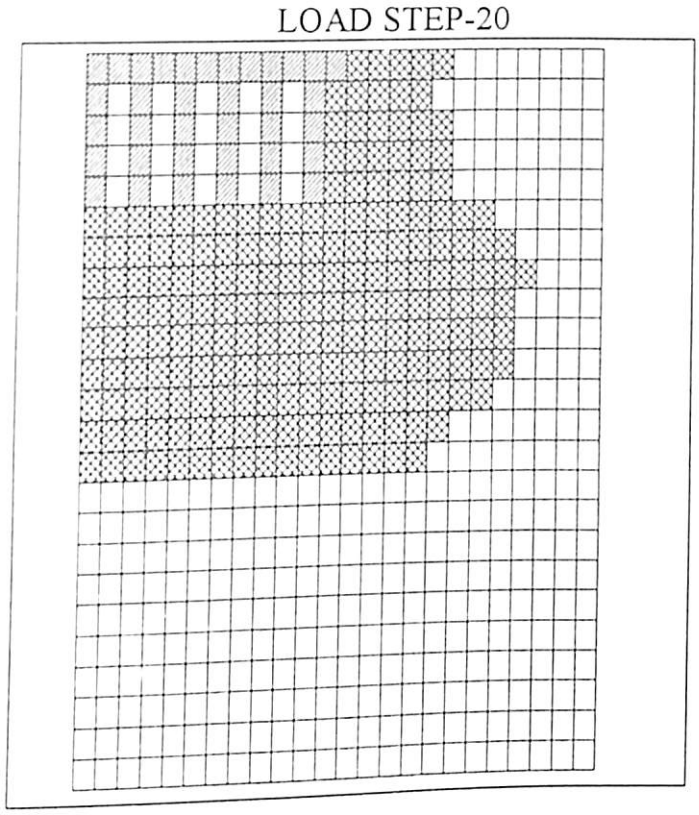

Figure 5.100 Yielding of Soil in a Piled Raft Foundation
(D = 10 m, s/d = 2.5, L = 10 m, t = 0.1 m, E_s = 22000 kN/m^2)

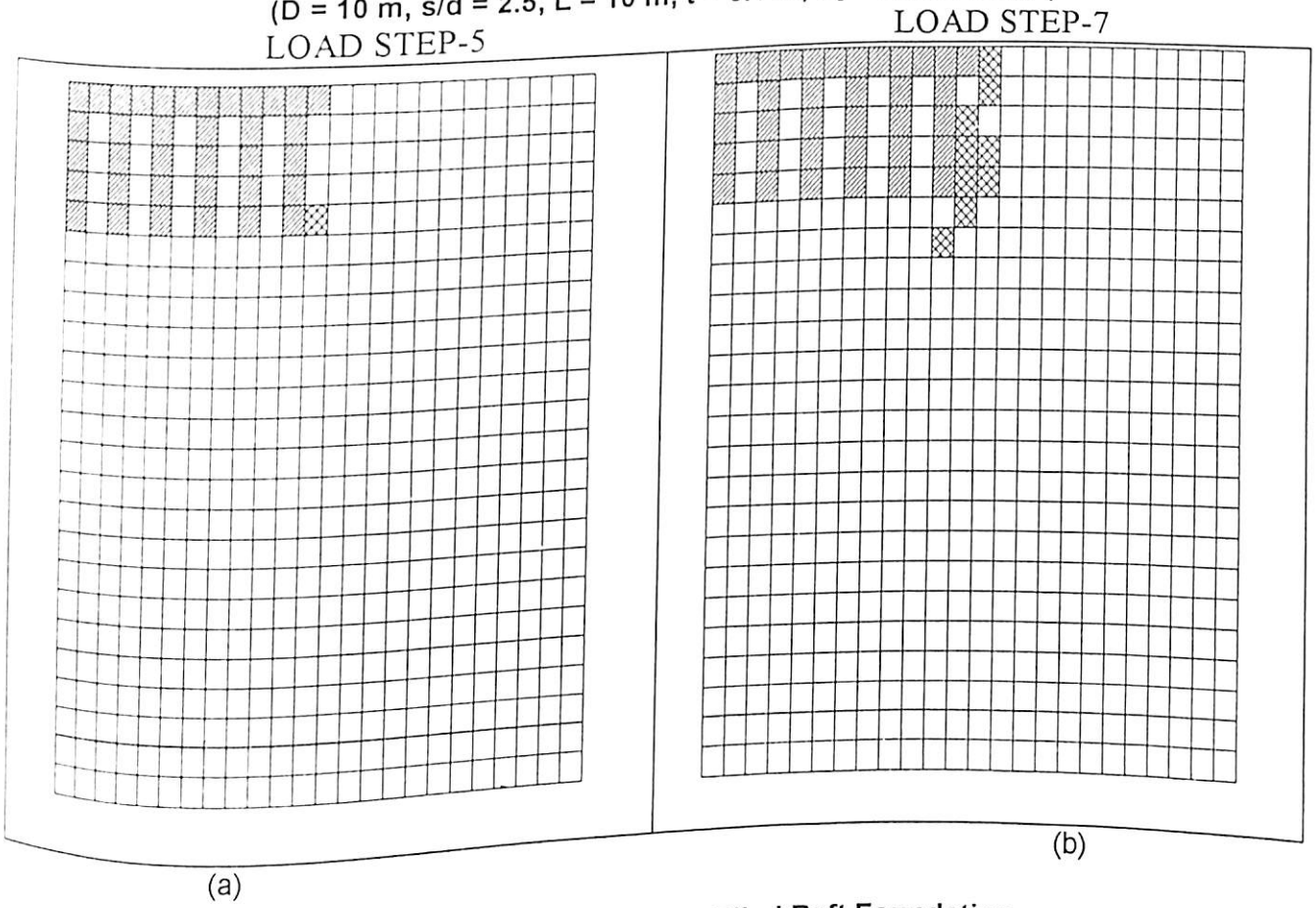

Figure 5.101 Yielding of soil in Piled Raft Foundation
(D = 10 m, s/d = 2.5, L = 10 m, t = 4.0 m, E_s = 22000 kN/m^2)

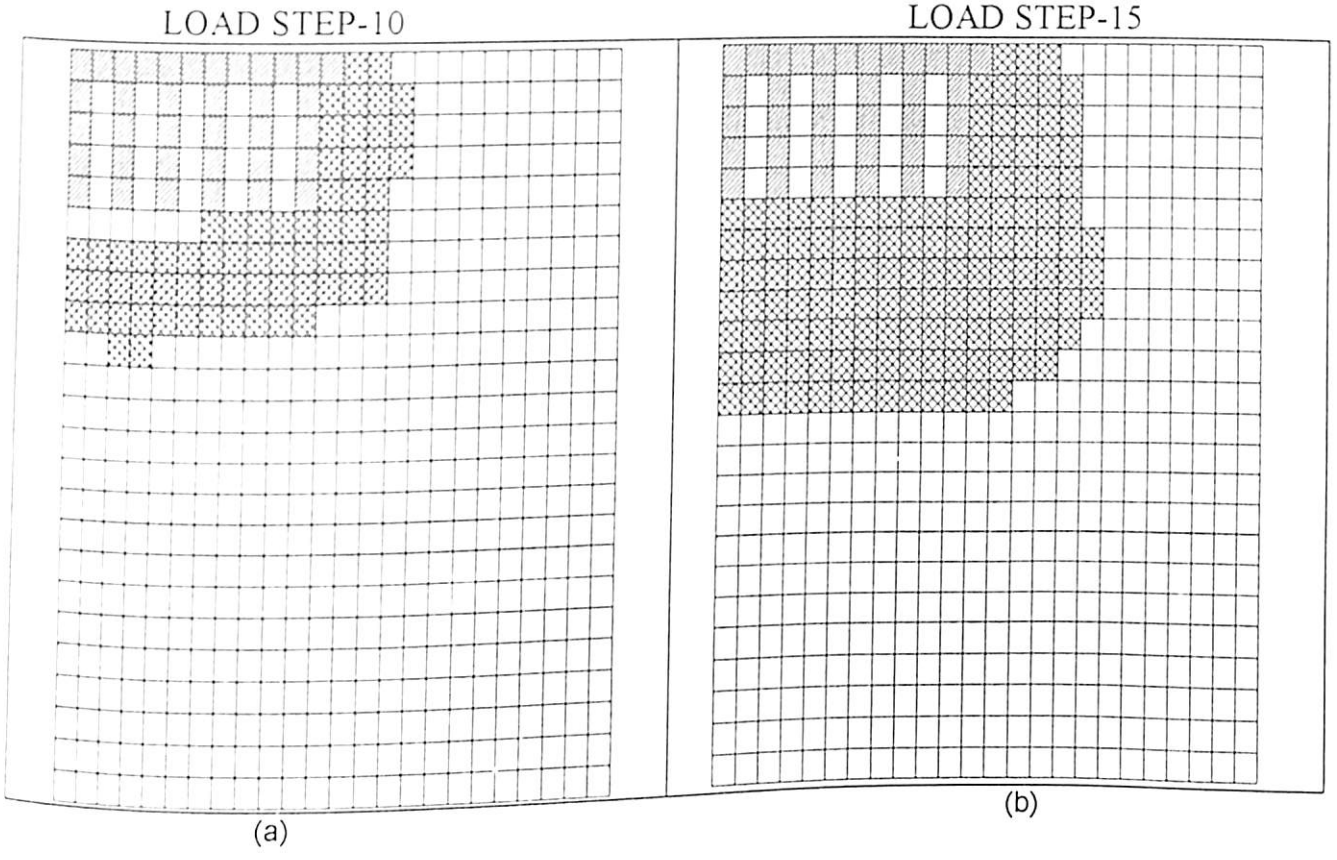

Figure 5.102 Yielding of Soil in a Piled Raft Foundation
(D = 10 m, s/d = 2.5, L = 10 m, t = 4.0 m, E_s = 22000 kN/m^2)

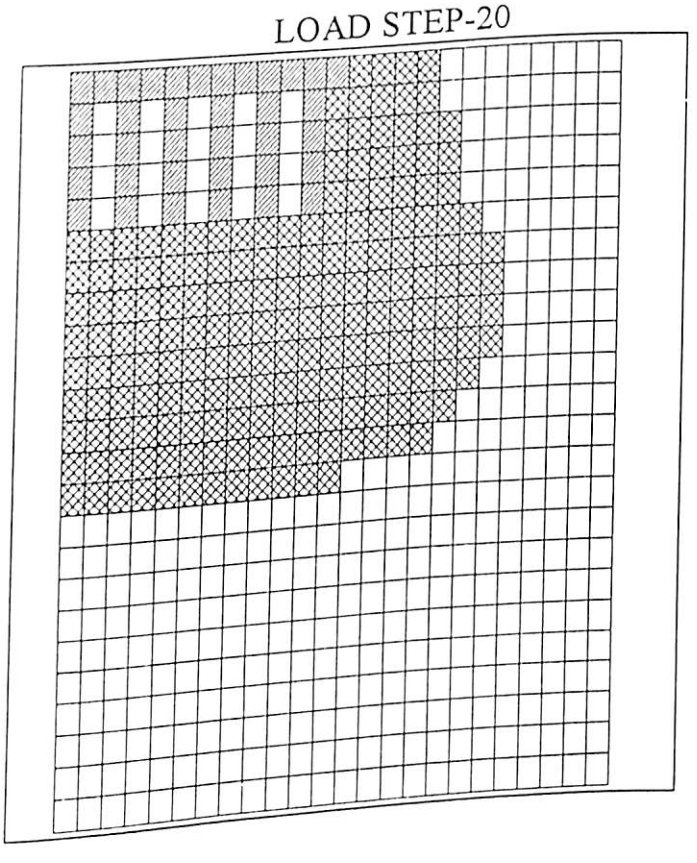

Figure 5.103 Yielding of Soil in a Piled Raft Foundation
(D = 10 m, s/d = 2.5, L = 10 m, t = 4.0 m, E_s = 22000 kN/m^2)

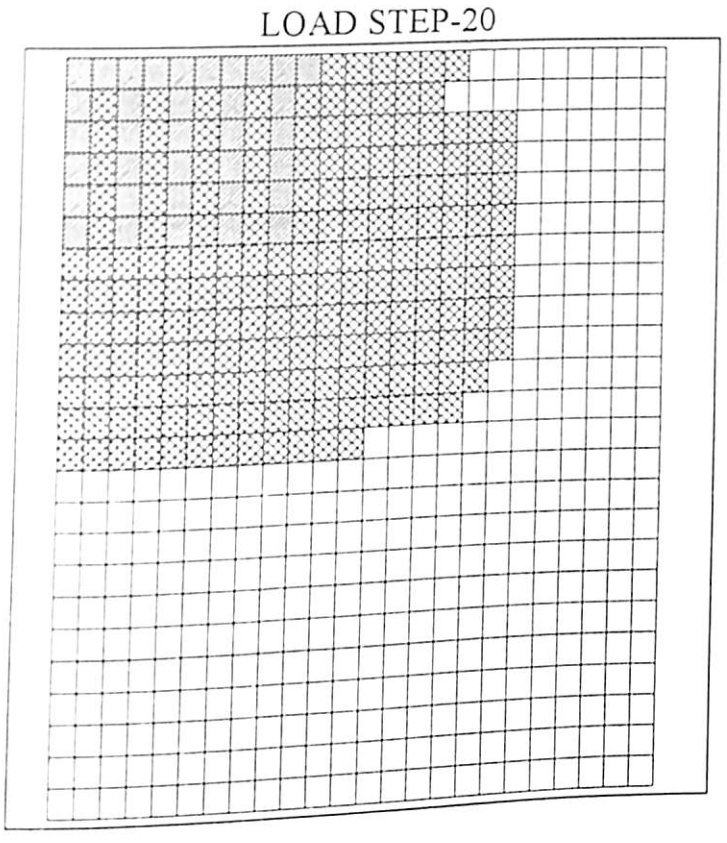

Figure 5.106 Yielding of Soil in a Piled Raft Foundation
(D = 30 m, L = 30 m, s/d = 7.5, t = 1.0 m, E_s = 130000 kN/m^2)

Figures 5.107 (a), (b) show the development of yielding of soil for a piled raft foundation of raft diameter 30 metre, spacing to diameter ratio of 7.5, soil modulus of 22000 kN/m^2 and raft thickness of 1.0 metre with 90 m length of pile. The yielding of soil starts at the edge of the raft (load step 4) and moves in the lateral direction (load step 7). With further increase in load step (10), Figure 5.108 (a), the yielding of soil is seen below the raft and in between the piles. At load step 15 as shown in Figure 5.108 (b), the yielding completely reaches up to the bottom of the raft and also spreads in the lateral direction. At load step 20, Figure 5.109, the yielding of soil is seen up to larger length of pile. Also near the base of the pile yielding of soil is seen.

Figures 5.110 (a), (b) show the yielding of soil for a piled raft foundation of raft diameter 30 metres, spacing to diameter ratio between piles of 7.5, pile length 90 metres. The yielding of soil is seen at the edge of the raft (load steps 5 and 7). The yielding is seen in between the piles (and spreads over a larger length of pile Figures 5.111 (a), (b) (load steps 10 and 15). Figure 5.112 shows the yielding up to a larger length of pile and also up to larger area in the lateral direction.

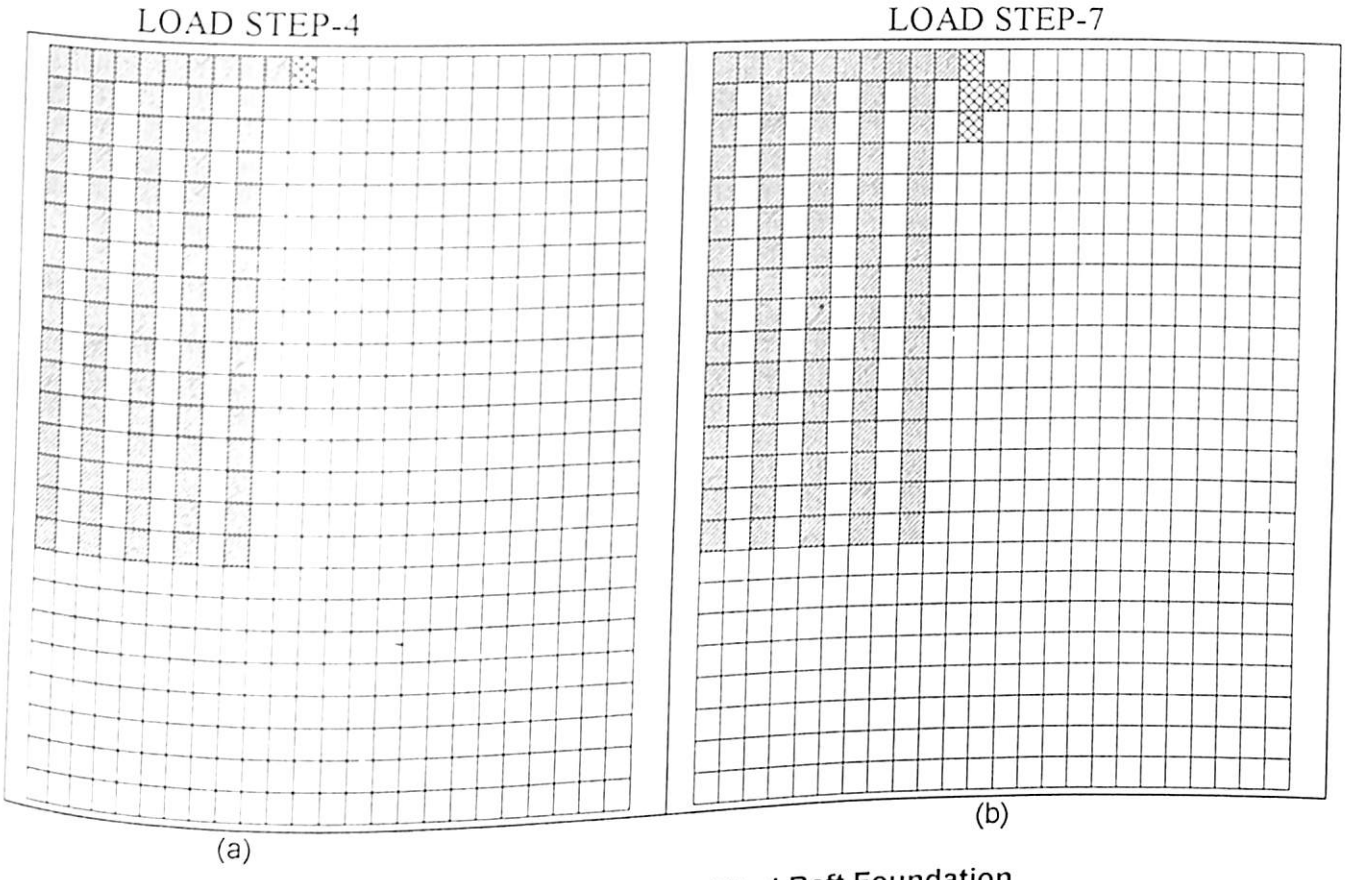

Figure 5.107 Yielding of Soil in a Piled Raft Foundation
(D = 30 m, L = 90 m, s/d = 7.5, t = 1.0 m, E_s = 22000 kN/m^2)

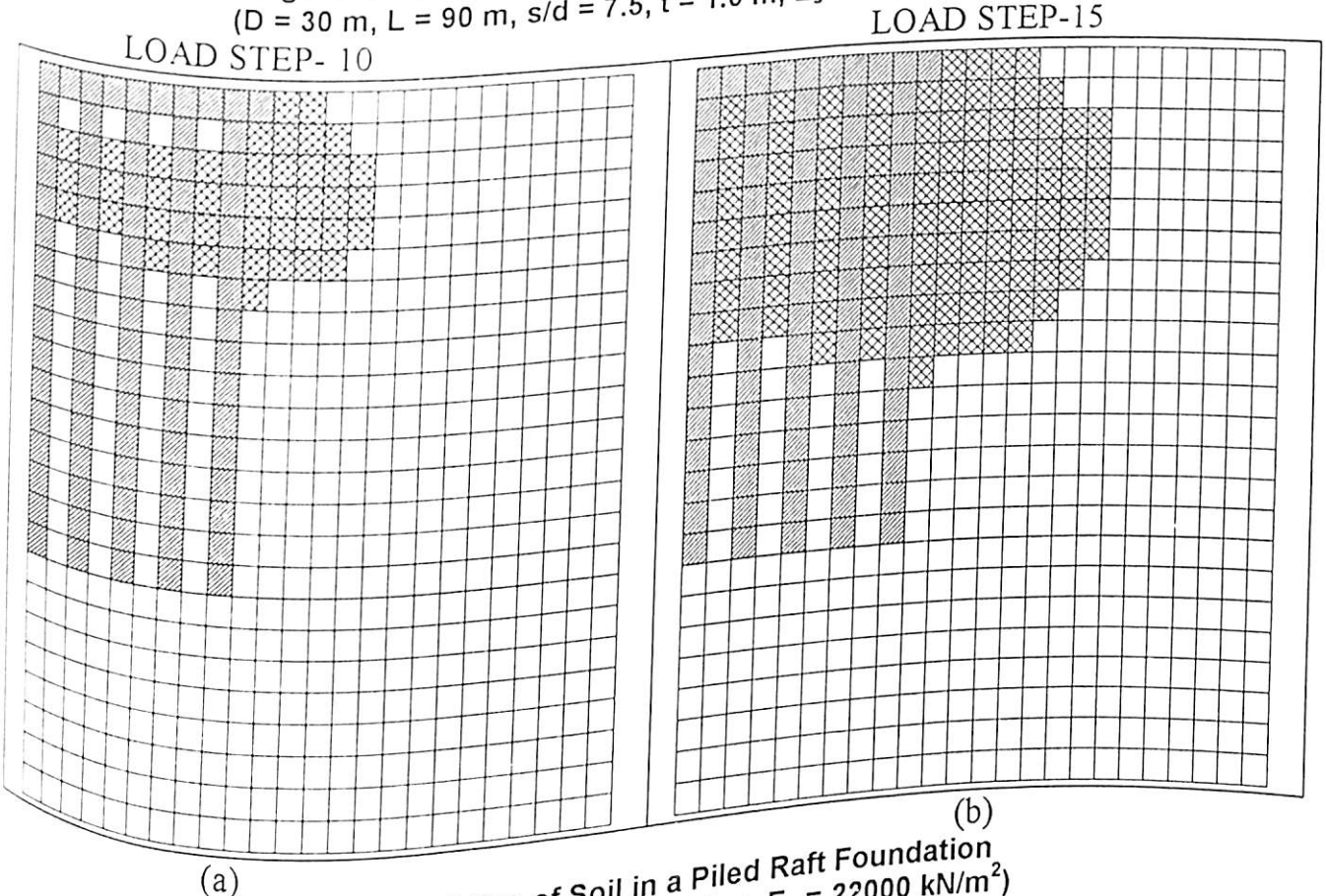

Figure 5.108 Yielding of Soil in a Piled Raft Foundation
(D = 30 m, L = 90 m, s/d = 7.5, t = 1.0 m, E_s = 22000 kN/m^2)

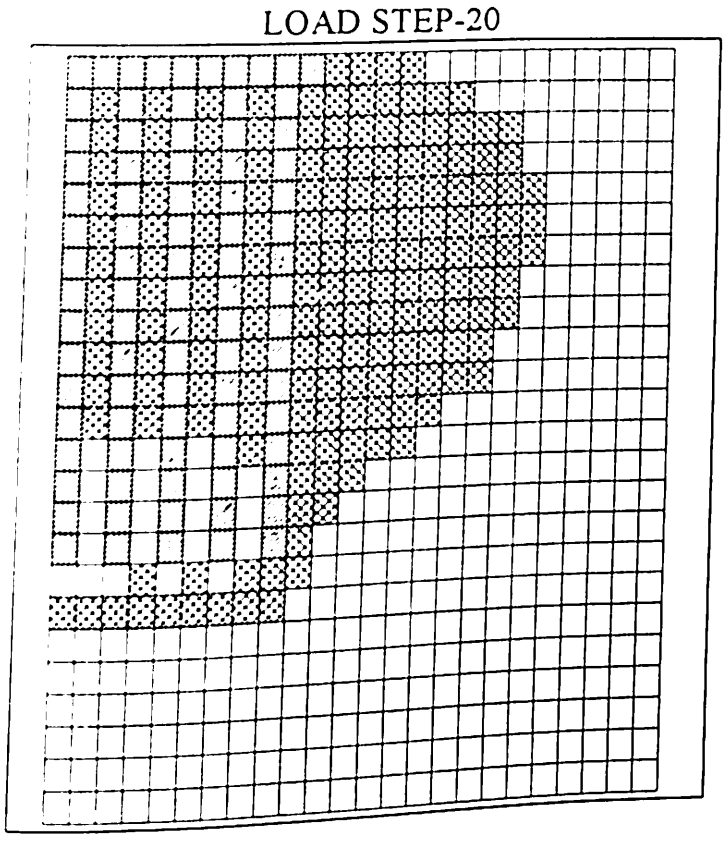

Figure 5.109 Yielding of Soil in a Piled Raft Foundation
(D = 30 m, L = 90 m, s/d = 7.5, t = 1.0 m, E_s = 22000 kN/m^2)

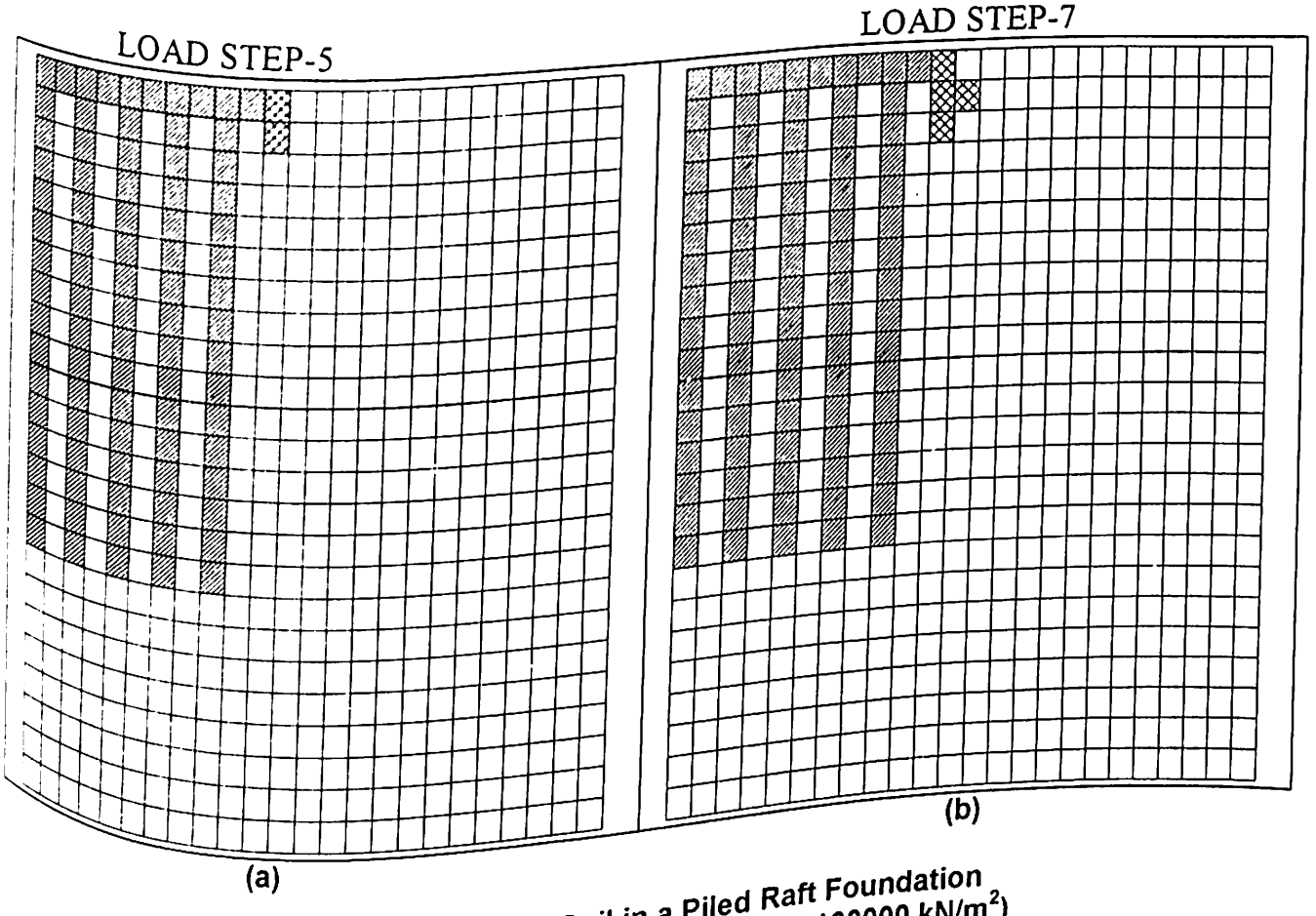

Figure 5.110 Yielding of Soil in a Piled Raft Foundation
(D = 30 m, L = 90 m, s/d = 7.5, t = 1.0 m, E_s = 130000 kN/m^2)

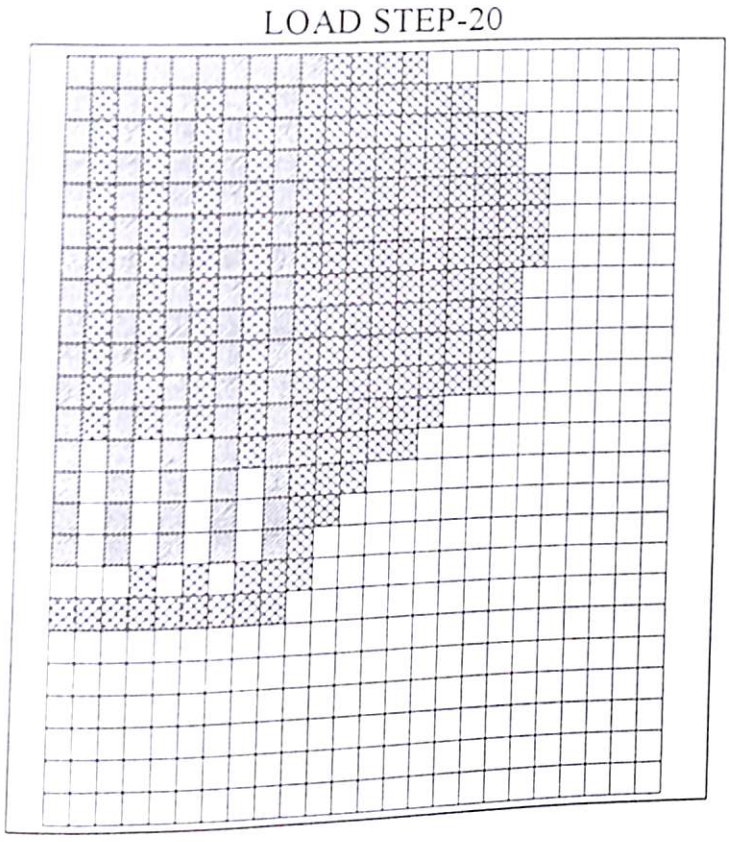

Figure 5.109 Yielding of Soil in a Piled Raft Foundation
(D = 30 m, L = 90 m, s/d = 7.5, t = 1.0 m, E_s = 22000 kN/m^2)

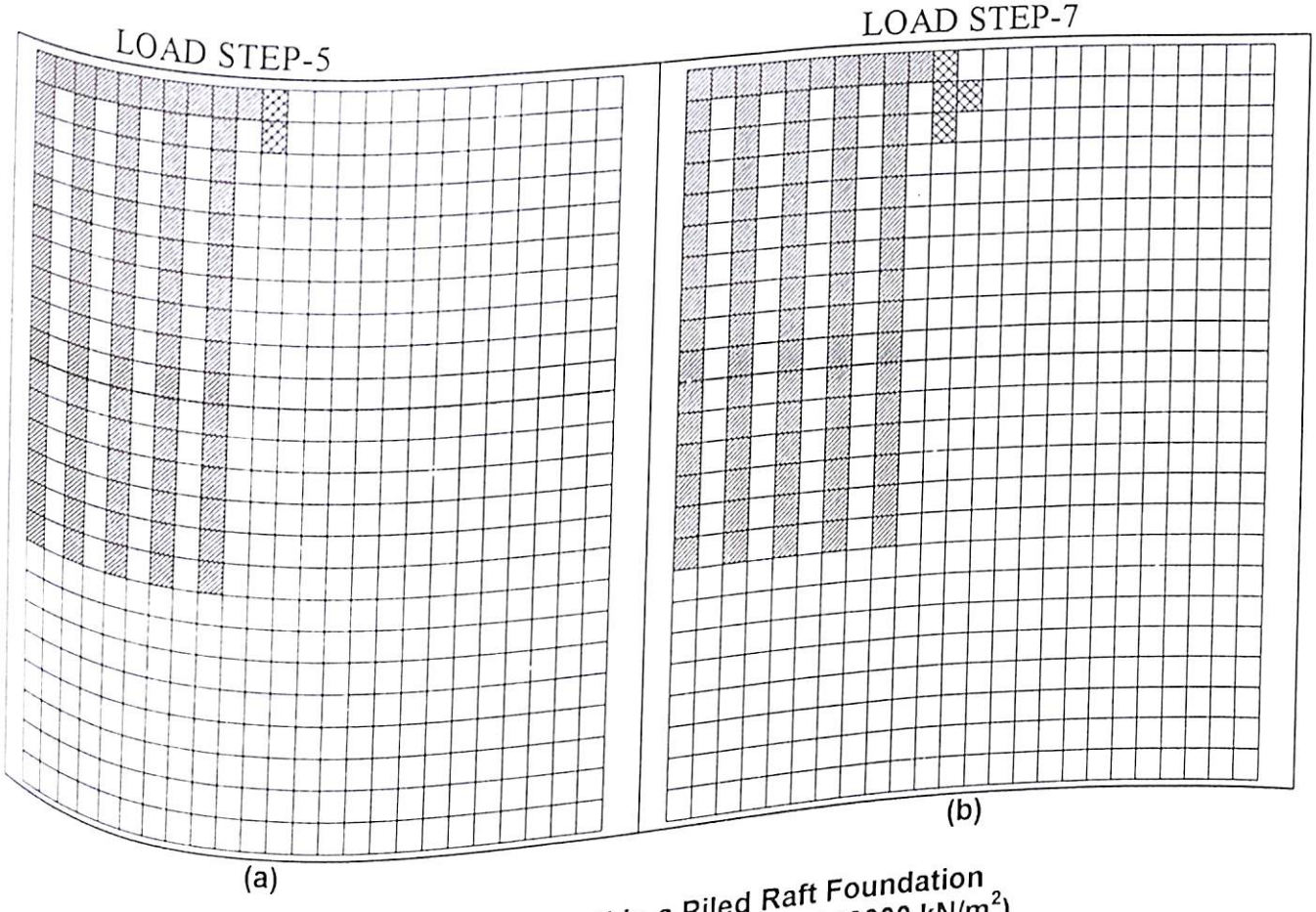

Figure 5.110 Yielding of Soil in a Piled Raft Foundation
(D = 30 m, L = 90 m, s/d = 7.5, t = 1.0 m, E_s = 130000 kN/m^2)

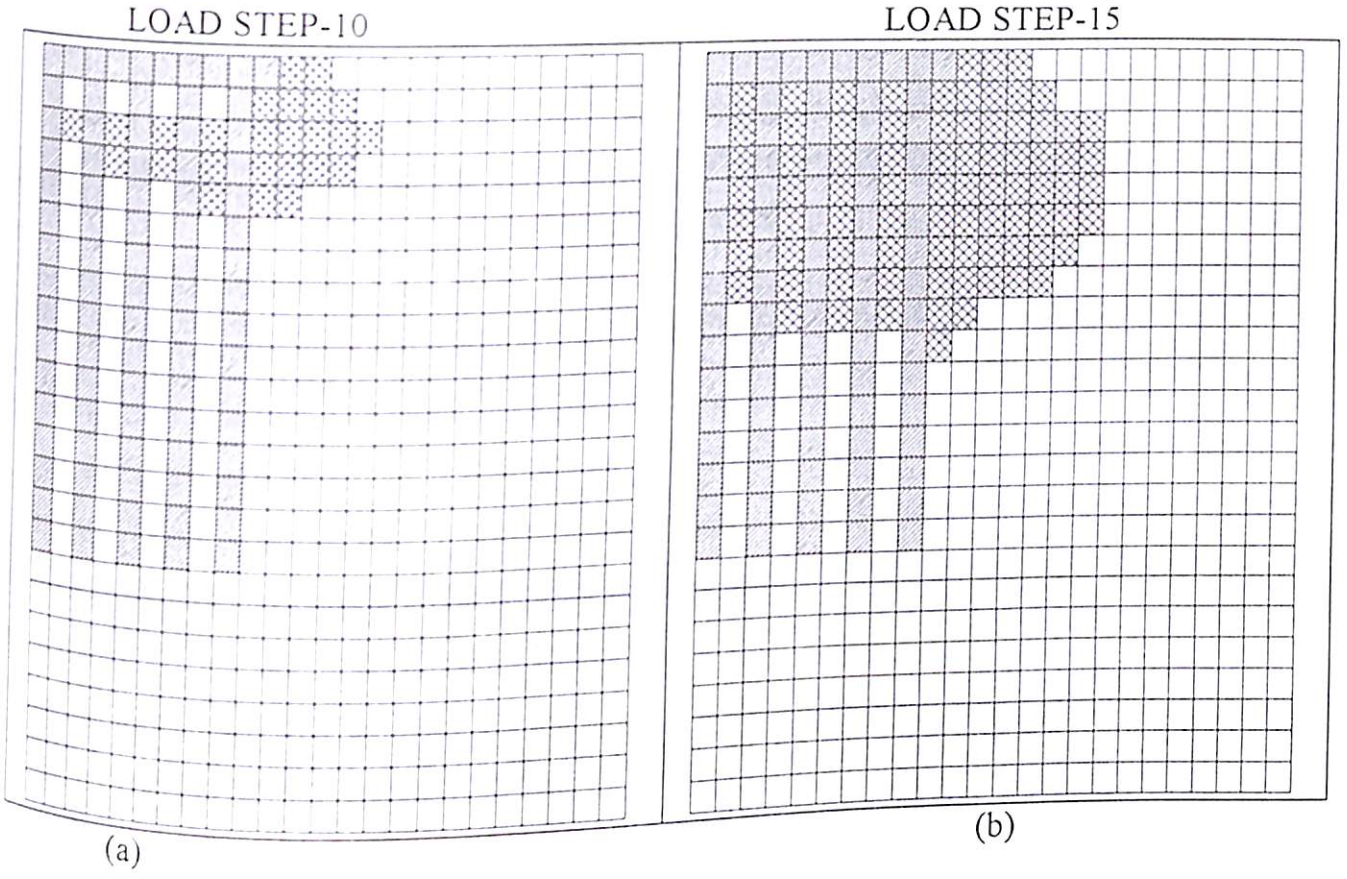

Figure 5.111 Yielding of Soil in a Piled Raft Foundation
(D = 30 m, L = 90 m, s/d = 7.5, t = 1.0 m, E_s = 130000 kN/m^2)

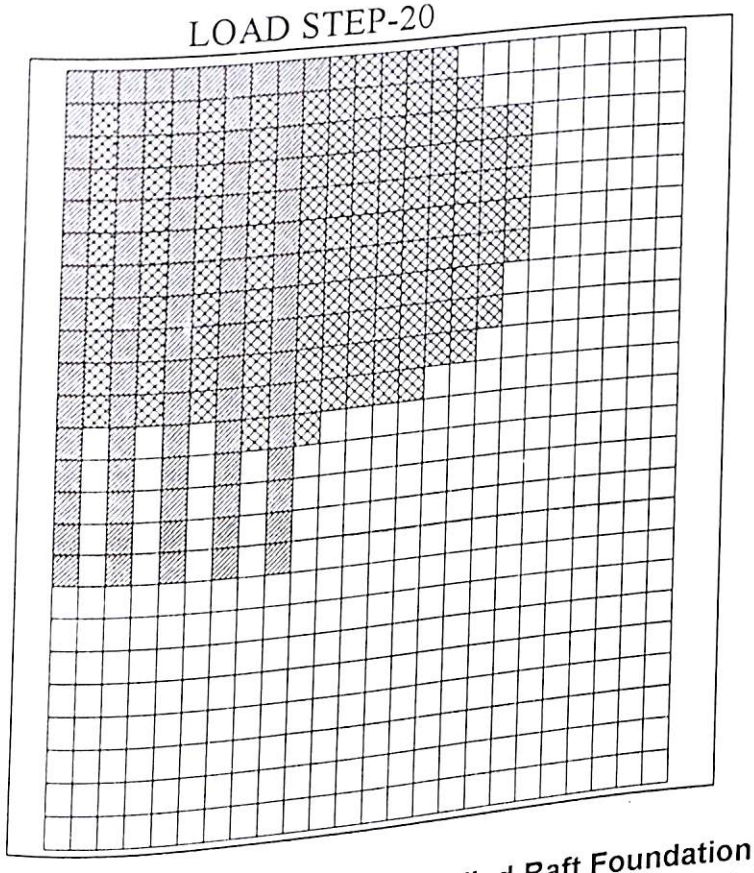

Figure 5.112 Yielding of Soil in a Piled Raft Foundation
(D = 30 m, L = 90 m, s/d = 7.5, t = 1.0 m, E_s = 130000 kN/m^2)

CHAPTER 6

NONLINEAR FINITE ELEMENT ANALYSIS OF PILED RAFT FOUNDATION UNDER PLANE STRAIN CONDITION

6.1 INTRODUCTION

Three dimensional Raft and Piled raft foundation can be analysed by considering it as a plane strain problem as the pressure bulb corresponding to the load applied depends on the smaller dimension i.e. the width of the raft and piled raft. This saves a huge computational cost. Hence in order to understand the behaviour of foundations when loaded till failure, nonlinear finite element analysis has been done under plane strain condition for raft and piled raft foundation.

6.2 DEFINITION OF PROBLEM

In order to understand the behaviour of raft and piled raft foundation nonlinear finite element analysis is to be carried out for raft and piled raft foundation by varying parameters raft width, length of pile, soil modulus and spacing between the piles.

6.3 DETAILED PARAMETRIC STUDY

Detailed parametric study has been done for raft and piled raft foundation by varying the following parameters:

Width of Raft =10, 20, 30, 40, 50 meters
Thickness of the Raft = 0.1 m to 4.0 m
Length of Pile= 10, 20, 30, 40, 60, 90, 120 meter
Diameter of Pile = 0.4 m
Soil Modulus =22000, 76000, 130000 kN/m^2
Poisson's Ratio for Soil = 0.45
Modulus of Raft and Pile Material = 20000000 kN/m^2
Poisson's Ratio of Raft and Pile Material = 0.30

6.4 ANALYSIS OF RAFT

PSNLFEM software has been used to analyse the raft foundation under plane strain condition. The validation of the results obtained from this software has been shown in chapter 4. Figure 6.1 shows the finite element discretization considered for raft foundation. The raft and soil has been discretized into four noded isoparametric finite elements. The soil has been modeled as Von-Mises elasto-plastic material. From the centre of the raft a zone of soil equal to 5 times the size of the raft has been considered. Below the raft soil of depth equal to 200 meter has been considered. The boundary condition considered has been shown in Figure 6.1.

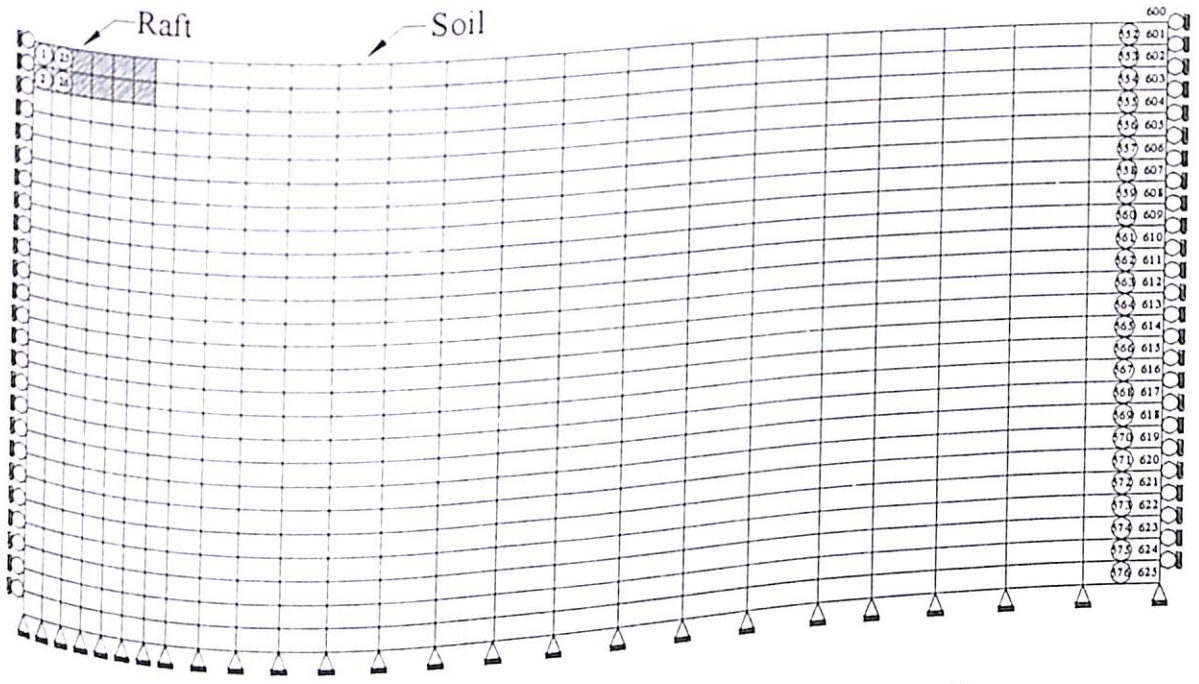

Figure 6.1 Finite Element Discretization for Raft

6.5 ANALYSIS OF PILED RAFT FOUNDATION

Finite element analysis for piled raft foundations under plane strain condition has been performed by PSNLFEM software. The results obtained from PSNLFEM software have been found in good agreement with standard finite element software. A strip of piled raft foundation of width equal to the spacing between the piles in the transverse direction has been considered in the analysis. The side of strip considered is equal to the width of the raft. Finite element discretization for typical piled raft foundation with the surrounding soil and the soil strata below has been shown in Figure 6.2. The raft, pile and soil have been discretized into four noded isoparametric finite elements. The number of nodes and elements considered are 625 and 576 respectively. The

material nonlinearity of soil has been idealised by Von-Mises Yield Criterion, which is very suitable for the clay under undrained condition. The depth of soil considered in the analysis is 200 meters. This depth has been kept constant for all the analyses. Soil domain equal to 5 times the width of raft has been considered from the center of the raft in the lateral direction. The bottom nodes have been considered completely fixed. All the nodes at center and edge boundaries have been allowed to undergo only vertical translation. Uniformly distributed load have been considered to act on the foundation. The uniformly distributed load considered has been applied as concentrated load on the respective nodes on the foundation.

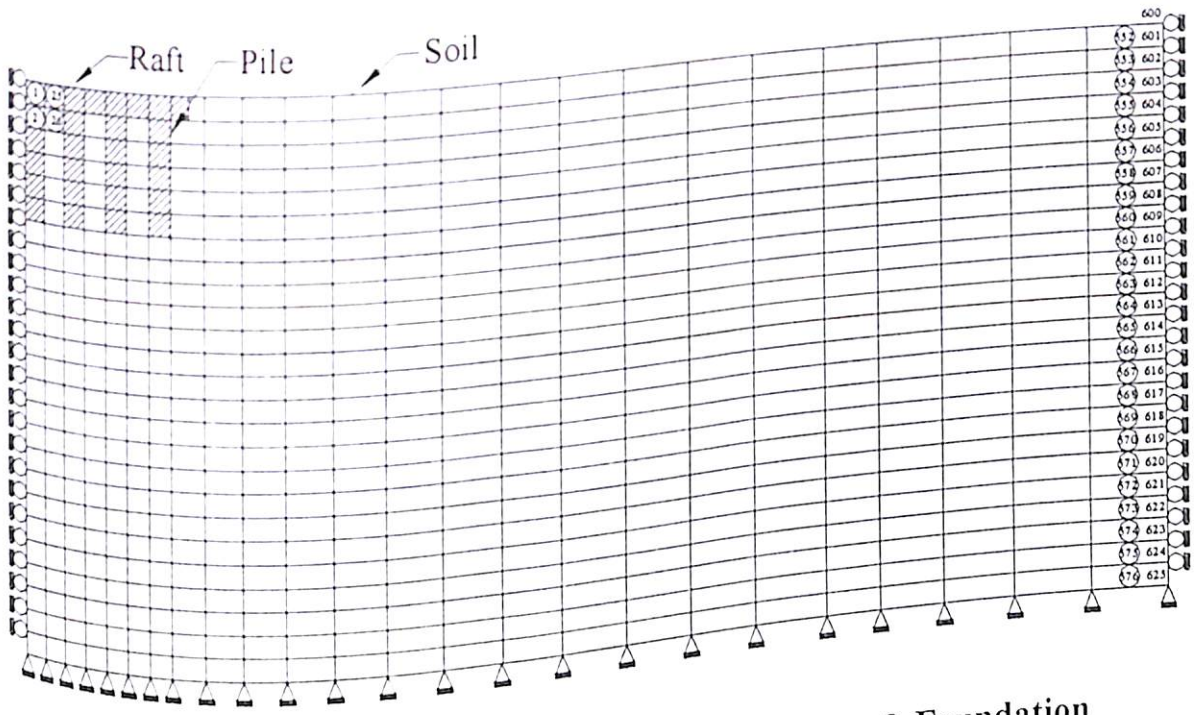

Figure 6.2 Finite Element Discretization for Piled Raft Foundation

6.6 RESULTS AND DISCUSSION

6.6.1 Load Settlement Curves for Raft

6.6.1.1 Effect of thickness

Figures 6.3 (a), (b), (c) show the load settlement curve of raft foundation of diameter 10 meters. The effect of thickness and soil modulus on load settlement behaviour of raft foundation has been shown in the same Figures. The effect of increase in thickness is found to increase the load carrying capacity of raft foundation. This effect is predominant at higher loading intensity. The effect of increase in soil modulus is to increase the load carrying capacity of raft foundation.

Figures 6.4 (a), (b), (c) show the load settlement curve of raft foundation of width 20 meters. The effect of thickness and soil modulus on load settlement behaviour of raft foundation has been shown in the same Figures. The effect of increase in thickness is found to increase the load carrying capacity of raft foundation. This effect is predominant at higher loading intensity. The effect of increase in soil modulus is to increase the load carrying capacity of raft foundation.

Figures 6.5 (a), (b), (c) show the load settlement curve of raft foundation of width 30 meter. The effect of thickness and soil modulus on load settlement behaviour of raft foundation has been shown in the same Figure. It can be observed from the graph that with increase in thickness, the load carrying capacity of raft foundation increases. This effect can be clearly seen at higher loading intensity. The effect of increase in soil modulus is found to reduce the settlement of raft foundation.

Figures 6.6 (a), (b), (c) show the load settlement curve of raft foundation of width 40 meter. Increase in thickness of the raft has been found to increase the load carrying capacity of raft foundation. Higher loading intensity clearly shows this effect. The effect of increase in soil modulus is seen to increase the load carrying capacity of raft foundation.

Figures 6.7 (a), (b), (c) show the load settlement curve of raft foundation of width 50 meter. The effect of thickness and soil modulus on load settlement behaviour of raft foundation has been shown in the same Figures. It is observed from the graphs that with increase in thickness of the raft settlement reduces and load carrying capacity of raft foundation increases. Higher loading intensity clearly shows this effect. The effect of increase in soil modulus is to increase the load carrying capacity of raft foundation.

6.6.1.2 Effect of soil modulus

The effect of soil modulus on the load settlement behaviour of piled raft foundation of width 10 meter has been shown in Figure 6.8 for varying thickness of the raft. The effect of increase in soil modulus is to increase the load carrying capacity of piled raft foundation. The effect of increase in thickness is to increase the load carrying capacity of piled raft foundation.

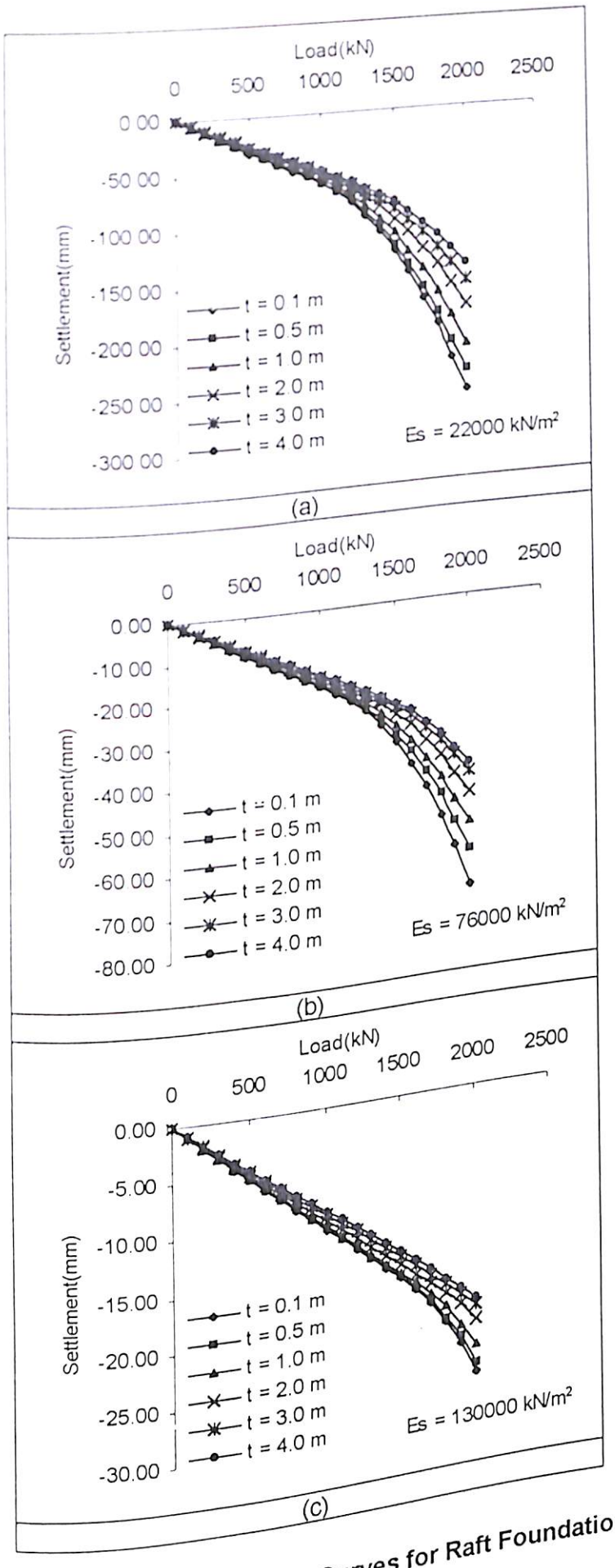

Figure 6.4 Load Settlement Curves for Raft Foundation (B = 20 m)

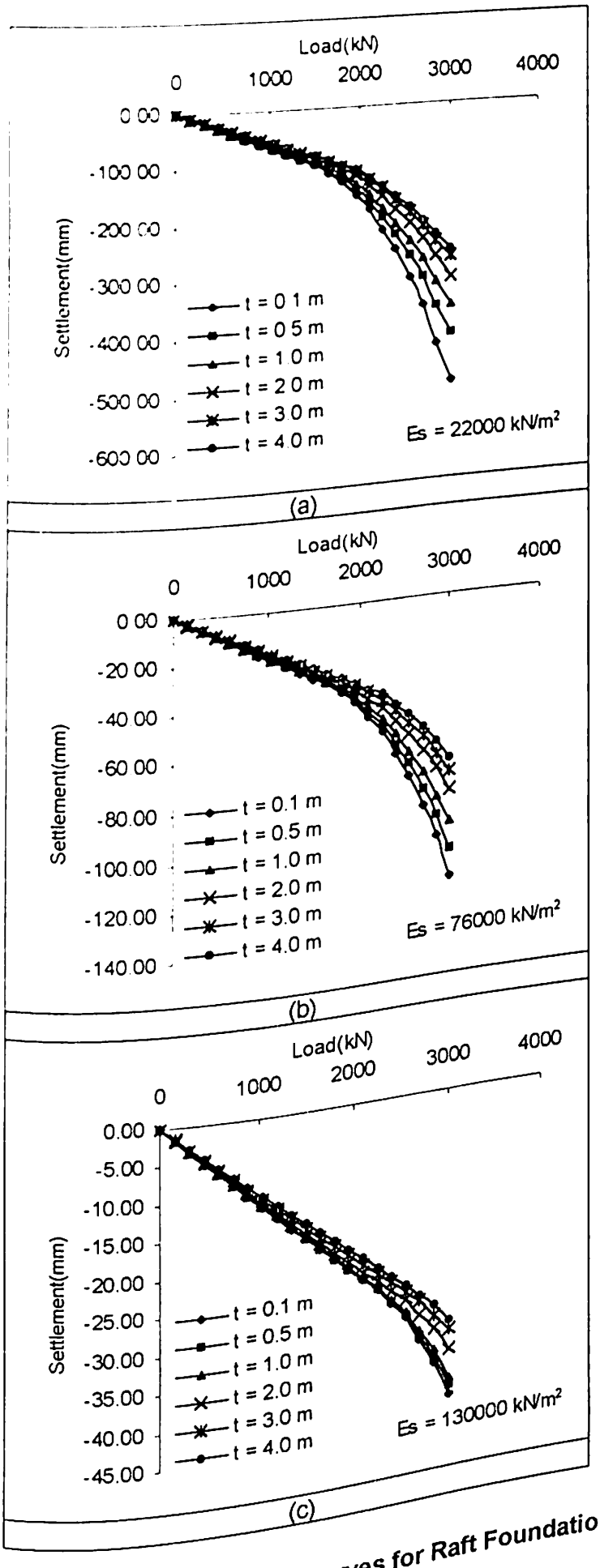

Figure 6.5 Load Settlement Curves for Raft Foundation (B = 30 m)

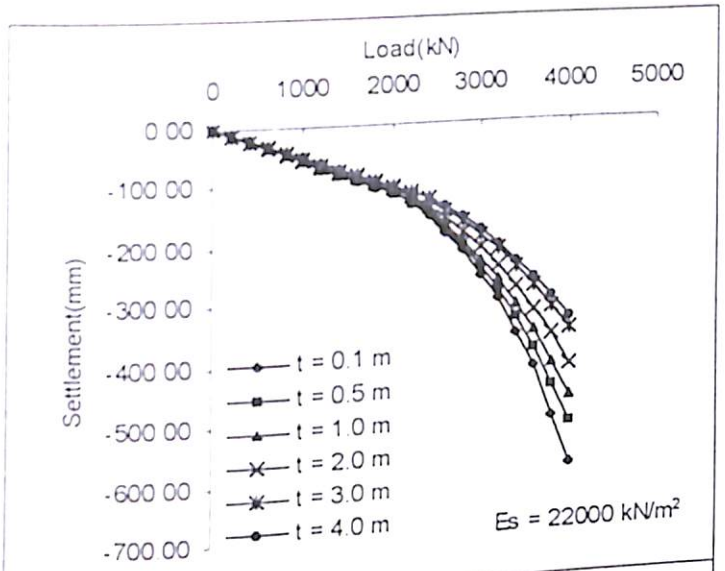
Load(kN)
0
1000
2000
3000
4000
5000
0.00
-100.00
-200.00
-300.00
-400.00
-500.00
-600.00
-700.00
Settlement(mm)
t = 0.1 m
t = 0.5 m
t = 1.0 m
t = 2.0 m
t = 3.0 m
t = 4.0 m
Es = 22000 kN/m²

(a)

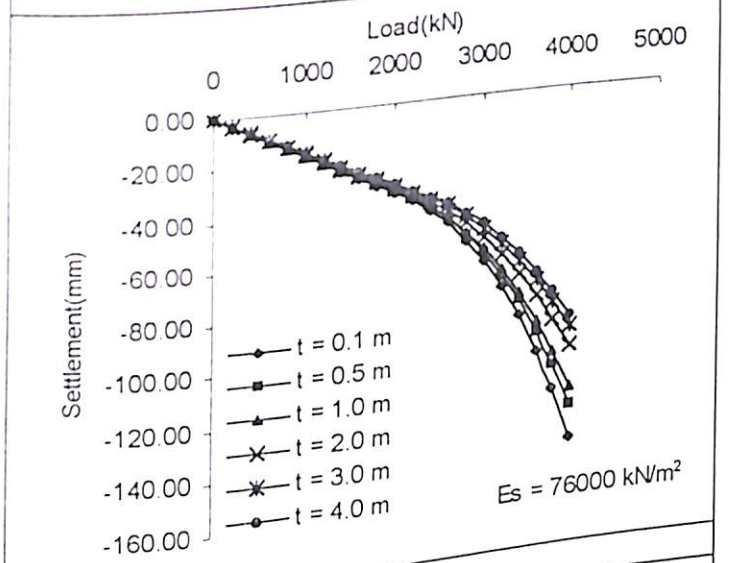
Load(kN)
0
1000
2000
3000
4000
5000
0.00
-20.00
-40.00
-60.00
-80.00
-100.00
-120.00
-140.00
-160.00
Settlement(mm)
t = 0.1 m
t = 0.5 m
t = 1.0 m
t = 2.0 m
t = 3.0 m
t = 4.0 m
Es = 76000 kN/m²

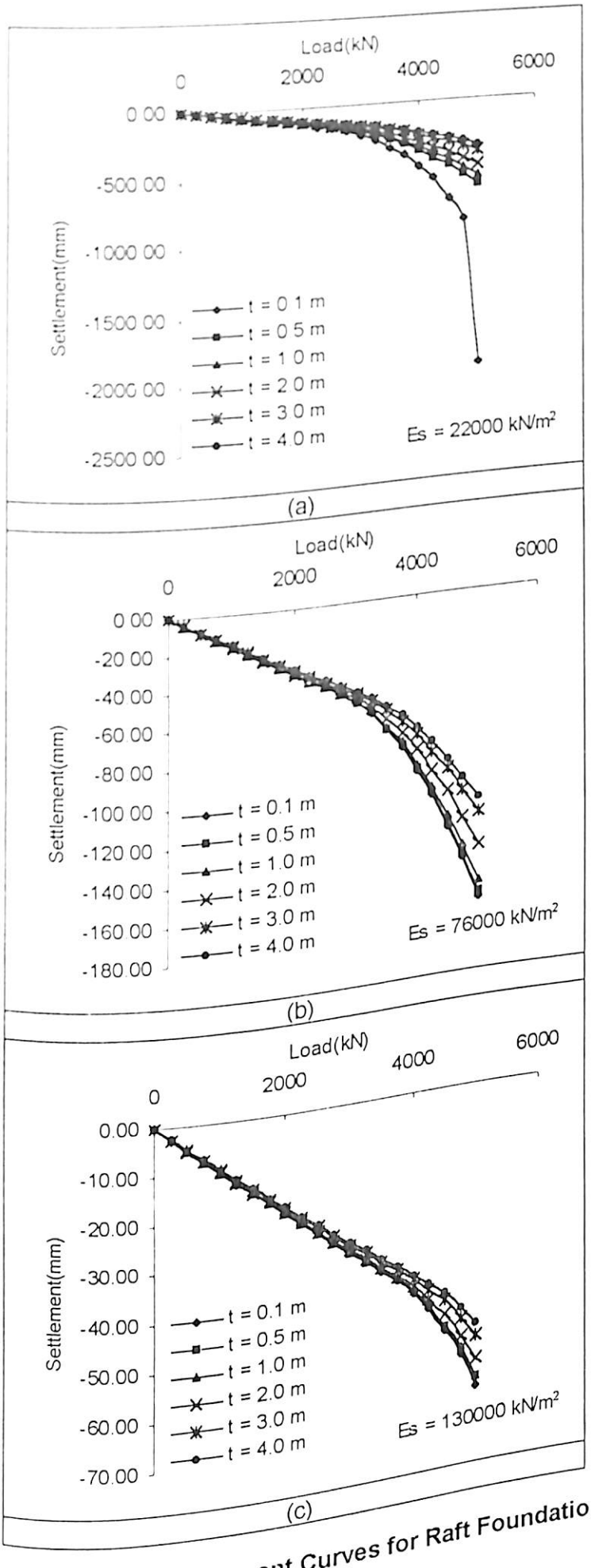

Figure 6.7 Load Settlement Curves for Raft Foundation (B = 50 m)

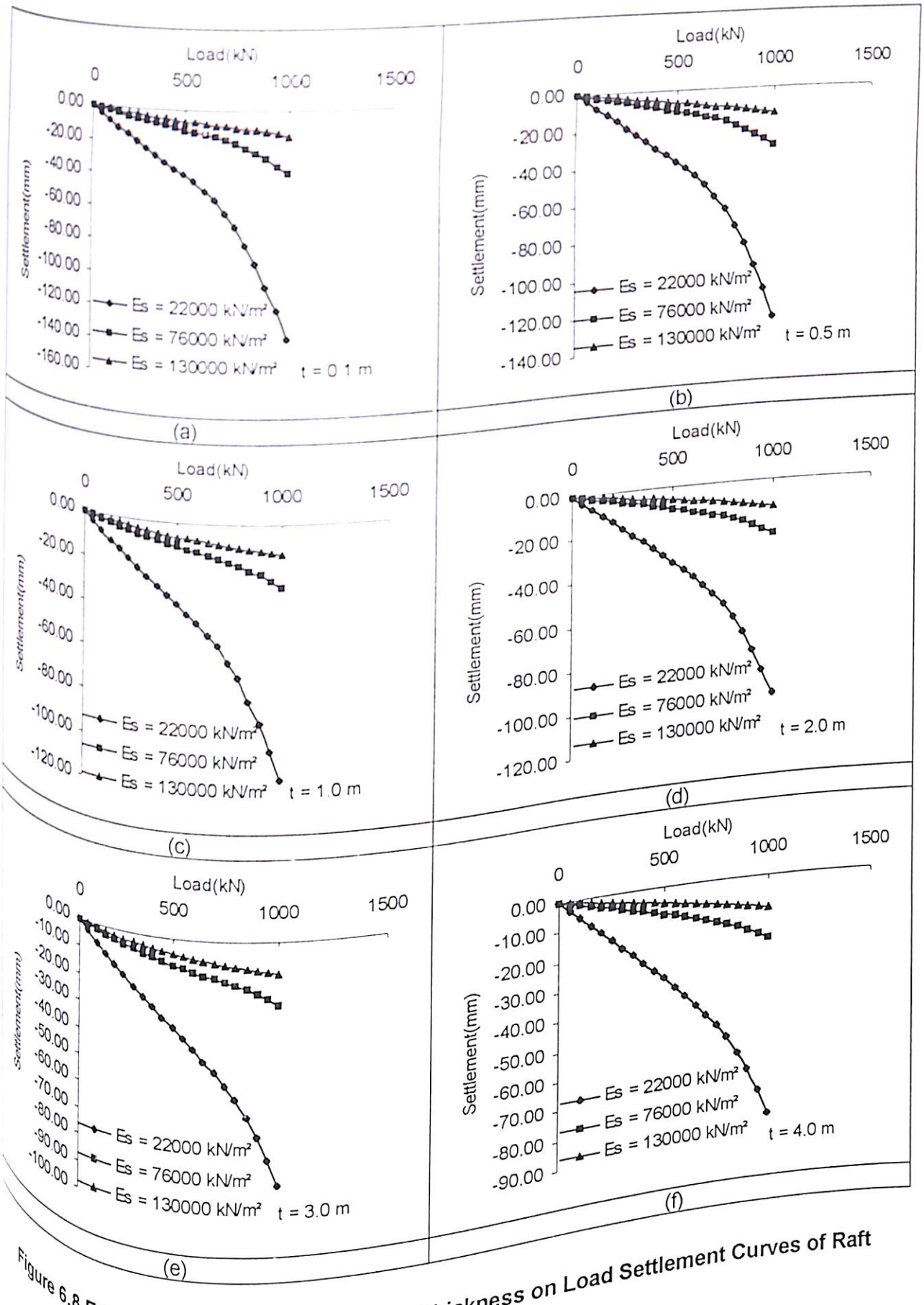

Figure 6.8 Effects of Soil Modulus and Raft Thickness on Load Settlement Curves of Raft Foundation (B = 10 m)

The effect of soil modulus on the load settlement behaviour of piled raft foundation of width 20 meter has been shown in Figure 6.9 for varying thickness of the raft. The effect of increase in soil modulus and thickness is to reduce the settlement and increase the load carrying capacity of piled raft foundation.

Figures 6.10 (a), (b), (c), (d), (e), (f) show the effect of soil modulus on the load settlement behaviour of piled raft foundation of width 30 meter for varying thickness of the raft. The load carrying capacity can be seen maximum at higher soil modulus and thickness. The load carrying capacity is minimum at smaller thickness and soil modulus. When the thicknesses of raft and soil modulus are increased, the load carrying capacity is found to increase. The increased soil modulus and thickness helps in reducing the overall settlement of the raft foundation.

The effect of soil modulus on the load settlement behaviour of piled raft foundation of width 40 meter has been shown in Figure 6.11 for varying thickness of the raft. For the range of thickness and soil modulus considered, the load carrying capacity is found maximum at larger thickness and higher soil modulus.

Figures 6.12 (a), (b), (c), (d), (e), (f) show the effect of soil modulus on the load settlement behaviour of piled raft foundation of width 50 meter for varying thickness of the raft. The load carrying capacity in this case is more than for the 40 meter width of raft. The effect of increase in thickness and soil modulus follows the similar trend as explained for Figure 6.11.

6.6.1.3 Effect of width of raft

The effect of width of raft on the load settlement behaviour of raft has been shown in Figure 6.13 for varying thickness of raft and soil modulus of 22000 kN/m^2. The effect of increase in width of raft is to increase the load carrying capacity of raft significantly. This increase is predominant at higher load. The raft of smaller dimension reaches to its ultimate capacity at lesser settlement while the raft of larger size reaches to its ultimate capacity at high settlement.

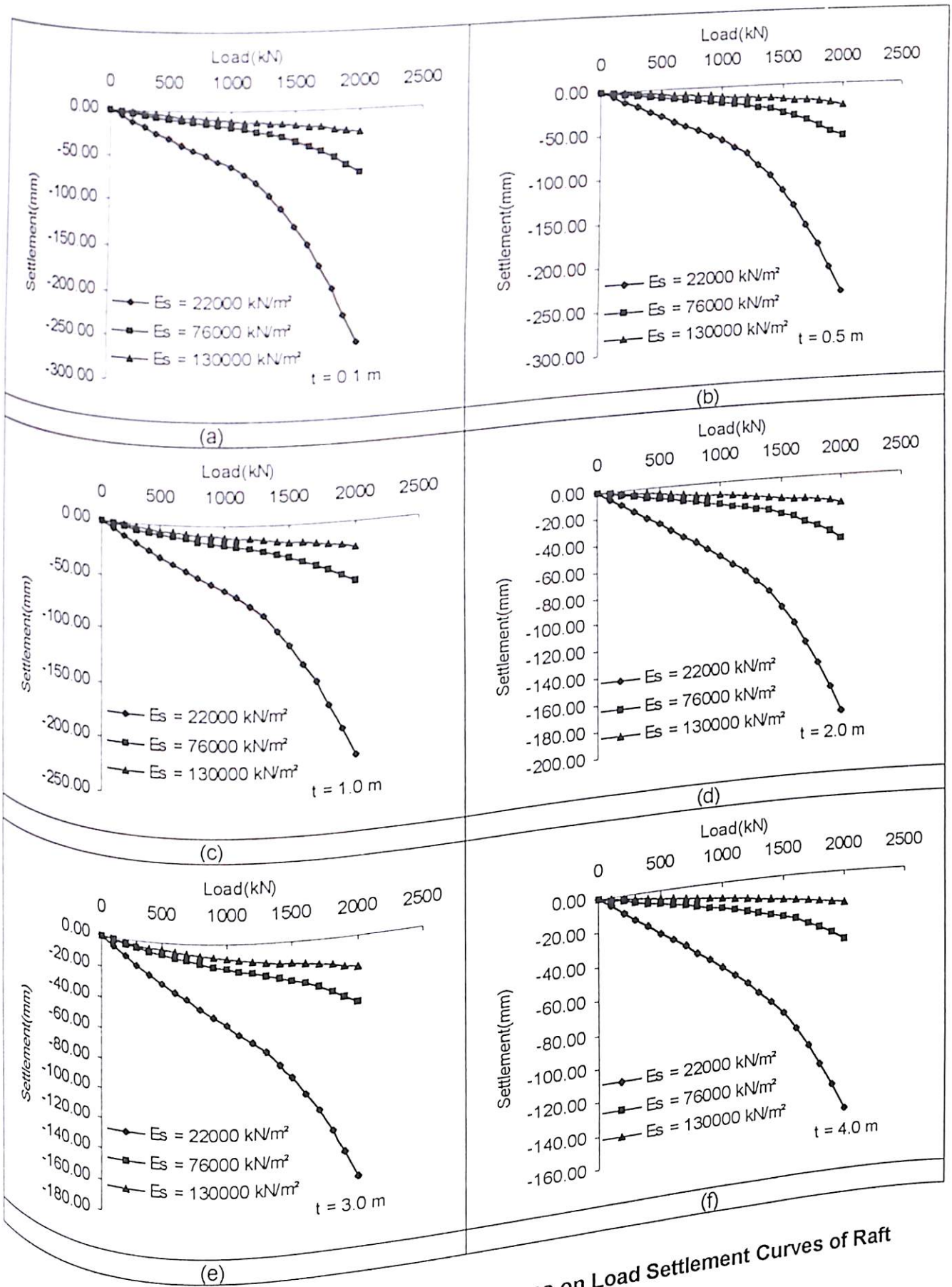

Figure 6.9 Effect of Soil Modulus and Raft Thickness on Load Settlement Curves of Raft Foundation (B = 20 m)

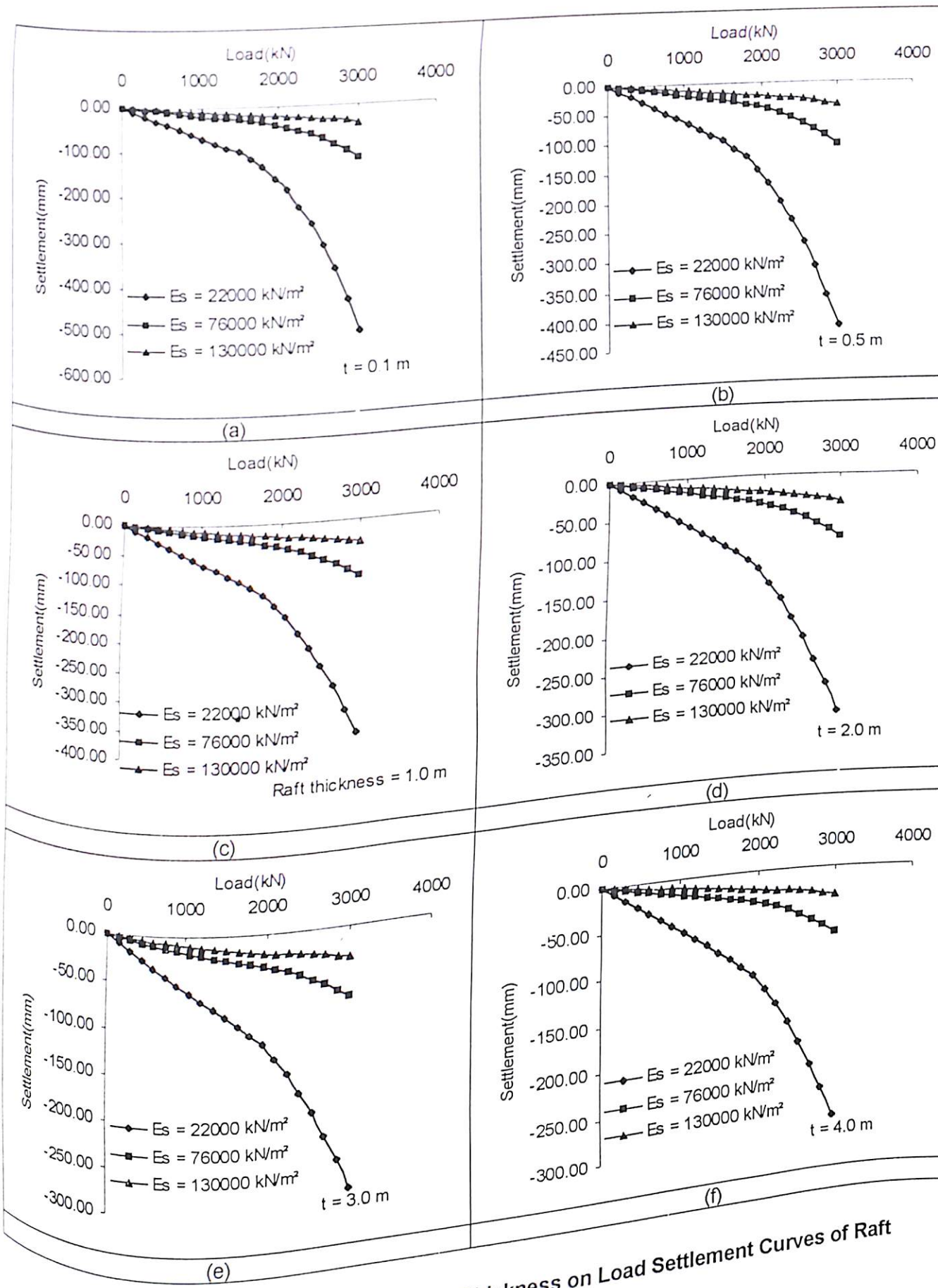

Figure 6.10 Effect of Soil Modulus and Raft Thickness on Load Settlement Curves of Raft Foundation (B = 30 m)

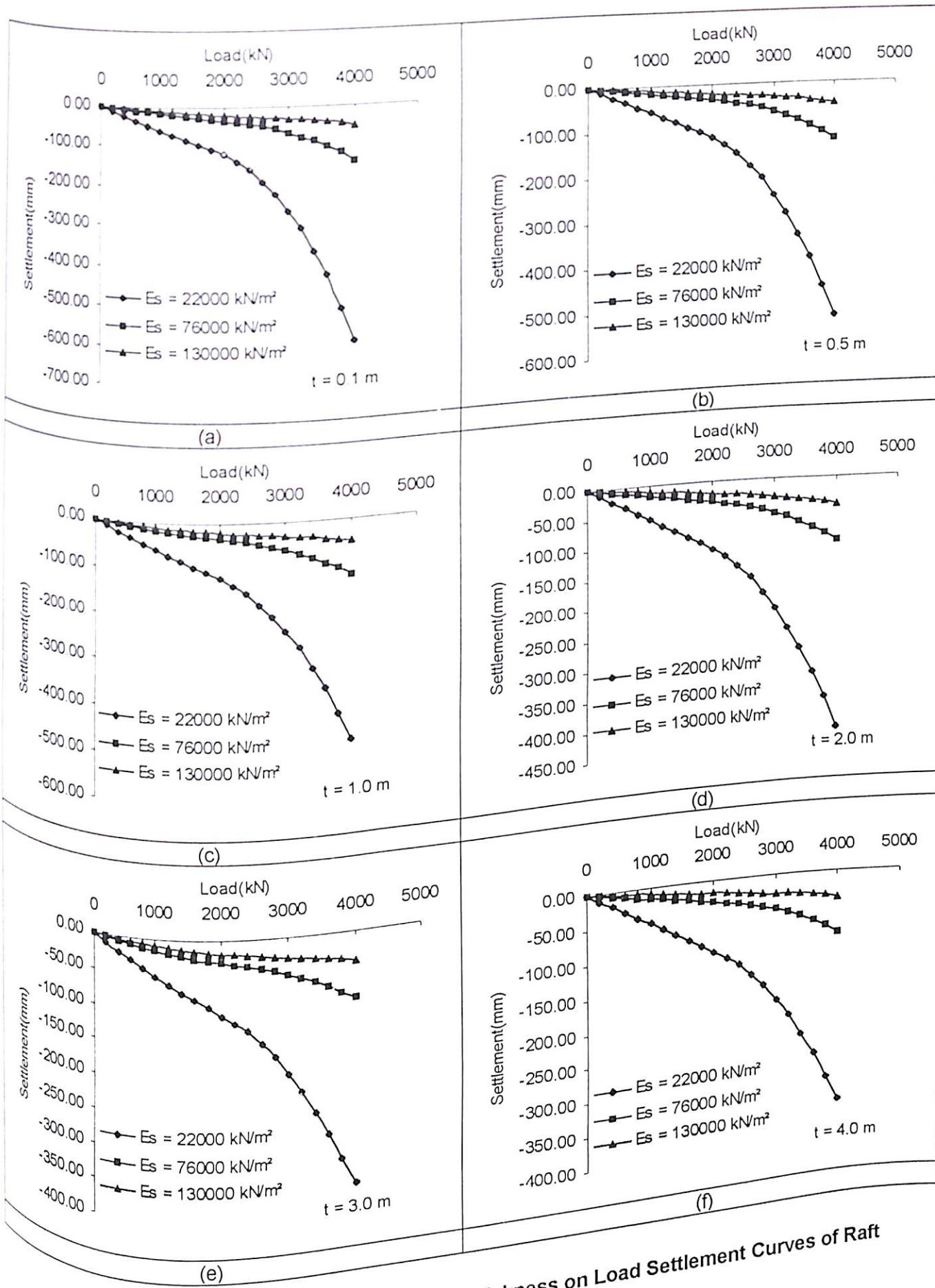

Figure 6.11 Effect of Soil Modulus and Raft Thickness on Load Settlement Curves of Raft Foundation (B = 40 m)

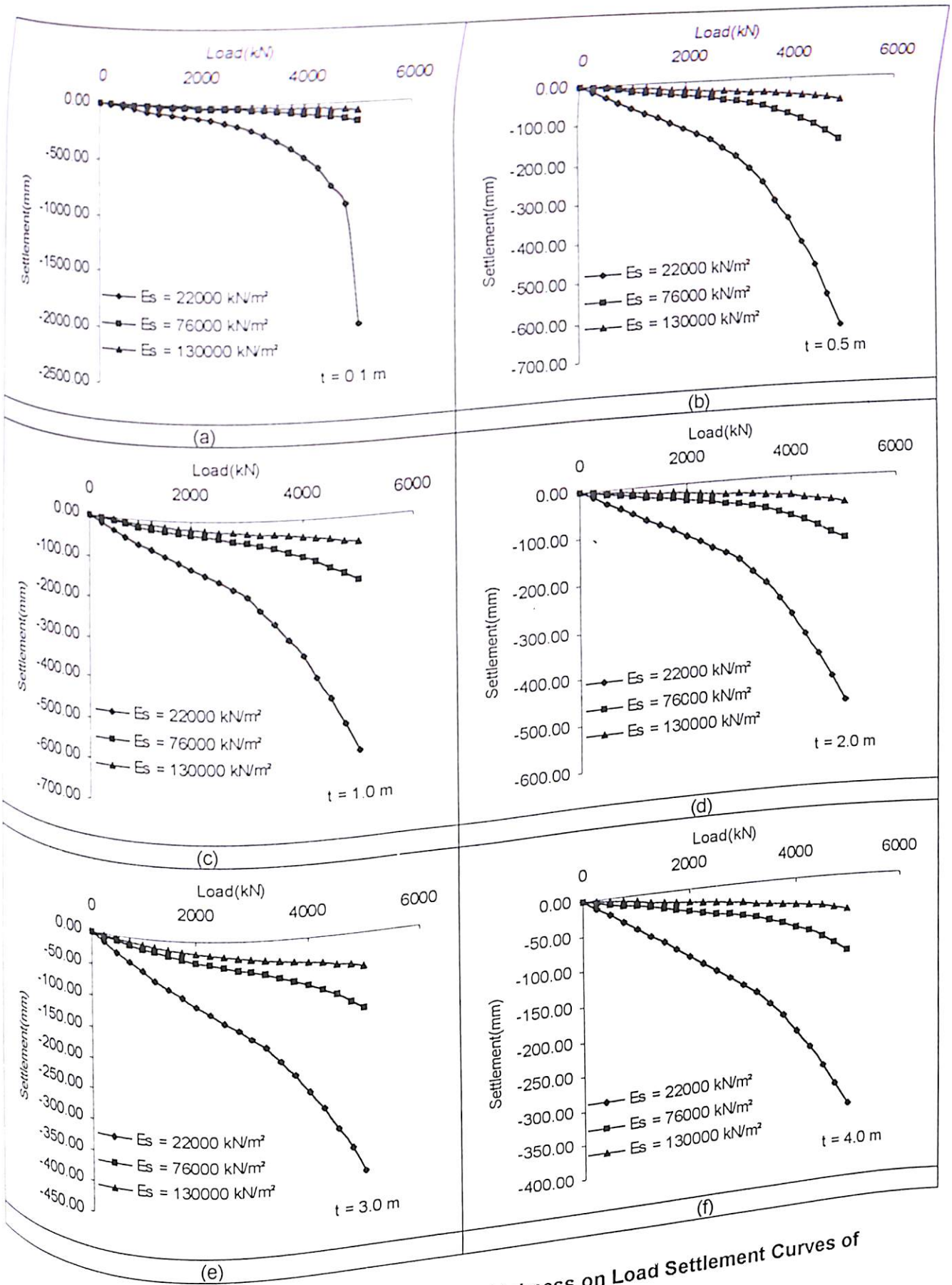

Figure 6.12 Effect of Soil Modulus and Raft Thickness on Load Settlement Curves of Raft Foundation (D = 50 m)

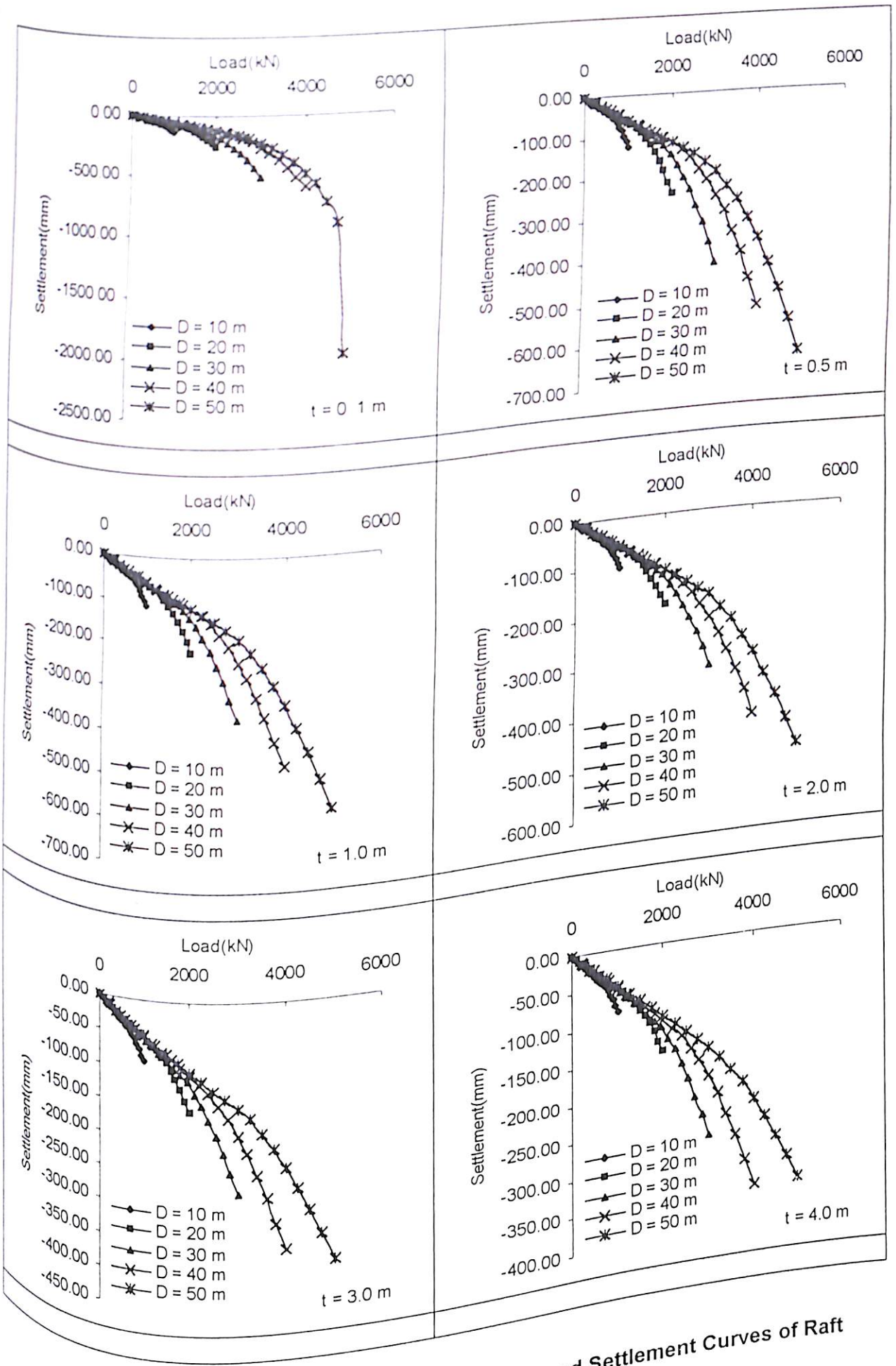

Figure 6.13 Effect of Raft Width on Load Settlement Curves of Raft Foundation (E_s = 22000 kN/m^2)

The effect of width of raft on the load settlement behaviour of raft has been shown in Figure 6.14 for varying thickness of raft and soil modulus of 76000 kN/m^2. Significant increase in load carrying capacity of raft is seen with increase in width of the raft. This increase is seen predominant at higher load. When settlement and load carrying capacity is compared for increased width of raft, it is found that the raft of larger width reaches to its ultimate capacity at larger settlement compared to the raft of lesser width..

6.6.2 Load Settlement Curve for Piled Raft Foundation

6.6.2.1 Effect of pile length

The effect of length of pile on the load settlement behaviour of piled raft foundation has been shown in Figure 6.15 for center to center spacing of 2.5 times the one side of the pile and raft width 10 meter. The increase in length of the pile significantly increases the load carrying capacity and reduces settlement of piled raft foundation. This increase in load carrying capacity of piled raft foundation is predominant at higher loading intensity. The effect of increase in soil modulus is to increase the load carrying capacity of piled raft foundation.

Figures 6.16 (a), (b), (c) show the effect of length of pile on the load settlement behaviour of piled raft foundation for center to center spacing of 5.0 times the one side of the pile and raft width of 10 meter. The increased length of pile is found effective in increasing the load carrying capacity and reducing the settlement of piled raft foundation. This is due to the fact that the length of mobilization of unit skin friction increases with increase in length of pile. With increase in soil modulus, the load carrying capacity of piled raft foundation increases. This is because there is increase in stiffness of soil with corresponding increase in modulus.

The effect of length of pile on the load settlement behaviour of piled raft foundation has been shown in Figure 6.17 for center to center spacing of 7.5 times the one side of the pile and raft width of 10 meter. The effect of increase in length and soil modulus on load carrying capacity is same as explained above.

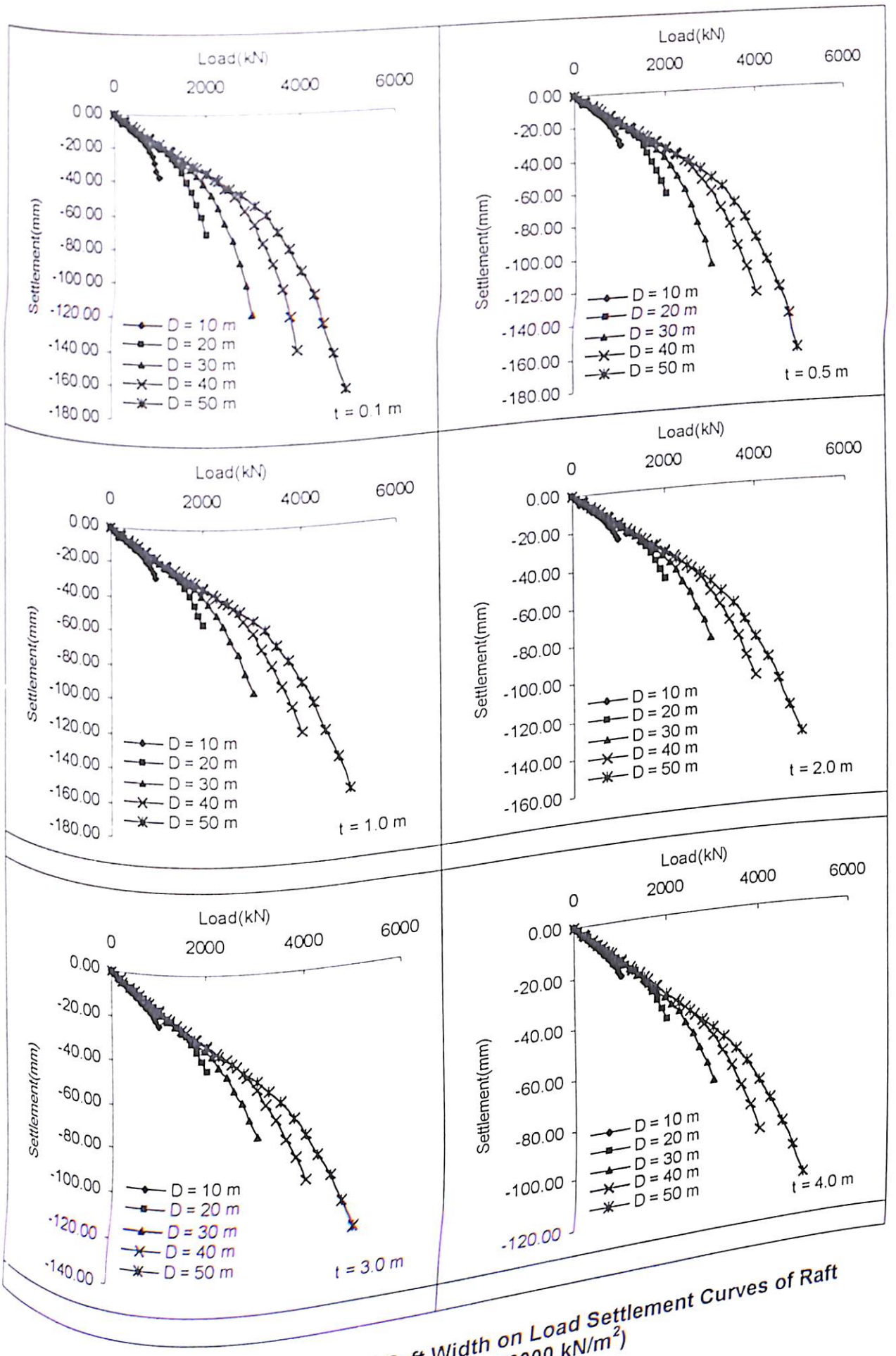

Figure 6.14 Effect of Raft Width on Load Settlement Curves of Raft Foundation (Es = 76000 kN/m^2)

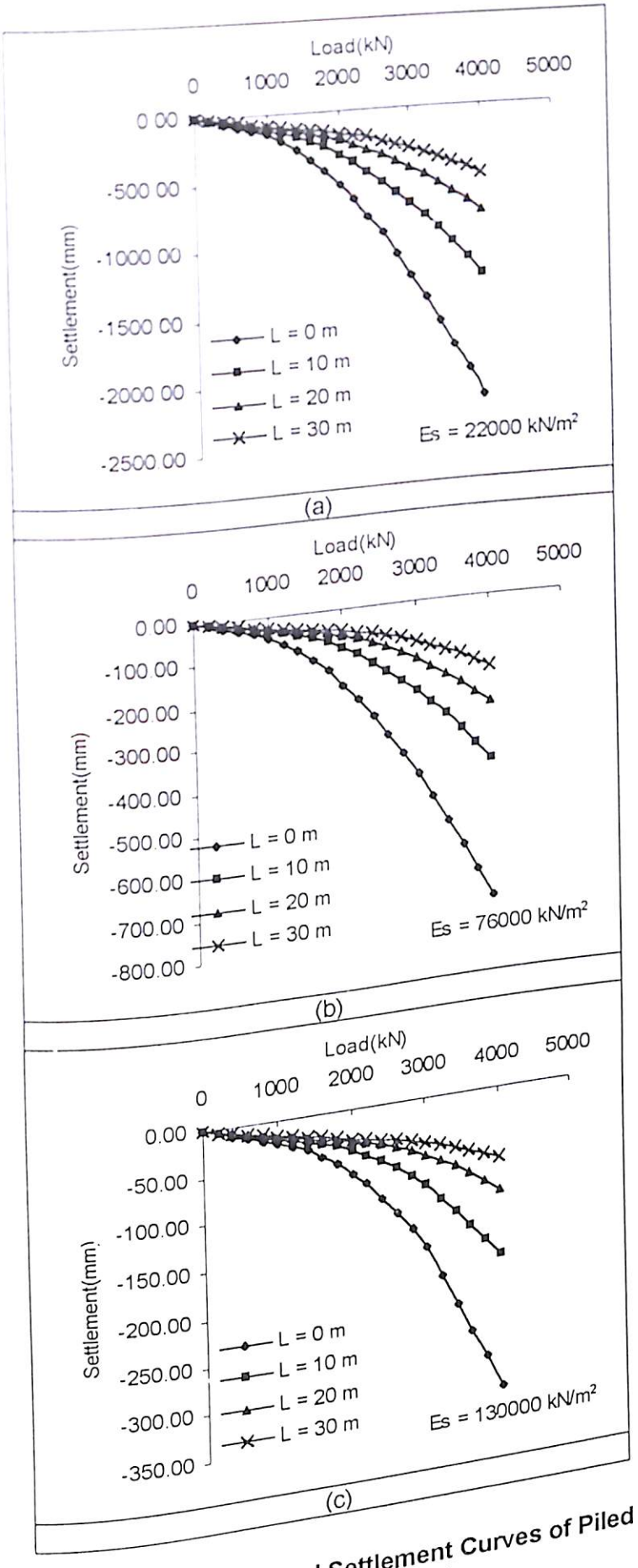

Figure 6.15 Effect of Pile Length on Load Settlement Curves of Piled Raft Foundation (B = 10 m, s/d = 2.5)

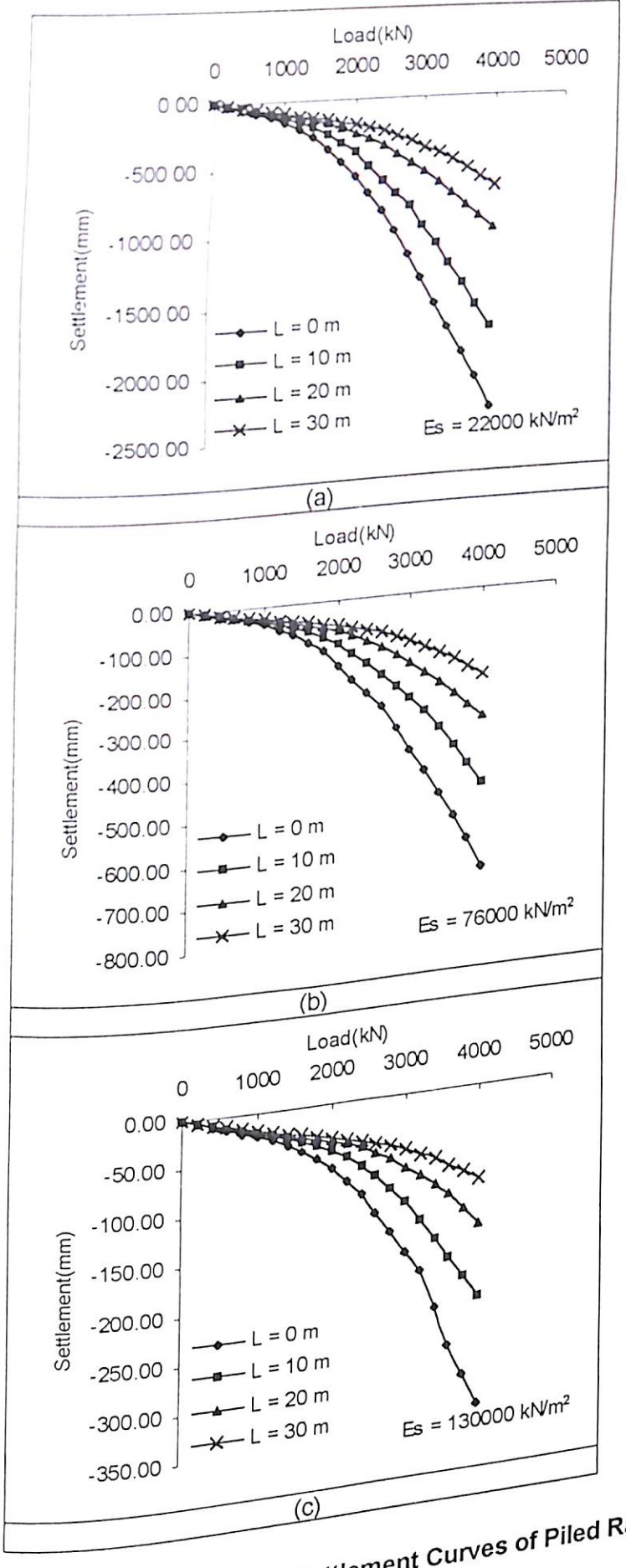

Figure 6.16 Effect of Pile Length on Load Settlement Curves of Piled Raft Foundation (B = 10 m, s/d = 5)

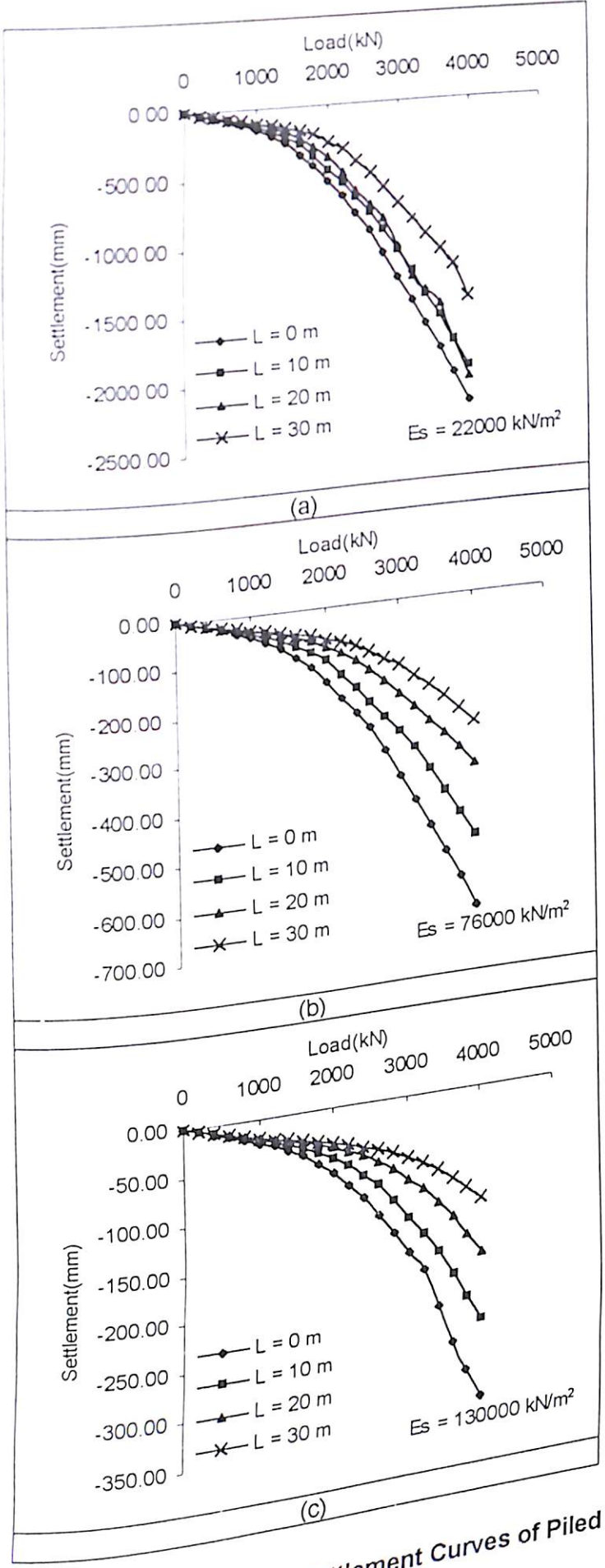

Figure 6.17 Effect of Pile Length on Load Settlement Curves of Piled Raft Foundation (B = 10 m, s/d = 7.5)

The effect of soil modulus on the load settlement behaviour of piled raft foundation of width 10 meter has been shown in Figure 6.18 for varying pile lengths and spacing equal to 2.5 times the one side of the pile. The load carrying capacity of piled raft foundation increases with increase in length of pile and soil modulus. This is because the stiffness of pile increases due to increase in length of pile and stiffness of soil increases due to increase in soil modulus

Figures 6.19 (a), (b), (c), (d) show the effect of soil modulus on the load settlement behaviour of piled raft foundation of width 10 meter for varying pile lengths and spacing equal to 5 times the one side of the pile. The increased length of pile and soil modulus improves load carrying capacity significantly.

The effect of soil modulus on the load settlement behaviour of piled raft foundation of width 10 meter has been shown in Figure 6.20 for varying pile lengths and spacing equal to 7.5 times the one side of the pile. The effect of increase in soil stiffness is to increase the load carrying capacity of piled raft foundation. With increase in pile length the range of mobilization of unit skin friction increases and hence has been found significant in increasing the load carrying capacity.

6.6.2.2 Effect of spacing

The effect of spacing on load settlement behaviour of piled raft foundation of width 10 meter has been shown in Figure 6.21 for soil modulus of 22000 kN/m^2 for varying length of the pile. The effect of increase in spacing is to reduce the overall load carrying capacity of piled raft foundation but increases the load carrying capacity of individual piles because the mobilization of skin friction increases with increase in spacing between the piles.

Figures 6.22 (a), (b), (c) show the effect of spacing on load settlement behaviour of piled raft foundation of width 10 meter and soil modulus of 76000 kN/m^2 for varying pile length. The load carrying capacity of piled raft foundation decreases with increase in pile spacing.

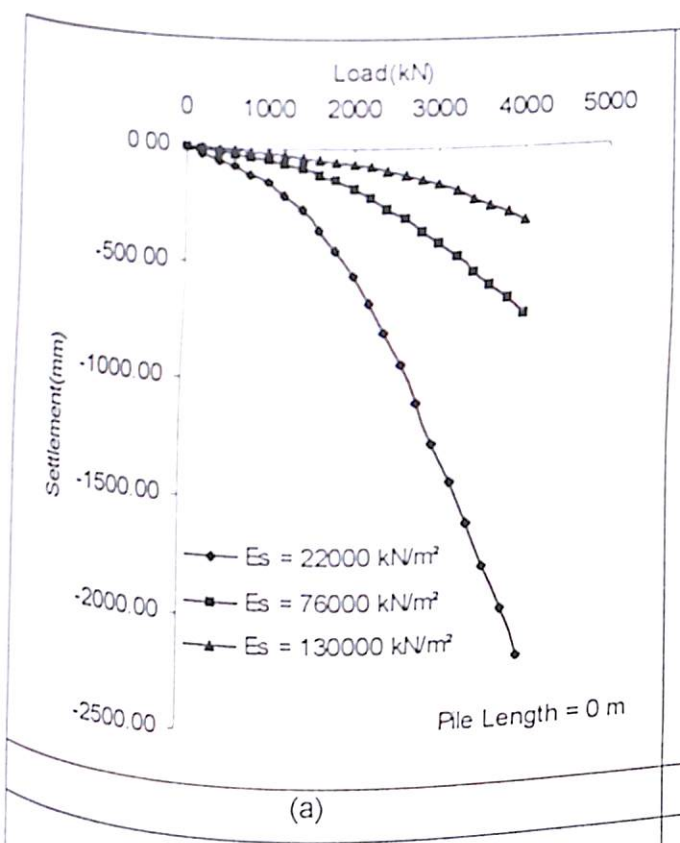
Load(kN)
0 1000 2000 3000 4000 5000
0.00
-500.00
-1000.00
-1500.00
-2000.00
-2500.00
Settlement(mm)
Es = 22000 kN/m²
Es = 76000 kN/m²
Es = 130000 kN/m²
Pile Length = 0 m

(a)

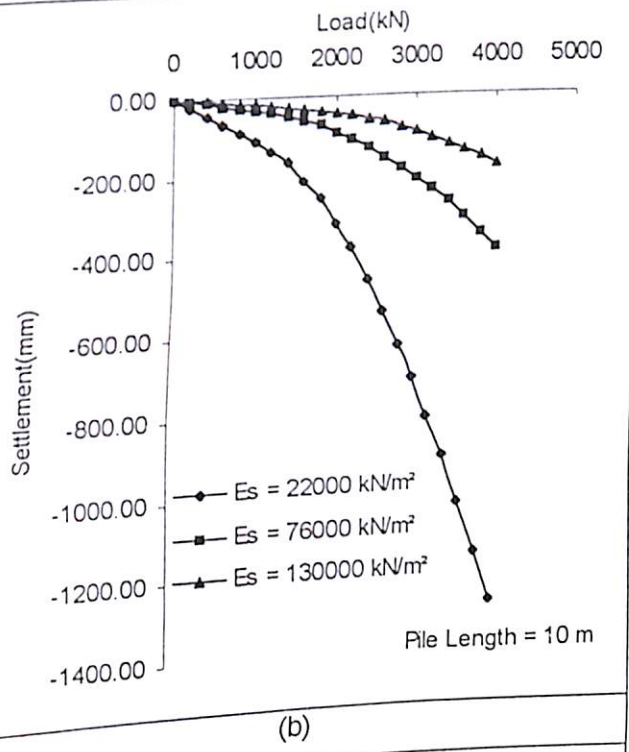
Load(kN)
0 1000 2000 3000 4000 5000
0.00
-200.00
-400.00
-600.00
-800.00
-1000.00
-1200.00
-1400.00
Settlement(mm)
Es = 22000 kN/m²
Es = 76000 kN/m²
Es = 130000 kN/m²
Pile Length = 10 m

(b)

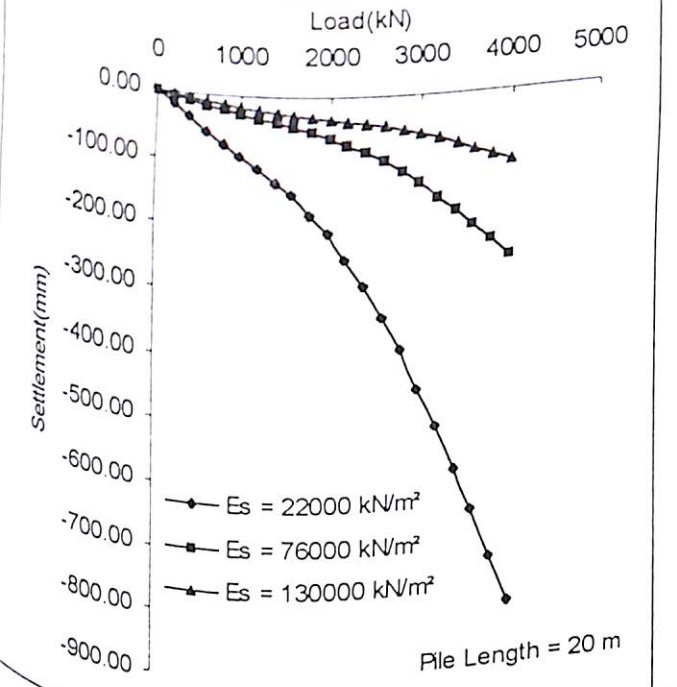
Load(kN)
0 1000 2000 3000 4000 5000
0.00
-100.00
-200.00
-300.00
-400.00
-500.00
-600.00
-700.00
-800.00
-900.00
Settlement(mm)
Es = 22000 kN/m²
Es = 76000 kN/m²
Es = 130000 kN/m²
Pile Length = 20 m

(c)

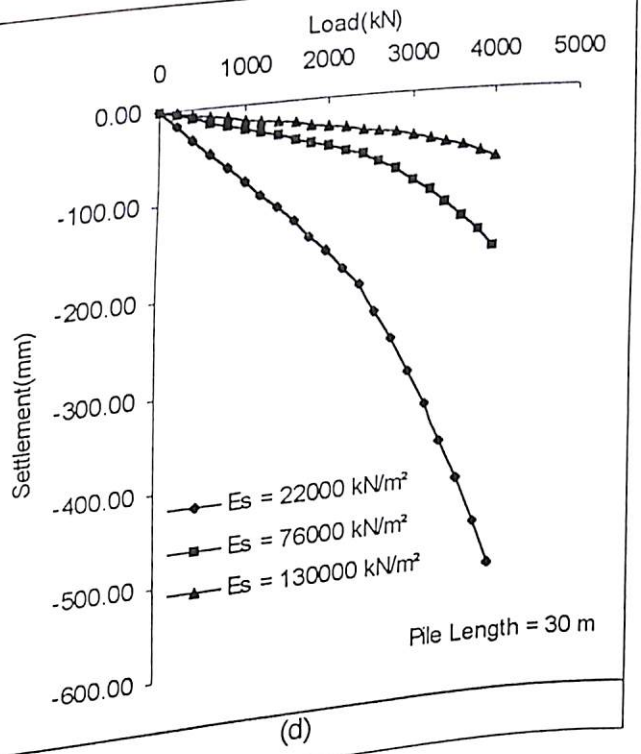
Load(kN)
0 1000 2000 3000 4000 5000
0.00
-100.00
-200.00
-300.00
-400.00
-500.00
-600.00
Settlement(mm)
Es = 22000 kN/m²
Es = 76000 kN/m²
Es = 130000 kN/m²
Pile Length = 30 m

(d)

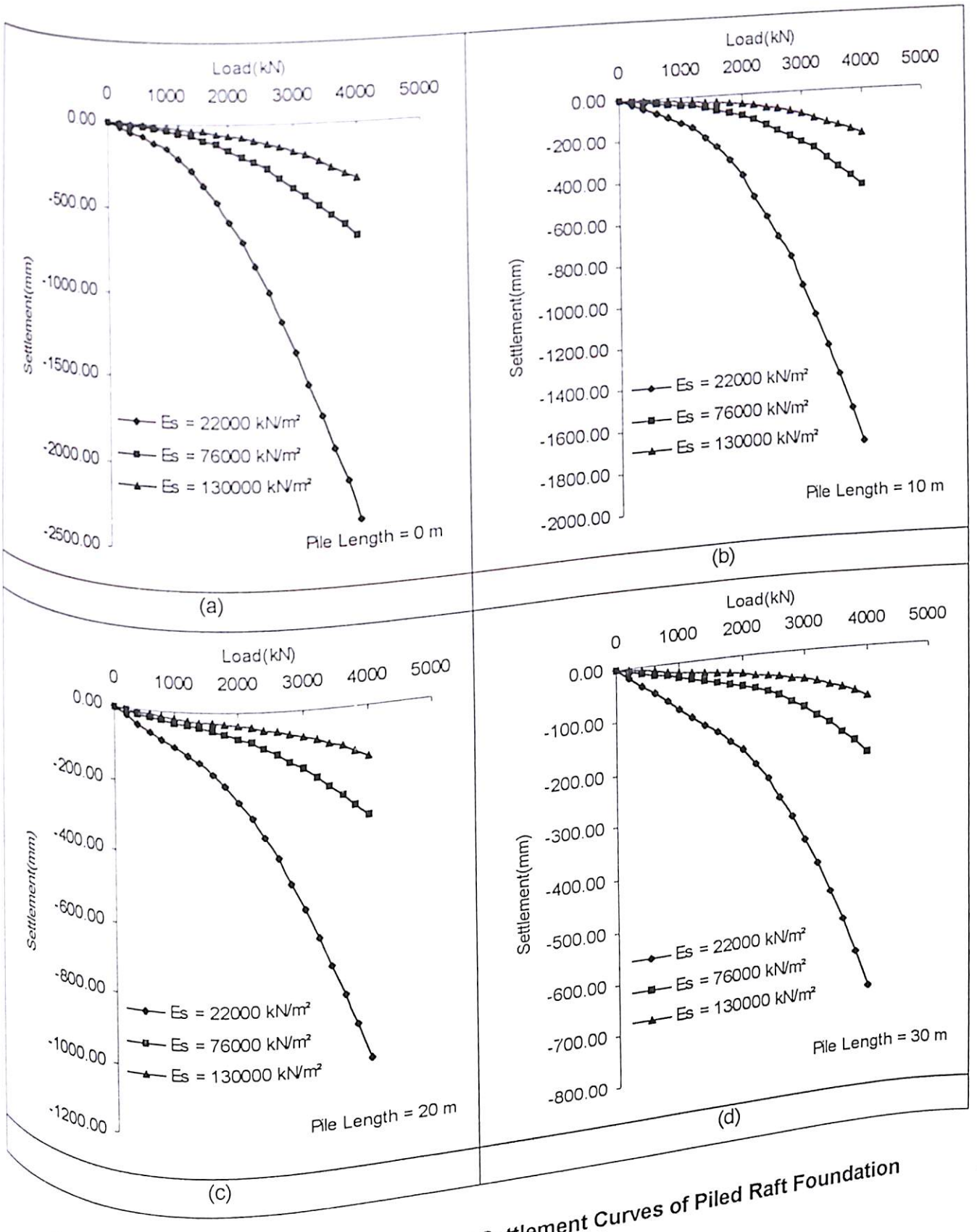

Figure 6.19 Effect of Soil Modulus on Load Settlement Curves of Piled Raft Foundation (B = 10 m, s/d = 5)

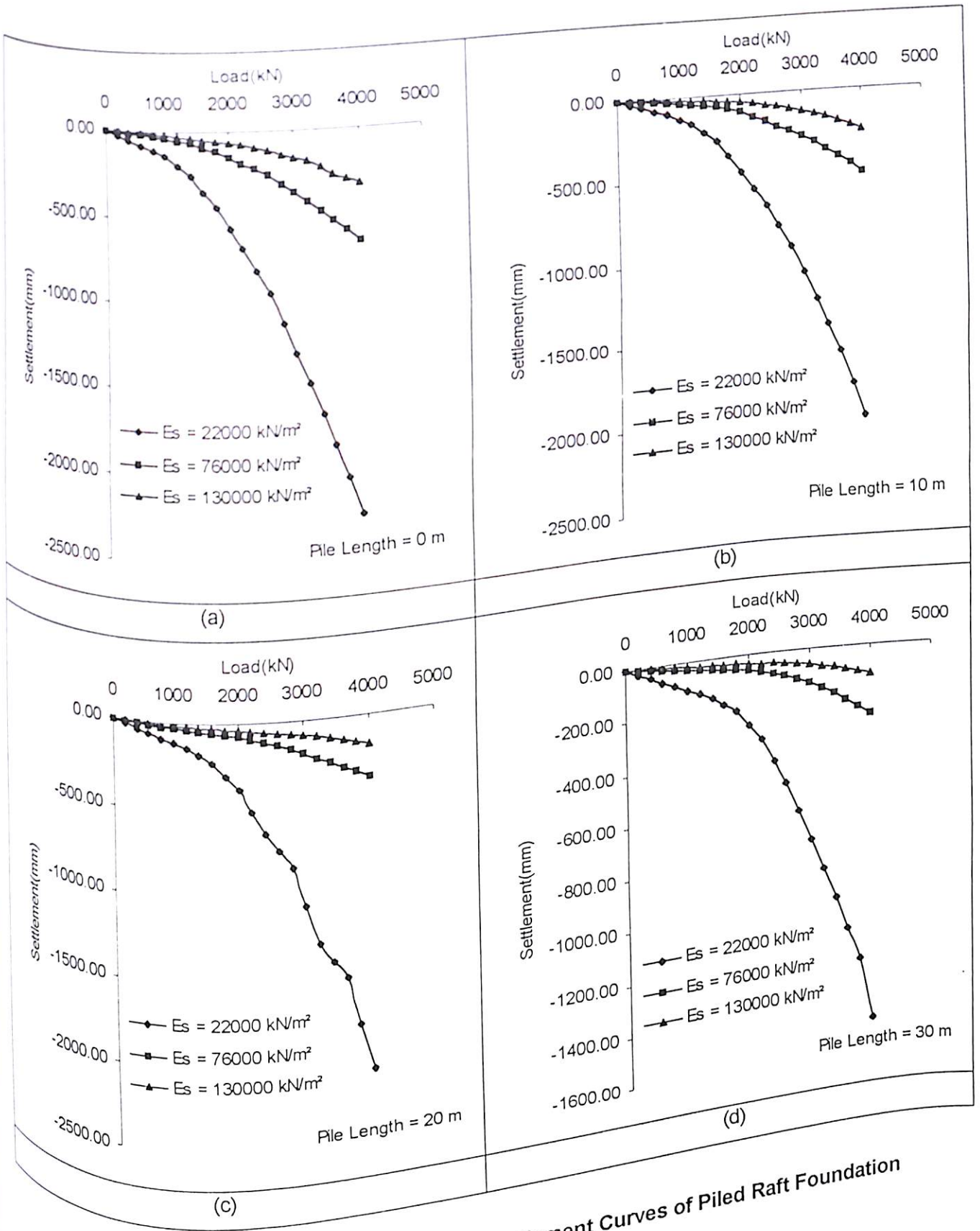

Figure 6.20 Effect of Soil Modulus on Load Settlement Curves of Piled Raft Foundation (B = 10 m, s/d = 7.5)

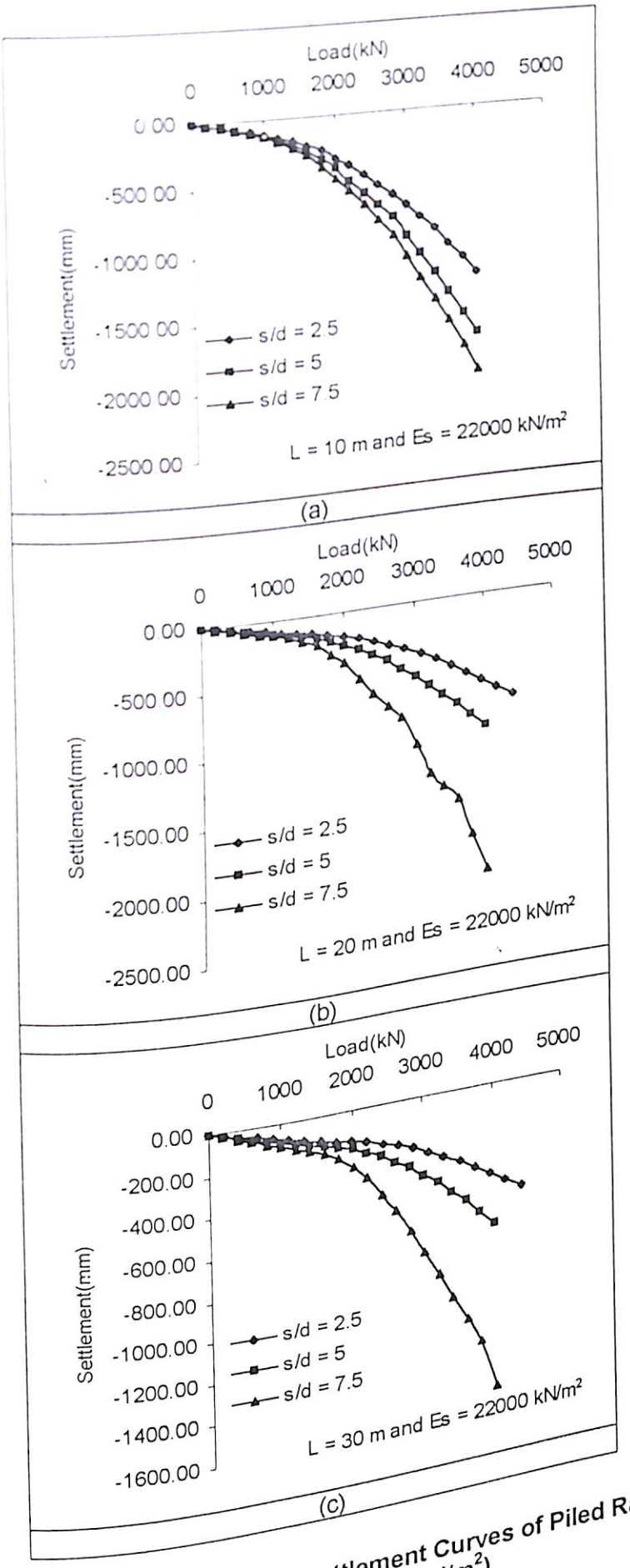

Figure 6.21 Effect of Spacing on Load Settlement Curves of Piled Raft Foundation ($B = 10$ m, $E_s = 22000$ kN/m^2)

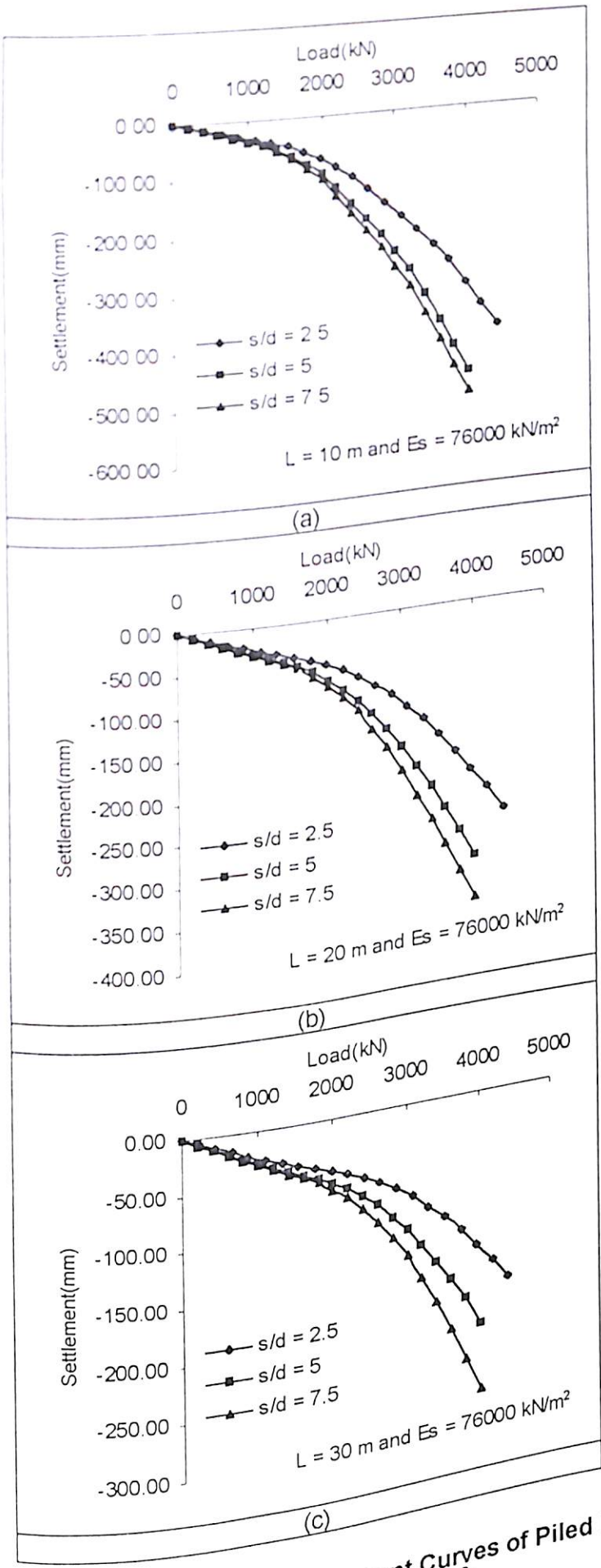

Figure 6.22 T... Load Settlement Curves of Piled Raft Foundation ...000 kN/m²)

Figures 6.23 (a), (b), (c) show the effect of spacing on load settlement behaviour of piled raft foundation of width 10 meter for soil modulus of 130000 kN/m^2 for varying pile length. The load carrying capacity decreases with increase in spacing between piles and increases with increase in soil modulus. The reason is same as explained earlier.

Raft width 20 m

The effect of length of pile on the load settlement behaviour of piled raft foundation has been shown in Figure 6.24 for raft width 20 meter and center to centre spacing to side ratio of pile equal to 5.0. The effect of spacing and pile length is same as explained earlier.

Figures 6.25 (a), (b), (c) show the effect of pile length on the load settlement behaviour of piled raft foundation for raft width 20 meter and center to centre spacing to side ratio of pile equal to 7.5. The load carrying capacity of piled raft foundation increases with increase in pile length due to the increased range of mobilization of unit skin friction.

The effect of length of pile on the load settlement behaviour of piled raft foundation has been shown in Figure 6.26 for raft width 20 meter and center to centre spacing to side ratio of pile equal to 10. The effect of increase in length of pile is same as explained above.

Figures 6.27 (a), (b), (c), (d) show the effect of soil modulus on the load carrying capacity of piled raft foundation for raft width 20 meter and spacing to side ratio of pile equal to 5. The load carrying capacity of piled raft foundation increases with increase in soil modulus. This is because the stiffness of soil increases with increase in soil modulus.

The effect of soil modulus on the load carrying capacity of piled raft foundation has been shown in Figure 6.28 for raft width 20 meter and spacing to side ratio of pile equal to 7.5. The effect of increase in soil modulus is same as explained above.

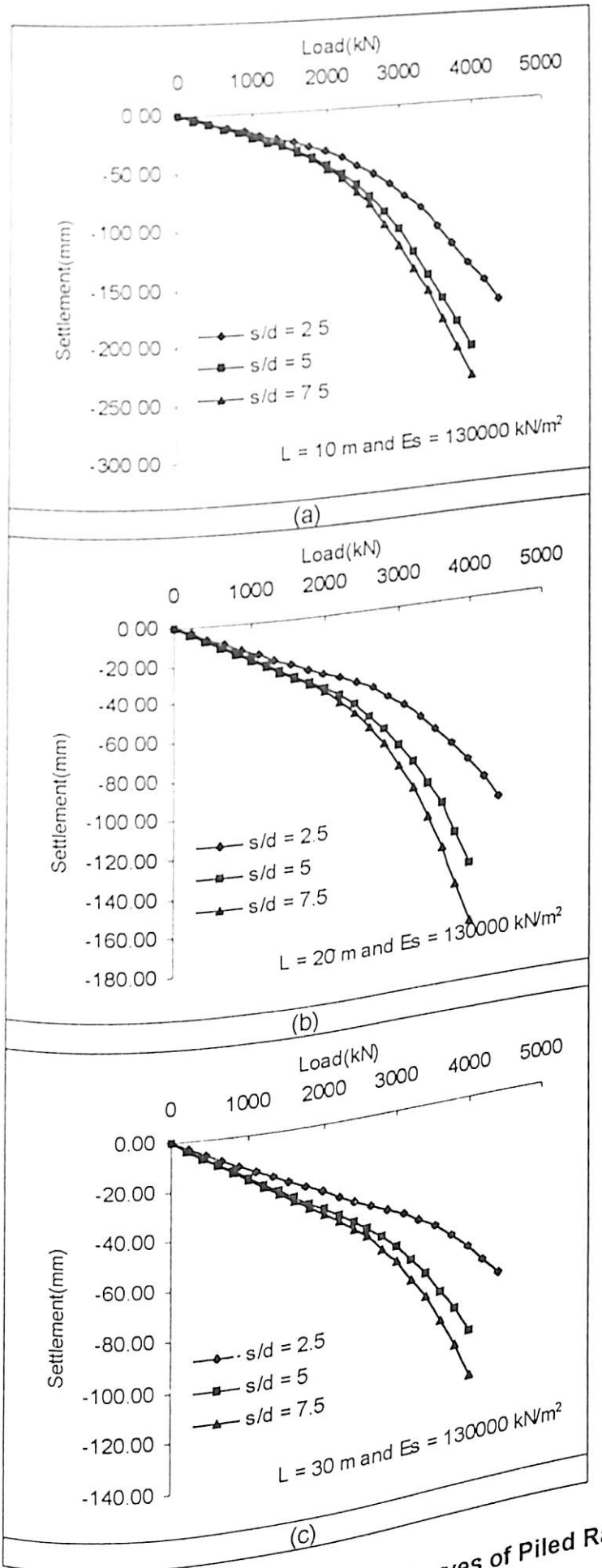

Figu

Curves of Piled Raft Foundation

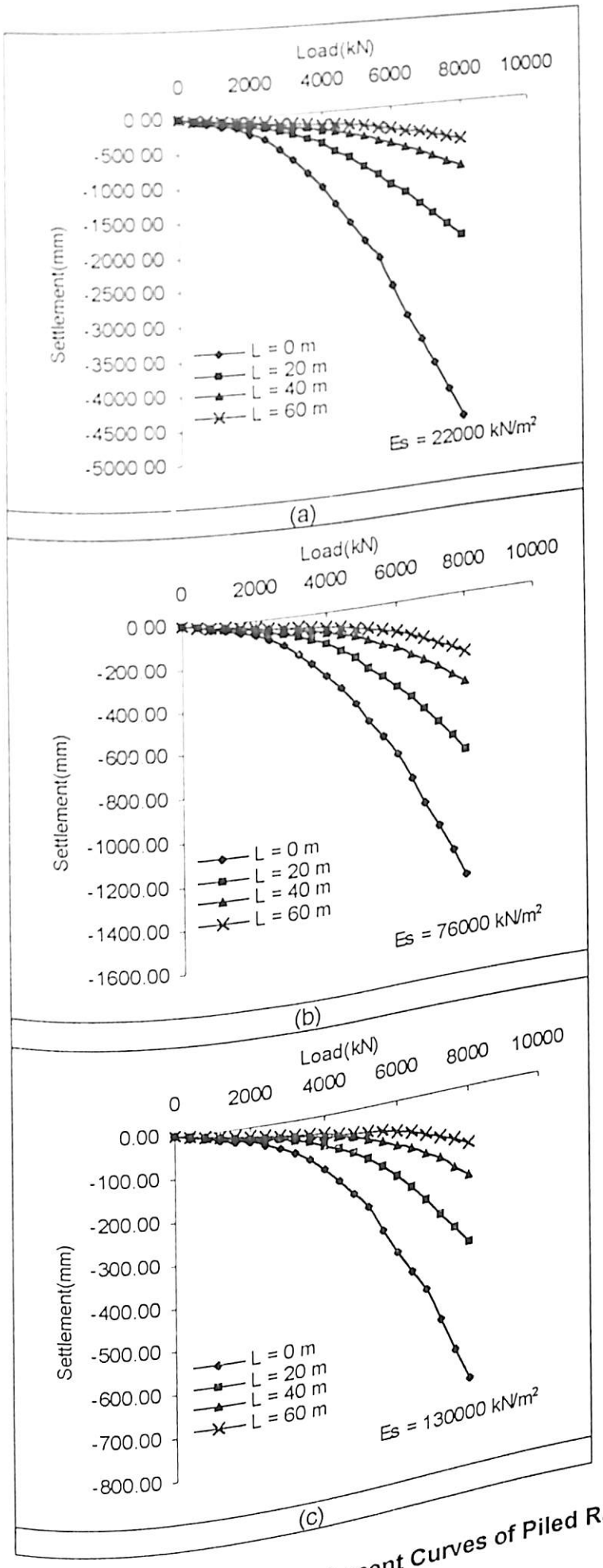

Figure 6.24 Effect of Pile Length Load Settlement Curves of Piled Raft Foundation (B = 20 m, s/d = 5)

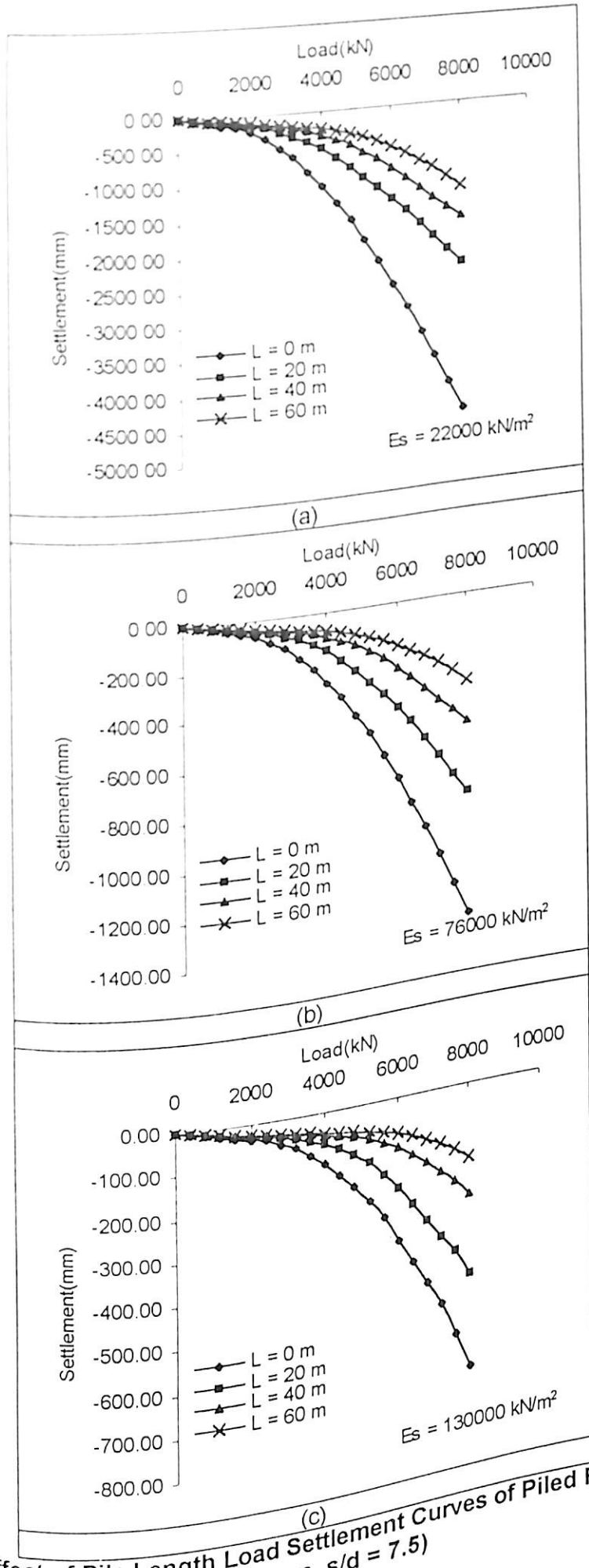

Figure 6.25 Effect of Pile Length Load Settlement Curves of Piled Raft Foundation (B = 20 m, s/d = 7.5)

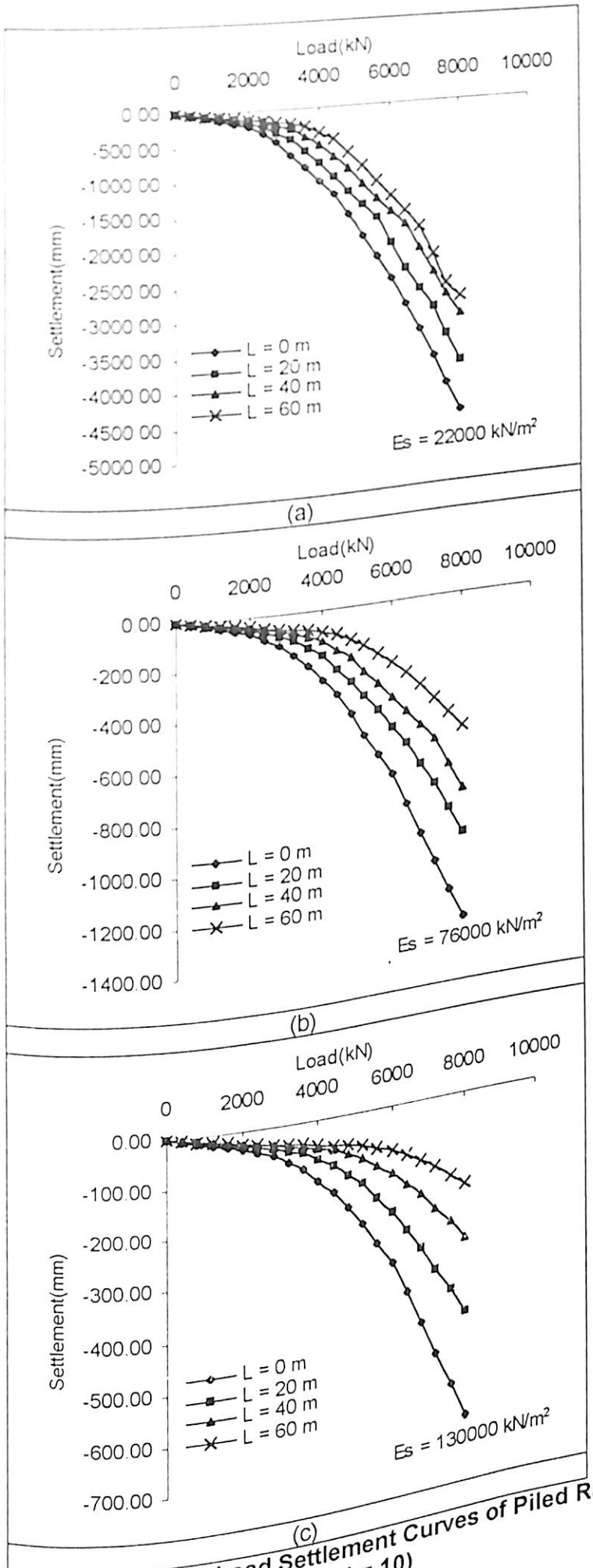

Figure 6.26 Effect of Pile Length Load Settlement Curves of Piled Raft Foundation (B = 20 m, s/d = 10)

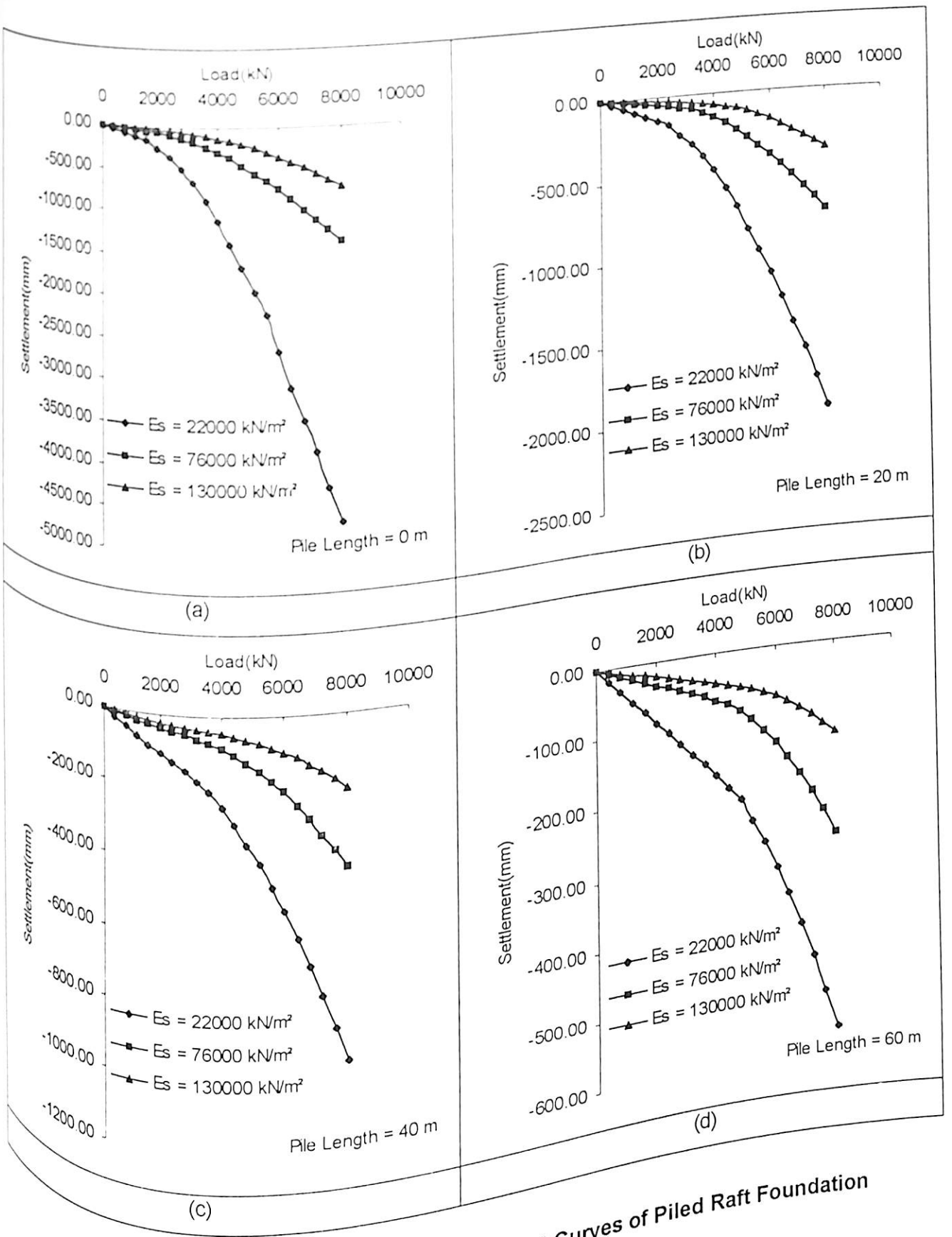

Figure 6.27 Effect of Soil Modulus Load Settlement Curves of Piled Raft Foundation (B = 20 m, s/d = 5)

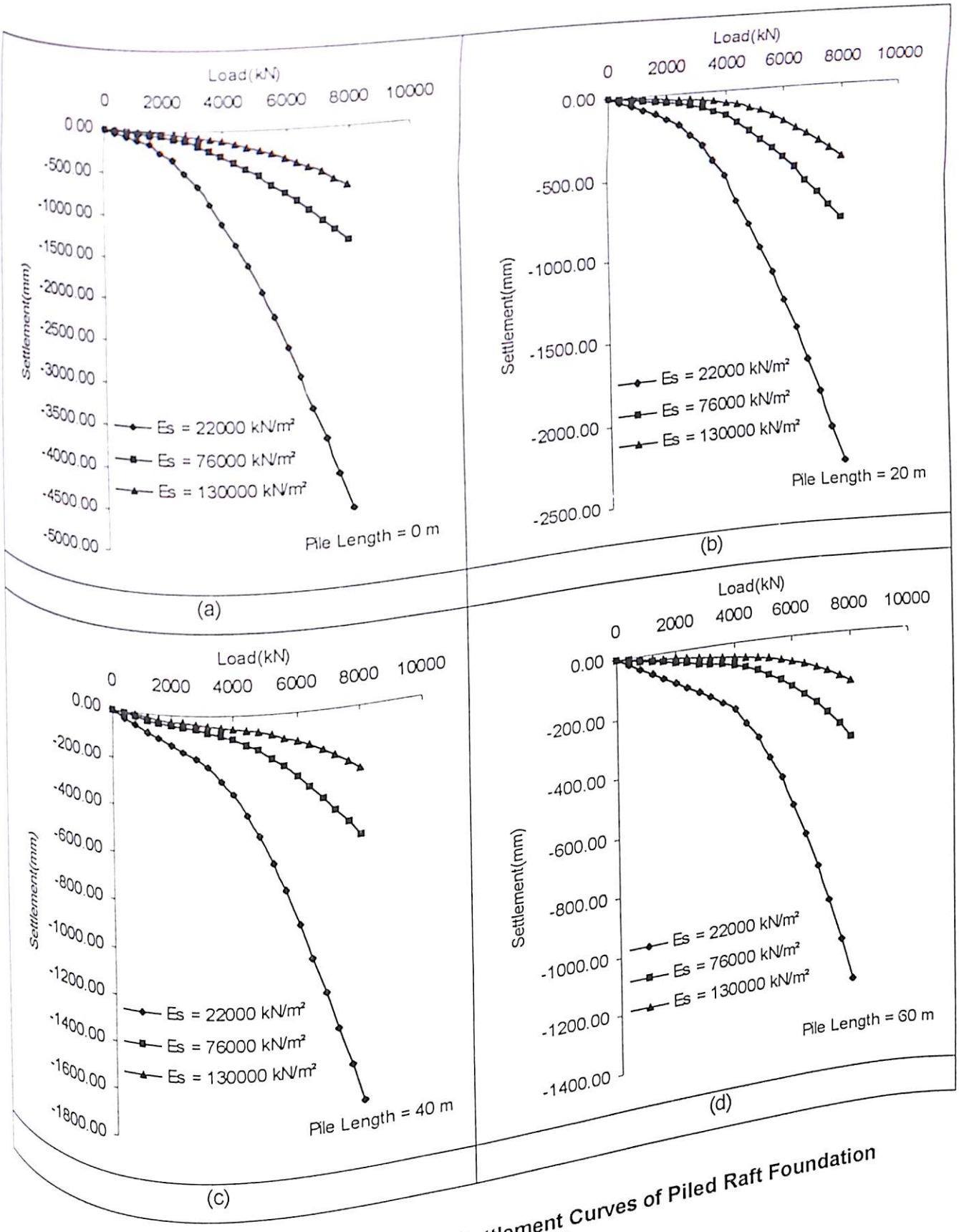

Figure 6.28 Effect of Soil Modulus Load Settlement Curves of Piled Raft Foundation (B = 20 m, s/d = 7.5)

The effect of soil modulus on the load carrying capacity of piled raft foundation has been shown in Figure 6.29 for raft width 20 meter and spacing to side ratio of pile equal to 10.0. The effect of increase in soil modulus is to increase the load carrying capacity of piled raft foundation

The effect of spacing on the load settlement behaviour of piled raft foundation of raft width 20 meter has been shown in Figure 6.30 for different pile length and soil modulus of 22000 kN/m^2. The effect of increase in spacing is to reduce the load carrying capacity of piled raft foundation

The effect of spacing on the load settlement behaviour of piled raft foundation of raft width 20 meter has been shown in Figure 6.31 for different pile length and soil modulus of 76000 kN/m^2. It can be observed from the graph that with increase in spacing between the piles, settlement of raft increases which results in lesser load carrying capacity.

The effect of spacing on the load settlement behaviour of piled raft foundation of raft width 20 meter has been shown in Figure 6.32 for different pile length and soil modulus of 130000 kN/m^2. Similar trends can be observed in this case also as it was for soil modulus 76000 kN/m^2.

Raft Width 30 m

The effect of length of pile on the load settlement behaviour of piled raft foundation has been shown in Figure 6.33 for raft width 30 meter and center to centre spacing to side ratio of pile equal to 7.5. The effect of increase in length of pile is to increase the load carrying capacity of piled raft foundation.

The effect of length of pile on the load settlement behaviour of piled raft foundation has been shown in Figure 6.34 for raft width 30 meter and center to centre spacing to side ratio of pile equal to 10.0. It can be observed from the graph that with increase in pile length settlement decreases and load carrying capacity of the foundation increases.

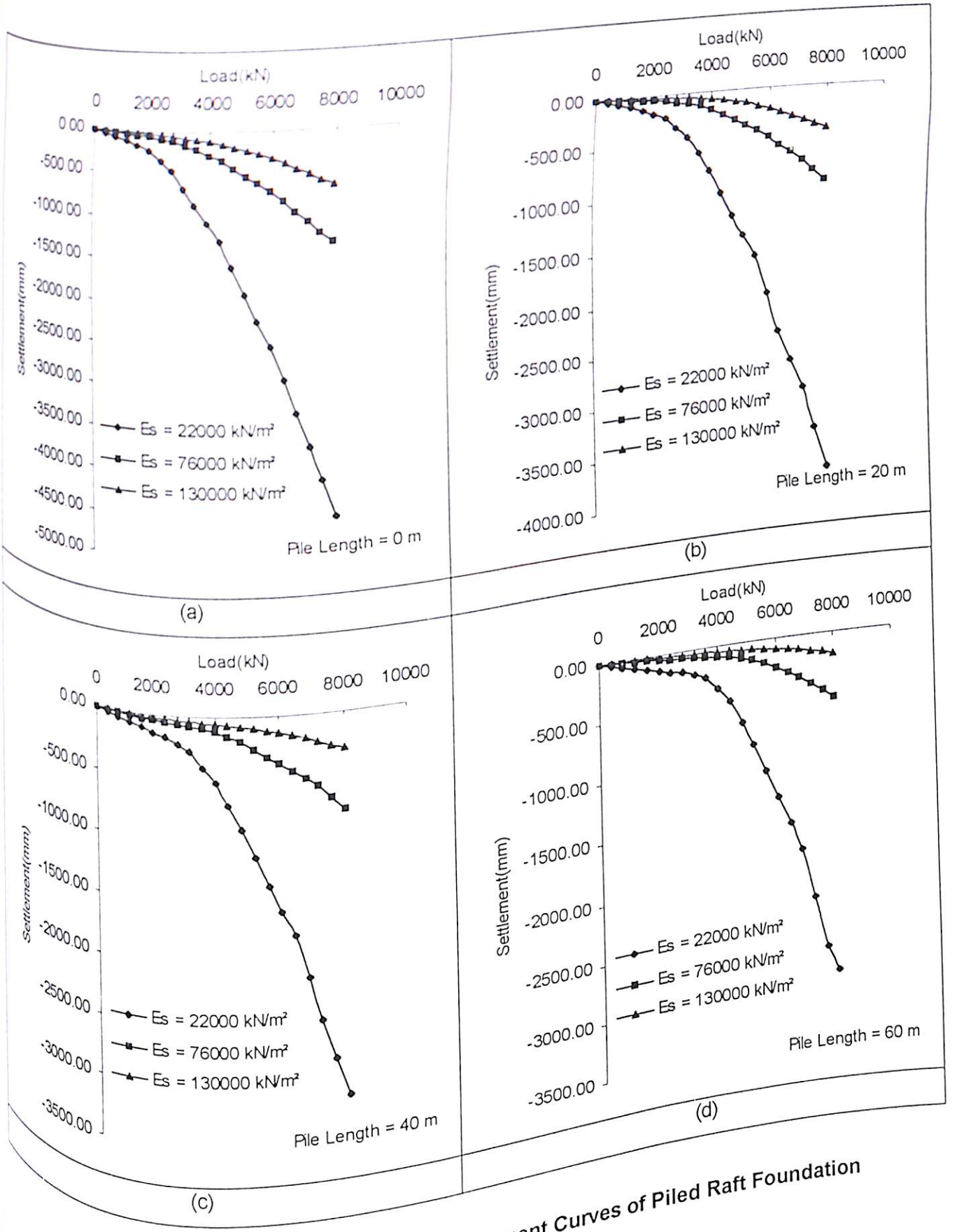

Figure 6.29 Effect of Soil Modulus Load Settlement Curves of Piled Raft Foundation (B = 20 m, s/d = 10)

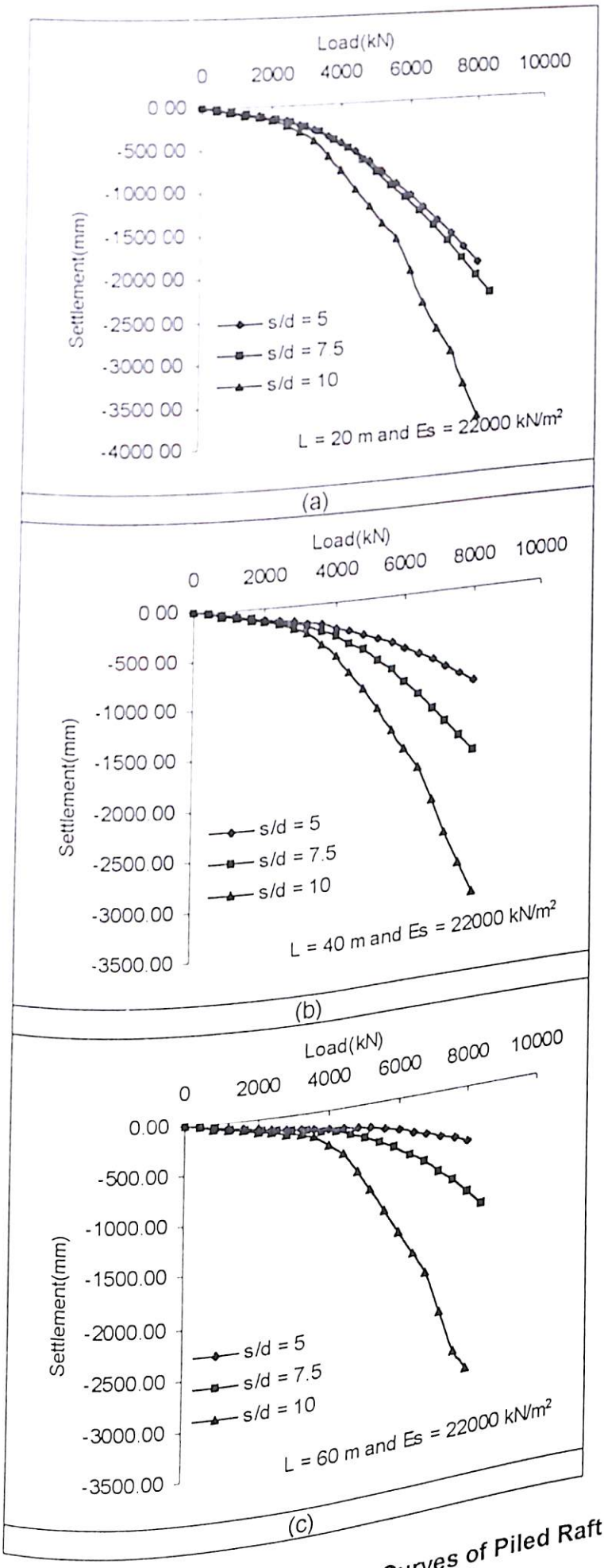

Figure 6.30 Effect of spacing Load Settlement Curves of Piled Raft Foundation ($B = 20$ m, $E_s = 22000$ kN/m²)

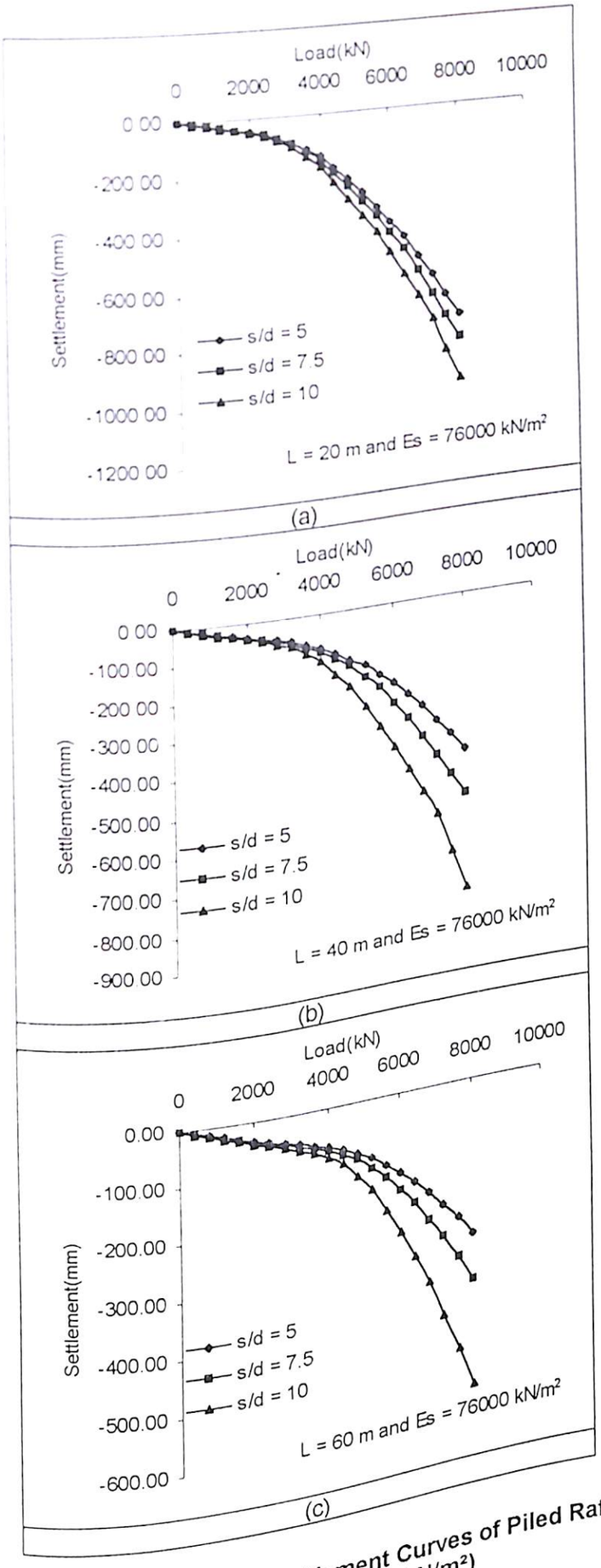

Figure 6.31 Effect of spacing Load Settlement Curves of Piled Raft Foundation ($B = 20$ m, $E_s = 76000$ kN/m²)

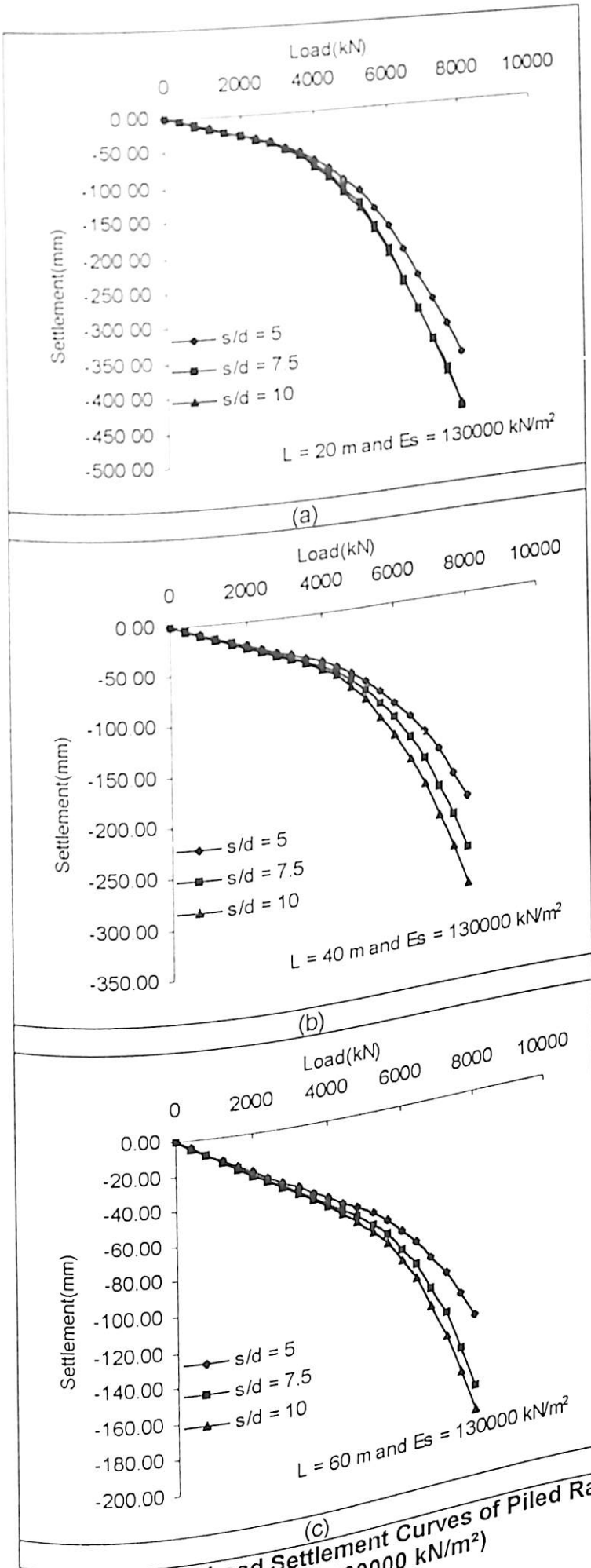

Figure 6.32 Effect of spacing Load Settlement Curves of Piled Raft Foundation (B = 20 m, Es = 130000 kN/m²)

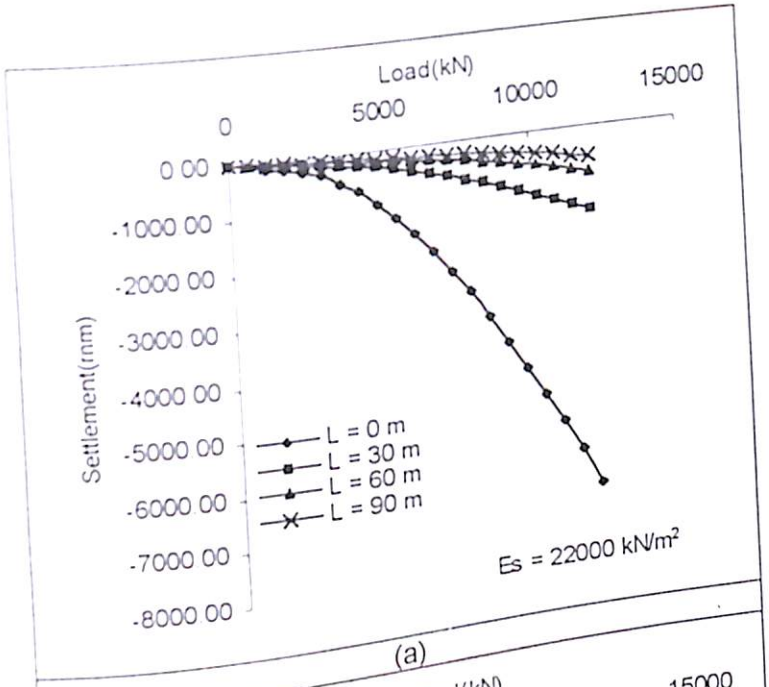
Load(kN)
0
5000
10000
15000
0 00
-1000 00
-2000 00
-3000 00
-4000 00
-5000 00
-6000 00
-7000 00
-8000 00
Settlement(mm)
L = 0 m
L = 30 m
L = 60 m
L = 90 m
Es = 22000 kN/m²
(a)
15000

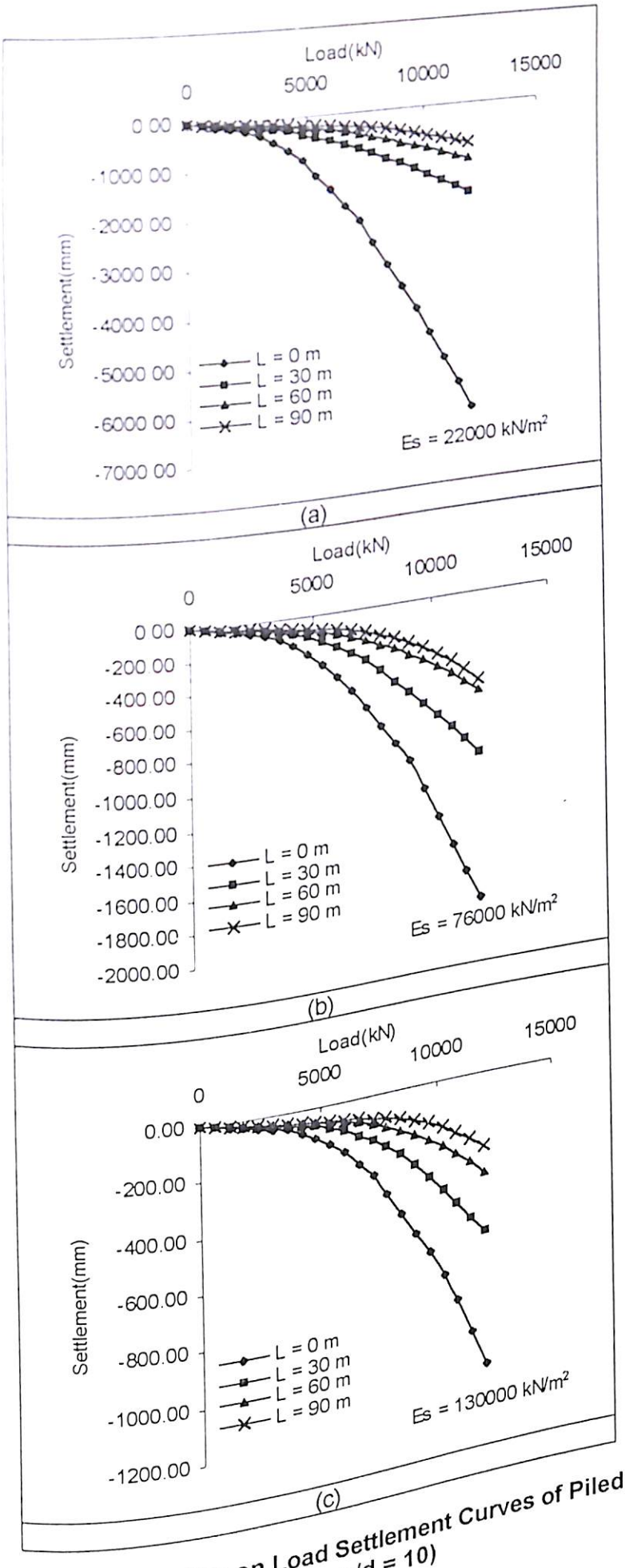

Figure 6.34 Effect of Length of Pile on Load Settlement Curves of Piled Raft Foundation (B = 30 m, s/d = 10)

The effect of soil modulus on the load carrying capacity of piled raft foundation has been shown in Figure 6.35 for raft width 30 meter and spacing to side ratio of pile equal to 7.5. It can be observed from the graph that increase in soil modulus improves the load carrying capacity of piled raft foundation significantly.

The effect of soil modulus on the load carrying capacity of piled raft foundation has been shown in Figure 6.36 for raft width 30 meter and spacing to side ratio of pile equal to 10.0. The effect of increase in soil modulus is same as explained earlier.

The effect of spacing on the load settlement behaviour of piled raft foundation of raft width 30 meter has been shown in Figure 6.37 for different pile length and soil modulus of 22000 kN/m^2. It can be clearly seen from the graph that with increase in spacing, load carrying capacity of piled raft foundation reduces

The effect of spacing on the load settlement behaviour of piled raft foundation of raft width 30 meter has been shown in Figure 6.38 (a), (b), (c) for different pile length and soil modulus of 76000 kN/m^2. The effect of increase in spacing is same as explained earlier.

The effect of spacing on the load settlement behaviour of piled raft foundation of raft width 30 meter has been shown in Figure 6.39 (a), (b), (c) for different pile length and soil modulus of 130000 kN/m^2. With increase in spacing between the piles, settlement increases, thereby reducing the load carrying capacity of piled raft foundation.

Raft width 40 m

The effect of length of pile on the load settlement behaviour of piled raft foundation has been shown in Figure 6.40 (a), (b), (c) for raft width 40 meter and center to centre spacing to side ratio of pile equal to 7.5. The effect of increase in length of pile is to increase the load carrying capacity of piled raft.

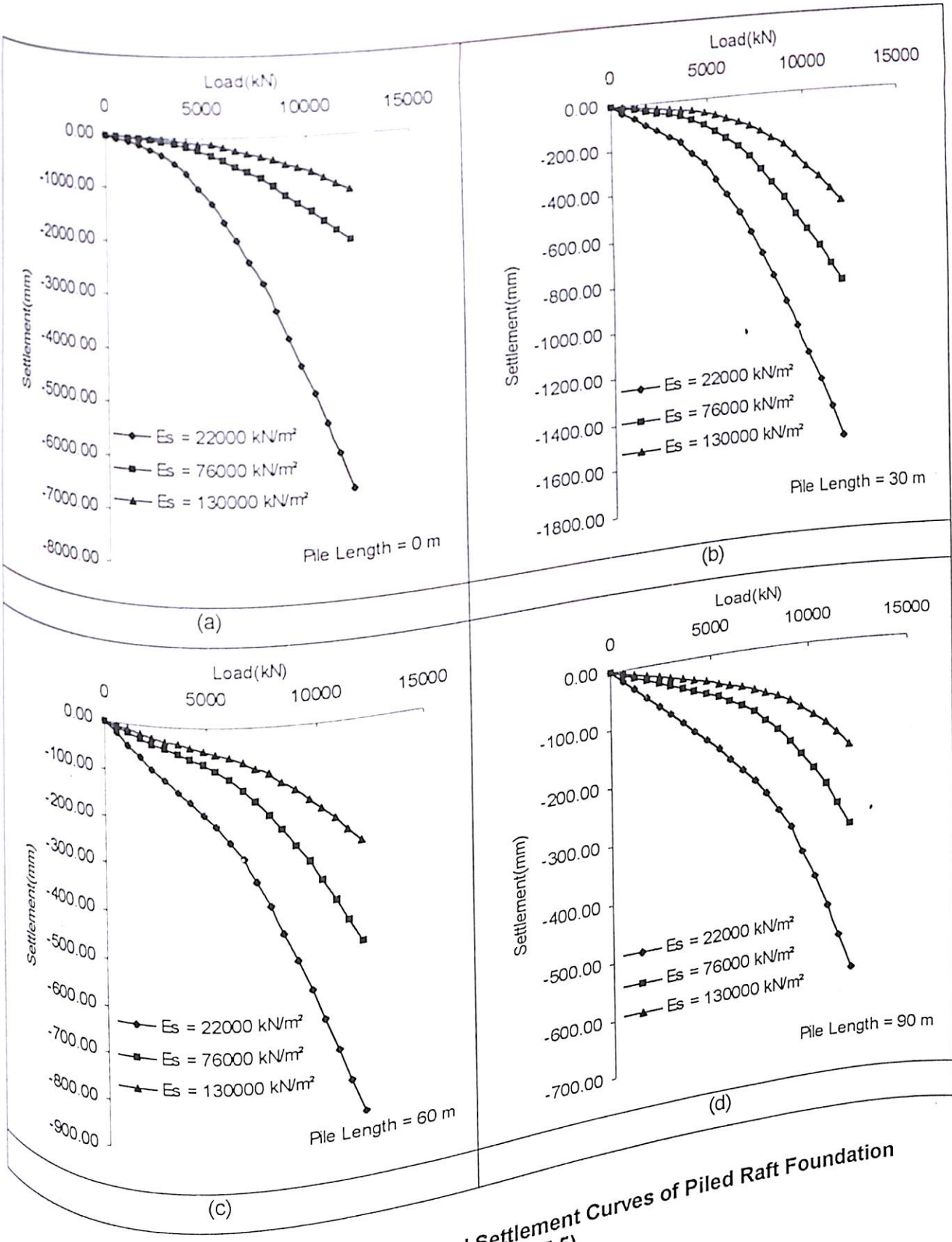

Figure 6.35 Effect of Soil Modulus on Load Settlement Curves of Piled Raft Foundation (B = 30 m, s/d = 7.5)

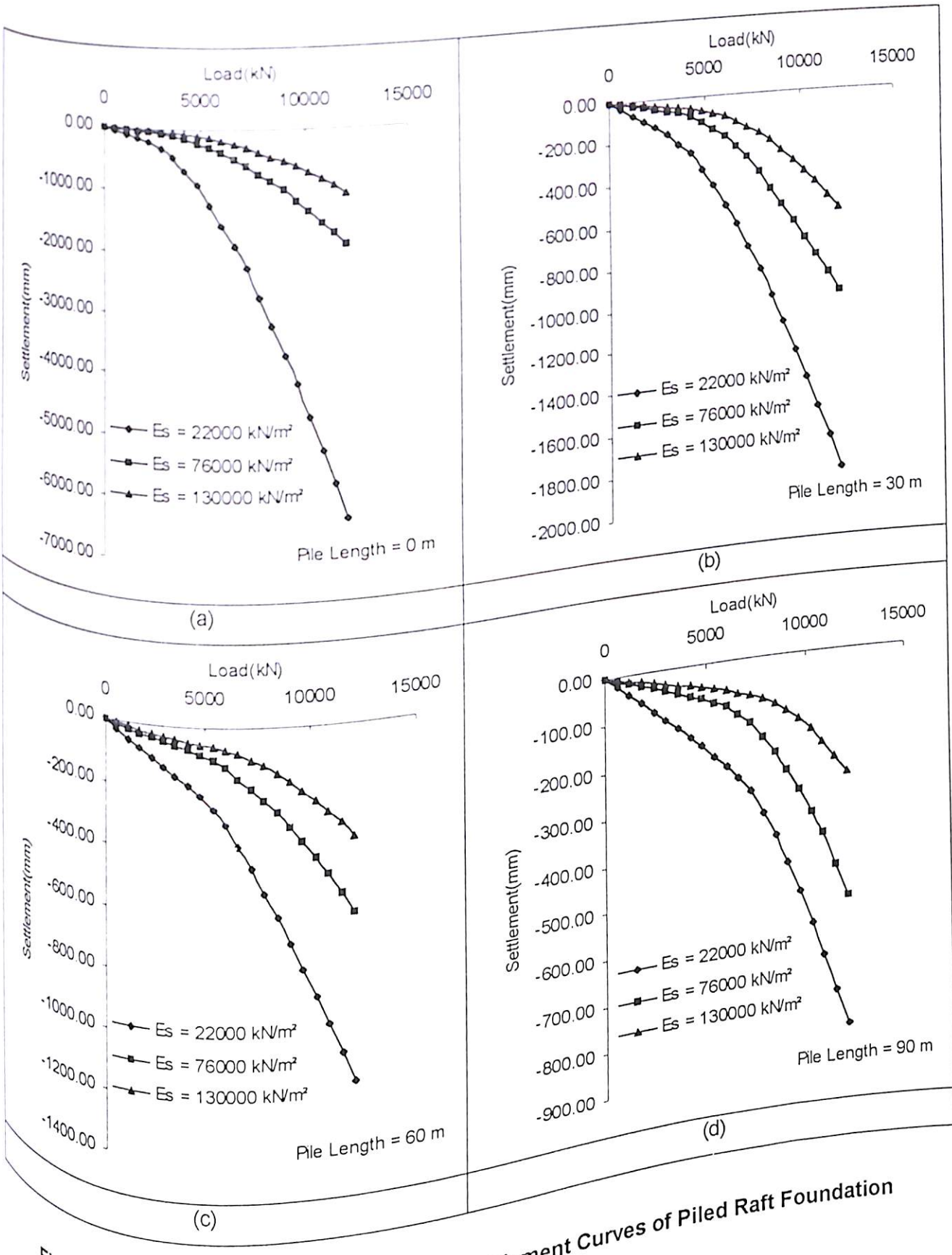

Figure 6.36 Effect of Soil Modulus on Load Settlement Curves of Piled Raft Foundation (B = 30 m, s/d = 10)

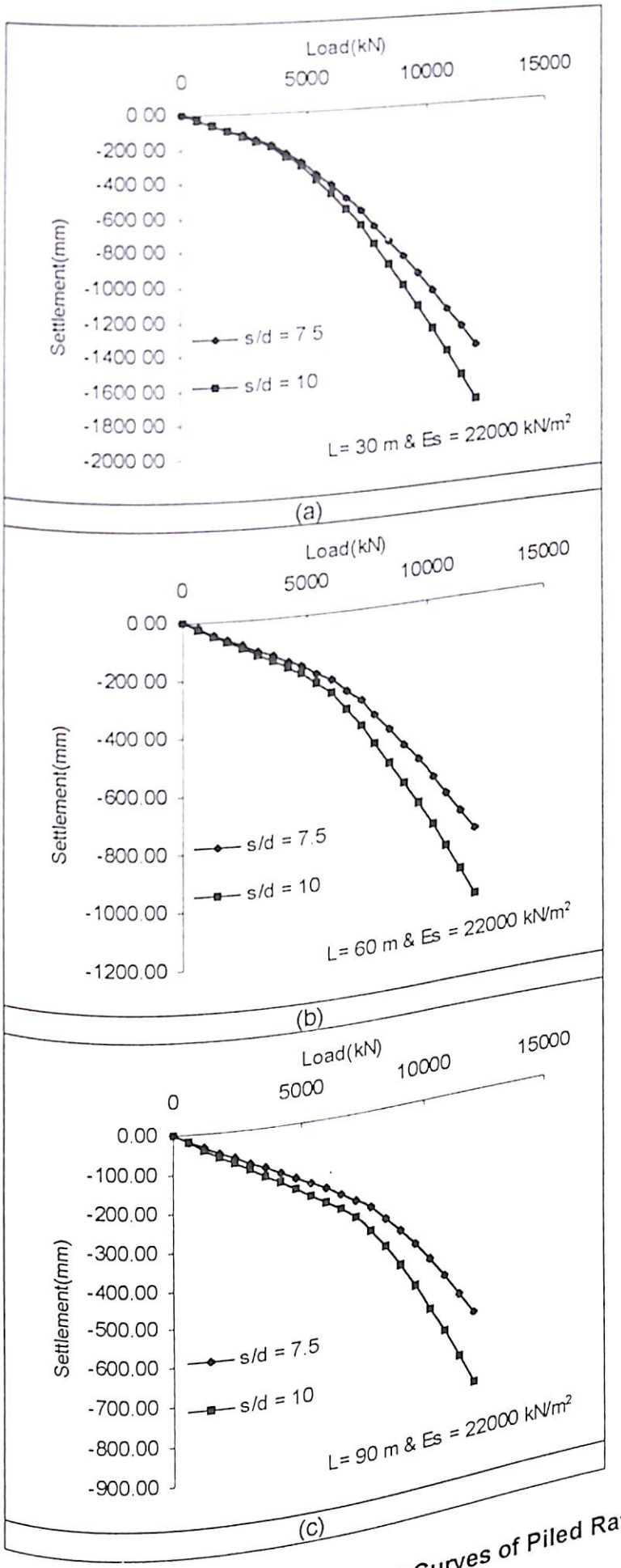

Figure 6.37 Effect of Spacing on Load Settlement Curves of Piled Raft Foundation (B = 30 m, Es = 22000 kN/m^2)

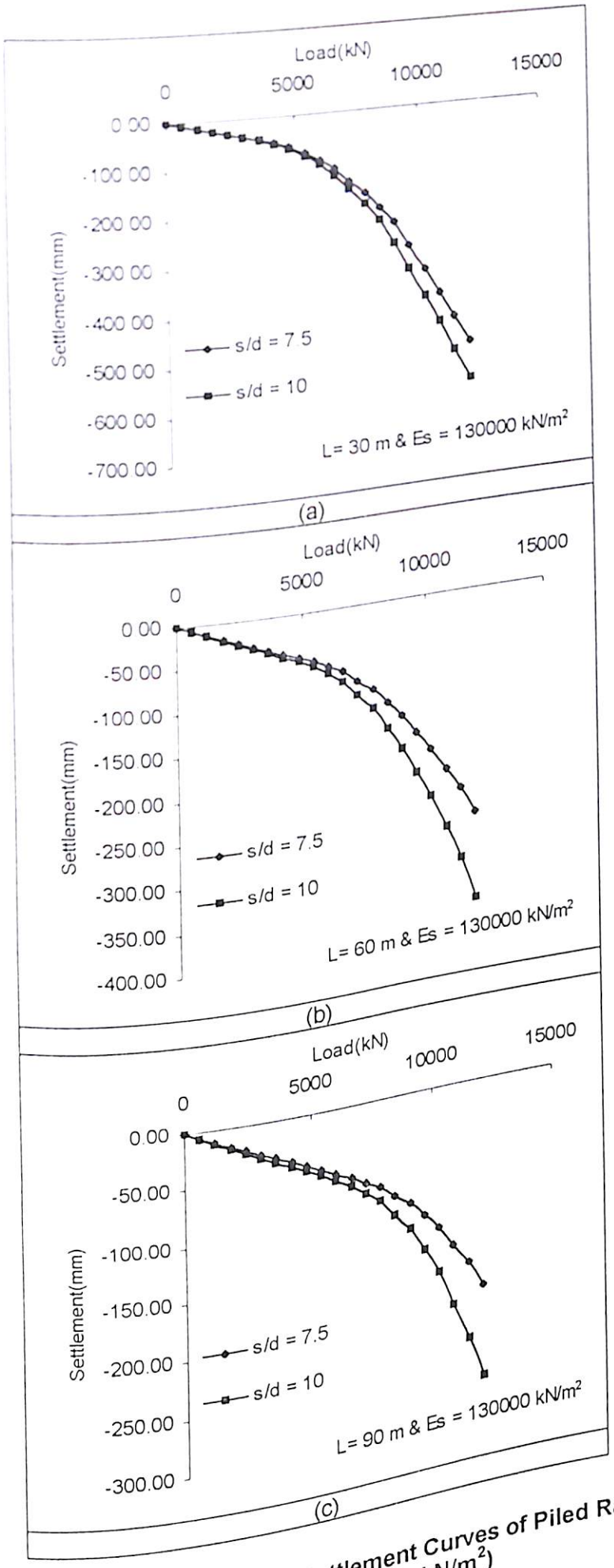

Figure 6.39 Effect of Spacing on Load Settlement Curves of Piled Raft Foundation (B = 30 m, Es = 130000 kN/m^2)

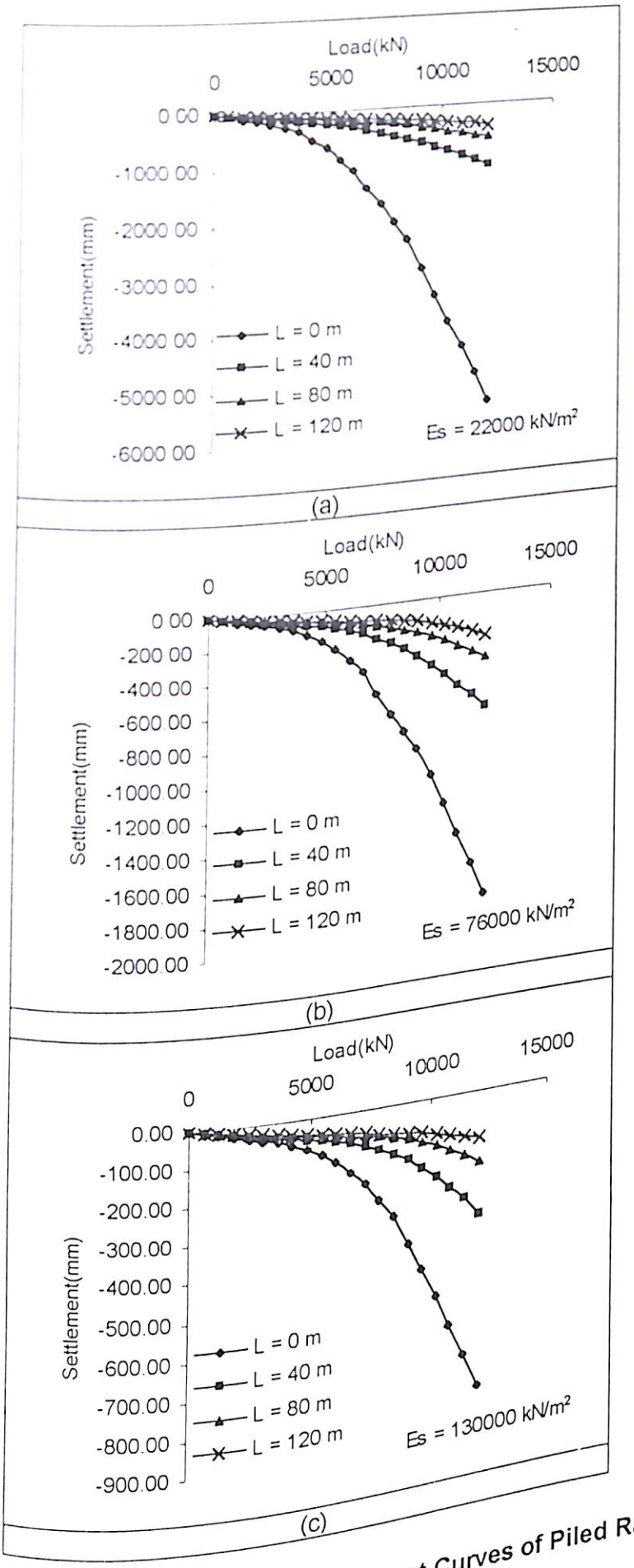

Figure 6.40 Effect of Pile Length on Load Settlement Curves of Piled Raft Foundation (B = 40 m, s/d = 7.5)

The effect of length of pile on the load settlement behaviour of piled raft foundation has been shown in Figure 6.41 (a), (b), (c) for raft width 40 meter and center to centre spacing to side ratio of pile equal to 10. It is observed form the graph that settlement decreases with increase in pile length.

The effect of length of pile on the load settlement behaviour of piled raft foundation has been shown in Figure 6.42 (a), (b), (c) for raft width 40 meter and center to centre spacing to side ratio of pile equal to 15. The load carrying capacity of piled raft foundation increases with increase in pile length due to the increased range of mobilization of unit skin friction.

The effect of soil modulus on the load carrying capacity of piled raft foundation has been shown in Figure 6.43 for raft width 40 meter and spacing to side ratio of pile equal to 7.5. The load carrying capacity of piled raft foundation increases with increase in soil modulus. This is because the stiffness of soil increases with increase in soil modulus.

The effect of soil modulus on the load carrying capacity of piled raft foundation has been shown in Figure 6.44 for raft width 40 meter and spacing to side ratio of pile equal to 10. The effect of increase in soil modulus is same as explained above.

The effect of soil modulus on the load carrying capacity of piled raft foundation has been shown in Figure 6.45 for raft width 40 meter and spacing to side ratio of pile equal to 15. The effect of increase in soil modulus is to increase the load carrying capacity of piled raft foundation.

6.6.3 Axial Load Distribution

Figures 6.46 (a), (b) show the effect of spacing on the axial load distribution for center pile in a piled raft foundation for piles of length 90 meter, raft width 30 meter, soil modulus 130000 kN/m^2. The axial load in piles first increases and then decreases with depth. This shows that in the top portion of piles the mobilization of skin friction is not

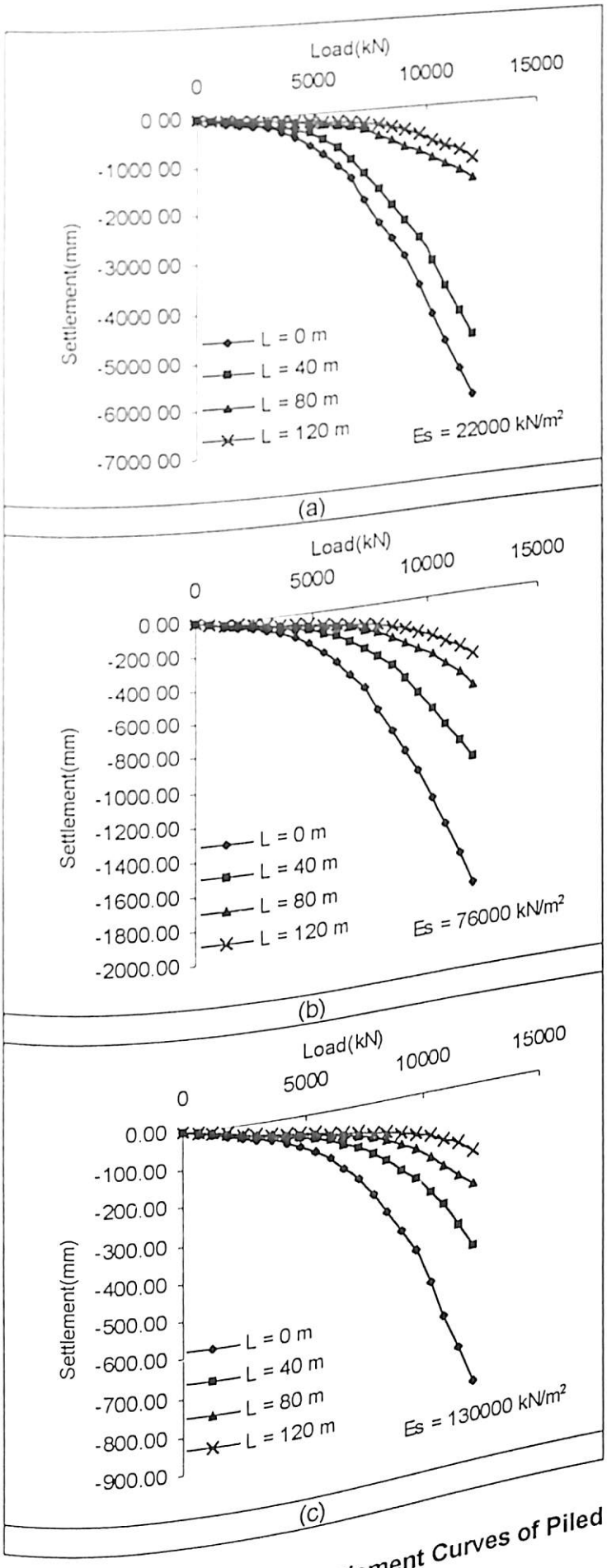

Figure 6.41 Effect of Pile Length on Load Settlement Curves of Piled Raft Foundation (B = 40 m, s/d = 10)

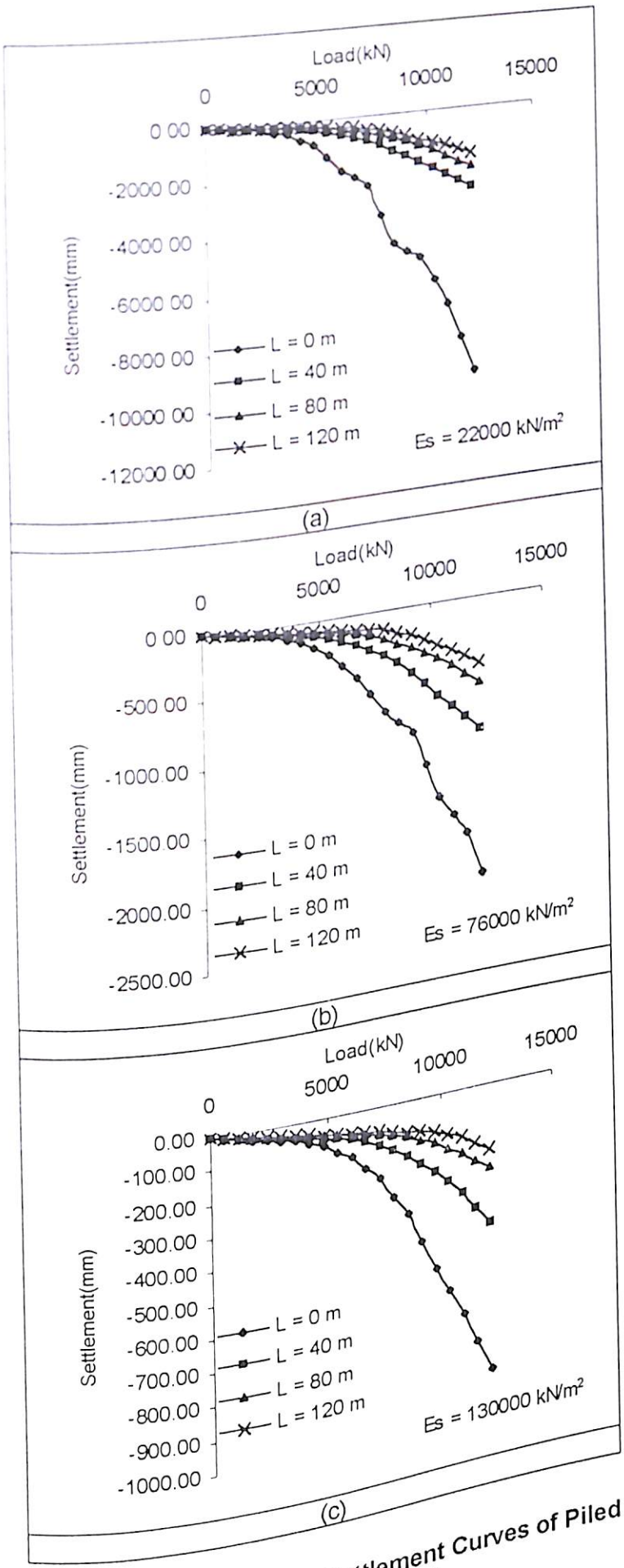

Figure 6.42 Effect of Pile Length on Load Settlement Curves of Piled Raft Foundation (B = 40 m, s/d = 15)

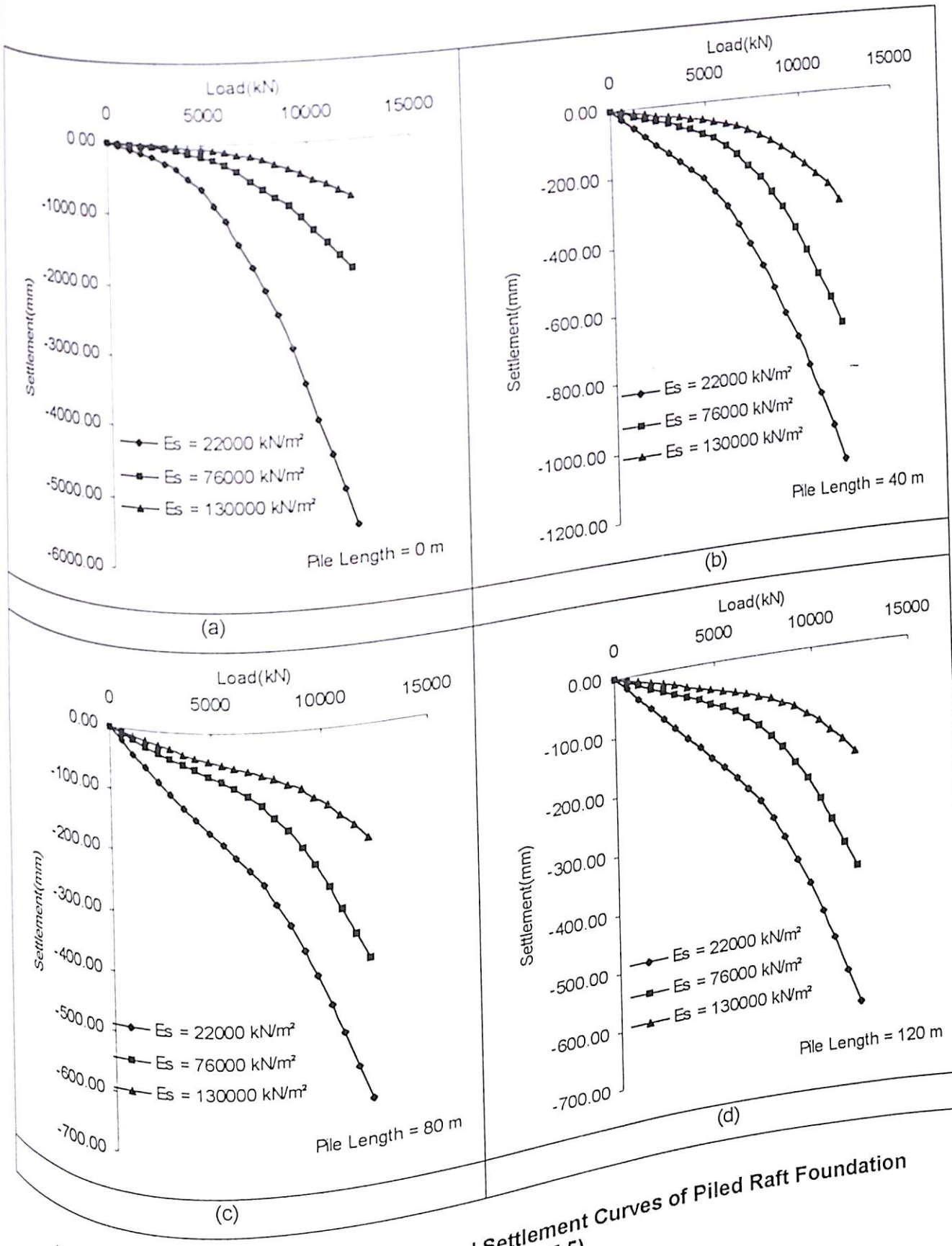

Figure 6.43 Effect of Soil Modulus on Load Settlement Curves of Piled Raft Foundation (B = 40 m, s/d = 7.5)

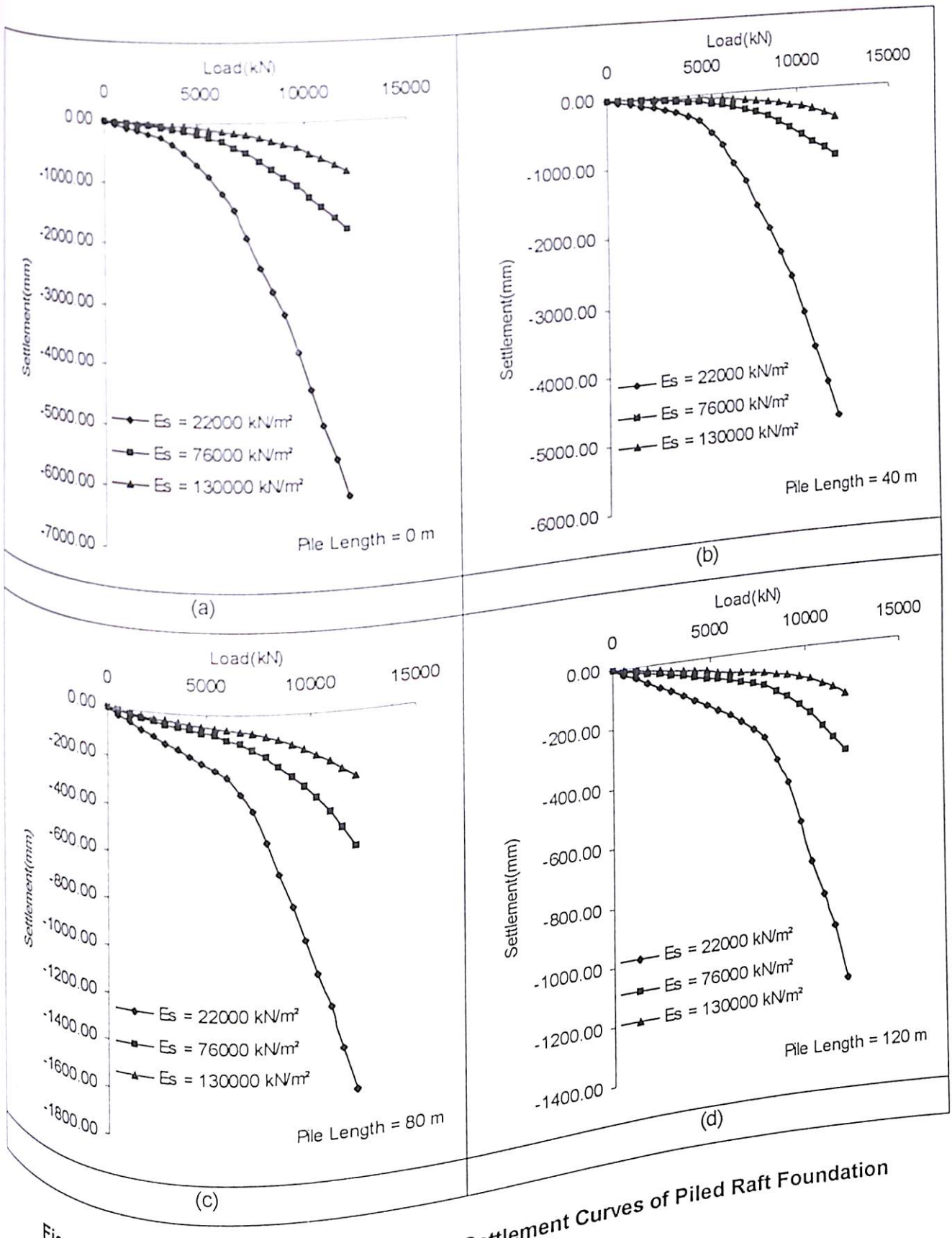

Figure 6.44 Effect of Soil Modulus on Load Settlement Curves of Piled Raft Foundation (B = 40 m, s/d = 10)

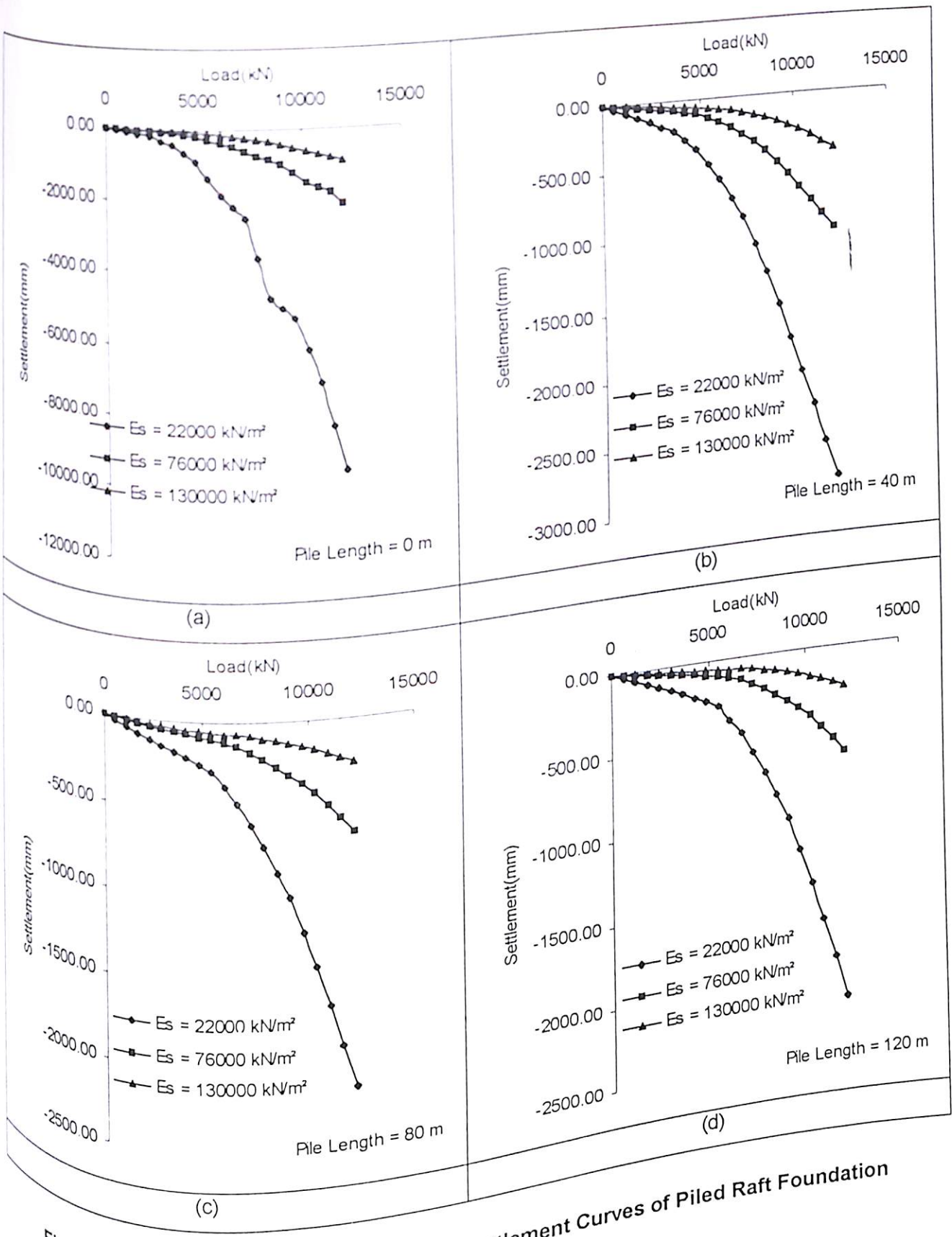

Figure 6.45 Effect of Soil Modulus on Load Settlement Curves of Piled Raft Foundation (B = 40 m, s/d = 15)

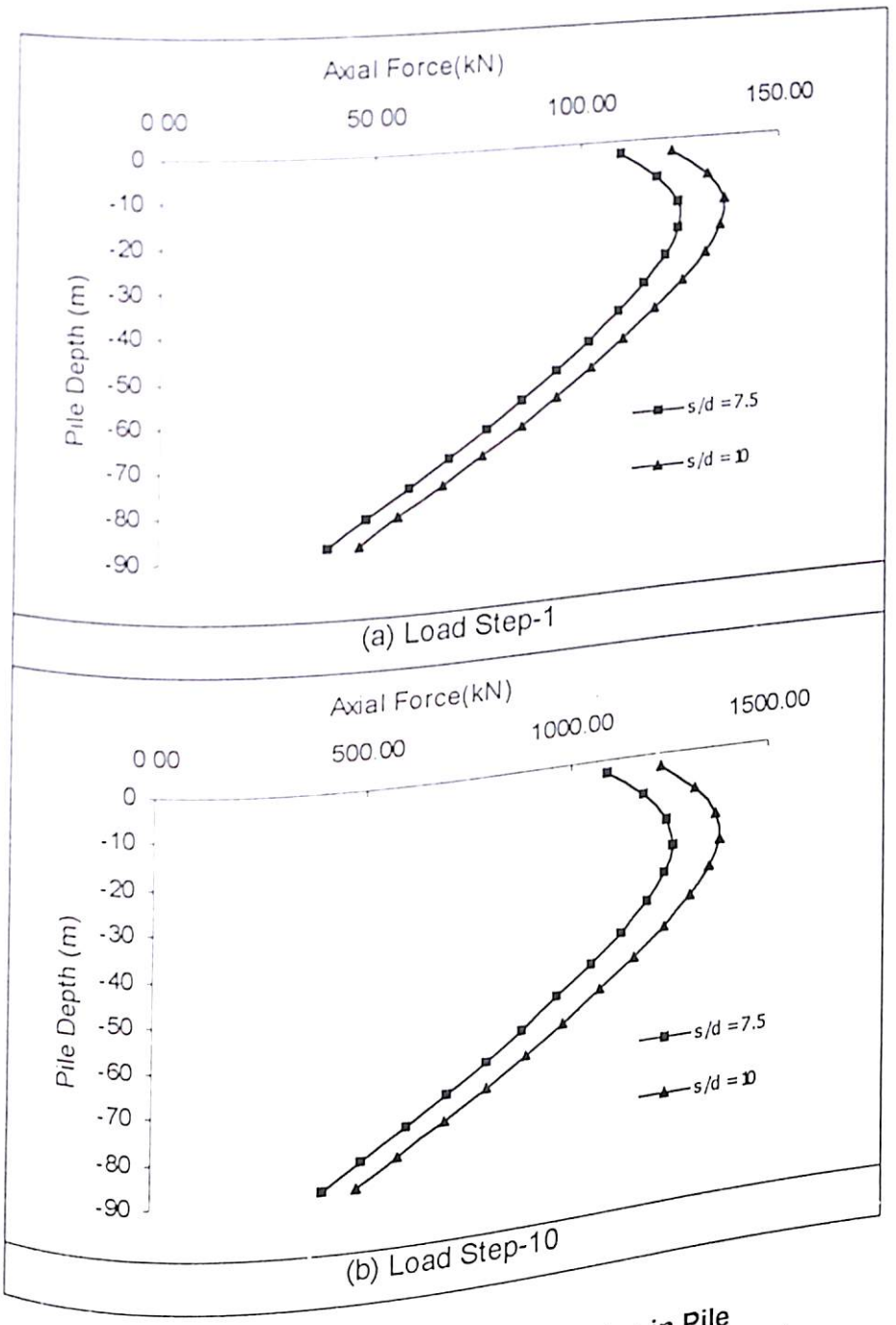

Figure 6.46 Axial Force Distribution in Pile
(B = 30 m, L = 90 m, Es = 130000 kN/m^2, Center Pile)

there. With increase in spacing the axial load in pile increases. Also with increase in load steps the axial load in pile increases.

Figures 6.47 (a), (b) show the effect of spacing on the axial load distribution for end pile in a piled raft foundation for piles of length 90 meter, raft width 30 meter, soil modulus 130000 kN/m^2 for load step one and ten. The axial load in piles first increases and then decreases with depth. This shows that in the top portion of piles the mobilization of skin friction is not there. With increase in spacing the axial load in pile increases. Also with increase in load steps the axial load in pile increases.

Figures 6.48 (a), (b) show the effect of soil modulus on the axial load distribution in center and edge piles for a pile of length 90 metre with spacing to one side ratio of 10 for load step one. The effect of increase in soil modulus is to increase the axial load carrying capacity of pile. Comparison of Fig 6.48(a) and (b) show that the axial load carrying capacity of end piles are more than that of the center pile.

Figures 6.49 (a), (b) show the effect of soil modulus on the axial load distribution in center and edge piles for a pile of length 90 metres with spacing to one side ratio of 10 for load step ten. The effect of increase in soil modulus is to increase the axial load carrying capacity of pile. Comparison of Fig 6.49 (a) and (b) show that the axial load carrying capacity of end piles are more than that of the center pile. When Figures 6.48 and 6.49 are compared it is found that with increase in load step, the axial load in piles increases.

6.6.4 Settlement Profile

6.6.4.1 Settlement profile for raft

Figures 6.50 (a), (b), (c) show the settlement profile for raft foundation of width 10 meter for varying thickness of the raft and soil modulus of 76000 kN/m^2. There is differential settlement in the raft at very small thickness of the raft. This differential settlement reduces with increase in thickness of the raft and becomes almost zero when the thickness of the raft is 4.0 meter.

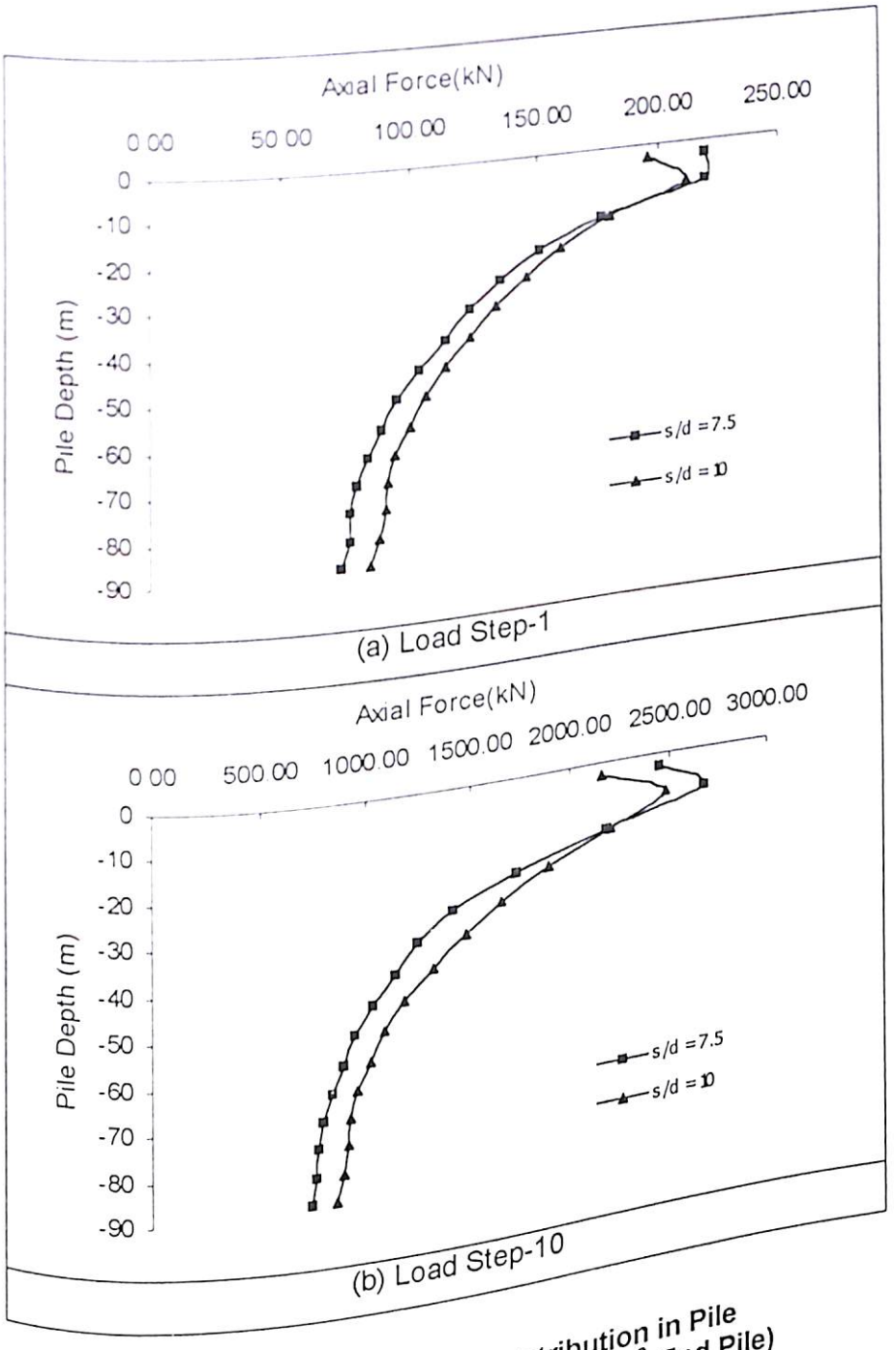

Figure 6.47 Axial Force Distribution in Pile
(B = 30 m, L = 90 m, Es = 130000 kN/m^2, End Pile)

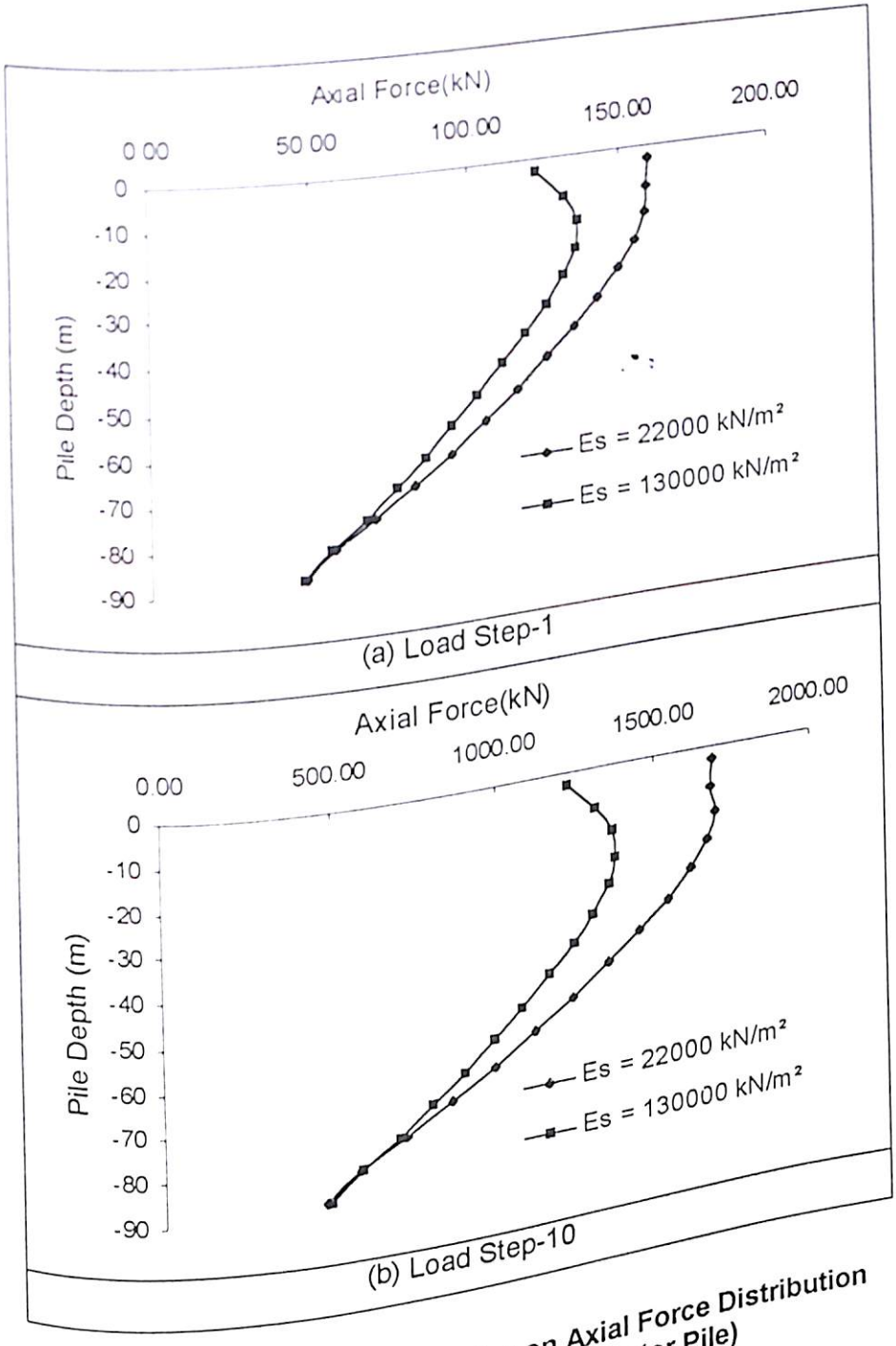

Figure 6.48 Effect of Soil Modulus on Axial Force Distribution (B = 30 m, L = 90 m, s/d = 10, Center Pile)

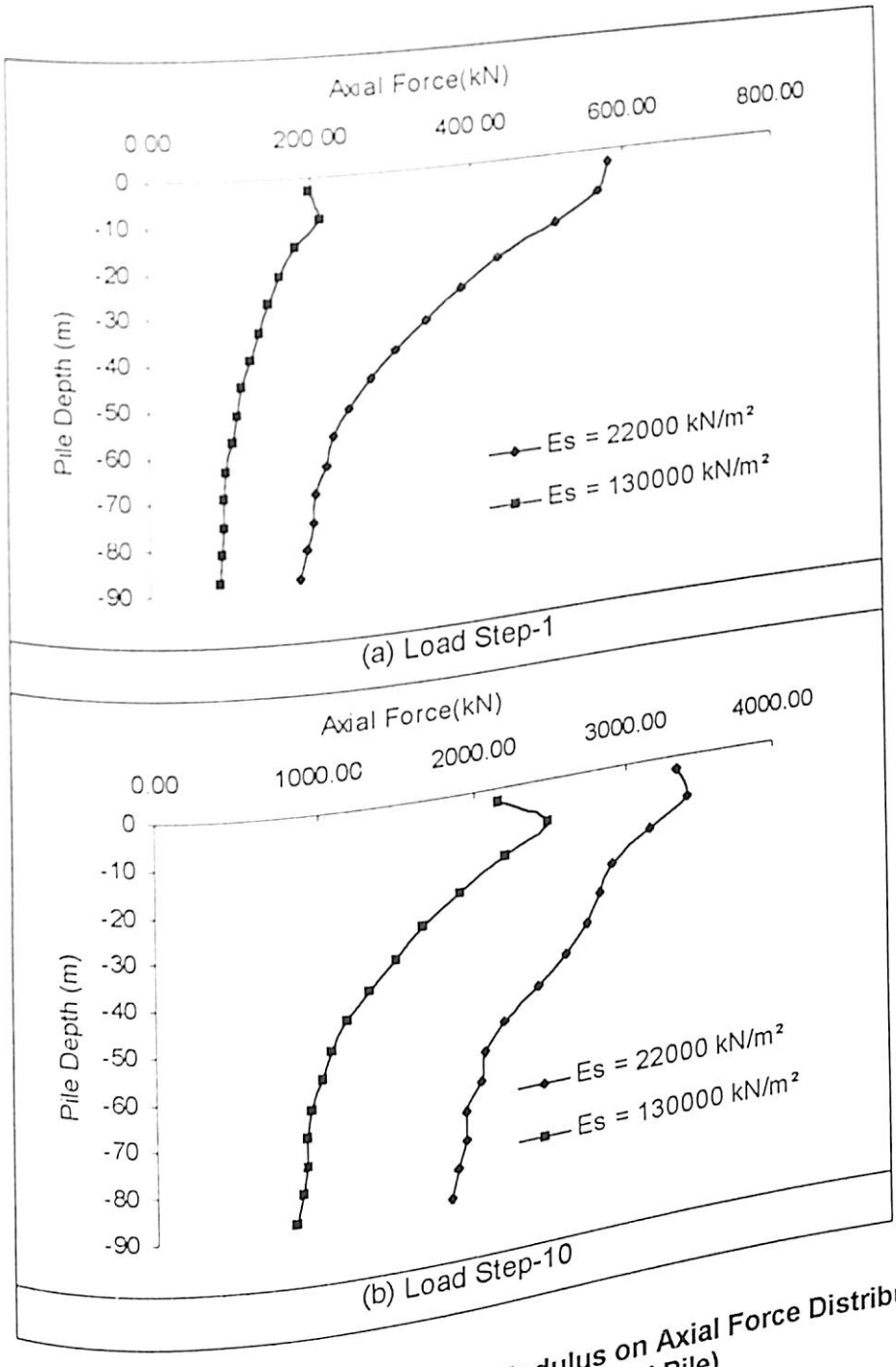

Figure 6.49 Effect of Soil Modulus on Axial Force Distribution (D = 30 m, L = 90 m, s/d = 10, End Pile)

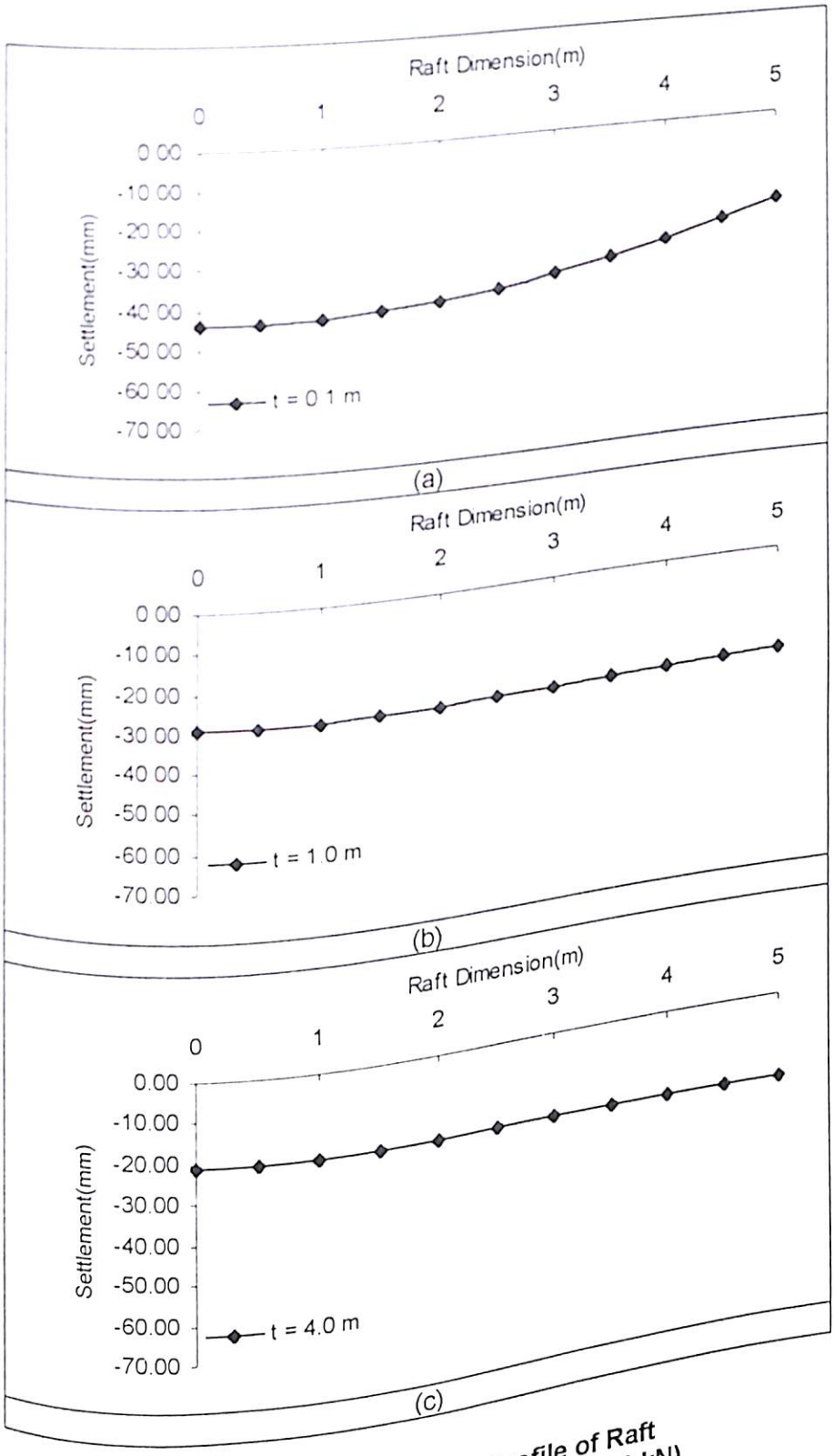

Figure 6.50 Settlement Profile of Raft
(B = 10 m, E_s = 76000 kN/m^2, P = 1000 kN)

Figures 6.51 (a), (b), (c) show the settlement profile for raft foundation of width 10 meter for varying thickness of the raft and soil modulus of 130000 kN/m^2. Differential settlement can be observed in the raft at very small thickness of the raft. Reduction in differential settlement occurs with increase in thickness of the raft and becomes almost zero when the thickness of the raft is 4.0 meter. When compared with Figure 6.50, the overall settlement reduces due to the increase in soil modulus.

Figures 6.52 (a), (b), (c) show the settlement profile for raft foundation of width 20 meter for varying thickness of the raft and soil modulus of 22000 kN/m^2. Similar trend can be observed for the settlement profile of the raft as it was seen in case raft diameter 10 m. Increase in the thickness of the raft is contributing significantly in reducing the differential settlement.

Figures 6.53 (a), (b), (c) show the settlement profile for raft foundation of width 20 meter for varying thickness of the raft and soil modulus of 76000 kN/m^2. For this soil modulus also differential settlement can be observed at smaller thickness of the raft. The reduction in differential settlement can be observed with increase in thickness of the raft and becomes almost zero when the thickness of the raft is 4.0 meter. When compared with Figure 6.52, the overall settlement reduces due to the increase in soil modulus.

Figures 6.54 (a), (b), (c) show the settlement profile for raft foundation of width 20 meter for varying thickness of the raft and soil modulus of 130000 kN/m^2. There is differential settlement in the raft at very small thickness of the raft. This differential settlement reduces with increase in thickness of the raft and becomes almost zero when the thickness of the raft is 4.0 meter. When compared with Figure 6.52, 6.53 the overall settlement reduces due to the increase in soil modulus

Figures 6.55 (a), (b), (c) show the settlement profile for raft foundation of width 30 meter for varying thickness of the raft and soil modulus of 22000 kN/m^2. There is differential settlement in the raft at very small thickness of the raft. This differential settlement reduces with increase in thickness of the raft and becomes almost zero when the thickness of the raft is 4.0 meter.

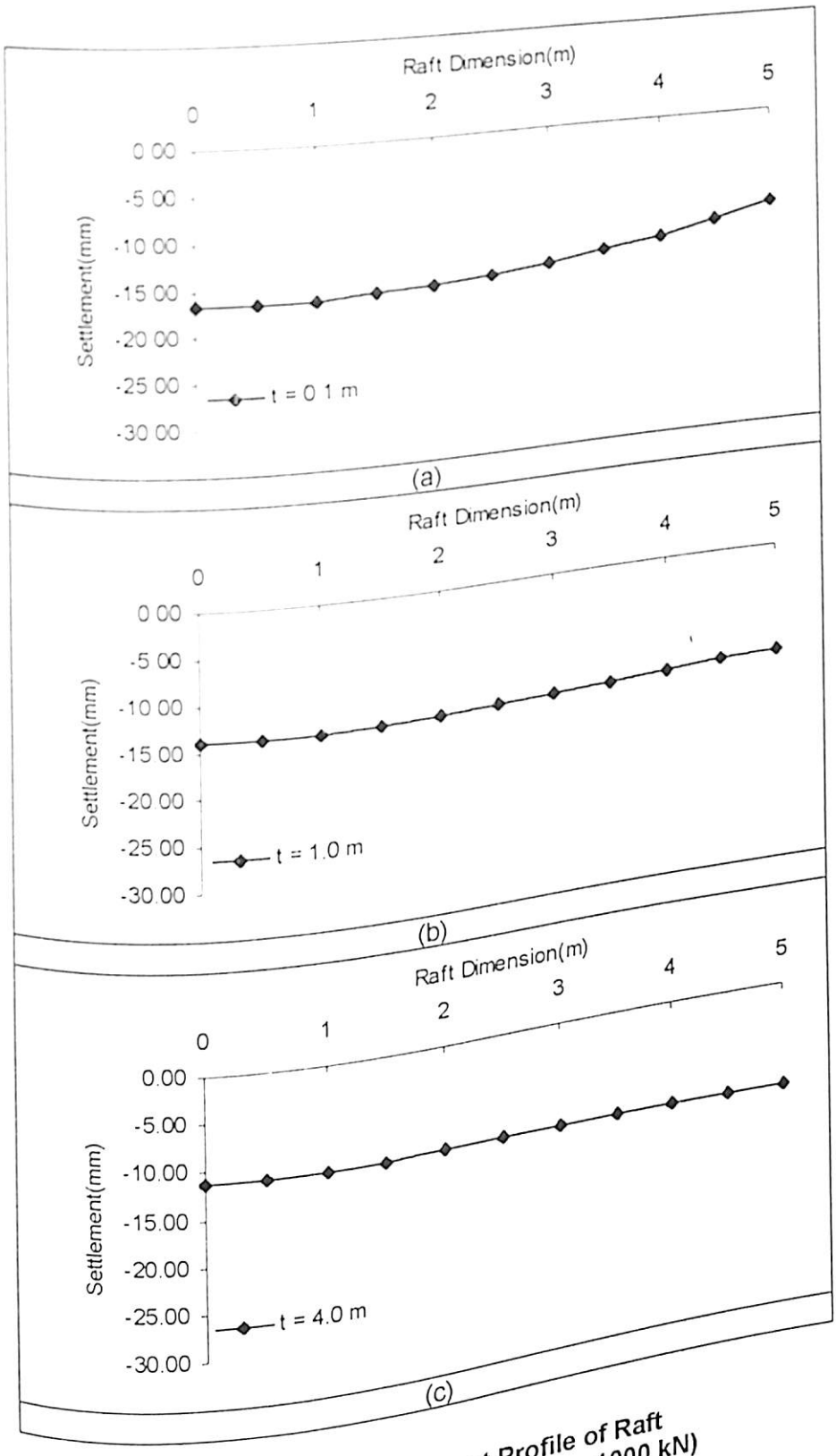

Figure 6.51 Settlement Profile of Raft
(B = 10 m, Es = 130000 kN/m^2, P = 1000 kN)

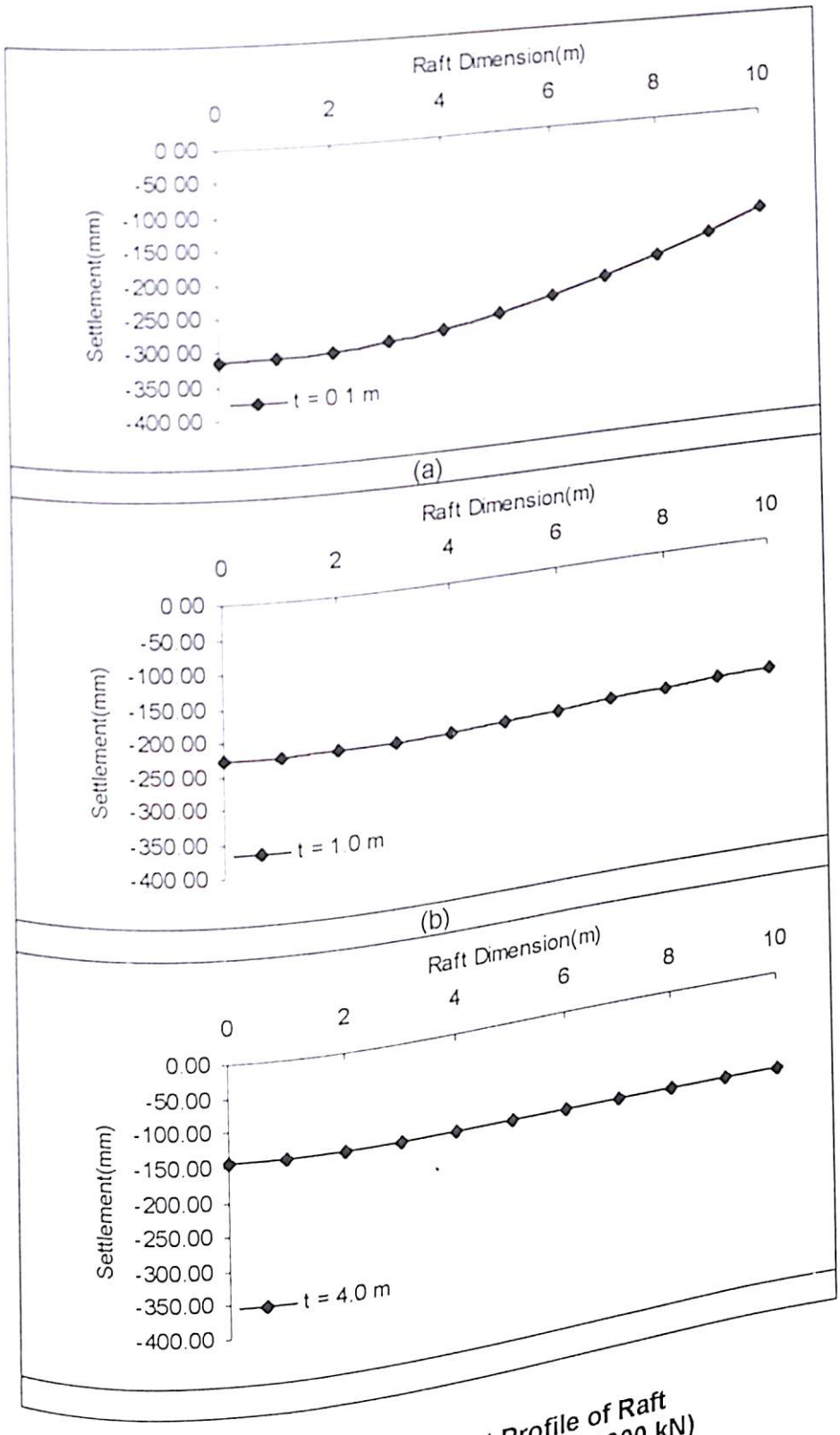

Figure 6.52 Settlement Profile of Raft
(B = 20 m, Es = 22000 kN/m^2, P = 2000 kN)

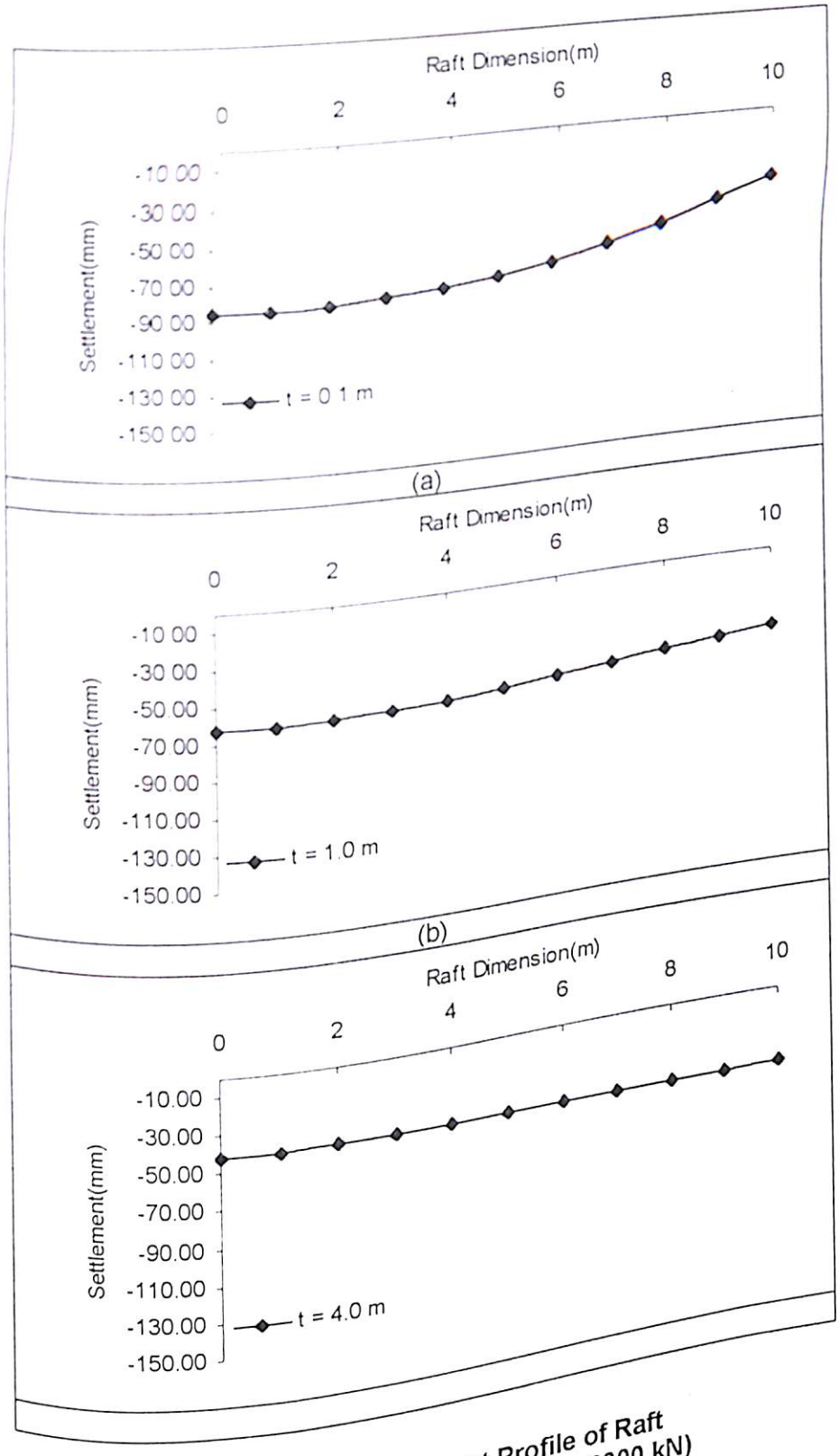

Figure 6.53 Settlement Profile of Raft
(D = 20 m, Es = 76000 kN/m^2, P = 2000 kN)

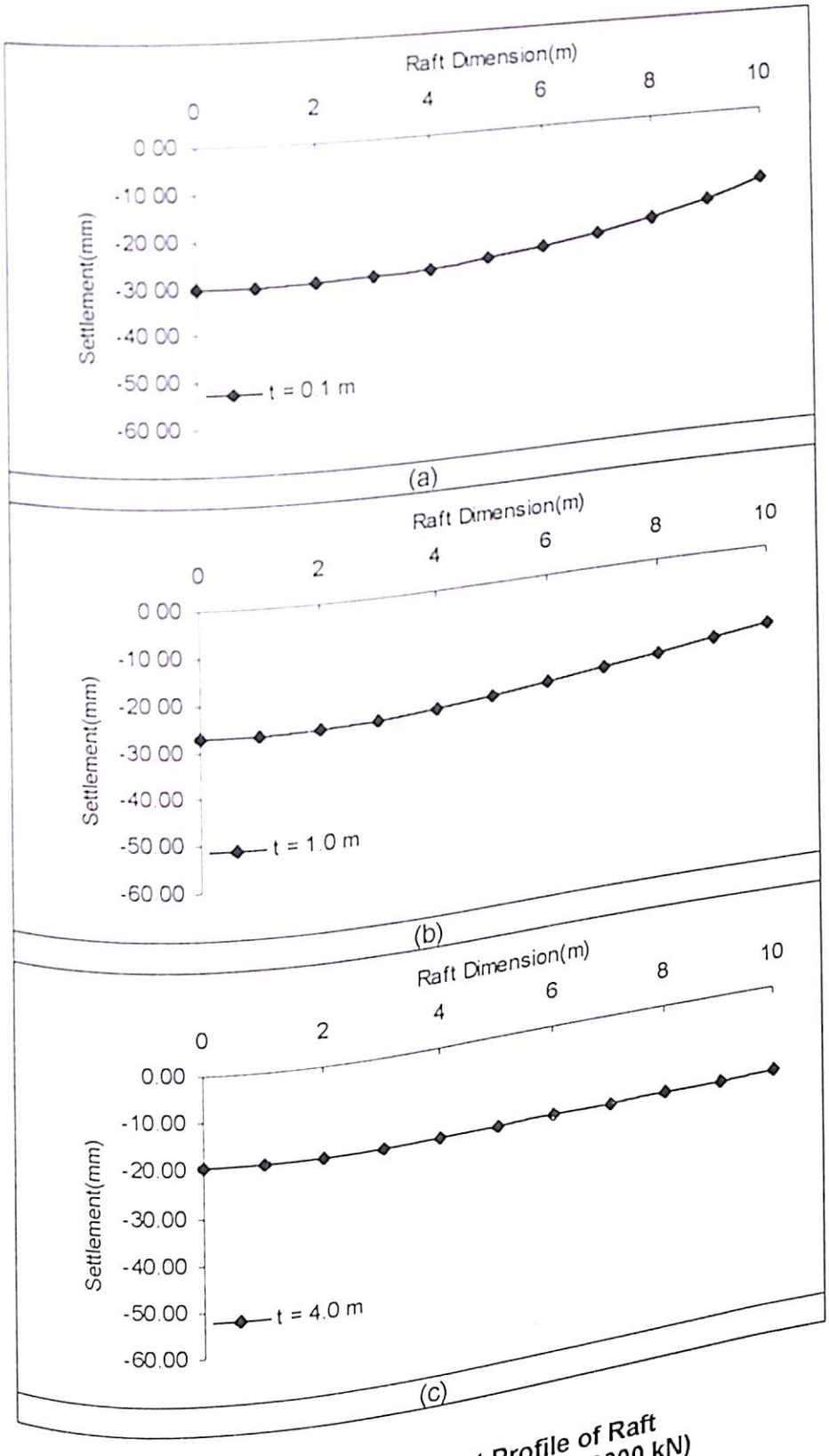

Figure 6.54 Settlement Profile of Raft
(B = 20 m, Es = 130000 kN/m^2, P = 2000 kN)

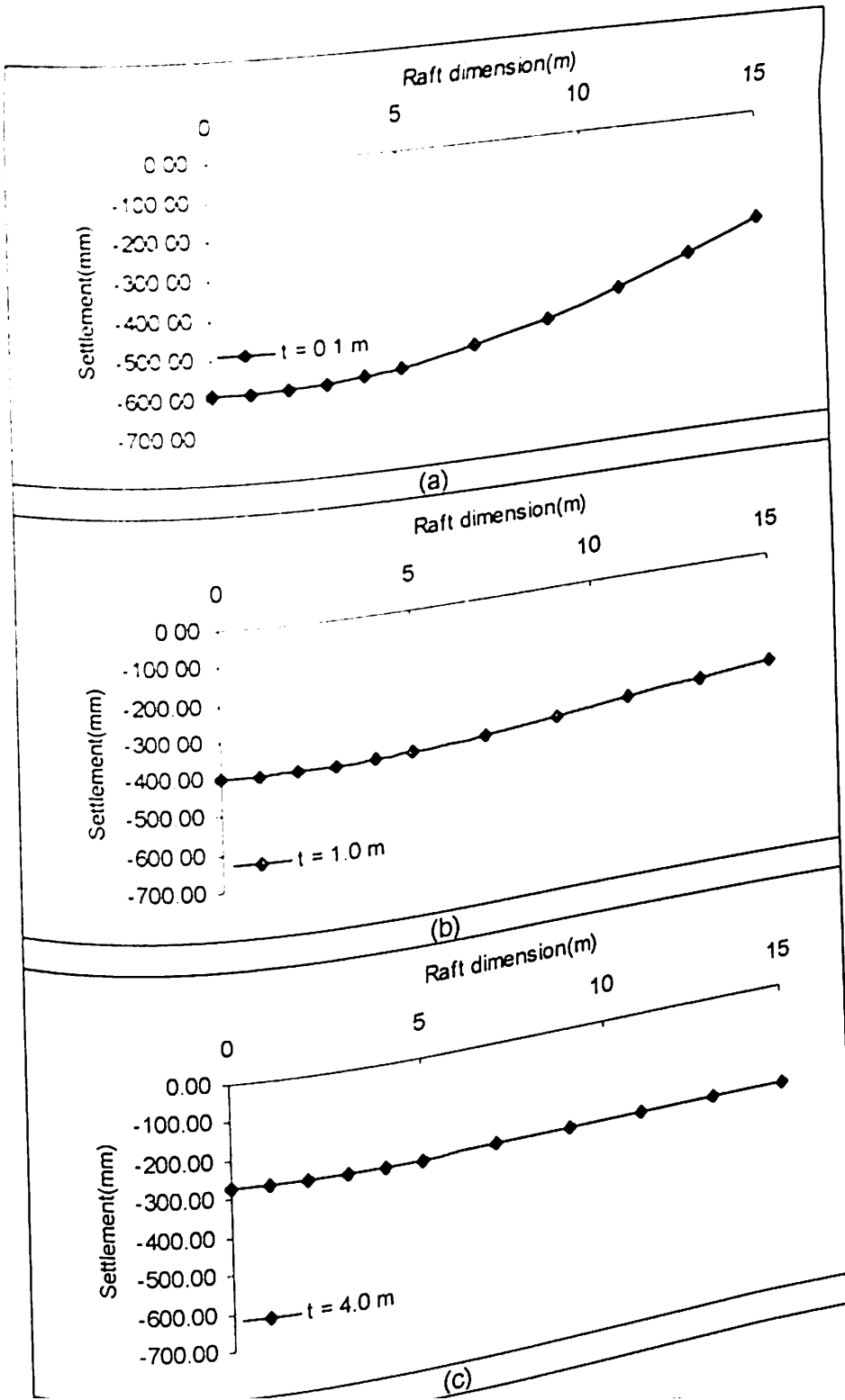
Raft dimension(m)
0
5
10
15
0.00
-100.00
-200.00
-300.00
-400.00
-500.00
-600.00
-700.00
Settlement(mm)
t = 0.1 m
(a)
Raft dimension(m)
0
5
10
15
0.00
-100.00
-200.00
-300.00
-400.00
-500.00
-600.00
-700.00
Settlement(mm)
t = 1.0 m
(b)
Raft dimension(m)
0
5
10
15
0.00
-100.00
-200.00
-300.00
-400.00
-500.00
-600.00
-700.00
Settlement(mm)
t = 4.0 m
(c)

Figures 6.56 (a), (b), (c) show the settlement profile for raft foundation of width 30 meter for varying thickness of the raft and soil modulus of 76000 kN/m^2. There is differential settlement in the raft at very small thickness of the raft. This differential settlement reduces with increase in thickness of the raft and becomes almost zero when the thickness of the raft is 4.0 meter. When compared with Figure 6.55, the overall settlement reduces due to the increase in soil modulus.

Figures 6.57 (a), (b), (c) show the settlement profile for raft foundation of width 30 meter for varying thickness of the raft and soil modulus of 130000 kN/m^2. Differential settlement is seen in the raft at very small thickness (0.1 m) of the raft. As the raft thickness increases and reaches to 4.0 m, the differential settlement reduces to almost zero. When compared with Figure 6.55, 6.56 the overall settlement is found to reduce due to the increase in soil modulus

Figures 6.58 (a), (b), (c) show the settlement profile for raft foundation of width 40 meter for varying thickness of the raft and soil modulus of 22000 kN/m^2. It can be observed form the graph that at smaller thickness (0.1 m), differential settlement is there in the raft. This differential settlement is minimum when thickness of raft reaches 4.0 meter.

Figures 6.59 (a), (b), (c) show the settlement profile for raft foundation of width 40 meter for varying thickness of the raft and soil modulus of 76000 kN/m^2. Similar trend can be seen for settlement profile of raft as it was for soil modulus 22000 kN/m^2. When compared with Figure 6.54, the overall settlement reduces due to the increase in soil modulus.

Figures 6.60 (a), (b), (c) show the settlement profile for raft foundation of width 40 meter for varying thickness of the raft and soil modulus of 130000 kN/m^2. Differential settlement can be observed in the raft at very small thickness. This differential settlement reduces with increase in thickness of the raft and becomes almost zero when the thickness of the raft is 4.0 meter.

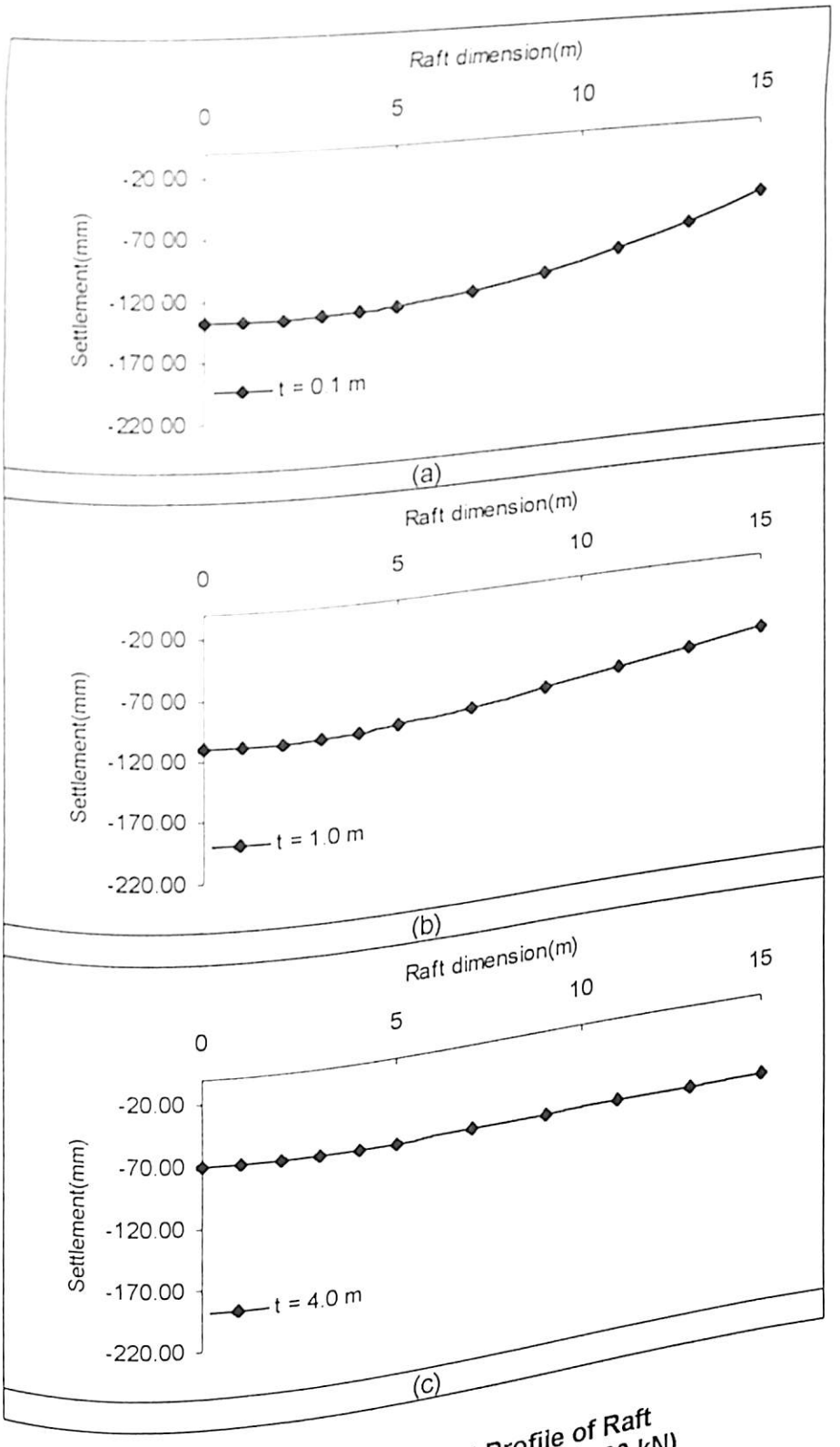

Figure 6.56 Settlement Profile of Raft
(B = 30 m, E_s = 76000 kN/m^2, P = 3000 kN)

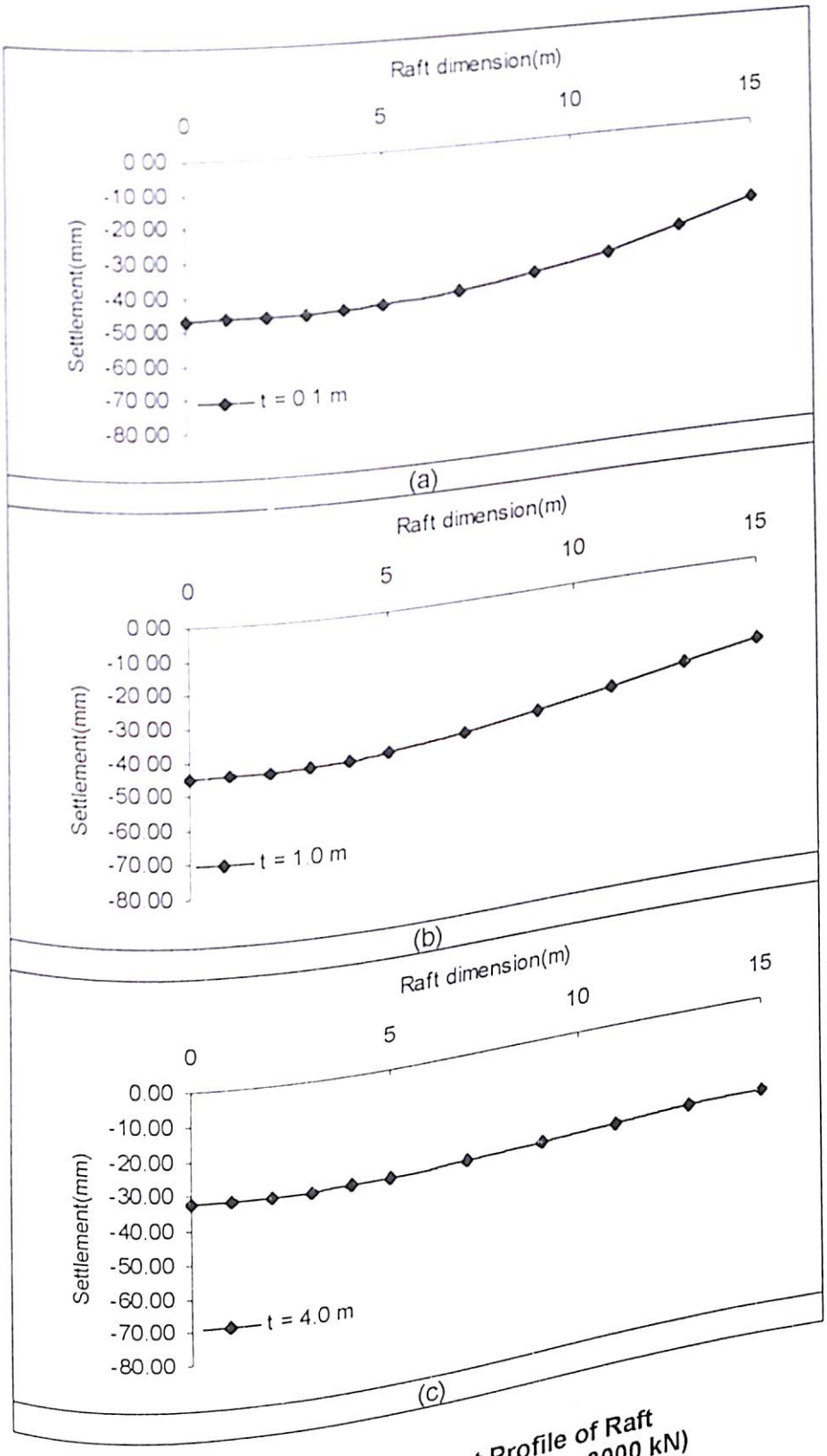

Figure 6.57 Settlement Profile of Raft
(B = 30 m, E_s = 130000 kN/m^2, P = 3000 kN)

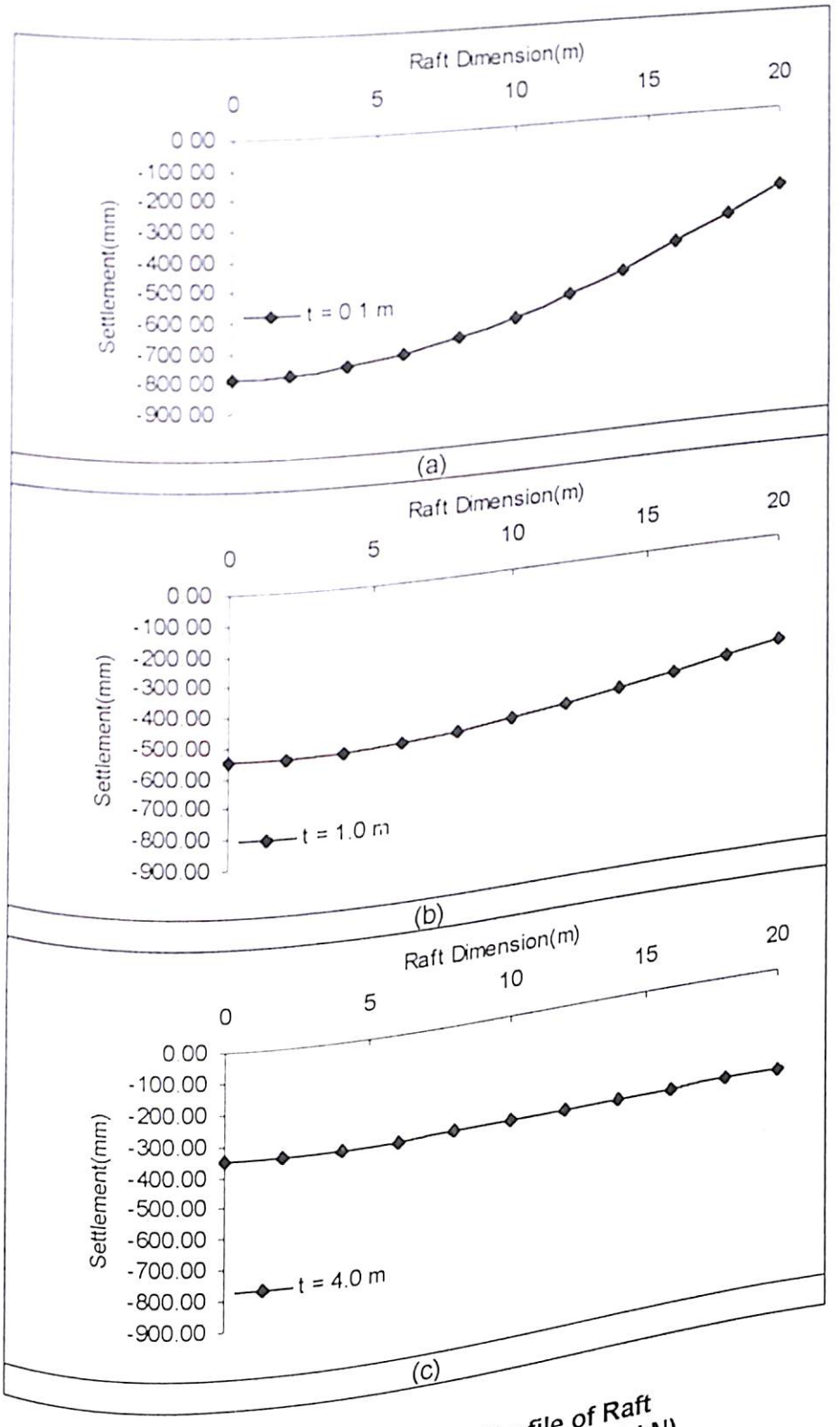

Figure 6.58 Settlement Profile of Raft
(B = 40 m, E_s = 22000 kN/m^2, P = 4000 kN)

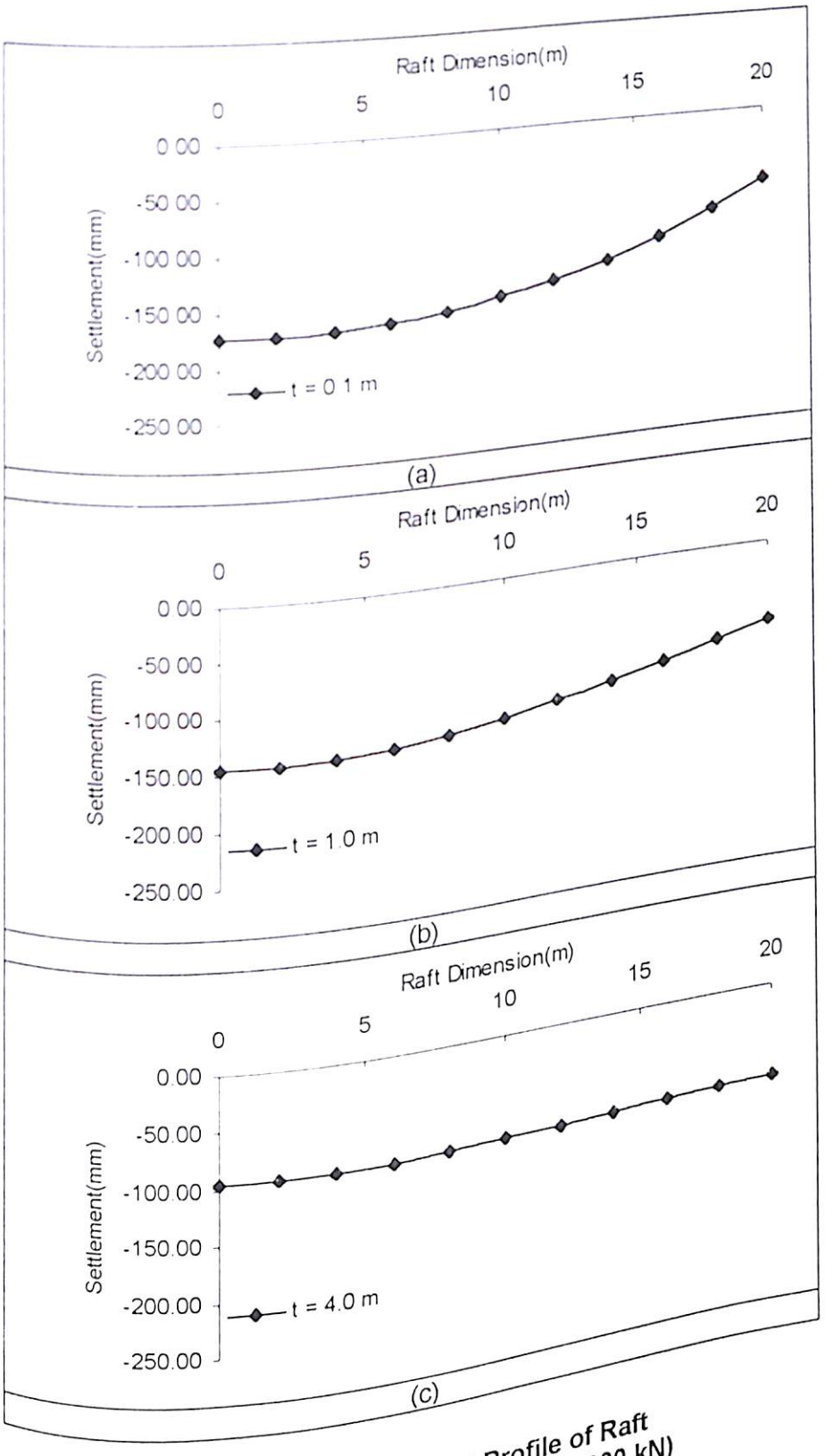

Figure 6.59 Settlement Profile of Raft
(B = 40 m, E_s = 76000 kN/m^2, P = 4000 kN)

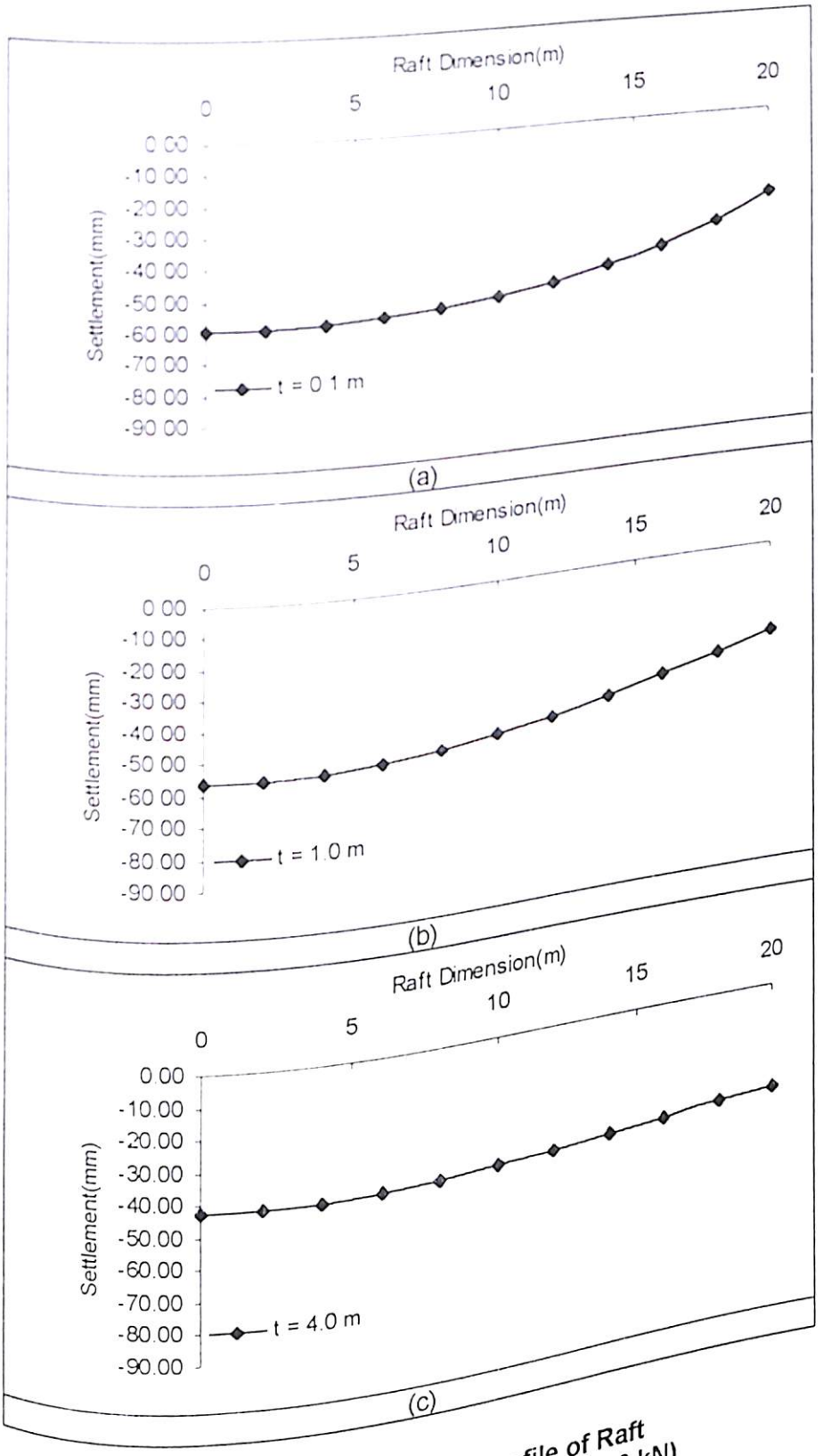

Figure 6.60 Settlement Profile of Raft
(B = 40 m, E_s = 130000 kN/m^2, P = 4000 kN)

When compared with Figure 6.58,6.59 the overall settlement reduces due to the increase in soil modulus

Figures 6.61 (a), (b), (c) show the settlement profile for raft foundation of width 50 meter for varying thickness of the raft and soil modulus of 22000 kN/m^2. The settlement profile of raft at smaller thickness (0.1 m) shows the presence of differential settlement. It is observed from the settlement profile that differential settlement reduces with increase in thickness of the raft and becomes almost zero when the thickness of the raft is 4.0 meter.

Figures 6.62 (a), (b), (c) show the settlement profile for raft foundation of width 50 meter for varying thickness of the raft and soil modulus of 76000 kN/m^2. There is differential settlement in the raft at very small thickness of the raft. This differential settlement reduces with increase in thickness of the raft and becomes almost zero when the thickness of the raft is 4.0 meter. When compared with Figure 6.61, the overall settlement reduces due to the increase in soil modulus.

Figures 6.63 (a), (b), (c) show the settlement profile for raft foundation of width 50 meter for varying thickness of the raft and soil modulus of 130000 kN/m^2. It can be clearly seen from the settlement profile that at smaller thickness of the raft, differential settlement is significant. However, differential settlement reduces with increase in thickness of the raft and becomes almost zero when the thickness of the raft is 4.0 meter. When compared with Figure 6.61,6.62 the overall settlement reduces due to the increase in soil modulus

6.6.4.2 Settlement Profile for Piled Raft Foundation

Figures 6.64 (a), (b), (c) show the settlement profile for piled raft foundation whose raft width is 10 meter for a soil modulus of 22000 kN/m^2 and spacing to one side ratio 2.5 for varying length of the pile. The effect of increase in length of pile is to reduce the differential settlement and overall settlement.

Figures 6.65 (a), (b), (c) show the settlement profile for piled raft foundation whose raft width is 10 meter for a soil modulus of 76000 kN/m^2 and spacing to one side ratio of 2.5

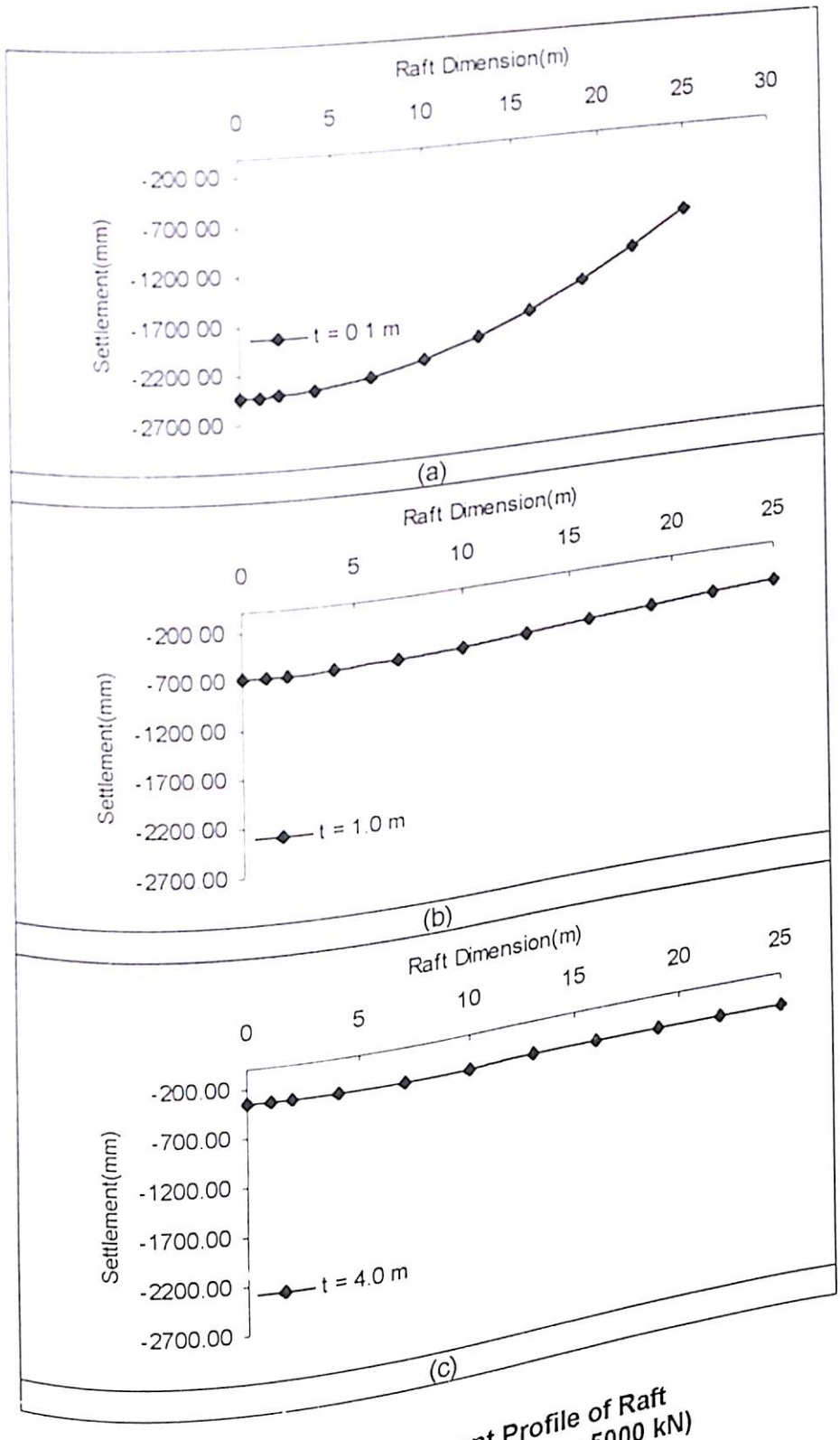

Figure 6.61 Settlement Profile of Raft
(B = 50 m, E_s = 22000 kN/m^2, P = 5000 kN)

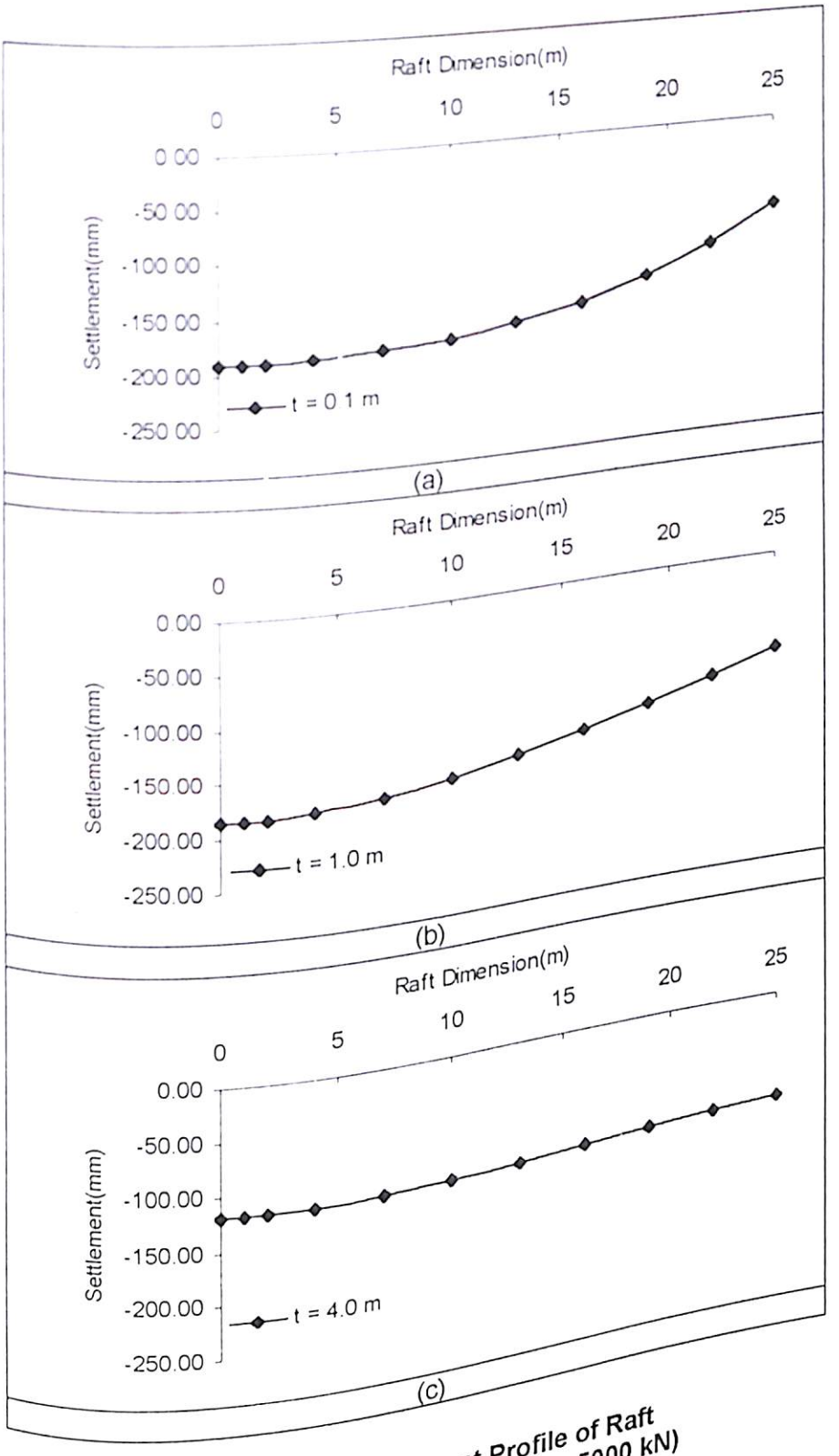

Figure 6.62 Settlement Profile of Raft
(B = 50, m E_s = 76000 kN/m^2, P = 5000 kN)

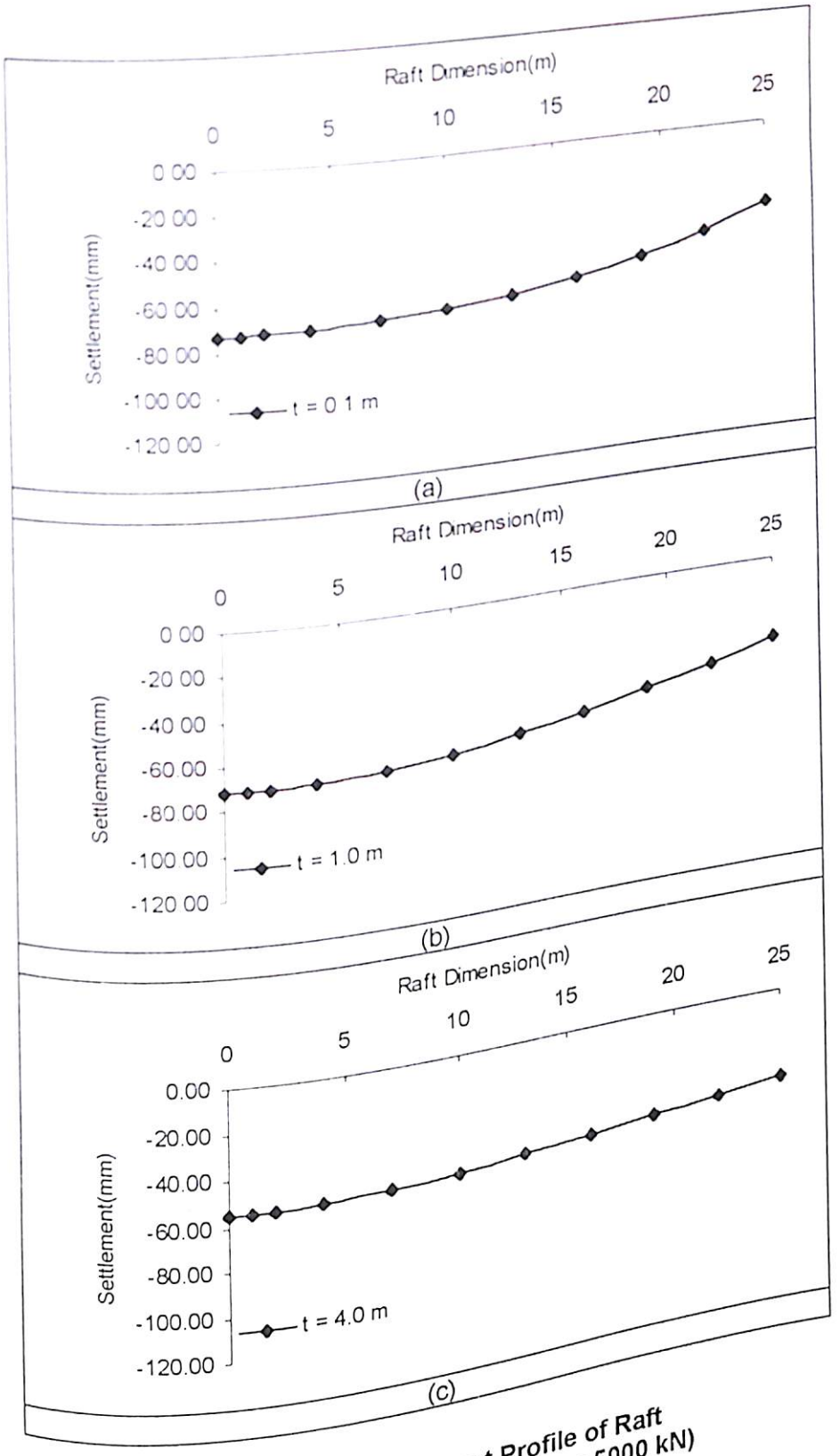

Figure 6.63 Settlement Profile of Raft
(B = 50 m, E_s = 130000 kN/m^2, P = 5000 kN)

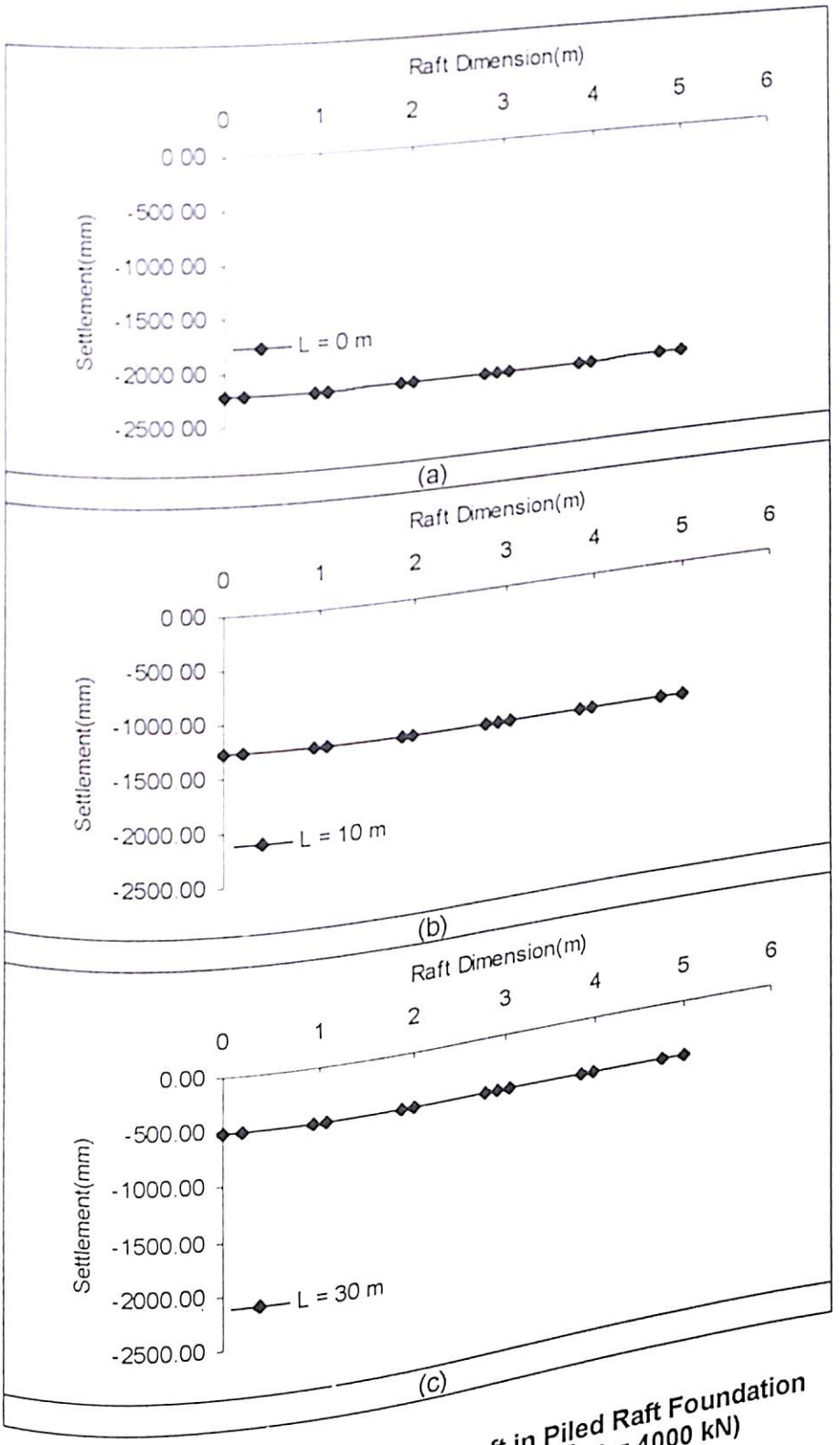

Figure 6.64 Settlement Profile of Raft in Piled Raft Foundation (B = 10 m, s/d = 2.5, E_s = 22000 kN/m^2, P = 4000 kN)

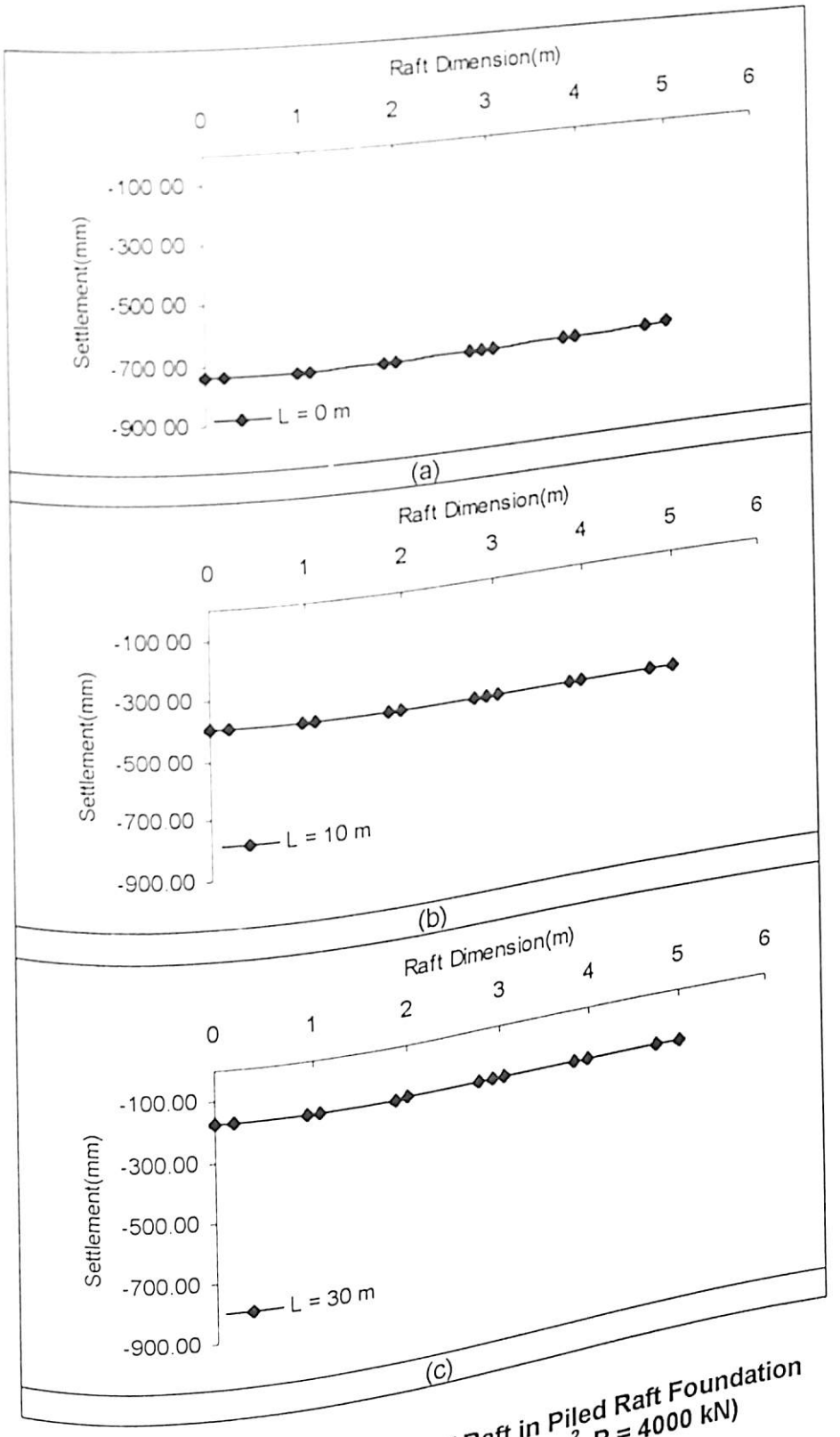

Figure 6.65 Settlement Profile of Raft in Piled Raft Foundation (B = 10 m, s/d = 2.5, E_s = 76000 kN/m^2, P = 4000 kN)

for varying length of the pile. The effect of increase in length of pile is to reduce the differential settlement and overall settlement. When compared with Figure 6.64, the overall settlement reduces with increase in soil modulus.

Figures 6.66 (a), (b), (c) show the settlement profile for piled raft foundation whose raft width is 10 meter for a soil modulus of 130000 kN/m^2 and spacing to one side ratio of 2.5 for varying length of the pile. The effect of increase in length of pile is to reduce the differential settlement and overall settlement. When compared with Figures 6.64 and 6.65 the overall settlement reduces with increase in soil modulus.

Figures 6.67 (a), (b), (c) show the settlement profile for piled raft foundation whose raft width is 10 meter for a soil modulus of 22000 kN/m^2 and spacing to one side ratio 5.0 for varying length of the pile. It can be observed from the graphs that with increase in pile length, differential settlement as well as overall settlement is reducing.

Figures 6.68 (a), (b), (c) show the settlement profile for piled raft foundation whose raft width is 10 meter for a soil modulus of 76000 kN/m^2 and spacing to one side ratio of 5.0 for varying length of the pile. The effect of increase in length of pile is to reduce the differential settlement and overall settlement and thereby increasing the load carrying capacity of the piled raft foundation. When compared with Figure 6.67, the overall settlement reduces with increase in soil modulus.

Figures 6.69 (a), (b), (c) show the settlement profile for piled raft foundation whose raft width is 10 meter for a soil modulus of 130000 kN/m^2 and spacing to one side ratio of 5.0 for varying length of the pile. The effect of increase in length of pile is to reduce the differential settlement and overall settlement. When compared with Figures 6.67 and 6.68 the overall settlement reduces with increase in soil modulus. When Figures 6.67, 6.68, 6.69 are compared with Figures 6.64, 6.65 and 6.66 it is found that the overall settlement increases with increase in spacing between the piles.

Figures 6.[illegible] settlement profile for piled raft foundation whose raft [illegible] spacing to one side ratio of 7.5

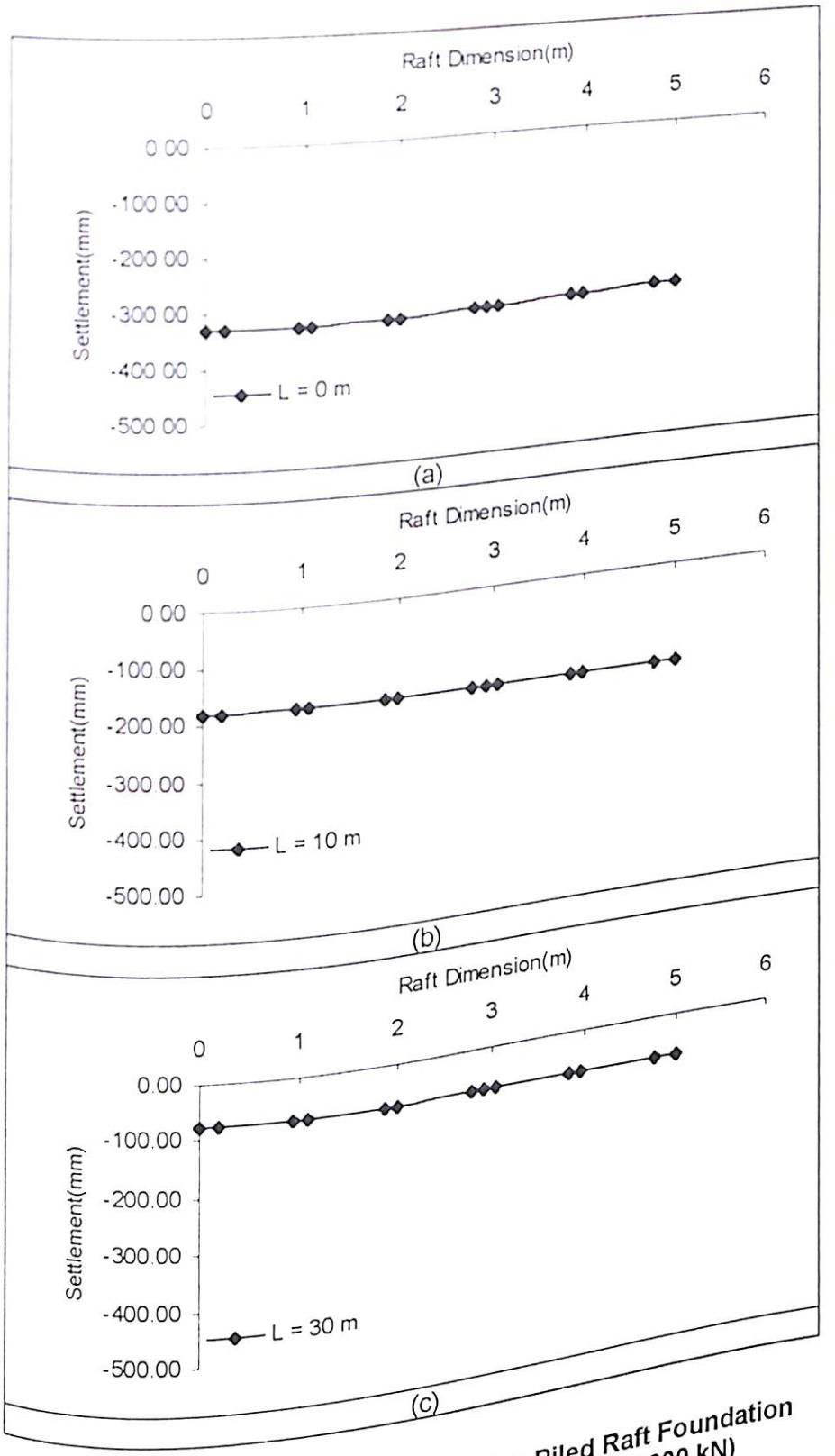

Figure 6.66 Settlement Profile of Raft in Piled Raft Foundation (B = 10 m, s/d = 2.5, E_s = 130000 kN/m^2, P = 4000 kN)

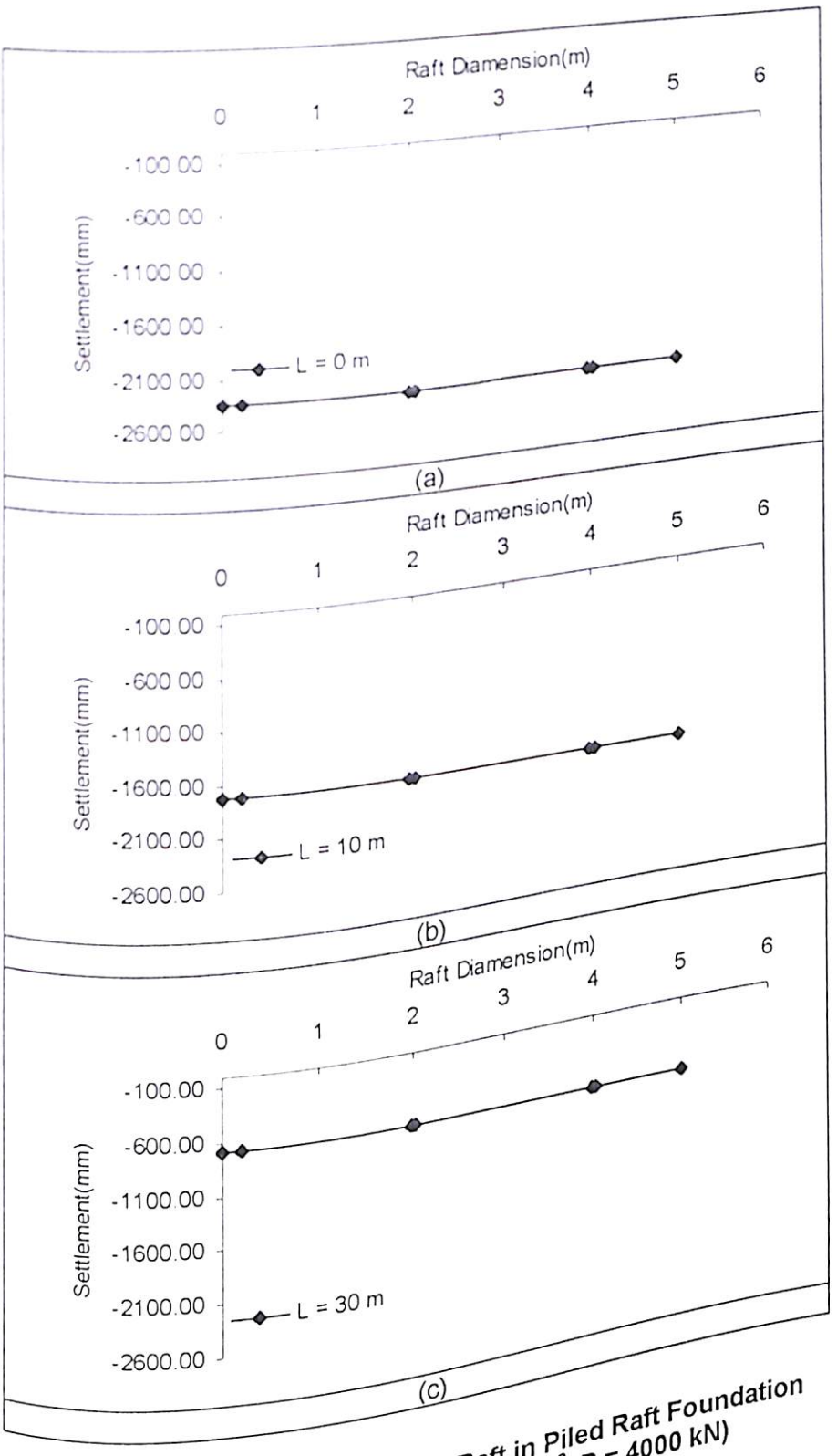

Figure 6.67 Settlement Profile of Raft in Piled Raft Foundation (B = 10 m, s/d = 5, E_s = 22000 kN/m^2, P = 4000 kN)

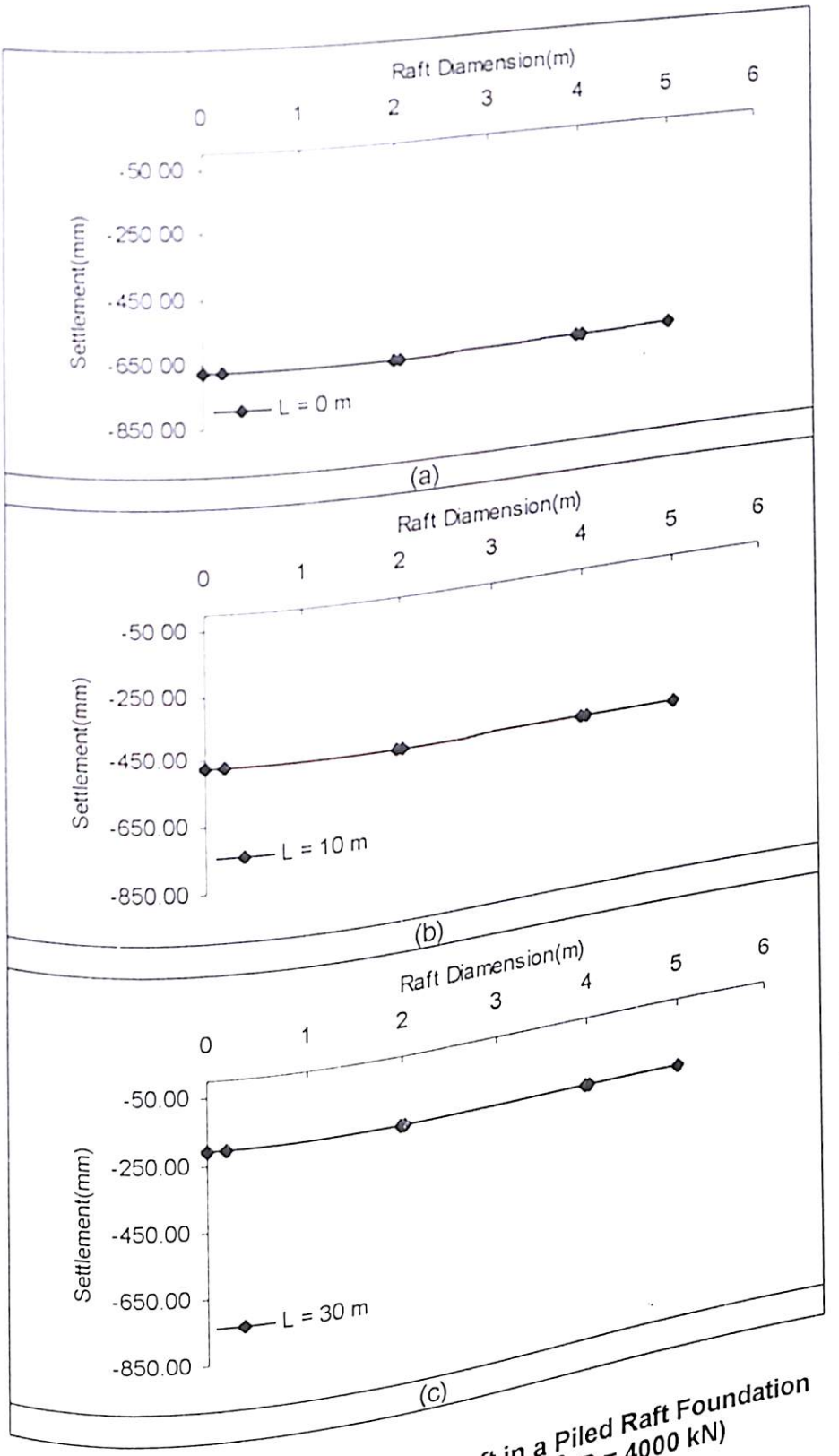

Figure 6.68 Settlement Profile of Raft in a Piled Raft Foundation (B = 10 m, s/d = 5, E_s = 76000 kN/m^2, P = 4000 kN)

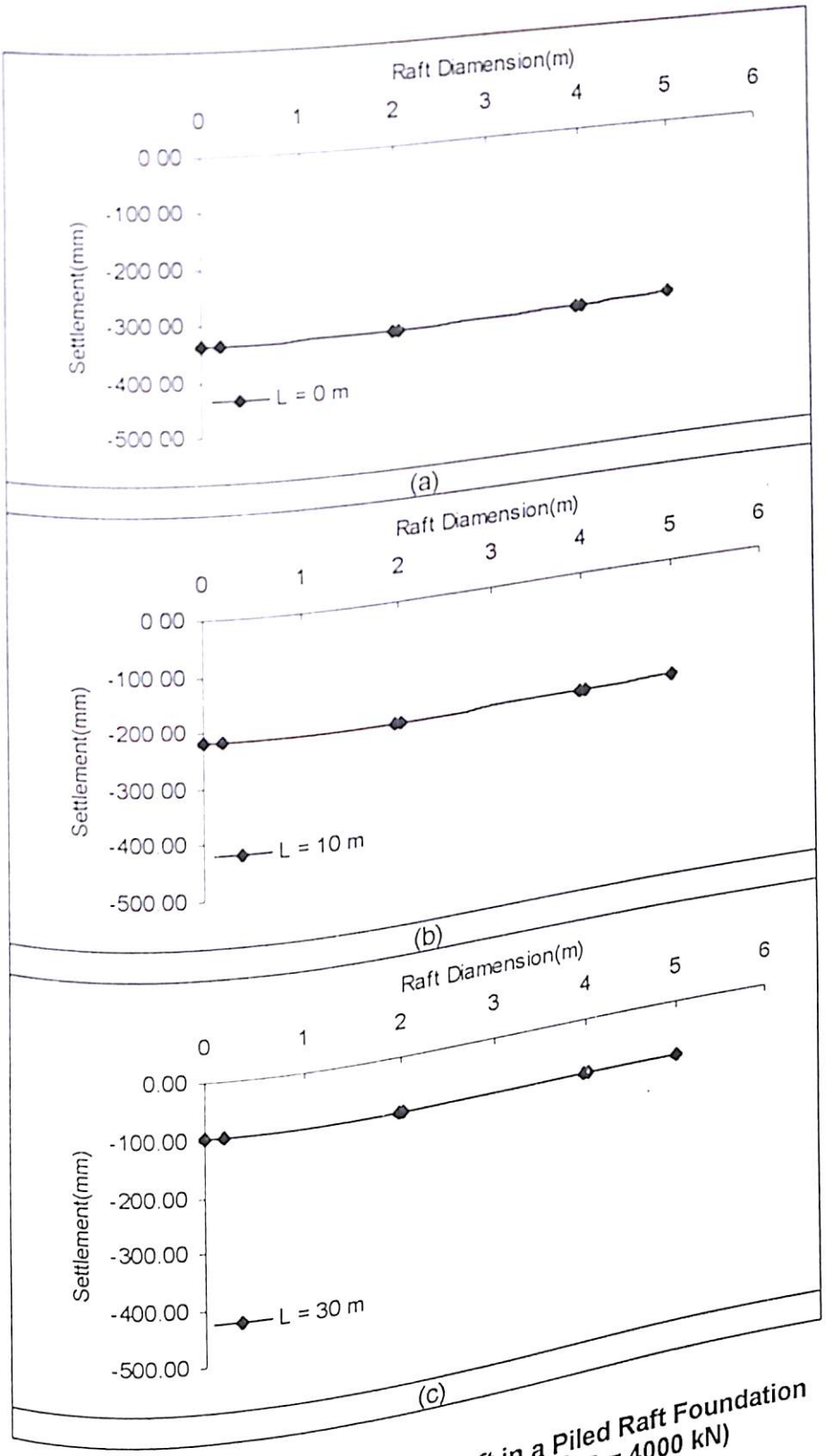

Figure 6.69 Settlement Profile of Raft in a Piled Raft Foundation (B = 10 m, s/d = 5, E_s = 130000 kN/m^2, P = 4000 kN)

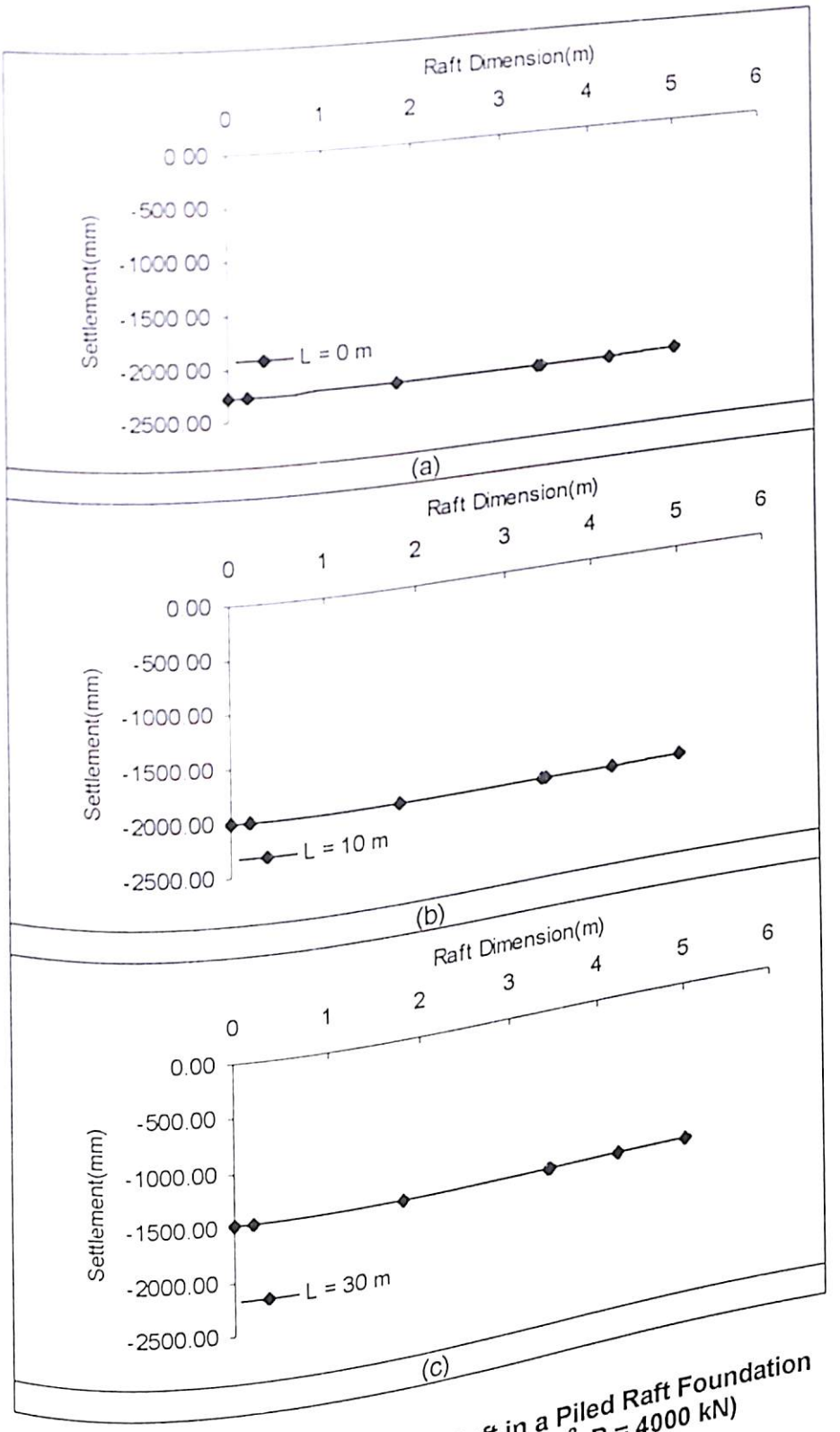

Figure 6.70 Settlement Profile of Raft in a Piled Raft Foundation (B = 10 m, s/d = 7.5, E_s = 22000 kN/m^2, P = 4000 kN)

for varying length of the pile. The effect of increase in length of pile is to reduce the differential settlement and overall settlement.

Figures 6.71 (a), (b), (c) show the settlement profile for piled raft foundation whose raft width is 10 meter for a soil modulus of 76000 kN/m^2 and spacing to one side ratio of 7.5 for varying length of the pile. The effect of increase in length of pile is to reduce the differential settlement and overall settlement. When compared with Figure 6.66, the overall settlement reduces with increase in soil modulus.

Figures 6.72 (a), (b), (c) show the settlement profile for piled raft foundation whose raft width is 10 meter for a soil modulus of 130000 kN/m^2 and spacing to one side ratio of 7.5 for varying length of the pile. The effect of increase in length of pile is to reduce the differential settlement and overall settlement. When compared with Figures 6.70 and 6.71 the overall settlement reduces with increase in soil modulus. When Figures 6.70,6.71,6.71 are compared with Figures 6.67, 6.68, 6.69 and 6.64, 6.65 and 6.66 it is found that the overall settlement increases with increase in spacing between the piles.

6.6.5 Yielding of Soil

Figures 6.73 (a), (b) show the yielding of soil for a piled raft foundation under plane strain condition for a raft of width 10m, spacing to one side ratio of 2.5, length of pile 10 meter, thickness of raft 0.1 metre and soil modulus 22000 kN/m^2. The yielding has started from load step 3 and yielding is first seen in the soil element at the edge of the raft and the tip of the boundary pile. In load step 5 the yielding is seen in the soil elements moving in the lateral direction and downward direction.

Figures 6.74 (a), (b) show the yielding in the soil mass at load step 7 and load step 10 respectively. Complete yielding of soil is seen below the tip of piles and also the soil surrounding the pile gets yielded. This has been found in load step 7. In load step 10 complete yielding of soil below the pile tip is seen and also the yielding is seen to progress upto the boundary. The block behaviour of piled raft foundation is found in this case.

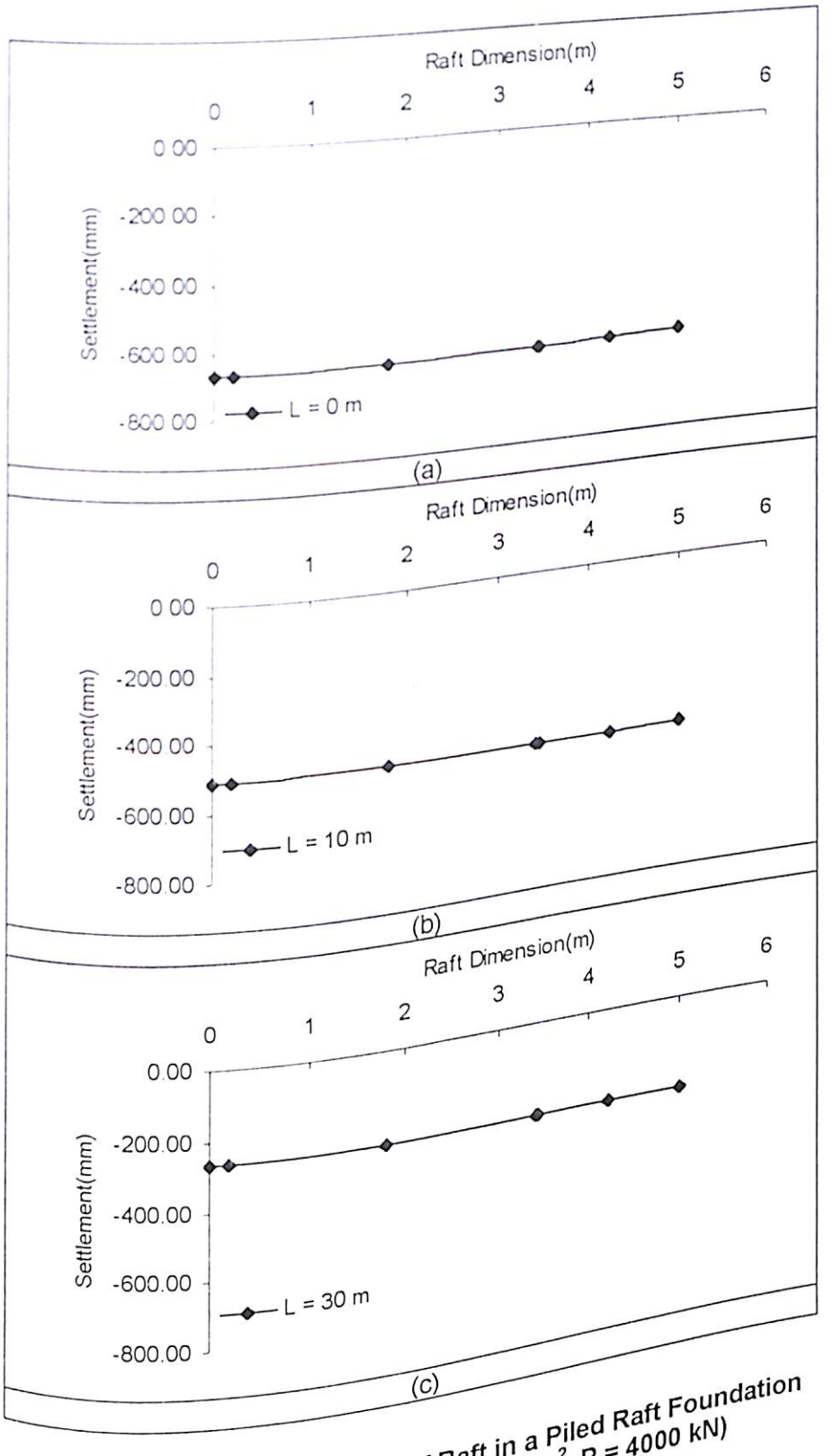

Figure 6.71 Settlement Profile of Raft in a Piled Raft Foundation (B = 10 m, s/d = 7.5, E_s = 76000 kN/m^2, P = 4000 kN)

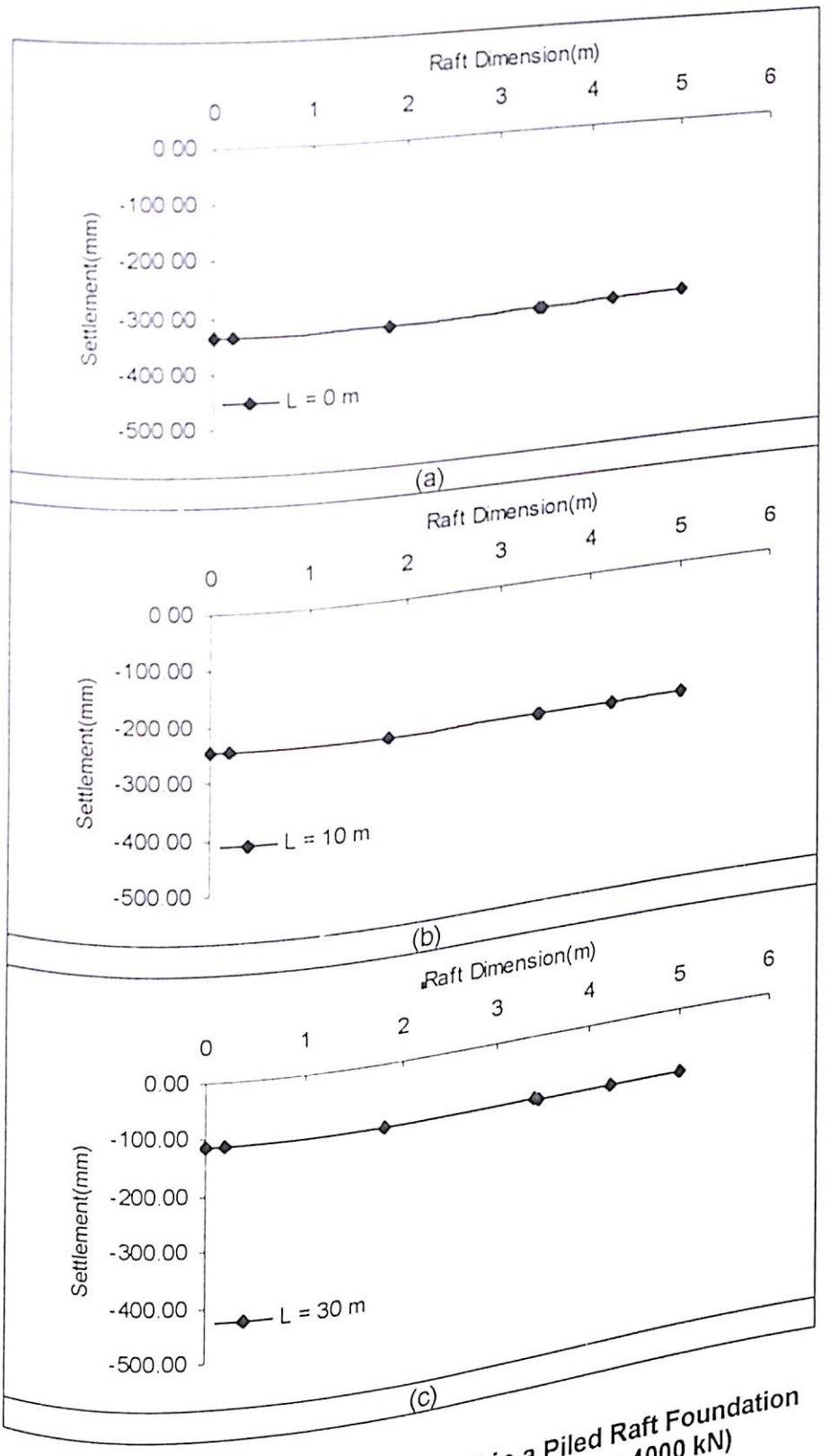

Figure 6.72 Settlement Profile of Raft in a Piled Raft Foundation (B = 10 m, s/d = 7.5, E_s = 130000 kN/m^2, P = 4000 kN)

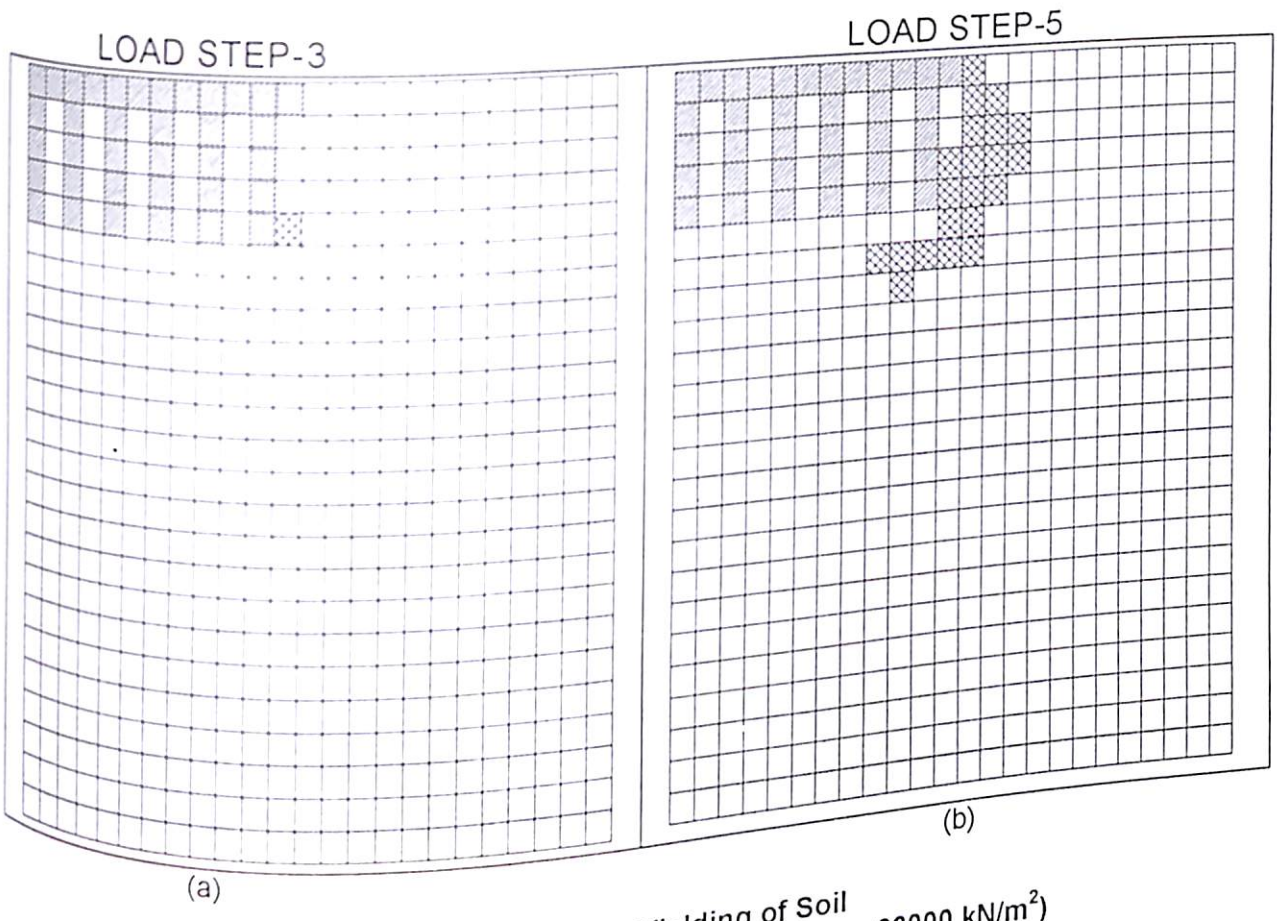

Figure 6.73 Yielding of Soil
(B = 10 m, L = 10 m, t = 0.1 m, s/d = 2.5, E_s = 22000 kN/m^2)

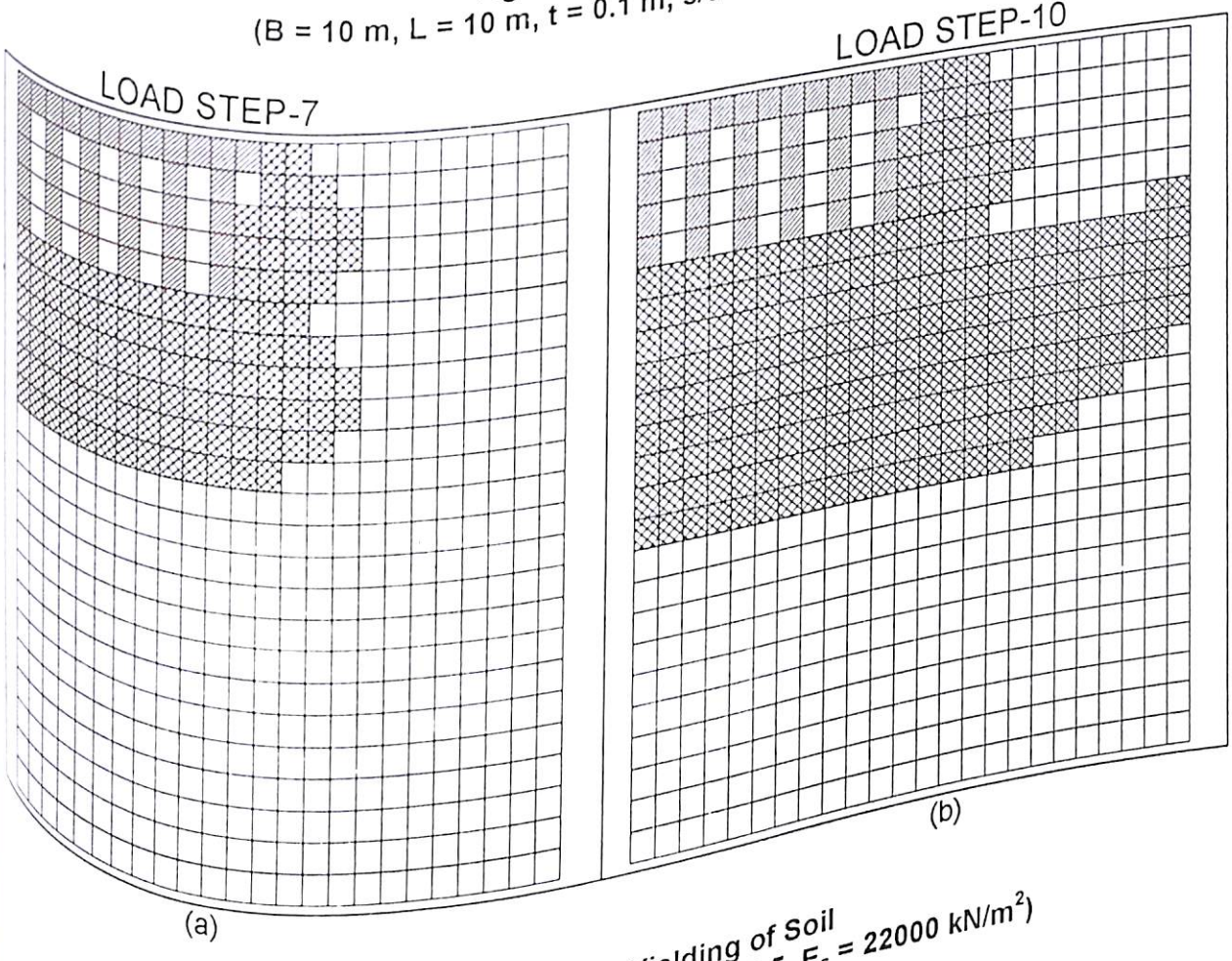

Figure 6.74 Yielding of Soil
(B = 10 m, L = 10 m, t = 0.1 m, s/d = 2.5, E_s = 22000 kN/m^2)

Figures 6.75 (a), (b) show the yielding of the soil in a piled raft foundation under plane strain condition for raft width of 10 meters, spacing to diameter of pile equal to 2.5, length of pile 10m, soil modulus 22000 kN/m^2 and the raft thickness of 1.0 metre. In load step 3 yielding is seen to start at the tip of the pile. In load step 5, the yielding is seen to progress downward and in lateral direction.

Figures 6.76 (a), (b) show the yielding of soil that has progressed from edge towards the center below the piles and also has moved in the lateral direction as well as in the downward direction. In load step 10, complete yielding of soil is seen below the pile and also in the lateral direction upto a wide range. The block behaviour of pile is seen even in this case.

Figures 6.77 (a), (b) show the development of yielding in the soil for a piled raft foundation of width 10 metres, length of pile 10 metres, and raft thickness of 4.0 metres and soil modulus of 22000 kN/m^2. In load step 4, the soil yielding is seen to start at the tip of the pile. In load steps 5, more soil elements have been found to yield.

Figures 6.78 (a), (b) show the yielding of the soil mass for load step 7, where the yielding of soil has progressed from boundary of pile towards the center pile and also in the lateral direction. This yielding is found to progress from the soil elements near the pile tip in the downward direction. This has been found in load step 7. In load step 10, maximum yielding is seen in the soil elements below the pile tip and also in the lateral direction. The zone of yielding keeps increasing with increase in load steps.

Figures 6.79 (a), (b) show the yielding of soil for a piled raft foundation of length 10 metres, spacing to one side ratio of 2.5, raft width 10 metre for a soil of modulus 130000 kN/m^2 and raft thickness of 0.1 metre. The yielding is seen in the soil at the tip of pile and also near the edge of the pile in load step 5. This yielding progresses in the down ward direction near the boundary piles. Also more soil elements in the lateral directions yield (load step 7).

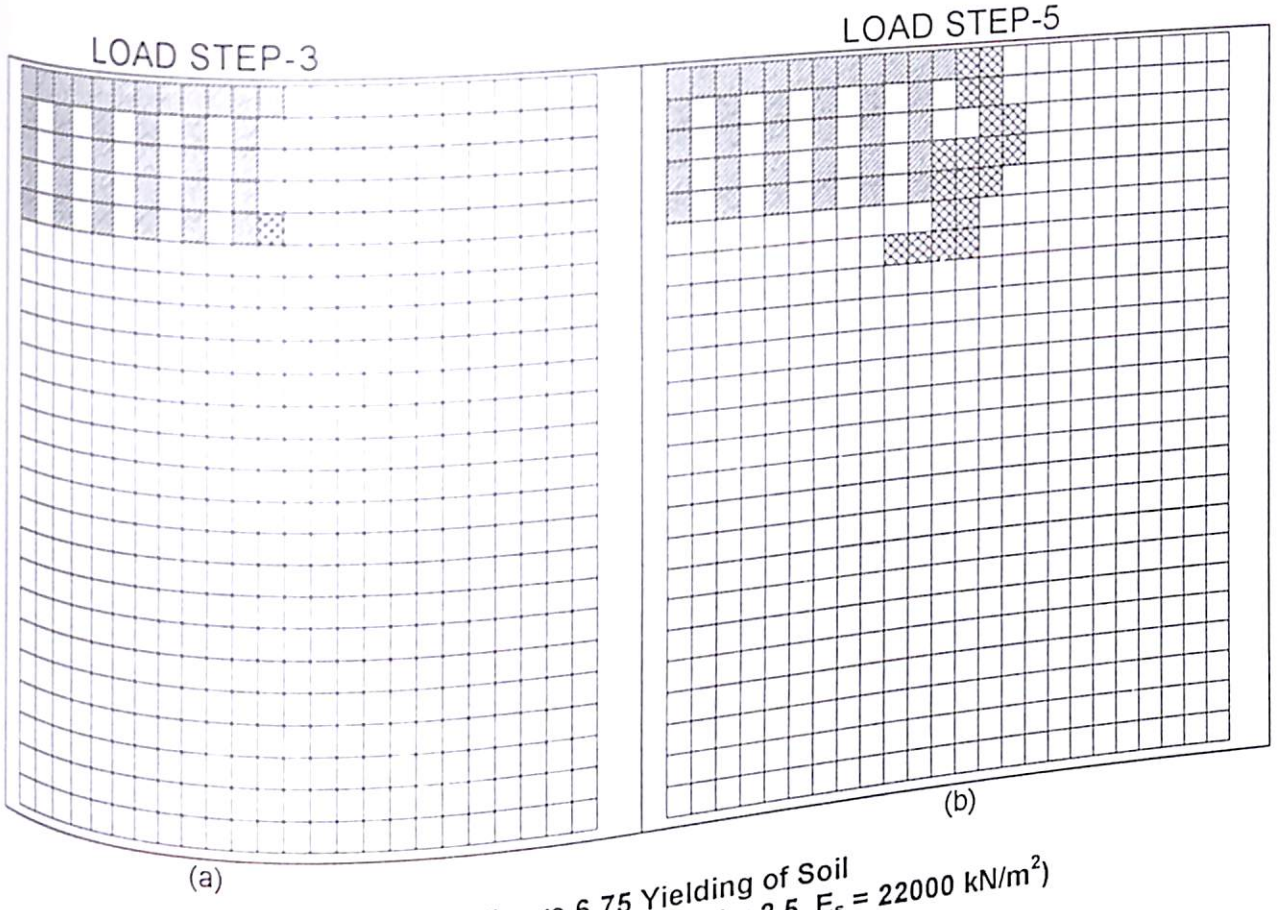

Figure 6.75 Yielding of Soil
(B = 10 m, L = 10 m, t = 1.0 m, s/d = 2.5, E_s = 22000 kN/m^2)

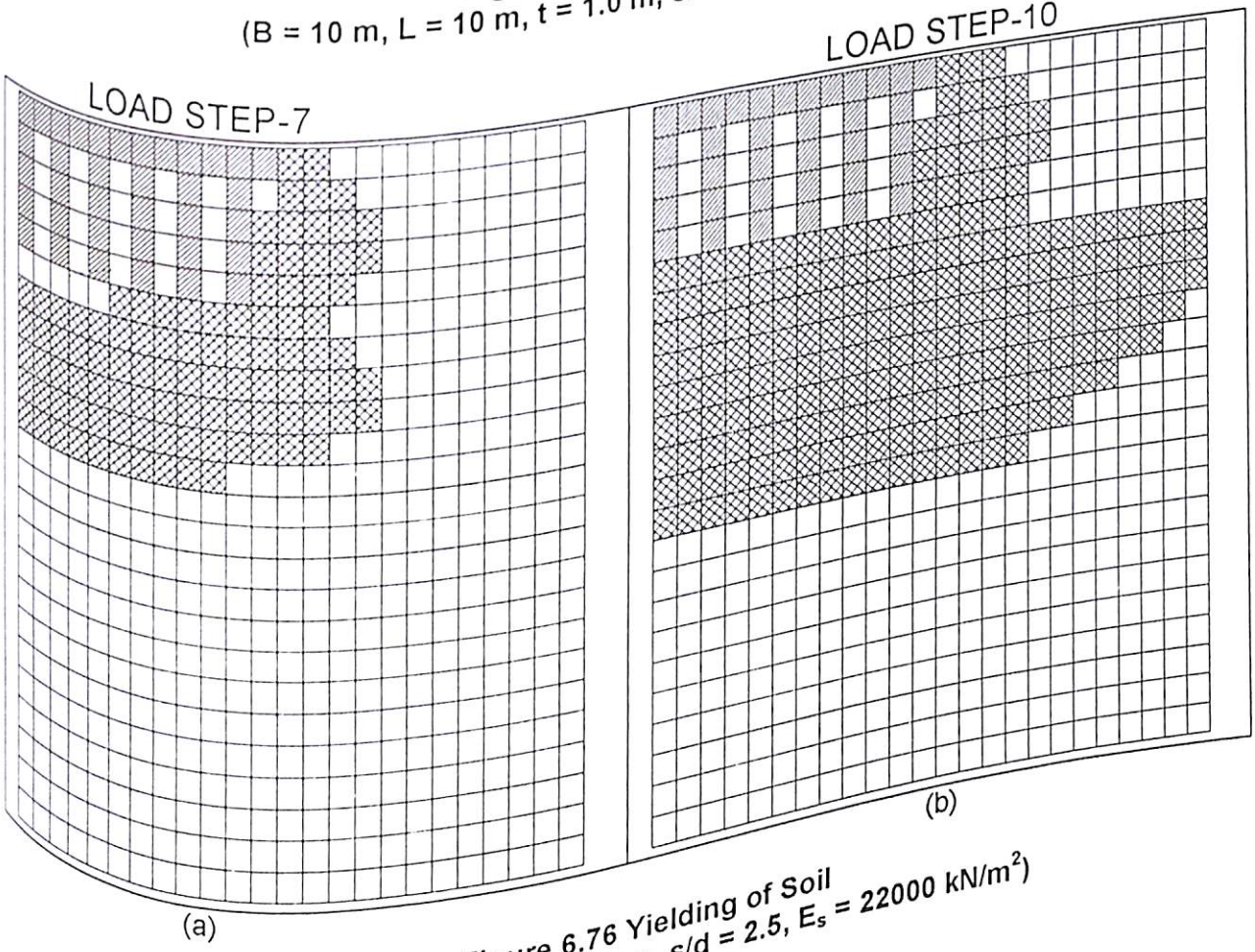

Figure 6.76 Yielding of Soil
(B = 10 m, L = 10 m, t = 1.0 m, s/d = 2.5, E_s = 22000 kN/m^2)

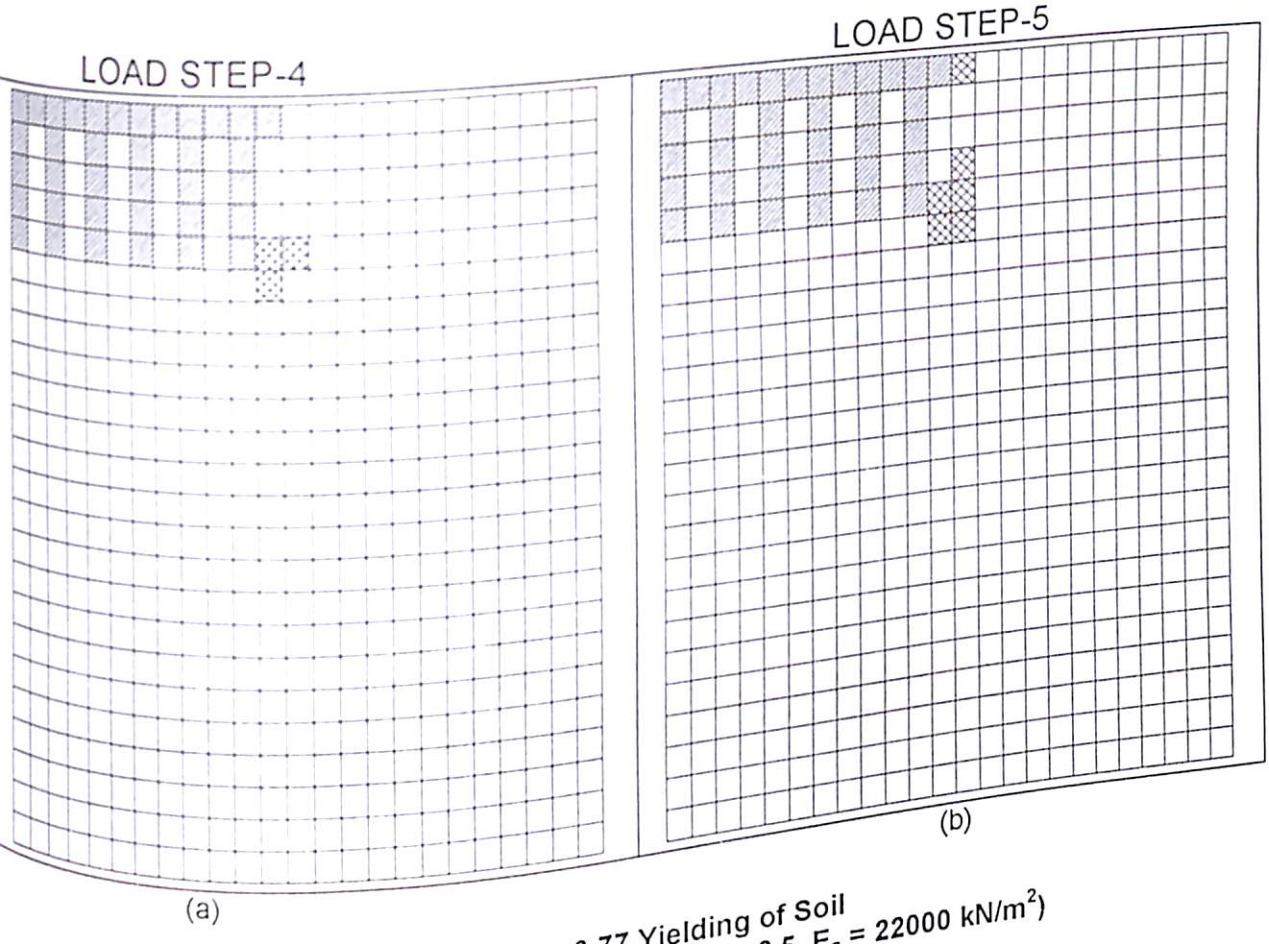

Figure 6.77 Yielding of Soil
(B = 10 m, L = 10 m, t = 4.0 m, s/d = 2.5, E_s = 22000 kN/m^2)

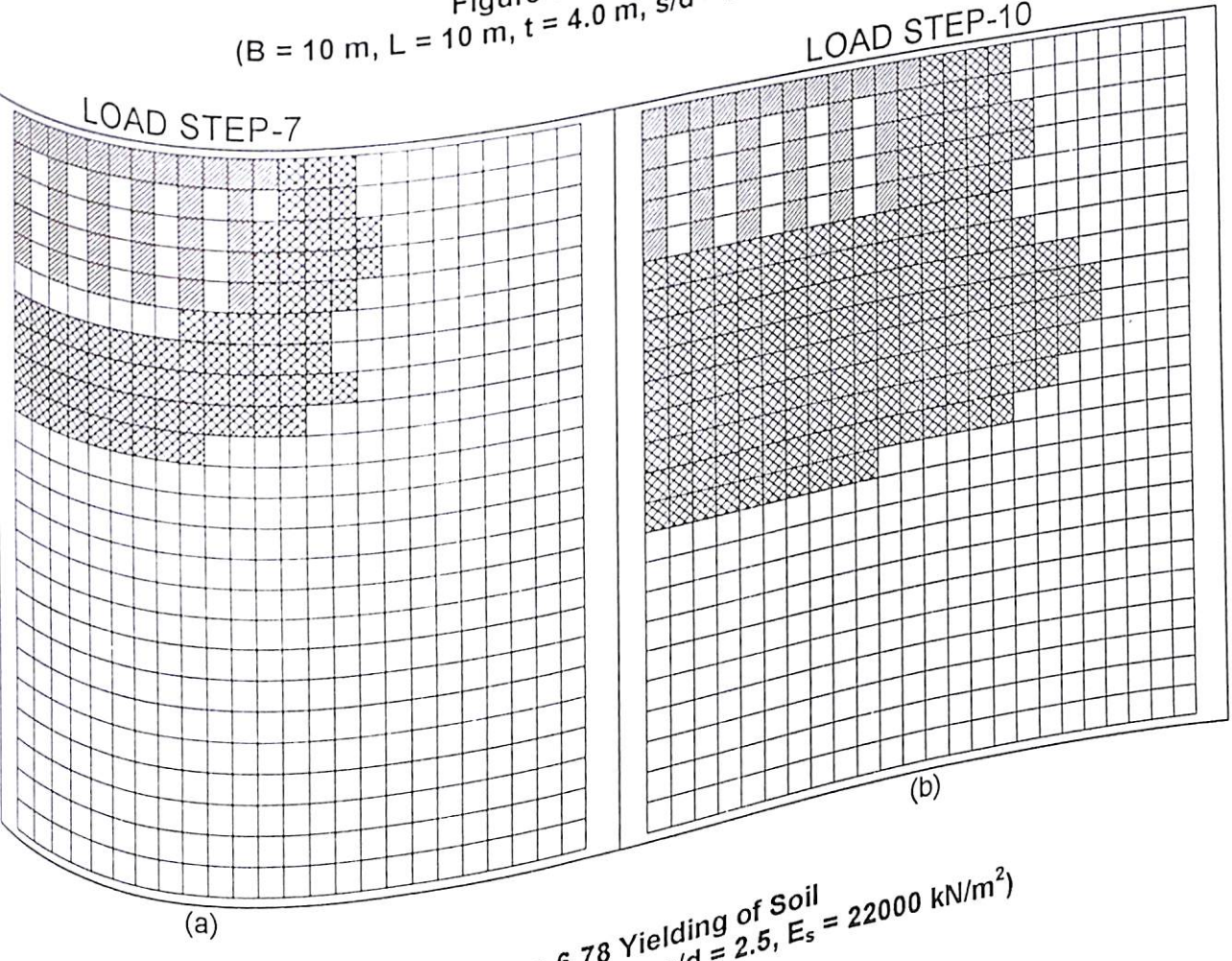

Figure 6.78 Yielding of Soil
L = 10 m, t = 4.0 m, s/d = 2.5, E_s = 22000 kN/m^2)

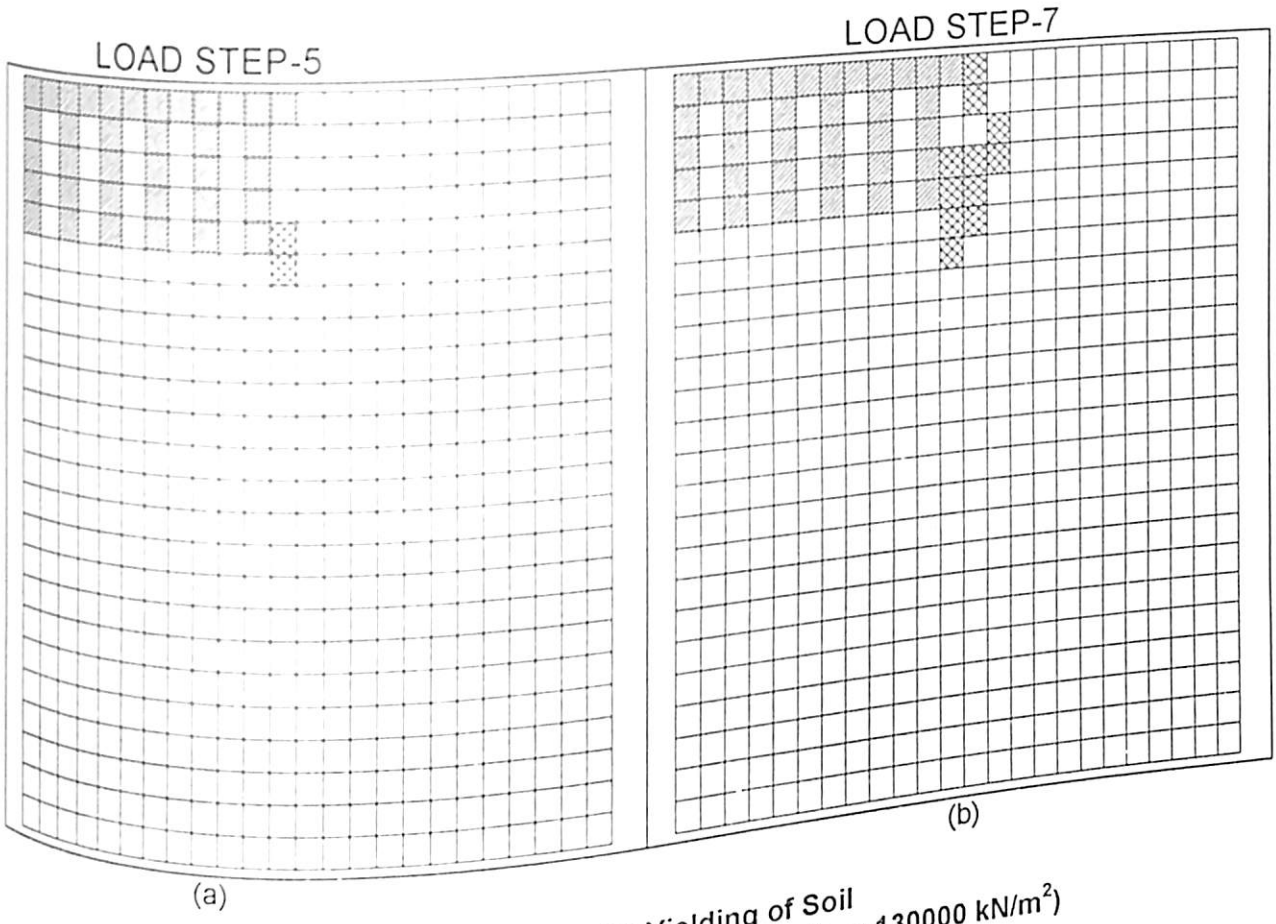

Figure 6.79 Yielding of Soil
(B = 10 m, L = 10 m, t = 0.1 m, s/d = 2.5, E_s = 130000 kN/m^2)

Figures 6.80 (a), (b) show the yielding of soil below the piled raft foundation for load step 10 and 15. In load step 10, complete yielding of soil elements below the pile tip is seen. Also the soil in between the piles is found yielded. This yielding of soil in between the piles is seen near the boundary piles. In load step 15, the soil elements in between the three rows of piles have been found to yield. Also this yielding is seen to spread upto the boundary considered.

Figures 6.81 (a), (b) shows the yielding of soil for a piled raft foundation of thickness 1.0 m, pile length of 10 metres, soil modulus of 130000 kN/m^2. In load step 5 yielding starts from the tip of the pile. In load step 7 the yielding is seen in more soil elements.

Figures 6.82 (a), (b) show the yielding of soil for load step 10 and load step 15. The yielding in soil is found to progress towards the center and below the pile tip and also in the lateral direction. Some of the soil elements in between the piles are also found to yield. In load step 15, complete yielding of soil is seen in between the boundary piles and also the soil elements below the pile is found to yield upto a larger depth. The yielding is also seen to reach upto the boundary considered in the analysis.

Figures 6.83 (a), (b) shows the yielding of soil for a piled raft foundation of pile length 30 metre, width of raft 10 metre, thickness of raft 0.1 metre and soil modulus of 22000 kN/m^2. In load step 5, the yielding of soil is seen below the pile tip. In load step 7 some more soil elements near the pile tip are found to yield.

Figures 6.84 (a), (b) show the yielding of soil for load step 10 and load step 15. The soil is found to yield near the boundary piles. The soil near the edge of the raft and also below the pile is found to yield. The soil element just below the pile has not been found to yield. In load step 15, almost all the soil elements are found to yield. Also the soil in between the boundary piles and near the boundary piles are found to yield.

Figure 6.85 shows the complete yielding of soil below the pile. The yielding of soil has spread over a larger area on the boundary piles. The yielding zone has reached upto the boundary considered in the analysis.

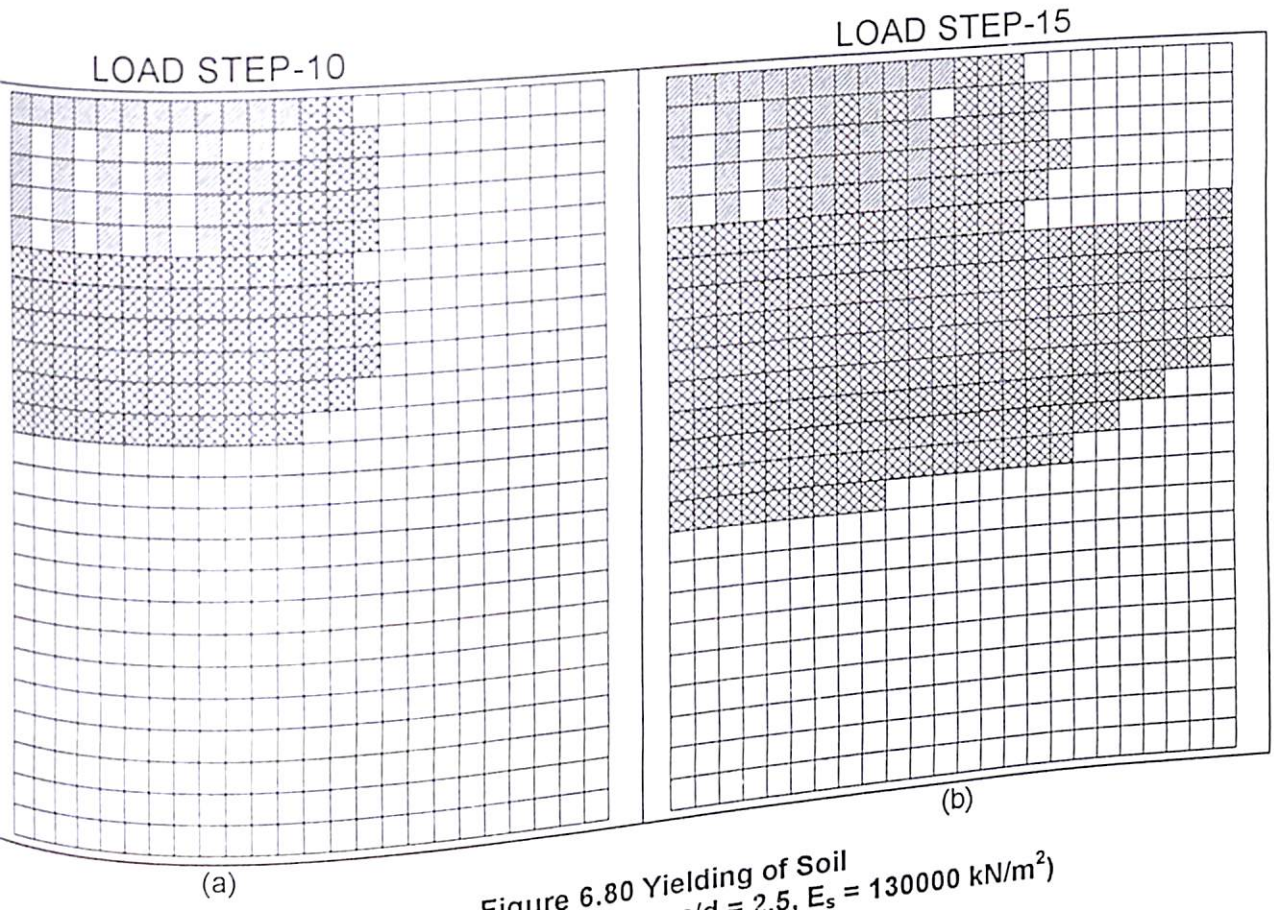

Figure 6.80 Yielding of Soil
(B = 10 m, L = 10 m, t = 0.1 m, s/d = 2.5, E_s = 130000 kN/m^2)

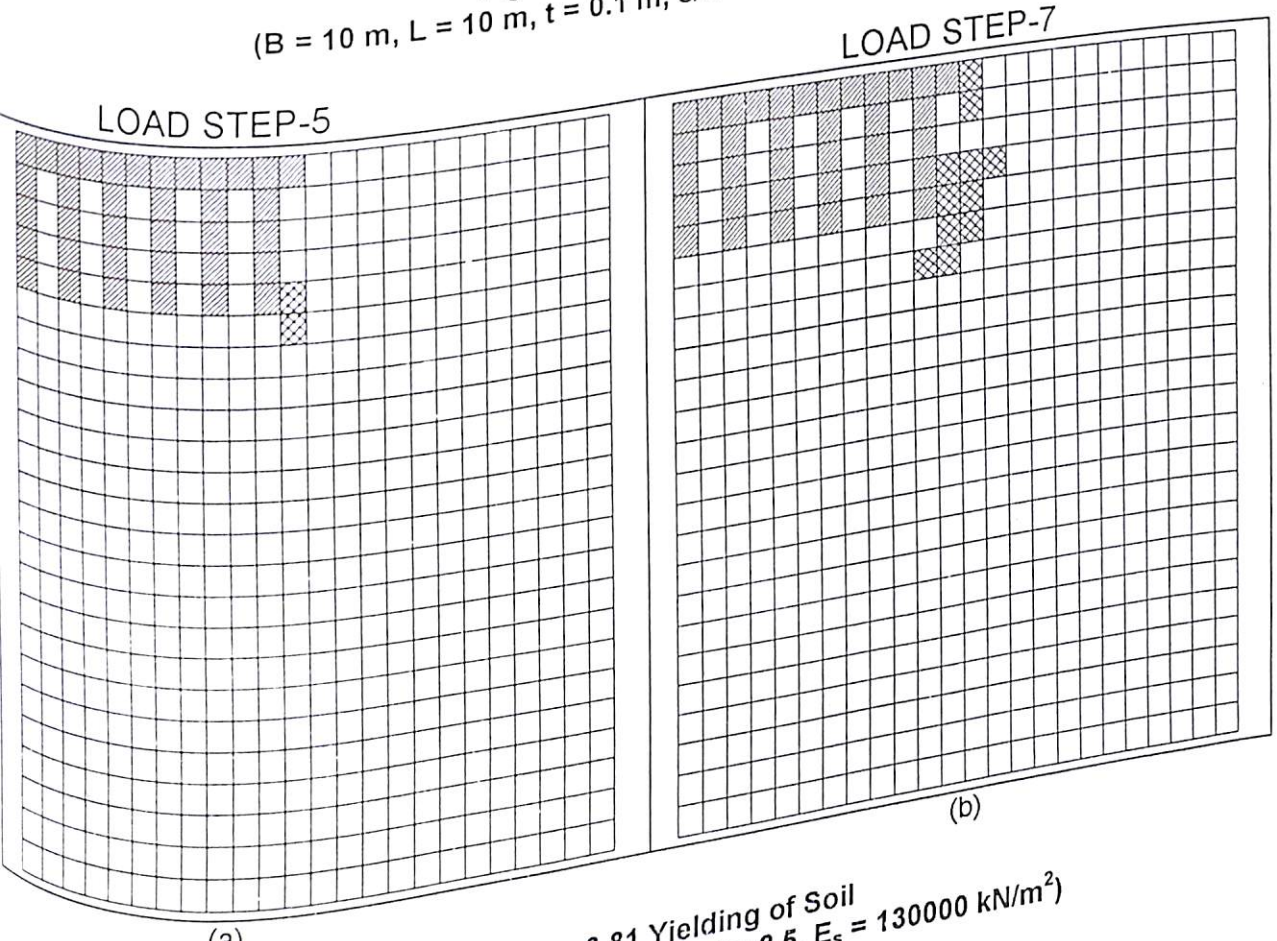

Figure 6.81 Yielding of Soil
(B = 10 m, L = 10 m, t = 0.1 m, s/d = 2.5, E_s = 130000 kN/m^2)

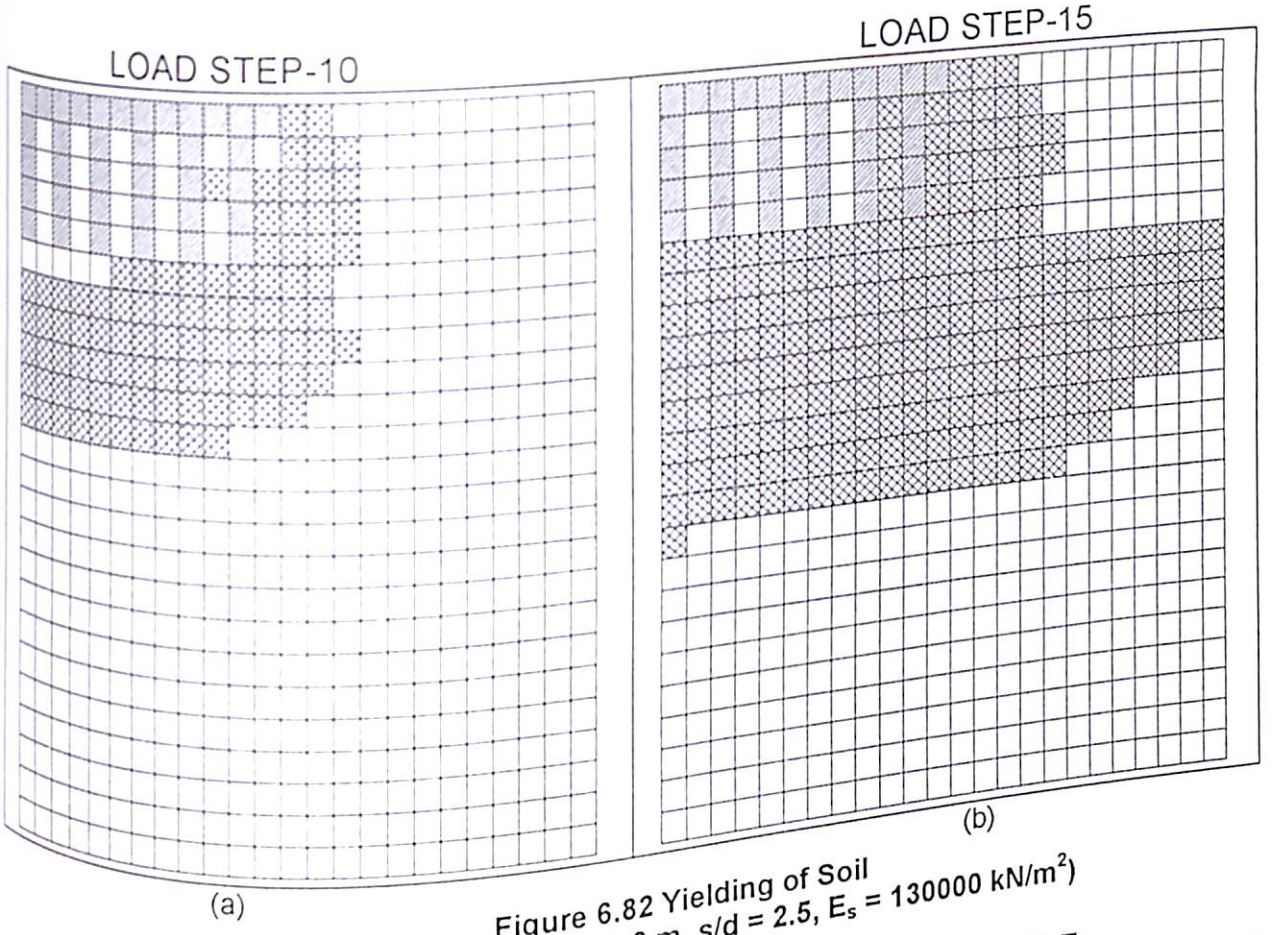

Figure 6.82 Yielding of Soil
(B = 10 m, L = 10 m, t = 1.0 m, s/d = 2.5, E_s = 130000 kN/m^2)

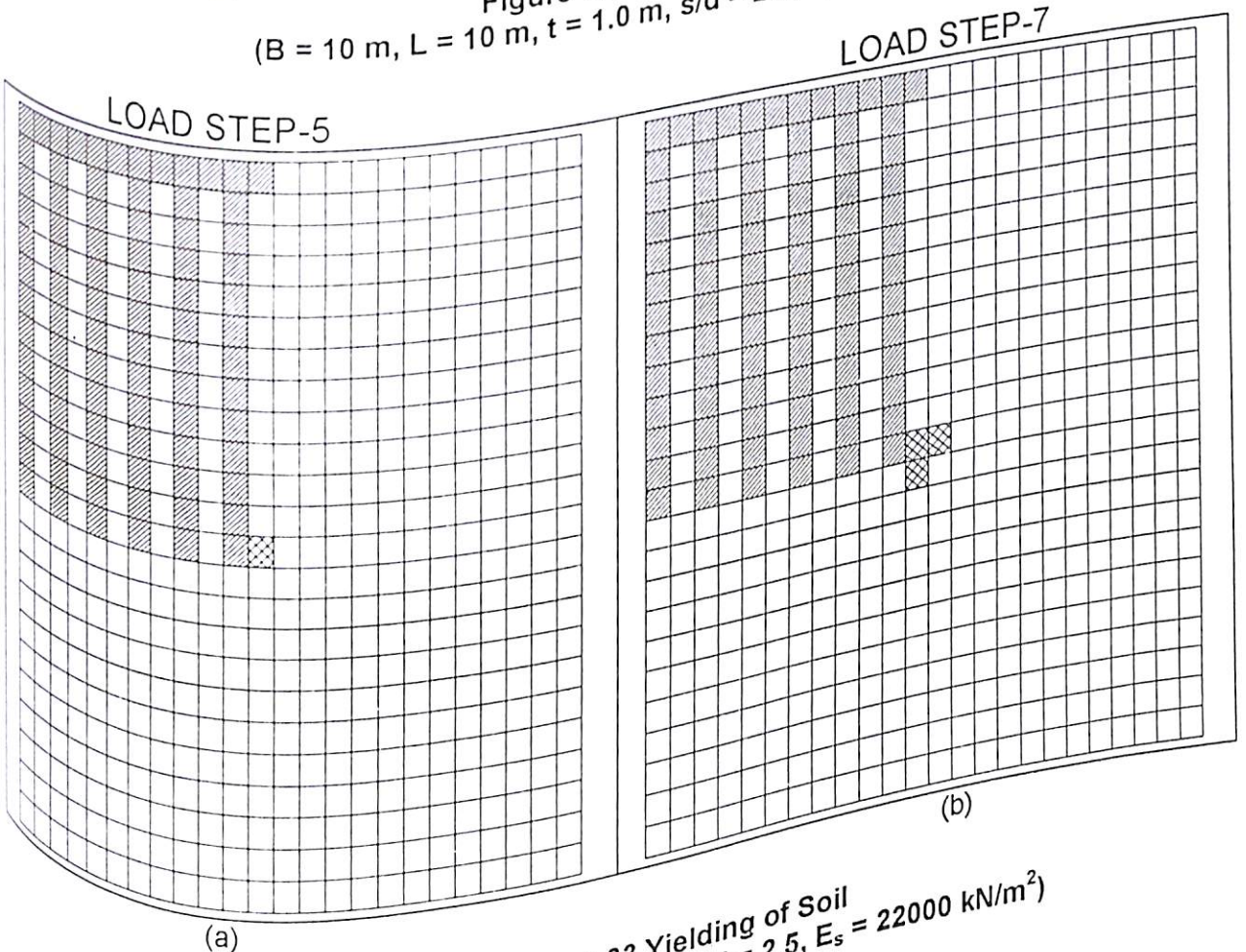

Figure 6.83 Yielding of Soil
(B = 10 m, L = 30 m, t = 1.0 m, s/d = 2.5, E_s = 22000 kN/m^2)

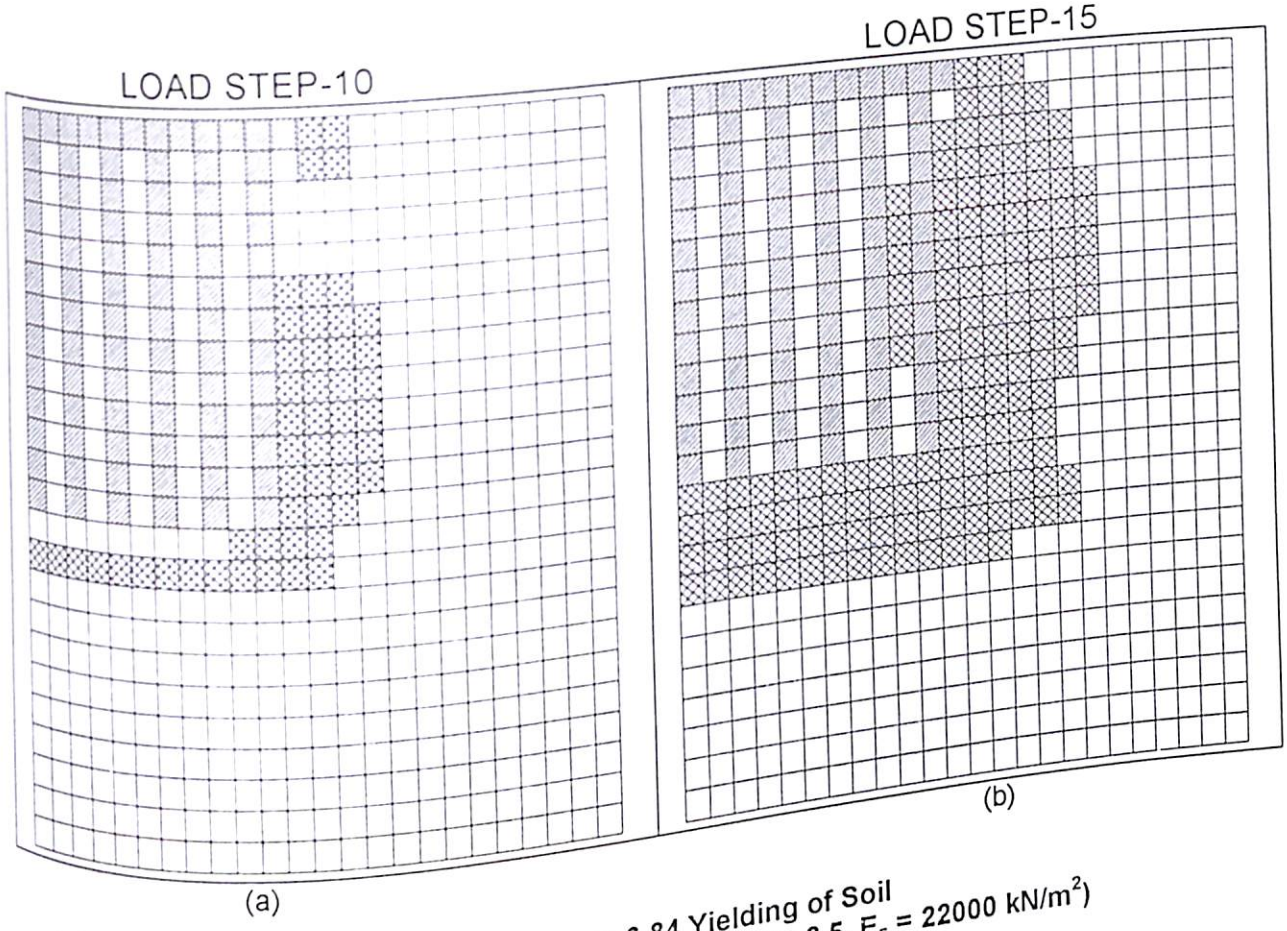

Figure 6.84 Yielding of Soil
(B = 10 m, L = 30 m, t = 1.0 m, s/d = 2.5, E_s = 22000 kN/m^2)

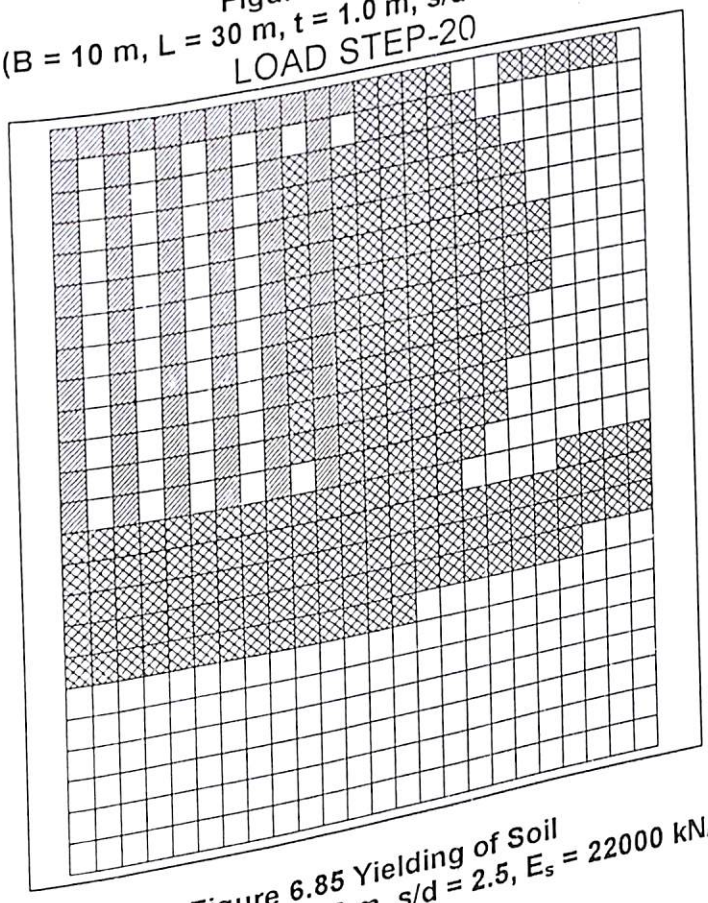

Figure 6.85 Yielding of Soil
(B = 10 m, L = 30 m, t = 1.0 m, s/d = 2.5, E_s = 22000 kN/m^2)

The soils in between the piles have also been found to yield.

Figures 6.86 (a), (b) show the yielding of the soil for a piled raft foundation of width 10 metre, length of pile 30 metre, spacing to one side ratio of pile 2.5, soil modulus of 22000 kN/m^2 and raft thickness of 4.0 metre. The yielding of soil is seen near the tip of pile (load step 6). The yielding is seen in more soil elements near the tip of the boundary piles (load step-8).

Figures 6.87 (a), (b) show the development of soil yielding for load step 10 and 15. In load step 10, more soil elements with respect to load step-8 are seen to yield near the tip of the boundary piles. In load step 15 the yielding is upto a larger area both in lateral and downward direction.

Figures 6.88 (a), (b) show the development of yield stress for a piled raft foundation for a spacing to one side ratio of 7.5, length of pile 10 metre, soil modulus 22000 kN/m^2 and raft thickness 0.1 metre. In load step 3, yielding is seen in soil element near the raft edge. In load step 5, the yielding is there in soil elements below the piles and also surrounding the pile. The yield surface is seen to form a pressure bulb.

Figures 6.89 (a), (b) show the development of yielding for load step 8 and 10. In load step 8, the soil element is seen to a larger area below the pile and surrounding the pile. Also the soil elements in between the piles are found to yield.

In load step 10 a very large area has been found to yield below and surrounding the pile. At the lower portion of pile and below it, in the lateral direction, the soil is found to yield upto the lateral boundary considered in the analysis.

Figures 6.90 (a), (b) shows the yielding of soil for a piled raft foundation of raft width 10 metre, spacing to diameter ratio of 7.5, pile length 10 metre, soil modulus 130000 kN/m^2 and raft thickness of 1.0 metre. As seen in above cases, the yielding of soil is near the edge of the raft in load step 4 while in load step 7, yielding is seen below the pile and surrounding the pile. The soil elements yielded can be seen in this Figure.

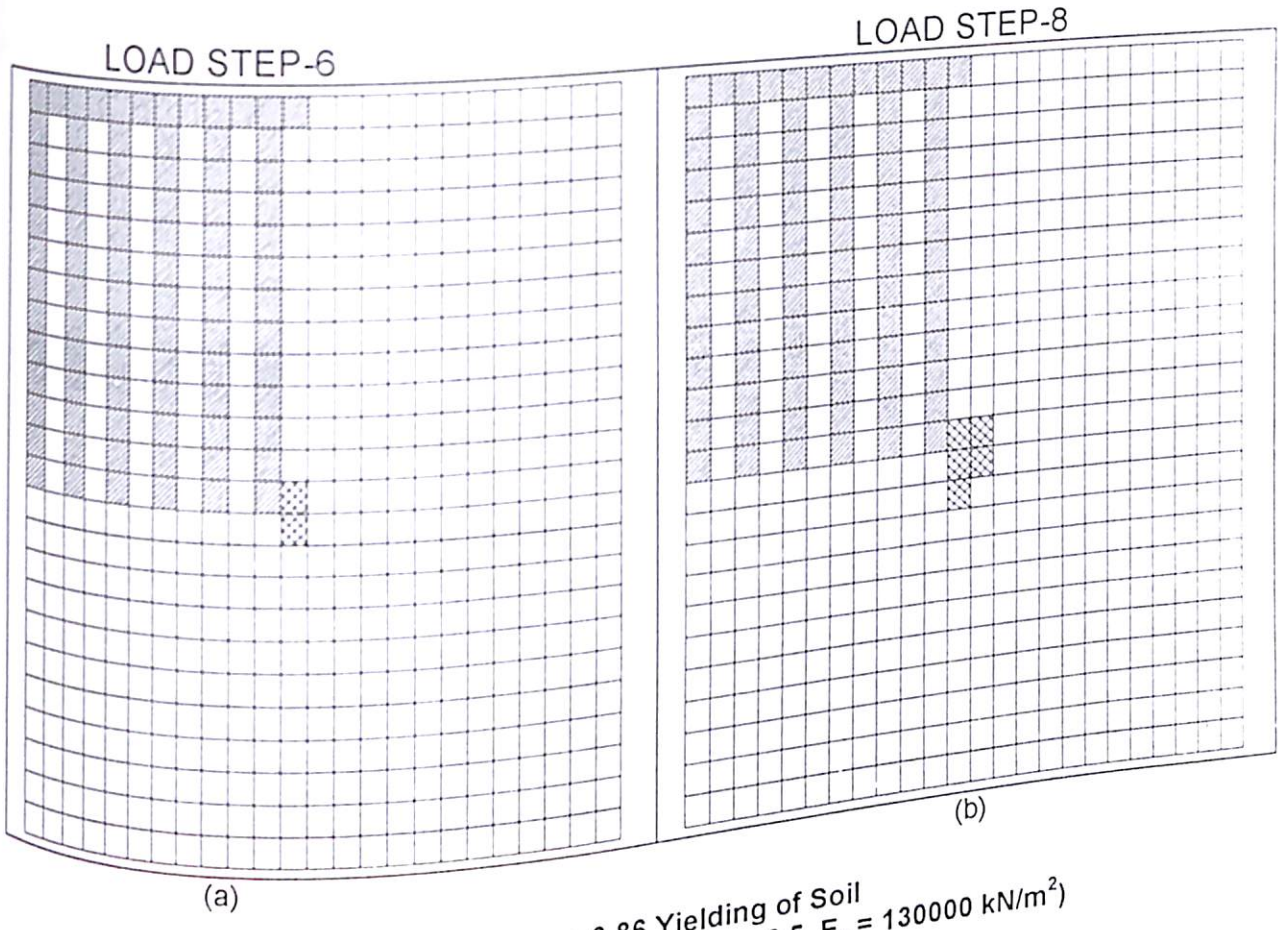

Figure 6.86 Yielding of Soil
(B = 10 m, L = 30 m, t = 4.0 m, s/d = 2.5, E_s = 130000 kN/m^2)

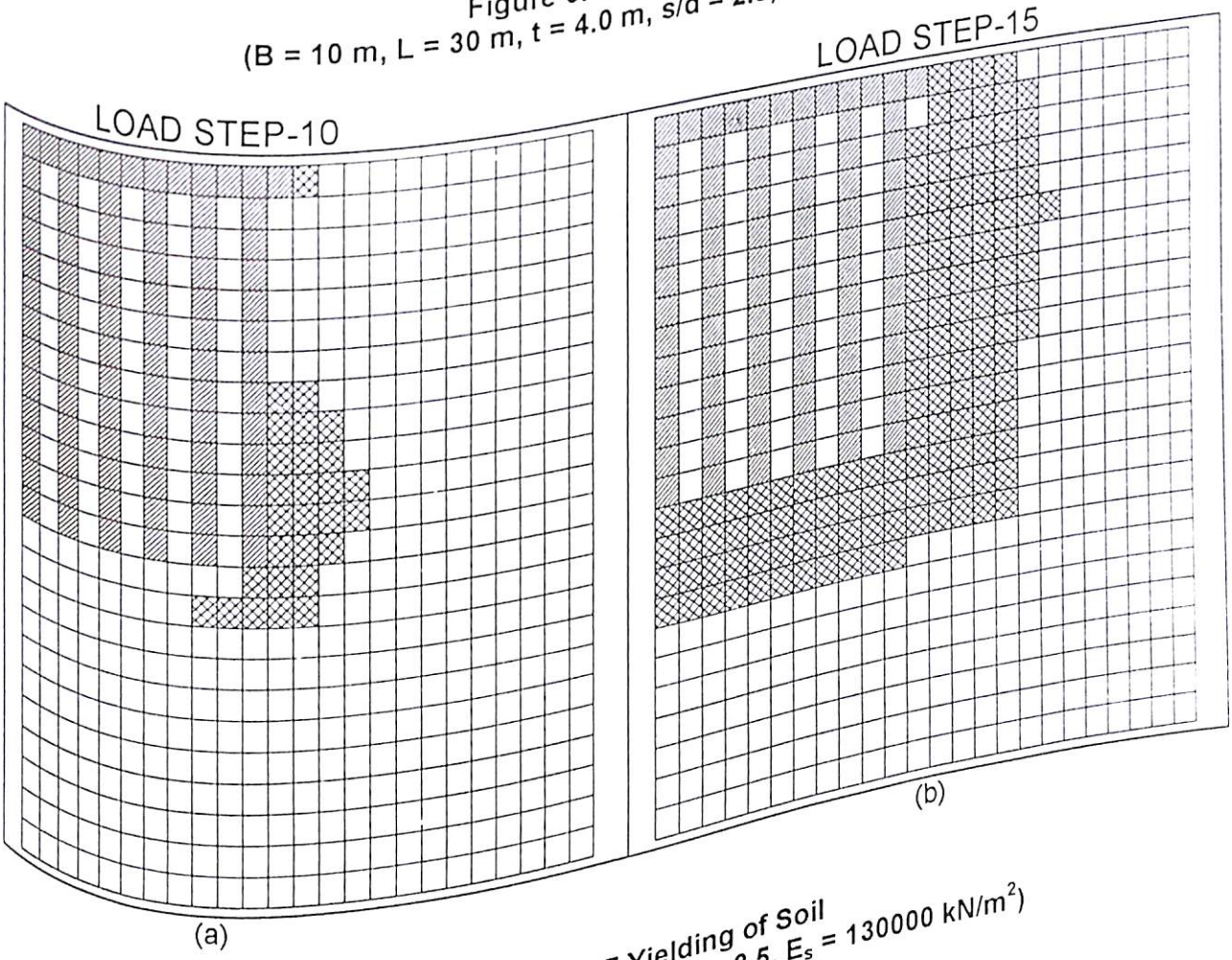

Figure 6.87 Yielding of Soil
(B = 10 m, L = 30 m, t = 4.0 m, s/d = 2.5, E_s = 130000 kN/m^2)

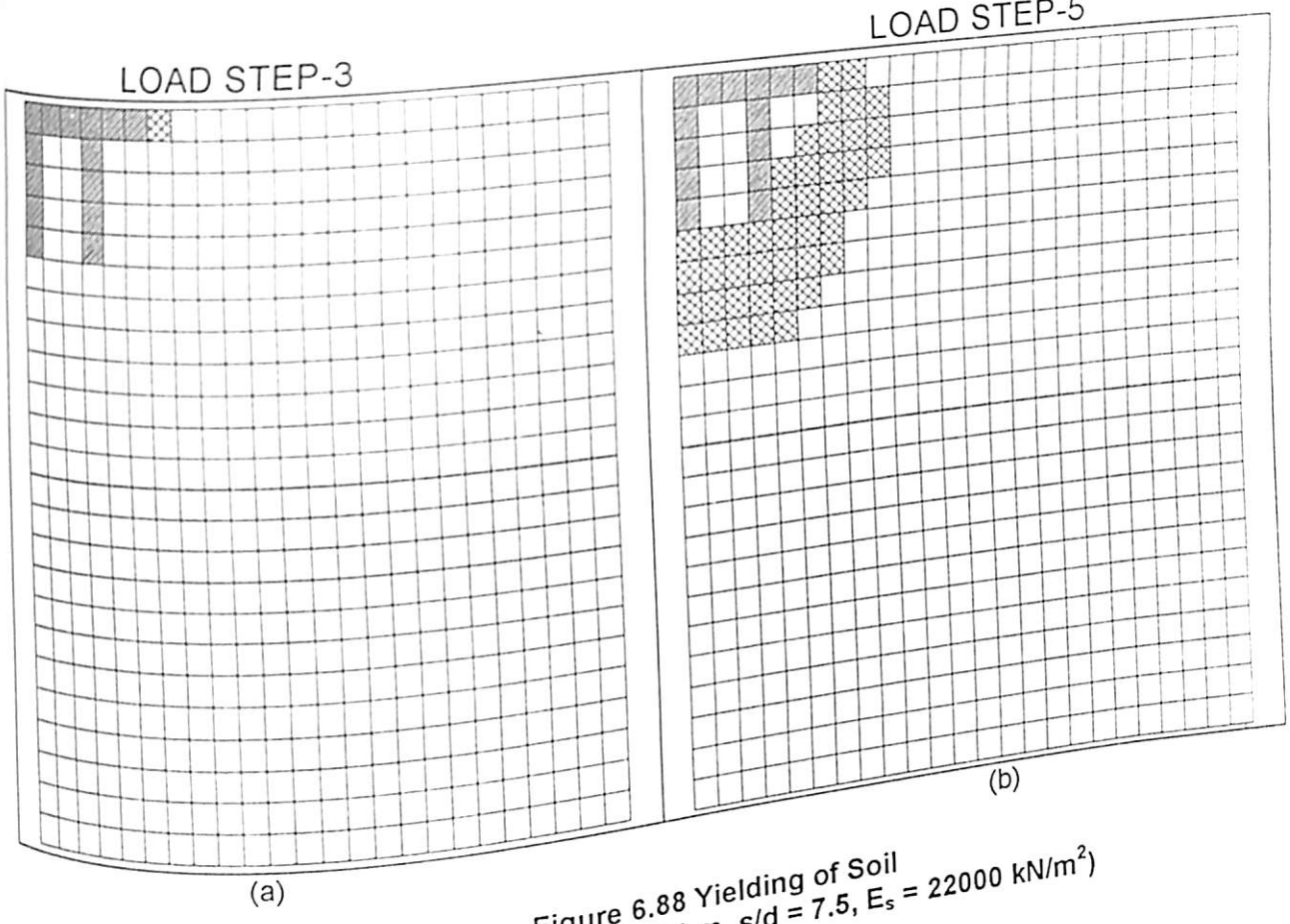

Figure 6.88 Yielding of Soil
(B = 10 m, L = 10 m, t = 0.1 m, s/d = 7.5, E_s = 22000 kN/m^2)

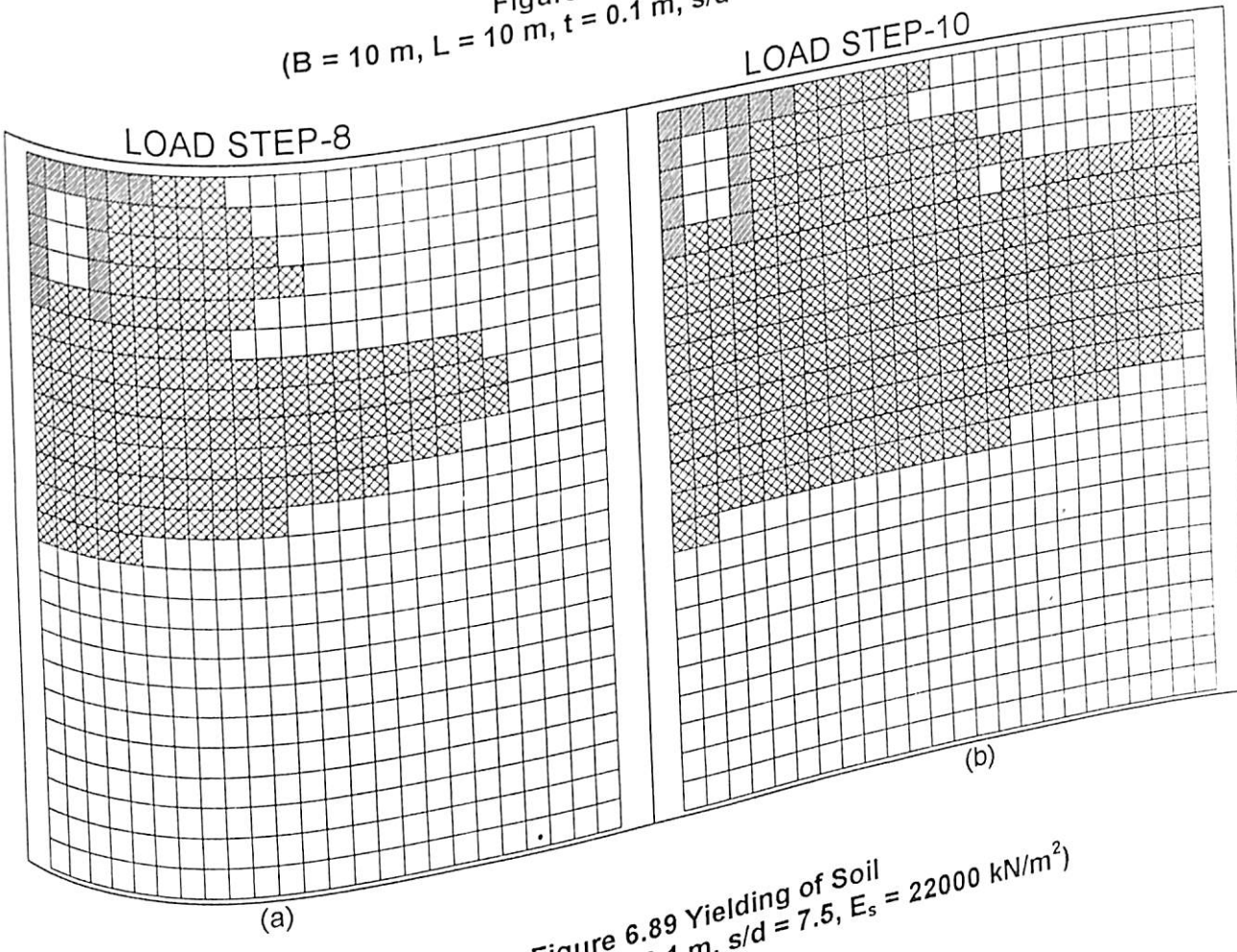

Figure 6.89 Yielding of Soil
(B = 10 m, L = 10 m, t = 0.1 m, s/d = 7.5, E_s = 22000 kN/m^2)

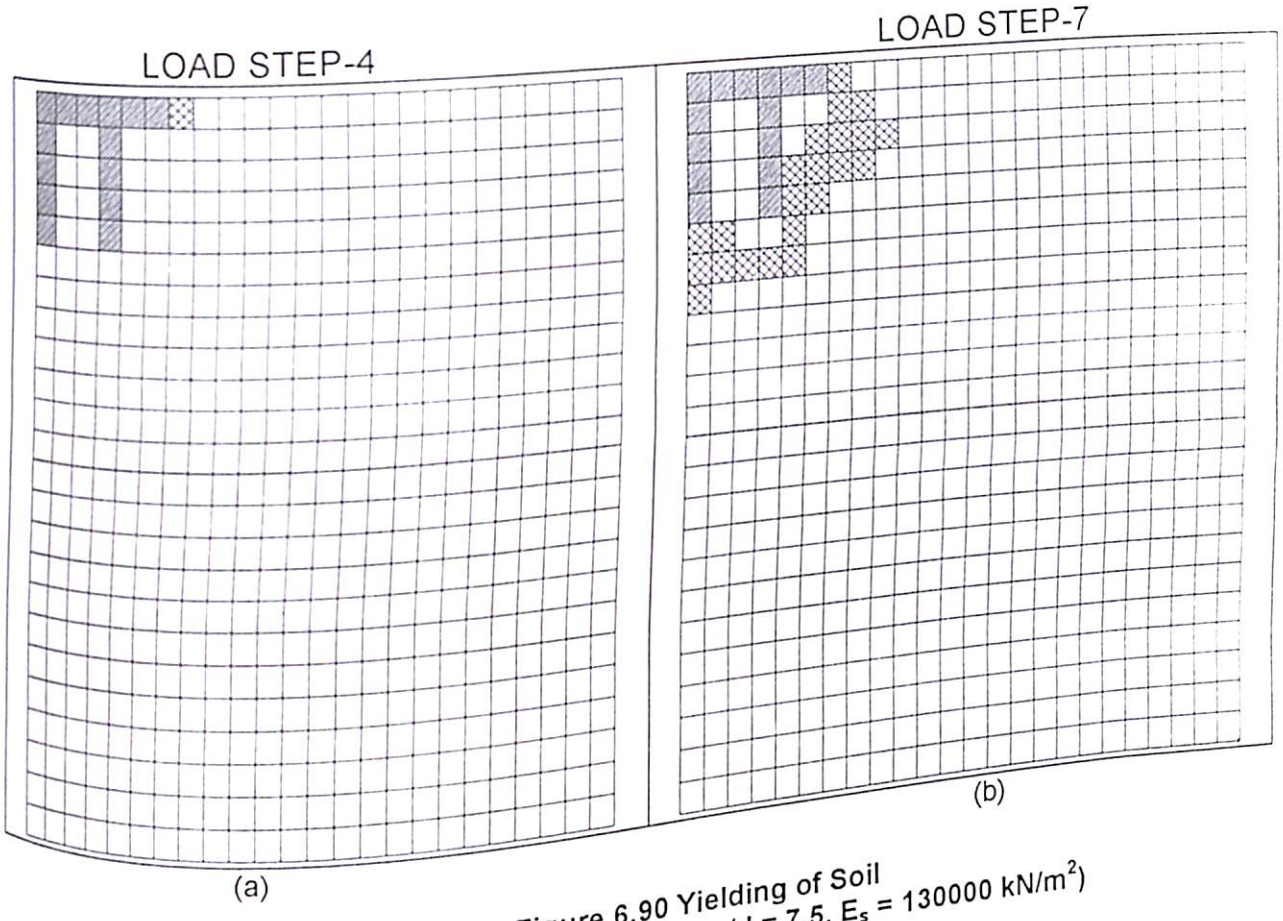

Figure 6.90 Yielding of Soil
($B = 10$ m, $L = 10$ m, $t = 1.0$ m, $s/d = 7.5$, $E_s = 130000$ kN/m^2)

Figures 6.91 (a), (b) show the yielding of soil for load step 10 and 15. In load step 10, the yielding has spread below the pile and surrounding the pile. The yielding is also seen in between the pile that reached upto the bottom of the raft. In load step 15, the yielding of soil is seen upto larger area. Near the lower portion of the pile, the yielding is seen upto the boundary considered in the analysis.

Figures 6.92 (a), (b) show the yielding of the soil for a piled raft foundation of raft width 10 metre, spacing to diameter 7.5, pile length 30 metre , soil modulus of 22000 kN/m^2 and raft thickness 1.0 metre. In load step 4 yielding is seen near the edge of the raft while in load step 6 yielding is seen near the edge of the raft and below the tip of the pile.

Figures 6.93 (a), (b) show the yielding of soil for load step 9 and 12. In load step 9, yielding is seen below the pile tips and also surrounding the pile. The maximum soil elements are seen to yield in the middle depth of the pile all around it. In load step 12, yielding is seen to in between the piles, which is upto half-length of pile. The soil surrounding the pile and also below the pile is found to yield.

Figure 6.94 shows the yielding of soil for load step 20. The yielding of soil is seen in large percentage of elements except few, which are below the bottom of the raft and in the extreme right top corner. The elements below the raft, which has not yielded shows, that in long piles the soil elements below the raft moves along with the pile showing zero frictional resistance offered by the pile.

Figures 6.95 (a), (b) show the yielding of soil for a piled raft foundation for a spacing to diameter ratio of 7.5, length of pile 30 metre, raft thickness of 1.0 metre and the soil modulus of 130000 kN/m^2. In load step 5 and soil elements near the edge of the raft are found to yield.

Figures 6.96 (a), (b) show the yielding of soil elements for load steps 12 and 16. In load step 12 the soil elements surrounding the pile in the top portion is found to yield. In load step 16 elements below the pile tip and also surrounding the pile are found to

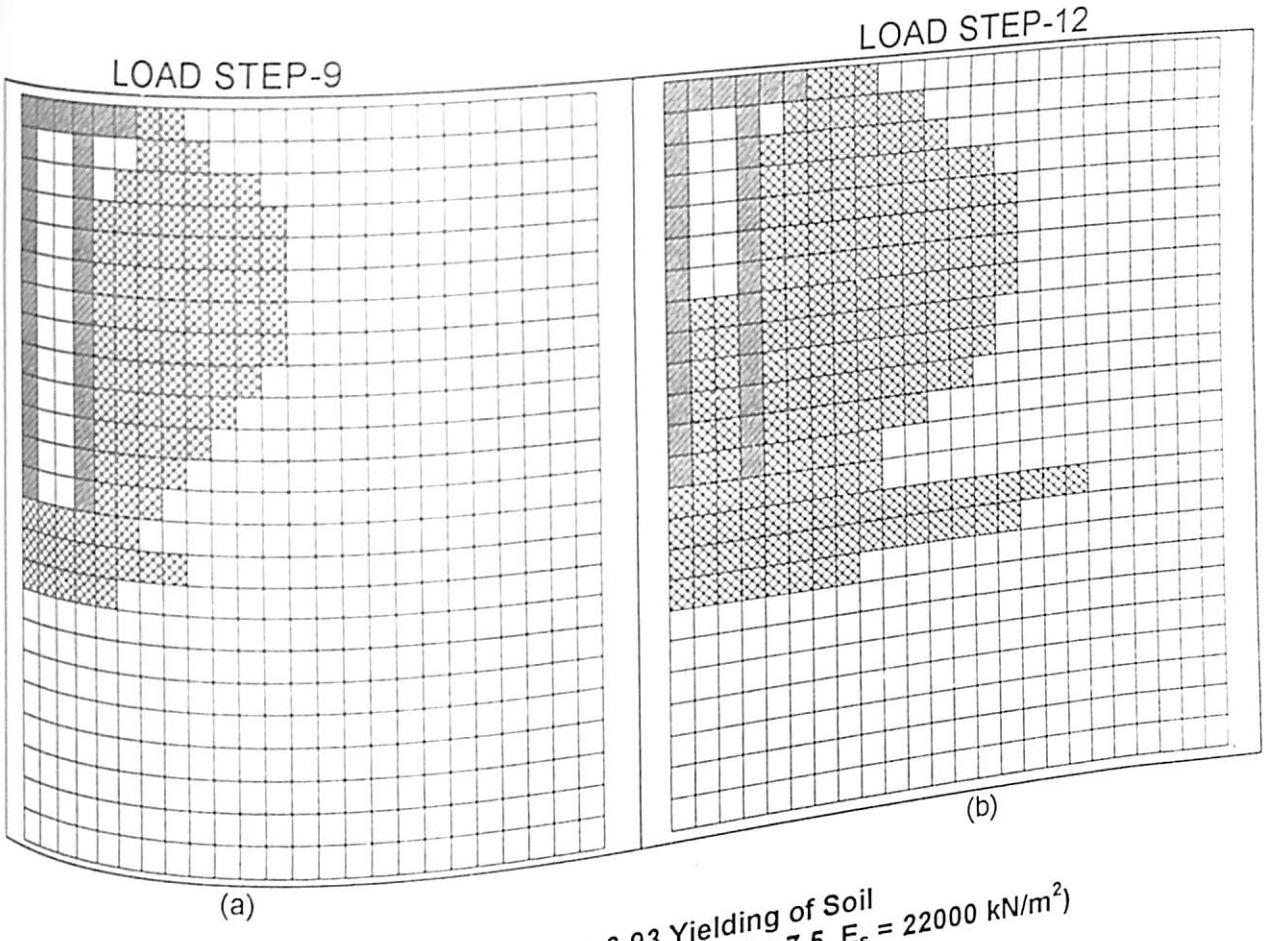

Figure 6.93 Yielding of Soil
(B = 10 m, L = 30 m, t = 1.0 m, s/d = 7.5, E_s = 22000 kN/m^2)

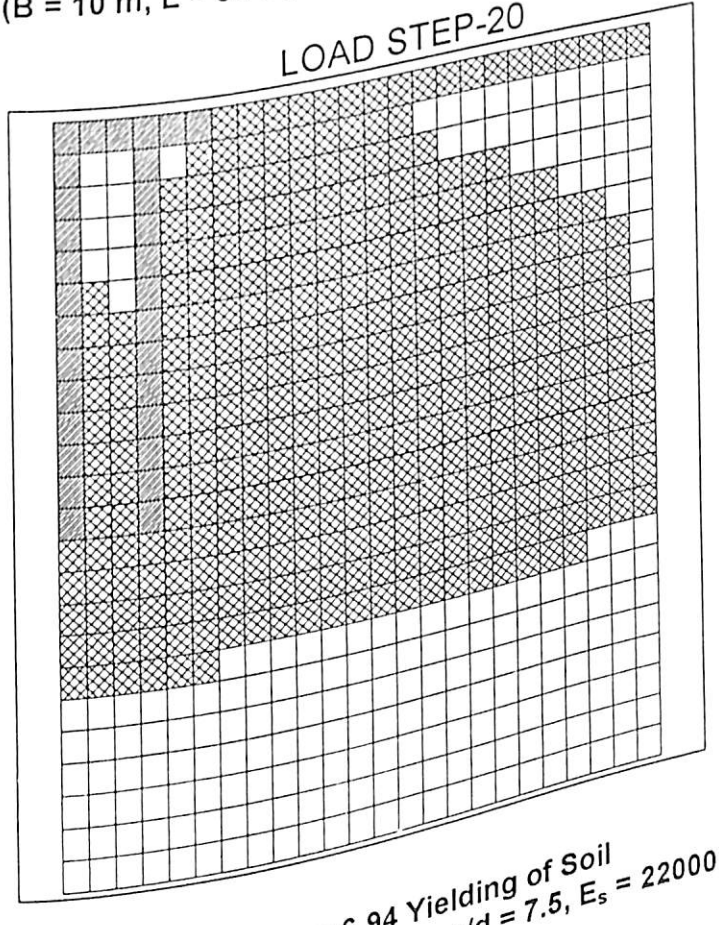

Figure 6.94 Yielding of Soil
(B = 10 m, L = 30 m, t = 1.0 m, s/d = 7.5, E_s = 22000 kN/m^2)

yield. Also the soil elements in between the piles are found to yield.

Figure 6.97 shows the yielding of the soil for load step 20. The soil elements in between the piles have yielded upto the larger length of the pile. The soil elements surrounding the pile have yielded upto a larger area.

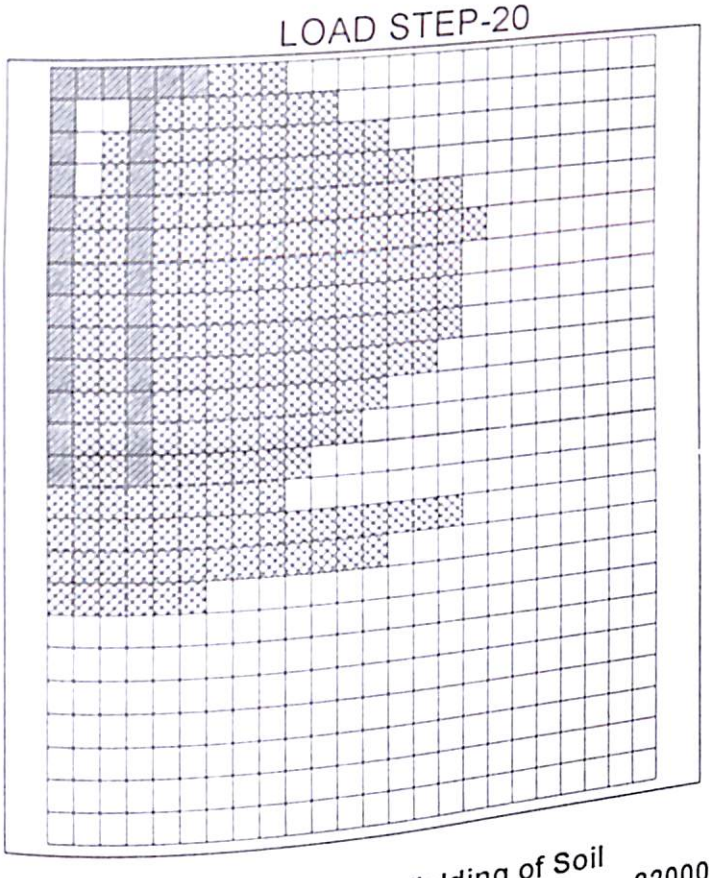

Figure 6.97 Yielding of Soil
(B = 10 m, L = 30 m, t = 1.0 m, s/d = 7.5, E_s = 22000 kN/m^2)

CHAPTER 7

APPLICATION OF LOAD SETTLEMENT CURVE

7.1 INTRODUCTION

In order to design a foundation, the load and settlement are the two important factors. For a known dimension of a foundation, allowable load can only be applied on the foundation. Also the settlement corresponding to the applied load should not exceed the permissible value. On the other hand if the allowable load or the permissible settlement is known, the dimension of the foundation can be designed for known soil properties. The foundation can be of shallow or deep or the combination of the two. Here a combination of the two types of foundations, which is an axisymmetric piled raft foundation as well as piled raft foundation under plane strain condition, have been considered. The spacing between piles is an important factor, which must be considered while designing a piled raft foundation. The permissible settlement considered is 125 mm, which is for multistoreyed building as per IS: 1904 - 1986.

7.2 EXAMPLES

7.2.1 Axisymmetric Piled Raft Foundation

7.2.1.1 Example-1

An axisymmetric piled raft foundation of raft diameter 10 metre is to be designed in a soil mass of modulus 22000 kN/m^2 and poisson's ratio 0.45 for a uniformly distributed load of 500 kN/m^2. The piles below the raft is to be placed at a spacing equal to 5 times the diameter of the pile. Suggest the length of the pile such that the settlement does not exceed the permissible value. Consider diameter of pile of 0.40 meter.

Solution:

Modulus of soil (E_s)=22000 kN/m^2

Poisson's ratio of soil (μ) =(0.45)

Uniformly distributed load on raft (udl)=500 kN/m^2

Diameter of raft (D)=10 meter

Spacing to diameter ratio of pile (s/d)=5

Diameter of pile =0.40 meter

The area of raft (a) = $\pi D^2/4$ = 78.539 m^2 [After putting the value of D in the equation]

Hence the load on the raft = a x udl

= 78.539 x 500 kN= 39269.908 kN

For the load applied on the raft of 39269.908, Diameter of raft (D)=10 meter and soil modulus (E_s) of 22000 kN/m^2, the settlement for different length of pile obtained from Figure 7.1 is given below.

Table 7.1 Settlement for different length of Pile
(D =10 m, s/d =5, E_s = 22000 kN/m^2)

Length of Pile	Settlement
0 m	329.52
10 m	153.40
20 m	102.28
30 m	68.20

For multistoreyed structures the permissible settlement is 125 mm. From the results obtained it is found that raft without pile and the raft with pile of length 10 meters undergoes more settlement than the permissible value. Hence pile of length 20 meter and 30 meters are suitable here. To be more specific one should go for 20-meter length of pile as the 30-meter length of pile is going to increase the cost of pile.

7.2.1.2 Example-2

A foundation is to be designed in a soil mass of modulus 76000 kN/m^2 and poisson's ratio 0.45 for a uniformly distributed load of 500 kN/m^2. The option is that the designer can go for

a raft or piled raft foundation under axisymmetric condition such that the raft diameter is 10 meter. The piles below the raft is to be placed at a spacing equal to 5 times the diameter of the pile. Suggest whether one should go for raft or a piled raft foundation. Consider diameter of pile of 0.40 meter.

Solution:

Modulus of soil (E_s)=76000 kN/m^2

Poisson's ratio of soil (μ) =(0.45)

Uniformly distributed load on raft (udl)=500 kN/m^2

Diameter of raft (D)=10 meter

Spacing to diameter ratio of pile (s/d)=5

Diameter of pile =0.40 meter

The area of raft (a) = $\pi D^2/4$ = 78.539 m^2 [After putting the value of D in the equation]

Hence the load on the raft = a x udl

= 78.539 x 500 kN= 39269.908 kN

For the load applied on the raft of 39269.908, Diameter of raft (D)=10 meter and soil modulus (E_s) of 76000 kN/m^2, the settlement for different length of pile obtained from Figure 7.2 is given below.

Table 7.2 Settlement for different length of Pile (D =10 m, s/d =5, E_s = 76000 kN/m^2)

Length of Pile	Settlement
0 m	88.90
10 m	38.88
20 m	29.17
30 m	25.00

For multistoreyed structures the permissible settlement is 125 mm. From the results obtained it is found that in all the cases the settlement obtained is less than the permissible value. Even raft undergoes settlement less than the permissible value. Hence even raft foundation is suitable for this soil.

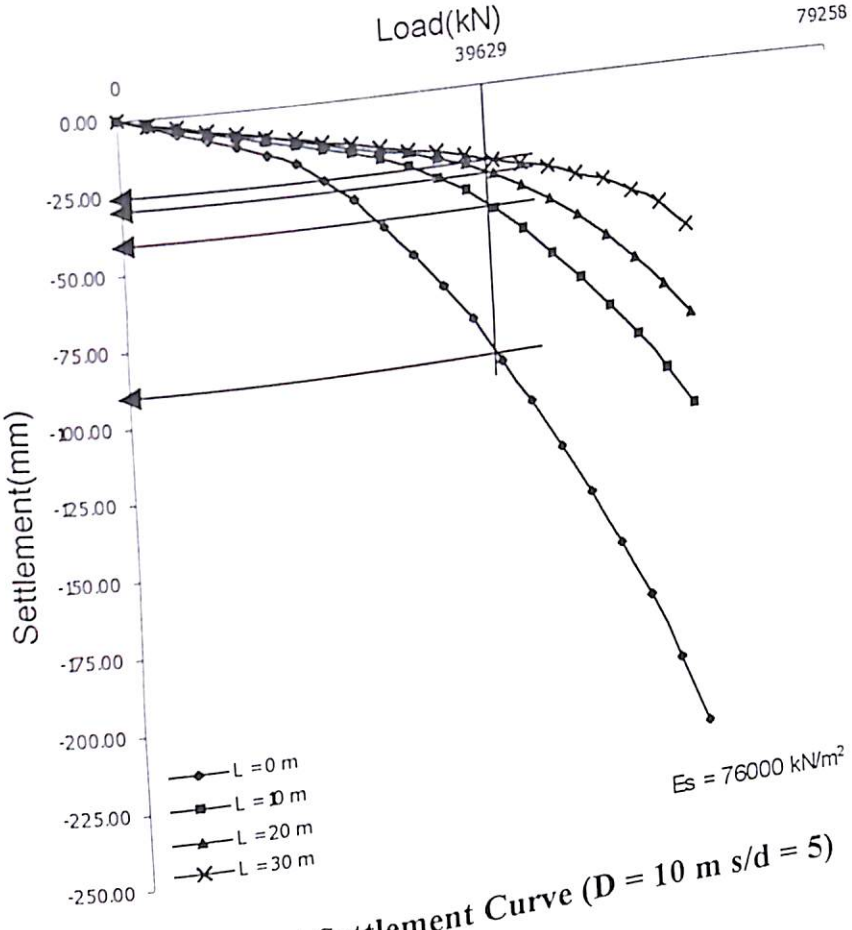

Figure 7.2 Load Settlement Curve (D = 10 m s/d = 5)

7.2.1.3 Example-3

Find the load that a piled raft foundation can take for the permissible settlement of 125 mm if the proposed diameter of raft is 10m and the possible length of piles are 10m, 20m and 30 m. The possible two construction sites are having soil with modulus 22000 kN/m^2 and 76000 kN/m^2.

Solution:

Permissible settlement= 125 mm

Diameter of raft (D)=10 m

Elastic modulus of soil (E_s)=22000, 76000 kN/m^2.

The lengths of piles (L) = 10, 20 and 30 m.

For the data given above, the load carried by the piled raft foundation can be obtained from Figure 7.3. The values obtained have been tabulated below.

Table 7.3 Permissible Loads Obtained for Different Length of Pile and the Soil Modulus (D = 10 m s/d = 5)

Length of Pile (m)	Load Carried by Piled Raft Foundation (kN)	
	E_s=22000 kN/m^2	E_s=76000 kN/m^2
0	23200	46428.61
10	35600	-
20	42800	-
30	53200	-

The table above provides the load carried by piled raft foundation for different length of pile and the soil modulus for the permissible settlement of 125 mm. The designers are suggested to select the best option depending upon the site condition and the total load coming from the superstructure. If the load coming from the superstructure is less, the first option can be selected which is nothing but the raft foundation. If the load coming from the superstructure is more the second or third or fourth option can be selected depending upon the load. The table makes clear that if site condition is good, the same options as discussed above is going

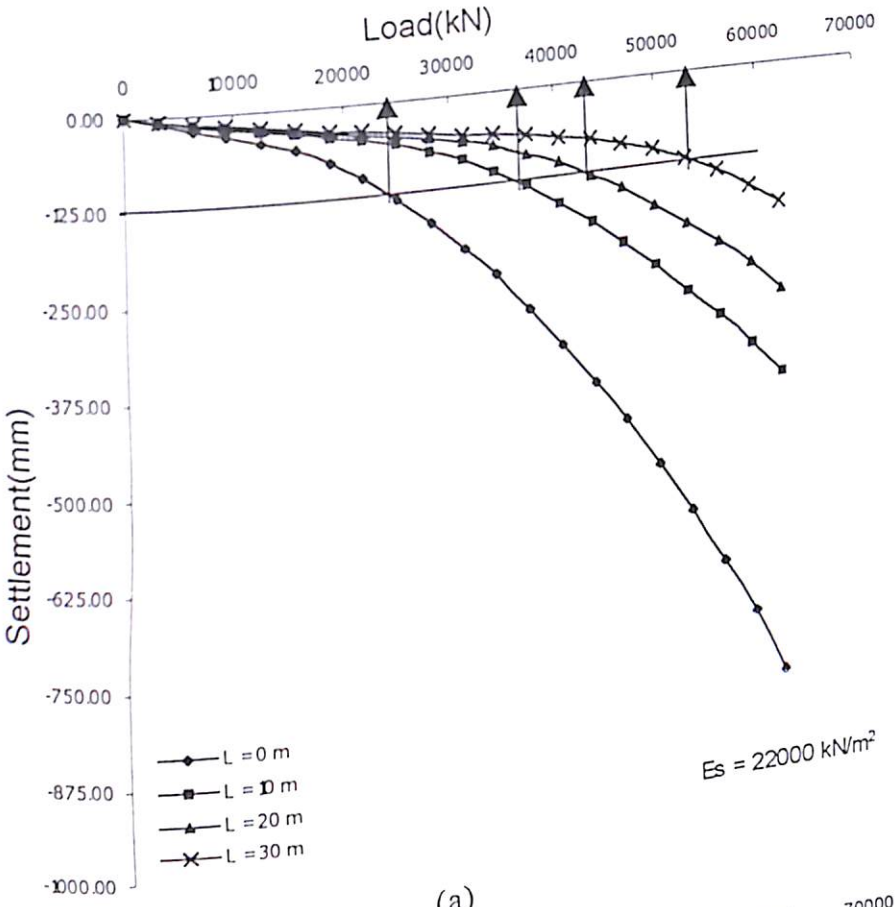

(a)

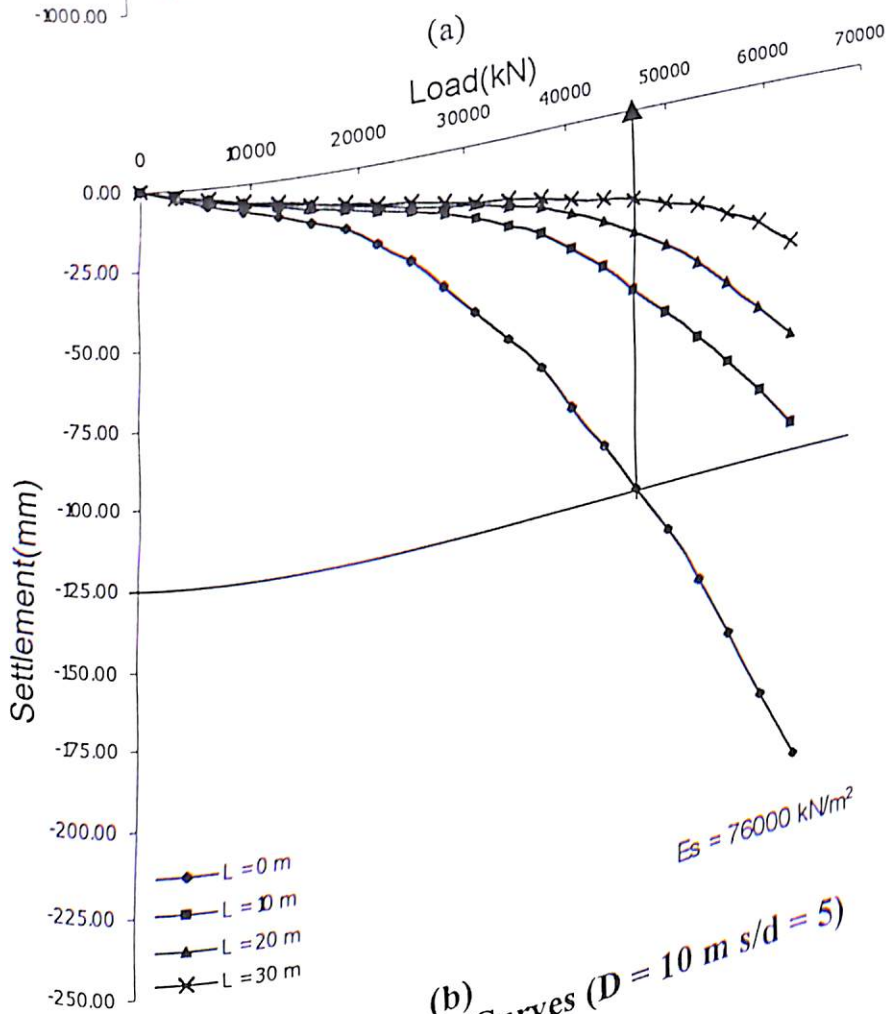

(b)

Figure 7.3 Load Settlement Curves (D = 10 m s/d = 5)

to provide better load carrying capacity of the piled raft foundation at permissible settlement.

7.2.1.4 Example 4

An axisymmetric piled raft foundation with raft diameter 30 metre, centre to centre spacing between piles equal to 5 times the diameter of pile is to be designed such that the settlement of the piled raft foundation does not exceed the permissible value. Suggest the suitable length of pile for a wide range of soil modulus. What is the maximum permissible load and hence the loading intensity on the foundation for each case. What is the possible number of storey in each case if the loading intensity per storey is assumed to be of 10 kN/m^2?

Solution

Diameter of raft (D)=30 m

Spacing to diameter ratio (s/d)=5

The permissible settlement for the multi storey building =125 mm

For raft diameter (D) 30m, s/d=5 and 125 mm settlement, the pile length, load and loading intensity have been obtained from Figure 7.4 (a) and Figure 7.4 (b) and shown in table below:

Table 7.4 Permissible Load and Loading Intensity obtained for Different Length of Pile and the Soil Modulus (D =30 m s/d =5)

Pile Length (m)	Permissible Load and Loading Intensity obtained for Different Length of Pile and the Soil Modulus					
	E_s=22000 kN/m^2		E_s=76000 kN/m^2		E_s=130000 kN/m^2	
	Load (kN)	UDL (kN/m^2)	Load (kN)	UDL (kN/m^2)	Load (kN)	UDL (kN/m^2)
30	206250.00	291.78	358620.675	507.344	493750.294	698.51
60	284375.00	402.31	472413.80	668.33	-	-
90	353125.00	499.57	541379.30	765.89	-	-

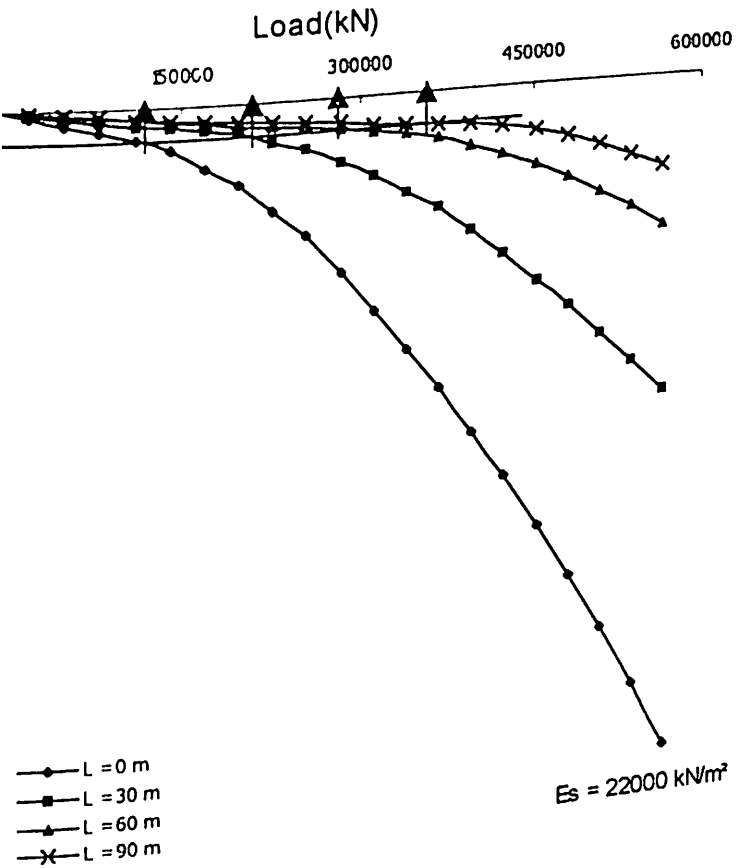
Load(kN)
150000
300000
450000
600000
L = 0 m
L = 30 m
L = 60 m
L = 90 m
Es = 22000 kN/m²

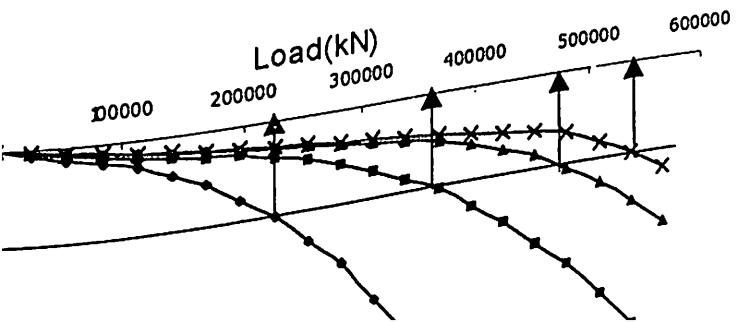
Load(kN)
100000
200000
300000
400000
500000
600000

From the table piles of desired length can be selected corresponding to the permissible load or loading intensity coming on the foundation. Generally in a multistory building, the loading intensity per storey considered is 10 kN/m^2. Hence the number of storey of buildings which is possible depending upon the length of pile of 30, 60 and 90 metre are 28, 39, 51 storey in a soil whose modulus is 22000 kN/m^2 and 50, 67 and 75 storey in a soil whose modulus is 76000 kN/m^2. For the soil with modulus of 130000 kN/m^2, even with pile of length 30 metre, 69 storey of building is possible. Other lengths of pile have not been shown as the piled raft settlement has been found to be less than the permissible value.

7.2.1.5 Example 5

An axisymmetric piled raft foundation with raft diameter 50 metre, centre to centre spacing between piles equal to 7.5 times the diameter of pile is to be designed such that the settlement of the piled raft foundation does not exceed the permissible value. Suggest the suitable length of pile for soil modulus 22000 kN/m^2 and 76000 kN/m^2. What is the maximum permissible load and hence the loading intensity on the foundation for each case? What is the possible number of storey of building in each case if the loading intensity per storey is assumed to be of 10 kN/m^2? What is the improvement in the number of storey when piles are added to the raft foundation?

Solution

Diameter of raft (D)=50 m

Spacing to diameter ratio (s/d)=7.5

The permissible settlement for the multi storey building =125 mm

For raft diameter (D) 50m, s/d=5 and 125 mm settlement, the pile length, load and loading intensity have been obtained from Figure 7.5 and shown in table 7.5 below:

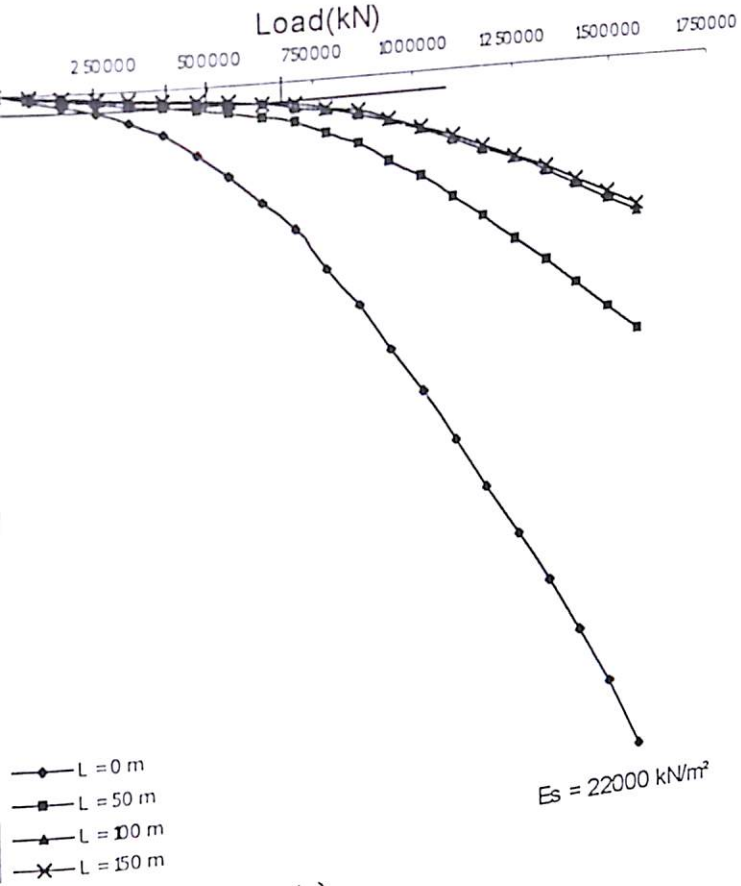

(a)

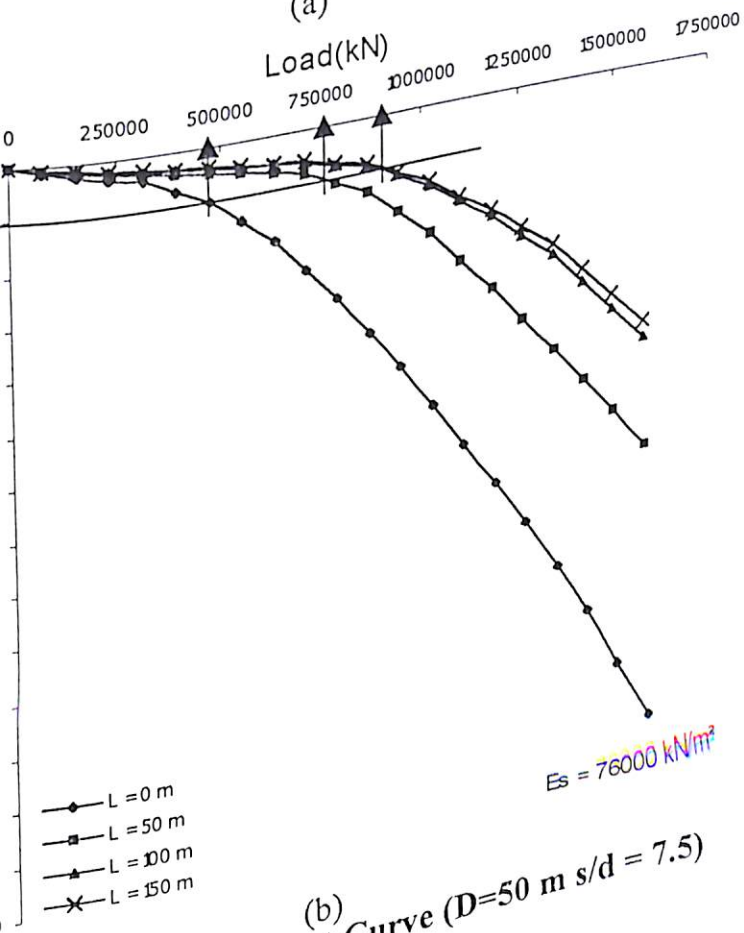

(b)

e 7.5 Load Settlement Curve (D=50 m s/d = 7.5)

Table 7.5 Permissible Load and Loading Intensity obtained for Different Length of Pile and the Soil Modulus (D =50 m s/d = 7.5)

Pile Length (m)	Permissible Load and Loading Intensity obtained for Different Length of Pile and the Soil Modulus			
	E_s = 22000 kN/m^2		E_s=76000 kN/m^2	
	Load (kN)	UDL (kN/m^2)	Load (kN)	UDL (kN/m^2)
0	189189.18	96.35	472727.28	240.76
50	348648.69	177.57	772727.27	393.55
100	459459.51	234.00	927272.74	472.26
150	627027.05	319.34	927272.74	472.26

From the table piles of desired length can be selected corresponding to the permissible load ... As the loading intensity per storey given is 10 ... the length of

Table 7.5 Permissible Load and Loading Intensity obtained for Different Length of Pile and the Soil Modulus (D =50 m s/d = 7.5)

Pile Length (m)	Permissible Load and Loading Intensity obtained for Different Length of Pile and the Soil Modulus			
	E_s = 22000 kN/m^2		E_s=76000 kN/m^2	
	Load (kN)	UDL (kN/m^2)	Load (kN)	UDL (kN/m^2)
0	189189.18	96.35	472727.28	240.76
50	348648.69	177.57	772727.27	393.55
100	459459.51	234.00	927272.74	472.26
150	627027.05	319.34	927272.74	472.26

From the table piles of desired length can be selected corresponding to the permissible load or loading intensity coming on the foundation. As the loading intensity per storey given is 10 kN/m^2, the number of storey of buildings which is possible depending upon the length of pile of 0, 50, 100 and 150 metre are 10, 18, 23 and 31 storey in a soil whose modulus is 22000 kN/m^2 and 24, 39, 47 and 49 storey in a soil whose modulus is 76000 kN/m^2. Here zero length of pile means the raft alone. It can be seen from the table that when piles of length even equal to the raft diameter has been added to the raft, the number of storey has increased from 10 to 18 in a soil of modulus 22000 kN/m^2 while this increase is from 24 to 39 in a soil of modulus 76000 kN/m^2. When piles of length 100 m have been provided, the number of storey has increased from 10 to 23 in case of soil with modulus 22000 kN/m^2 while this increase is from 24 to 47 in case of soil with modulus 76000 kN/m^2.

7.2.2 Piled Raft Foundation Under Plane Strain Condition

7.2.2.1 Example 1

A piled raft foundation of raft width 20 metre, centre to centre spacing between piles equal to 5.0 times the side of pile is to be designed such that the settlement of the piled raft foundation does not exceed the permissible value. Suggest the suitable length of pile for soil modulus 22000 kN/m^2, 76000 kN/m^2, and 130000 kN/m^2. What is the maximum permissible load and hence the loading intensity on the foundation for each case? What is

the possible number of storey of building in each case if the loading intensity per storey is assumed to be of 10 kN/m^2? What is the improvement in the number of storey when piles are added to the raft foundation?

Solution:

Width of raft (B)=20 m

Spacing to side ratio (S/d)=5

Soil modulus (E_s)=22000, 76000, 130000 kN/m^2.

The permissible settlement for the multi storey building =125 mm

For raft width (B)= 20m, S/d=5 and 125 mm settlement, the pile length, load and loading intensity have been obtained from Figures 7.6 (a) , (b) and shown in table below

Table 7.6 Permissible Load and Loading Intensity obtained for Different Length of Pile and the Soil Modulus (D =30 m s/d =5)

Pile Length (m)	Permissible Load and Loading Intensity obtained for Different Length of Pile and the Soil Modulus					
	Es = 22000 kN/m^2		Es = 76000 kN/m^2		Es = 130000 kN/m^2	
	Load (kN)	UDL (kN/m^2)	Load (kN)	UDL (kN/m^2)	Load (kN)	UDL (kN/m^2)
0	1307.69	68.3845	3000.00	150.00	4087.50	204.375
20	1923.08	96.154	4316.16	215.818	6000.00	300
40	2500.00	125.00	5363.64	268.182	7500.00	375
60	3038.46	151.923	6409.095	320.45	-	-

From the table given above for soil modulus 22000 kN/m^2, the possible number of storey of buildings for pile lengths 0,20,40 and 60 meters are 7,10,12 and 15 respectively. The addition of piles of length 20,40 and 60 meters improves the number of storey by 3,5,8 respectively.

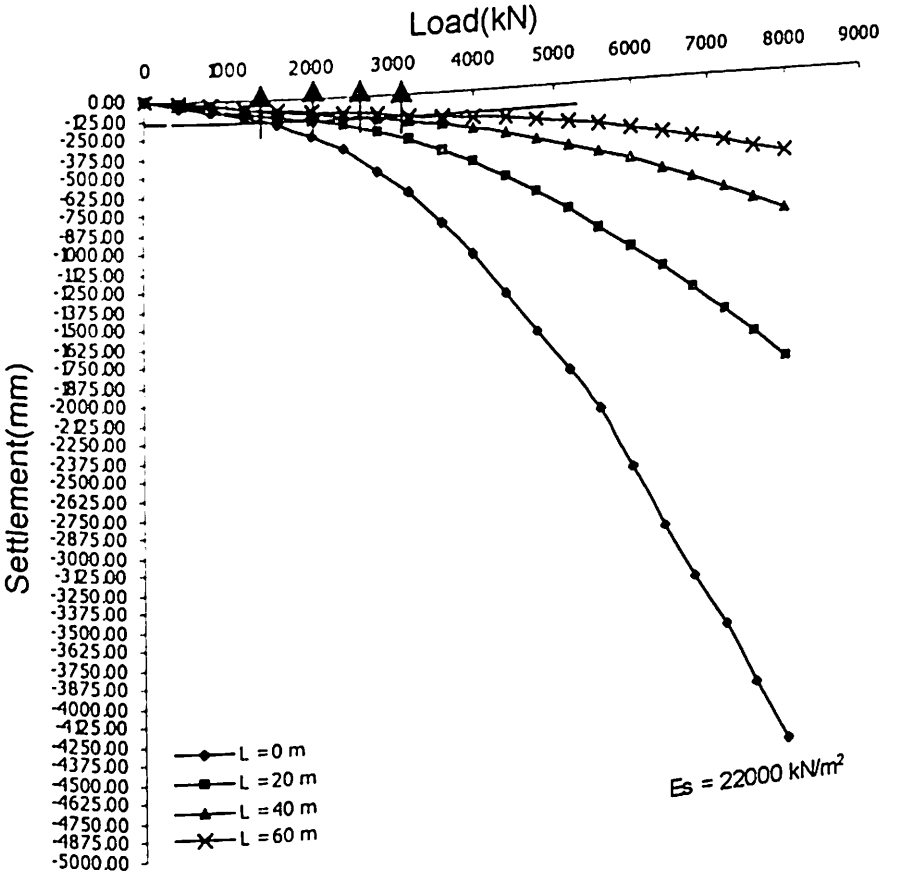

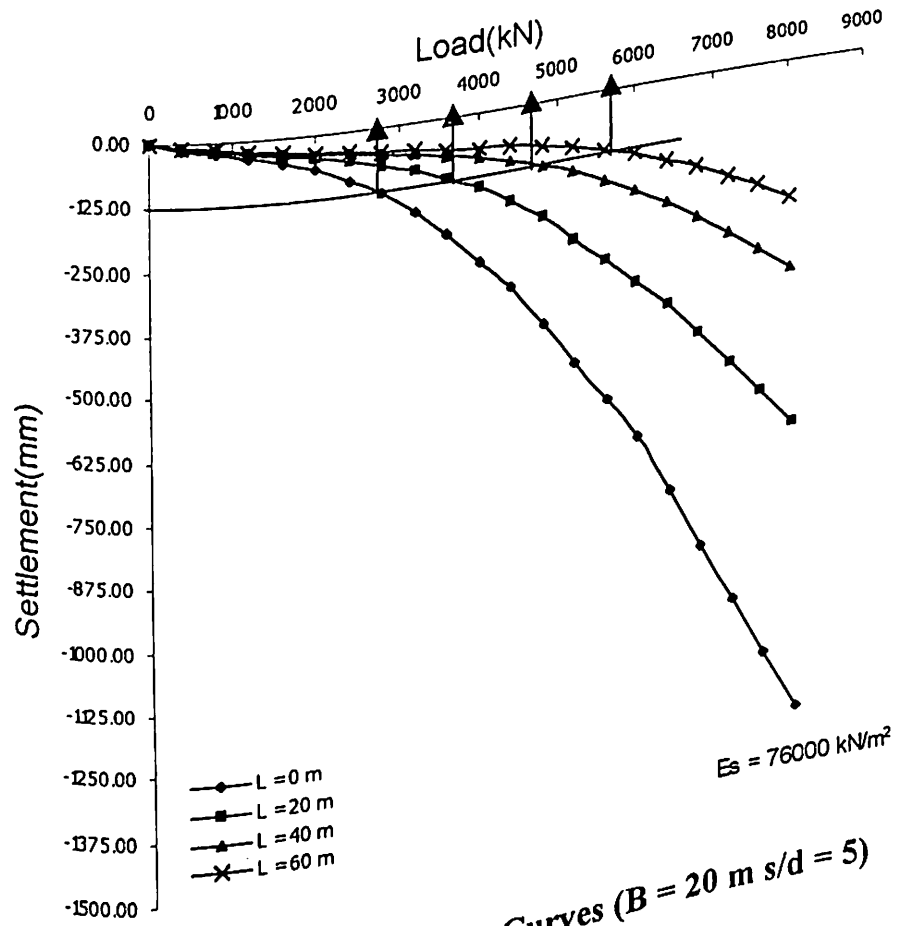

Figure 7.6 (a) Load Settlement Curves (B = 20 m s/d = 5)

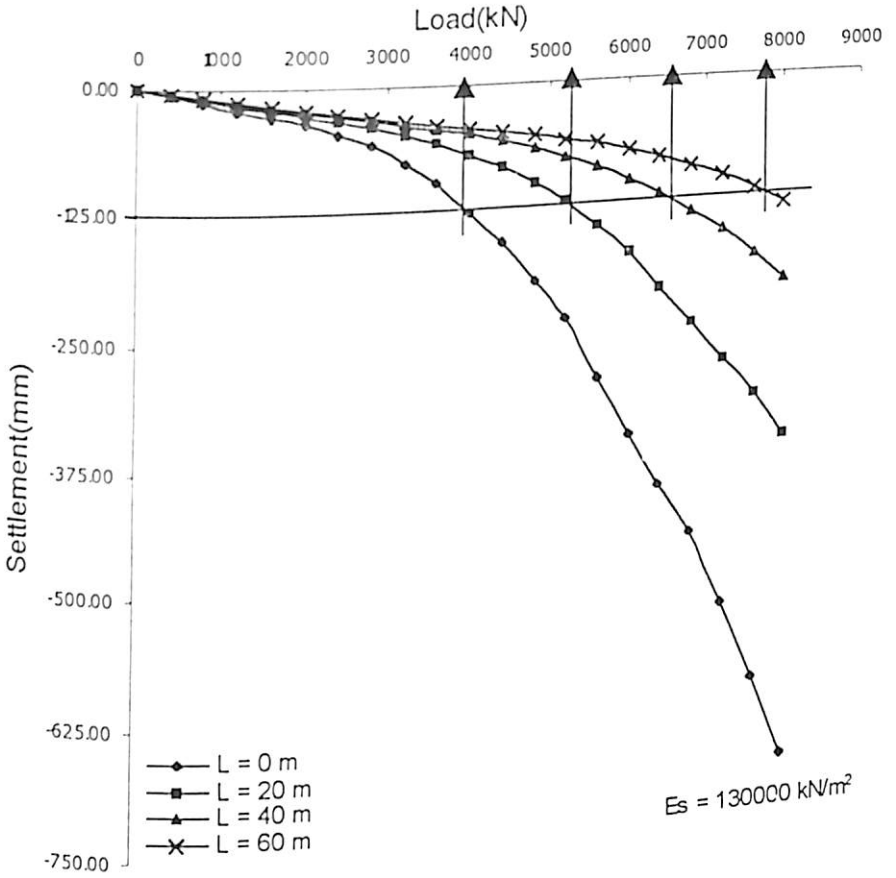

Figure 7.6 (b) Load Settlement Curves (B = 20 m s/d = 5)

From the table 7.6 for soil modulus 76000 kN/m^2, the possible number of storey of buildings for pile lengths 0,20,40 and 60 meters are 15,21,27 and 32 respectively. The addition of piles of length 20,40 and 60 meters improves the number of storey by 6,12,17 respectively.

From the table 7.6 for soil modulus 130000 kN/m^2, the possible number of storey of buildings for pile lengths 0,20,40 meters are 20,30,37 respectively. The addition of piles of length 20,40 meters improves the number of storey by 10,17 respectively.

7.2.2.2 Example 2

A piled raft foundation of raft width 20 metre, centre to centre spacing between piles equal to 7.5 times the side of pile is to be designed such that the settlement of the piled raft foundation does not exceed the permissible value. Suggest the suitable length of pile for soil modulus 22000 kN/m^2, 76000 kN/m^2, and 130000 kN/m^2. What is the maximum permissible load and hence the loading intensity on the foundation for each case? What is the possible number of storey of building in each case if the loading intensity per storey is assumed to be of 10 kN/m^2? What is the improvement in the number of storey when piles are added to the raft foundation?

Solution:

Width of raft (B)=20 m

Spacing to side ratio (S/d)=7.5

Soil modulus (E_s)=22000, 76000, 130000 kN/m^2.

The permissible settlement for the multi storey building =125 mm

For raft width (B)= 20m, S/d=7.5 and 125 mm settlement, the pile length, load and loading intensity have been obtained from Figures 7.7 (a) and (b) and shown in table 7.7 below

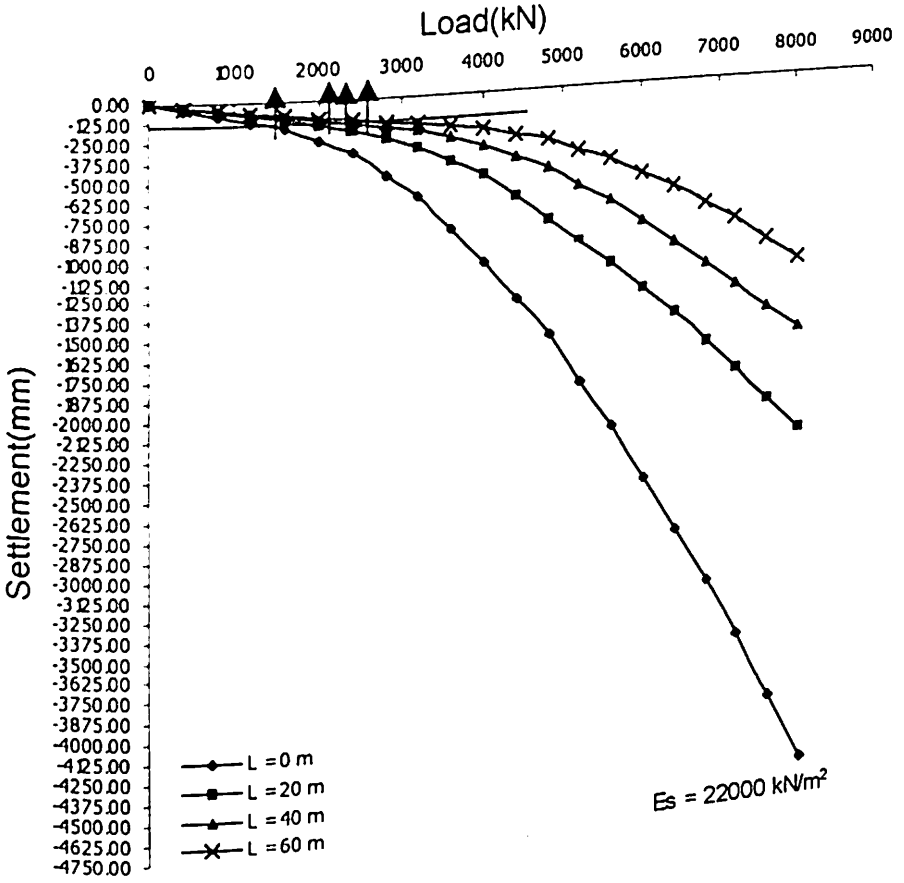

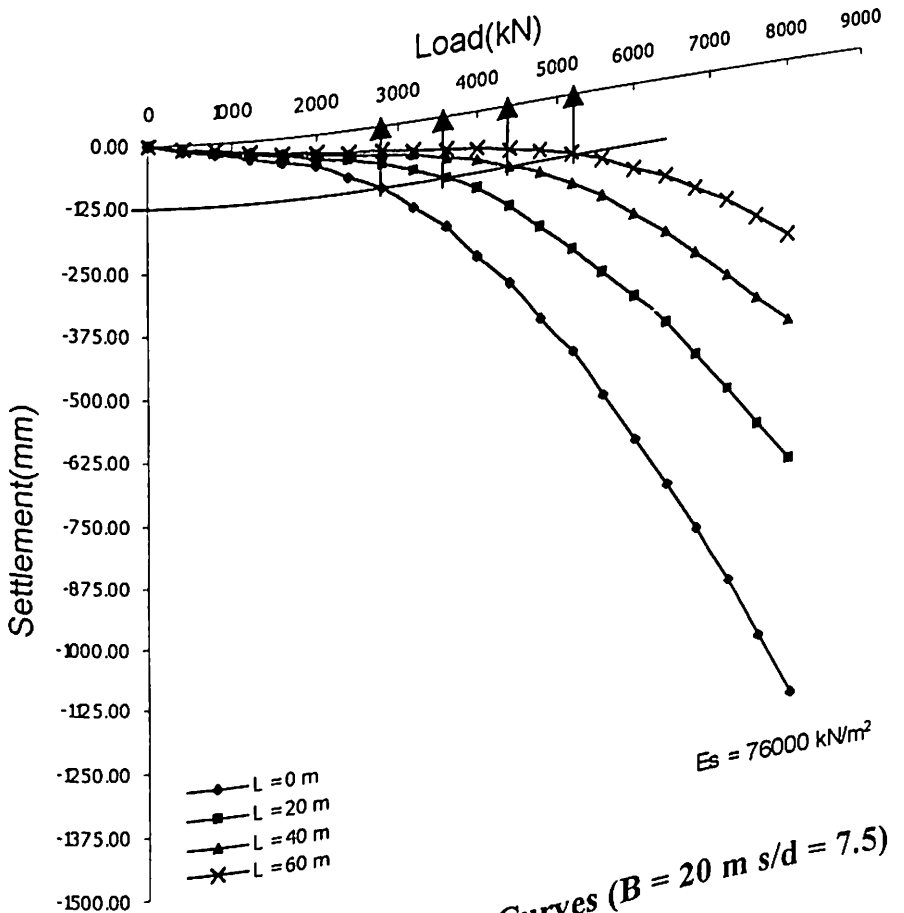

Figure 7.7 (a) Load Settlement Curves (B = 20 m s/d = 7.5)

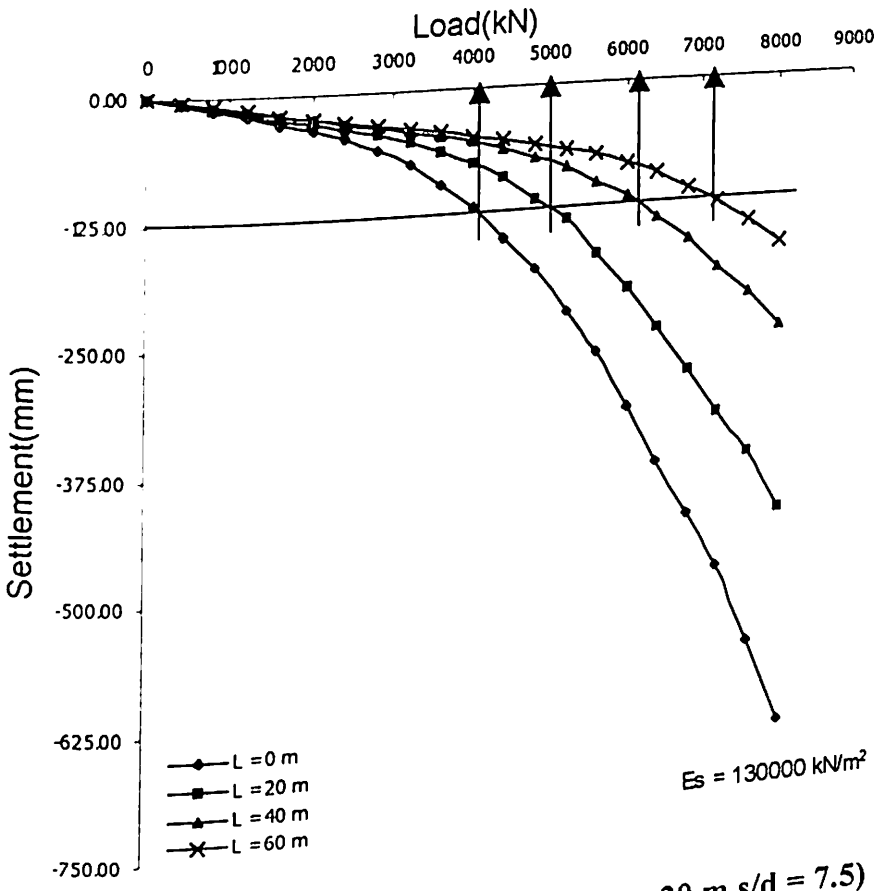

Figure 7.7 (b) Load Settlement Curves (B = 20 m s/d = 7.5)

Table 7.7 Permissible Load and Loading Intensity obtained for Different Length of Pile and the Soil Modulus (D =20 m s/d = 7.5)

Pile Length (m)	Permissible Load and Loading Intensity obtained for Different Length of Pile and the Soil Modulus					
	Es = 22000 kN/m^2		Es = 76000 kN/m^2		Es = 130000 kN/m^2	
	Load (kN)	UDL (kN/m^2)	Load (kN)	UDL (kN/m^2)	Load (kN)	UDL (kN/m^2)
0	1300.00	65.00	2923.08	146.154	4148.148	207.4074
20	1750.00	87.50	3692.32	184.62	5071.42	253.571
40	2112.50	105.63	4461.52	223.076	6142.84	307.142
60	2375.00	118.75	5307.68	265.38	7142.84	357.142

From the table given above for soil modulus 22000 kN/m^2, the possible number of storey of buildings for pile lengths 0,20,40 and 60 meters are 6,9,10 and 12 respectively. The addition of piles of length 20,40 and 60 meters improves the number of storey by 3,4,6 respectively.

From the table given above for soil modulus 76000 kN/m^2, the possible number of storey of buildings for pile lengths 0,20,40 and 60 meters are 14,18,22 and 26 respectively. The addition of piles of length 20,40 and 60 meters improves the number of storey by 4,8,12 respectively.

From the table given above for soil modulus 130000 kN/m^2, the possible number of storey of buildings for pile lengths 0,20,40 and 60 meters are 21,25,31 and 36 respectively. The addition of piles of length 20,40 and 60 meters improves the number of storey by 4,10,15 respectively.

7.2.2.3 Example 3

A piled raft foundation of raft width 20 metre, centre to centre spacing between piles equal to 10.0 times the side of pile is to be designed such that the settlement of the piled raft foundation does not exceed the permissible value. Suggest the suitable length of pile for soil modulus 22000 kN/m^2, 76000 kN/m^2, and 130000 kN/m^2. What is the maximum

permissible load and hence the loading intensity on the foundation for each case? What is the possible number of storey of building in each case if the loading intensity per storey is assumed to be of 10 kN/m^2? What is the improvement in the number of storey when piles are added to the raft foundation?

Solution:

Width of raft (B)=20 m

Spacing to side ratio (S/d)=10

Soil modulus (E_s)=22000, 76000, 130000 kN/m^2.

The permissible settlement for the multi storey building =125 mm

For raft width (B)= 20m, S/d=10 and 125 mm settlement, the pile length, load and loading intensity have been obtained from Figures 7.8 (a) and (b) and shown in table 7.8 .

Table 7.8 Permissible Load and Loading Intensity obtained for Different Length of Pile and the Soil Modulus (D = 20 m s/d = 10)

Pile Length (m)	Permissible Load and Loading Intensity obtained for Different Length of Pile and the Soil Modulus					
	Es = 22000 kN/m^2		Es = 76000 kN/m^2		Es = 130000 kN/m^2	
	Load (kN)	UDL (kN/m^2)	Load (kN)	UDL (kN/m^2)	Load (kN)	UDL (kN/m^2)
0	1250.00	62.50	2846.16	142.308	4076.92	203.846
20	1550.00	77.50	3384.60	169.23	4846.16	242.308
40	1825.00	91.25	4076.92	203.846	5769.24	288.462
60	2000	100	4807.7	240.385	6923.08	346.154

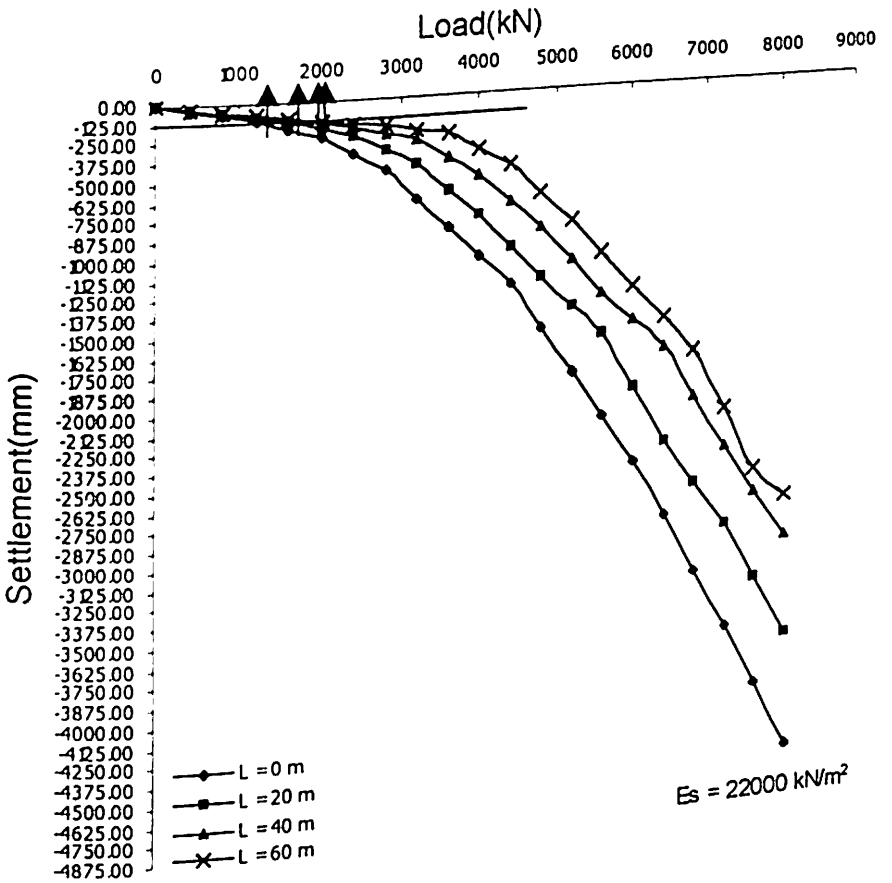

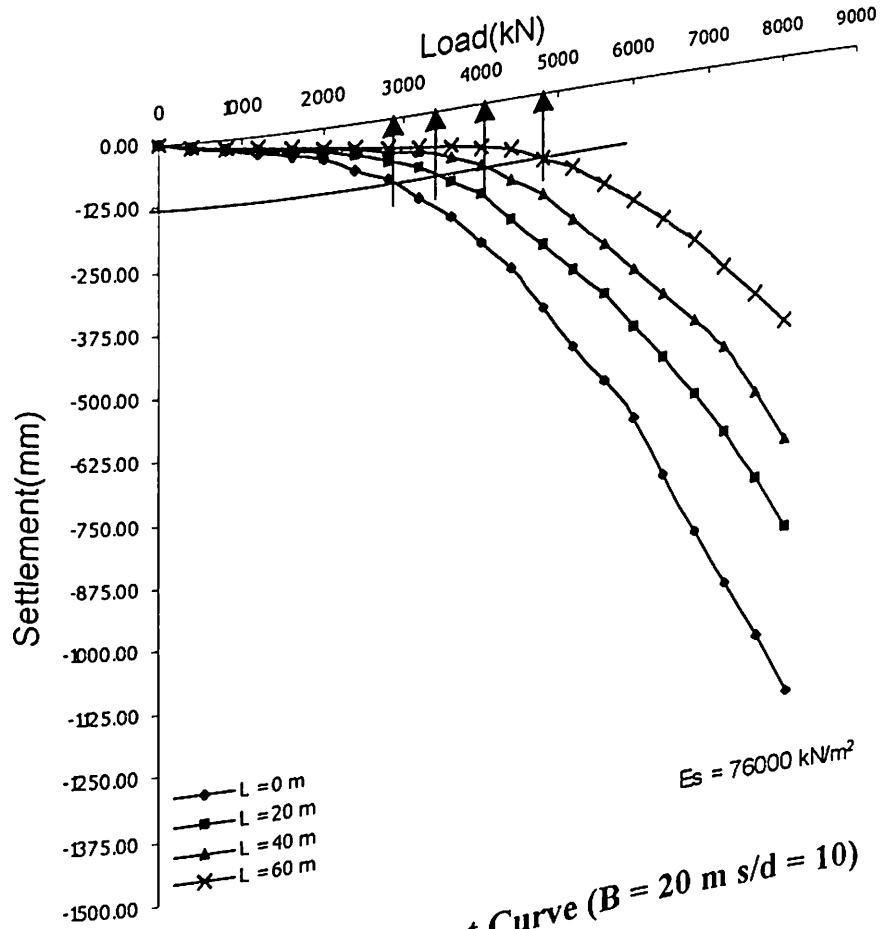

Figure 7.8 (a) Load Settlement Curve (B = 20 m s/d = 10)

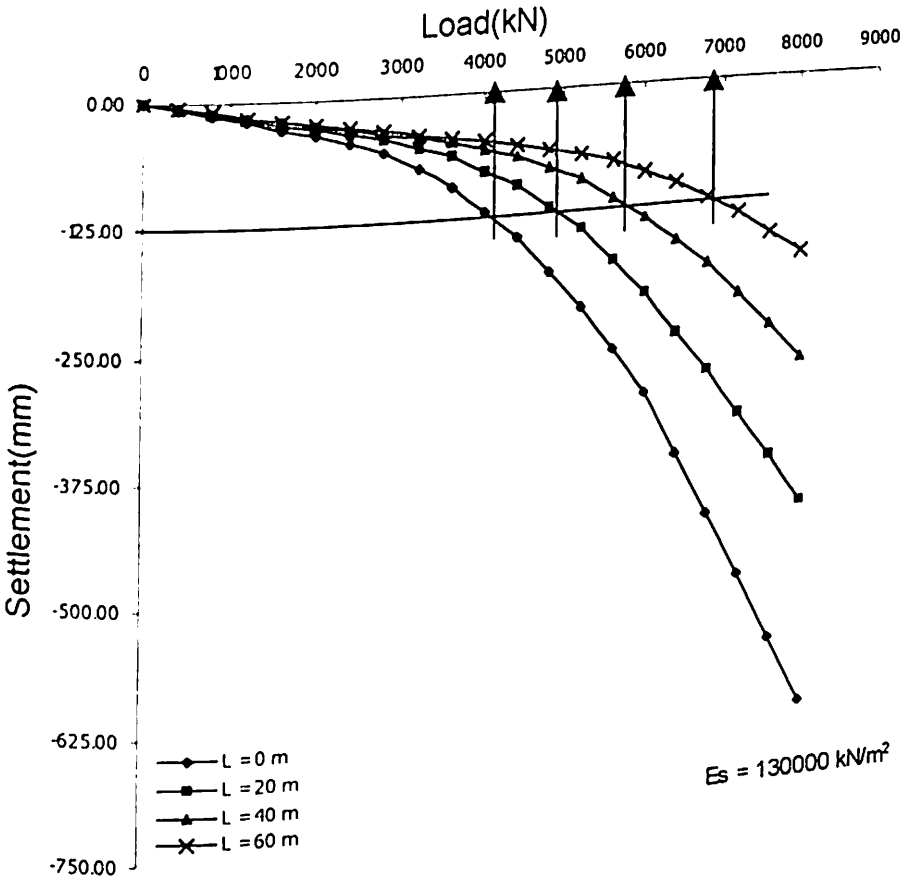

Figure 7.8 (b) Load Settlement Curve (B = 20 m s/d = 10)

From the table 7.8 for soil modulus 22000 kN/m^2, the possible number of storey of buildings for pile lengths 0,20,40 and 60 meters are 6,8,9 and 10 respectively. The addition of piles of length 20,40 and 60 meters improves the number of storey by 2,3,4 respectively.

From the table 7.8 for soil modulus 76000 kN/m^2, the possible number of storey of buildings for pile lengths 0,20,40 and 60 meters are 14,17,20 and 24 respectively. The addition of piles of length 20,40 and 60 meters improves the number of storey by 3,6,10 respectively.

From the table 7.8 for soil modulus 130000 kN/m^2, the possible number of storey of buildings for pile lengths 0,20,40 and 60 meters are 20,24,29 and 35 respectively. The addition of piles of length 20,40 and 60 meters improves the number of storey by 4,9,15 respectively.

Note: From the different load settlement curves, one can find out the load carried by raft and pile separately. Curves with zero length of pile represent the load carried by raft. Other curves represent the load carried by raft and pile. By subtracting the load taken by raft from the total load taken by piled raft, the load carried by pile can easily be obtained.

CHAPTER-8

SUMMARY AND CONCLUSIONS

Based on the results of nonlinear finite element analysis of raft, piled raft foundation under axisymmetric and plane strain condition, the summary and conclusions are as follows:

1. The load transfer mechanism in piled raft foundation is different than the conventional piled foundation. Based on the yielding of soil it has been found that in piled raft foundation, the load transfer is first at the tip of pile than it moves upward.
2. In case of piled raft foundation with rigid raft, the yielding of soil is seen first near the tip and in between the boundary piles and then it moves towards the centre piles. This means that when rigid raft is there the load transfer is seen first for the boundary pile and then it moves towards the centre piles.
3. When the spacing between the piles is very small, the yielding of soil shows that the group of piles shows block behaviour forming a bulb shape of yielded zone of soil.
4. When the spacing between the piles is large, the soil element in between the piles are found to yield. This shows that load transfer has increased with increase in spacing. At large spacing, this load transfer is found maximum.
5. The nonlinear finite element method predicts the load settlement curves, which resembles with the observed field behaviour.
6. The load carrying capacity of raft increases with increase in thickness of raft
7. The effect of addition of piles even of length equal to the diameter/width of raft has been found to increase the load carrying capacity of raft significantly.
8. The effect of increase in length of pile has been found to increase the load carrying capacity of piled raft foundation significantly.
9. The effect of increase in spacing has been found to decrease the load carrying capacity of piled raft foundation.
10. The effect of increase in thickness of raft has been found to increase the load carrying capacity of piled raft foundation.

11. The effect of increase in diameter/size of raft keeping the pile spacing same has been found to increase the overall load carrying capacity significantly.
12. When the thickness of raft is very small (0.1 to 0.5 metre) dish shape of deflection is seen for the axisymmetric raft foundation. For the raft foundation under plane strain condition, maximum deflection is found at the centre and minimum at the edge of the raft. Differential settlement is found maximum in this case.
13. With increase in thickness of raft this differential settlement reduces and at high thickness of raft, this differential settlement is found almost zero.
14. This differential settlement of raft is also found to reduce with increase in length of pile and found almost zero at larger length of pile.
15. The axial force in pile has been found maximum in the top of pile and minimum at the bottom of the pile for all load steps. At higher load steps the axial load distribution curves have been found to overlap each other showing that the piles have reached to almost its ultimate load carrying capacity.
16. In case of piles in a piled raft foundation under plane strain condition, in some cases the axial force in the pile has been found to increase first, then decreasing with depth and then increases near the tip of the pile. This may be due to the bending of pile.
17. The effect of increase in spacing has been found to increase the load carrying capacity of pile showing that the mobilization of frictional resistance increases with increase in spacing between the piles.
18. The load settlement curves produced can be directly be used for predicting the load for permissible settlement. Also for the allowable load, the settlement experienced can be found. This is true for both raft and piled raft foundation under axisymmetric and plane strain condition.
19. From the parameters thickness of raft, diameter/raft size, pile length, spacing between piles, soil modulus, load applied, settlement, any one unknown parameters can be obtained if the other six parameters are known.

20. The application of load settlement curves shows that for permissible settlement, an option can be selected for raft or piled raft foundation depending upon the load coming from the superstructure.
21. From the load settlement curves obtained and based on the permissible settlement, when the load has been calculated and converted into uniformly distributed load, it is found that a 20 to75 storey multistory building can be constructed on the soil range considered in this thesis.
22. In case of an axisymmetric piled raft foundation with large thickness of raft, the boundary piles carry maximum load followed by the middle piles while the centre piles carry minimum load.
23. In case of piled raft foundation which is under plane strain condition having large raft thickness the edge piles carry maximum load followed by the middle piles while the centre piles carry minimum load
24. For earlier load steps, the raft takes most of the load. With increase in load steps the load gets transferred to the piles. This is true when the piles are of larger length with respect to diameter/width of the raft. For piled raft foundation in which pile is small compared to the raft size, the piles first reaches to its ultimate capacity and then the raft.

Future Scope of the Work

The work can be extended to composite piled raft foundation. In regions where high wind load acts and option for providing piled raft foundation is there, the analysis of piled raft foundation under lateral load is a must including the vertical load also. Option for analysing the piled raft foundation using probabilistic approach is also there. Detailed boundary element method with nonlinear technique can also be adopted for the same. For structures with few storeys, dynamic analysis can also be done.

REFERENCES

1. **Akinmusuru, J.O. (1981)** Interaction of piles and cap in piled footing, *Journal of Geotechnical Engineering*, Proceedings of ASCE, Vol.106, No. GT1, pp 263-268.

2. **Aucilio, E. and Counte, E. (1999)** Settlement rate of foundations on unsaturated soils *Canadian Geotech. Journal*, Vol 36, pp940-946.

3. **Baguelin, F and Frank, R. (1980)** Theoretical Studies of Piles using the Finite Element Method. *Proceedings Conference Numerical Methods in Offshore Piling, London.* Institution of Civil Engineers, Vol.7, No.8, pp83-91.

4. **Balaam, N.P., Poulos, H.G. and Booker, J.R. (1975)** Finite Element Analysis of the Effects of Installation on Pile Load-Settlement Behaviour. *Journal of Geotechnical Engineering*, Vol.6, No.1, pp33-48.

5. **Baumgartl (1986)** Gruppenwirkung bei V-Last. Beiträge zum symposium Pfahlgründungen, Institut für Grundbau, Boden - and Felsmechanik der Technischen Hochschule Darmstadt, März.

6. **Bowles, J.E.** (1988) *Foundation Analysis and Design*, McGraw-Hill International Editions, Singapore.

7. **Bowles J E (1986)** Mat design, *ACI Journal*, Vol.83, pp1010-1017.

8. **Brown, P.T. (1969)** Numerical analysis of uniformly loaded circular rafts on deep elastic foundations. *Geotechnique* Vol.19, No.3, pp 399-404.

9. **Brown, P.T. and Wiesner, T.J. (1975)** The behaviour of uniformly loaded piled strip footing. *Soils and Foundations*, Vol.15, No.4, pp13-21.

10. **Brown, P.T. and Wiesner, T.J. (1980)** Laboratory tests on model piled raft foundations, *Journal of Geotechnical Engineering, ASCE*, Vol.106, No.7, pp 767-783.

11. **Butterfield, R. and Banerjee, P.K. (1971)** The problem of pile group and pile cap interaction, *Geotechnique* Vol 21, No.2, pp 135-142.

12. **Burd H.J. and Frydman, S. (1997)** Bearing capacity of plane-strain footings on layered soils *Canadian Geotech. Journal*, Vol. 34, pp 241-253

13. **Byrne, B.W. and Cassidy, M.J. (2002)** "Investigating The Response of Offshore Foundations in Soft Clay Soils" Proceedings of OMAE'02 21st

International Conference on Offshore Mechanics and Arctic Engineering June 23-28, 2002 – Oslo, Norway OMAE2002-28057, pp1-13

14. **Castelli, F. and Maugeri, M. (2002)** Simplified Nonlinear Analysis for Settlement Prediction of Pile Groups, *Journal of Geotechnical and Geoenvironmental Engineering*, Vol.128, No.1, pp 76-84.

15. **Chen, W.F. (1990)** Nonlinear analysis in soil mechanics: Theory and implementation, Elsevier Publications.

16. **Clancy, P. and Randolph, M.F.** (1996) Simple design tools for piled raft foundations, *Geotechnique*, The Institution of Civil Engineers, London, U.K., Vol. XLVI, No. 2, 1996, pp 313-328.

17. **Chow, Y.K. (1987)** Three-dimensional analysis of pile groups. *Journal of Geotechnical Engineering* Vol. 113, No.6, pp 637-651.

18. **Chow, Y.K.** (1992) Pile-cap-pile group interaction in nonhomogeneous soil, *Journal of Geotechnical Engineering, ASCE*, Vol.117, No.11, pp 1655-1667.

19. **Clough, R.W. (1969)** Comparison of three-dimensional elements *Application of FEM in Civil Engineering, ASCE*, pp 13-14.

20. **Cooke, R.W., Bryden-Smith, D.W. and Gooch, M.N. (1981)** Some observations of the foundation loading and settlement of a multi-storey building on piled raft foundation in London Clay. *Proceedings, Institution of Civil Engineers*, 1, pp 433-460.

21. **Cooke, R.W (1986)** Piled raft foundations on stiff clays-a contribution to design philosophy, *Geotechnique*, Vol.36, No.2, pp169-203.

22. **D'Appolonia, D.J. and Lambe, T.W. (1971)** Performance of four foundations on end bearing piles, *Journal of the Soil Mechanics and Foundations Division.* Proceedings of the ASCE, Vol.97, No.SM1. pp 77-93.

23. **Desai, C.S.** (1981) Pile cap-pile group-soil interaction, *Journal of Geotechnical Engineering, ASCE*, Vol.107, No.5, pp 817-834.

24. **Desai, C.S., Muqtadir, A. and Scheele, F. (1986)** Interaction analysis of anchor-soil systems, *Geotechnical engineering Journal*, Vol.112, pp 537-553.

25. **Desai, C.S. and Abel, J.F. (1972)** *Introduction to the Finite Element Method: A Numerical Method for Engineering Analysis*, An East-West Edition.

26. **Driscoll, R.M. (1982)** Discussion on some observations of the foundation loading and settlement of a multistorey building on a piled raft foundation in London clay, *Proceedings Institution of Civil Engineers*, Vol.1, No.72, pp 696-699, U.K.

27. **Duncan, J.M. and Chang. C.Y. (1970)** Nonlinear analysis of stress and strains in soils, *Journal of the Soil Mechanics and Foundation Division*, Proceeding of the ASCE, pp.1629-1653.

28. **Drucker D.C. and Prager W. (1952)**, Soil Mechanics and Plastic Analysis of Limit Design, *Quart. Applied Mathematics* Vol.10, No.2.

29. **El-Mossallamy (1989),** Analysis of Pile-Raft Soil Interaction. M.Sc Thesis, Faculty of Engineering, Ain Shams University, Cairo, published in extracts in *Proceeding First International Conference on a Structural Engineering* of Ain Shams University under the same title and the names of El-Kadi, El-Nahhas, El-Mossallamt.

30. **Franke, E. (1991)** Measurements beneath piled rafts, *Keynote lecture to the ENPC-Conference on Deep Foundations*, Paris, pp1-28.

31. **Fraser, R.A. and Wardle, L.J. (1976)** Numerical analysis of rectangular rafts on layered foundation, *Geotechnique*, Vol.26, No.4, pp613-630.

32. **Gandhi and Maharaj (1996)** Analysis of piled raft foundation, Sixth International Conference on Piling and Deep Foundations, Bombay, India, pp 1.11.1-1.11.7.

33. **Hain, S.J. and Lee I.K. (1974)** Rational analysis of raft foundation, *Journal of Geotechnical Engineering* Vol.100, No.GT7, pp843-859.

34. **Hain, S.J. and Lee, I.K. (1978)** The analysis of flexible raft pile system, *Geotechnique*, vol.28, No.1, pp 65-83.

35. **Hannink, G. (1994)** Settlement of high-rise building in Rotterdam. *XIII International Conference on Soil Mechanics and Foundation Engineering*, New Delhi, India, pp 441-444.

36. **Hongladaromp, T., Chen, N. and Lee, S. (1973)** Load distribution in rectangular footings on piles, *Geotechnical Engineering*, Vol. 4, pp 77-90.

37. **Hooper, J.A** (1973) Observations on the behaviour of a piled raft foundation in London clay, *Proceeding of Institution of Civil Engineers*, Vol. 55, No.2, pp 855-877.

38. **Horvath, J.S. (1983)** New subgrade model applied to mat foundations, *Journal of Geotechnical Engineering*, Vol.109, No.12, pp1567- 1587.

39. **Jack I. Clark (1998)** The settlement and bearing capacity of very large foundations on strong soils: 1996 R.M. Hardy keynote address *Canadian Geotech. Journal*, Vol. 35, pp131-145.

40. **Kraft, L.M., Ray, R.P. and Kagawa, T.K. (1981)**, Theoretical t-z curves, *Journal of Geotechnical Engineering Division, ASCE*, Vol. 107, No.GT11, pp 1543-1561.

41. **Kay and Cavagnaro (1983)** Settlement of Raft Foundations, *Journal of Geotechnical Engineering* Vol.109, No.11, pp1367-1381.

42. **Kuppusamy, T. (1985)** Three-Dimensional Stress Analysis of Anisotropic Layered Soils. *International Conference. Finite Elements in Computational Mechanics*, Bombay, India, December 2-6.

43. **Kuwabara, F. (1989)** An elastic analysis for piled raft foundations in a homogeneous soil, *Soils and Foundations*, Vol.29, No.1, pp82-92.

44. **Lambe, T.W. (1968)** The behaviour of foundations during construction. *Journal of Soil Mechanics and Foundations Division*, Proceedings of ASCE, Vol.98, No. SM1, pp.93-129.

45. **Lambe, T. W., and Whitman, R. V. (1979)** , Soil Mechanics. S. I. version., Wiley Eastern Limited, New-Delhi, Bangalore, Bombay, Calcutta, Madras.

46. **Landva, A.O., Valsangkar, A.J., Alkins, J.C. and Charalambous, P.D. (1987)** Performance of a Raft Foundation Supporting a Multistorey Structure, *Canadian Geotechnical Journal*, Vol.25, pp138-149.

47. **Lianga, F., Chena, L. and Shib X (2003)** Numerical analysis of composite piled raft with cushion subjected to vertical load, *Computers and Geotechnique*, Vol. 30, pp443–453

48. **Liu. W. And Novak, M.** (1991) Soil-pile-cap static interaction analysis by finite and infinite elements, *Canadian Geotechnical Journal*, pp771-783.

49. **Lytton, R.L. and Meyer, K.T. (1971)** Stiffened mat on expansive clay. *Journal of Soil Mechanics and Foundations Division. Proceedings* ASCE, Vol.97, No.SM7, pp999-1019.

50. **Madhav, M.R. and Karmarkar, R.S.(1982)** Elasto-plastic settlement of rigid footings , *Journal of the Geotechnical Engineering Division*, ASCE, Vol.108, No.GT3, pp.483-488.

51. **Maharaj, D.K. (1996)** Application of elastic and elasto-plastic analysis for piled raft foundation, Ph.D Thesis, IIT, Madras, Chennai, India.

52. **Maharaj, D.K. (2000) AXINLFEM**-Axisymmetric Nonlinear Finite Element Software, Civil Engineering Group, Birla Institute of Technology and Science, Pilani, Rajasthan-333031

53. **Maharaj, D.K. (2000) PSNLFEM**-Plane Strain Nonlinear Finite Element Software, Civil Engineering Group, Birla Institute of Technology and Science, Pilani, Rajasthan-333031

54. **Maharaj, D.K. (2003)** Load-Settlement Behaviour of Piled Raft Foundation by Three-Dimensional Nonlinear Finite Element Analysis. *Electronic Journal of Geotechnical Engineering*, Vol. 8, Bundle (C), ppr 2003-0334

55. **Maharaj, D.K. and Gandhi, S.R. (2003)** Piled raft foundation behaviour by nonlinear finite element analysis, *Geotechnique* (Under Peer Review)

56. **Maharaj and Gandhi (2003)** "*Design chart for piled raft foundation by finite element method* " Proceedings Geotechnical Engineering, Institution of Civil Engineers, London (Accepted).

57. **Mattes N.S. and Poulos (1969)** Settlement of single compressible pile. *Journal of the Soil Mechanics and Foundations* Division Proceedings of ASCE, Vol.95, No.SM1, pp189-207.

58. **McKeen R.G. and Johnson L.D. (1990)** Climate-controlled soil design parameters for mat foundations. *Foundation Journal of Geotechnical Engineering* Vol.116, No.7, pp843-859.

59. **Noura,.A., Slimani, A. Laouami A (2002)** Foundation settlement statistics via. Finite element analysis, *Computers and Geotechnique* Vol.29, pp 641–672

60. **Ottaviani M. (1975)** Three-dimensional finite element analysis of vertically loaded pile groups, *Geotechnique* Vol.25, No.2, pp159-174.

61. **Owen, D.R.J. and Hinton, E. (1980)** Finite Elements in Plasticity: Theory and Practice. Pineridge Press, Swansea.

62. **Pender, M.J.(1994)** Components of the stiffness of pile-raft foundations, *XIII International conference on Soil Mechanics Foundation Engineering*, New Delhi, India, pp 923-928.

63. **Polo J.M. and Clemente L.M. (1988)** Pile-Group Settlement Using Independent Shaft and Point Loads, *Journal of Geotechnical Engineering* Vol. 114, No.4, pp 469-487.

64. **Poterasu, V.F. and Mihalache, N. (1985)** "FEM and BEM in elasto-plastic problems for soil-structure interaction" *International Conference. Finite Elements in Computational Mechanics*, Bombay, India, December 2-6.

65. **Potts, D.M. and Martins, J.P. (1982)** The shaft resistance of axially loaded piles in clay, *Geotechnique*, Vol.32, No.4, pp369-386.

66. **Poulos, H.G. and Davis, E.H. (1974)***"Elastic solutions for soil and rock mechanics"*, Chichester: Wiley.

67. **Poulos, H.G., and Davis, E.H. (1972)** "The analysis of pile raft systems", *Australian Geomechanics Journal*, (1), pp82-92.

68. **Poulos, H.G. and Davis, E.H. (1980)** *Pile Foundation Analysis and Design*, New York, Wiley.

69. **Poulos, H. G. (1993)** Piled raft in swelling or consolidating soils, *Journal of Geotechnical Engineering, ASCE*, Vol.119, No.2, pp374-380.

70. **Moora, P.J. and Spencer, G.K. (1969)** Settlement of building on deep compressible soil, *Proceedings of ASCE*, Vol. 95, No. SM3, pp 769-790.

71. **Poulos, H.G. (1994)** Alternative design strategies for piled raft foundations. *3rd International conference on DEEP FOUNDATION PRACTICE* incorporating PILETALK, Singapore.

72. **Poulos, H.G. (2001)** Piled raft foundations: design and applications, *Geotechnique*, Vol.51, No.2, pp95-113.

73. **Prevost, J.H. (1978)** Plasticity theory for soil stress-strain behaviour. *Journal of Engineering Mechanics Division*, ASCE, Vol.104, pp1177-1194.

74. **Randolph, M.F.** (1994) Design methods for pile group and piled raft, *XIII International Conference on Soil Mechanics and Foundation Engineering*, New Delhi, India, Vol.5, pp 1-21.

75. **Sahara1 M, Akino, N. and Tominaga, K. (2002)** Experimental Results and Elasto-plastic Analysis of the Vertical Behavior of a Single Model Pile, *Journal of Asian Architecture and Building Engineering* ,March 2002/73 Vol.1, No.1,pp 65-73

76. **Sasha D. Milovic (1998)** A comparison between observed and calculated large settlements of raft foundations *Canadian Geotech. Journal* Vol.35, pp251-263

77. **Schwab, H.H., Gundling, N. and Lutz, B. (1991)** Monitoring pile raft soil interaction. *Proc. of symposium on Field Measurements in Geotechnique*, Sorum, Balkema, Rotterdam, pp.117-127.

78. **Seed, B.R. (1989)** Numerical simulation of excavation in elasto-plastic soils, *International Journal Numerical and Analytical Methods in Geomechanics*, Vol.13, pp231-249.

79. **Severn R.T. (1966)** The solution of foundation mat problems by finite-element methods. *Structural Engineer* Vol.44, No.6, pp 223-228.

80. **Shukla S.N. (1984)** A simplified method for the design of mat on elastic foundation. *ACI Journal* Vol.81, pp 469-475.

81. **Silvestri, V. (2000)** Performance of shallow foundations on clay deposits in Montreal Island *Canadian. Geotech. Journal* Vol.37. pp218-237

82. **Simons, N.E. and Rodrignes, J.S.N. (1975)** F.E.A of surface deformation due to uniform loading on a layer of Gibson soil resting on a smooth rigid base, *Geotechnique*, Vol.25, No.2, pp375-379.

83. **Siriwardane, H.J. and Desai, C.S. (1983)** Computational procedures for nonlinear three-dimensional analysis with some advanced constitutive laws, *International Journal for Numerical and Analytical Methods in Geomechanics*, Vol.7, pp143-171.

84. **Tomono, M., Kakurai, M. and Yamashita, K. (1987)** Analysis of settlement behaviour of piled raft foundation, *Takenaka Technical Research Report*, May 87.

85. **Trochanis, A.M., Bielak, J. and Christiano, P. (1991)** Three-dimensional nonlinear study of piles, *Journal of Geotechnical Engineering, ASCE*, Vol.117, No.3, pp429-447.

86. **Whitmen, R.V. and Hoeg, K. (1966)** Development of plastic zone beneath a footing, report by M.I.T., Department of civil engineering to US army eng. waterways experiment station.

87. **Wiesner** *et al.*, **(1980)** Laboratory Tests on Model Piled Raft Foundations, *Journal of Geotechnical Engineering, ASCE*, Vol.106, No.7, pp767-783.

88. **Yamashita, K., Kakurai, M. and Yamada, T. (1994)** Investigation of a piled raft foundation on stiff clay, *XIII International Conference on Soil Mechanics and Foundation Engineering, New Delhi*, India, pp 543-546.

89. **Zeevaert, L (1957)** Foundation design and behaviour of Tower Latino Americana in Mexico city, *Geotechnique*, Vol.7, No.1, pp115-133.

90. **Zienkiwicz, O.C. and Chen, A.H. (1990)** Generalized plasticity and the modeling of soil behaviour. *International Journal Analytical and Numerical Methods in Geomechanics*. Vol.14, pp151-190.

91. **Zienkiwicz, O.C. (1990)** *The finite element method.* Tata McGraw-Hill Publishing Company Limited.

APPENDIX-I

Equivalent Piles Incase of Axisymmetric Piled Raft Foundation and Piled Raft Foundation under Plane Strain Condition

A circular raft foundation and piled raft foundation of varying diameter and thickness have been analyzed by nonlinear finite element method. In case of piled raft foundation, each concentric row of piles has been considered as an annulus having same stiffness and volume as that of the piles. The length of pile and that of the annulus have been considered same. The thickness of each annulus has been calculated based on following formula.

$$2\pi \times s_i \times t \times L = N \times \frac{\pi}{4} \times d^2 \times L$$

$$t = \frac{n \times \frac{\pi}{4} \times d^2}{2 \times \pi \times s_i}$$

Where i = 1 to n

n = Number of pile

d = diameter of pile

s_i = radius of the annulus

H = Length of Pile/ Length of annulus

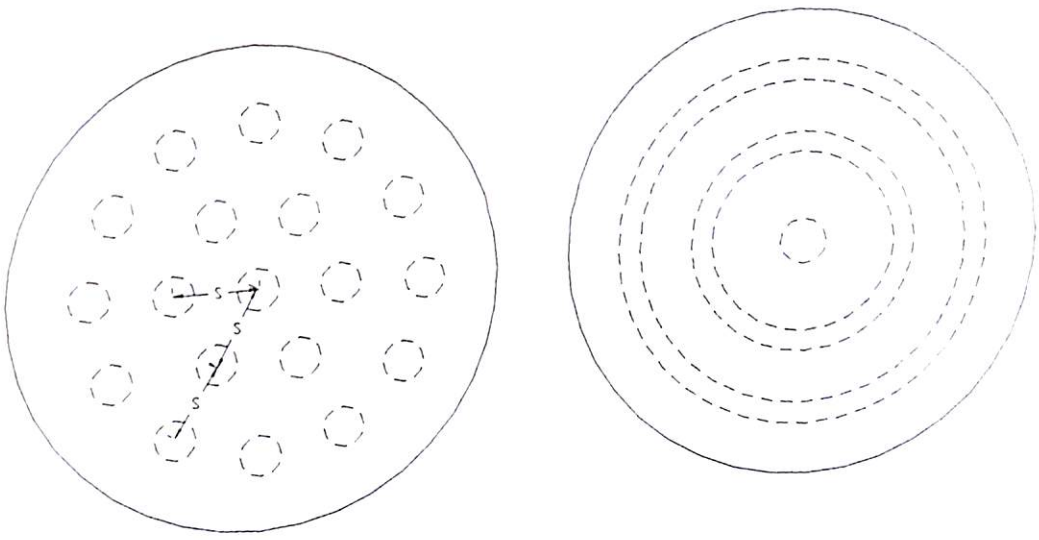

(a) Piles in Piled Raft Foundation

(b) Piles as Equivalent Annulus of same volume

Figure 1 Conversion of Piles into Equivalent Annulus of Same Volume

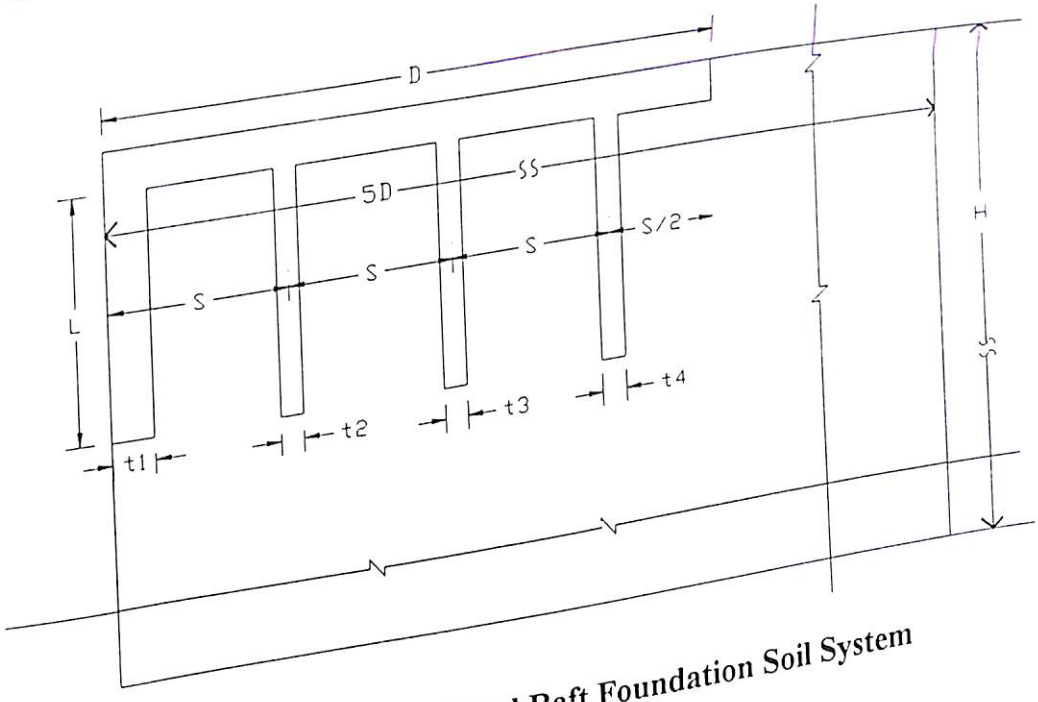

Figure 2 Axisymmetric Piled Raft Foundation Soil System

PLANE STRAIN CONDITION

Thickness can be computed from the following formula.

$(t \times s) \times L = d \times d \times L$

$t = d^2 / s$

Where

t is the thickness of the equivalent strip corresponding to a single pile in a spacing s.

s is the spacing between the piles

d is one side of the pile

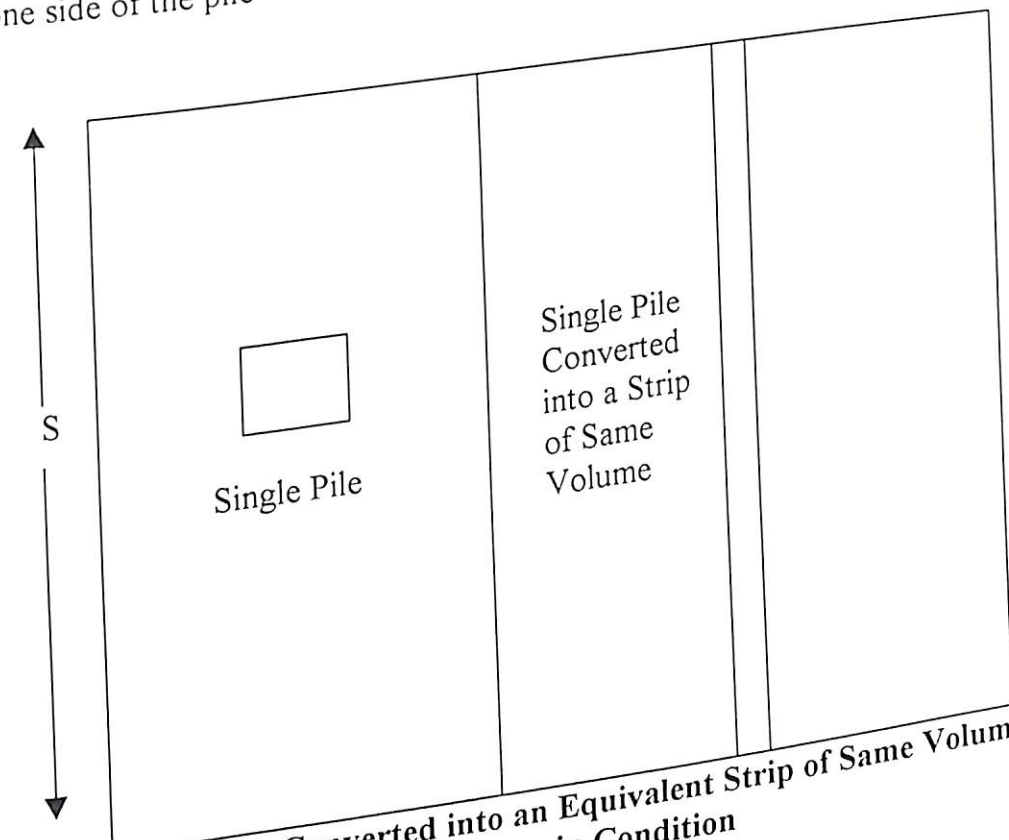

Figure 3 Single Pile Converted into an Equivalent Strip of Same Volume Under Plane Strain Condition

Table 1 Number of piles considered for various diameters of Piled Raft for different s/d

Raft Diameter ↓ S/d →	Number of Piles for Different Spacing to Diameter Ratio (s/d)				
	2.5	5.0	7.5	10.0	15.0
10	91	19	7	-	-
20	-	91	37	19	-
30	-	169	61	37	
40	-	-	127	91	37

APPENDIX-II

COST ANALYSIS

(i) AXISYMMETRIC PILED RAFT FOUNDATION

Based on nonlinear finite element analysis by considering different parameters as discussed in Chapter-5 it has been found that the effective length of pile corresponding to diameter of raft of 10, 20, 30, 40 and 50 metre are 20, 40,60, 80 and 100 metre respectively. Hence in cost analysis comparison with conventional piled foundation has been done corresponding to these effective lengths of piles of piled raft foundation. Below is discussed the method of calculation of saving in concrete volume when piled raft foundation is used instead of the conventional piled foundation.

$$\text{Volume of Concrete in case of piled raft foundation} = N \times \frac{\pi}{4} \times d^2 \times L$$

$$\text{Volume of Concrete in case of piled foundation} = N \times \frac{\pi}{4} d^2 \times L'$$

$$\% \text{ Saving in Concrete} = \frac{\left(N \times \frac{\pi}{4} d^2 \times L'\right) - \left(N \times \frac{\pi}{4} \times d^2 \times L\right)}{\left(N \times \frac{\pi}{4} \times d^2 \times L\right)}$$

$$= \left(\frac{L'-L}{L}\right)$$

Where

N = number of piles

L = length of the pile

d = Diameter of the pile

In this thesis the depth of soil layer considered is 200 m, which is nothing, but the length of the conventional pile considered. So in our case L' = 200 m

Based on the above equation the saving in concrete for effective length of pile considered are tabulated below

Diameter of Piled Raft	10	20	30	40	50
Effective Pile Length	20	40	60	80	100
% Saving in Concrete	900	400	233.33	150	100

(ii) PILED RAFT FOUNDATION UNDER PLANE STRAIN CONDITION

In case of piled raft foundation under plane strain condition no well defined length of the piles have been found beyond which there is no change in load settlement curve for the range of parameters considered in the analysis. Hence comparison has been made under the same length as considered in case of piled raft foundation under axisymmetric condition. Below is discussed the method of calculation of saving in concrete volume when piled raft foundation is used instead of the conventional piled foundation.

Volume of concrete per unit width for piled raft foundation= $N \times (t \times s) \times L$

Volume of concrete per unit width for piled raft foundation= $N \times (t \times s) \times L'$

$$\% \text{ Saving in concrete} = \frac{(N \times (t \times s) \times L') - (N \times (t \times s) \times L)}{(N \times (t \times s) \times L)}$$

$$= \left(\frac{L'-L}{L}\right)$$

Where

N = number of piles in the strip

t = thickness of equivalent strip of piles

L'= length of pile for conventional piled foundation

L = length of pile in piled raft foundation

s = spacing between the piles

The length of piles in conventional piled foundation is 200 meter. Hence L'=200 meter.

Based on above formula the saving of concrete is tabulated below

Width of Piled Raft	10	20	30	40	50
Pile Length	20	40	60	80	100
% Saving in Concrete	900	400	233.33	150	100

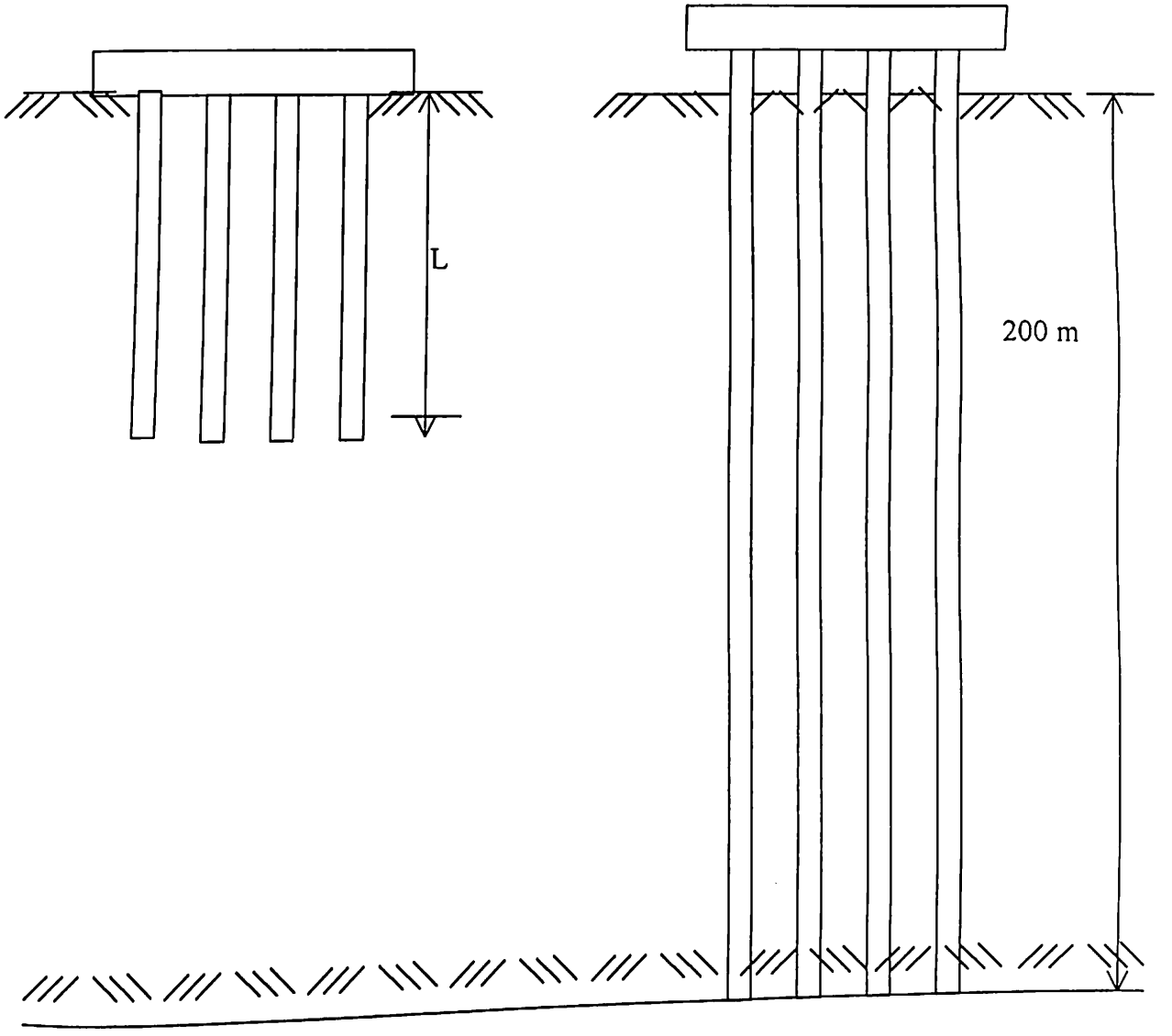
L
200 m

APPENDIX-III
FINITE ELEMENT SOFTWARE

PSNLFEM

1. Type of Analysis: This software can perform
   - i) Linear Finite Element Analysis
   - ii) Nonlinear Finite Element Analysis

2. Type of Element: Four noded isoparametric element
   - i) Rectangular shape
   - ii) Square Shape

3. Constitutive Model
   - i) Linear constitutive model
   - ii) Nonlinear constitutive model

     -Von-Mises yield Criterion

     -Through Von-Mises Yield criterion, Drucker-Prager yield criterion can be simulated for the clay.

4. Solution Technique Used

   Modified Newton Raphson Iterative Procedure

5. Input Details:
   - i) Number of elements in x-direction
   - ii) Number of elements in y-direction
   - iii) Total number of elements
   - iv) Half Band width
   - v) Number of restrained degree of freedom
   - vi) Number loaded degree of freedom
   - vii) Element coordinates in x-direction
   - viii) Element coordinates in y-direction

ix) Element properties (Modulus of elasticity, poisson's ratio of material and yield stress)

x) Boundary condition (Node number, 1 for restrained and 0 for displacement allowed)

xi) Degree of freedom number and load applied

6. Output Details:

i) Displacements of nodal points for each element

ii) Stresses in an element

iii) Von-Mises Stresses and Strains

AXINLFEM

1. Type of Analysis: This software can perform
   a. Linear Finite Element Analysis
   b. Nonlinear Finite Element Analysis

2. Type of Element: Four noded isoparametric element
   a. Rectangular shape
   b. Square Shape

3. Constitutive Model
   a. Linear constitutive model
   b. Nonlinear constitutive model
      -Von-Mises yield Criterion
      -Through Von-Mises Yield criterion, Drucker-Prager yield criterion can be simulated for the clay.

4. Solution Technique Used

   Modified Newton Raphson Iterative Procedure

5. Input Details:
   a. Number of elements in x-direction

b. Number of elements in y-direction
c. Total number of elements
d. Half Band width
e. Number of restrained degree of freedom
f. Number loaded degree of freedom
g. Element coordinates in x-direction
h. Element coordinates in y-direction
i. Element properties (Modulus of elasticity, poisson's ratio of material and yield stress)
j. Boundary condition (Node number, 1 for restrained and 0 for displacement allowed)
k. Degree of freedom number and load applied

6. Output Details:
   a. Displacements of nodal points for each element
   b. Stresses in an element
   c. Von-Mises Stresses and Strains

APPENDIX-IV
DISCRETIZATION DETAILS

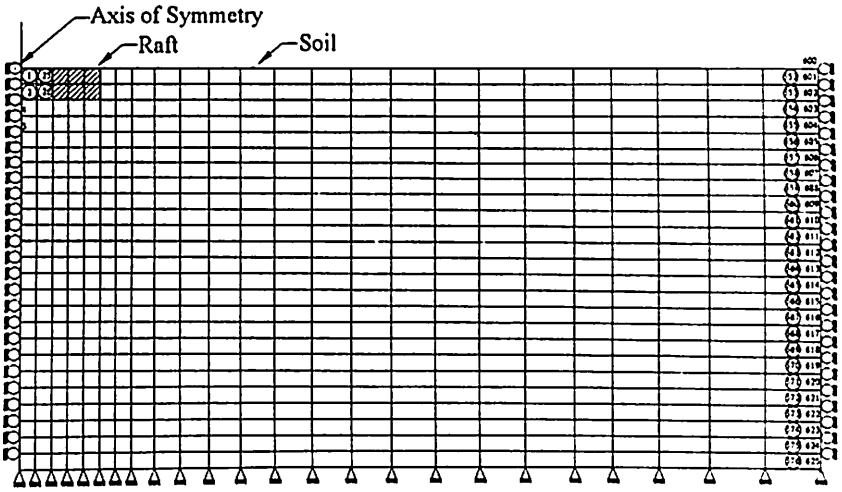

The dimensions of each element are given in Table 1 below for raft of diameter 10 m.

Table 1 Dimensions of elements for D =1 0 m, t= 1.0 m

Horizontal Direction

Element Number	Dimension (m)
1	0.5
2	0.5
3	0.5
4	0.5
5	0.5
6	0.5
7	0.5
8	0.5
9	0.5
10	0.5
11	0.5
12	1.0
13	2.0
14	2.0
15	3.0
16	4.0
17	4.0
18	4.0
19	4.0
20	4.0
21	4.0
22	4.0
23	4.0
24	6.0

Vertical Direction

Element Number	Dimension (m)
1	0.5
2	0.5
3	0.5
4	0.5
5	0.5
6	0.5
7	3.0
8	3.0
9	12.0
10	12.0
11	12.0
12	12.0
13	12.0
14	12.0
15	12.0
16	12.0
17	12.0
18	12.0
19	12.0
20	12.0
21	12.0
22	12.0
23	12.0
24	12.0

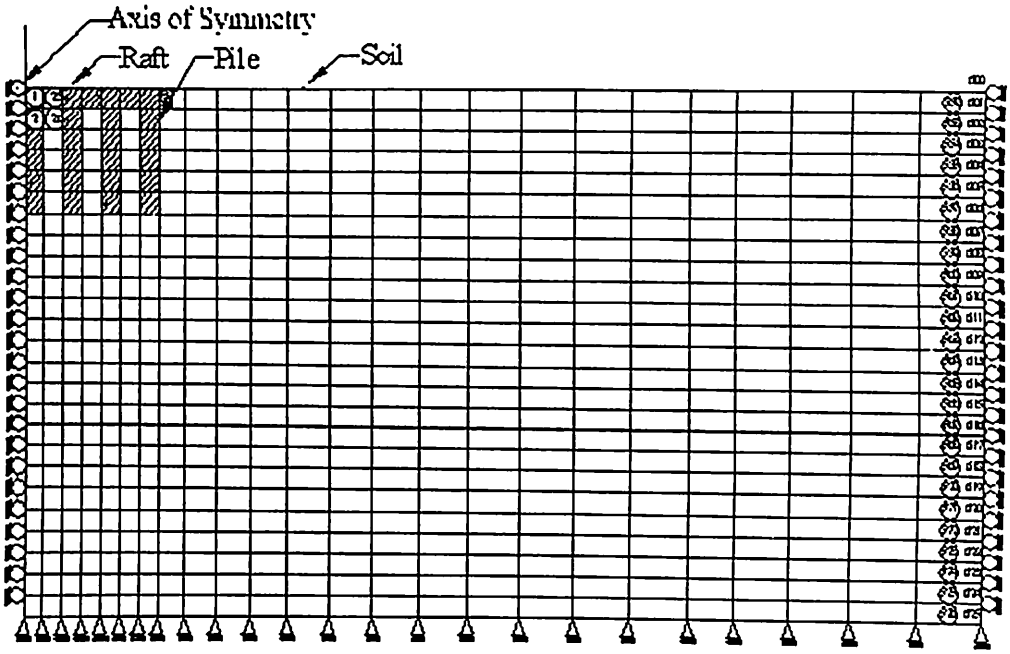

The Table 2 gives the dimensions of the elements for piled raft of diameter 30 m, s/d =2.5 and pile length as 30m.

Table 2 Dimension of Elements for D = 30m, s/d =2.5 and L = 30 m

Horizontal Direction

Element Number	Dimension (m)
1	0.2
2	1.77
3	0.06
4	1.94
5	0.06
6	1.94
7	0.06
8	1.94
9	0.06
10	1.94
11	0.06
12	1.94
13	0.06
14	1.94
15	0.06
16	0.97
17	2.0
18	10.0
19	18.0
20	20.0
21	20.0
22	20.0
23	30.0
24	30.0

Vertical Direction

Element Number	Dimension (m)
1	1.0
2	6.0
3	6.0
4	6.0
5	6.0
6	6.0
7	6.0
8	6.0
9	6.0
10	6.0
11	6.0
12	6.0
13	6.0
14	6.0
15	6.0
16	6.0
17	6.0
18	14.0
19	14.0
20	14.0
21	14.0
22	14.0
23	14.0
24	20.0

APPENDIX-IV
DISCRETIZATION DETAILS

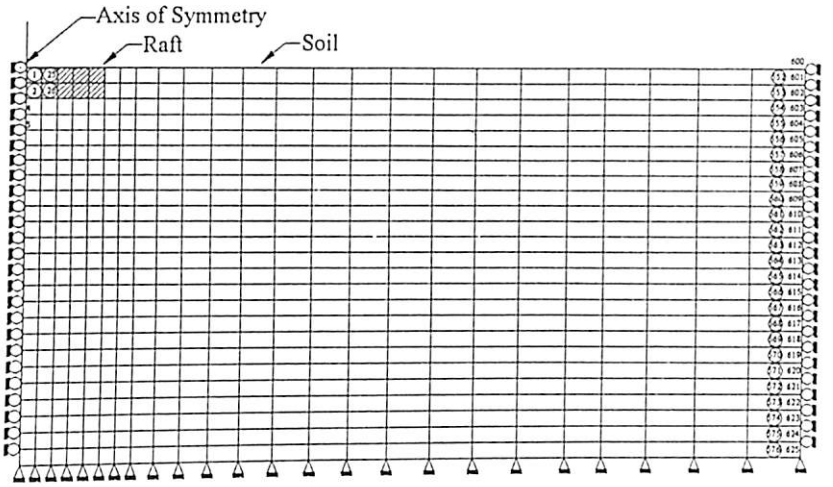

The dimensions of each element are given in Table 1 below for raft of diameter 10 m.

Table 1 Dimensions of elements for D =1 0 m, t= 1.0 m

Horizontal Direction

Element Number	Dimension (m)
1	0.5
2	0.5
3	0.5
4	0.5
5	0.5
6	0.5
7	0.5
8	0.5
9	0.5
10	0.5
11	0.5
12	1.0
13	2.0
14	2.0
15	3.0
16	4.0
17	4.0
18	4.0
19	4.0
20	4.0
21	4.0
22	4.0
23	4.0
24	6.0

Vertical Direction

Element Number	Dimension (m)
1	0.5
2	0.5
3	0.5
4	0.5
5	0.5
6	0.5
7	3.0
8	3.0
9	12.0
10	12.0
11	12.0
12	12.0
13	12.0
14	12.0
15	12.0
16	12.0
17	12.0
18	12.0
19	12.0
20	12.0
21	12.0
22	12.0
23	12.0
24	12.0

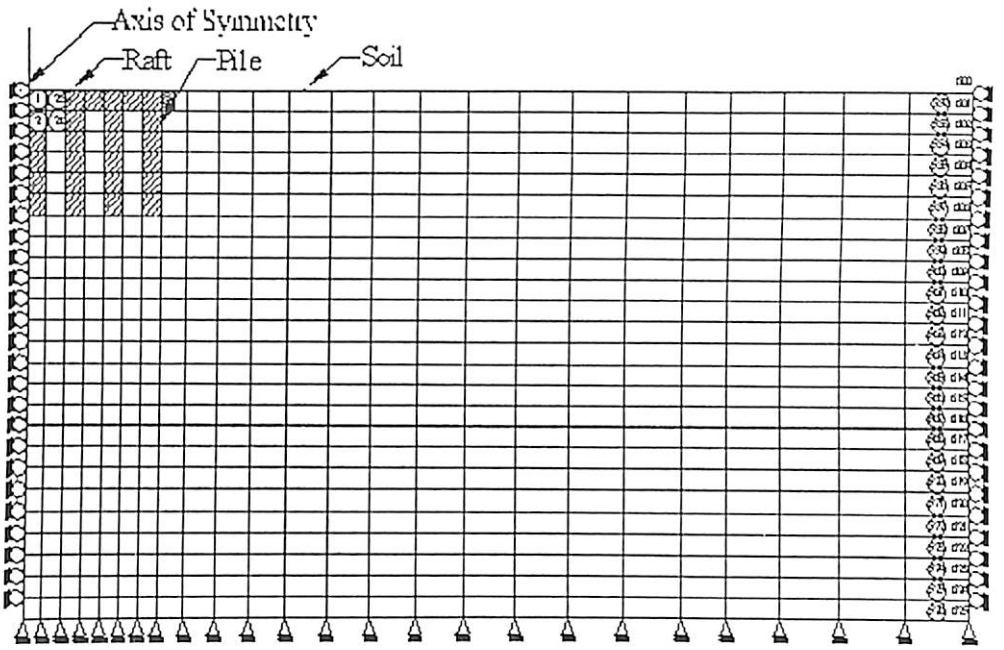

The Table 2 gives the dimensions of the elements for piled raft of diameter 30 m, s/d =2.5 and pile length as 30m.

Table 2 Dimension of Elements for D = 30m, s/d =2.5 and L = 30 m

Horizontal Direction

Element Number	Dimension (m)
1	0.2
2	1.77
3	0.06
4	1.94
5	0.06
6	1.94
7	0.06
8	1.94
9	0.06
10	1.94
11	0.06
12	1.94
13	0.06
14	1.94
15	0.06
16	0.97
17	2.0
18	10.0
19	18.0
20	20.0
21	20.0
22	20.0
23	30.0
24	30.0

Vertical Direction

Element Number	Dimension (m)
1	1.0
2	6.0
3	6.0
4	6.0
5	6.0
6	6.0
7	6.0
8	6.0
9	6.0
10	6.0
11	6.0
12	6.0
13	6.0
14	6.0
15	6.0
16	6.0
17	6.0
18	14.0
19	14.0
20	14.0
21	14.0
22	14.0
23	14.0
24	20.0

APPENDIX-V

LIST OF PUBLICATIONS

1. Maharaj, D.K., Anshuman, Banerjee, S. (2001) Nonlinear Finite Element Analysis of an Axisymmetric Raft Foundation, Indian Geotechnical Conference, 14-16 December, Organized by Indian Geotechnical Society, Indore Chapter in Association with Shri G S Institute of Technology and Science, Indore, India, pp 151-153

2. Maharaj, D.K. and Anshuman (2003) Behaviour of an axisymmetric raft foundation. All India Seminar on EMERGING TRENDS IN STRUCTURAL MECHANICS AND COMPOSITES (ETSMC-2003) organized by Department of Civil Engineering, National Institute of Technology, NIT, Rourkela and Institution of Engineers (I), 1-2 November.

3. Maharaj, D.K. and Anshuman (2003) Analysis of piled raft foundation. Under plane strain Condition, All India Seminar on EMERGING TRENDS IN STRUCTURAL MECHANICS AND COMPOSITES (ETSMC-2003) organized by Department of Civil Engineering, National Institute of Technology, NIT, Rourkela and Institution of Engineers (I), 1-2 November.

4. Maharaj, D.K. and Anshuman (2003) Behavior of Axisymmetric Piled Raft Foundation on Elastoplastic Soil, International e Conference on Modern Trends in Foundation Engineering: Geotechnical Challenges and Solutions, Organized by IIT Madras, Chennai, January 26-30,2004.

5. Maharaj, D.K. and Anshuman (2004) The Effect of Raft Size and Pile Length on Load-Settlement Behaviour of Axisymmetric Piled Raft Foundation, Electronic Journal of Geotechnical Engineering, Vol.9A, http://www.ejge.com/2004/Ppr0351/Ppr0351.htm.